

# Improving Design Phase Evaluations for High Pile Rebound Sites Final Report

FDOT Contract BDV 28-977-01

FIT Contract 201699

May 30, 2016

Principal Investigator: Paul J. Cosentino, Ph.D., P.E.  
Florida Institute of Technology  
150 W. University Blvd.  
Civil Engineering Department  
Melbourne FL 32901-6975  
cosentin@fit.edu  
Direct 321-674-7555  
Office 321-674-8048

DSR Contact: John Politano  
Florida Institute of Technology  
150 W. University Blvd.  
Office of Sponsored Programs  
Melbourne FL 32901-6975  
jpolitano@fit.edu  
321-674-7239

Project Manager: David Horhota, Ph.D., P.E.  
Florida Department of Transportation  
State Materials Office  
5007 NE 39<sup>th</sup> Ave.  
Gainesville, FL 32609  
David.Horhota@dot.state.fl.us  
352-955-2924

# Disclaimer

---

The opinions, findings, and conclusions expressed in this publication are those of the authors and not necessarily those of the State of Florida Department of Transportation.

## Metric Conversion Table

Symbol		Multiply By	To Find	Symbol
<b>LENGTH</b>				
in	inches	25.4	millimeters	mm
ft	feet	0.305	meters	m
<b>AREA</b>				
in <sup>2</sup>	square inches	645.2	square millimeters	mm <sup>2</sup>
ft <sup>2</sup>	square feet	0.093	square meters	m <sup>2</sup>
yd <sup>2</sup>	square yards	0.836	square meters	m <sup>2</sup>
<b>VOLUME</b>				
ft <sup>3</sup>	cubic feet	0.028	cubic meters	m <sup>3</sup>
<b>MASS</b>				
oz	ounces	28.35	grams	g
lb	pounds	0.454	kilograms	kg
T	short tons (2,000 l(b))	0.907	megagrams ("metric ton")	Mg (or "t")
<b>UNIT WEIGHT</b>				
pcf	lbf/ft <sup>3</sup>	16.02	kilograms/cubic meter	kg/m <sup>3</sup>
<b>TEMPERATURE (exact degrees)</b>				
°F	Fahrenheit	5 (F-32)/9 or (F-32)/1.8	Celsius	°C
<b>FORCE and PRESSURE or STRESS</b>				
lbf	pound force	4.45	newtons	N
kip	1,000 lbf	4.45	kilonewtons	kN
ton	2,000 lbf	8.90	kilonewtons	kN
lbf/in <sup>2</sup>	pound force/ square inch	6.89	kilopascals	kPa
ksi	kips / square inch	6.89	megapascals	MPa
tsf	tons/square foot	95.76	kilopascals	KPa

## Technical Report Documentation Page

1. Report No.	2. Government Accession No.	3. Recipient's Catalog No.	
4. Title and Subtitle Improving Design Phase Evaluations for High Pile Rebound Sites		5. Report Date May 31 2016	
		6. Performing Organization Code FIT Index 201699	
7. Author(s) Paul J. Cosentino, Edward H. Kalajian, Yahya S. Eldeen, Albert M. Bleakley, Brian Wisnom, Ali Omar, Hadeel Dekhn, Thaddeus J. Misilo, Alaa M. Shaban		8. Performing Organization Report No.	
9. Performing Organization Name and Address Florida Institute of Technology Civil Engineering Department 150 West University Blvd. Melbourne, FL 32901-6975 (321) 674-7555		10. Work Unit No. (TRAIS)	
		11. Contract or Grant No. Contract Number BDV28-977-01	
12. Sponsoring Agency Name and Address Florida Department of Transportation 605 Suwannee Street Tallahassee, Florida 32399-0450		13. Type of Report and Period Covered Final Report June 2013 – May 2016	
		14. Sponsoring Agency Code	
15. Supplementary Notes			
16. Abstract <p>A testing program performed to help determine typical soils properties encountered during pile installation when high rebound occurs produced a decision matrix for geotechnical engineers. High pile rebound (HPR) occurred at numerous sites in Florida. Samples from standard penetration test (SPT) borings and thin-walled tube sample borings were used in addition to cone penetrometer with pore pressure (CPTu) data to determine soil properties trends.</p> <p>Relationships between rebound and (a) SPT blow counts (N), (b) CPTu pore water pressure, and (c) fines content (FC) from previous studies were evaluated. Based on a large number of data points, weak correlations exist between inspector's rebound based and N, with rebound decreasing as N increased. There could be a relationship between rebound and FC up to about 35%; however, beyond this threshold, there is no clear relationship. A weak correlation exists between CPTu pore water pressure and rebound.</p> <p>FDOT Specification 455-5.10.3 based 0.25-inch rebound criterion was originally used but produced inclusive comparisons; therefore 0.5 inch rebound was used to yield these results. Grain size data show that rebound may be a function of certain grain sizes, implying that engineers could inexpensively locate HPR soils. The dry unit weights of the cohesive HPR soils are much lower than expected, with many values being less than the density of water. Although there was no difference in the Unified Soils Classification System or American Association of State Highway and Transportation Officials Classifications between HPR or nonHPR soils, as both classified as SM or A-4/A-2-4, the following differences were observed: (a) The average silt content for the HPR soils is more than twice as high as nonHPR soils, while both <math>D_{30}</math> and <math>D_{60}</math> are three times higher in the HPR soils than in the nonHPR soils; (b) the Atterberg limits of the HPR cohesive soils produced an average plastic index nearly twice that of the soils that displayed low to nonHPR problems; (c) the presence of silts significantly affects HPR; (d) clay content of cohesionless soils may be an effective index for predicting HPR; and (e) the Atterberg limits PI and clay content clearly showed differences between HPR and nonHPR soils. FC in the 30 to 40 % range could be an indicator of rebound greater than 0.5 inches. Sands with fines from 12 to 50% showed the greatest rebound potential.</p> <p>Permeability of HPR soils was one or two orders of magnitude lower than the nonHPR soils. Cyclic triaxial testing indicated that HPR soils are much more resilient than nonHPR soils. HPR and nonHPR soils plotted in somewhat distinct regions on soil behavior type charts. The rebound soils plotted as cemented silty fine sand with trace phosphate and shell or as cemented clayey fine sand with fines. Rebound soils are dilative while non-rebound soils are contractive.</p>			
17. Key Word High Pile Rebound, Bouncing Piles, Pore Water Pressures, Cone Penetrometer Test, Standard Penetration Test, Soil Behavior Chart.		18. Distribution Statement Document is available to the U.S. public through the National Technical Information Service, Springfield, Virginia 22161	
19. Security Classif. (of this report) Unclassified	20. Security Classif. (of this pag(e)) Unclassified	21. No. of Pages 484	22. Price

## Acknowledgements

---

This work was completed under FDOT contract number BDV28-977-01. The authors would like to acknowledge the following people for their invaluable guidance and help in the completion of this study: Dr. David Horhota, Jose Hernando, and Glenn Johnson from FDOT SMO; Robert Hipworth and Kathy Gray FDOT District 5; Samuel Weede FDOT District 3; and Brian Bloomfield from Southern Earth Sciences.

# Executive Summary

---

A comprehensive lab and field-testing program was performed to help engineers determine typical soil properties of the soils encountered during pile installation during which excessive rebound occurs. High pile rebound (HPR), as this phenomenon is termed, occurred at numerous sites in the Florida panhandle, as well as in northeastern and central Florida. Disturbed soil samples obtained from standard penetration test (SPT) borings, and test-borings with undisturbed thin-walled tube samples, were used in addition to in situ data from a cone penetrometer with pore pressure (CPTu) soundings to determine trends based on soil properties.

Evidence that relationships existed between rebound and (a) SPT blow counts (N), (b) CPTu pore water pressure, and (c) fines content (FC) (i.e., % passing #200 sieve) from previous studies was partially substantiated. Based on the large number of data points from 25 PCPs from 11 sites, a very weak correlation may exist between rebound based on inspector's set and SPT N values, with rebound decreasing as N increases. The original N-rebound correlation was based on about 30 data points with only four above N-values of 40. SPT testing invariably produces a large scatter when used for correlations. Based on several evaluations of rebound versus FC, there could be a relationship between these variables up to FC values of about 35%; however, beyond this threshold, there is no clear relationship. A weak correlation exists between CPTu pore water pressure and rebound.

Evaluation of numerous grain size distribution parameters shows that rebound greater than 0.5 inches may be a function of certain grain sizes, implying that engineers could inexpensively locate HPR soils and zones in properly completed soil borings. The standard FDOT Specification 455-5.10.3 rebound criterion of 0.25 inches was originally used for comparisons, however; unclear findings were produced. When 0.5 inches was used the findings became clear. Although there was no difference in the Unified Soils Classification System or American Association of State Highway and Transportation Officials Classifications between HPR or nonHPR soils, as both classified as SM or A-4/A-2-4, the following differences were observed:

1. The average silt content for the HPR soils is more than twice as high as nonHPR soils, while both  $D_{30}$  and  $D_{60}$  are three times higher in the HPR soils than in the nonHPR soils.

2. The Atterberg limits of the HPR cohesive soils tested produced an average plastic index nearly twice that of the soils that displayed low to nonHPR problems.
3. The presence of the silts significantly affects HPR. Below 20% silt, in cohesionless soils, HPR may not be clearly identified; however, above 20%, all 10 samples produced HPR. For cohesive soils, only HPR was evident between 20 and about 35%. With silt contents greater than about 50%, HPR is approximately the same as HPR below 20%.
4. The clay content of cohesionless soils may be an effective index for predicting HPR. Cohesive soils with clay contents less than about 30% produced nonHPR, while cohesive soils with clay contents above about 35% produced HPR.
5. The Atterberg limits PI and clay content clearly showed differences between HPR and nonHPR soils, with higher PIs and clay contents than the nonHPR soils. The Atterberg limits clearly showed differences between HPR and nonHPR soils, with higher PIs and LLs than the nonHPR soils.
6. HPR of cohesionless soils is more dependent upon silt content than clay content.

FC in the 30 to 40% range could be an indicator of rebound greater than 0.5 inches. By dividing the soils into three groups – a) FC below 12%; (b) FC between 12 and 50%, and (c) FC above 50% – the reevaluation of rebound versus  $N_{ES}$  reduced with the FDOT standard correction of process (i.e.,  $N_{auto} \times 1.24 = N_{ES}$ ) was performed. The following conclusions were obtained:

1. Sands with FC less than 12% generally did not produce rebound greater than 1 inch; and at  $N_{ES}$  above 20, they produced rebound less than 0.50 inches.
2. Soils with FC greater than 50% produced multiple instances of rebound greater than 1 inch when  $N_{ES}$  was less than 4, but they did not exceed 0.35 inches at  $N_{ES}$  greater than 24.
3. Sands with 12 to 50% fines showed the greatest potential for rebound, as rebound above 1 inch occurred up to an  $N_{ES}$  of 18 and remained high between 0.75 and 1 inch as  $N_{ES}$  increased to refusal.

In general, the permeability of the HPR soils was one or two orders of magnitude lower than the nonHPR soils. Specifically, HPR soils have permeabilities below  $5 \times 10^{-6}$ , while the nonHPR permeabilities were larger than  $1.2 \times 10^{-5}$  cm/s. The permeability of the cohesive HPR

soils is on the order of  $10^{-8}$  cm/s, or one order of magnitude lower than the nonHPR cohesive soils ( $10^{-7}$  cm/s).

The lower end of the range of dry unit weights of the HPR soils (104 pcf) is about 10% lower than the lower end of the range of dry unit weights of the nonHPR soils (111 pcf).

HPR soils required many more cycles to produce 1, 2.5, 5, 10, and 15% strains than the nonHPR soils and are therefore termed more resilient. The cyclic failure strains for nonHPR soils are typically higher (*with nearly all failing at 15% strain*) than the cyclic failure strains of HPR soils (*which mostly failed in the 1 to 5% range*). HPR specimens have lower pore water pressure ratios ( $\Delta u/\sigma_3'$ ) at failure than nonHPR specimens.

There are consistent trends indicating that increased CPTu pore pressures in fine silty sands with clays correlate to HPR for large diameter PCPs. The CPT pore water pressures ( $u_2$ ) may be linearly correlated to the pile rebound. The pore water pressures during CPTu testing are very high.

HPR and nonHPR soils plot in somewhat distinct regions on soil behavior type (SBT) charts. The rebound soils plot as fine dilative-cemented while non-rebound soils plot as either coarse or fine contractive soils on Robertson's 2012 SBT chart. Most SBT charts give some indication of type and behavior of rebound and non-rebound soils; however, these trends are sensitive to density and therefore overburden pressures.

Loose to medium dense silty sands with clay contents greater than 15% produce high rebound and were accompanied by acceptable set, which was defined as enough set to allow the pile to be driven. Medium dense to very dense silty sands have dilative response, produced rebound, and may lead to refusal. Soft to very stiff clays can produce rebound in excess of 2 inches. Rebound reduces as clays become harder.

# Table of Contents

---

1. INTRODUCTION .....	1
1.1. PROJECT OBJECTIVE.....	1
1.2. SUPPORTING TASKS AND DELIVERABLES .....	2
2. LITERATURE SEARCH .....	6
2.1. OVERVIEW .....	6
2.2. PILE MOVEMENT DURING DRIVING .....	6
2.3. DEFINITION OF HIGH PILE REBOUND.....	7
2.4. FACTORS AFFECTING PILE DRIVING IN HPR SOILS.....	8
2.5. METHODS FOR MEASURING REBOUND .....	9
2.5.1. <i>Manual Method</i> .....	9
2.5.2. <i>Dynamic Method: Pile and Soil Model by Wave Equation</i> .....	10
2.5.3. <i>High-speed Visual Measurement System of Pile Penetration and Rebound</i> .....	15
2.5.4. <i>He-Cd Laser Beam Measuring System</i> .....	17
2.6. HIGH PILE REBOUND CASE STUDIES .....	17
2.6.1. <i>Indian River Bridge over State Road 528 (Hussein et al., 2006)</i> .....	17
2.6.2. <i>Coastal North Carolina (Murrell et al., 2008)</i> .....	18
2.6.3. <i>Montreal and Timmons Ontario, Canada (Authier &amp; Fellenius, 1980)</i> .....	18
2.6.4. <i>Seattle, WA, and Florida (Likins, 1983)</i> .....	18
2.6.5. <i>High Quake in Washington’s Potomac Formation</i> .....	18
2.6.6. <i>North Sea Pile Drivability Issues in Dense Silty Sand</i> .....	19
2.6.7. <i>Escambia Bay, Pensacola, Florida</i> .....	20
2.6.8. <i>Summary of HPR Case Studies</i> .....	21

2.7. STANDARD PENETRATION TESTING .....	23
2.7.1. <i>Correcting SPT Blow Counts to N<sub>60</sub> Values</i> .....	23
2.7.2. <i>Normalized SPT N Values in Sands to Standard Overburden Pressure</i> .....	24
2.7.3. <i>Liquefaction Potential in Sandy Soils</i> .....	29
2.8. LABORATORY STUDIES OF SOIL CONSTITUENTS .....	34
2.8.1. <i>Effect of Particle Shape on the Engineering Properties of Granular Soils</i> .....	34
2.8.2. <i>Pile Drivability Using One-dimensional Wave Propagation Theory</i> .....	37
2.8.3. <i>Effect of Particle Size Distribution on Pile Tip Resistance in Calcareous Sand</i> .....	37
2.9. EFFECT OF CYCLIC LOADING .....	42
2.9.1. <i>The Use of Cyclic Deviator Stress to Evaluate Soil Behavior</i> .....	42
2.9.2. <i>Soil Behavior Under Repeated Vertical and Horizontal Stresses</i> .....	43
2.9.3. <i>The Influence of Fines Content on Pore Pressure Generation under Cyclic Loading</i>	44
2.9.4. <i>The Effects of Non-Plastic and Plastic Fines on the Liquefaction of Soil</i> .....	45
2.9.5. <i>The Effects of Non-plastic Fines on the Generation of Pore Water Pressure during Cyclic Loading</i> .....	45
2.9.6. <i>SPT N Value versus Liquefaction Potential</i> .....	48
2.9.7. <i>Development of Pore Water Pressures during Pile Driving</i> .....	49
2.9.8. <i>Summary of Cyclic Loading</i> .....	55
2.10. GEOLOGY OF FLORIDA.....	56
2.10.1. <i>Hawthorn Group</i> .....	56
2.10.2. <i>Geologic Traits of the Top of the Hawthorn Group</i> .....	57
2.10.3. <i>Engineering Properties of the Hawthorn Group near Okeechobee, Florida</i> .....	59

2.11. ESTIMATION OF SOIL PROPERTIES USING CPTu DATA .....	61
2.11.1. <i>Basic CPT Description</i> .....	61
2.11.2. <i>CPT Correlations and Soil Behavior Charts</i> .....	63
2.11.3. <i>Fines Content CPT Correlations</i> .....	72
2.12. EFFECT OF SILT CONTENT AND VOID RATIO ON SOIL HYDRAULIC CONDUCTIVITY .....	80
2.13. CORRELATIONS FROM SOIL AND SITE CHARACTERISTICS TO HPR IN FLORIDA.....	81
2.13.1. <i>Selection of Florida High Rebound Sites for Study</i> .....	81
2.13.2. <i>Using Fines Content and SPT Blow Counts to Predict High Pile Rebound</i> .....	82
2.13.3. <i>Identifying High Pile Rebound Using CPTu Pore Water Pressure</i> .....	87
2.14. SUMMARY OF CASE STUDY LITERATURE FINDINGS .....	89
3. METHODOLOGY, DESCRIPTION OF TESTING SITES, AND DATA COLLECTION.....	91
3.1. METHODOLOGY.....	91
3.1.1. <i>Identifying Testing Sites</i> .....	91
3.1.2. <i>Development of Testing Program</i> .....	92
3.1.3. <i>Collection of Existing PDA Data</i> .....	93
3.1.4. <i>Analysis of Design Phase PDA Data and Identification of Rebound Zones</i> .....	93
3.1.5. <i>Field Tests and Sampling</i> .....	94
3.1.6. <i>Field Site Data Processing</i> .....	95
3.2. DESCRIPTION OF SITES AND FIELD TESTING DATA.....	95
3.2.1. <i>I-4 / US-192 Interchange</i> .....	95
3.2.2. <i>State Road 417 International Parkway I-4 Interchange</i> .....	102
3.2.3. <i>State Road 50 over State Road 436</i> .....	107
3.2.4. <i>I-4 / State Road 408 Interchange, Ramp B</i> .....	111

3.2.5. Anderson Street Overpass .....	115
3.2.6. I-4 Widening Daytona.....	119
3.2.7. State Road 83 over Ramsey Branch Bridge.....	123
3.2.8. Saint Johns Heritage Parkway, Brevard County, Florida .....	127
3.2.9. I-10 Chaffee Road, Duval County, Florida .....	131
3.3. SUMMARY OF ALL FIELD TESTING RESULTS.....	133
4. ANALYSIS OF CPTU FIELD TESTING DATA .....	136
4.1. OVERVIEW OF THE CPTU ANALYSIS.....	136
4.2. ESTIMATION OF SOIL STRATIGRAPHY USING CPTU DATA .....	137
4.3. ANALYSIS OF THE ESTIMATED SOIL PROPERTIES .....	153
4.4. ANALYSIS OF CPTU PORE WATER PRESSURES .....	154
4.5. EVALUATION OF EXISTING CORRELATIONS BETWEEN HPR AND CPTU PORE WATER PRESSURE .....	157
4.6. ANALYSIS OF SOIL PROPERTIES' EFFECT ON THE INDUCED PORE WATER PRESSURES DURING PILE DRIVING.....	160
4.6.1. Shear-Induced Pore Water Pressure .....	161
4.6.2. Compression-Induced Pore Water Pressure.....	169
4.7. ESTIMATION AND ANALYSIS OF FINES CONTENT.....	172
4.7.1. Validation of Yi's (2014) Equation.....	172
4.7.2. Profiles of Measured and CPTu Predicted Fines Content .....	173
4.7.3. Effect of Fines Content on Pile Rebound .....	180
5. ANALYSIS OF SPT DATA.....	185
5.1. EVALUATION OF EXISTING SPT AND FINES CONTENT CORRELATIONS.....	185
5.1.1. Reevaluation of <i>N</i> versus Rebound.....	186

5.1.2. <i>FC versus Rebound</i> .....	187
5.2. REBOUND VERSUS SAFETY HAMMER EQUIVALENT SPT N VALUES.....	189
5.3. PDA REBOUND VERSUS SPT (N1)60 VALUES .....	191
5.4. PDA REBOUND VERSUS FINES CONTENT .....	192
5.5. PREDICTING CONTRACTIVE AND DILATIVE TRENDS FROM N1(60) VERSUS REBOUND.....	195
6. ANALYSIS OF LABORATORY DATA .....	197
6.1. ANALYSIS OF GRAIN SIZE PROPERTIES FOR HPR AND NONHPR SITES .....	197
6.2. EVALUATING HPR TRENDS FROM GRAIN SIZE AND CLASSIFICATION DATA.....	197
6.2.1. <i>Cohesionless Soils</i> .....	199
6.2.2. <i>Cohesive Soils</i> .....	200
6.3. EVALUATING SILT CONTENT EFFECTS ON REBOUND.....	203
6.3.1. <i>Cohesionless Soil</i> .....	203
6.3.2. <i>Cohesive Soil</i> .....	203
6.4. EVALUATING CLAY CONTENT EFFECTS ON HPR AND NONHPR SOILS.....	206
6.4.1. <i>Cohesionless Soil</i> .....	206
6.4.2. <i>Cohesive Soils</i> .....	207
6.5. EVALUATING SAND CONTENT EFFECTS ON HPR AND NONHPR SOILS .....	209
6.5.1. <i>Cohesionless Soils</i> .....	209
6.5.2. <i>Cohesive Soils</i> .....	210
6.6. EVALUATING SILT CONTENT VERSUS SAND CONTENT FOR HPR AND NONHPR SOILS.....	211
6.6.1. <i>Cohesionless Soils</i> .....	211
6.6.2. <i>Cohesive Soils</i> .....	212
6.7. EVALUATING SILT CONTENT VERSUS CLAY CONTENT FOR HPR AND NONHPR SOILS .....	213

6.7.1. Cohesionless Soils.....	213
6.7.2. Cohesive Soils.....	214
6.8. EVALUATION OF THE SILT CONTENT AND GRAIN SIZE DISTRIBUTION FACTORS $D_{10}$ , $D_{30}$ , $D_{60}$ ON HPR AND NONHPR SOILS .....	216
6.8.1. Cohesionless Soils.....	216
6.8.2. Cohesive Soils.....	219
6.9. EVALUATION OF FINE CONTENT VERSUS SILT CONTENT FOR HPR AND NONHPR SOILS .....	220
6.9.1. Cohesionless Soil.....	220
6.9.2. Cohesive Soils.....	221
6.10. EVALUATION THE EFFECT OF CLAY CONTENT AND PLASTICITY INDEX ON HPR AND NONHPR IN COHESIVE SOILS.....	222
6.11. EVALUATION THE EFFECT OF PLASTICITY INDEX AND LIQUID LIMIT ON HPR AND NONHPR IN COHESIVE SOILS.....	223
6.12. EVALUATING SILT CONTENT VERSUS PERMEABILITY FOR HPR AND NONHPR SOILS .....	224
6.12.1. Cohesionless Soils.....	224
6.12.2. Cohesive Soils.....	225
6.13. EVALUATION OF THE SILT CONTENT VERSUS UNIT WEIGHT ON HPR AND NONHPR SOILS....	226
6.13.1. Cohesionless Soil.....	226
6.13.1. Cohesive Soils.....	227
6.14. HPR BEHAVIOR DURING CYCLIC LOADING.....	228
6.14.1. The Effect of Number of Cycles on Axial Strain for HPR and NonHPR Soils.....	229
6.14.2. Evaluation of Failure Strain and Pore Water Pressure during Cyclic Loading ....	231
6.15. SOIL BEHAVIOR CHART TRENDS .....	233

7. ANALYSIS OF SOIL BEHAVIOR TYPE .....	237
7.1. BASIC APPROACH .....	237
7.2. SOIL BEHAVIOR TYPE CLASSIFICATION (ROBERTSON, 1990).....	237
7.2.1. <i>Normalized Cone Resistance versus Normalized Friction Ratio</i> .....	237
7.2.2. <i>Cone Resistance versus Pore Pressure Ratio</i> .....	239
7.3. SOIL BEHAVIOR TYPE CLASSIFICATION (ROBERTSON, 2012).....	242
7.4. SOIL CLASSIFICATION USING SCHNEIDER ET AL. (2008) .....	244
7.5. SOIL CLASSIFICATION USING ESLAMI AND FELLENIUS (1997) .....	246
7.6. SUMMARY OF SOIL BEHAVIOR TYPE CLASSIFICATION .....	247
8. CONCLUSIONS AND RECOMMENDATIONS .....	249
8.1. CONCLUSIONS.....	249
8.1.1. <i>Re-evaluations of Correlations</i> .....	249
8.1.2. <i>Grain Size Trends</i> .....	249
8.1.3. <i>Permeability and Density Trends</i> .....	251
8.1.4. <i>Cyclic Triaxial Trends</i> .....	251
8.1.5. <i>CPTu Trends</i> .....	252
8.1.6. <i>SBT Chart Trends</i> .....	253
8.2. RECOMMENDATIONS.....	254
9. REFERENCES.....	260

# List of Figures

---

FIGURE 2-1: CLASSIFICATION OF DYNAMIC PROBLEMS (AFTER ISHIHARA, 1996).....	7
FIGURE 2-2: RESISTANCE VS. PENETRATION WITH QUAKE FOR ONE HAMMER BLOW (MODIFIED AFTER SMITH, 1960).....	8
FIGURE 2-3: PILE DISPLACEMENT AND REBOUND RECORDED BY THE MANUAL METHOD (FROM HATTORI 1974, COURTESY OF GRL LIBRARY) .....	10
FIGURE 2-4: PILE-SOIL MODEL FOR WAVE EQUATION ANALYSIS (AFTER SMITH, 1960) .....	11
FIGURE 2-5: (A) PDA STRAIN GAGE AND ACCELEROMETERS ATTACHED TO A PILE AND (B) PDA EQUIPMENT WITH CAPWAP® (COURTESY OF PILE DYNAMICS, INC.).....	12
FIGURE 2-6: PDA OUTPUT MEASURED FORCE AND VELOCITY VERSUS TIME FROM A HAMMER BLOW (COURTESY OF PILE DYNAMIC, INC.) .....	13
FIGURE 2-7: CAPWAP® ITERATIVE PROCESS (COURTESY OF GRL & ASSOCIATES).....	14
FIGURE 2-8: TYPICAL PDA PILE TOP DISPLACEMENT VERSUS TIME DIAGRAM FROM ONE HAMMER BLOW FOR AN FDOT HPR SITE (COSENTINO ET AL., 2010).....	15
FIGURE 2-9: MARKING PAPER AND LINE SCAN CAMERA SETUP DURING PILE DRIVING (OLIVEIRA ET AL., 2013).....	16
FIGURE 2-10: COMPARISON BETWEEN ELASTIC REBOUND RESULTS OBTAINED WITH CONVENTIONAL MANUAL METHOD AND THE PDR SYSTEM (OLIVEIRA ET AL., 2013). .....	17
FIGURE 2-11: CN FACTORS FROM VARIOUS AUTHORS (AFTER DAS, 2014).....	27
FIGURE 2-12: COHESIONLESS AND COHESIVE UNIT WEIGHT ESTIMATES (CDOT, 2014) .....	28
FIGURE 2-13: EFFECT OF PARTICLE SHAPE ON MINIMUM AND MAXIMUM VOID RATIOS (HOLUBEC & D’APPOLONIA, 1972).....	35
FIGURE 2-14: EFFECT OF PARTICLE SHAPE ON ANGLE OF INTERNAL FRICTION (HOLUBEC & D’APPOLONIA 1972).....	36
FIGURE 2-15: EFFECT OF PARTICLE SHAPE ON STRESS-STRAIN CURVES FROM CONSTANT CELL PRESSURE TESTS (HOLUBEC, & D’APPOLONIA, 1972).....	36
FIGURE 2-16: INITIAL QUIOU SAND GRADATION CURVES (MCDOWELL & BOLTON, 2000) .....	38
FIGURE 2-17: CAMBRIDGE CENTRIFUGE CONTAINING THE 850 MM DIAMETER STEEL TUB WITH FOUR 190 MM DIAMETER SAMPLES (MCDOWELL & BOLTON, 2000).....	39

FIGURE 2-18: TIP RESISTANCE (kPA) AS A FUNCTION OF DEPTH (MM) FOR EACH OF THE FOUR SOIL SAMPLES (MCDOWELL & BOLTON, 2000).....	40
FIGURE 2-19: PARTICLE SIZE DISTRIBUTIONS FOR SAMPLES 1 AND 2 AT DEPTHS LESS THAN AND GREATER THAN THE INSTABILITY DEPTH (MCDOWELL & BOLTON, 2000).....	41
FIGURE 2-20: RESULTS OF CYCLIC TRIAXIAL TESTS: (A) SILT CONTENTS VERSUS CYCLES REQUIRED TO GENERATE 100% EXCESS PORE WATER PRESSURE; (B) LOADING CYCLES VERSUS EXCESS PORE PRESSURE RATIO (DASH & SITHARAM, 2009).....	48
FIGURE 2-21: CPTu PORE PRESSURES DISSIPATION TESTS AT THE ALEX FRASER BRIDGE (ROBERTSON ET AL., 1990).....	50
FIGURE 2-22 RELATIONSHIP BETWEEN MEASURED PORE PRESSURES FROM CPT <sub>u</sub> AND MP PIEZOMETERS WITH NORMALIZED RADIAL DISTANCE FROM PILE (ROBERTSON ET AL., 1990).....	51
FIGURE 2-23: PORE WATER PRESSURE CHANGES DUE TO PILE DRIVING (EIGENBROD & ISSIGONIS, 1996).....	52
FIGURE 2-24: EXCESS PORE PRESSURE VERSUS DRIVING DEPTH FOR THE THREE SENSOR LOCATIONS (BINGJIAN, 2011).....	53
FIGURE 2-25: EXCESS PORE PRESSURE VERSUS RADIAL DISTANCE AT DISCRETE DRIVING DEPTHS CURVE (FROM BINGJIAN, 2011).....	54
FIGURE 2-26: CHANGE IN PORE PRESSURE VERSUS TIME FOR THE THREE SENSOR LOCATIONS (BINGJIAN, 2011).....	55
FIGURE 2-27 TOP ELEVATION CONTOURS OF THE HAWTHORN GROUP WITH APPROXIMATE HIGH PILE REBOUND SITE LOCATIONS [AFTER SCOTT (1990)].....	60
FIGURE 2-28: TYPES OF CPT PROBES (FROM LEFT: 2 CM <sup>2</sup> , 10 CM <sup>2</sup> , 15 CM <sup>2</sup> , 40 CM <sup>2</sup> ) (ROBERTSON & CABAL, 2010).....	62
FIGURE 2-29: CPTu PORE PRESSURE TRANSDUCER POSITIONS: AT THE CONE POINT (U <sub>1</sub> ), BEHIND THE CONE TIP (U <sub>2</sub> ), AND ON THE SHAFT BETWEEN THE CONE AND SLEEVE (U <sub>3</sub> ).....	62
FIGURE 2-30: OVERVIEW OF THE CONE PENETRATION TEST PER ASTM D5778-95.....	63
FIGURE 2-31: NORMALIZED SOIL BEHAVIOR TYPE CHART (SBTN) BASED ON CPT NORMALIZED CONE RESISTANCE (Q <sub>TN</sub> ) AND NORMALIZED FRICTION RATIO (F <sub>R</sub> ) (ROBERTSON, 1990).....	65
FIGURE 2-32: RELATIONSHIP BETWEEN CPT RESULTS AND DIMENSIONLESS SOIL UNIT WEIGHT (ROBERTSON & CABAL, 2010).....	67
FIGURE 2-33: ROBERTSON (1990) CONE RESISTANCE VERSUS PORE PRESSURE RATIO SBT CHART.....	68
FIGURE 2-34: NORMALIZED SBT CHART DEVELOPED BY SCHNEIDER ET AL. (2008).....	69
FIGURE 2-35: ESLAMI AND FELLENIUS' (1997) SBT CHART.....	70

FIGURE 2-36: SCHEMATIC OF VOID RATIO VERSUS STRAIN USED TO DETERMINE THE STATE PARAMETER .....	71
FIGURE 2-37: UPDATED NORMALIZED CONE RESISTANCE VERSUS FRICTION RATIO SBT CHART WITH SOIL BEHAVIOR (ROBERTSON, 2012) .....	72
FIGURE 2-38: MEASURED VERSUS ESTIMATED FC (%) FOR 95% CONFIDENCE LEVEL (YI, 2014).....	74
FIGURE 2-39: EXPERIMENTAL CORRELATION BETWEEN $T_{50}$ AND FINES CONTENT (MOAYED, 2006).....	75
FIGURE 2-40: SUGGESTED VARIATION OF SOIL PERMEABILITY (K) AS A FUNCTION OF SOIL BEHAVIOR TYPE INDEX $I_c$ (ROBERTSON, 2010).....	79
FIGURE 2-41: STATE PARAMETER CONTOURS ON THE ROBERTSON (1990) NORMALIZED SBT CHART (ROBERTSON, 2009).....	80
FIGURE 2-42: HYDRAULIC CONDUCTIVITY FOR VARIOUS SILT CONTENTS (BANDINI & SATHISKUMAR, 2009).....	81
FIGURE 2-43: (A) GENERALIZED SOIL PROFILE, (B) PDA DIAGRAM, (C) $N_{SPT}$ , AND (D) PERCENT FINES CONTENT FOR SITE 1 ANDERSON STREET OVERPASS (JARUSHI ET AL., 2013). .....	84
FIGURE 2-44 (A) CORRELATION BETWEEN REBOUND, NSPT, AND FINES CONTENT, AND (B) CORRELATION BETWEEN PERMANENT-SET, $N_{SPT}$ AND FINES CONTENT (JARUSHI ET AL., 2013). .....	85
FIGURE 2-45: PREDICTED REBOUND USING $N_{SPT}$ AND FINES CONTENT VERSUS ACTUAL PDA REBOUND (JARUSHI ET AL., 2013) .....	86
FIGURE 2-46: (A) GENERALIZED SOIL PROFILE, (B) PDA DIAGRAM AND (C) CPTU PORE-WATER PRESSURE ( $U_2$ ) FOR SITE 3 I- 4/US.192 (COSENTINO ET AL., 2013).....	88
FIGURE 2-47: CORRELATIONS BETWEEN REBOUND, PERMANENT-SET AND (A) CPTU PORE WATER PRESSURE, AND (B) RATIO OF CPTU PORE PRESSURE ( $U_2$ ) AND HYDROSTATIC PRESSURE ( $U_0$ ) (COSENTINO ET AL., 2013). .....	89
FIGURE 3-1: TEST PILES, SPT BORING, AND CPTU SOUNDING LOCATIONS FOR I-4/US-192 INTERCHANGE .....	96
FIGURE 3-2: DIGITAL SET, PILE REBOUND, AND $N_{PD}$ VERSUS DEPTH FOR (A) PIER 6/PILE 16, (B) PIER 7/PILE 10 AND (C) PIER 8/PILE 4 FOR I-4/US 192 INTERCHANGE .....	97
FIGURE 3-3: GENERAL SOIL PROFILE WITH USCS CLASSIFICATION AND THE ACTUAL NUMBER OF BLOWS (N) FROM SPT BORINGS B-39, B-40, AND B-41 FOR I-4/US 192 INTERCHANGE .....	99
FIGURE 3-4: CPTU $Q_c$ , $F_s$ , AND $U_2$ VERSUS DEPTH FROM CPTU-4 NEAR PIER 6/PILE 16 AT I-4/US 192 .....	100
FIGURE 3-5: CPTU $Q_c$ , $F_s$ , AND $U_2$ VERSUS DEPTH FROM CPTU-3 NEAR PIER 7/PILE 10 AT I-4/US 192 .....	101

FIGURE 3-6: CPTU $Q_c$ , $F_s$ , AND $U_2$ VERSUS DEPTH FROM CPTU-2 NEAR PIER 8/PILE 4 AT I-4/US 192.....	101
FIGURE 3-7: TEST PILES, SPT BORING, AND CPTU SOUNDING LOCATIONS FOR SR 417 INTERNATIONAL PARKWAY I-4 INTERCHANGE.....	103
FIGURE 3-8: DIGITAL SET, PILE REBOUND, AND $N_{PD}$ VERSUS DEPTH FOR ((A) B1/PILE 14 AND ((B) B2/PILE 5 AT SR 417 INTERNATIONAL PARKWAY I-4 INTERCHANGE .....	104
FIGURE 3-9: GENERAL SOIL PROFILE WITH USCS CLASSIFICATION AND $N_{SPT}$ FROM SPT BORINGS SPT-B1 AND SPT-B2 FOR SR 417 INTERNATIONAL PARKWAY I-4 INTERCHANGE .....	105
FIGURE 3-10: CPTU $Q_c$ , $F_s$ , AND $U_2$ VERSUS DEPTH FROM CPT-1 NEAR B1/PILE 14 AT SR 417 INTERNATIONAL PARKWAY I-4 INTERCHANGE.....	106
FIGURE 3-11: CPTU $Q_c$ , $F_s$ , AND $U_2$ VERSUS DEPTH FROM CPT-3 NEAR B2/PILE 5 AT SR 417 INTERNATIONAL PARKWAY ...	107
FIGURE 3-12: TEST PILES, SPT BORING, AND CPTU SOUNDING LOCATIONS FOR SR50/SR436 .....	108
FIGURE 3-13: DIGITAL SET, PILE REBOUND, AND $N_{PD}$ VERSUS DEPTH FOR PILE 5 FOR THE WESTBOUND SIDE OF SR 50 / SR 436 .....	109
FIGURE 3-14: GENERAL SOIL PROFILE WITH USCS CLASSIFICATION AND THE ACTUAL $N_{SPT}$ FROM SPT BORING TH-4B NEAR PILE 5 AT THE WESTBOUND SIDE OF SR50/SR436.....	110
FIGURE 3-15: CPTU $Q_c$ , $F_s$ , AND $U_2$ VERSUS DEPTH FROM CPT-1 NEAR PILE 5 AT THE WESTBOUND SIDE OF SR 50 / SR436.	111
FIGURE 3-16: TEST PILE, SPT BORING, AND CPTU SOUNDING LOCATIONS FOR I-4/SR 408 (RAMP B) .....	112
FIGURE 3-17: DIGITAL SET, PILE REBOUND, AND $N_{PD}$ VERSUS DEPTH FOR PIER 2/PILE 5 AT RAMP B OF I-4 / SR 408.....	113
FIGURE 3-18: GENERAL SOIL PROFILE WITH USCS CLASSIFICATION AND THE ACTUAL NUMBER OF BLOWS (N) FROM SPT BORING B-101 NEAR PIER 2/PILE 5 AT RAMP B OF I-4/SR 408.....	114
FIGURE 3-19: CPTU $Q_c$ , $F_s$ , AND $U_2$ VERSUS DEPTH FROM CPT B-109 NEAR PIER 2/PILE 5 AT RAMP B OF I-4/SR 408.....	115
FIGURE 3-20: TEST PILES, SPT BORING, AND CPTU SOUNDING LOCATIONS FOR THE ANDERSON STREET OVERPASS .....	116
FIGURE 3-21: DIGITAL SET, PILE REBOUND, AND $N_{PD}$ VERSUS DEPTH FOR (A) PIER 6/PILE 6 AND (B) PIER 6/PILE 5 AT THE ANDERSON STREET OVERPASS.....	117
FIGURE 3-22: GENERAL SOIL PROFILE WITH USCS CLASSIFICATION AND THE ACTUAL $N_{SPT}$ FROM SPT BORING SPT P6-3 NEAR PIER 6 AT THE ANDERSON STREET OVERPASS .....	118
FIGURE 3-23: CPTU $Q_c$ , $F_s$ , AND $U_2$ VERSUS DEPTH FROM CPT-5 NEAR PIER 6 AT THE ANDERSON STREET OVERPASS .....	119

FIGURE 3-24: TEST PILES, SPT BORING, AND CPTU SOUNDING LOCATIONS FOR I-4 WIDENING DAYTONA .....	120
FIGURE 3-25: DIGITAL SET, PILE REBOUND, AND $N_{PD}$ VERSUS DEPTH FOR EB3/PILE 5 AT I-4 WIDENING DAYTONA.....	121
FIGURE 3-26: GENERAL SOIL PROFILE WITH USCS CLASSIFICATION AND THE ACTUAL $N_{SPT}$ FROM SPT BORING SPT DC-1 NEAR EB3/PILE 5 AT I-4 WIDENING DAYTONA.....	122
FIGURE 3-27: CPTU $Q_c$ , $F_s$ , AND $U_2$ VERSUS DEPTH NEAR EB3/PILE 5 AT I-4 WIDENING DAYTONA .....	123
FIGURE 3-28: TEST PILE, SPT BORING, AND CPTU SOUNDINGS LOCATIONS FOR SR 83/RAMSEY BRANCH BRIDGE .....	124
FIGURE 3-29: DIGITAL SET, PILE REBOUND, AND $N_{PD}$ VERSUS DEPTH FOR EB5/PILE 2 AT SR 83/RAMSEY BRANCH BRIDGE	125
FIGURE 3-30: GENERAL SOIL PROFILE WITH USCS CLASSIFICATION AND THE ACTUAL $N_{SPT}$ FROM SPT BORING B-3 NEAR EB5/PILE 2 AT SR 83/ RAMSEY BRANCH BRIDGE.....	126
FIGURE 3-31: CPTU $Q_c$ , $F_s$ , AND $U_2$ VERSUS DEPTH FROM CPT-1 NEAR EB5/PILE 2 AT SR 83/ RAMSEY BRANCH BRIDGE.....	128
FIGURE 3-32: CPTU $Q_c$ , $F_s$ , AND $U_2$ VERSUS DEPTH FROM CPT-2 NEAR EB5/PILE 2 AT SR 83/RAMSEY BRANCH BRIDGE .....	128
FIGURE 3-33: SITE LOCATION AND TEST PILE, SPT BORING AND CPTU SOUNDING LOCATIONS FOR HERITAGE PARKWAY, BREVARD COUNTY, FLORIDA .....	129
FIGURE 3-34: (A) FDOT AND TH-6 SOIL PROFILE, (B) PDA DIAGRAM, (C) NSAFE AND FC FOR HERITAGE PARKWAY TEST PILE B3P1 .....	130
FIGURE 3-35: COMBINED CPTU DATA FROM HERITAGE PARKWAY.....	131
FIGURE 3-36: SITE LOCATION, SPT BORING AND CPT SOUNDING FOR I-10 CHAFFEE ROAD INTERCHANGE, DUVAL COUNTY, FLORIDA.....	132
FIGURE 3-37: (A) SOIL PROFILE, (B) PDA DIAGRAM, (C) NSAFE AND FC FOR I-10 CHAFFEE ROAD INTERCHANGE TEST PILE B3 EB 1.....	133
FIGURE 4-1: SATURATED DENSITY VERSUS DEPTH FOR I-4/US 192 AT (A) PIER 6/PILE 16, (B) PIER 7/PILE 10, AND (C) PIER 8/PILE 4 RESPECTIVELY WITH HPR ZONES SHADED .....	138
FIGURE 4-2: SATURATED DENSITY VERSUS DEPTH FOR SR 417 INTERNATIONAL PARKWAY AT (A) B1/PILE 14 (B) B2/PILE 5 .....	139
FIGURE 4-3: SATURATED DENSITY VERSUS DEPTH FOR SR 50/SR436 AT WESTBOUND/PILE 5 WITH HPR ZONES SHADED ...	139
FIGURE 4-4: SATURATED DENSITY VERSUS DEPTH FOR I-4/SR408 AT PIER 2/PILE 5 .....	140

FIGURE 4-5: SATURATED DENSITY VERSUS DEPTH FOR ANDERSON STREET AT PIER 6/PILES 5 AND 6 WITH HPR ZONES SHADED .....	140
FIGURE 4-6: SATURATED DENSITY VERSUS DEPTH FOR I-4 WIDENING DAYTONA AT EB3/PILE 5 WITH HPR ZONES SHADED	141
FIGURE 4-7: SATURATED DENSITY VERSUS DEPTH FOR SR 83/RAMSEY BRANCH BRIDGE AT EB5/PILE 2 WITH HPR ZONES SHADED .....	141
FIGURE 4-8: NORMALIZED SOIL BEHAVIOR TYPE INDEX AND TYPICAL GEOTECHNICAL SECTION FOR I-4/US 192 AT PIER 6/PILE 16 WITH HPR ZONE SHADED (GSE = 109.6 FT) .....	143
FIGURE 4-9: NORMALIZED SOIL BEHAVIOR TYPE INDEX AND TYPICAL GEOTECHNICAL SECTION FOR I-4/US 192 AT PIER 7/PILE 10 WITH HPR ZONE SHADED (GSE = 108.6 FT) .....	144
FIGURE 4-10: NORMALIZED SOIL BEHAVIOR TYPE INDEX AND TYPICAL GEOTECHNICAL SECTION FOR I-4/US 192 AT PIER 8/PILE 4 WITH HPR ZONE SHADED (GSE = 90.2 FT) .....	145
FIGURE 4-11: NORMALIZED SOIL BEHAVIOR TYPE INDEX AND TYPICAL GEOTECHNICAL SECTION FOR SR 417 INTERNATIONAL PARKWAY AT B1/PILE 14 (GSE = 72.3 FT) .....	146
FIGURE 4-12: NORMALIZED SOIL BEHAVIOR TYPE INDEX AND TYPICAL GEOTECHNICAL SECTION FOR SR 417 INTERNATIONAL PARKWAY AT B2/PILE 5 (GSE = 72.3 FT).....	147
FIGURE 4-13: NORMALIZED SOIL BEHAVIOR TYPE INDEX AND TYPICAL GEOTECHNICAL SECTION FOR SR 50/SR436 AT WEST BOUND/PILE 5 WITH HPR ZONE SHADED (GSE = 99.0 FT) .....	148
FIGURE 4-14: NORMALIZED SOIL BEHAVIOR TYPE INDEX AND TYPICAL GEOTECHNICAL SECTION FOR I-4/SR408 AT PIER 2/PILE 5 (GSE = 106 FT) .....	149
FIGURE 4-15: NORMALIZED SOIL BEHAVIOR TYPE INDEX AND TYPICAL GEOTECHNICAL SECTION FOR ANDERSON STREET OVERPASS AT PIER 6/PILE 5, 6 WITH HPR ZONE SHADED (GSE = 104 FT) .....	150
FIGURE 4-16: NORMALIZED SOIL BEHAVIOR TYPE INDEX AND TYPICAL GEOTECHNICAL SECTION FOR I-4 WIDENING DAYTONA AT EB3/PILE 5 (GSE = 42.0 FT).....	151
FIGURE 4-17: NORMALIZED SOIL BEHAVIOR TYPE INDEX AND TYPICAL GEOTECHNICAL SECTION FOR SR 83 OVER RAMSEY BRANCH BRIDGE AT EB 5/PILE 2 WITH HPR ZONE SHADED (GSE = 1.0 FT).....	152
FIGURE 4-18: ZONES AFFECTED BY CONE PENETRATION (FROM BURNS & MAYNE, 1999).....	155
FIGURE 4-19: PILE REBOUND FOR 24 24-INCH PRECAST CONCRETE PILES VERSUS CPT <sub>u</sub> U <sub>2</sub> (JARUSHI ET AL., 2013).....	157
FIGURE 4-20: DIGITAL REBOUND VERSUS CPT <sub>u</sub> PORE PRESSURE FROM SIX TEST SITES .....	159

FIGURE 4-21: DIGITAL REBOUND VERSUS CPTu PORE PRESSURE FROM SIX TEST SITES WITH REBOUND > 0.5 INCHES.....	160
FIGURE 4-22: SOIL LAYERS DEFORMATIONS AROUND A DRIVEN PILE .....	161
FIGURE 4-23: TYPICAL SHEAR STRESS VERSUS SHEAR STRAIN FOR GRANULAR AND COHESIVE SOILS (DAS, 2008) .....	162
FIGURE 4-24: UNDRAINED SHEAR STRENGTH FOR I-4/US 192 AT (A) PIER 6/PILE 16, (B) PIER 7/PILE 10, AND (C) PIER 8/PILE 4 WITH HPR ZONES SHADED.....	163
FIGURE 4-25: UNDRAINED SHEAR STRENGTH FOR SR 417 INTERNATIONAL PARKWAY AT (A) B1/PILE 14 AND (B) B2/PILE 5.....	164
FIGURE 4-26: UNDRAINED SHEAR STRENGTH FOR SR 50/SR 436 AT WESTBOUND/PILE 5 WITH HPR ZONE SHADED .....	165
FIGURE 4-27: UNDRAINED SHEAR STRENGTH FOR I-4/SR 408 AT PIER 2/PILE 5.....	166
FIGURE 4-28: UNDRAINED SHEAR STRENGTH FOR ANDERSON STREET AT PIER 6 WITH HPR ZONE SHADED.....	167
FIGURE 4-29: UNDRAINED SHEAR STRENGTH FOR I-4 WIDENING DAYTONA AT EB3/PILE 5 .....	168
FIGURE 4-30: UNDRAINED SHEAR STRENGTH FOR SR 83/RAMSEY BRANCH BRIDGE AT EB 5/PILE 2 WITH HPR ZONES SHADED (A) CPT1, (B) CPT2 .....	169
FIGURE 4-31: PLASTIC AND ELASTIC ZONES AROUND SINGLE DRIVEN PILE (WREN, 2007).....	170
FIGURE 4-32: GUI AND JENG 'S (2009) MAXIMUM COMPRESSION-INDUCED PORE WATER PRESSURE DUE TO DRIVING 24-INCH PRESTRESSED CONCRETE PILES WITH HPR ZONES SHADED FOR I-4/US 192 AT (A) PIER 6/PILE 16, (B) PIER 7/PILE 10, AND (C) PIER 8/PILE 4.....	172
FIGURE 4-33: VERIFICATION OF FINES CONTENT ESTIMATION PROCEDURE BASED ON 80 DATA POINTS FROM ALL SITES.....	173
FIGURE 4-34: PREDICTED AND MEASURED FINES CONTENT VERSUS DEPTH FOR I-4/US 192 AT (A) PIER 6/PILE 16 (B) PIER 7/PILE 10 (C) PIER 8/PILE 4 WITH HPR ZONES SHADED.....	174
FIGURE 4-35: PREDICTED AND MEASURED FINES CONTENT VERSUS DEPTH FOR SR 417 INTERNATIONAL PARKWAY AT (A) B1/PILE 14 (B) B2/PILE 5.....	175
FIGURE 4-36 FOR PREDICTED AND MEASURED FINES CONTENT VERSUS DEPTH FOR SR 50/SR 436 AT WESTBOUND/PILE 5 WITH HPR.....	176
FIGURE 4-37 FOR PREDICTED AND MEASURED FINES CONTENT VERSUS DEPTH FOR I-4/SR 408 AT PIER 2/PILE 5.....	177
FIGURE 4-38 FOR PREDICTED AND MEASURED FINES CONTENT VERSUS DEPTH FOR THE ANDERSON STREET OVERPASS AT PIER 6/PILE 5, 6 WITH HPR ZONE SHADED .....	178

FIGURE 4-39 FOR PREDICTED AND MEASURED FINES CONTENT VERSUS DEPTH FOR I-4 WIDENING DAYTONA AT EB 3/PILE 5 WITH HPR ZONE SHADED.....	179
FIGURE 4-40: PREDICTED AND MEASURED FINES CONTENT VERSUS DEPTH FOR SR 83 OVER RAMSEY BRANCH BRIDGE AT EB 5/PILE 2 WITH HPR ZONE SHADED.....	180
FIGURE 4-41: PILE REBOUND VERSUS CPTU FC FOR DIFFERENT SOIL TYPES.....	182
FIGURE 4-42: CPTU PORE WATER PRESSURE ( $U_2$ ) VERSUS FC FOR DIFFERENT SOIL TYPES.....	184
FIGURE 5-1: REBOUND VERSUS N AND FC BY COSENTINO ET AL. (2011).....	186
FIGURE 5-2: CURRENT STUDY REBOUND VS $N_{ES}$ FOR SITES REVIEWED BY COSENTINO ET AL. (2011) AND JARUSHI (2013)....	187
FIGURE 5.3: CURRENT STUDY REBOUND VS FC FOR SITES REVIEWED BY COSENTINO ET AL. (2011).....	188
FIGURE 5.4: MINIMUM FC BOUNDARY WITH ASSOCIATED REBOUND (FC > 35% OMITTED).....	189
FIGURE 5.5: REBOUND VS $N_{ES}$ FOR ALL SITES AND SOILS.....	190
FIGURE 5.6: REBOUND VS $(N1)60$ FOR SANDS.....	192
FIGURE 5.7: REBOUND VS FC FOR ALL SITES AND SOILS.....	193
FIGURE 5.8: FREQUENCY DISTRIBUTION OF FC FOR (A) REBOUND > 0.50 INCHES AND (B) REBOUND < 0.50 INCHES.....	194
FIGURE 5.9: SOIL PREDICTED REACTION TO SPT EQUIVALENT $(N1)60$ AFTER WISNOM (2015) FOR (A) REBOUND > 0.50 INCHES AND (B) REBOUND < 0.50 INCHES.....	196
FIGURE 6.1: GRAIN SIZE DISTRIBUTION CURVES FOR HIGH PILE HPR COHESIONLESS SOIL.....	200
FIGURE 6.2: GRAIN SIZE DISTRIBUTION CURVES FOR NONHPR COHESIONLESS SOILS.....	200
FIGURE 6.3: GRAIN SIZE DISTRIBUTION CURVES FOR HIGH PILE HPR COHESIVE SOILS.....	202
FIGURE 6.4: GRAIN SIZE DISTRIBUTION CURVES FOR LOW TO NONHPR COHESIONLESS SOILS.....	202
FIGURE 6.5: SILT CONTENT (%) VS. PDA HPR (IN) – COHESIONLESS SOILS (SM) FROM ALL SITES.....	205
FIGURE 6.6: SILT CONTENT (%) VS. PDA HPR (IN) – COHESIVE SOILS (CH, CL) FROM ALL SITES.....	206
FIGURE 6.7: CLAY CONTENT (%) VS. PDA HPR (IN) – COHESIONLESS SOILS (SM) FROM ALL SITES.....	207
FIGURE 6.8: CLAY CONTENT (%) VS. PDA HPR (IN) – COHESIVE SOILS (CH, CL) FROM ALL SITES.....	208
FIGURE 6.9: SAND CONTENT (%) VS. PDA HPR (IN) – COHESIONLESS SOILS (SM) FROM ALL SITES.....	210

FIGURE 6.10: SAND CONTENT (%) VS. PDA HPR (IN) – COHESIVE SOILS (CH, CL) FROM ALL SITES .....	211
FIGURE 6.11: SILT CONTENT (%) VS. SAND CONTENT (%) – COHESIONLESS SOILS (SM) FROM ALL SITES .....	212
FIGURE 6.12: SILT CONTENT (%) VS. SAND CONTENT (%) – COHESIVE SOILS (CH, CL) FROM ALL SITES.....	213
FIGURE 6.13: SILT CONTENT (%) VS. CLAY CONTENT – COHESIONLESS SOILS (SM) FROM ALL SITES.....	214
FIGURE 6.14: SILT CONTENT (%) VS. CLAY CONTENT – COHESIVE SOILS (CH, CL) FROM ALL SITES.....	216
FIGURE 6.15: SILT CONTENT (%) VS. D <sub>10</sub> CONTENT – COHESIONLESS SOILS (SM) FROM ALL SITES .....	217
FIGURE 6.16: SILT CONTENT (%) VS. D <sub>30</sub> CONTENT – COHESIONLESS SOILS (SM) FROM ALL SITES .....	218
FIGURE 6.17: SILT CONTENT (%) VS. D <sub>60</sub> CONTENT – COHESIONLESS SOILS (SM) FROM ALL SITES .....	219
FIGURE 6.18: CLAY CONTENT (%) VS. D <sub>60</sub> CONTENT – COHESIVE SOILS (CH, CL) FROM ALL SITES.....	220
FIGURE 6.19: SILT CONTENT (%) VS. FINES CONTENT (%) – COHESIONLESS SOILS (SM) FROM ALL SITES.....	221
FIGURE 6.20: SILT CONTENT (%) VS. FINES CONTENT (%) – COHESIVE SOILS (CH, CL) FROM ALL SITES.....	222
FIGURE 6.21: CLAY CONTENT (%) VERSUS PLASTIC INDEX (PI) .....	223
FIGURE 6.22: LIQUID LIMIT (LL) VERSUS PLASTIC INDEX, (PI) FOR COHESIVE (CL, CH) SOILS.....	224
FIGURE 6.23: PERMEABILITY VS. SILT CONTENT – COHESIONLESS SOILS (SM) FROM ALL SITES .....	225
FIGURE 6.24: PERMEABILITY VS. SILT CONTENT – COHESIVE SOILS (CH, CL) FROM ALL SITES .....	226
FIGURE 6.25: DRY UNIT WEIGHT VS. SILT CONTENT – COHESIONLESS SOILS (SM) FROM ALL SITES .....	227
FIGURE 6.26: DRY UNIT WEIGHT VS. SILT CONTENT – COHESIVE SOILS (CH, CL) FROM ALL SITES .....	228
FIGURE 6.27: NUMBER OF CYCLES REQUIRED TO ACHIEVE 1%, 2.5%, 5%, 10%, AND 15% STRAIN FOR COHESIONLESS SOILS SUSCEPTIBLE TO HPR AND NONHPR .....	230
FIGURE 6.28: NUMBER OF CYCLES REQUIRED TO ACHIEVE 1%, 2.5%, 5%, 10%, AND 15% STRAIN FOR COHESIVE SOILS SUSCEPTIBLE TO HPR AND NONHPR.....	231
FIGURE 6.29: CYCLIC TRIAXIAL FAILURE STRAIN VERSUS NUMBER OF CYCLES FROM CYCLIC TRIAXIAL TESTS PERFORMED ON COHESIONLESS HPR AND NONHPR SOILS .....	232
FIGURE 6.30: PORE WATER PRESSURE RATIO VERSUS NUMBER OF CYCLIC LOADINGS FROM CYCLIC TRIAXIAL TESTS ON HPR AND NONHPR COHESIONLESS SOILS.....	233

FIGURE 6.31 AVERAGED CPT <sub>u</sub> CONE TIP RESISTANCE NEAR THIN-WALLED TUBE SAMPLE VERSUS CYCLIC TRIAXIAL DEVIATOR STRESS AT FAILURE FROM CORRESPONDING SAMPLE .....	234
FIGURE 6.32: ESTIMATED SOIL BEHAVIOR BASED ON REGRESSION EQUATION FROM HPR AND NONHPR LABORATORY SAMPLES ON ROBERTSON'S (2012) UPDATED NORMALIZED CONE RESISTANCE VERSUS FRICTION RATIO SBT CHART .....	235
FIGURE 6.33: ESTIMATED SOIL BEHAVIOR BASED ON CPT RESULTS MATCHED TO HPR AND NONHPR LABORATORY SAMPLE ELEVATIONS ON ROBERTSON'S (2012) UPDATED NORMALIZED CONE RESISTANCE VERSUS FRICTION RATIO SBT CHART .....	236
FIGURE 7.1: HPR DATA OVERLAID ON ROBERTSON'S (1990) NORMALIZED CONE RESISTANCE VERSUS NORMALIZED FRICTION RATIO SBT CHART WITH THE NORMALLY CONSOLIDATED ZONE SHOWN .....	238
FIGURE 7.2: NONHPR DATA OVERLAID ON ROBERTSON'S (1990) NORMALIZED CONE RESISTANCE VERSUS NORMALIZED FRICTION RATIO SBT CHART WITH THE NORMALLY CONSOLIDATED ZONE SHOWN.....	239
FIGURE 7.3: HPR DATA OVERLAID ON ROBERTSON'S (1990) CONE RESISTANCE VERSUS PORE PRESSURE RATIO SBT CHART	241
FIGURE 7.4: NONHPR DATA OVERLAID ON ROBERTSON'S (1990) CONE RESISTANCE VERSUS PORE PRESSURE RATIO SBT CHART .....	241
FIGURE 7.5: HPR DATA OVERLAID ON ROBERTSON'S (2012) UPDATED NORMALIZED CONE RESISTANCE VERSUS FRICTION RATIO SBT CHART .....	243
FIGURE 7.6: NONHPR DATA OVERLAID ON ROBERTSON'S (2012) UPDATED NORMALIZED CONE RESISTANCE VERSUS FRICTION RATIO SBT CHART.....	244
FIGURE 7.7: HPR DATA OVERLAID ON SCHNEIDER ET AL.'S (2008) SBT CHART .....	245
FIGURE 7.8: NONHPR DATA OVERLAID ON SCHNEIDER ET AL.'S (2008) SBT CHART .....	246
FIGURE 7.9: HPR DATA OVERLAID ON ESLAMI AND FELLENIUS' (1997) SBT CHART.....	248
FIGURE 7.10: NONHPR DATA OVERLAID ON ESLAMI AND FELLENIUS' (1997) SBT CHART .....	248

# List of Tables

---

TABLE 1-1: TOTAL NUMBER OF SITES TESTED FOR HPR RESEARCH .....	2
TABLE 1-2: PHASE II TESTING SUMMARIES .....	3
TABLE 2-1: PILE DRIVING VARIABLES .....	9
TABLE 2-2: HIGH PILE REBOUND LITERATURE AND CASE HISTORY SUMMARY .....	22
TABLE 2-3: $\Delta(N1)60T$ CORRECTION BASED ON FC (AFTER TOKIMATSU & YOSHIMI, 1983) .....	33
TABLE 2-4: LIQUEFACTION POTENTIAL BASED ON $(N1)60$ . (SEED ET AL., 1985) .....	34
TABLE 2-5: VARIATION IN RELATIVE DENSITY (DASH & SITHARAM, 2009) .....	47
TABLE 2-6: ESTIMATED SOIL RESPONSE TO CYCLIC SHEARING BASED ON $(N1)60TA$ .....	49
TABLE 2-7: SUMMARY OF CRITICAL CYCLIC PARAMETERS .....	56
TABLE 2-8: HAWTHORN GROUP CHARACTERISTICS .....	59
TABLE 2-9 HAWTHORN LAYER ENGINEERING PROPERTIES (AFTER BROWN ET AL., 2005) .....	61
TABLE 2-10: SBTn ZONES CORRESPONDING TO THE SBTn INDEX ( $I_c$ ) AFTER ROBERTSON (1990) .....	66
TABLE 2-11: ESTIMATED PERMEABILITY BASED ON NORMALIZED SOIL BEHAVIOR TYPE, SBTn (LUNNE ET. AL, 1997) .....	78
TABLE 2-12: FDOT HIGH PILE REBOUND SITES .....	82
TABLE 3-1: SUMMARY OF HPR TESTING SITES AND TESTING PROGRAM.....	91
TABLE 3-2: SUMMARY OF FIELD TESTING DATA FOR ALL LOCATIONS .....	135
TABLE 3-3: AVERAGE RESULTS FOR NONHPR AND HPR SITES .....	135
TABLE 4-1 SPT AND CPTU TESTING SITES .....	136
TABLE 5-1: LIST OF HIGH PILE REBOUND SITES AND CORRESPONDING TESTING .....	186
TABLE 5.2 PERCENT FC OCCURRENCES BASED ON REBOUND > AND < 0.50 INCHES .....	194
TABLE 5.3: PERCENT LIQUEFACTION POTENTIAL OCCURRENCES BASED ON REBOUND > AND < 0.5 INCHES.....	196
TABLE 6.1: PHYSICAL PROPERTIES OF COHESIONLESS SOIL SAMPLES .....	198

TABLE 6.2: PHYSICAL PROPERTIES OF COHESIVE SOIL SAMPLES .....204

TABLE 7-1: RANGES FROM ROBERTSON'S (1990) SOIL BEHAVIOR TYPE CLASSIFICATION CHARTS FOR HPR AND NONHPR  
ZONES AT ALL SITES.....242

# 1. Introduction

Pile driving is a complex interaction between the pile, soil, hammer, and driving procedures. To resist high lateral loads, piles in hurricane zones have become wider, while the most economical and lightest (i.e., diesel) hammers have typically been used. When these large diameter displacement piles are driven into certain soil profiles, they can bounce or rebound excessively after each hammer blow. The engineering term most commonly used to describe this phenomenon is high pile rebound (HPR). The Florida Department of Transportation (FDOT) has encountered HPR at numerous sites throughout the state (Cosentino et al., 2010, Jarushi et al., 2013).

If HPR is excessive, pile-driving contractors sometimes require thousands of hammer blows and/or change hammers to drive the pile. During HPR, the hammer can be damaged and the excessive hammer blows result in high compressive stresses that can damage the piles.

Research has been conducted to help identify the soils potentially causing HPR before construction (i.e., during the design phase site investigation). HPR is a function of many variables (pile size, hammer type, soil type); however, Cosentino et al., (2010) and Jarushi et al., (2013) presented findings that indicate that Standard Penetration Test (SPT) N-values, the fines content (i.e., % passing #200 sieve) and the Cone Penetrometer Test (CPT) pore water pressures can be correlated to HPR. However, due to the limited number and location of sites evaluated, these correlations need to be verified. Data from additional sites needed to be added to the existing database to validate the correlations so that engineers might use them.

Proposed Phase II HPR Study: From FDOT contract BDK81-977-01, thorough lab and field-testing was conducted on the three sites (Cosentino et al., 2010). Following this work, FDOT assisted in additional testing and retrieval of more data on eight additional sites, but only SPT and CPTu as well as limited grain size testing were performed (Jarushi et al., 2013). It is the intent of this Phase II project to validate these new findings and correlations and to modify them if necessary by performing additional sampling and testing at more sites both with and without HPR.

## 1.1. Project Objective

The objective of this project is to validate the new correlations developed by the research team such that engineers can use them to help predict HPR.

## 1.2. Supporting Tasks and Deliverables

The following tasks were completed to achieve the research objective.

**Task 1. Literature Search:** The literature on pile rebound was reviewed and a summary was prepared. This summary, which is presented in Chapter 2, includes information on the Pile, Hammer, Soil Types, and Profiles. The soil types typically encountered during pile rebound are summarized along with their index, pore pressure responses, and strength-deformation properties. Soil classification charts based on Cone Penetrometer Test (CPT) data, such as the one developed by Robertson and Campanella (1983), were used to determine if the rebound soils plotted within certain regions of these plots.

**Task 2. Develop Locations of New Testing Sites:** Of the 11 sites that have been studied, only one has no rebound, while three have rebound with acceptable set (See Table 1-1). Acceptable set is defined as any permanent set that allows the piles to be successfully driven. To solidify the correlations, developed during the Florida Institute of Technology (FIT) research, additional sites with no or minimal rebound and HPR with acceptable set were sought.

Table 1-1: Total Number of Sites Tested for HPR Research

Total Number of Sites		
HPR with Unacceptable Set	HPR with Acceptable Set	No HPR with Acceptable Set
7	3	1

To complete this new Phase II work, three new sites (or locations within existing sites) were identified through coordinated efforts with FDOT and consulting personnel. Table 1-2 contains a summary of the lab and field-testing for the existing and new sites. The three sites tested during BDK81-977-01 are shown as sites 1 through 3, the eight sites tested by Jarushi et al. (2013) are shown as sites 3 through 11, and the three new sites are shown as sites 12 to 14. None of the existing 11 sites had the complete series of tests conducted. Note that when CPT<sub>u</sub> tests exist, no standard CPT tests (i.e., without pore pressure) are needed. There are five sites from which Shelby tube samples have been obtained. For this new testing, a complete set of lab

and field tests were conducted, excluding the pocket penetrometer. This test was omitted because many of the disturbed samples could not be tested with this device.

Table 1-2: Phase II Testing Summaries

Site		Field Testing						Lab Testing						
Abbreviation	No	SPT	CPT	CPTu	DMT	Shelby Tubes	Pocket Penetrometer	Grain Size	% passing 200	Atterberg Limits	Natural Moisture	Permeability	Shear Strength	Cyclic Triaxial
ASO	1	√	√	√	√	√	√	√	√	√	√	√	√	X
JYP	2	√	√	√	√	√	√	√	√	√	√	√	√	X
RBB SR 83	3	√	√	√	√	√	√	√	√	√	√	√	√	X
SR50/SR436	4	√	X	√	□	□	□	□	√	□	□	□	□	□
I4/US192	5	√	X	√	☒	☒	□	☒	√	☒	☒	☒	☒	☒
I4/OP	6	√	X	√	☒	☒	□	☒	√	☒	☒	☒	☒	☒
I4/SR417	7	√	X	√	☒	☒	□	☒	√	☒	☒	☒	☒	☒
JYPExt	8	√	X	√	□	□	□	□	√	□	□	□	□	□
I10Chaffee	9	√	X	√	☒	☒	□	☒	√	☒	☒	☒	☒	☒
I4/SR408 B	10	√	X	√	☒	☒	□	☒	√	☒	☒	☒	☒	☒
SR528	11	√	√	X	□	□	□	□	√	□	□	□	□	□
I-4 Widening	12	☒	X	☒	☒	☒	X	☒	☒	☒	☒	☒	☒	☒
RBB SR 83 II	13	☒	X	☒	☒	☒	X	☒	☒	☒	☒	☒	☒	☒
Heritage Pky	14	☒	X	☒	☒	☒	X	☒	☒	☒	☒	☒	☒	☒

- ☒ Phase II Testing Samples Obtained or Testing Completed
- Phase II Testing Requested
- √ Completed Testing
- X No Testing

**Abbreviation**

**Description**

- ASO Anderson Street Overpass for I-4 SR 408
- JYP John Young Parkway over I4
- RBB SR 83 Ramsey Branch Bridge US 331
- SR50/SR436 State Road 50 over State Road 46
- I4/US192 I4/US 192 Ramp CA
- I4/OP I4/ Osceola Parkway Ramp D2 over D1
- I4/SR417 I4/State Road 417 Ramp
- JYPExt John Young Parkway Extension to SR 423
- I10Chaffee I10 Chaffee Road Overpass
- I4/SR408 B I4/State Road 408 Ramp B
- SR528 State Road 528 Bridge Over Indian River
- I-4 Widening I-4 Over Deer Crossing NO HIGH Pile Rebound
- RBB SR 83 II Ramsey Branch Bridge US 331 Revisited Summer 2014
- Heritage Pky Palm Bay Parkway over C-1 Canal City of Palm Bay

**Task 3. Test Program for New Field Testing Sites:** In addition to the lab and field-testing data, PDA data from the test-pile(s) was obtained. The testing program for the new sites included the following field tests (See Table 1-2):

1. SPT (with both automatic and safety hammers)
2. CPT with pore water pressure measurements

3. Dilatometer (DMT) testing including pore pressures
4. Thin-walled tube samples

The testing program for the new sites will also include the following laboratory tests on either disturbed split spoon samples or undisturbed thin-walled tube samples:

5. Grain Size Distribution with silt clay and fines content from split spoon samples
6. Atterberg Limits from split spoon samples
7. Permeability testing on thin-walled tube samples
8. Consolidated Drained Triaxial Shear Testing of thin-walled tube samples
9. Cyclic Triaxial Testing with Pore Water Pressure Measurements of thin-walled tube samples

**Task 4. Field Data Reduction:** The SPT, CPT, and DMT data were reduced from their raw field format to applicable engineering formats used for further analysis.

**Task 5. Laboratory Testing and Reduction of Disturbed Samples:** The disturbed samples obtained from the split barrel samples during the SPT borings were used to perform the following tests (shown in Task 3):

1. Grain Size Distribution with silt, clay, and fines content
2. Atterberg Limits

The main purpose of this testing was to produce soil properties that allow the HPR and nonHPR soils to be characterized and related to the amount and or probability of rebound.

**Task 6. Data Reduction and Analysis of Thin-walled Tube Results:** The test data obtained from this task was analyzed to determine which engineering properties, trends, and correlations are associated with HPR. As a companion effort, FDOT's State Materials Office (SMO) received the thin-walled tube samples obtained during field sampling at the new sites and conducted the following tests:

1. Consolidated Undrained Flexible Wall Permeability according to the procedure specified by ASTM D 5084. Confining stresses will be varied from 10 to 30 psi to simulate samples from 20 to about 60 feet deep.
2. Triaxial Shear: Following permeability testing, each sample will be sheared at a strain rate based on recommendations in ASTM D 4767. Confining stresses will be varied from 10 to 30 psi to simulate samples from 20 to about 60 feet deep.

3. Cyclic Triaxial Testing with Pore Water Pressure Measurements of thin-walled tube samples. Samples will be confined to stresses similar to the confining stresses associated with the sampling depths; then 1000 cycles will be conducted at stress-levels determined as a percentage of the CU Triaxial Failure Stress. It is anticipated that these stress levels will be 10, 20, 40, 60, and if possible, 80 percent of the failure strength. Data from the testing will include load and deflection versus time and cycle number plus variation in pore water pressure with time and cycle number. The stress levels are assumed to change from those associated with elastic behavior (10, 20 and 40%) to those associated with plastic behavior (60 and 80%).

This testing produced soil properties that allow the HPR and nonHPR soils to be characterized and related to the amount and/or probability of rebound.

**Task 7. Analyze Reduced Laboratory Data from Disturbed Testing:** The reduced lab data from the grain size and Atterberg limit testing was analyzed to determine if there are any indicators associated with HPR.

**Task 8. Analyze Reduced Field Data:** The reduced SPT, DMT, and CPT data was analyzed to determine trends and correlations with HPR. This data was added to the existing correlations so that they could be improved and verified according to the research objective.

## **2. Literature Search**

### **2.1. Overview**

Pile driving is a complex interaction between soil properties, hammer types, and driving procedures. The constraints developed by the design engineer must be met during the driving process and each location can pose different and sometimes unique problems. One of the more complex pile-driving phenomena occurs when piles reach a certain depth during the installation but begin to rebound after each hammer blow rather than continue to progress. This problem becomes severe when the upward movement (rebound) exceeds about  $\frac{1}{4}$  inch and there is no or minimal pile penetration into the soil. The engineering phrase most commonly used to describe this problem is high pile rebound (HPR) although some engineers term it as bounce (Cosentino et al., 2010, Murrell et al., 2008).

The Florida Department of Transportation (FDOT) previously funded research under Contract BDK-81 977-01 titled *Design Phase Identification of High Pile Rebound Soils* to try to determine which soil properties may be causing this problem (Cosentino et al., 2010). Three Florida sites, which experienced high rebound, were examined. At all three sites, single acting diesel hammers were used to drive large diameter high displacement piles to depths greater than 40 feet. Based on limited soil data from these sites, it was concluded that HPR occurred in very dense saturated silty fine sand or clayey fine sand soil layers. This current follow-on study expands on the earlier research to better define parameters that will predict HPR so that designers and construction contractors can anticipate and prevent issues during construction.

The literature review focused on six areas: 1) Methods of measuring rebound, 2) historical case studies of HPR sites, 3) laboratory testing related to rebound, 4) effects of cyclic loading on soils, 5) geology of Florida associated with HPR, and 6) correlations between soil or site parameters and HPR.

### **2.2. Pile Movement during Driving**

Smith (1960) used a hybrid linear elastic-plastic model to depict pile load-displacement movement from a single hammer blow. Figure 2-2 shows the actual and modeled energy rebound during a single hammer cycle. The elastic compression of the soil or rock below the pile point

results in an upward displacement (i.e., rebound) of the pile after the hammer blow. Rebound is typically associated with the reaction of the soil as opposed to the pile. Quake is the modeling parameter describing the displacement required to reach the limit of the soil's initial elastic movement (i.e., similar to rapid earthquake movements) from the dynamic energy resulting from a single hammer blow (Smith, 1960). Stated another way, quake is the pile displacement when the soil behavior changes from elastic to plastic (Murrell et al., 2008).

Soils are often exposed to different forms and therefore durations of cyclic loading from either natural forces or construction activities, as shown in Figure 2-1. The static loads occur over a low number of cycles; however, the various dynamic loads occur over a large number of cycles. Pile driving waves are similar in duration to those found from earthquake, traffic, and machine foundations.

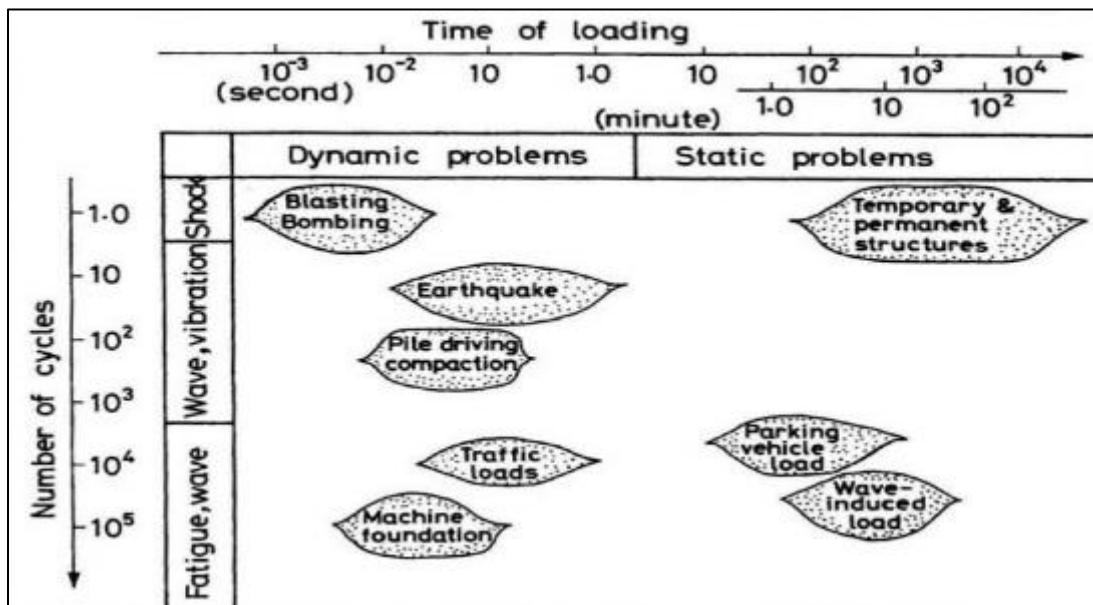


Figure 2-1: Classification of dynamic problems (after Ishihara, 1996)

### 2.3. Definition of High Pile Rebound

Due to the magnitude of the hammer force and the elastic properties of the pile and surrounding soils, some elastic rebound is always expected. Rebound is not a problem as long as the permanent set (downward penetration) is sufficiently large and the pile driving is not at refusal (i.e., less than or equal to 2 inches with the hammer operating at its highest setting determined by the engineer). Occasionally during the installation of large-diameter displacement

piles, the pile movement is almost entirely elastic, resulting in a small or negligible permanent set. FDOT considers the rebound to be excessive if it exceeds ¼ inch (FDOT Road and Bridge Construction Specifications, 455-5.10.3). Hussein et al. (2006) use the term “high-rebound,” to describe this condition while others (Murrell et al., 2008) use the term “bounce.” During this research, excessive rebound will be termed “high pile rebound” or HPR. Authier and Fellenius (1980) related HPR to “large” quake or “high” quake (i.e., greater than 0.35 inches).

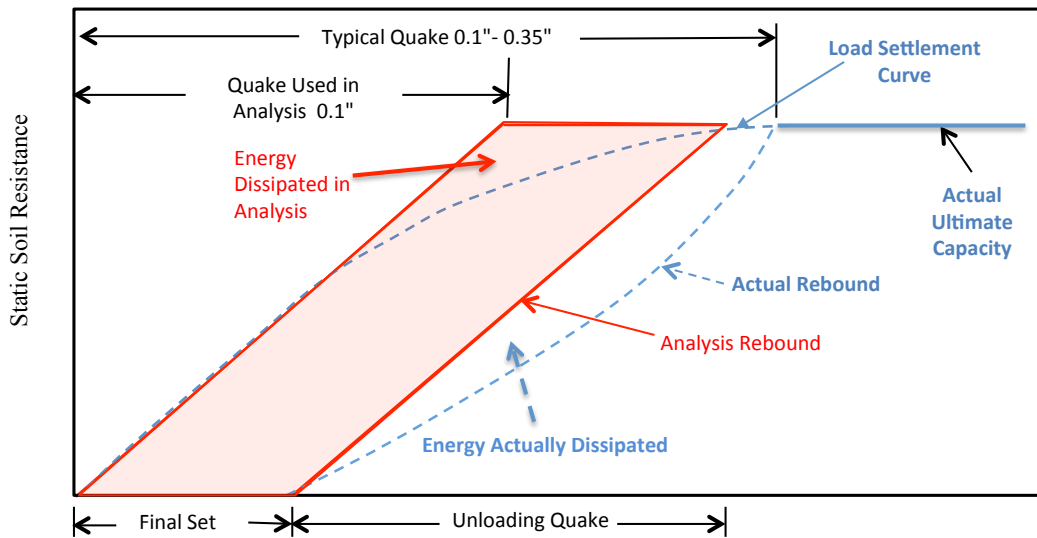


Figure 2-2: Resistance vs. penetration with quake for one hammer blow (modified after Smith, 1960)

## 2.4. Factors Affecting Pile Driving in HPR Soils

There are numerous variables associated with pile driving. Table 2-1 contains a list of 19 variables grouped into categories for piles, hammers, soils, and sites. Variables related to the piles include material type, dimensions, shape, and unsupported length during driving. Variables related to the hammers include type, stroke height, and efficiency. The soil variables include basic index properties such as grain size and shape; density; pore water pressures during lab and field-testing and pile driving; strength deformation behavior under constant strain and cyclic loading; and permeability. Site related variables include geologic stratification, pile installation order, and HPR zone confining stresses. The variables being evaluated during this research are

noted with a check mark. The soil related variables are being evaluated either with field tests such as the SPT, CPT, or DMT or with lab tests on disturbed and thin-walled tube samples.

Table 2-1: Pile Driving Variables

Variable		HPR
Category	Description	Phase II
Piles	Material Type	
	Diameter	
	Length	
	Unsupported Length	
Hammers	Shape	
	Type	
	Stroke Height	
Soils	Efficiency	
	Grain Size Distribution	✓
	Density	✓
	Pore Water Pressure	✓
	Particle Shape	✓
	Consolidation Behavior	✓
	Permeability	✓
	Static Shear Behavior	✓
Cyclic Shear Behavior	✓	
Site	Geologic Stratification	✓
	Confining Stresses	✓
	Installation Order	

✓ = variables evaluated during this research

## 2.5. Methods for Measuring Rebound

### 2.5.1. Manual Method

The manual method of measuring pile displacement and rebound consists of taping paper onto the pile near a reference board or beam. As the pile is driven, a pencil moved horizontally across the edge of the reference board records the pile's movement, as illustrated in Figure 2-3. The resulting graphs show each hammer-blow's maximum displacement and rebound. While the method is simple, it requires a high degree of dexterity and lacks the precision needed for complex engineering investigations. In addition, there is also a risk of injury to the operators.

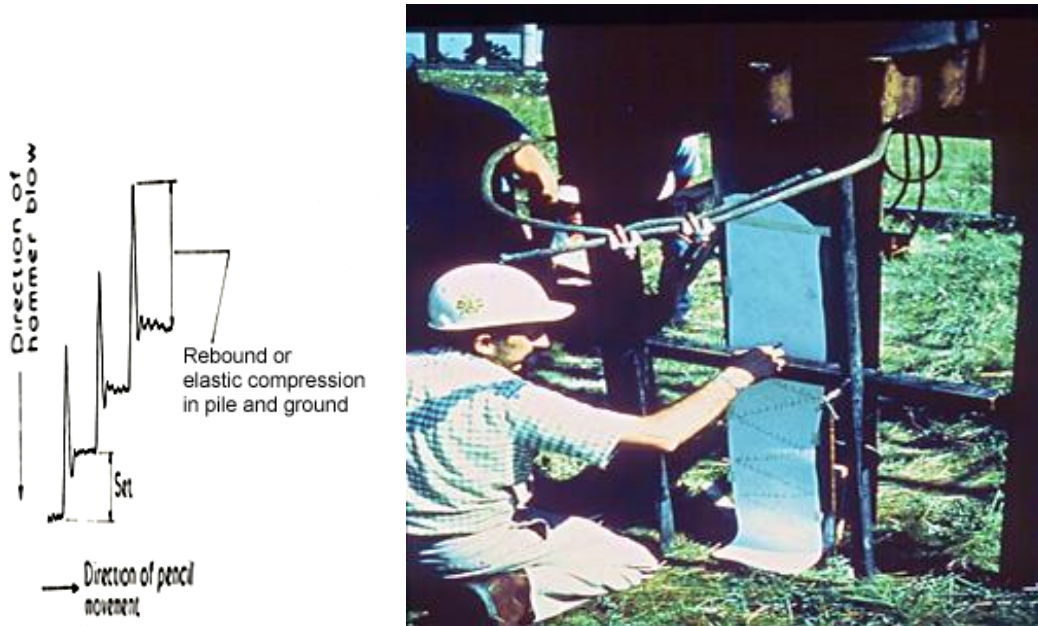


Figure 2-3: Pile displacement and rebound recorded by the manual method (from Hattori 1974, Courtesy of GRL Library)

### 2.5.2. Dynamic Method: Pile and Soil Model by Wave Equation

Smith (1960) developed the discretized spring and dashpot model, shown in Figure 2-4, to represent the pile and hammer system. It consists of a hammer and anvil ram, cushion material for the hammer and pile (if concrete), a pile cap, the pile, and the surrounding soils. Springs are used to represent elastic materials, while spring and dashpot combinations are used to represent elasto-plastic materials such as soils. Smith (1960) also included soil damping ( $J$ ), along with quake ( $q$ ), to help describe the system. The viscous soil damping ( $J_v$ ) and the wave speed are proportional to the force or dynamic pile resistance ( $R(t) = J_v * v(t)$ ). Historically, three damping coefficients have been defined for the dynamic pile soil model: Smith's damping coefficient ( $J_s$ ) has units of 1/velocity, the viscous soil damping ( $J_v$ ) has units of force/velocity, and the Case damping coefficient ( $J_c$ ) is dimensionless since pile impedance ( $Z$ ) is included ( $R(t) = J * Z * v(t)$ ). The impedance is found by using Young's Modulus multiplied by the pile cross-sectional area and then divided by the wave speed, resulting in units of force/velocity.

Dynamic testing is performed only during pile driving when real-time measurements are required. The dynamic testing system, as presented in Figure 2-5, consists of: (a) field testing utilizing specialized equipment such as strain gauges and accelerometers and (b) pile wave signal matching software such as the CAsE Pile Wave Analysis Program (CAPWAP<sup>®</sup>).

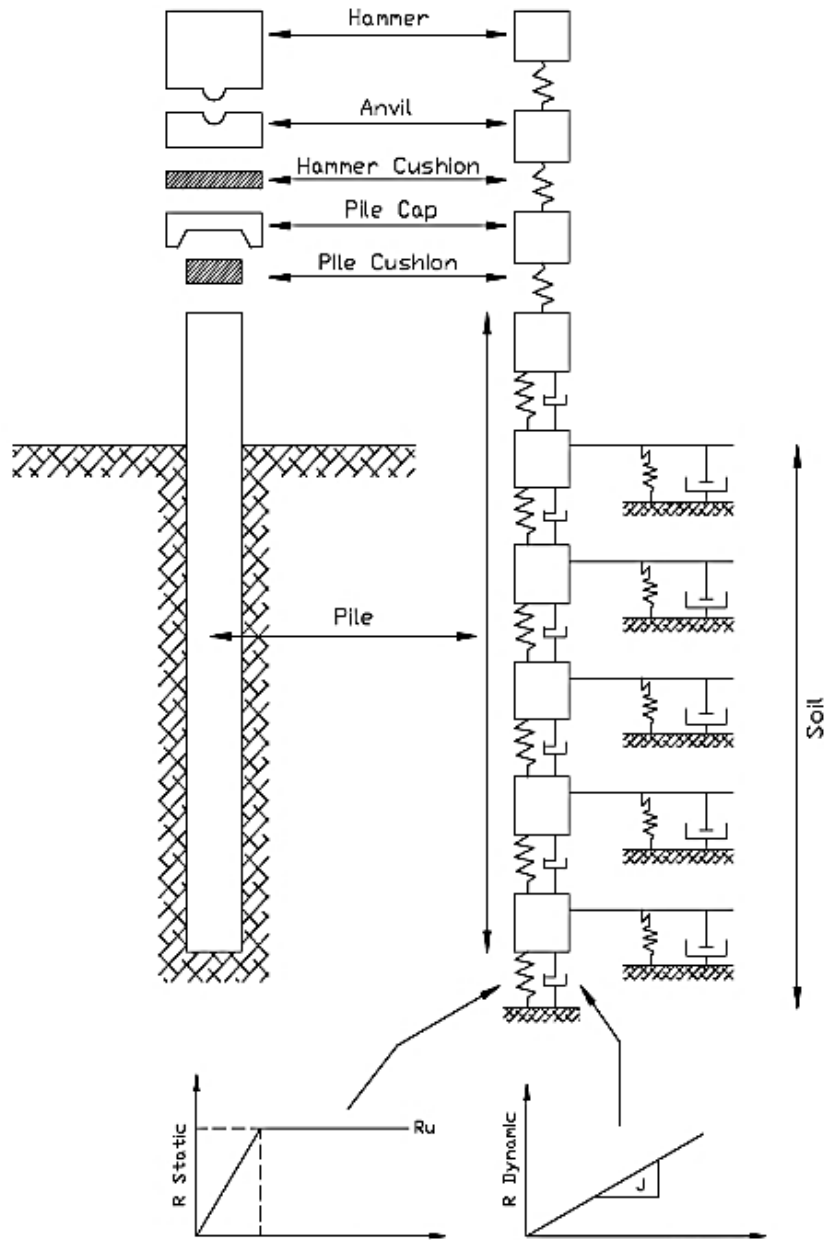
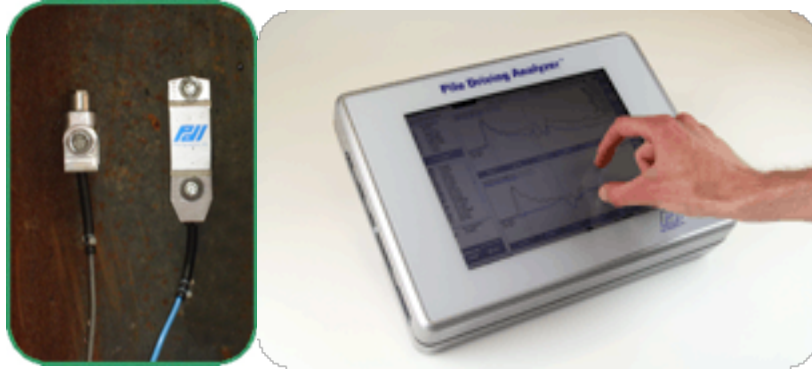


Figure 2-4: Pile-soil model for wave equation analysis (after Smith, 1960)



(a)

((b)

Figure 2-5: (a) PDA Strain Gage and Accelerometers attached to a pile and (b) PDA equipment with CAPWAP<sup>®</sup> (Courtesy of Pile Dynamics, Inc.)

The signals from the accelerometers and strain gauges, placed within two feet of the pile head, are used with data acquisition in a software package called the Pile Driving Analyzer (PDA). Accelerations are integrated once to produce velocity traces versus time and a second time to produce deflections versus time. The strains are used along with the known pile properties (area and elastic modulus) to produce the force in the pile versus time at the gauge location. Based on Hooke's Law ( $E=\sigma/\epsilon$ ), the strain ( $\epsilon$ ) and elastic modulus ( $E$ ) are used to determine the stress ( $\sigma$ ), and then the area of the pile is used to determine the force. PDA force and velocity versus time data from a hammer blow are depicted in Figure 2-6.

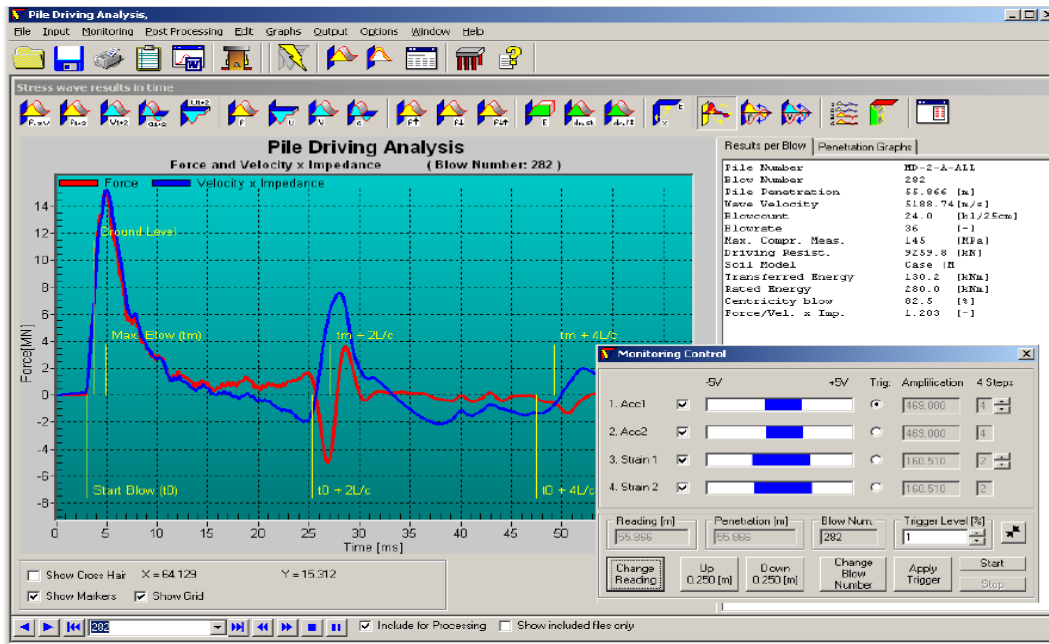


Figure 2-6: PDA output measured force and velocity versus time from a hammer blow (Courtesy of Pile Dynamic, Inc.)

CAPWAP<sup>®</sup> is a software package with a signal matching procedure that primarily uses ultimate resistance values, soil damping factors, and quakes in a series of equations to match computed with measured PDA force and velocity signals. The CAPWAP<sup>®</sup> program has various operator adjustable variables in the computation of its force versus time curves including: side quake, toe quake, side damping, toe damping, static resistance along the pile shaft, and static resistance at the pile toe.

The operator adjusts these variables to produce a match between the actual force trace and the computed force curve (Authier & Fellenius, 1980). After the measured force has been obtained for each hammer blow (Figure 2-6), engineers use the CAPWAP<sup>®</sup> signal matching process along with these forces to predict force versus time curves. This predicted curve is then compared to the actual force trace generated during pile driving. Figure 2-7 demonstrates five iterations of this matching process. Damping was added after the first iteration, then the capacity was increased, and finally the quakes were adjusted. This process produced a good match by iteration 5.

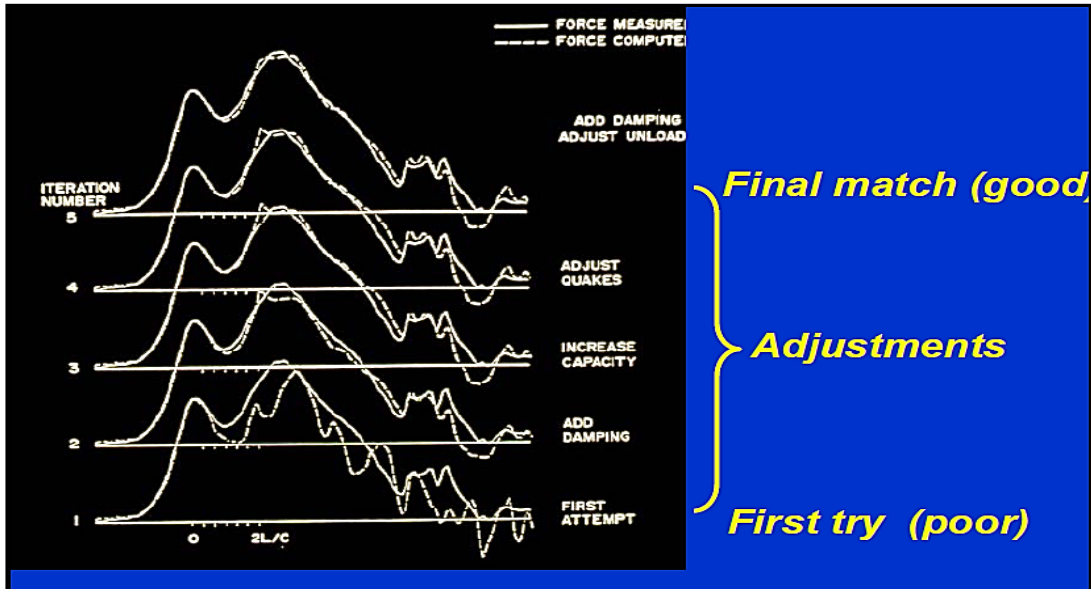


Figure 2-7: CAPWAP® iterative process (Courtesy of GRL & Associates)

Figure 2-8 presents typical HPR PDA data from an FDOT site. The plot, with displacement recorded in inches on the vertical axis and time recorded in milliseconds on the horizontal axis, shows a maximum displacement (DMX) of 1 inch, a digital set (dSet) of 0.27 inches, and an inspector set (iSet) of 0.11 inches. Note that the inspector set is the average set over one-foot and is found by taking the inverse of the number of blows per foot. The digital set from the PDA output (DFN or dSet) is recorded over 200 milliseconds, with approximately 1.5 seconds occurring between hammer blows for typical diesel hammers. The final pile set occurs after the digital signal has ended. This discrepancy between the dSet and iSet has caused most engineers to assume the inspector set to be more reliable. Assuming that the inspector set is reliable, a rebound of 0.89 inches would be measured. The rebound based on dSet would be 0.73-inches.

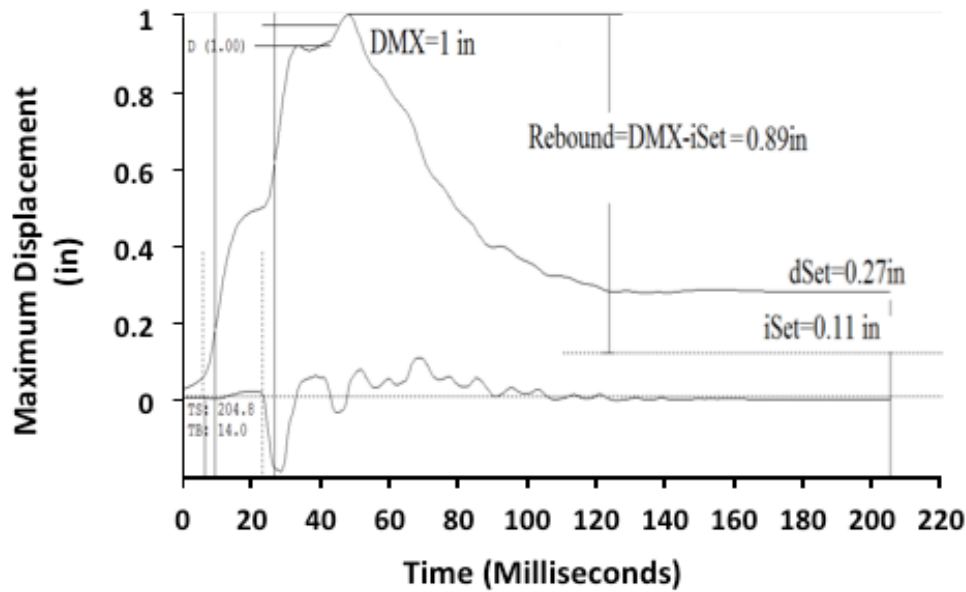


Figure 2-8: Typical PDA pile top displacement versus time diagram from one hammer blow for an FDOT HPR site (Cosentino et al., 2010)

### 2.5.3. High-speed Visual Measurement System of Pile Penetration and Rebound

Bum-Jae et al. (2002) have a patented approach for measuring pile movement during installation by using a high-speed camera. The measurement system, portrayed in Figure 2-9, consists of special marking paper, a high-speed line scan camera equipped with a zoom lens, and a personal computer. Line scan cameras use a single line of pixels to scan images and therefore, require less processing than conventional digital cameras. Fax machines are an example of line scan cameras. The method is based on two-dimensional motion achieved by stacking alternating white and black right-angled triangles on paper, as shown in Figure 2-9. As the pile is driven, the line-scan camera produces a line image by scanning from the top to the bottom of the attached marking paper. The height of each triangle is 40 mm and the width is 200 mm. The line-scanned image is used to determine a location along the pile. This methodology shows promise in measuring pile movement and rebound during driving.

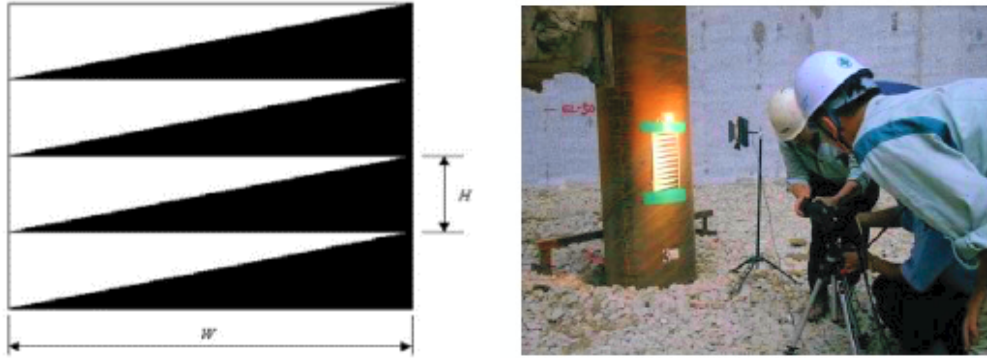


Figure 2-9: Marking paper and line scan camera setup during pile driving (Oliveira et al., 2013)

Oliveira et al., (2011) developed a fast tool to measure the rebound and the final set for driven prestressed concrete piles (PCPs) with diameters varying from 60 to 80 cm and lengths varying from 20 to 50 m. Three coastal locations were used, one in Rio de Janeiro, another in Sepetiba, and the third in Itajai, Brazil. All three test locations had known soil profiles and  $N_{SPT}$  values. Measurements were performed using digital image processing techniques. An A4-size sheet laminated with a printed pattern was fixed to the pile, and then a standard video camera (30 Hz sampling rate) was used to capture the images. An optical rebound analyzer (termed PDR by the authors) consisting of both a charged couple device (CCD) camera, mounted on a tripod, and a computer was placed so that it faced towards the pile at a distance of approximately 5 to 10 m. This spacing ensured that there was no significant effect from driving vibrations on the results.

A comparison between rebound values obtained by the PDR and the manual method is exhibited in Figure 2-10. These results indicated good agreement between the two methods. The manual method produced slightly higher rebound predictions at values over 10 mm than the PDR method (Figure 2-10). The authors termed this rebound “elastic.”

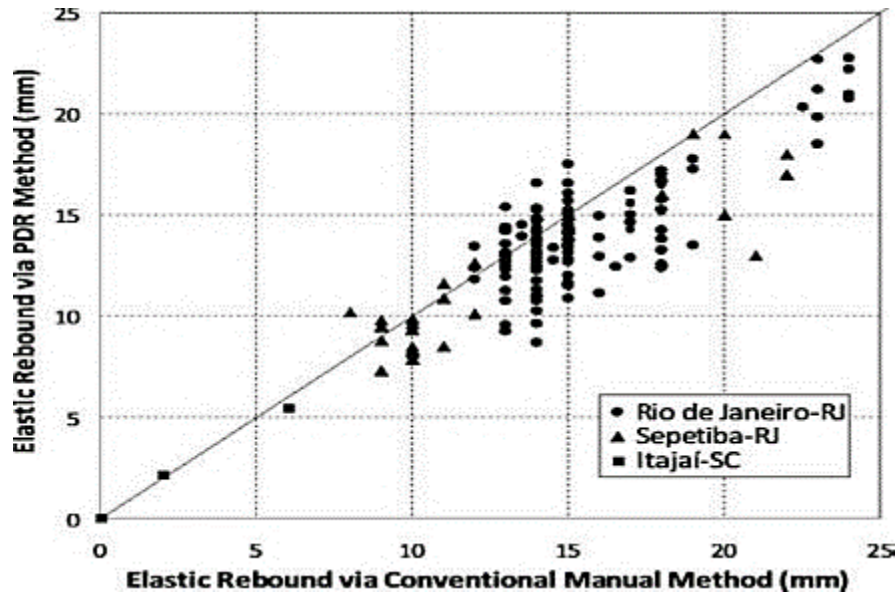


Figure 2-10: Comparison between elastic rebound results obtained with conventional manual method and the pdr system (Oliveira et al., 2013).

#### 2.5.4. He-Cd Laser Beam Measuring System

Another method to physically measure pile displacements and rebound was proposed by Hattori (1974). A Helium-Cadmium (He-Cd) laser beam, used in conjunction with photosensitive oscillograph paper attached to the pile, produces traces of the pile movement. The laser beam has a high energy density and the proper convergence characteristics that allow it to transmit and focus the beam onto a point at a distance of 10 to 20 meters. During a field trial, the laser beam produced visual traces of pile movement including rebound after only a few minutes.

### 2.6. High Pile Rebound Case Studies

The literature review provided multiple case histories of pile rebound at locations throughout North America. The case histories were reviewed and are described in detail in Chapter 2 of the Contract BDK81 Work Order 977-01 final report. An abbreviated summary of this information is provided to complete this literature review.

#### 2.6.1. Indian River Bridge over State Road 528 (Hussein et al., 2006)

Hussein et al. (2006) evaluated HPR while driving 115 long, 30-inch square PCPs along Central Florida’s Indian River Bridge over State Road 528. The HPR soils were described as hard clayey sand to sandy clay, with Unified Soil Classification System (USCS) symbols of SC

and CL. Hussein et al. attributed the HPR to the build-up of excess pore water pressure during the driving process. Due to the limitations of the data collected during the construction process, this conclusion could not be supported analytically. In order to decrease rebound and the tensile stresses in the pile, the plywood cushion thickness used with the diesel hammer was increased.

### **2.6.2. Coastal North Carolina (Murrell et al., 2008)**

In the Murrell et al. (2008) coastal North Carolina case study, 12- and 18-inch square PCP piles (55 and 70 feet long), which were driven into stiff clays, were described as bouncing. The piles developed circumferential cracks from excessive driving stresses. Changing the hammer to one with a larger ram and a shorter stroke with a longer contact time per blow reduced both the tensile stresses and rebound. Murrell et al. (2008) also indicated that the CPT testing with pore pressures showed that the soil layers with pore pressures greater than 20 tsf (1915 kPa) likely caused the bouncing.

### **2.6.3. Montreal and Timmons Ontario, Canada (Authier & Fellenius, 1980)**

Authier and Fellenius (1980) conducted a case study of HPR in 41-foot-long piles that were smaller than others found in the literature (12.75 inches). They were driven into glacial till described as very dense sandy silty or dense clayey silty. Authier and Fellenius concluded that HPR piles produced excessive toe quake.

### **2.6.4. Seattle, WA, and Florida (Likins, 1983)**

Likins (1983) studied one HPR case in Washington State and two cases in Florida in which the piles experienced large quake and high tensile stresses. These piles ranged from 18- to 24-inch-diameter square PCPs between 70 and 122 feet long. The soils were described as hard silty clays or dense fine sand with some silt or clay.

### **2.6.5. High Quake in Washington's Potomac Formation**

Regan and Higgins (2009) discussed some of the challenges faced with driving large displacement piles in the Potomac Formation in Washington, DC. This formation is the oldest sedimentary deposit in that region. It consists of very dense sands interbedded with layers of high

plasticity overconsolidated clays. This deposit is typically the bearing stratum for the deep foundations in the region.

Square 355 mm (14 in) PCPs were installed using a Delmag single-acting diesel hammer as part of the foundation for the National Harbor Hotel. The piles were dynamically load tested and monitored during driving using the PDA equipment. Significant elastic compression (quake) and HPR (0.64 to 1 inches) (16.3 to 25.4 mm) was observed during the driving process.

These large quakes affected the efficiency of the pile/hammer/soil system. Extra energy, in terms of increased stroke height, was required to overcome the elastic rebound. This also increased the total number of blows needed to fully mobilize the pile resistance. High blow counts and the subsequent high compressive stresses within the pile caused five of seventeen piles to rupture within the lower 1/3 to 1/2 of the pile. The authors attributed these ruptures to high tensile stresses as the wave reflected up from the pile toe during the early driving portion of the installation, while little tip resistance existed. Driving problems were overcome by controlling the ram weight and stroke to minimize early driving tensile stresses, allowing the piles to be successfully installed. The authors related the large soil rebound to the degree of overconsolidation of this bearing stratum and to the increase of excess pore water pressure during driving.

#### **2.6.6. North Sea Pile Drivability Issues in Dense Silty Sand**

Mes and McDermot (1976) discussed pile installation problems for large diameter open-ended pipe piles driven into dense silty sand to support a North Sea oil platform. The pile design called for pile penetration of approximately 140 feet in the sea floor. All of the twenty piles experienced refusal at approximately 70 feet of penetration into a sandy silt layer before reaching design capacities. Even with the heaviest hammer, the piles did not reach the desired depth. A drill was inserted in the original open-ended primary piles to drill to the original design depth. Smaller secondary piles were driven inside of the primary piles and then grouted into the primary piles. Pile capacities were reduced to account for the modified placement.

Mes and McDermot (1976) proposed several reasons for these problems. When very dense sand or silt deforms, it expands in volume (i.e., dilation occurs) reducing pore pressures and possibly producing negative pore pressures. The combination of increased volume and

decreased pore pressure causes sandy soil shear strength to increase. As a result, pile tip resistance and side friction increase, both inside and outside pipe piles, which then prevent the piles from further penetration.

### **2.6.7. Escambia Bay, Pensacola, Florida**

Stevens (2012) presented a case history where large quake and rebound were observed during the driving of PCPs in Escambia Bay, Pensacola, Florida. A 20-inch (508 mm) PCP was driven through soils that consisted of very soft to soft clay to a depth of 40 ft (12.2 m), underlain by medium dense to dense fine sand to a depth of 78 ft (24 m), which was underlain by dense to very dense silty sand. Eighteen piles were installed with a Delmag D62-23 single-acting diesel hammer with plywood cushions of either 4 or 6 inches (101 or 152 mm) thickness.

Preliminary analysis using the basic wave equations was conducted for each site. The results were then modified to match field data acquired through CAPWAP<sup>®</sup> analyses. Eighteen piles were monitored with PDA sensors and the Case method using the CAPWAP<sup>®</sup> analysis was used to estimate the pile capacity.

The ground surface elevation at this site is 0 feet (0 m). Twenty-inch (508 mm) square PCPs, 86 feet long were installed. Pile IN-16 for pier 24 experienced large rebounds during both easy and hard driving conditions. During the first 38 feet (11.6 m), the pile was driven with low blow counts. Between 38 and 58 feet, blow counts increased until they reached 79 blows/foot (0.3 m) at 58 feet (17.7 m), with the hammer operating at fuel setting 2. The blow count increased to 87 blows/foot (0.30 m) with a set of 0.13 inches (3.3 mm) at 68 feet (20.7 m). The final blow count was 122 blows/foot (0.30 m) at 76-foot penetration (23 m). Because of the high blow counts, driving was suspended. Driving was resumed after 14 days. The final 3 feet (1 m) to specified depth was achieved at 124, 106 and 113 blows/foot (0.30 m) at the highest hammer fuel setting. Pile displacement and rebound were recorded manually using a pencil trace. During easy driving, rebound ranged from 0.44 to 0.50 inches (11 to 12.7 mm) and during hard driving from 0.53 to 0.62 inches (13.46 to 15.72 mm). Large quakes, which were estimated using the CAPWAP<sup>®</sup> software procedures, ranged from 0.27 to 0.50 inches (6.85 to 12.7 mm). Also CAPWAP<sup>®</sup> output indicated that these sands produced a high Smith damping factor of 0.40 sec/ft in comparison to a typical sand damping of 0.15 sec/ft. Due to high quake and rebound,

practical refusal occurred at blow counts lower than expected. Initial estimation of pile capacities using a typical damping factor of 0.15 yielded excessively overestimated pile capacities (a more than 200-ton difference).

A microscopic grain size texture analysis conducted on seven samples of dense to very dense silty sand from this site indicated that these sands had angular to subangular grains. The internal friction for the angular grains is 6 to 8 degrees higher than for the subangular soils, which implies that angular soils require more energy to reach their failure state. The author concluded that the only unusual soil feature that may have contributed to high quake and rebound was the angularity.

### **2.6.8. Summary of HPR Case Studies**

Table 2-2 is a summary of the case studies. Several common factors were present at most of the HPR sites:

- Piles were large diameter displacement piles;
- Soils in the rebound layers typically contained silts and clays;
- Soils in the rebound zone were dense to very dense or stiff;
- Piles were longer than 40 feet;
- Pile driving hammers were single acting diesel;

Table 2-2: High Pile Rebound Literature and Case History Summary

Author	Site Name	Location	Pile Type/Shape	Rebound Soils	
				Density	Description
Hussein et al. 2006	SR.528 over Indian River	Brevard County, Florida	30 inch square PCP, 18 inch circular hollow core	Hard	Clayey sand to sandy clay
Murrell et al. 2008	Coastal North Carolina	North Carolina	12 and 20 inch square PCP	Firm to stiff	Clay
Authier and Fellenius 1980	Site 1	Timmons Ontario, Canada	Closed-toe 12.75 inch pipe piles	Very dense	Sandy silty glacial till
	Site 2	Montreal, Canada	12 inch square PCP	Dense	Clayey silty glacial till
Likins 1983	Site 1	Seattle, WA	24 inch octagonal hollow PCP	Hard	Silty clay
	Site 2	Florida	24 inch square PCP	Dense	Light gray sand
	Site 3	Florida	18 inch square PCP	Dense	Fine sand with some silt or clay
Regan et al. 2009	Washington, DC	District of Columbia	20 inch square PCP	Very dense or Hard	Overconsolidated clay
Mes and McDermot 1976	Oil platform	North Sea	Large diameter pipe piles	Dense to very dense	Silty sand
Stevens 2012	Escambia Bay	Pensacola, Florida	20 inch square PCP	Dense to very dense	Silty fine sand

## **2.7. Standard Penetration Testing**

Standard Penetration tests follow testing method ASTM D1586. Representative disturbed samples are obtained by progressively driving a split spoon sampler deeper into the ground at intervals ranging from 5 feet to continuous. N values, the number of blows per 6 inches, are counted for three 6-inch increments and recorded for the final 12 inches. Dropping a 140-pound hammer a distance of 30 inches provides the energy applied to the sampler.

Though the SPT is commonly used, and was proposed as a “standardized” test, research through the years has shown that results can be very inconsistent. Schmertmann (1975) points out that some engineers believe the word “test” is too dignified a term to use for the N-value. An advantage of the SPT has always been that its soil samples allow for visual and laboratory classification. Because of the ease at which it is conducted, as well as the multitude of available data, SPT research and its use will continue into the future.

### **2.7.1. Correcting SPT Blow Counts to N<sub>60</sub> Values**

By the 1980s, many different SPT driving systems had been developed throughout the world. Skempton (1986), having evaluated many case studies in the total energy transmission efficiency of an SPT test, proposed a standardized blow count correlation factor. His N<sub>60</sub> value corrects N to a system efficiency of 60%. It is assumed this correction factor was based on a majority of testing methods used at the time, which ranged in hammer efficiencies from 55 to 65%.

SPT hammers are dropped from a standardized height of 30 inches and weigh 140 pounds, but the full theoretical free fall energy is not transmitted to the sampler for penetration. Depending on the release type (trip or slip-rope), friction reduces the hammer’s free fall potential force and reduces the magnitude of the anvil strike. Additionally, the efficiency of the hammer is dependent on the size of the hammer and the area of the anvil it strikes. Dynamic losses occur from the anvil to rod system, further reducing the applied hammer force.

Schmertmann (1978) found that the transmission of compression and reflected tensile waves in the SPT rods were affected by rod length. Gibbs and Holtz (1957) previously had found that increased rod length affected N values, but since the magnitude was relatively small,

compared to the overburden pressure effects to N, rod length influences were excluded initially. Seed et al. (1985) showed that American SPT split spoon samplers without liners had higher N values by an average of 20%. Borehole diameters had previously been found to influence SPT N blow counts in sand, but Skempton (1986) suggested conservative correction factors until more information was available (borehole correction factors have remained as originally proposed).

Coduto (2001) summarized N correction to N<sub>60</sub> by an equation in the form of:

$$N_{60} = \frac{EM * CB * CS * CR * N}{0.60} \quad \text{Equation 2-1}$$

where

EM = Hammer rod efficiency (automatic, safety, etc.)

CB = Borehole diameter correction

CS = Sampler diameter correction

CR = Rod length correction

N = N<sub>spt</sub>

### 2.7.2. Normalized SPT N Values in Sands to Standard Overburden Pressure

The effective overburden pressure ( $\sigma'_{vo}$ ) on the soil being tested affects SPT N values. Skempton (1986), in reviewing full scale laboratory results by Gibbs and Holtz (1957) and Marcuson and Beiganousky (1977), showed that for any particular sand, at an  $\sigma'_{vo}$  less than 2 ton/ft<sup>2</sup> and within a D<sub>r</sub> range of 40 to 80%, SPT N values in sands were influenced directly by D<sub>r</sub>. Skempton (1986) pointed to three observations that state the following:

- a. The blow count N increases almost linearly with  $\sigma'_{vo}$  at a constant D<sub>r</sub>.
- b. At a constant  $\sigma'_{vo}$ , N increases roughly with D<sub>r</sub><sup>2</sup>.
- c. At a given D<sub>r</sub> and  $\sigma'_{vo}$ , N is higher for sands with a larger mean grain size (D<sub>50</sub>).

As the SPT test penetrates deeper,  $\sigma'_{vo}$  increases, and the number of blows to penetrate the split spoon sampler into the same sand increases. It then becomes necessary to normalize N values to a constant overburden pressure. Normalized SPT N value (N<sub>1</sub>) guidelines are contained in ASTM D6066 and have been used extensively in liquefaction studies. N<sub>spt</sub> or N<sub>60</sub> are normalized to an  $\sigma'_{vo}$  of 2000 psf (or 100 kPa) by use of a correction factor (C<sub>N</sub>) through use of:

$$N1 = CN * N_{spt} \quad \text{or} \quad (N1)_{60} = CN * N_{60} \quad \text{Equation 2-2}$$

where

CN = Correction factor determined by normalization formulas

ASTM D6066 limits the use of normalization to granular cohesionless soils with the Unified Soils Classification System (USCS) classifications SM, SW, SP, SP-SM, and SW-SM.

### 2.7.2.1. Overburden (CN) Correction Factors for SPT in Sand

Many authors have proposed a number of correlations. Das (2014) cites five correction factors (CN) used to determine (N1)<sub>60</sub>. They include:

Liao and Whitman (1986):

$$CN = \sqrt{\frac{Pa}{\sigma'_{vo}}} \quad \text{or} \quad (Pa/\sigma'_{vo})^k \quad \text{Equation 2-3}$$

where

$$k = 0.4 - 0.6 \text{ (0.5 standard)}$$

Skempton (1986)

$$(A) \quad CN = \frac{2}{1 + \left(\frac{\sigma'_{vo}}{Pa}\right)} \quad \text{(for normally consolidated fine sand)} \quad \text{Equation 2-4}$$

$$(B) \quad CN = \frac{3}{2 + \left(\frac{\sigma'_{vo}}{Pa}\right)} \quad \text{(for normally consolidated coarse sand)} \quad \text{Equation 2-5}$$

$$(C) \quad CN = \frac{1.7}{0.7 + \left(\frac{\sigma'_{vo}}{Pa}\right)} \quad \text{(for overconsolidated sand)} \quad \text{Equation 2-6}$$

Seed et al. (1979)

$$CN = 1 - 1.25 \log\left(\frac{\sigma'_{vo}}{Pa}\right) \quad \text{Equation 2-7}$$

Peck et al. (1974)

$$CN = 0.77 \log\left[\frac{20}{\left(\frac{\sigma'_{vo}}{Pa}\right)}\right] \quad \text{(for } \frac{\sigma'_{vo}}{Pa} \geq 0.25) \quad \text{Equation 2-8}$$

Bazaraa (1967)

$$CN = \frac{4}{1+4\left(\frac{\sigma'_{vo}}{Pa}\right)} \quad \left(\text{for } \frac{\sigma'_{vo}}{Pa} \leq 0.75\right) \quad \text{Equation 2-9}$$

$$CN = \frac{4}{3.25+\left(\frac{\sigma'_{vo}}{Pa}\right)} \quad \left(\text{for } \frac{\sigma'_{vo}}{Pa} \geq 0.75\right) \quad \text{Equation 2-10}$$

where

Pa = Vertical Effective stress standard (2000 psf or 100 kPa).

Liao and Whitman (1986), found that numerous  $CN$  factors were either overly conservative at lower depths, had slope discontinuities, or did not equal one at  $\sigma'_{vo}$  of 2000 psf. In 1986, they proposed their  $CN$  as a possible standard. Their experimental basis was developed through analysis of normally consolidated, uncemented, unaged, primarily quartz clean sands. Equation 2.3 was developed with a fitting parameter ( $k$ ) that ranges from 0.4 to 0.6. They noted that  $k$  is likely a function of  $D_r$ , as had been determined by Marcuson and Bieganousky (1977) and Seed et al. (1975). They also note that, given the crudeness and lack of accuracy of SPT penetration resistance, a value of  $k = 0.5$  would be appropriate, and standard practice is to assume a value of  $k = 0.5$ .

Though this was a tentative recommendation in 1986, Das (2014) points out that Liao and Whitman's  $CN$  formula (Equation 2.3) is recommended, and as such is specified in ASTM D 6066. Coduto (2001) recognized the importance of adjusting  $N_{spt}$  values to depth, but placed a limit on the magnitude of  $CN$  (Liao and Whitman 1986 do not), suggesting the maximum  $N_{1(60)}$  value not be greater than two times  $N_{60}$ . Figure 2.6, after Das (2014), shows comparisons of the  $CN$  values using the relationships from the various authors above.

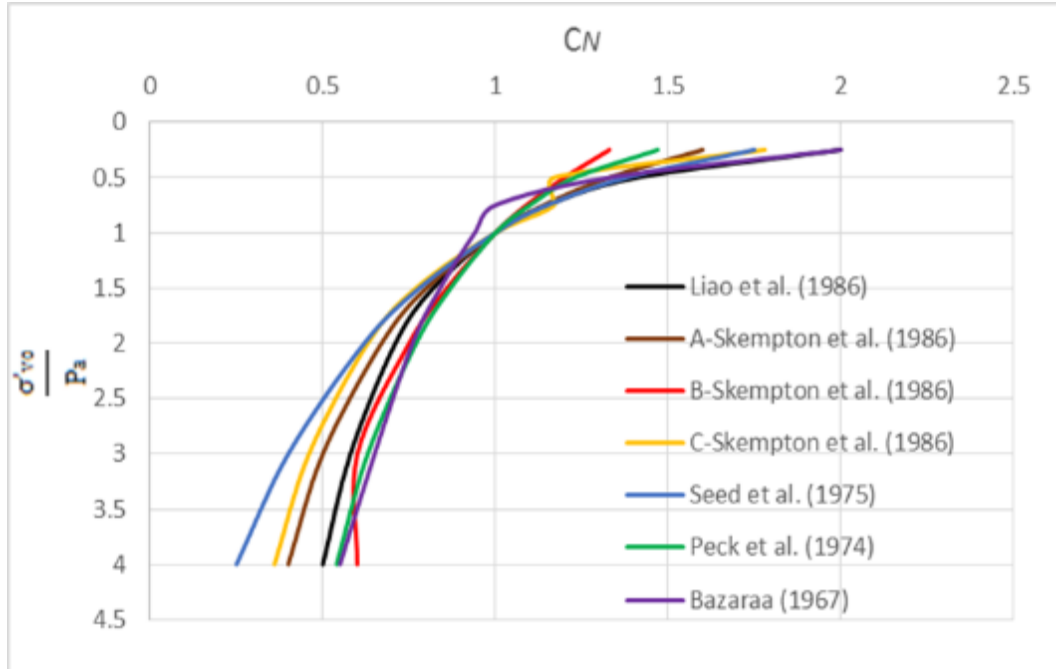


Figure 2-11: CN factors from various authors (after Das, 2014)

### 2.7.2.2. Estimating Soil Unit Weight

To determine the  $\sigma'_{vo}$  of a soil sample at depth, soil weights are estimated, assumed, or determined from undisturbed samples. Standardized unit weight ( $\gamma$ ) estimations are available in many forms, but accuracy in determining a clearly defined  $\gamma$  is not established. Commonly, a broad range of  $\gamma$ 's are listed per soil type or N value. Bowles (1977) and the Naval Facilities Engineering Command (NAVFAC) soil mechanics design manual 7.01 (1971) both present  $\gamma$  values in lb/ft<sup>3</sup>. Bowles compares  $\gamma$  in cohesionless and cohesive soils to N, while NAVFAC 7.01 references soil index properties to  $\gamma$ . Coduto (2001) lists soil dry ( $\gamma_{dry}$ ) and moist unit weight ( $\gamma_{sat}$ ) ranges given N and USCS soil classification. Though not identified, it was assumed for the purpose of this study that the the N referenced by the above authors and used in  $\gamma$  correlations was N60.

The California Department of Transportation (CDOT) (2014) compares (N1)60 to  $\gamma_{dry}$  and  $\gamma_{sat}$  for both cohesionless and cohesive soils. For cohesionless soils, three ranges are provided and  $\gamma$  is rounded to the nearest 5 lb/ft<sup>3</sup> based on the following guidelines:

- Use higher values for well-graded sands and gravels and average values for poorly-graded sands and gravels.

- Use lower values for elastic silt, and clayey or silty sands as well as gravel plus deduct up to 20% for dry soils.

For cohesive soils, three values (high, average, and low) are also provided and  $\gamma$  is again determined by  $(N1)_{60}$ . No further directions are provided, but it can reasonably be assumed that clay plasticity and sensitivity play a major role in selecting, which values apply. Figure 2.7 shows both cohesive and cohesionless charts used by CDOT (2014).

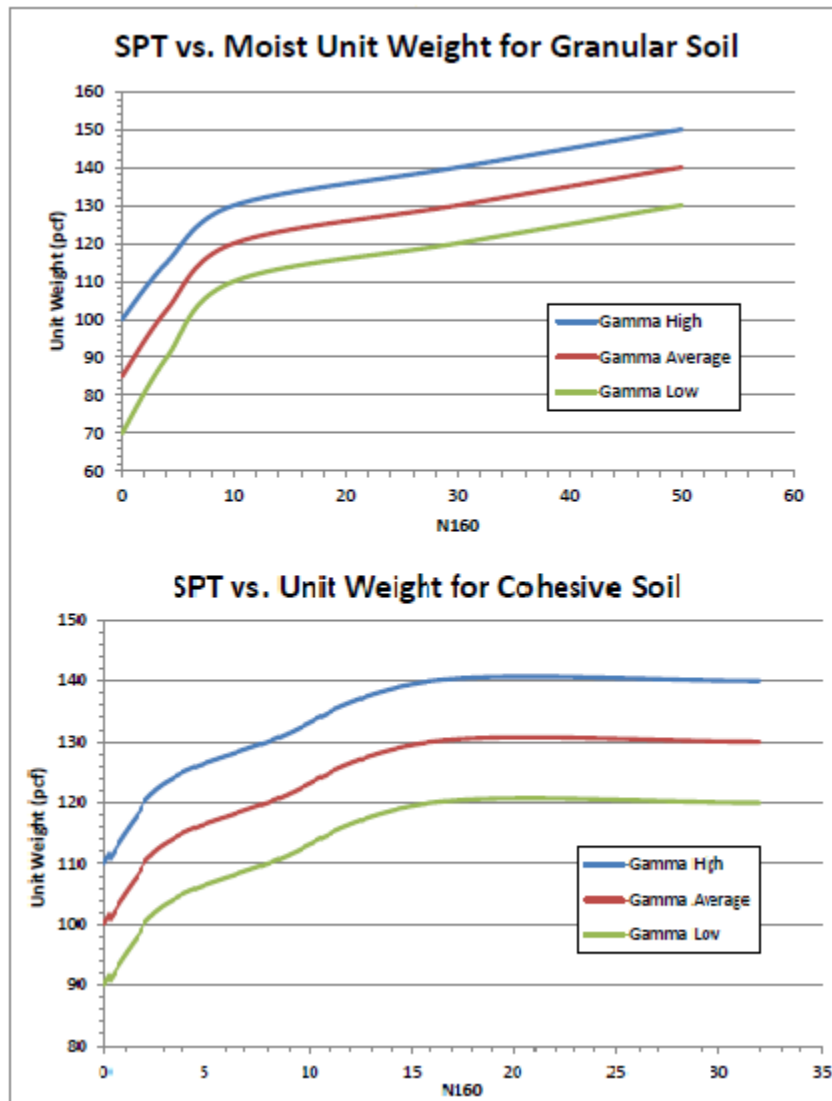


Figure 2-12: Cohesionless and cohesive unit weight estimates (CDOT, 2014)

### 2.7.3. Liquefaction Potential in Sandy Soils

The SPT has a long history in developing correlations with soil liquefaction potential and assessing soil vulnerability to earthquakes. SPT blow counts reflect stress and strain history effects, soil fabric, vertical and horizontal  $\sigma'$ , and  $D_r$ . All are known to influence the resistance of sands to liquefaction (Tokimatsu & Yoshimi, 1983). Research in Japan has been carried out due to an abundance of SPT borings and extensive historical earthquake records. Damage caused by liquefaction is easily verified by field observations, which give correlations great merit as they directly relate to field performance under real stress conditions (Seed et al., 1985).

Liquefaction is a phenomenon in which a cohesionless soil loses strength during an earthquake or rapid loading and acquires a degree of mobility sufficient to permit movements. It occurs in saturated soils and primarily results from a buildup of  $\Delta u$  that develops when shear stresses are applied in a cyclic manner. Seed and Hon (1987) suggest, based on 20 years of research, that there is a limiting pore pressure ratio ( $r_u$ ), between  $\Delta u$  and  $\sigma'_{vo}$ , where liquefaction generally occurs in a soil that is susceptible to liquefaction. They suggest that a  $r_u$  less than 60% does not lead to soil liquefaction, and a  $r_u$  greater than 100% does.

Liquefaction does not occur until certain criteria, soil, and loading conditions result in high  $r_u$  readings. Lee and Seed (1967) simulated earthquake loading using isotropically-consolidated undrained tests with cyclic deviator stress applications on uniform Sacramento River Sand. They found that the stress conditions inducing failure of saturated sands were influenced by:

1. The magnitude of the cyclic stress or strain
2. The number of stress or strain cycles
3. The void ratio of the sand
4. The confining pressure to which the sand is subjected
5. The failure criteria used

The failure criteria used can vary. Practical problems may suggest that excessive deformations constitute failure. In reality, liquefaction can appear as settlement, small boils, or complete failure in the form of large slides or building collapses. Four categories have been previously recognized by Lee and Seed (1967) in cyclic loading problems and include:

1. Initial Liquefaction – Soil first exhibits any degree of partial liquefaction during cyclic loading
2. Partial Liquefaction – Soil exhibits no resistance to deformation over a strain range considered less than failure. Saturated sand may be in partial liquefied condition over a substantial number of stress cycles.
3. Complete Liquefaction – Soil exhibits no resistance to deformation over a wide strain range. Any saturated sand that undergoes complete liquefaction has failed for practical purposes.
4. Failure – Strains become excessive and are considered to have occurred when the strains attain a double amplitude of 20%.

Additionally, when considering liquefaction, the number of stress cycles, stress magnitudes, soil densities, and confining pressure, Lee and Seed (1967) found the following:

1. Cyclic Stress applications will induce liquefaction or partial liquefaction of saturated sands over a considerable range of densities.
2. The higher the cyclic stress or strain, the smaller the stress cycles required to induce failure.
3. The lower the confining pressure, the lower the cyclic stress, strains, or number of cycles required to induce liquefaction.
4. When sands liquefy under cyclic stresses of constant amplitude, deformations immediately become very large.
5. Dense sands may develop a condition of partial liquefaction in which the effective confining pressure and the resistance to deformation are zero over some range of strain amplitude, although they are appreciable over other ranges of deformation. (Partial liquefaction is then accompanied by failure.)
6. The cyclic stresses required to induce liquefaction or failure of initially unstressed elements of saturated sand are considerably smaller than those required to induce failure under static loading conditions.

### 2.7.3.1. SPT N Correlations with Liquefaction Resistance

#### 2.7.3.1.1. N Value Corresponding to Liquefaction and Non-liquefaction Soils

Koizuma (1966) referenced N values from pre-earthquake SPT borings with those completed after the Niigata Earthquake of 1964. He looked at soils and the related damage in terms of critical void ratio ( $e_{crit}$ ), and the associated critical N value ( $N_{cr}$ ). He found that loose sands tended to contract when sheared, increasing the pore pressures and resulting in the loss of shear strength. Post-earthquake settlement was then documented as  $\Delta u$  dissipated, as were increased N values in SPTs taken afterwards. Dense sands dilated during the earthquake resulted in no loss of soil stability, negative pore water pressures, and lower N values in post-quake borings. He developed a plot valid at depths greater than four meters, which divided a sand response (contraction or dilation) to cyclic loading based on  $N_{cr}$ . The following equation, which is a simplified linear expression, correlates  $N_{cr}$  with depth.

$$N_{cr} = [1.9743 \times \text{Depth (m)}] - 0.4698 \quad \text{Equation 2-11}$$

Finn (1982) reviewed case studies from China where innovative lab testing correlated liquefaction with N. Triaxial tests mounted on a vibrator, which applied cyclic deviator stresses under constant confining pressure, and drained cyclic tests used to model pore water changes in undrained conditions were carried out. In 1974, an empirical equation based on SPT field data was adopted to provide  $N_{cr}$ . The formula is given by:

$$N_{cr} = \dot{N} \{1 + 0.125(D_s - 3) + 0.05(D_w - 2)\} \quad \text{(Finn, 1982)} \quad \text{Equation 2-12}$$

where

$D_s$  = depth to sand layer under consideration (m)

$D_w$  = depth to water table below ground surface (m)

$\dot{N}$  = function of shaking intensity or acceleration which relate to earthquake magnitude (blows/ft) according to the table below

Intensity	Acceleration	$\dot{N}$
VII	0.075	6
VIII	0.15	10
IX	0.30	16

Seed et al. (1983), using field data from liquefied and non-liquefied sites, showed that the cyclic stress required to cause liquefaction increased as  $N_1$  increased in sands. In addition, silty sands were found to have significantly higher liquefaction resistance, at similar  $N_1$  values, than coarse-grained sands. The authors suggested that coarse-grained sands had an equivalent  $N_1$  value 7.5 blows per foot higher than that of silty sands. Silty and coarse-grained sands were categorized based on  $D_{50}$  ( $D_{50} < 0.15$  mm and  $D_{50} > 0.25$  mm respectively), which corresponded to an approximate FC of 30%.

Clay soils are found to have a much higher resistance to liquefaction than those without the presence of clays. In fact, clay soils have been considered non-vulnerable (Seed et al., 1983) as long as the clay's plasticity is not low and the clay content is above a certain percent. Seed et al. (1983) proposed that a soil with minimum clay contents of 15% would generally not liquefy. Tokimatsu and Yoshimi (1983) proposed minimum clay contents of 20%.

#### **2.7.3.1.2. Influence of Fine Content on N Value**

Tokimatsu and Yoshimi (1983) proposed using FC as an index property for soil liquefaction, and plotted liquefaction based on FC,  $D_{50}$ , and  $N_1$  values. It was shown that the mean normalized  $N$  value at which liquefaction occurred decreased as FC increased and was a better indicator of soil behavior than  $D_{50}$ . Kishida (1969) previously proposed that the coefficient of uniformity,  $C_u$ , played an important role in liquefaction resistance, which agrees with a general trend that  $C_u$  tends to exceed five when FC exceeds 10% (Tokimatsu & Yoshimi, 1983).

Tokimatsu and Yoshimi (1983) proposed corrections to  $(N_1)_{60}$  based on FC as shown in Table 2-3. These ranges would increase measured  $N_1$  values to account for the reduced blow counts associated with FC induced pore water pressures during SPT sampling. It was assumed that SPT hammer systems utilized were the “tombi” (Japanese version of the trip monkey), therefore requiring equivalent trip monkey SPT ( $N_{\text{trip}}$ ) blow counts adjusted to  $N_{60}$ .

Table 2-3:  $\Delta(N_1)_{60t}$  Correction Based on FC (after Tokimatsu & Yoshimi, 1983)

FC	$\Delta (N_1)_{60t}$
0-5	0
5-10	Interpolate between 0 and 5
>10	$0.1(F(C))+4$

### 2.7.3.1.3. $(N_1)_{60}$ correlated to Liquefaction Damage

Seed et al. (1985) proposed approximate  $(N_1)_{60}$  ranges with respect to the severity of liquefaction damage. He noted that liquefaction at varying  $(N_1)_{60}$  values take on different forms of failure. Previously, liquefaction had been separated into two descriptions: liquefaction (large deformations) and cyclic mobility (boils and cracks) with limiting strain potential (Seed, 1975). DeAlba et al. (1976) confirmed this by demonstrating that dense sands would only undergo limited amounts of cyclic strain, even if  $r_u$  reached 100% under cyclic loading conditions. The proposed ranges of  $(N_1)_{60}$  are included in Table 2-4.

Table 2-4: Liquefaction Potential Based on  $(N_1)_{60}$ . (Seed et al., 1985)

$(N_1)_{60}$	Potential Damage
0-20	High
20-30	Intermediate
>30	No significant damage

## 2.8. Laboratory Studies of Soil Constituents

### 2.8.1. Effect of Particle Shape on the Engineering Properties of Granular Soils

Holubec and D'Appolonia (1972) studied the effect of particle shape on the engineering properties of granular soils. Experiments were conducted on four sands with different particle shapes and angularity. Results shown in Figure 2-13, Figure 2-14, and Figure 2-15 indicate that the maximum void ratio, friction angle, and shear strength all increase with increasing particle angularity. It was concluded that the particle shape has a pronounced effect on void ratio, friction angle, and shear behavior.

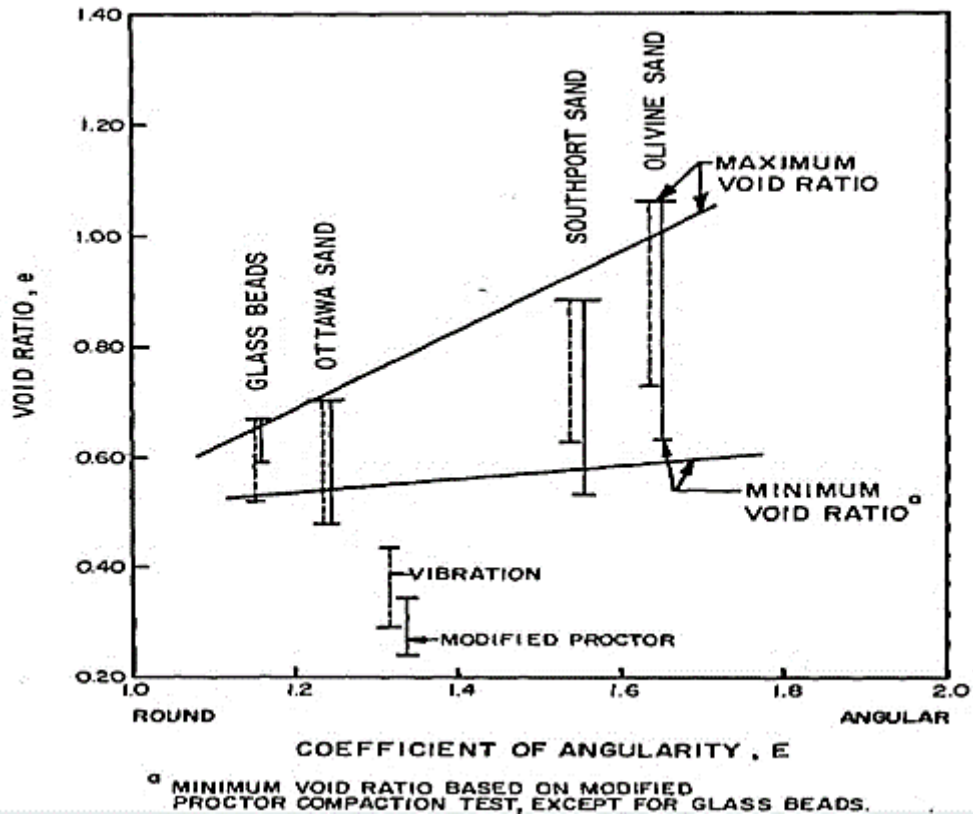


Figure 2-13: Effect of particle shape on minimum and maximum void Ratios (Holubec & D'Appolonia, 1972)

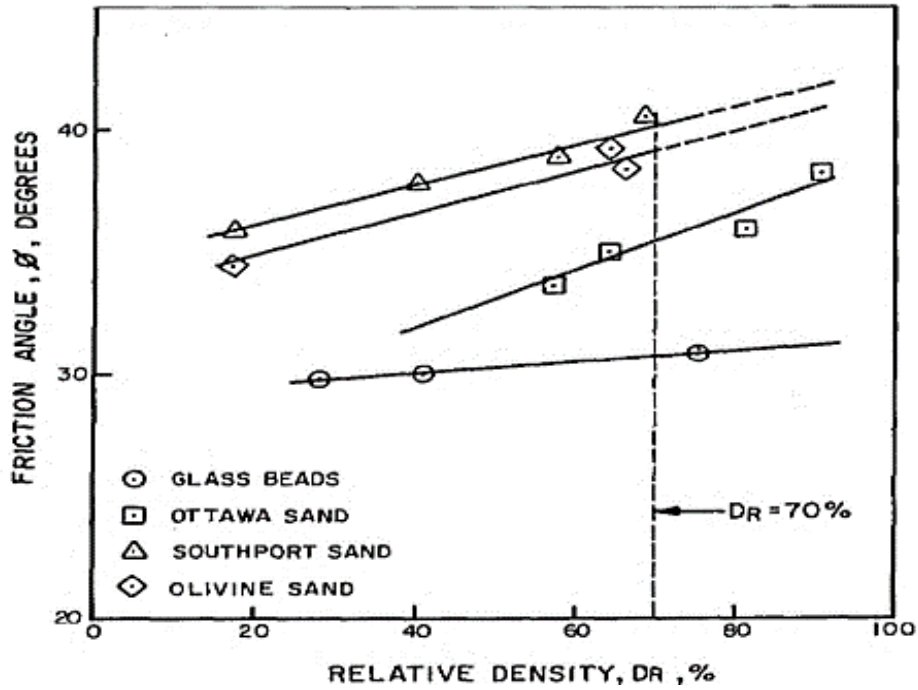


Figure 2-14: Effect of particle shape on angle of internal friction (Holubec & D'Appolonia 1972)

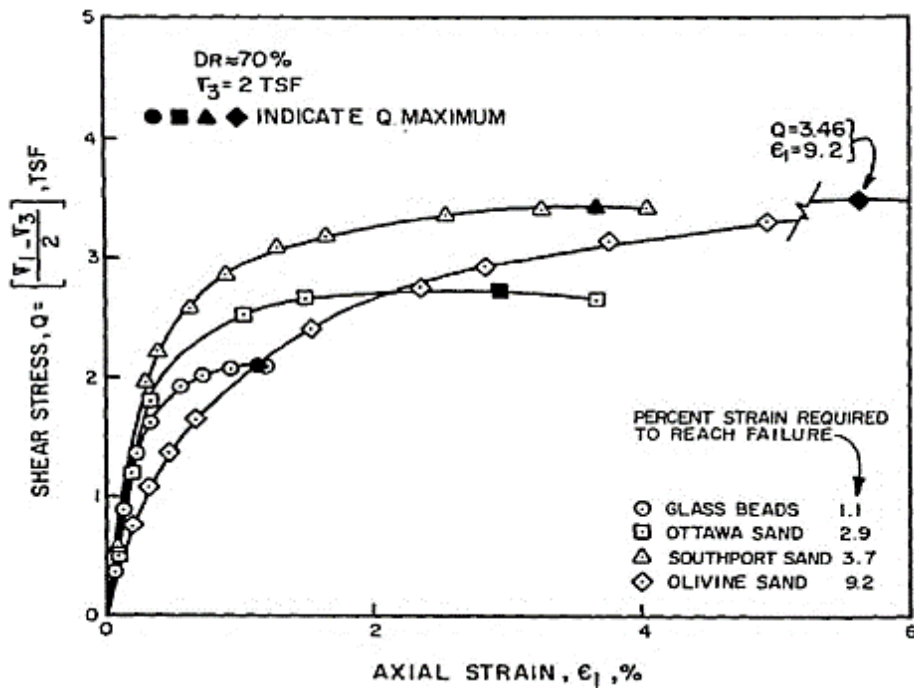


Figure 2-15: Effect of particle shape on stress-strain curves from constant cell pressure tests (Holubec, & D'Appolonia, 1972)

### **2.8.2. Pile Drivability Using One-dimensional Wave Propagation Theory**

Chen and Chen (2001) presented a model to study pile drivability using a one-dimensional wave propagation theory and the wave equation developed by Smith (1960). This model included the ram impact force, cushion stiffness, and pile impedance. The pile movements of maximum displacement and rebound were discussed and presented. The one-dimensional wave propagation theory was used to solve the kinematic equation for the pile toe.

The results presented the influence of driving system parameters on pile drivability. Chen and Chen (2001) concluded that as the tip resistance increased, rebound also increased; however, as the skin resistance increased, the rebound decreased. Additionally, as more mass/spring/dashpot segments were added to more finely discretize the model, predicted skin resistance increased and rebound decreased. The model results showed that as hammer mass and drop height increased, the pile penetration increased linearly. The model also suggests that the longer the hammer impact time, the larger the penetration. An increase of pile impedance leads to a higher peak force and a shorter impact duration, which damages the pile and leads to fatigue. It was concluded that the method developed helps engineers to select the proper equipment, estimate the driving blow counts, penetration, and pile stresses.

### **2.8.3. Effect of Particle Size Distribution on Pile Tip Resistance in Calcareous Sand**

McDowell and Bolton (2000) used the Cambridge centrifuge to investigate the effect of particle size distribution on pile end bearing resistance in calcareous sand. Quiou sand with two different grain size distributions was used, as shown in Figure 2-16. Two samples from each gradation were used. The first consisted of particles smaller than 0.5 mm, while the second grade included particles with nominal sizes ranging from 0.15mm to 0.5 mm.

Initial particle size distributions for the two gradings of soil

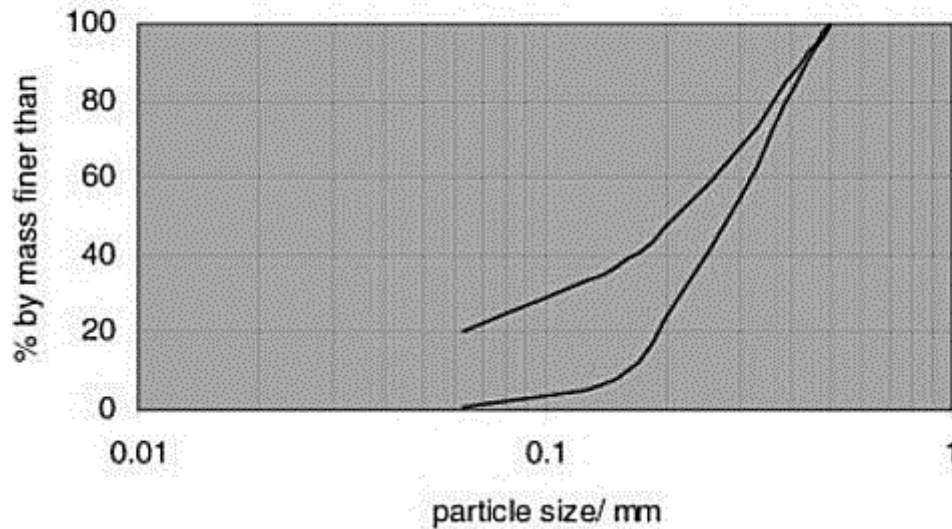


Figure 2-16: Initial Quiou sand gradation curves (McDowell & Bolton, 2000)

All four samples were placed in 190 mm (7.48 in) diameter 260 mm (10.2 in) high plastic tubes. Samples were compacted to their maximum density using vibration under a 5 Kg (11 l(b) weight. The samples were placed in an 850 mm (33.5 in) plastic tube, which was attached to a Cambridge beam centrifuge, as shown in Figure 2-17.

The samples were subjected to a vertical stress at the top and bottom soil boundaries. A 10 mm (0.39 in) diameter model pile with a 60° conical tip was driven 235 mm (9.25 in) at 1 mm/sec (0.039 in/sec penetration rate into the samples. This rate was chosen to make crushing unlikely; however, the authors still found it. The model pile was driven from an initial height of 275 mm (10.8 in) above the base of the tube to ensure that the pile penetration stopped 40 mm (1.57 in) above the base of the tube. This centrifuge testing corresponded to a 0.7 m (2.30 ft) diameter pile being driven at a rate of 7.0 cm/sec (2.75 in/se(c) into the soil, a rate much slower than typically found during actual pile driving.

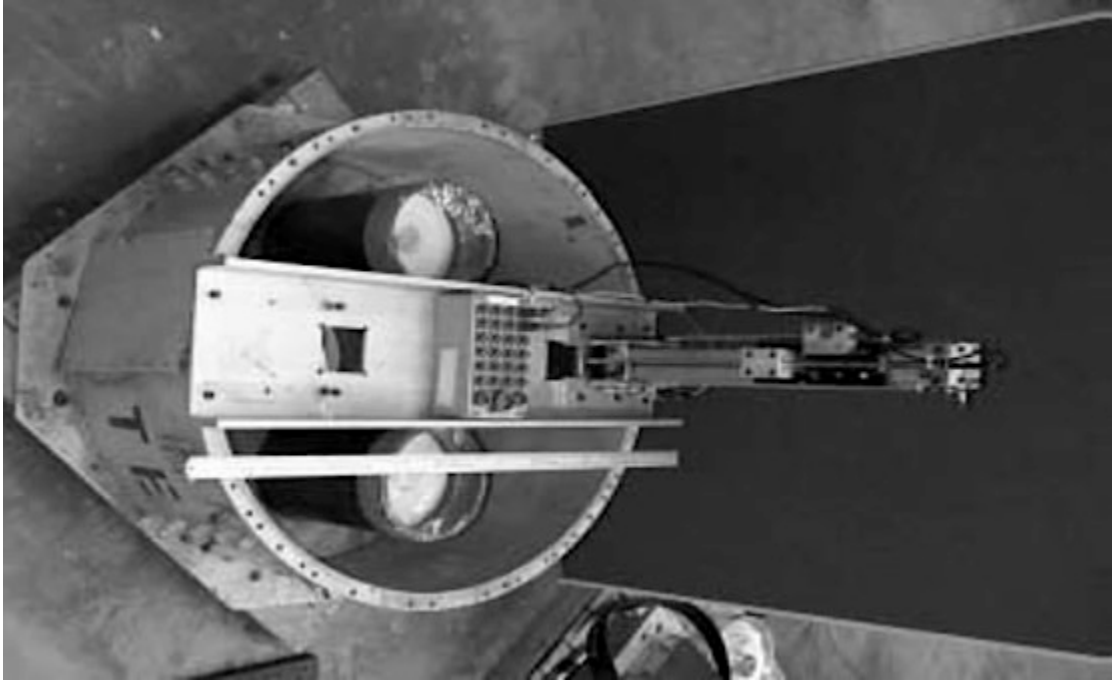


Figure 2-17: Cambridge centrifuge containing the 850 mm diameter steel tub with four 190 mm diameter samples (McDowell & Bolton, 2000)

The tip resistance ( $q_c$ ) for the model pile was plotted as a function of depth as shown in Figure 2-18. During each test, the tip resistance reached a maximum at a specific depth (termed the depth of instability) and then decreased as penetration continued. The maximum tip resistance was about 20 MPa (2,900 psi) for the well-graded soils near a penetration of about 60 mm (2.36 in) (a) and (b) and 10 MPa (1,450 psi) for the uniform soils near a penetration approaching 100 mm (3.94 in) (c) and (d). It was concluded that the peak resistance is a function of the initial particle size distribution.

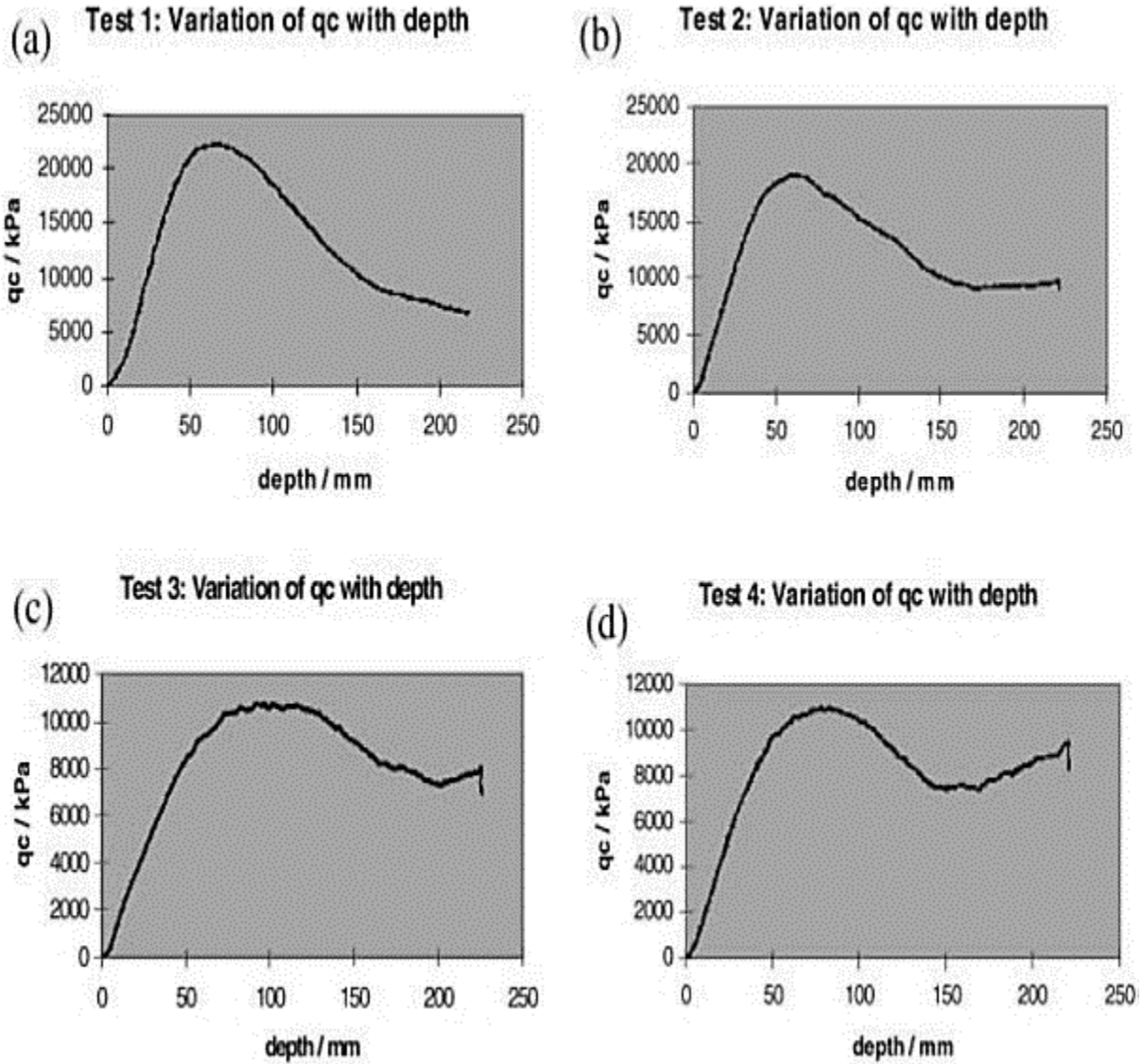


Figure 2-18: Tip resistance (kPa) as a function of depth (mm) for each of the four soil samples (McDowell & Bolton, 2000)

Following the centrifugal driving process, a 10 mm (0.394 in) hollow tube attached to a vacuum pump was used to retrieve the particles adjacent to the pile. The associated particle size distributions for the well-graded soil samples at depths less than and greater than the instability depth were plotted, as shown in Figure 2-19. This figure shows no appreciable particle size changes above the depth of instability but rather large changes below this depth. The maximum particle size changes occurred below the depths of instability (60 and 100 mm) (2.36 and 3.93 in) at about 0.2 mm (0.00787 in) as the percent fines increased from about 50 to 60%. The authors

concluded that there was insignificant particle crushing in the soil above the instability depth, but some crushing below the instability depth.

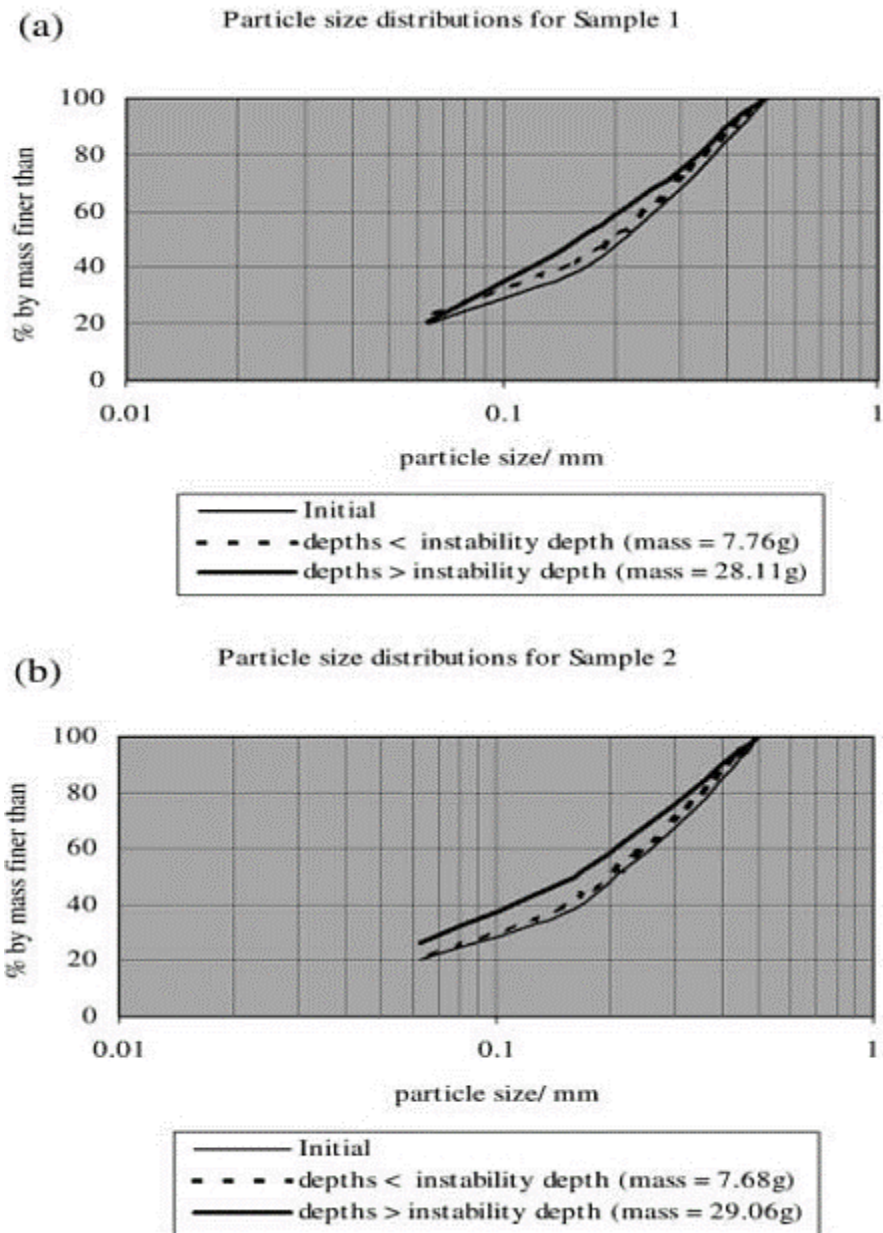


Figure 2-19: Particle size distributions for samples 1 and 2 at depths less than and greater than the instability depth (McDowell & Bolton, 2000)

## **2.9. Effect of Cyclic Loading**

A summary of the experimental studies that have been performed with the intention of describing the behavior of soils subjected to cyclic loading is presented. The majority of this research found that soils failed at stress levels below the maximum static failure deviator stresses.

### **2.9.1. The Use of Cyclic Deviator Stress to Evaluate Soil Behavior**

The Critical Stress Level (CSL) is expressed as a percentage of the static deviator stress at failure. Below the CSL, the soil primarily deforms elastically; above the CSL, the soil deforms plastically. At stress levels above the CSL, each load cycle results in additional non-recoverable deformation and ultimate failure (Frost et al., 2004; Awad 1975; Putri et al. 2012; Shahin et al. 2011; Wilson & Greenwood, 1974).

Frost et al. (2004) concluded that applying cyclic deviator stresses at levels below 50% of the static deviator failure stress ( $\sigma_{df}$ ) resulted in fairly constant and small increases in permanent deformation. If the applied cyclic deviator stresses exceeded this level, rapid increases in deformations occurred. Putri et al. (2012) reported that the threshold (CSL) stress of compacted clay with sand ranged from 30% to 38.6% of  $\sigma_{df}$  at low and high confining pressures, respectively.

Puppala et al. (2004) used deviatoric stress levels of 0.2, 0.4, and 0.6  $\sigma_{df}$  and carried out 10,000 repeated cyclic triaxial loadings at 1 Hz loading frequency on sandy clay (CL) with 38% passing through a number 200 sieve. The authors evaluated both the elastic and plastic deformations during the testing. The findings confirmed the existence of a CSL near 60% of the failure stress.

Okur et al. (2008) concluded that pore water pressures were induced when cyclic loading was applied to particular types of saturated soils. As the pore pressure builds, the soils start to lose their shear strength and large deformations occur, causing soil failure. This phenomenon is called liquefaction in sandy soils and cyclic softening in saturated fine soils. The research team performed undrained cyclic tests using cyclic stress ratios of up to 0.35 and loading frequencies of 0.1 Hz (10 seconds per cycle). The researchers concluded that soil specimens with high

plasticity indices produced the highest resistance to cyclic failure and excess pore pressure generation. High cyclic stress ratios (up to  $0.8 \sigma_{df}$ ) were required for cyclic softening to occur.

## **2.9.2. Soil Behavior Under Repeated Vertical and Horizontal Stresses**

Awad (1975) investigated the cyclic behavior of silty clay under relatively slow repeated vertical stresses using conventional triaxial tests. To produce a loading rate of one cycle per minute, load durations of 45 seconds were followed by a rest of 15 seconds. One thousand cycles were performed during each triaxial test. The samples were subjected to two types of repeated loadings. The first was cyclic vertical stress with a constant cell pressure and the second was cyclic vertical stress with varied cell pressures.

Awad (1975) found CSL values, which varied from 0.37 to  $0.5 \sigma_{df}$ . Within the elastic range (below the CSL), the pore water pressures increased during the first 10 cycles and then decreased due to the soil dilation. In contrast, once the stresses reached the plastic range (above the CSL), the pore water pressures continued to increase up to the time of failure. In some samples with an applied cyclic deviator load equal to  $0.60 \sigma_{df}$ , failure occurred after only one cycle due to a sudden increase in the pore water pressures.

Moses and Rao (2003) performed a study on the influence of cyclic loading on the strength and deformation behavior of cemented marine clay using cyclic triaxial tests. Using loading frequencies of 0.05, 0.083, and 0.17 Hz (6, 12, and 20 seconds per cycle), the authors selected CSLs from 0.25 to 0.7. The authors concluded that both the pore water pressure and strain increased dramatically within the first 2,000 loading cycles and then stabilized, showing no additional increase with the remaining cycles. When they conducted cyclic triaxial tests at 0.7 CSR, some samples failed within a few cycles, while minimal deformation occurred to soils for CSRs up to 0.35.

Shahin et al. (2011) studied the behavior of soft clay during undrained cyclic loading. Different cyclic deviator stresses were applied below and above the CSR. All samples were tested at a loading frequency of 1 Hz with CSLs between 0.36 and 0.71 using 150,000 cycles. The results showed that under CSRs up to 0.63 both the excess pore water pressures and axial strains increased with an increasing number of cycles up to about 100,000, after which they remained relatively constant. For a CSL of 0.71, the soil failed after the first few cycles. The

study confirmed that testing soil at deviator stresses higher than the CSR led to the generation of pore water pressures and non-recoverable deformation, which led to soil failure. When tested at a deviator stress less than the CSL soil reached a state of equilibrium with no sign of failure.

### **2.9.3. The Influence of Fines Content on Pore Pressure Generation under Cyclic Loading**

A significant amount of laboratory research has been conducted to clarify the effects of silt and clay content on pore pressure response during cyclic loading. Loose sands subjected to short duration cyclic loading produced a sudden and complete loss of strength leading to liquefaction. Boulanger and Idriss (2008) concluded that, as a result of cyclic loading, cohesive fine-grained soils experienced considerable loss in shear strength despite the fact that the effective stress was not zero. Cohesionless fine-grained soils, on the other hand, completely lost their shear strength during cyclic loading as result of built-up pore water pressures that produced zero effective stresses.

Moses and Rao (2003) found that when dynamic loads were applied in soft clays, the pore water pressure began to increase, causing a decrease in effective stress and strength. This process led to a breakdown of the soil structure, resulting in a significant reduction in stiffness and strength.

Historical data proves that liquefaction produces a significant reduction of the stiffness and strength in soils other than clean, uniform, loose saturated sands. In addition, a vast range of soil gradation and consistencies have been linked with shear strength reduction during undrained cyclic loading (Koester, 1993).

In general, the presence of plastic or clayey fines increases the soil liquefaction potential during dynamic loading (Polito, 1999). Additionally, as the silt content in sand increases to a limiting value, the liquefaction resistance increases. Past this limiting silt content, the liquefaction resistance decreases.

Cyclic triaxial tests were conducted by Sandoval-Shannon (1989) to evaluate the characteristics of silt. The results indicate that low plasticity silts and fine uniform sands produced liquefaction when the pore water pressure reached the effective confining pressure.

Arab and Belkhatir (2012) studied the influence of low plasticity fines on the cyclic behavior of silty sand. They concluded that liquefaction potential of silty sand increased as fines content increased up to a maximum of 20%, and then decreased when the fines content increased to 40%. Koester (1993) found that sands containing 20%-26% fines were strongly susceptible to strength loss. The cyclic triaxial strength dropped for specimens composed of 20% plastic fines.

#### **2.9.4. The Effects of Non-Plastic and Plastic Fines on the Liquefaction of Soil**

Bray et al. (2004) suggested that the most effective indicator of the liquefaction of fine-grained soils is their plasticity index. The authors found that if fine grained soils have a Plastic Index (PI) less than or equal to 12, and a ratio of the water content to liquid limit ( $w_c/LL$ ) greater than 0.85, then it will be prone to liquefaction, thus significant strength loss. Also, if a fine-grained soil has  $PI > 20$ , then it will not undergo liquefaction.

Boulanger et al. (2006) suggested that the term liquefaction be reserved for identifying the development of significant strains or strength loss in fine-grained soils exhibiting sand-like behavior, while the term cyclic softening failure is used to define similar phenomena in fine-grained soils exhibiting clay-like behavior. They concluded that fine grained soils with a  $PI \geq 7$  showed cyclic softening, while those with a  $PI < 7$  experienced liquefaction.

Guo and Prakash (1999) studied the liquefaction of silts and silt-clay mixtures under cyclic loading. Their results indicate that the liquefaction resistance of silt clay mixtures decreased as PI increased, within the low plasticity range. This trend was reversed in the high plasticity range.

Seed et al. (1985) stated that sands containing more than 5% fines had significant strength loss resulting in liquefaction of these sandy soils. Other studies by Osipov et al. (2005) and Koester (1994) produced the same conclusion: that soil resistance improved as fines content increased. However, low plasticity soils were very vulnerable to liquefaction.

#### **2.9.5. The Effects of Non-plastic Fines on the Generation of Pore Water Pressure during Cyclic Loading**

Hazirbaba (2005) defined the limiting fines content (LFC) as the transition point beyond which there are sufficient fines to prevent the coarse soil particles from being in contact. In this

situation, the fines dominate the behavior of the soils and become the main skeleton that carries the shear stresses.

The limiting fines content (LFC) of a soil is generally calculated using the following equation:

$$\text{LFC} = W_{\text{fines}} / (W_{\text{sand}} + W_{\text{fines}}) \quad \text{Equation 2-13}$$

where

$W_{\text{fines}}$  = solid weight of the fines portion and

$W_{\text{sand}}$  = solid weight of the sand portion

Dash and Sitharam (2009) studied the effects of non-plastic fines on the generation of pore water pressure during cyclic loading. The researchers analyzed the generation of pore water pressure based on the cycle ratio, the ratio of loading cycles to the loading cycles required to cause initial liquefaction. The research team conducted 289 undrained cyclic triaxial tests on isotropically consolidated sand-silt mixtures with silt contents from 5% to 75%. Note that only silt was used; therefore, the LFC is actually the limiting silt content for this work. Data was organized such that the relative density (RD) was determined as the silt content was increased. Two sets of tests were performed with initial void ratios of 0.44 and 0.54. As silt was added, the RD range (i.e.  $\gamma_{\text{min}}$  to  $\gamma_{\text{max}}$ ) increased; therefore, the RD values decreased even though the overall densities at each blend increased. The results showed that the rate of generation of excess pore water pressure increased as the silt content increased.

The trend was reversed when the silt content exceeded an LFC of 21%. The authors examined the increase in pore water pressure to the initial decrease in relative densities up to the limiting silt content. As the silt content increased beyond the limiting fines content, the relative densities started to increase, as shown in Table 2-5.

Table 2-5: Variation in Relative Density (Dash & Sitharam, 2009)

Silt Content (%)	RD (%) at $e_c = 0.44$	RD (%) at $e_c = 0.54$
0	92	53.8
5	63.3	32.6
10	55.8	26.6
15	49.3	21.6
20	42.7	15.7
25	60.1	37.3
30	62.5	40.7
35	70	49.8
40	78.7	60.5
50	88.8	73.1
60	90.5	77
75	No Data	97.3

The presence of silt produced a significant effect on the cyclic resistance and pore pressure of all sand silt mixtures, as demonstrated in Figure 2-20. A steep decline was observed in the limiting silt content during the cyclic resistance when conducting undrained cyclic triaxial tests on sand-silt mixtures with silt contents from 0% to 60%. This sharp decrease in cyclic resistance reversed when the silt contents were beyond the transition point (15 to 25 %) where the silts make up the predominate percentage of the soil skeleton.

The testing showed that as the pore water pressures increased, the specimens got weaker and lost strength up to the transition point. Beyond the transition point, the specimens gained strength with increasing silt content beyond the limiting fines content (LFC) of 21%.

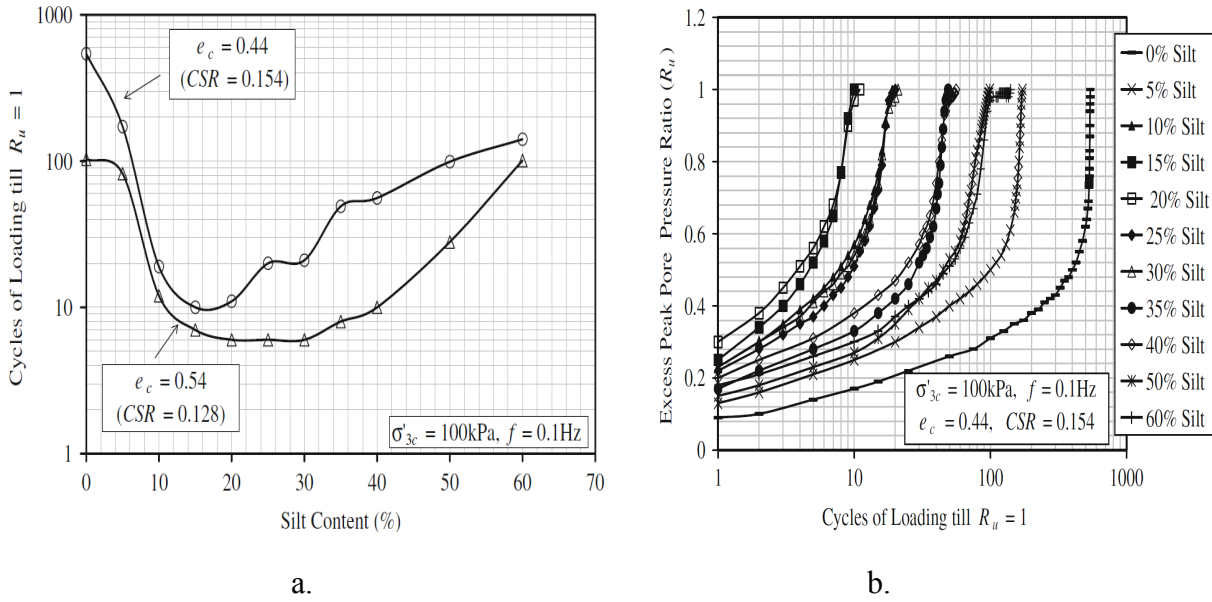


Figure 2-20: Results of cyclic triaxial tests: (a) Silt contents versus cycles required to generate 100% excess pore water pressure; (b) Loading cycles versus excess pore pressure ratio (Dash & Sitharam, 2009)

### 2.9.6. SPT N Value versus Liquefaction Potential

Seed et al. (1985) proposed correlations with  $(N_1)_{60}$  and the potential damage caused from liquefaction, which has been termed liquefaction potential for this study. Based on Koizuma's description of liquefied and non-liquefied soils after the 1964 Niigata Earthquake, Seed et al. (1985) proposed damage potential for N values from 0-20, 20-30, and  $> 30$  were changed to soil responses to account for a soil's contractive or dilative response. It was assumed that Seed et al. (1985) used N values developed from Japanese trip monkey hammers when comparing liquefaction damage. Table 2-6 presents Japanese trip-monkey-derived  $(N_1)_{60}$  values adjusted for FC [ $(N_1)_{60ta}$ ] in comparison to a coarse grained granular soil's response when sheared.

Table 2-6: Estimated Soil Response to Cyclic Shearing Based on (N1)<sub>60ta</sub>

(N1) <sub>60ta</sub>	Soil Response
0-20	Contraction
20-30	Intermediate
>30	Dilative

### 2.9.7. Development of Pore Water Pressures during Pile Driving

Robertson et al. (1990) studied the distribution of excess pore water pressures and drainage conditions around 915 mm (36.0 inch) diameter open-ended steel piles. These piles were driven to a depth of approximately 90 m (295 ft) through normally consolidated marine clayey silt as a component of the foundations for the Alex Fraser Bridge in British Columbia. A multi-point piezometer was installed close to the pile group in order to measure the pore water pressures before and after driving. Eighteen hours after completion of driving, a cone penetration sounding, with pore pressure measurements (CPT<sub>u</sub>) was performed 5 m (16.4 ft) from one of the piles. During this sounding, CPT<sub>u</sub> dissipation tests were performed at various depths to record the equilibrium pore pressures throughout the marine silt deposits. The dissipation data, in terms of pore water pressures versus log time in minutes was recorded for the different elevations, as presented in Figure 2-21. CPT<sub>u</sub> cylindrical dissipation theory (Robertson et al., 1990) was used to estimate the excess pore pressures 5 m (16.4 ft) from the pile immediately after driving. The time factor (T) associated with the CPT geometry can be determined using the following equation:

$$T = C_h t / R^2 \quad \text{Equation 2-14}$$

where

$C_h$  is the coefficient of consolidation in the radial direction,

$t$  is the time

$R$  is the radius of the probe.

The CPTu dissipation data indicates that the average time required to achieve 95% degree of dissipation was between 35 and 45 minutes. For the same degree of dissipation and an assumed constant value of  $C_h$ , the following relationship holds:

$$\frac{t_{95} (pile)}{t_{95} (CPTu)} = \frac{R^2 (pile)}{R^2 (CPTu)} \quad \text{Equation 2-15}$$

Using the known 915 mm (36 inch) pile diameter and the standard CPTu diameter of 35.7 mm (1.40 inch) and associated  $t_{95}$  for the CPTu, the time required for 95% pressure dissipation for the pile was estimated to be 16 to 21 days.

The multi-point (MP) piezometer provided a series of pore pressure measurements at discrete depths over an extended period of time. The results were compared with the  $CPT_u$  results and showed excellent agreement as displayed in Figure 2-21. It was concluded that the excess pore pressures generated due to pile driving extend laterally a distance of 25 to 35 times the pile radius.

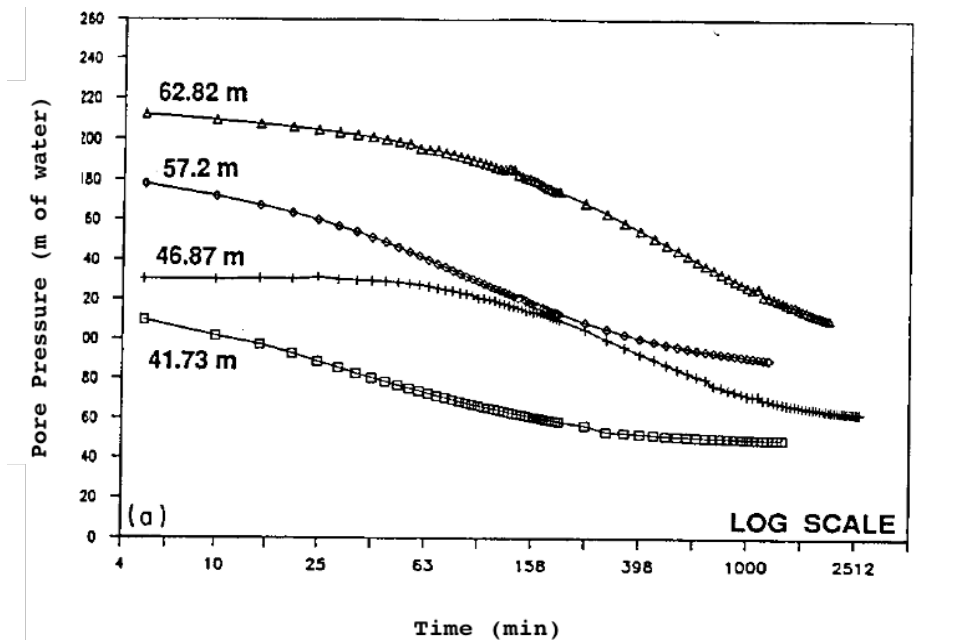


Figure 2-21: CPTu pore pressures dissipation tests at the Alex Fraser Bridge (Robertson et al., 1990)

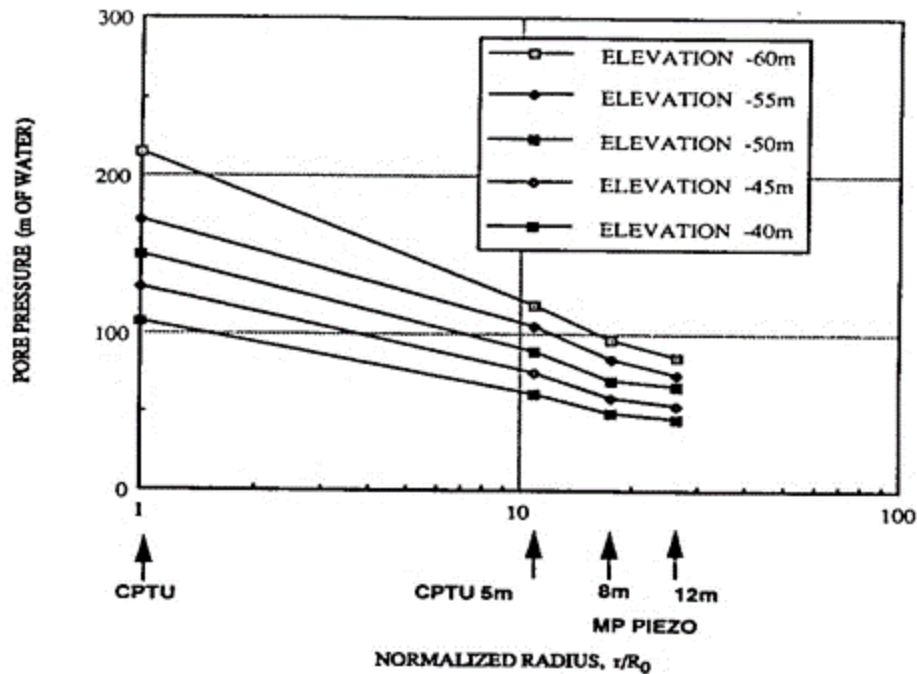


Figure 2-22 Relationship between measured pore pressures from  $CPT_u$  and MP piezometers with normalized radial distance from pile (Robertson et al., 1990)

Eigenbrod and Issigonis (1996) monitored pore water pressure responses recorded during driving of steel piles through soft, sensitive clay into very dense sand and gravel. Data was recorded from two piezometers installed from about 4 to 12 m (13.2 to 39.6 ft) from the piles at two different depths, 9 m (29.5 ft) and 18 m (59 ft), in three boreholes at the site. Since the piles were too long (22 m) (72.2 ft) to be driven as a single segment, two segments were welded and driven consecutively to provide the required design length. During the driving of the first segment to a depth of approximately 14 m (45.9 ft), very small pore water pressures were observed. However, high pore water pressures were observed in the clay during the driving of the second segment, as depicted in Figure 2-23.

Stress and pore water pressure changes were analyzed by evaluating the driving force as a flexible load applied over the surface of an elastic half-space (the soft clay layer). The authors concluded that the clay layer was experiencing rebound or upward stresses from the underlying very dense sand and gravel as the piles were driven into this very dense layer. The pore water pressure changes were accompanied by equivalent increases in total stresses causing changes in effective stresses and pile capacity. However, this was not the case when the pore water pressures increased during driving from the dynamic loading. In this case, the total stresses

remained constant while the pore water pressure increased. This ultimately led to a significant decrease in effective stresses and a loss in bearing capacity.

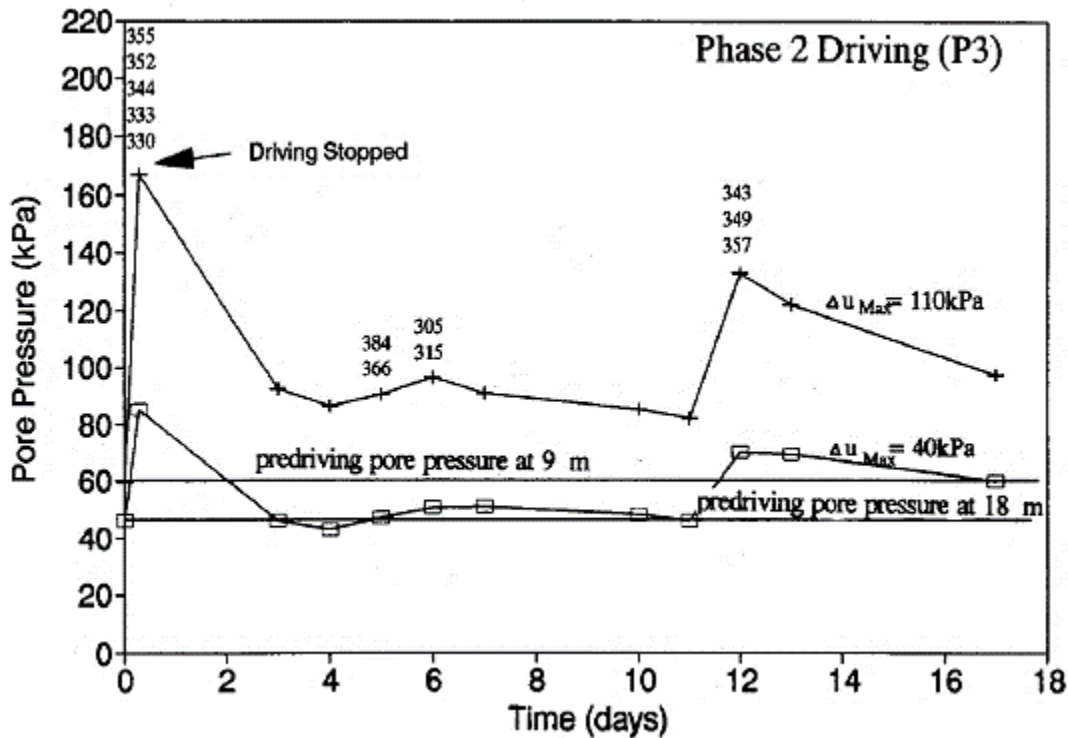


Figure 2-23: Pore water pressure changes due to pile driving (Eigenbrod & Issigonis, 1996)

Bingjian (2011) studied the pore water pressure variation in saturated soft soil due to the driving of a PCP. Two existing residential buildings were selected for this case study. The soils at the site were characterized as silty clay to mucky clay with a water table 0.9-1.6 m (2.95 – 5.25 ft) below the ground surface. The soils had high natural moisture content, void ratio, and compressibility, as well as low strength and permeability. The foundation consisted of 500 mm (19.7 inch) diameter prefabricated concrete tubular piles 48-50 m (157-164 ft) long. Each had an ultimate capacity of 4,000 kN (900 kips). During driving, as the pile penetrated into the saturated soft clay, a combination of consolidation and excess pore water pressures was developed since the water could not dissipate quickly due to the fast loading and low coefficient of permeability. In order to measure these pressures, six pore pressure transducers with vibrating wire strain gauges were installed radially and symmetrically on both sides of the pile at radial distances of 0.9 m (2.95 ft), 1.9 m (6.24 ft), and 2.9 m (9.51 ft) at a depth of 14.5 m (47.6 ft). The variation of pore water pressure ( $u$ ) recorded by the three gauges at 14.5 m (47.6 ft) was plotted versus the

driven depth (H) of the pile, as illustrated in Figure 2-24. This figure shows a significant increase in the pore pressures at about 11 meters (36 ft). It also shows that the pore pressures nearest the pile are much higher than those 2.9 m (9.51 ft) from the pile. The variation of pore water pressure at discrete driving depths (H) in terms of radial distance from the pile at the gauge locations is shown in Figure 2-25. This plot shows that the excess pore pressures decreased rapidly from the 0.9 m (2.95 ft) to 1.9 m (6.24 ft) radial distance and that the pore pressures at the larger depths are much higher than those for the shallower depths. The author concluded that the radius of influence was about 3 m, which for the 0.5 m pile equates to about six times the pile diameter.

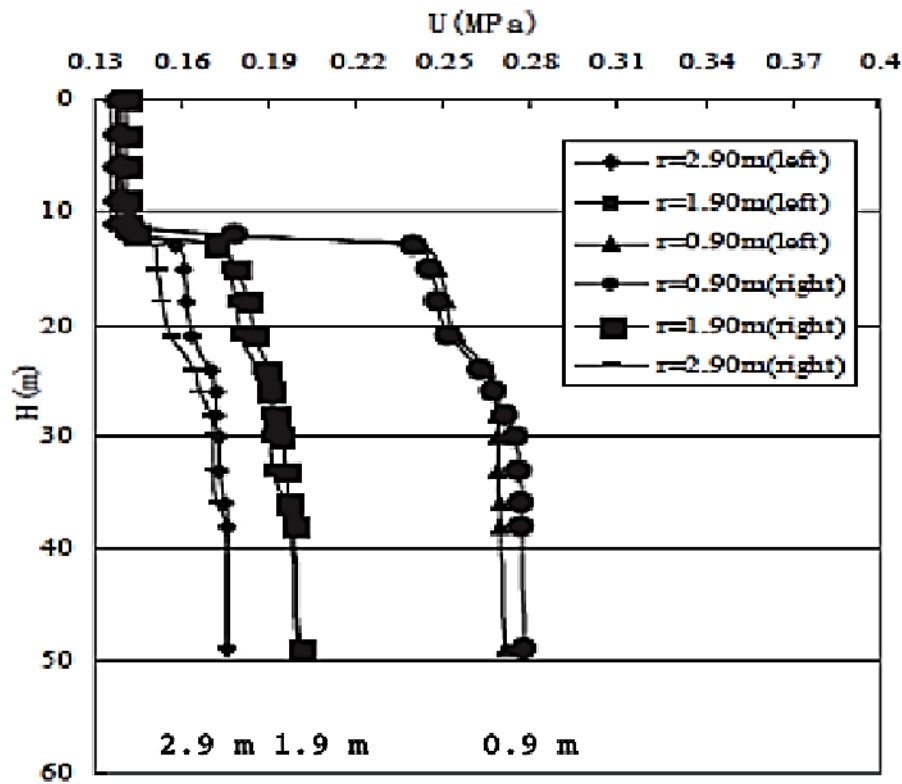


Figure 2-24: Excess pore pressure versus driving depth for the three sensor locations (Bingjian, 2011)

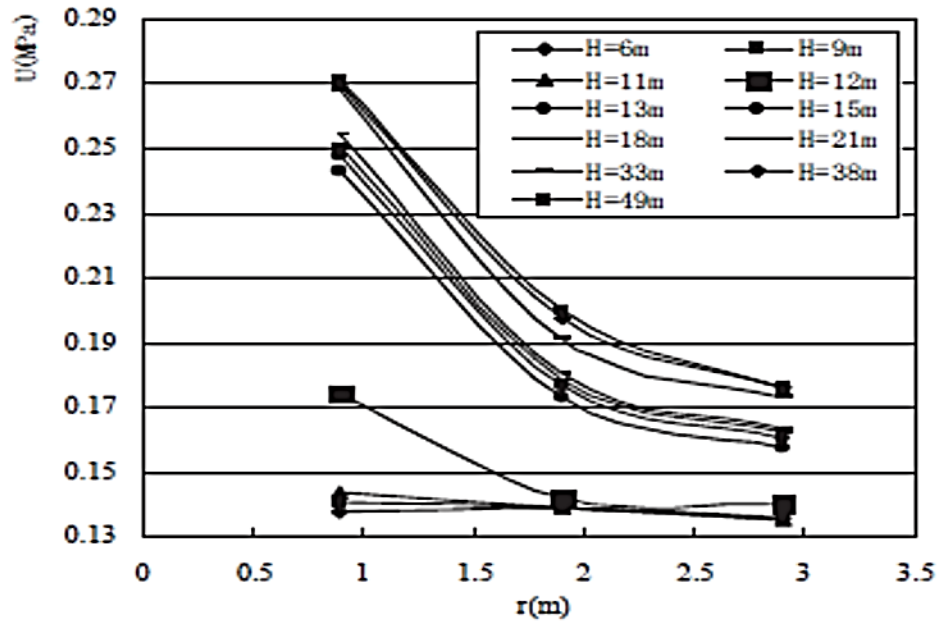


Figure 2-25: Excess pore pressure versus radial distance at discrete driving depths curve (From Bingjian, 2011)

After the pile driving was completed, the dissipation of the excess pore water pressures was observed over the next 40 days (1,000 hours). There were a total of fifteen observations for each gauge, as illustrated in Figure 2-25. This figure shows the variation of excess pore water pressure with time at the 0.9 m (2.95 ft), 1.9 m (6.24 ft), and 2.9 m (9.51 ft) radial distances from the pile. After about 400 hours (16.7 days), the excess pore pressures for the 1.9m (6.24 ft) and 2.9 m (9.51 ft) locations had nearly dissipated to hydrostatic pressure (0.13 MPa). The excess pore pressures at 0.9 m (2.95 ft) nearly dissipated at about 600 hours (25 days).

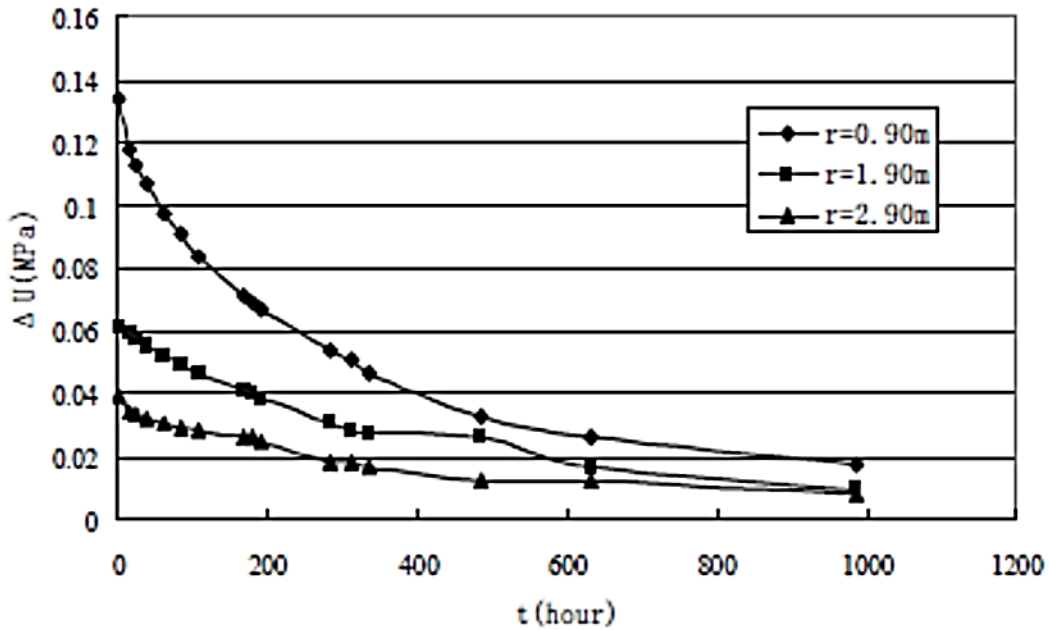


Figure 2-26: Change in pore pressure versus time for the three sensor locations (Bingjian, 2011)

### 2.9.8. Summary of Cyclic Loading

Research on cyclic behavior of soils has identified the CSL above which soils undergo plastic deformations and below which they undergo elastic deformations. As shown in Table 2-7, CSLs generally range from 0.2 to 0.8. The most common CSL is about 0.6. Limiting fines content (LFC) has predominantly been studied as a predictor for the susceptibility of soils to liquefaction under cyclic loading. Unfortunately, not much research is available with both CRL and LFC information.

The cyclic testing reported in the literature typically used load durations much longer than the load durations associated with pile driving (typically less than 1 second). The resilient modulus test conducted in accordance with the American Association of State Highway and Transportation Officials (AASHTO) T307 specifies a 1 Hz cycling rate with a 0.1 second loading duration and a 0.9 second unloading time. The soil descriptions, load durations, CSL, and LFC results from the studies discussed above are summarized in Table 2-7.

Table 2-7: Summary of Critical Cyclic Parameters

Reference	CSL	LFC	Loading Duration (s)	Soil Description
Putri et al. (2012)	0.3-0.38	N/A	N/A	Clay with sand
Awad (1975)	0.37-0.5	N/A	45	Silty clay
Moses and Rao (2003)	0.25-0.7	N/A	6, 12, 20	Marine clay
Puppala et al. (2004)	0.2, 0.4, 0.6	N/A	1	Sandy clay soils
Shahin et al. (2011)	0.36, 0.71	N/A	1	Soft clay
Okur et al. (2008)	0.35	N/A	10 to 10,000	Fine grain soils
Dash and Sitharam (2009)	0.03, 0.08, 0.14	21%	1	Silty sand

## 2.10. Geology of Florida

High pile rebound may be related to geology. In Florida, the top of a geologic formation named the Hawthorn Group often matches the initial elevation associated with rebound. The Hawthorn Group is an aquiclude (permeability  $k \approx 0$ ) preventing Florida's surficial aquifers from extending to the deep Florida aquifer (Hoenstine, 1984). In regions where the Hawthorn Group is absent, the surficial aquifers extend to the Florida aquifer system.

### 2.10.1. Hawthorn Group

The Hawthorn Group is one of many geological formations in the Florida peninsula. The Hawthorn Group was formed in the middle of the Miocene (in Greek "less recent") epoch. The sediments were placed after the erosion of the karstic limestone surface of Florida. The Hawthorn sediments deposition ended in the Early Pliocene era (Scott & MacGill, 1981). The group occurs eastward of the Apalachicola River, northward to Berkeley County in South Carolina, and southward through the Peninsula of Florida. In some parts of Florida, this formation has been entirely eroded.

The Hawthorn Group is a combination of alluvial, terrestrial, marine, and deltaic beds. Generally, the group contains a combination of sand, silt, clay, phosphate, limestone, and dolomite. Phosphate is present in the formation, as much as 60 percent in some cases, but the mineral is absent in other locations (Scott, 1990). A silty, sandy, phosphatic dolomite is the most common constituent in this group. The sizes of this mineral vary; the most common size is 0.002 to 0.005 inch (0.0625 mm to 0.125 mm). It has a yellowish-gray to white color (Scott & MacGill, 1981). The limestone in the formation contains varying amounts of sand, clay, and phosphate.

The limestone is mainly white or yellowish-gray to very pale orange. Limestone is not found everywhere in the formation; it is scattered throughout the region, changing its thickness from two to thirty feet.

Clay soils represent less than five percent of the Hawthorn Group. In the group, clay beds have different colors from yellowish-gray to light green to moderately dark gray. The clay beds contain quartz silt and sand, dolomite, and phosphate in different percentages (Scott & MacGill, 1981). The abundant clays in the group are montmorillonite and palygorskite (Houstine, 1984).

The Hawthorn Group sand beds can vary in color from light gray to very pale orange to dusky yellow-green. They also contain quartz particles with angular to subangular shapes. The sand beds have some phosphate and silt present; usually these beds have a thickness of two to three feet.

The successive marine inundations that the Florida peninsula experienced around a million years ago led to the presence of fossils in the Hawthorn Group. When the formation was created, marine life was present in the soil. Bioturbation (the stirring or mixing of sediments by organisms) may have caused the Hawthorn Group's distinct types of beds (Scott & MacGill, 1981).

### **2.10.2. Geologic Traits of the Top of the Hawthorn Group**

Soil minerals, such as calcareous or dolomitic phosphatic sand, are typically used to identify the top of the Hawthorn Group. These sediments are normally an olive-green color (Hoenstine, 1984) and are often composed of a clayey phosphatic residuum.

Table 2-8 contains a summary of the Hawthorn Group's characteristics including the different beds found in this geologic formation. Figure 2-27 shows the elevation of the top of the Hawthorn Group throughout Florida with the approximate locations of the FDOT high rebound sites.

The elevation of the top of the Hawthorn Group varies in the state of Florida. In the northwest, it is at a higher elevation of approximately 100 to 200 ft (30.5 to 61 m) above sea level. In the northeast, it is at an elevation of 0 ft to minus 100 ft (30.5 m) below sea level. In Central Florida, the elevation is approximately 0 ft to 50 ft (15.3 m) above sea level. In the south, it is at an elevation of 100 ft to 150 ft (30.5 to 45.7 m) below sea level.

The Hawthorn Group is the thickest in the southernmost part of Florida, ranging from 700 to 900 ft (213 to 274 m). In Central Florida, the thickness decreases to 100 to 300 ft (30.5 to 91 m). Northeast Florida (100 to 500 ft) (30.5 to 152 m) has thicker sediments than the northwest (100 to 250 ft) (30.5 to 76.2 m) (Scott, 1990). In the Panhandle, due to marine erosion, many of the middle Miocene (Hawthorn Group) and Pliocene layers are largely missing (Scott & MacGill, 1981).

Table 2-8: Hawthorn Group Characteristics

<b>Top of Hawthorn Group in Florida</b>	<ul style="list-style-type: none"> <li>•normally olive green clayey phosphatic residuum</li> <li>•calcareous or dolomitic sand</li> <li>•impervious in some parts</li> <li>•elevation 200-100 ft above sea level (north), 100-200 ft below sea level (south).</li> </ul>
<b>Clay Beds with Quartz Silt, Sand, Dolomite &amp; Phosphate</b>	<ul style="list-style-type: none"> <li>•yellow-gray or light green to dark gray</li> <li>•less than 5 % of formation</li> <li>•montmorillonite or palygorskite</li> </ul>
<b>Phosphate Beds 10 to 25 % of Central Florida Formation</b>	<ul style="list-style-type: none"> <li>•black to tan &amp; white</li> <li>•over 10 billion tons</li> <li>•up to 60% in some places</li> </ul>
<b>Phosphatic Dolomite</b>	<ul style="list-style-type: none"> <li>•0.0625 to 0.125 mm grain sizes</li> <li>•yellow gray to white</li> </ul>
<b>Limestone</b>	<ul style="list-style-type: none"> <li>•white yellow-gray to pale orange</li> <li>•between 2 ft and 30 ft</li> <li>•scattered through region</li> </ul>
<b>Chert with Fossils</b>	<ul style="list-style-type: none"> <li>•2 inches to 2 ft thick</li> <li>•medium to dark gray</li> <li>•scattered throughout formation</li> </ul>

### 2.10.3. Engineering Properties of the Hawthorn Group near Okeechobee, Florida

Brown et al. (2005) reported engineering properties of the Hawthorn Group soils for deep wells in the Okeechobee region of South Florida. The properties are summarized in Table 2-9. In general, the soils at depths below 200 ft (61 m), are overconsolidated, have very low permeabilities, and Atterberg limits that average 46 for the liquid limit and 22 for the PI.

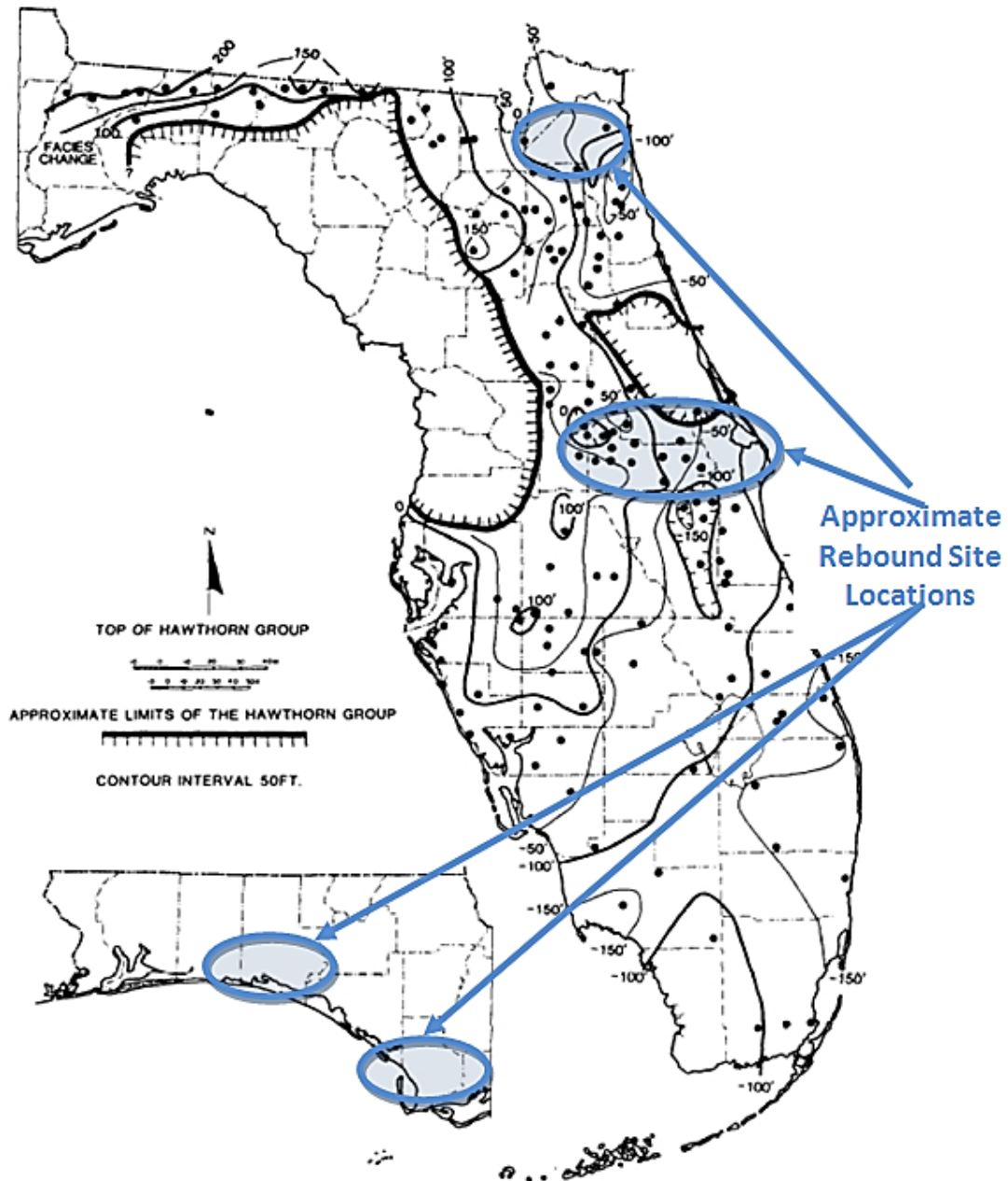


Figure 2-27 Top elevation contours of the Hawthorn Group with approximate high pile rebound site locations [after Scott (1990)]

Table 2-9 Hawthorn Layer Engineering Properties (after Brown et al., 2005)

Sample Depth (ft)	Natural Moisture (%)	Moist Unit Weight (PCF)	Liquid Limit (%)	Plastic Limit (%)	Specific Gravity	Effective Overburden Pressure (psf)	OCR	Compression Index	$e_o$	Kv (cm/sec)
220	23.7	111.49	40	22	2.647	10800	2.42	0.08	0.708	3.80E-09
220	18.8	115.73	77	55	2.625	11733	2.05	0.04	0.576	2.60E-09
292	20.9	112.94	26	4	2.692	14758	1.77	0.04	0.682	4.70E-07
292	21.6	114.98	29	8	2.653	15353	1.69	0.04	0.632	1.50E-07
380	16.0	116.98	52	22	2.757	20740	1.24	0.04	0.608	2.00E-09
380	20.2	113.40	55	21	2.657	19380	1.23	0.05	0.645	2.70E-09
218	20.2	108.30	65	41	2.681	10006	2.04	0.13	0.749	
285	22.8	117.13	28	5	2.692	15598	1.08	0.03	0.633	
382	21.6	112.18	40	18	2.723	19016	0.87	0.05	0.722	
Average	20.6	113.68	46	22	2.681	15265	1.60	0.06	0.662	1.05E-07

## 2.11. Estimation of Soil Properties Using CPTu Data

### 2.11.1. Basic CPT Description

CPTu test data is used for in situ soil investigations due to its repeatability, economic efficiency, and the availability of continuous data with depth (Yi 2014). Several probe sizes with tip areas ranging from 2 to 40 cm<sup>2</sup> exist, as shown in Figure 2-28. The most common 10-cm<sup>2</sup> probe was used in this research. The pore pressure transducer on a CPTu can be placed at three positions, as shown in Figure 2-29. The  $u_2$  position, which is also the most common, was used in this work.



Figure 2-28: Types of CPT probes (from left: 2 cm<sup>2</sup>, 10 cm<sup>2</sup>, 15 cm<sup>2</sup>, 40 cm<sup>2</sup>) (Robertson & Cabal, 2010)

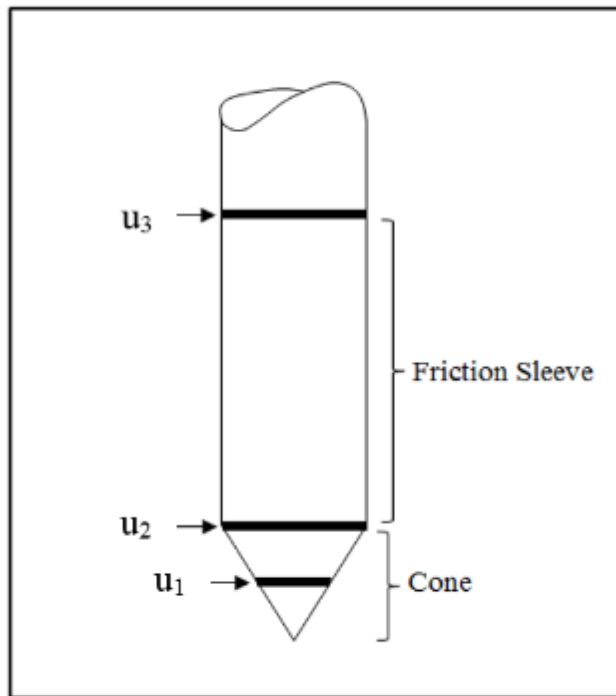


Figure 2-29: CPTu Pore pressure transducer positions: at the cone point ( $u_1$ ), behind the cone tip ( $u_2$ ), and on the shaft between the cone and sleeve ( $u_3$ )

The electric cone is typically advanced in one-meter increments at a constant rate of 2 cm/sec using the hydraulic press of a specialized cone truck. A schematic of a complete CPTu test system is shown in Figure 2-30. During penetration, voltage signals from the point and

sleeve load cells are transmitted to the surface through a cable housed within the cone rod. Specialized data acquisition hardware and software are used to record readings from the transducers at a frequency of approximately five readings per second. These electrical signal readings are then converted to engineering units of stress using device-specific calibration factors.

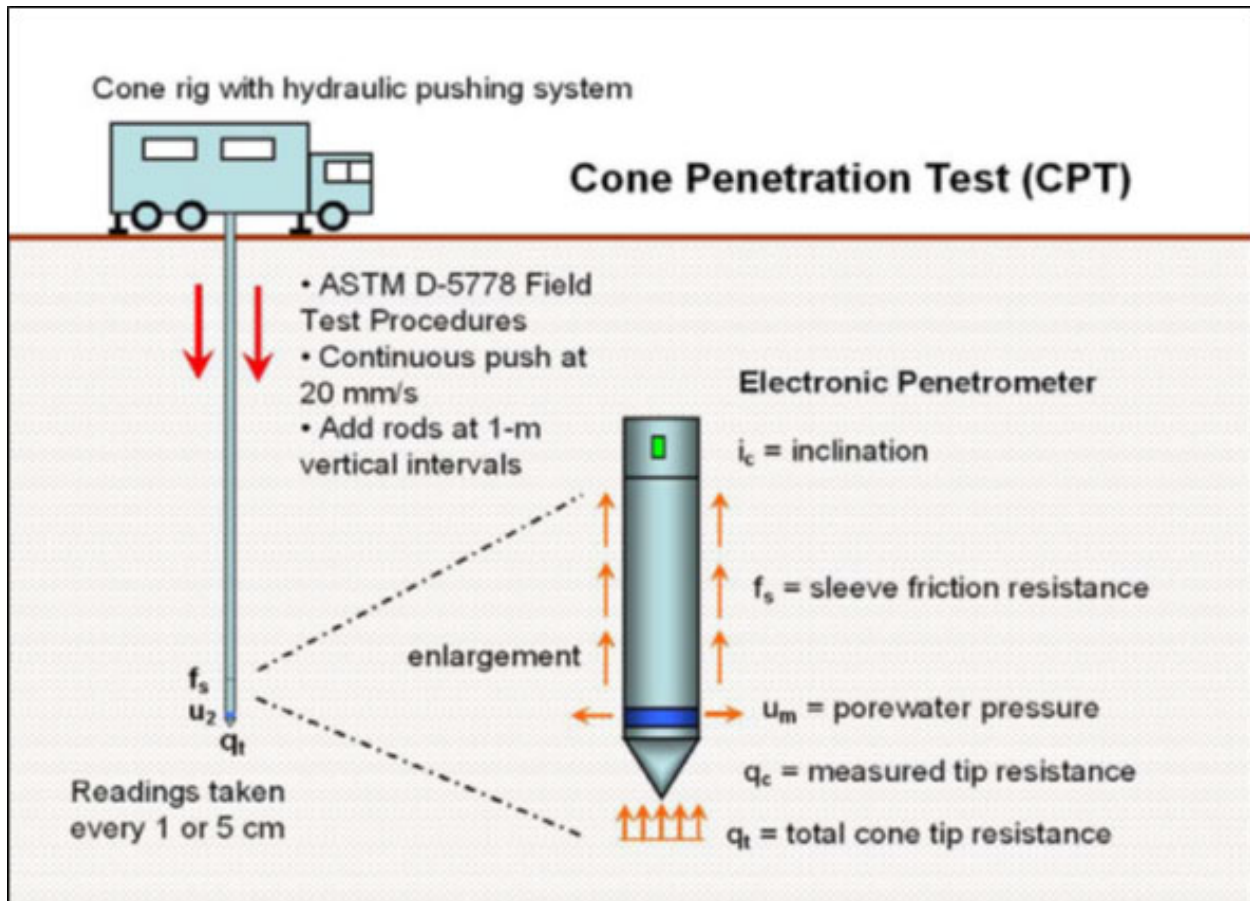


Figure 2-30: Overview of the cone penetration test per ASTM D5778-95

### 2.11.2. CPT Correlations and Soil Behavior Charts

Three key parameters are measured continuously with depth during the CPTu test: cone resistance ( $q_c$ ), side friction ( $f_s$ ), and excess pore water pressure ( $u$ ). Pore water pressures are developed during the steady, 2 cm/s penetration of the cone into the soil. These data can be used to determine soil types, stratigraphy and engineering properties (Schneider et al., 2008).

The recorded  $q_c$  values must be corrected for pore water pressures acting on unequal tip areas of the cone, especially in stiff clays and silts where significant pore pressures are typically

generated. In dense granular soils and clean sands, this correction does not tend to be critical (Lunne et al., 1997). The corrected cone resistance or total cone tip resistance is designated as  $q_t$ , and is determined using:

$$q_t = q_c + (1 - a_n) u_2 \quad \text{Equation 2-16}$$

where

$q_t$  = cone resistance corrected for pore water pressure at cone shoulder,

$q_c$  = measured cone tip resistance,  $q_c = q_t$  in sandy soil,

$u_2$  = pore pressure measured at cone shoulder,

$a_n$  = net area ratio for the cone, typical range between 0.70 and 0.85

### 2.11.2.1. Robertson 1990 SBT Chart

Although Robertson and Campanella (1983) presented a CPT soil-based classification chart, Robertson et al. (1986) modified this work and presented a soil classification chart based on the basic CPTu parameters. Since both  $q_c$  and  $f_s$  are affected by an increase in the effective overburden stress, the CPTu data was normalized to account for the influence of overburden stress (Robertson 1990). Wroth (1984) and Houlsby (1988) suggested that CPTu data could be normalized using the following equations:

$$Q_{tn} = \frac{q_t - \sigma_{vo}}{\sigma'_{vo}} \quad \text{Equation 2-17}$$

$$F_r = \frac{f_s}{q_t - \sigma_{vo}} \times 100\% \quad \text{Equation 2-18}$$

where

$Q_{tn}$  = normalized cone tip resistance

$F_r$  = normalized friction ratio

$\sigma_{vo}$  = total overburden stress

$\sigma'_{vo}$  = effective overburden stress

and other terms as previously defined

Using these CPTu parameters, a normalized soil behavior type index ( $I_c$ ) was proposed by Robertson (1990) and incorporated into the SBT chart.  $I_c$  is determined according to:

$$I_c = [(3.47 - \log Q_t)^2 + (\log F_r + 1.22)^2]^{0.5} \quad \text{Equation 2-19}$$

The normalized soil behavior type (SBTn) chart shown in Figure 2-31 was developed using the normalized soil behavior type index ( $I_c$ ). It has nine soil types with varying regions of consolidated, cementation, age, sensitivity, and  $I_c$ . Table 2-1 shows the corresponding soil descriptions and the range of  $I_c$  for each of the nine SBTn zones. Figure 2-31 findings typically have between good to excellent reliability (Robertson & Cabal, 2010).

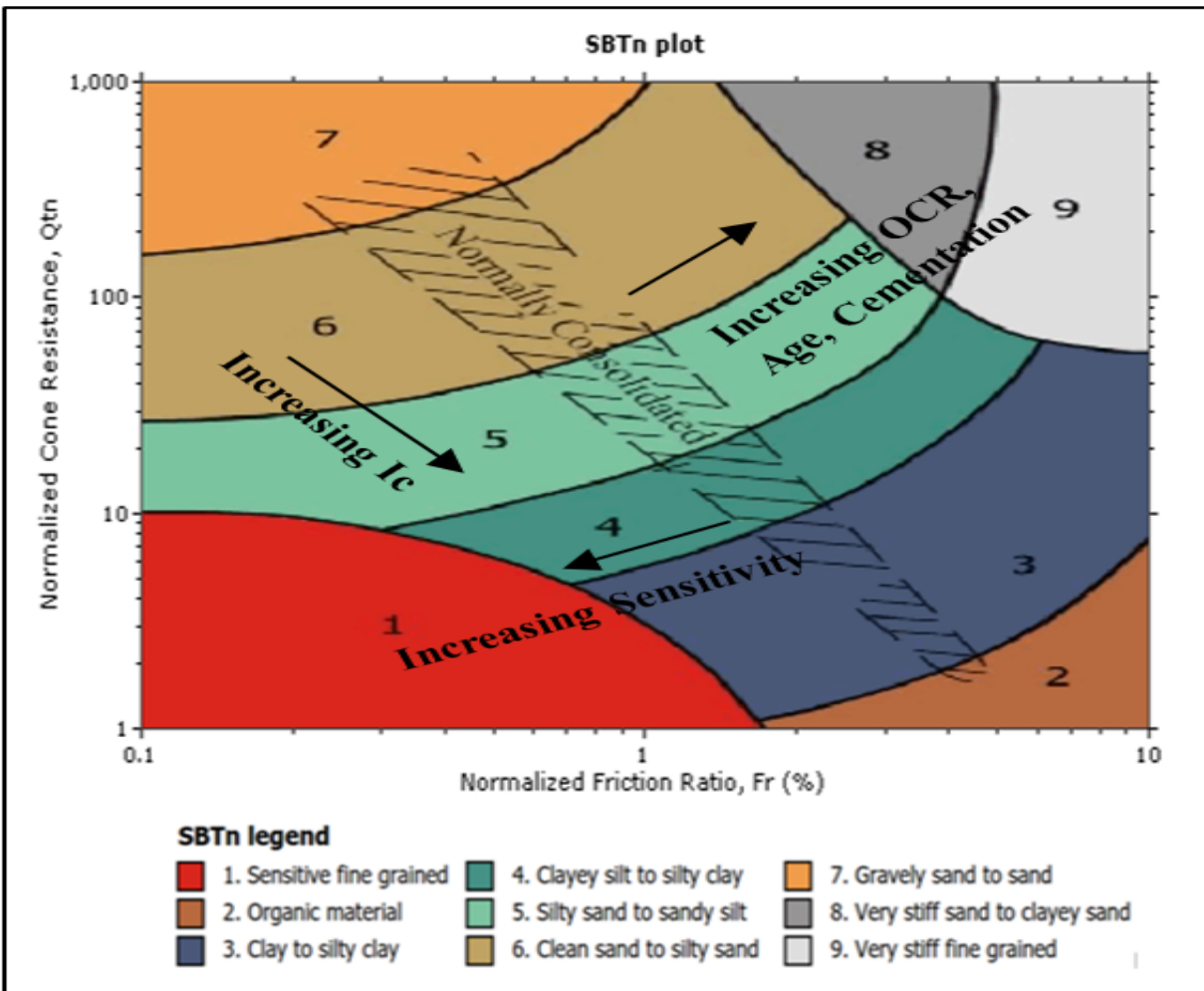


Figure 2-31: Normalized soil behavior type chart (SBTn) based on CPT normalized cone resistance ( $Q_{tn}$ ) and normalized friction ratio ( $F_r$ ) (Robertson, 1990)

Table 2-10: SBTn Zones Corresponding to the SBTn Index ( $I_c$ ) after Robertson (1990)

Zone	$I_c$	Soil Behavior Type
1	N/A	Sensitive fine-grained
2	> 3.6	Clay-organic soil
3	2.95 – 3.6	Clays: clay to silty clay
4	2.60 – 2.95	Silt mixtures: clayey silt and silty clay
5	2.05 – 2.60	Sand mixtures: silty sand to sandy silt
6	1.31 – 2.05	Sands: clean sand to silty sand
7	< 1.31	Dense sand to gravelly sand
8	N/A	Stiff sand to clayey sand*
9	N/A	Stiff fine-grained*

\* Overconsolidated or cemented

### 2.11.2.2. Robertson and Cabal (2010) SBT Chart

Using the basic SBT format from Robertson and Campanella (1983), Robertson and Cabal (2010) added lines representing soil unit weight. This 1983 chart has 12 zones instead of the nine shown in the previous figure. The resulting graph is shown in Figure 2-32. The chart is dimensionless because the cone resistance was divided by atmospheric pressure ( $p_a$ ) and the unit weight was divided by the unit weight of water ( $\gamma/\gamma_w$ ). The straight lines in the figure show that the dimensionless soil unit weight increases with increasing cone resistance. The lines were developed using:

$$\gamma/\gamma_w = 0.27 [\log R_f] + 0.36 [\log(q_t/p_a)] + 1.236 \quad \text{Equation 2-20}$$

where

$$R_f = \text{measured cone friction ratio, } R_f = (f_s/q_c) \times 100$$

$p_a$ : the atmospheric pressure in the same units of  $q_t$ .  
 and other terms as previously defined

Data were collected from sites where CPTu results and measured soil unit weight were available to verify the proposed equation. The results showed a good agreement between the measured unit weight and the estimated unit weight.

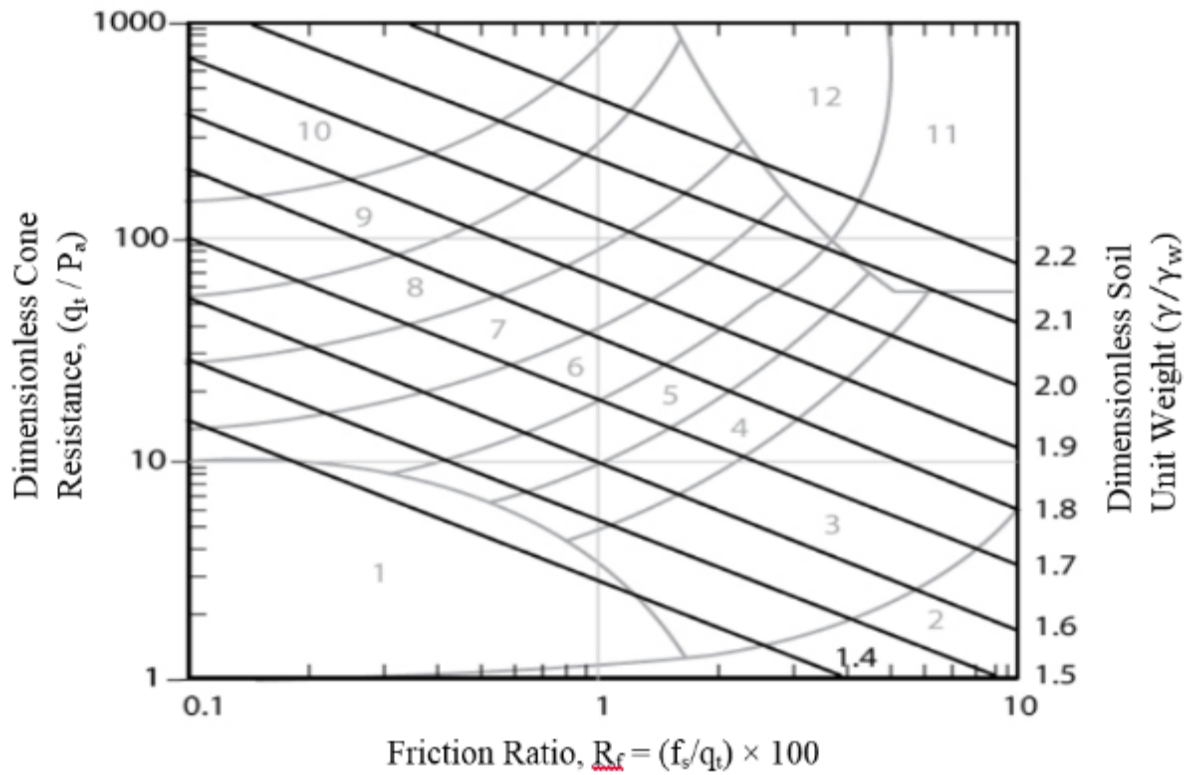


Figure 2-32: Relationship between CPT results and dimensionless soil unit weight (Robertson & Cabal, 2010)

### 2.11.2.3. Robertson 2009 SBT Chart

Robertson (2009) developed the normalized pore pressure SBTn chart, shown in Figure 2-33. Normalization of pore pressures first requires separation of pore pressures that are a function of soil response and those existing in the ground prior to the penetration. Measured penetration pore pressure ( $u_2$ ) represents the sum of the in situ or hydrostatic pore pressure ( $u_0$ ) and the excess pore pressure ( $\Delta u_2$ ) (Schneider et al., 2008). A pore pressure normalization ratio (Bq) suggested by Wroth (1984) is presented in:

$$B_q = \frac{\Delta u}{q_t - \sigma_{v0}} = \frac{u_2 - u_0}{q_t - \sigma_{v0}} \quad \text{Equation 2-21}$$

where

$u_0$  = in situ pore pressure  
and other terms as previously defined

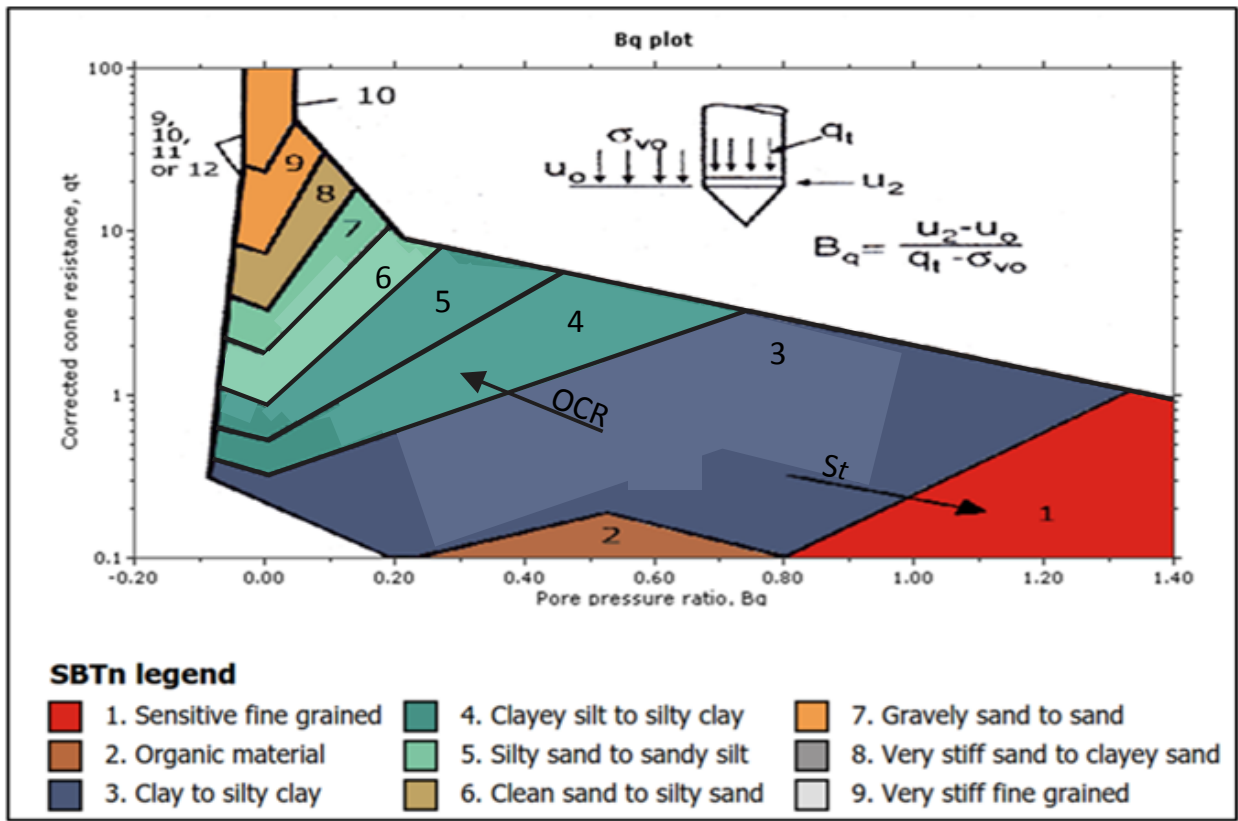


Figure 2-33: Robertson (1990) Cone resistance versus pore pressure ratio SBT chart

#### 2.11.2.4. Schneider et al.'s (2008) SBT Chart

Schneider et al. (2008) developed the normalized SBT chart shown in Figure 2-34. The cone tip resistance was normalized by dividing by the vertical effective stress,  $\sigma'_{v0}$ , using (Wroth 1984), while the pore pressure ( $u_2$ ) was normalized using:

$$\text{Normalized pore water pressure} = \frac{\Delta u_2}{\sigma'_{v0}} = \frac{u_2 - u_0}{\sigma'_{v0}} \quad \text{Equation 2-22}$$

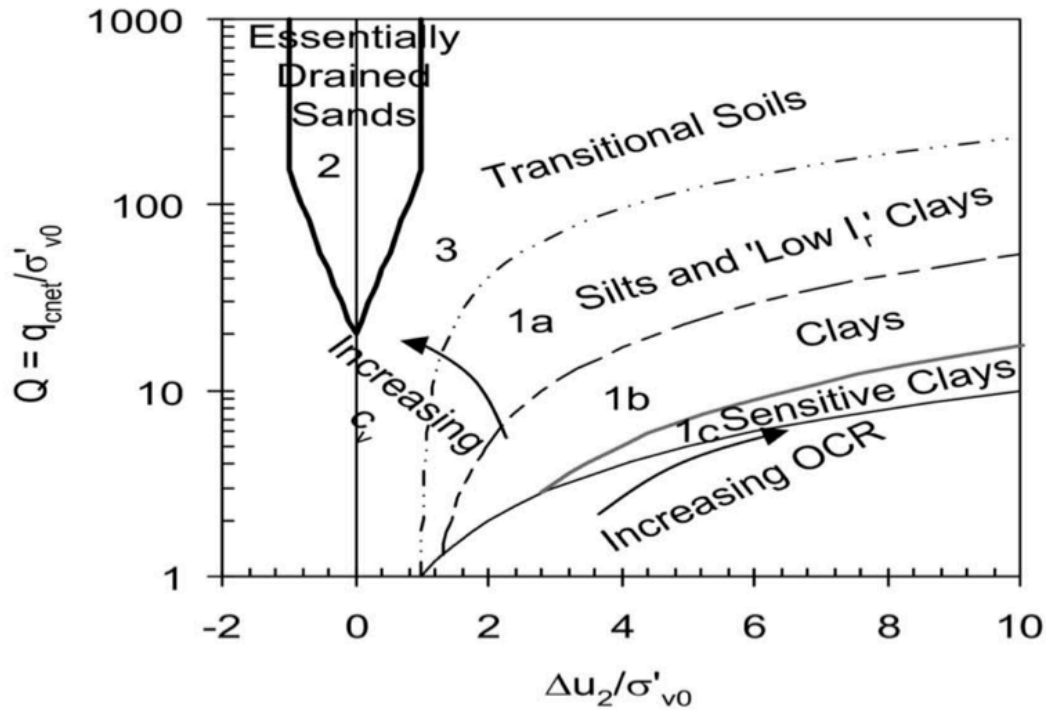


Figure 2-34: Normalized SBT chart developed by Schneider et al. (2008)

#### 2.11.2.5. Eslami and Fellenius' (1997) SBT Chart

Eslami and Fellenius (1997) developed a soil profiling method to classify the soil using CPT data. This method depends on the CPT parameters measured directly during the test (i.e.,  $q_t$  or  $q_c$ ,  $f_s$ , and  $u_2$ ). Therefore, it can be developed directly during the CPT sounding because the normalization by division with effective overburden stress is not required.

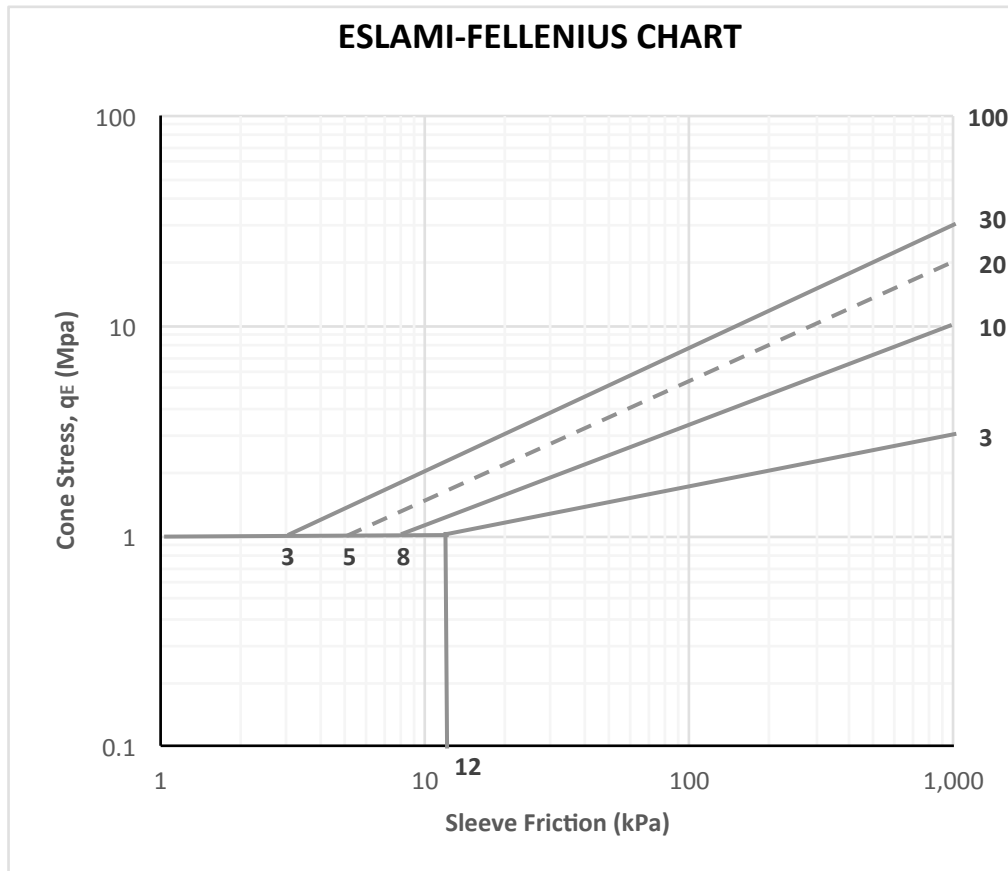


Figure 2-35: Eslami and Fellenius' (1997) SBT Chart

#### 2.11.2.6. Robertson's (2012) SBT Chart

Robertson (2012) developed an SBT chart, which accounts for soil dilation and contraction during cone penetration. This chart allows engineers to classify the soil as either dilative or contractive and is an updated version of the  $Q_{tn} - F_r$  earlier chart by Robertson (1990). Two regions were identified using the state parameter ( $\psi$ ) and OCR. The state parameter ( $\psi$ ) is defined as the difference between the initial void ratio,  $e$ , and the void ratio at critical state,  $e_{cs}$ . The critical state of a soil is the state at which the shear stress remains constant while the shear strain increases (Holtz & Kovacs, 1981). Figure 2-36 shows that loose sands contract while dense sands dilate above and below the critical void ratio respectively. The state parameter is negative for dense sands and positive for loose sands.

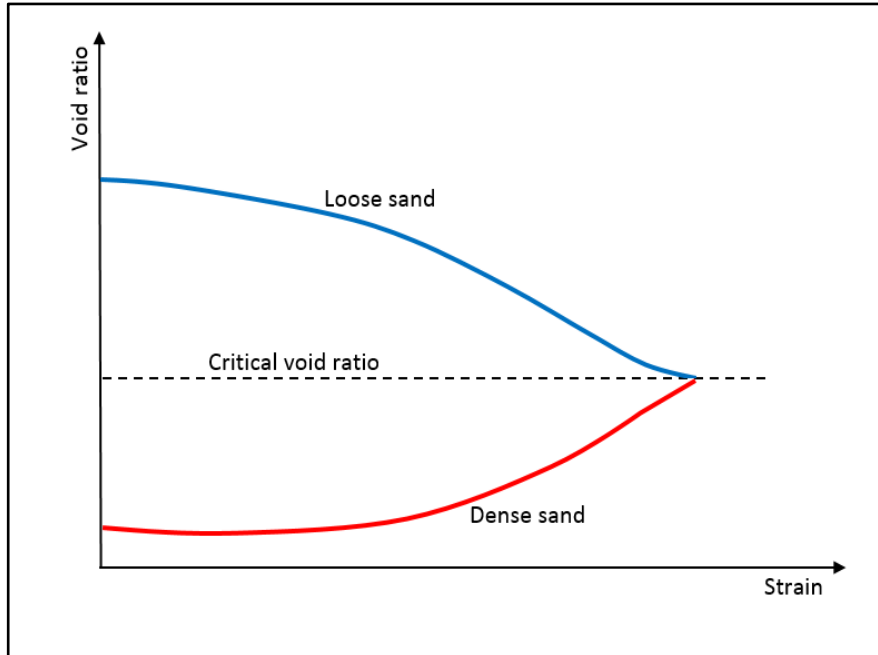


Figure 2-36: Schematic of void ratio versus strain used to determine the state parameter

Coarse-grained soils with a state parameter less than  $-0.05$  and fine-grained soils with an OCR greater than 4 are dilative at large strains (i.e., typical of pile driving and CPT testing). Robertson (2012) divided each region into three sub-regions based on drainage: undrained, transitional, and drained. The undrained region included fine-grained soils while the drained region included coarse-grained soils. The transitional region represents mixed soils (i.e., coarse and fine). Therefore, four major groups of soil behavior were identified on this chart: fine dilative (FD), coarse dilative (CD), fine contractive (FC), and coarse contractive (CC).

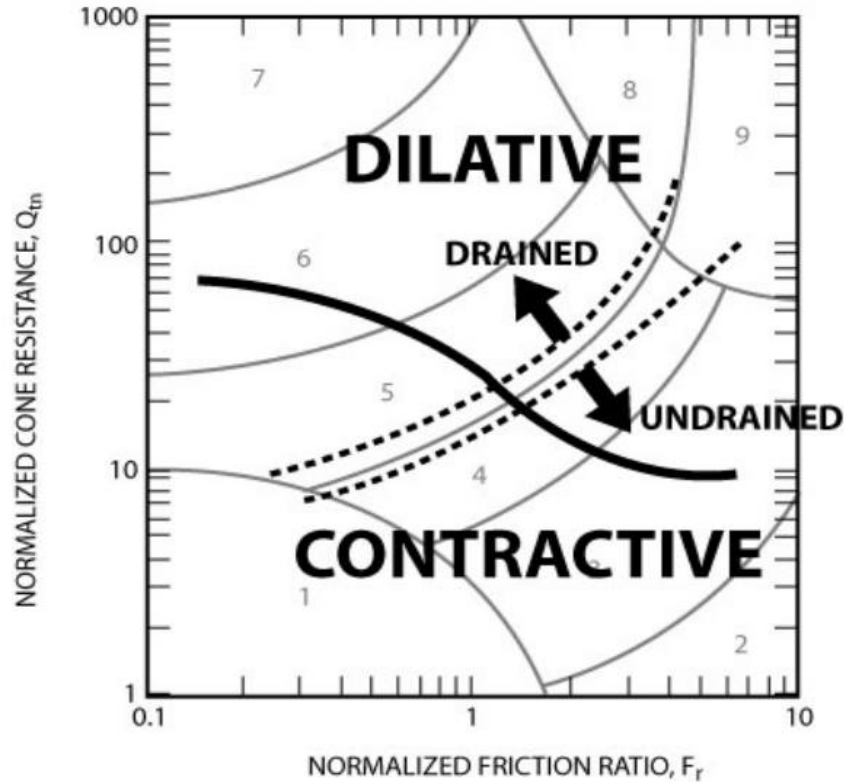


Figure 2-37: Updated normalized cone resistance versus friction ratio SBT chart with soil behavior (Robertson, 2012)

### 2.11.3. Fines Content CPT Correlations

#### 2.11.3.1. Yi's 2014 CPT Fines Content Correlation

Yi (2014) conducted a study in order to verify correlations used to estimate fines content (FC) from CPT data. Three SPT borings and three CPT soundings were conducted at a chosen site. Each CPT was very close to an SPT to produce representative data. Disturbed soil samples were collected every 2.5 ft during SPT borings and FC (%) were measured by washing them on #200 sieve following ASTM specifications. Cone tip resistance ( $q_c$ ) and sleeve friction ( $f_s$ ) from each CPT sounding were used to estimate FC using existing correlations developed by Robertson and Wride (1998), Idriss and Boulanger (2007) and Cetin and Ozan (2009). The measured and estimated FC's from the three locations were presented graphically versus depth. The results show that the measured FC (%) values were generally higher than estimated values. Yi (2014) presented the following FC correlation based on the Robertson and Wride (1998) SBT index  $I_c$ :

$$I_c = [(3.47 - \log_{10} Q_t)^2 + (\log_{10} F_r + 1.22)^2]^{0.5} \quad \text{Equation 2-23}$$

where

$$Q_t = [(q_t - \sigma_{vo})/\sigma'_{vo}] \quad \text{Equation 2-24}$$

$$F_r = [f_s/(q_t - \sigma_{vo})] \quad \text{Equation 2-25}$$

$Q_t$  = normalized tip resistance

$F_r$  = normalized friction ratio

$q_t$  = corrected tip resistance

$f_s$  = cone sleeve friction

$\sigma_{vo}$  = total overburden stress

$\sigma'_{vo}$  = effective overburden stress

In order to produce a more representative correlation, 133 samples of measured FC from a total of eleven sites, including the site mentioned above, were collected and utilized. Yi's (2014) new proposed correlation is presented in Figure 2-38.

Yi (2014) concluded that both Robertson and Wrides' (1998) and Idriss and Boulanger's (2008) methods underestimate FC, especially for measured FC higher than approximately 25%, while Cetin and Ozan's (2009) method may overestimate FC (%) for values greater than approximately 15%. He proposed the following equations for FC (%) based on  $I_c$ :

$$I_c < 1.31, \quad FC (\%) = 0 \quad \text{Equation 2-26}$$

$$1.31 \leq I_c < 2.5, \quad FC (\%) = 42.0 I_c - 55.0 + 10 \sin \left( \left( \frac{I_c - 2.5}{1.19} \right) \pi \right) \quad \text{Equation 2-27}$$

$$2.5 \leq I_c < 3.1, \quad FC(\%) = 83.3 I_c - 158.3 \quad \text{Equation 2-28}$$

$$I_c \geq 3.2, \quad FC (\%) = 100 \quad \text{Equation 2-29}$$

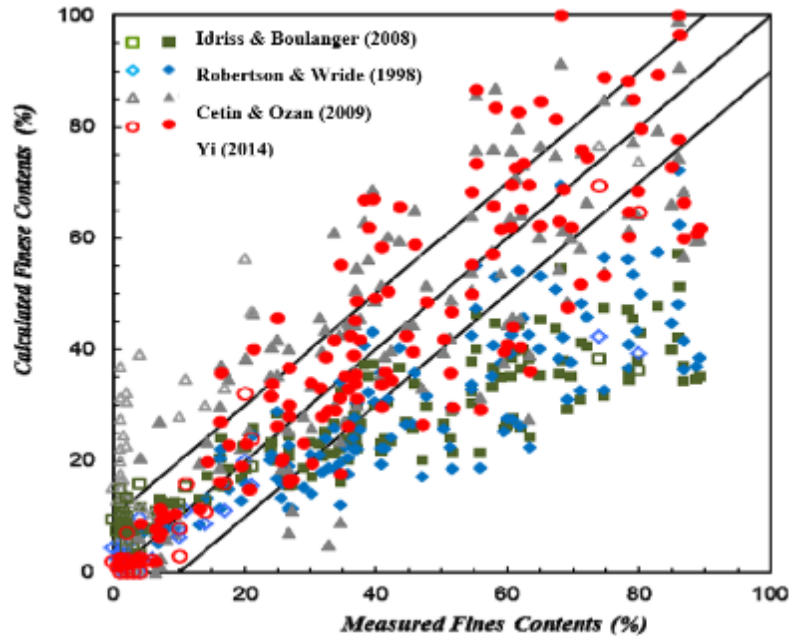


Figure 2-38: Measured versus estimated FC (%) for 95% confidence level (Yi, 2014)

### 2.11.3.2. Moayed's 2006 CPT Fines Content Correlation

Moayed (2006) developed an approach to evaluate the FC of soil layers based on CPTu results. FC was correlated with time for 50% dissipation of pore water pressure ( $t_{50}$ ). For this purpose, eleven CPT soundings were performed in silty sand samples with several different silt contents from 0% to 50% using 5% increments in the calibration chamber. The testing chamber consisted of a rigid thick-wall steel cylinder of 0.76 m internal diameter and 1.5 m height with removable top and bottom plates. Clean fine sand with a specific gravity of 2.6 was used. This sand was rounded to sub-angular fine-grained quartz sand with  $D_{50} = 0.4$  mm and  $C_u = 3.0$ . Before filling the testing chamber with a dry sample, a soil filter grading from coarse sand to fine gravel was formed at the bottom, and another filter layer was formed at the top of the soil. In order to saturate the soil specimen, the top plate was fixed on the chamber and a vacuum was applied inside the chamber for 30 minutes. Then the bottom water supply was opened until a uniform slow upward flow was reached. The standard CPTu used in this investigation has a 10 cm<sup>2</sup> tip area and 150 cm<sup>2</sup> friction sleeve area with the filter element located immediately behind the cone tip to record pore water pressure. The CPTu was advanced through the soil by a hydraulic system at a constant rate of 20 mm/sec. Tip resistance, friction resistance, and pore water pressure were recorded continuously during sounding at each 1 cm of depth. The pore

pressure dissipation tests were also carried out at the midpoint of each sample. The  $t_{50}$  parameter was determined for each sample containing different silt content. The relationship between  $t_{50}$  and FC is presented in Figure 2-39. It was concluded that  $t_{50}$  increases as FC increases, especially for content greater than 30%. There was a good correlation between  $t_{50}$  and fines content as presented in:

$$t_{50} = 10.235 e^{0.079 (FC)} \quad \text{Equation 2-30}$$

where

$t_{50}$  = time required for 50% dissipation for pore water pressure

$e$  = void ratio

FC = fines content (%)

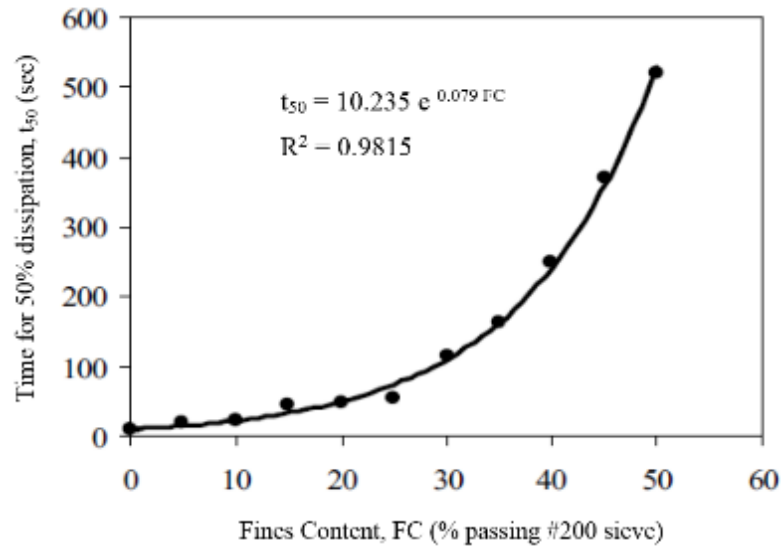


Figure 2-39: Experimental correlation between  $t_{50}$  and fines content (Moayed, 2006)

Jamiolkowski et al. (2003) correlated the penetration resistance of the cone penetration tests ( $q_c$ ) to the relative density of sand. The CPT soundings were performed on three types of silica sand in a calibration chamber with a diameter and height of 1.2 m and 1.5 m respectively. The testing samples were reconstituted and subjected to the one-dimensional compression in order to apply the desired consolidation stress level and stress-history. The penetration test was performed using the cylindrical Fugro-type electrical cone tips having diameters ( $d_o$ ) equal to 35.6, 25.4, 20, 11, and 10 mm to investigate the influence of the calibration chamber diameter ( $D_o$ ) to ( $d_o$ ) ratio ( $R_d$ ) on the cone tip resistance ( $q_c$ ). The measured penetration resistance

appeared to be independent of the  $R_d$  and as a result, the penetration resistance measured in the calibration chamber matches the field value. The experimental data was used to develop the following relationship to estimate the relative density based on CPT tip resistance and the effective stress:

$$D_r\% = 100 \cdot \left[ 0.268 \cdot \ln \left( \frac{q_t/\sigma_{atm}}{\sqrt{\sigma'_{vo}/\sigma_{atm}}} \right) - 0.675 \right] \quad \text{Equation 2-31}$$

where

$q_t$  = corrected tip resistance

$\sigma_{atm}$  = atmospheric pressure in the same units of  $q_t$

$\sigma'_{vo}$  = effective overburden stress

Robertson et al. (1983) discussed the interpretations of the piezometer cone data that had been used to estimate soil properties and its engineering applications. In situ piezometer cone testing had been carried out by the In situ Testing Group at the University of British Columbia at sites near Vancouver, B.C. Soil at these sites were deltaic sands, silts, and clays or glaciomarine clays and silty clays. Different types of piezometer cones had been used, and undrained shear strength and sensitivity measurements were obtained at these sites. Piezometer cone data from four of these sites were used to present soil classification, undrained shear strength ( $S_u$ ), sensitivity, and stress history (OCR). For soil classification, it was recommended that all cone data ( $q_c$ ,  $f_s$ , and  $u$ ) as well as pore pressure dissipation data be used to define soil behavior type more accurately. The cone data should be normalized to account for the effect of increasing overburden pressure in case of cone soundings deeper than 30 m. The dissipation data obtained during pauses in the cone penetration can be used to improve soil classification and to provide an index on the soil permeability and consolidation characteristics. No unique relationship between CPT data and  $S_u$  was found for all soil types. The undrained shear strength is strongly influenced by stress history, sensitivity, and stiffness; therefore, an iterative approach was recommended to estimate shear strength. Sensitivity was found to have a significant effect on the measured pore pressure. Increasing sensitivity caused pore water pressure to increase proportionally.

Chen and Mayne (1996) conducted a statistical analysis between CPTu measurements and “stress history of clays” to evaluate various CPTu parameters in interpreting the stress history of clay. Large field data of CPTu soundings from 205 clay sites around the world had been collected to develop statistical correlations. Most of the data was collected from the eastern and western United States, southern Canada, western Europe, and southeastern Asia, where CPTu penetration tests have been used more frequently than in other parts of the world. The collected CPTu data included tip resistance ( $q_t$ ) and the pore pressures measured at the tip apex ( $u_1$ ) and behind the tip ( $u_2$ ). In addition to the CPT field data, data of soil properties with an emphasis on the index properties including natural water content, liquid limit, plasticity index, and sensitivity was gathered. “Preconsolidation pressure” data from oedometer testing was included to make a comparison with the estimated preconsolidation pressure from CPT parameters. “Stress history” was measured in terms of preconsolidation pressure,  $\sigma'_p$ , and the overconsolidation ratio. The authors used simple linear, logarithm, and multiple regression methods and examined correlations between the stress history and several frequently used CPTu parameters. Direct correlations for  $\sigma'_p$  with stress difference ( $q_t - \sigma_{vo}$ ),  $\Delta u_1$ , and  $(q_t - u_1)$  were developed. The plasticity index was also incorporated to develop multiple regression analysis. This multiple regression improved statistical correlations by increasing the correlation coefficient.

Robertson (2010) presented an updated correlation to estimate the coefficient of permeability using CPT test results. The correlation evaluated the suggested soil permeability by Lunne et al (1997) with a range of  $k$  values for each Soil Behavior Type (SBT), as shown in Table 2-11. The suggested and modified  $k$  by Lunne et al (1997) and Robertson (2010) are shown in Figure 2-40 and simplified as

$$1.0 < I_c \leq 3.27, \quad k = 10^{(0.952 - 3.04 I_c)} \quad \text{m/sec} \quad \text{Equation 2-32}$$

$$3.27 < I_c \leq 4.0, \quad k = 10^{(-4.52 - 1.37 I_c)} \quad \text{m/sec} \quad \text{Equation 2-33}$$

where

$I_c$  = soil behavior type index

$k$  = coefficient of permeability

Table 2-11: Estimated Permeability Based on Normalized Soil Behavior Type, SBTn (Lunne et al, 1997)

SBTn Zone	Soil Type	Range of k (cm/sec)	SBTn Index ( $I_c$ )
1	Sensitive fine-grained	$3 \times 10^{-8}$ to $3 \times 10^{-6}$	NA
2	Organic soil-clay	$1 \times 10^{-8}$ to $1 \times 10^{-6}$	$I_c > 3.60$
3	Clay	$1 \times 10^{-8}$ to $1 \times 10^{-7}$	$2.95 < I_c < 3.60$
4	Silt mixture	$3 \times 10^{-7}$ to $1 \times 10^{-5}$	$2.60 < I_c < 2.95$
5	Sand mixture	$1 \times 10^{-5}$ to $1 \times 10^{-3}$	$2.05 < I_c < 2.60$
6	Sand	$1 \times 10^{-3}$ to $1 \times 10^{-1}$	$1.31 < I_c < 2.05$
7	Dense sand to gravelly sand	$1 \times 10^{-1}$ to $1 \times 10^2$	$I_c < 1.31$
8	Very dense / Stiff soil	$1 \times 10^{-6}$ to $1 \times 10^{-1}$	NA
9	Very stiff fine grained soil	$1 \times 10^{-7}$ to $1 \times 10^{-5}$	NA

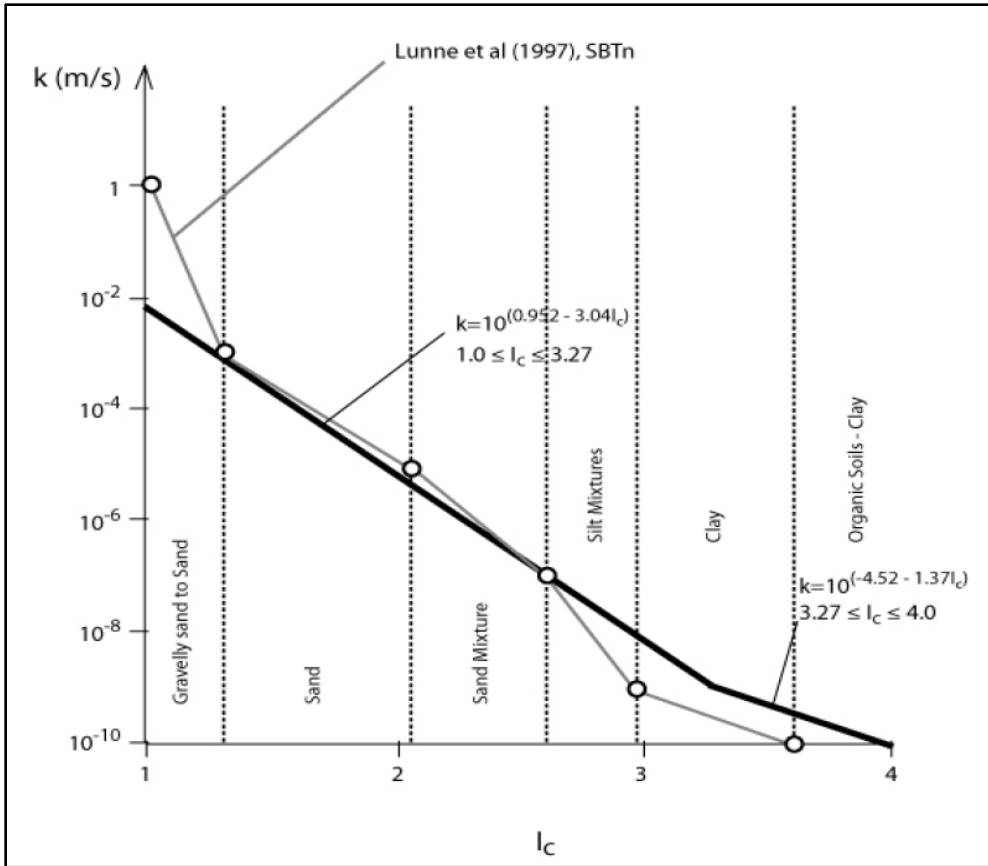


Figure 2-40: Suggested variation of soil permeability ( $k$ ) as a function of soil behavior type index  $I_c$  (Robertson, 2010)

A simplified method has been recently developed to estimate the state parameter ( $\psi$ ) from the normalized cone tip resistance. Based on field and laboratory data, Robertson (2009) developed contours of state parameter ( $\psi$ ) on the normalized soil behavior type (SBT) chart presented earlier in Figure 2-31. The SBT chart with the state parameter contours is shown in Figure 2-41. Robertson (2010) suggested the following approximate relationship between the state parameter and the clean sand equivalent normalized cone resistance ( $Q_{tn,cs}$ ):

$$\psi = 0.56 - 0.33 \log Q_{tn,cs} \quad \text{Equation 2-34}$$

where

$Q_{tn,cs}$  = clean sand equivalent normalized cone resistance, which is a function of soil behavior type index ( $I_c$ ).

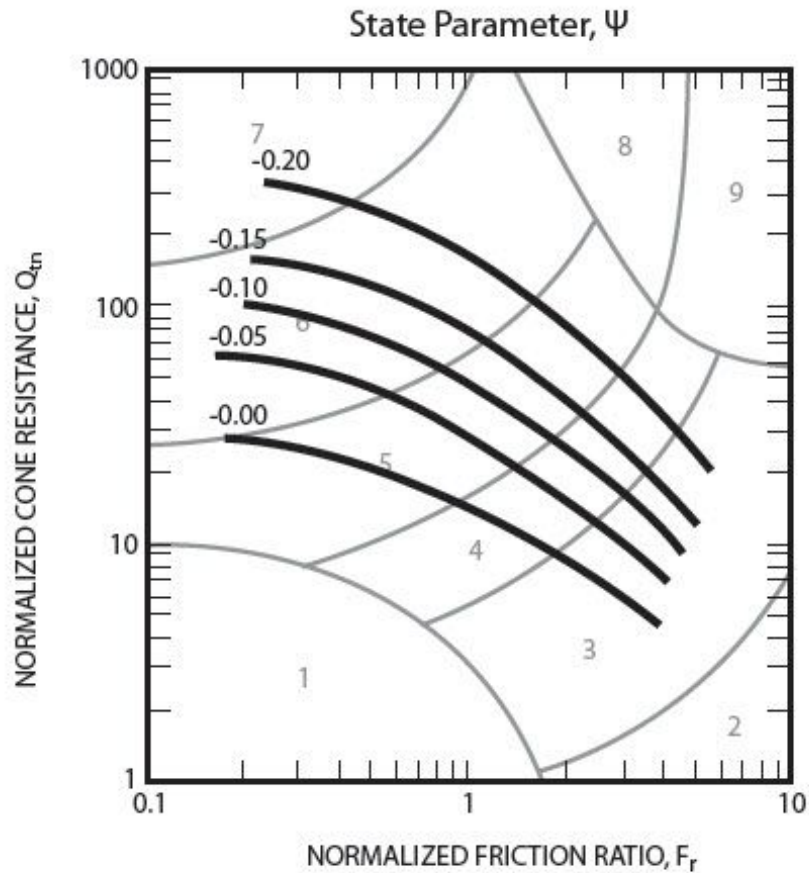


Figure 2-41: State parameter contours on the Robertson (1990) normalized SBT chart (Robertson, 2009)

## 2.12. Effect of Silt Content and Void Ratio on Soil Hydraulic Conductivity

Bandini and Sathiskumar (2009) studied the effect of silt content and void ratio on the saturated hydraulic conductivity and compressibility of sand-silt mixtures. Two poorly graded quartz sands with rounded grains and a specific gravity of 2.65 were used and called host sands as they constitute the sand matrix hosting the fines. Ottawa sand, which has coefficients of uniformity ( $C_u$ ) and curvature ( $C_c$ ) of 1.87 and 1.04, respectively, was used as the host sand in the first set of tests. The second host sand was prepared by mixing equal parts, by dry weight, of Ottawa sand and ASTM 20-30 sand (C-778-93(A) and was called 50-50 sand. This sand has  $C_u = 2.46$  and  $C_c = 1.09$ . Sand-silt mixtures were prepared by adding Sil-Co-Sil #106 with specific gravity of 2.65 to the host sands with different percents in order to determine the effect of silt content on the hydraulic conductivity and compressibility. Flexible wall permeameter tests were

performed on 60 specimens of the two types of host sands with 0, 5, 10, 15, 20, and 25% silt. The  $e_{\max}$  and  $e_{\min}$  values of the sand-silt mixtures were found for each type of sand. It was noticed that as the silt content increases,  $e_{\max}$  and  $e_{\min}$  of these mixtures decrease up to approximately 20 and 25% silt content, respectively. Hydraulic conductivity measurements were conducted at different effective confining stresses for all specimens. The experimental results show that the saturated hydraulic conductivity of sands with 25% silt can be, on average, two orders of magnitude smaller than those of clean sands with 0% silt content, as shown in Figure 2-42. For a given silt content,  $k$  varies mostly within one order of magnitude, depending on the void ratio of the soil.

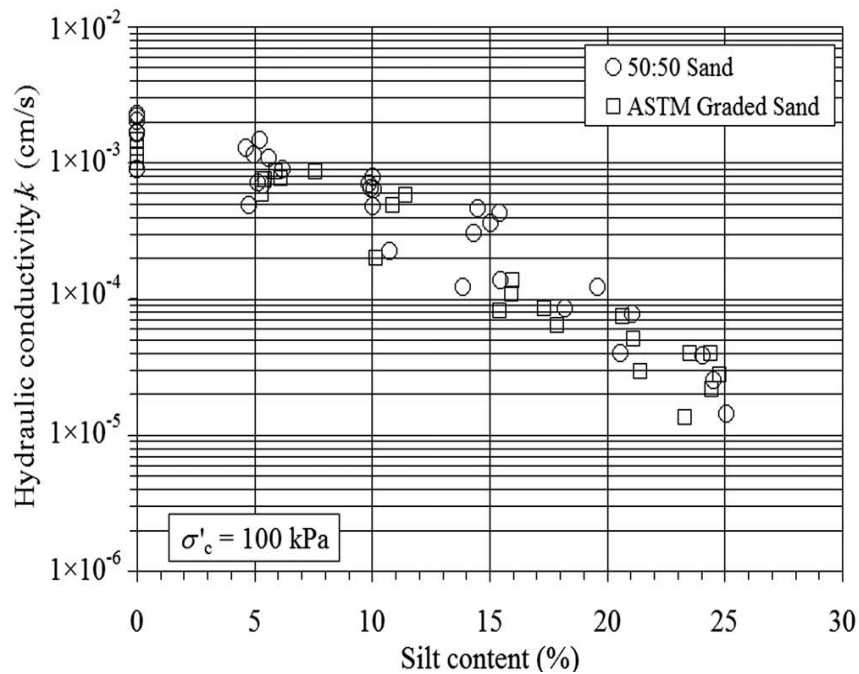


Figure 2-42: Hydraulic conductivity for various silt contents (Bandini & Sathiskumar, 2009)

## 2.13. Correlations from Soil and Site Characteristics to HPR in Florida

### 2.13.1. Selection of Florida High Rebound Sites for Study

During the investigation phase of the research, FDOT personnel and consultants identified 14 problematic rebound sites in Florida. Three sites were located in the Florida Panhandle, nine in the Orlando area of Central Florida, one in Jacksonville, and one near the Cape Canaveral area of Central Florida. Six representative sites were chosen for further analysis.

Three of these sites were selected for case study evaluations and three others selected for both case study evaluations and an extensive retesting program. Sites 2, 5, and 7 were chosen for the case study evaluations as representative. Sites 1, 3, and 11 were chosen for both the case study and retesting program. These sites were the most easily accessible of the known sites and had the most extensive existing information available.

Table 2-12: FDOT High Pile Rebound Sites

Sites No.	Description	County
1	Anderson St. Overpass at I-4/SR-408	Orange
2	I-4/SR-408 Ramp B	Orange
3	I-4/US-192	Osceola
4	I-4 Osceola Parkway	Osceola
5	I-4/SR-423 John Young Parkway	Orange
6	I-4/SR-482 Sand Lake Rd.	Orange
7	SR-50 and SR-436	Orange
8	SR -417 and International Drive	Osceola
9	SR-528 and US 441	Orange
10	SR-20 over Rocky Bayou WB	Okaloosa
11	SR-83 Ramsey Branch	Walton
12	SR-71 West Arm Lake	Gulf
13	SR-528 over Indian River	Brevard
14	I-10 at Chaffee Road	Jacksonville

Jarushi (2011) evaluated data from the six sites including gradation, pore water pressures, and field data from standard penetration and cone penetrometer test to predict potential HPR sites. The results of this study were published in two papers, which are summarized below.

### 2.13.2. Using Fines Content and SPT Blow Counts to Predict High Pile Rebound

Jarushi et al. (2011) developed correlations between HPR, fines content (percent passing #200 sieve) and SPT blow counts ( $N_{SPT}$ ) during the installation of PCPs at the six sites discussed in the previous section.

The piles were square displacement piles from 18 to 24 inches (457 to 610 mm) wide, approximately 95 feet (29 m) long, and driven with a single acting diesel hammer. Soils at the sites were mainly sands with varying percentages of silt and clay. Most soils in the HPR layers

had high fines content (over 15%) with natural moisture contents less than the liquid limit and all plotted near the A-Line on the Casagrande Plasticity Chart. These soils displayed an olive green to light green color.

The pile movements were obtained from test piles at each site, instrumented with the PDA, strain gauges, and accelerometers. The accelerations recorded during the pile movements from each hammer blow were integrated twice to produce displacement versus time data. This data includes DMX, which was subtracted from the pile set (inspector set or iSet) to produce the rebound per hammer blow. Digital set (dSet) and iSet were both evaluated. Digital set values were determined by subtracting DFN from DMX, where DFN is the final set from the PDA data (See Figure 2-8). Better correlations were obtained using iSet values.

Profiles with the following information were developed for each site: (a) soil types, (b) PDA-based pile DMX, rebound, and iSet rebound, (c)  $N_{SPT}$ , and (d) fines content. The fines content is the percent passing the number 200 sieve. The profiles included a dashed line at the FDOT minimum limit for HPR of 0.25 inches. Figure 2-43 shows a typical profile from the Anderson Street Overpass. The elevations corresponding to rebound over 0.25 inches near elevation 10 ft (3.0 m) consistently correlated with the elevations where the  $N_{SPT}$  and fines content increased.

Data from Hussein et al. (2006) was added to the data from the six sites. It was developed from the PDA results for the test pile chosen for the SR528 Bridge over the Indian River. Correlations using  $N_{SPT}$  and fines content from the seven sites were used to develop a design equation to predict pile rebound. Figure 2-44 contains plots displaying the correlations between rebound and permanent set versus the  $N_{SPT}$  values and fines content. Both  $N_{SPT}$  and fines content produced strong correlations to rebound ( $R^2 = 0.80$ ). Weak correlations ( $R^2 = 0.25$ ) were produced between  $N_{SPT}$ , fines content, and permanent set.

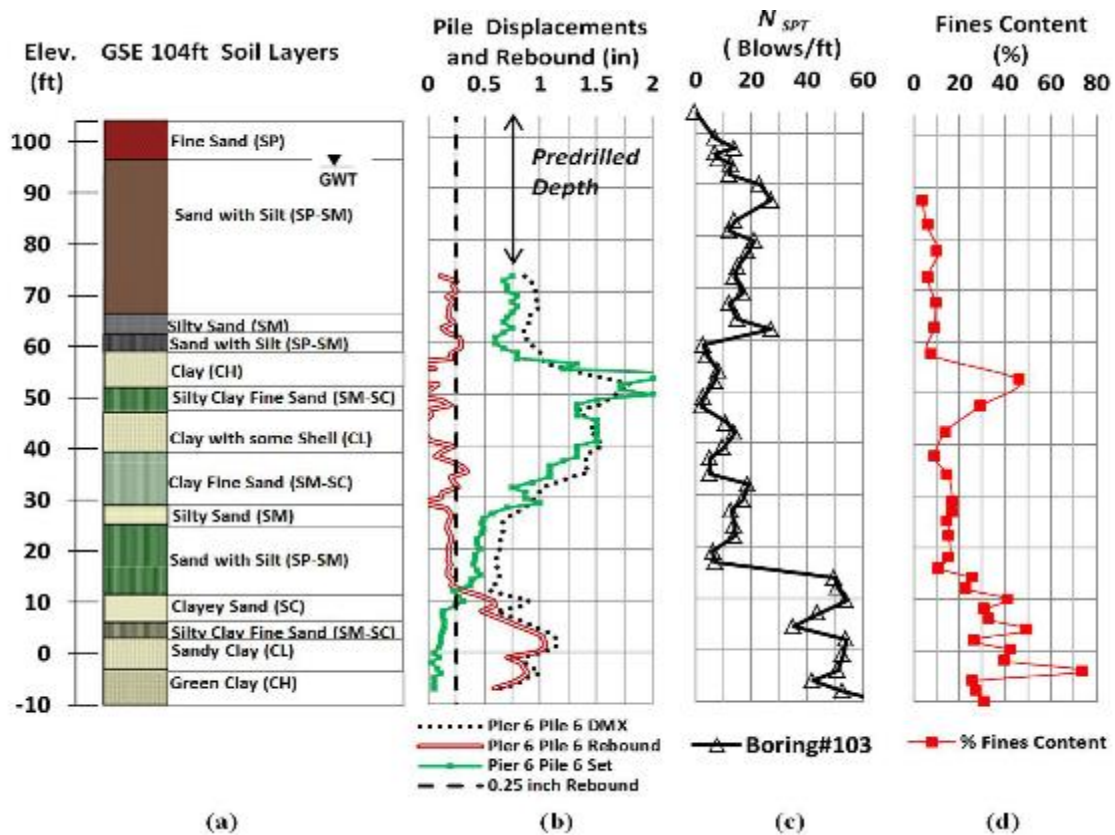


Figure 2-43: (a) Generalized soil profile, (b) PDA diagram, (c)  $N_{SPT}$ , and (d) percent fines content for site 1 Anderson Street Overpass (Jarushi et al., 2013).

Evaluation of these plots showed changes in pile movement at several blow count and fines content locations. Acceptable permanent set with minimal rebound occurred in soil conditions where  $N_{SPT}$  was below 15 blows/ft and fines content was below 25 percent. When  $N_{SPT}$  values were between 15 and 40 blows/ft, and fines content was between 25 and 40 percent, permanent set remained acceptable but pile rebound was measured at between 0.25 and 0.6 inches. When  $N_{SPT}$  exceeded 40 blows/ft with fines content greater than 40 percent, permanent set dropped to unacceptable or near zero and pile rebound exceeded 0.6 inches. The authors were not able to determine whether these relationships between  $N_{SPT}$ , fines content, and permanent set applied to soils outside of the study areas.

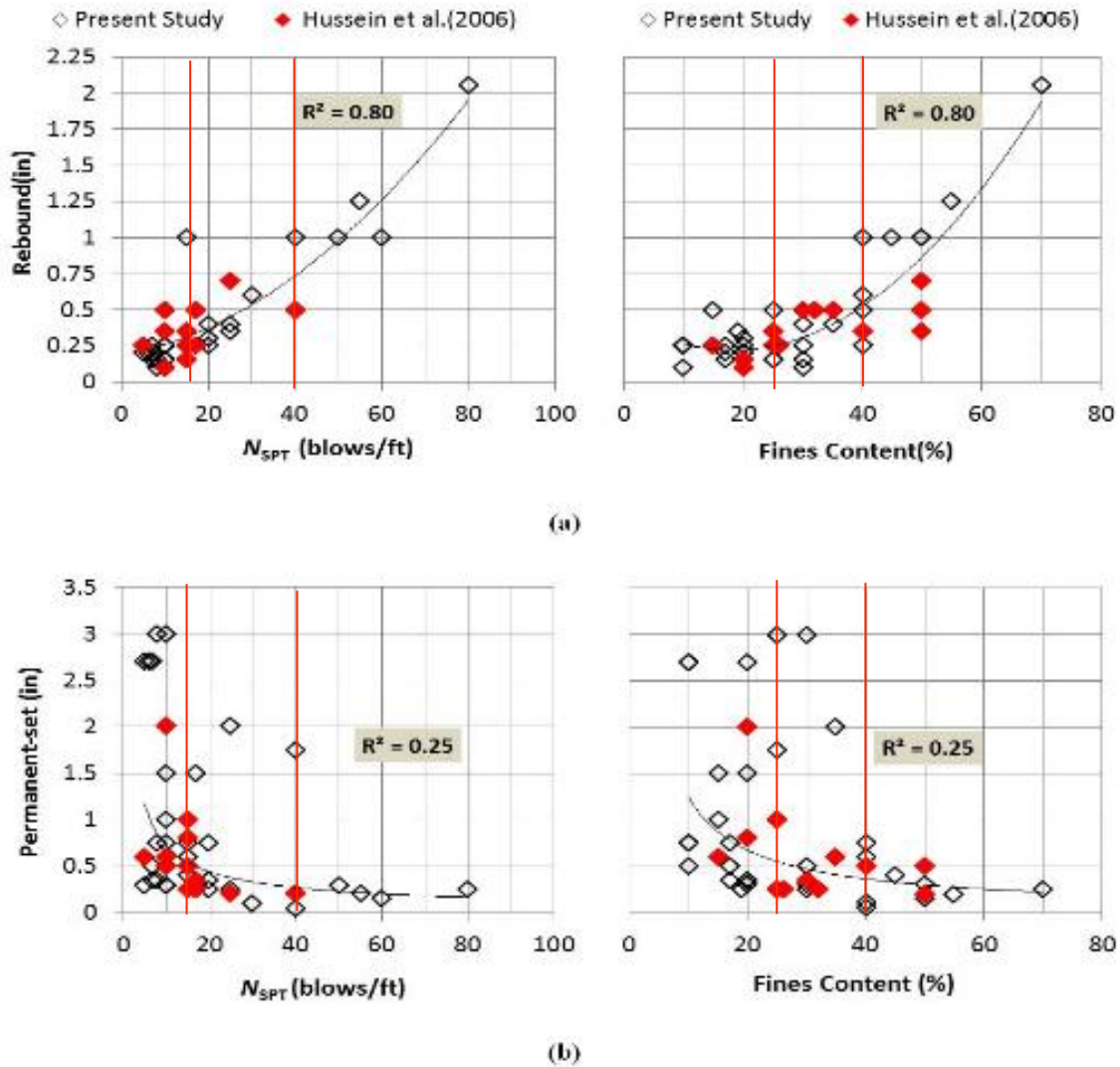


Figure 2-44 (a) Correlation between rebound, NSPT, and fines content, and (b) correlation between permanent-set,  $N_{SPT}$  and fines content (Jarushi et al., 2013).

A regression analysis of the data was performed to develop an empirical equation for predicting HPR (Jarushi et al., 2011). It is intended specifically to predict rebound of 18- or 24-inch square PCPs driven with single-acting diesel hammers, a common pile/hammer combination in Florida. Predicted rebound was evaluated against the observed rebound from the sites used in this case study plus additional FDOT HPR sites. The predicted and observed rebound values are shown in Figure 2-45. The data produced an  $R^2$  value of 0.80, indicating a strong correlation between predicted and observed rebound.

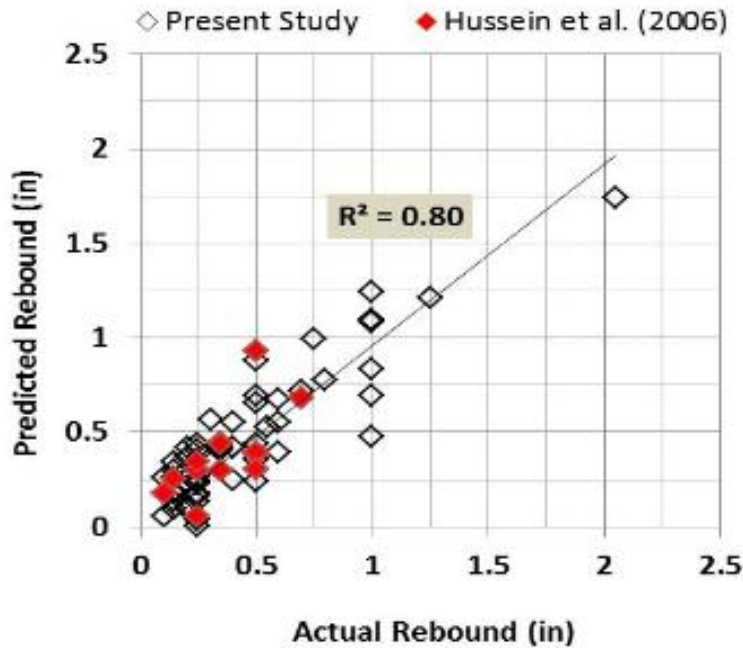
$$R = -0.166 + 0.016N_{SPT} + 0.009FC$$

Equation 2-35

where

R= rebound (inch)

$N_{SPT}$  = uncorrected SPT blow counts (blows/ft), for 5 blow/ft or higher



FC = fines content (percent) for 12 percent or higher

Figure 2-45: Predicted rebound using  $N_{SPT}$  and fines content versus actual PDA rebound (Jarushi et al., 2013)

The combined data from this study and from the site presented by Hussein et al. (2006) consistently showed that HPR might occur when all of the following conditions are present:

- high displacement piles
- single-acting diesel hammers
- pile tip below ground water table
- soils with high fines content (> 40%)
- soils with high  $N_{SPT}$  values.

### **2.13.3. Identifying High Pile Rebound Using CPTu Pore Water Pressure**

In a companion study to Jarushi (2013), Cosentino et al. (2010) investigated possible correlations between HPR and pore water pressure during the installation of PCPs at the same six Central Florida sites discussed in Section 2.13.2.

Pore water pressures obtained during CPT testing were used, with the pore pressure readings taken from behind the cone tip (i.e.,  $u_2$ ) during penetration of the cone. The pile movements were obtained from test piles at each site, instrumented with the PDA strain gauges and accelerometers. The accelerations, recorded during the pile movements from each hammer blow, were integrated twice to produce displacement versus time data. This data in turn produced DMX, which was subtracted from the inspector set (iSet) to produce the rebound per hammer blow.

Soil profile charts, which included pile displacements, rebound, and pore water pressure versus elevation, were developed and used to determine correlations between pile rebound, iSet, and excess pore water pressure. As is shown in Figure 2-46, these charts showed that the elevations corresponding to rebound greater than 0.25 inches (6.35 mm) matched the elevations (35 ft) (10.7m) where the CPTu values increased.

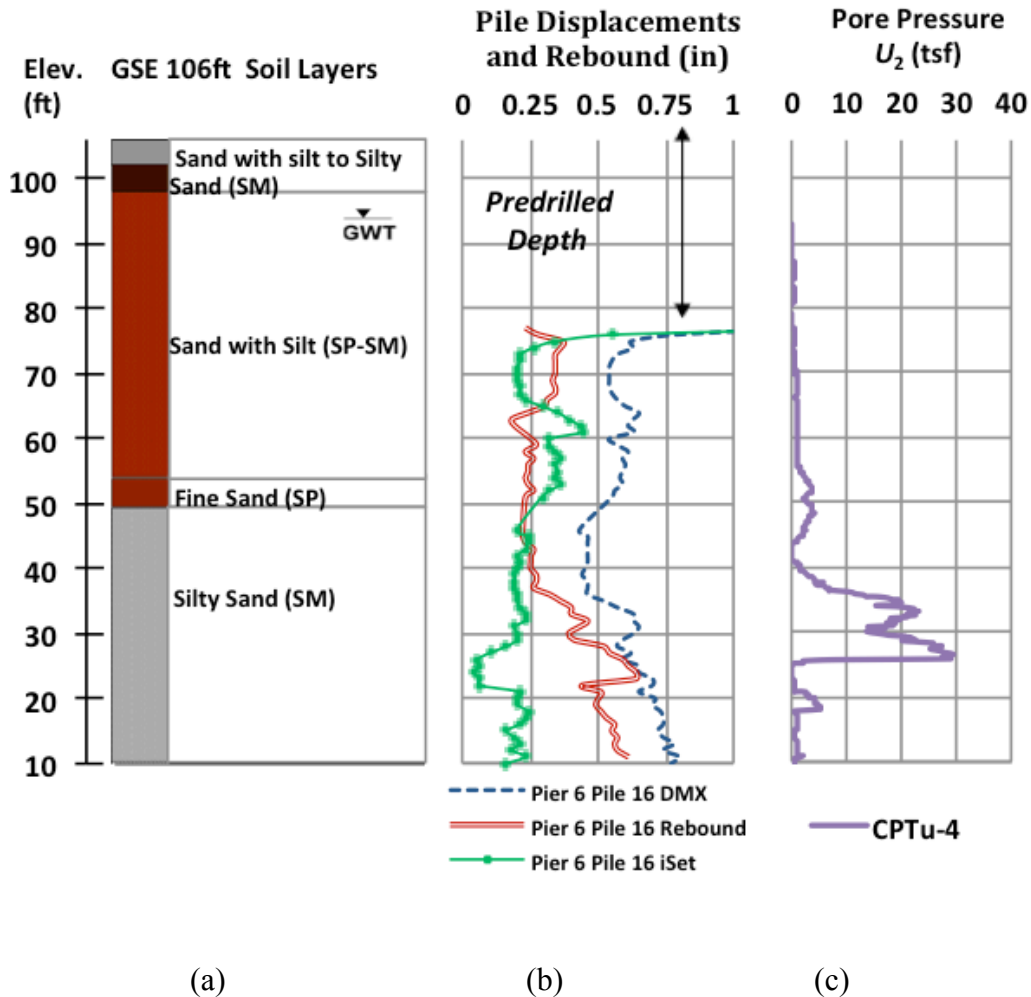


Figure 2-46: (a) Generalized soil profile, (b) PDA diagram and (c) CPTu pore-water pressure ( $u_2$ ) for Site 3 I-4/US.192 (Cosentino et al., 2013).

Pile rebound and iSet were plotted versus  $u_2$  and a normalized pore pressure of  $u_2/u_0$  ( $u_0$  is the hydrostatic pressure) to obtain linear correlations. The Central Florida data were combined with Murrell et al's (2008) data. The combined data consistently produced strong linear correlations with regression coefficients greater than 0.6 (Figure 2-47). In general, rebound increased and iSet decreased as  $u_2$  and  $u_2/u_0$  increased. Rebound versus either pore pressure or  $u_2/u_0$  nearly plots through the origin, indicating that rebound (inches) would equal approximately 2.5% of the  $u_2$  value (tsf) or 5.5 % of the  $u_2/u_0$  ratio (dimensionless).

Evaluation of the plots showed changes in pile movement at several pore pressure levels. When  $u_2$  was less than 5 tsf, pile rebound was below 0.25 inches and permanent set was acceptable. When  $u_2$  was between 5 tsf and 20 tsf, HPR occurred but was acceptable (i.e., the

pile was advancing without excessive blows and stresses). When  $u_2$  was greater than 20 tsf, excessive rebound occurred with minimal or no permanent set.

CPTu pore water pressures increase from near zero to high positive values in all HPR zones. Strong correlations between rebound and pore pressure as well as permanent-set and pore pressure indicated that permanent-set decreases and rebound increases linearly with either pore pressure,  $u_2$ , or normalized pore pressure,  $u_2/u_0$ .

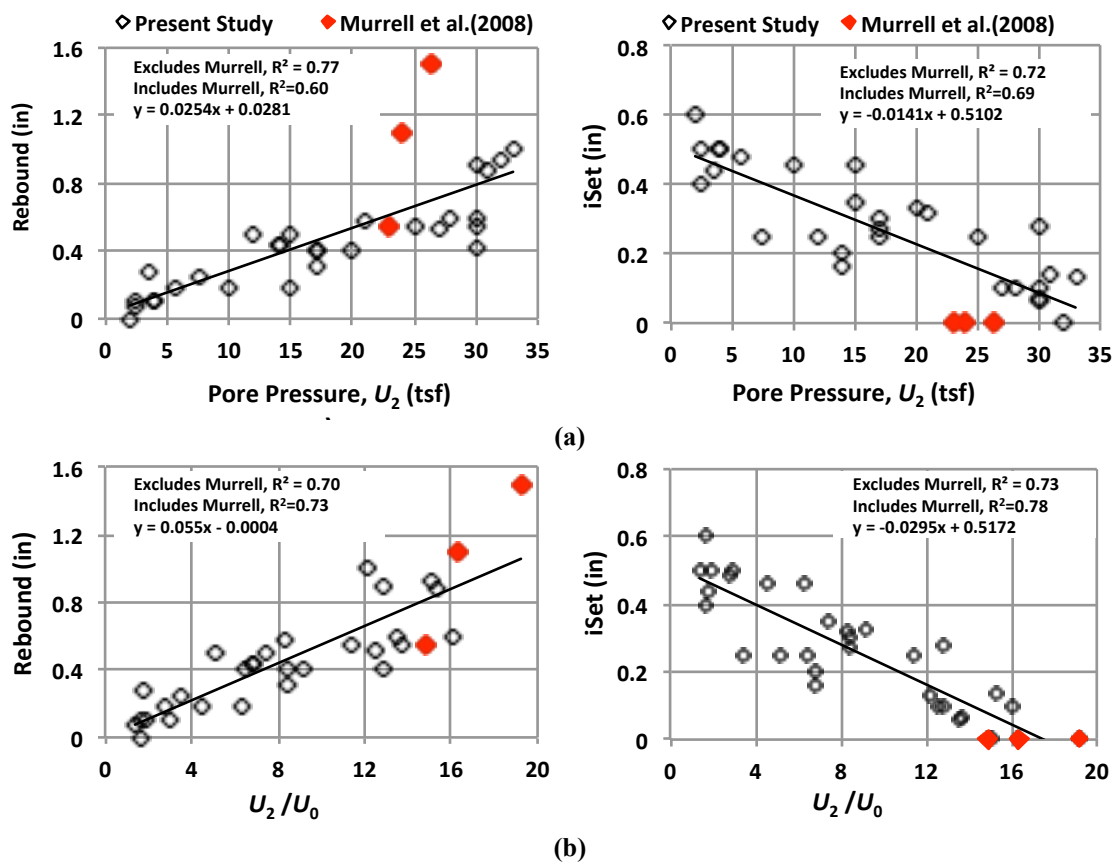


Figure 2-47: Correlations between rebound, permanent-iSet and (a) CPTu pore water pressure, and (b) ratio of CPTu pore pressure ( $u_2$ ) and hydrostatic pressure ( $u_0$ ) (Cosentino et al., 2013).

## 2.14. Summary of Case Study Literature Findings

Based on multiple High Pile Rebound case studies both within and outside of Florida, HPR is a recognized problem that occurs most commonly when high displacement piles are driven into dense fine sands with silty or clayey fines. These conditions are frequently associated

with a geologic formation known as the Hawthorn layer, which exists throughout Florida and parts of Georgia and the Carolinas.

There are several methods of measuring pile rebound and permanent set in order to quantify HPR. The most common are the manual method and automated PDA systems. PDA data is very useful in defining the HPR zones. Large quake displacements are typically determined using CAPWAP<sup>®</sup> analyses when HPR occurs.

Several laboratory studies have proposed (a) percentage and type of fines in soils, (b) soil dilatancy, and (c) susceptibility to large changes in pore pressure, as indicators of potential HPR. Dynamic loading effects on soil structure and stress response have also been studied; however, the variety of cyclic loading techniques employed makes drawing clear conclusions difficult. Table 2-7, the summary of cyclic loading parameters, indicates that a CSL of between 12.8 and 70% of the failure stress exists and that below this level, small changes in pore pressure occur while above it large changes occur. This table also shows that a limited number of studies have focused on load durations of 1 second per cycle.

Based on previous studies of HPR sites within Florida, SPT N-values, changes in silt content between soil layers, and CPTu pore pressures have been correlated to HPR, with strong positive correlations from both sets of test data. SPT versus rebound correlations were nonlinear, while the CPTu versus rebound correlations were linear. These latter correlations indicated that rebound might be a problem when CPTu pressures exceeded 20 tsf.

### 3. Methodology, Description of Testing Sites, and Data Collection

#### 3.1. Methodology

##### 3.1.1. Identifying Testing Sites

Throughout Central Florida, North Florida, and the Florida Panhandle, ten sites, as shown in Table 3-1, were identified for SPT, CPTu, DMT, undisturbed testing, and data analysis to support the research objectives. The selection was based on the following criteria:

- a) The fact that these sites were clearly identified by FDOT as having some rebound.
- b) They were easily accessible for performing field-testing.

The rebound may have been accompanied by minimal or zero set, which caused driving problems or by acceptable set, which allowed the piles to be driven.

Table 3-1: Summary of HPR Testing Sites and Testing Program

Number	Description	Testing			
		SPT	CPTu	DMT	Undisturbed
1	I-4 / US-192 Interchange / Osceola County / Florida.	✓	✓	⊗	✓
2	State Road 417 International Parkway / Osceola County / Florida.	✓	✓	⊗	✓
3	I-4 / Osceola Parkway / Osceola County / Florida.				✓
4	State Road 50 and State Road 436 / Orange County / Florida.	✓	✓		
5	I-4 / State Road 408 Ramp B / Orange County / Florida.	✓	✓		
6	Anderson Street Overpass at I-4/SR-408 / Orange County / Florida.	✓	✓		
7	I-4 Widening Daytona / Volusia County / Florida.	✓	✓		
8	State Road 83 over Ramsey Branch Bridge / Walton County / Florida.	✓	✓		✓
9	Saint Johns Heritage Parkway, Brevard County	✓	⊗	⊗	✓
10	I-10 Chaffee Road, Duval County Florida	✓	⊗		✓

Note: ✓ completed ⊗ partial data

The majority of these sites are in the Central Florida area, but two sites are not. Site 8 is located in the northern Panhandle of Florida where the soil composition is similar to that in Central Florida but the geologic deposit process produced less dense soils. Site 10 is in Jacksonville and again has similar soils to those found throughout Florida.

### 3.1.2. Development of Testing Program

In order to identify and evaluate the characteristics of soil deposits, which may cause HPR, geotechnical lab and field-testing were performed. The lab testing included both undisturbed and disturbed sampling. Undisturbed samples were obtained from six of the ten sites shown in Table 3-1, sites so that the following information could be determined:

1. Unit weight
2. Moisture Content
3. Permeability
4. Saturation
5. *In situ* Void Ratio
6. Triaxial shear strength
7. Undrained Cyclic Triaxial Pore Pressure Behavior.

The field data included retrieval of existing PDA, which was matched to SPT, and CPTu data that was collected and processed during this work. PDA results were used to identify the zones in the vertical soil profiles where HPR occurred. SPT data were used to develop soil profiles, provide disturbed samples for grain size evaluations, and yield N-values. The grain size and N-value information was then used to evaluate published correlations (Jarushi et al., 2013). CPTu  $q_c$ ,  $f_s$  and  $u_2$  data was used to determine a series of soil properties throughout each soil profile. CPTu soil properties at these sites included:

1. Unit weight ( $\gamma$ )
2. Permeability (k)
3. Relative density ( $D_r$ )
4. State parameter ( $\psi$ )
5. Undrained shear strength ( $S_u$ )
8. Overconsolidation ratio (OCR).

The correlations developed for predicting these parameters were programmed into the geotechnical software, CPeT-IT v.1.4 (2014), which was licensed to Florida Tech and used to process the CPTu data. Gregg Drilling and Testing, Inc., developed it in collaboration with Robertson and Cabel (2012). CPTu testing at Sites 9 and 10 proved problematic and could not be

used for correlations. In both cases, the sounding depths were too shallow for use in subsequent analyses.

Both the soil behavior type (SBT) and fines content (FC) were estimated from CPTu data. To verify FC, disturbed soil samples, obtained during the research SPT and design phase testing, were used to obtain measured FC. The results of all soil properties were presented versus depth as vertical profiles for each site. Using the PDA data, the rebound zones were highlighted on these profiles to investigate the difference between the rebound and non-rebound soil properties and to identify the soil properties that had a significant effect of soil rebound.

The second objective of this research was an evaluation of the accuracy of existing HPR correlations. These include correlations to  $u_2$ , FC, and  $N_{SPT}$ . To fulfill this objective, pore pressure ( $u_2$ ) – rebound correlations developed by Jarushi et al. (2013) were re-evaluated. The additional CPTu data from the seven sites was used for the re-evaluation.

By superimposing the CPTu results on several known SBT charts, graphical correlations were produced. This process was completed using the CPeT-IT v.1.4 (2014) software.

DMT testing was performed at three of the sites and produced very limited results. The main problem was pushing the wider DMT blade through the soils as it stopped well above any critical layers. Therefore, DMT testing was eliminated and excluded from further analysis.

### **3.1.3. Collection of Existing PDA Data**

FDOT and their contractors provided detailed geotechnical and construction data for each site. The data collected included project contract drawings, test pile locations, and PDA data as well as locations and data of existing SPT borings and CPT soundings.

### **3.1.4. Analysis of Design Phase PDA Data and Identification of Rebound Zones**

Test piles at these sites were instrumented with PDA accelerometers and strain transducers during construction, and this data was used to identify rebound zones. PDA data recorders collected the accelerations and strains for each hammer blow. The accelerations were integrated twice to produce displacements versus time data for each blow. This data was used to determine the maximum displacement (i.e., DMX) and digital final set (DFN). At the same time,

FDOT inspectors recorded the number of blows required to drive the pile each foot on the pile driving logs. The inspector set (iSet) in the units of inch/blow was calculated by taking the reciprocal of the number of blows ( $N_{PD}$ ). In cases where  $N_{PD}$  was over 240 blows/foot (i.e., 20 blow/inch), the test pile driving process was terminated. This situation is referred to as pile refusal. Since the precise pile location is not always known, the double integration may produce significant errors. For this study, the inspector set was used to calculate pile rebound by subtracting it from the DMX as follows:

$$\text{Rebound (in/blow)} = \text{DMX (in/blow)} - \text{inspector set (in/blow)} \quad \text{Equation 3-1}$$

Pile rebound (in/blow) for each test pile at each site was presented versus depth in order to identify rebound zones. Pile rebound varied and ranged from 0 to 1.5 inches per blow. Excessive rebound was considered to be any rebound exceeding FDOT's specification, Section 455, of 0.25 in/blow or  $N_{PD}$  exceeding 240 blow/ft

### **3.1.5. Field Tests and Sampling**

CPTu penetration tests were conducted at the FDOT sites using an electrical cone penetrometer with pore water transducer behind the cone tip. CPTu soundings were performed according to ASTM D-5778 near the associated test piles until refusal or desired depth was met. The CPT parameters  $q_c$ ,  $f_s$ , and  $u_2$  were plotted versus depth and used to estimate soil properties.

SPTs were performed by FDOT as near as possible to the test piles at each site. The SPT borings extended deeper than the associated test piles to provide a representative description of the soil at each site. SPT borings were performed according to ASTM D-1586. An automatic hammer was used to drive the SPT sampler. Disturbed soil samples were retrieved every five feet from the split spoon. These samples were packaged for further FDOT examination and laboratory testing. The number of blows required to drive the SPT sampler one foot was recorded as the N value ( $N_{SPT}$ ). No corrections were applied to  $N_{SPT}$ . When the number of blows exceeded 50 before the sampler was driven 1 foot, the number of blows was recorded as 50 blows per the distance driven, which is normally less than 1 foot. If  $N_{SPT}$  exceeded 50 blows over a depth of less than 12 inches (where D is the depth in inches), the number of blows was multiplied by (12/D) to extrapolate to an estimated  $N_{SPT}$ .

FDOT sponsored a study by Davidson (1999) to investigate SPT hammer efficiencies from 58 different drilling systems. Using SPT analyzer equipment (similar to PDA sensors) on both automatic and safety hammers, a common correction factor of 1.24 was adopted to convert automatic SPT N values to an equivalent safety hammer  $N_{ES}$  according to

$$N_{ES} = N_{auto} \times 1.24 \quad \text{Equation 3-2}$$

### **3.1.6. Field Site Data Processing**

A Google Maps<sup>®</sup> site location photo was developed for each site showing the SPT, CPTu, and the PDA test pile locations. A soil profile was developed from each SPT boring. The profile includes the soil type for each layer using both the Unified Soil Classification System (USCS) symbols (e.g., SP-SM) and the American Society for Testing and Materials (ASTM) soil descriptions (e.g., sand with silt).  $N_{SPT}$  was also graphically included versus depth for each boring. Drilling crews from Ardaman & Associates, Inc., and the FDOT State Materials Office (SMO) performed these tests. CPTu penetration test data, including  $q_c$ ,  $f_s$ , and  $u_2$ , were presented versus depth. These profiles were used to identify the rebound zones.

## **3.2. Description of Sites and Field Testing Data**

### **3.2.1. I-4 / US-192 Interchange**

#### **3.2.1.1. General Description and Field Testing Locations**

The I-4/US-192 interchange is located in Kissimmee, Florida, Osceola County (See Figure 3-1). The site consists of two ramps (CA and BD) and two bridges (US-192 Westbound and US-192 Eastbound). The approximate Ground Surface Elevation (GSE) ranges from 95 ft to 109 ft (North American Vertical Datum of 1988 or NAVD88). The ground water table (GWT) is located 10 to 15 feet below GSE. The bridge piers are supported by a group of 24-inch square PCPs, 115 ft long. Three test piles (pier 6/pile 16, pier 7/pile 10 and pier 8/pile 4) along ramp CA were analyzed (Figure 3-1). They were driven with an ICE 120 S single-acting diesel hammer with a rated energy of 120 ft-kips (139 kJ) using a 9-inch thick plywood pile cushion. Pile installation included predrilling 30 feet below GSE. SPT and CPTu tests were performed 15 ft to 20 feet from these test piles (Figure 3-1).

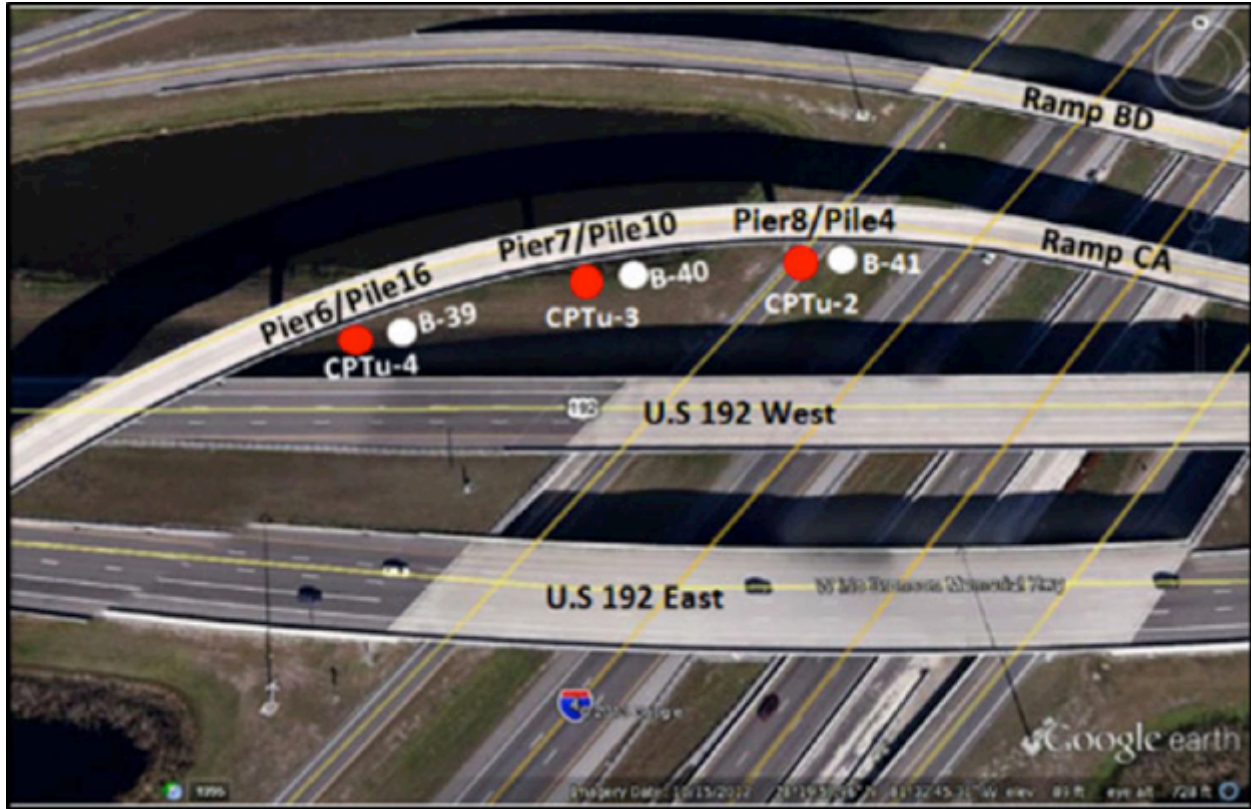


Figure 3-1: Test piles, SPT boring, and CPTu sounding locations for I-4/US-192 interchange

### 3.2.1.2. PDA Data and Identification of HPR Zones

The PDA data digital set and rebound per blow were plotted along with  $N_{PD}$  versus depth, as shown in Figure 3-2. Rebound of up to 0.25 in/blow occurred at depths between 40 and 70 ft for all three test-piles and the corresponding digital set ranged from 0.25 to 0.5 in/blow. As shown in Figure 3-2, the rebound zone was identified at depths between 70 and 100 ft. The rebound ranges from 0.25 to 0.92 inch/blow and set less than 0.25 inch/blow. This rebound zone also produced a rapid increase in the number of blows from an average of 50 blows/ft to 300 blows/ft.

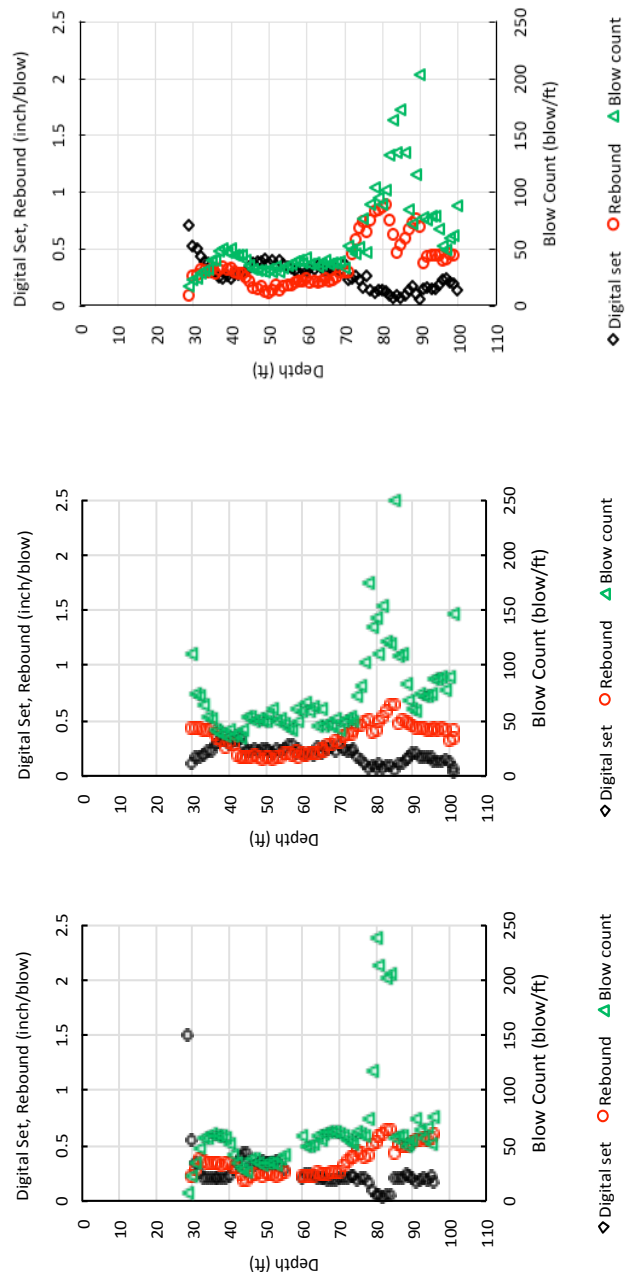


Figure 3-2: Digital set, pile rebound, and  $N_{PD}$  versus depth for (a) pier 6/pile 16, (b) pier 7/pile 10 and (c) pier 8/pile 4 for I-4/US 192 interchange

### 3.2.1.3. SPT Data and General Soil Profile

At I-4/US-192, three SPT borings (i.e., B-39, B-40, and B-41) were performed approximately 15 to 20 feet away from the associated test piles at piers 6, 7, and 8, respectively. A general soil profile showing soil stratification and  $N_{SPT}$  was developed, as illustrated in Figure 3-3. GSE varied due to fill for the embankment; therefore, borings B-39 and B-40 GSE were 109.6 and 108.6, respectively. Boring B-41 GSE was 90.2 ft, or 18 ft lower than those of borings B-39 and B-40. When the generalized profile was developed (Figure 3-3), the soil types and  $N_{SPT}$  values were based on the adjusted 18 ft depth. The SPT borings extended to a depth of 180 ft below the GSE.

The rebound zone at the I-4/US 192 interchange, between 70 ft and 100 ft, is characterized by cemented fine sand (SM) with trace phosphate and shell.  $N_{SPT}$  ranges from 15 to 25 blows/ft.

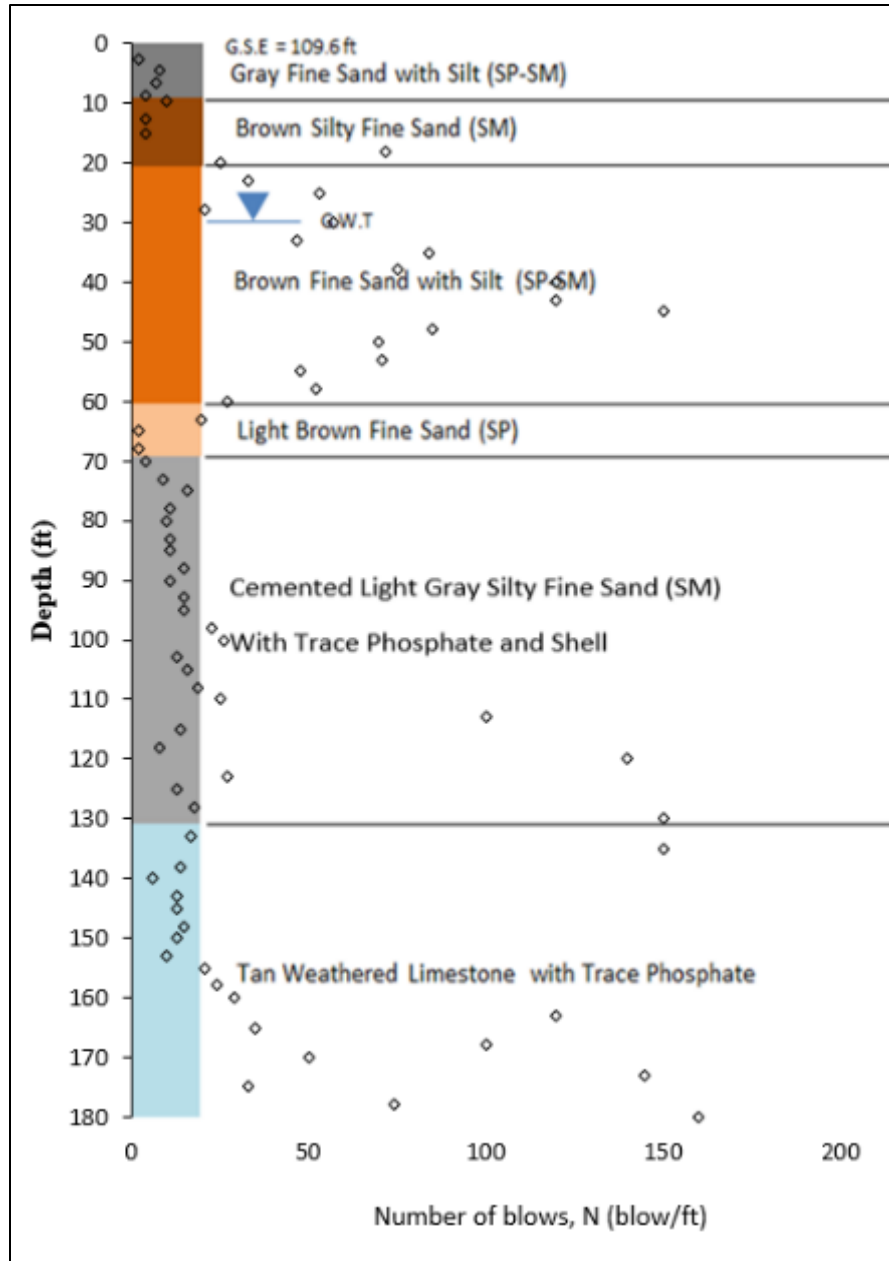


Figure 3-3: General soil profile with USCS classification and the actual number of blows (N) from SPT borings B-39, B-40, and B-41 for I-4/US 192 Interchange

### 3.2.1.4. CPTu Data

Three CPTu soundings, CPT-4, CPT-3, and CPT-2, were conducted about 15 ft to 20 ft from the test piles near ramp CA, pier 6/pile 16, pier 7/pile 10, and pier 8/pile 4 respectively. The CPTu soundings extended to a depth of 96 ft, 95 ft, and 105 ft near pier 6, pier 7, and pier 8, respectively. The data was presented versus depth as illustrated in Figure 3-4, Figure 3-5, and Figure 3-6. The rebound zones at all the test piles were highlighted in the CPTu profiles in order

to identify if there is any difference in the measured CPTu parameters (i.e.  $q_c$ ,  $f_s$ , and  $u_2$ ) at the rebound zones.

Figure 3-4, Figure 3-5, and Figure 3-6 each show that the  $q_c$  averages 100 tsf in the rebound zones (70 ft to 90 ft) and from 100 tsf to 600 tsf in the non-rebound zones. CPTu  $f_s$  increased from 1 tsf to 4 tsf in the rebound zones, and averaged 1 tsf in the upper non-rebound zone (30 ft to 70 ft). Note, a zone with high  $q_c$  and  $f_s$  is located at depth 10 ft to 30 ft. This zone was predrilled; therefore, no PDA information is available. The CPTu  $u_2$  depth profiles shown Figure 3-4, Figure 3-5, and Figure 3-6, indicate a rapid increase in  $u_2$  in the rebound zones, where  $u_2$  increased from near zero to 500 psi within a depth of about 10 ft.

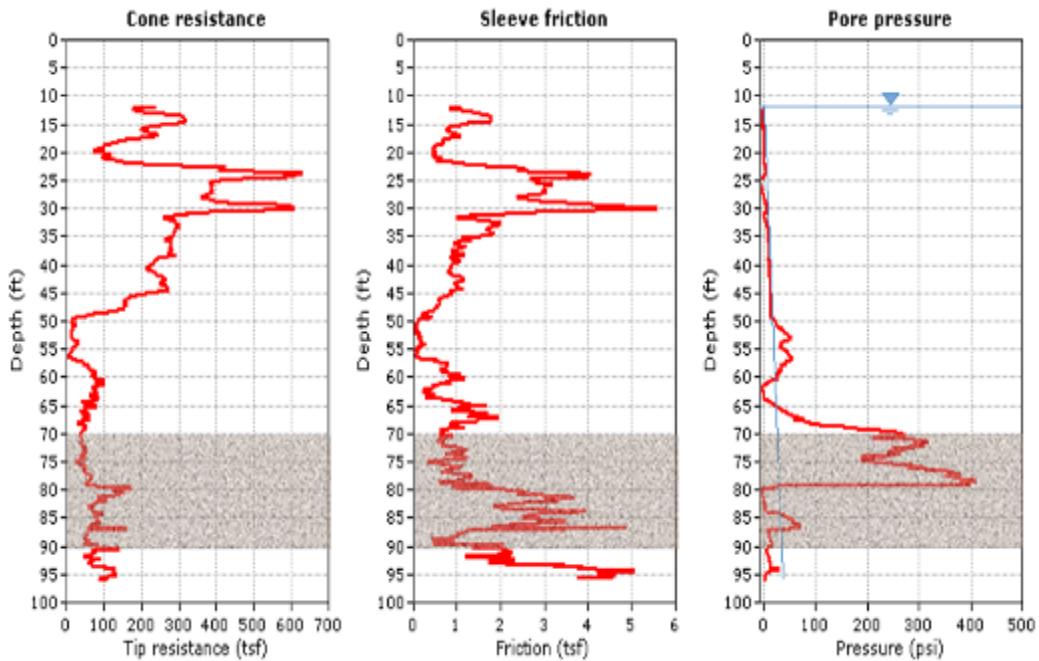


Figure 3-4: CPTu  $q_c$ ,  $f_s$ , and  $u_2$  versus depth from CPTu-4 near pier 6/pile 16 at I-4/US 192

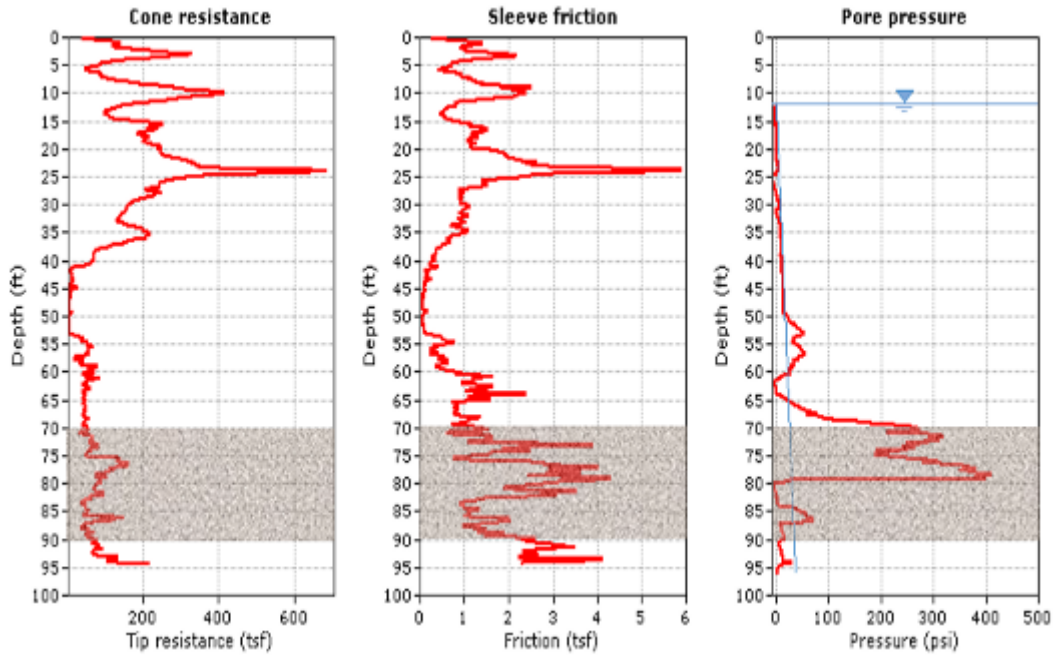


Figure 3-5: CPTu  $q_c$ ,  $f_s$ , and  $u_2$  versus depth from CPTu-3 near pier 7/pile 10 at I-4/US 192

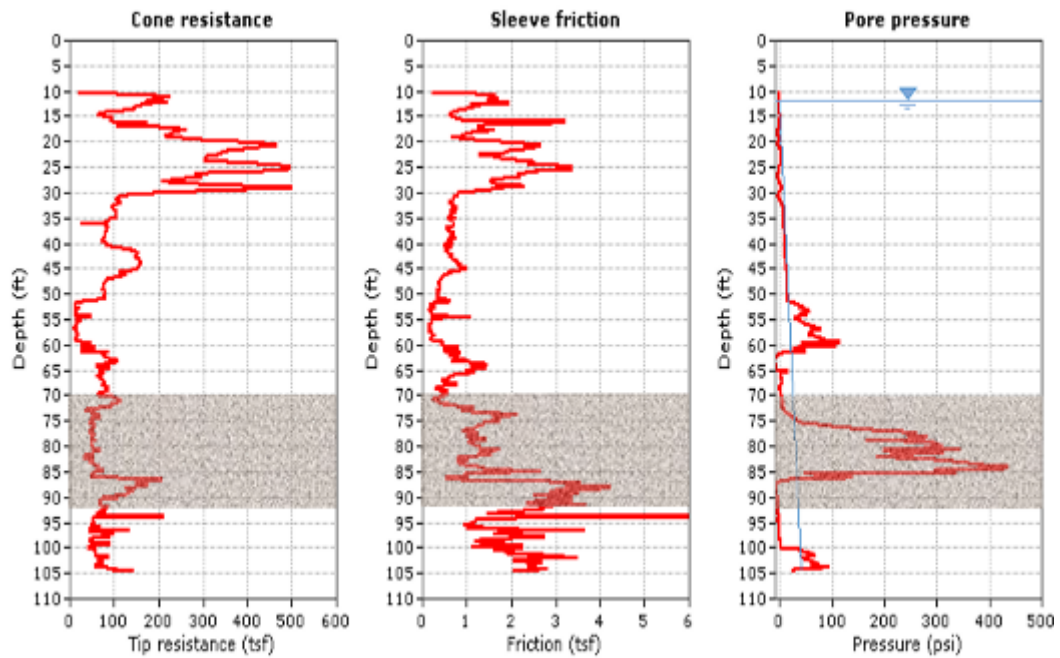


Figure 3-6: CPTu  $q_c$ ,  $f_s$ , and  $u_2$  versus depth from CPTu-2 near pier 8/pile 4 at I-4/US 192

## **3.2.2. State Road 417 International Parkway I-4 Interchange**

### **3.2.2.1. General Description and Field Testing Locations**

The SR 417 International Parkway I-4 Interchange is located in Osceola County, 15 miles north of Orlando in Lake Mary, Florida. It has one ramp and a bridge with two end bents (B1 and B2). It connects SR 417 westbound to I-4 westbound as shown in Figure 3-7. GSE at both end bents was 72.3 ft (NAVD88) and GWT is located at 6 ft below GSE. Groups of 100-foot long, twenty-four inch square PCPs were used to construct the two end bents. Two test piles were instrumented with PDA: Pile 14 at end bent B1 and Pile 5 at end bent B2. The piles at B1 and B2 were predrilled to 15 feet and 27 feet below GSE respectively and then driven with an APE, D 46-42 single-acting diesel hammer with a 120 ft-kips (139 kJ) rated energy. A nine-inch thick plywood pile cushion was used during pile driving. Two SPT borings and two CPTu soundings were conducted approximately 30 feet from the test piles as shown in Figure 3-7.

### **3.2.2.2. PDA Data and Identification for HPR Zones**

Rebound fluctuated from below 0.25 inch/blow to maximums near 0.5 inch/blow during test pile installation. Even though rebound occurred, the test piles were successfully driven; therefore, this site is considered a rebound site with acceptable set. From 30 to 40 feet, a rebound of about 0.35 inch/blow was recorded during driving of both piles. Rebound also exists from 40 to 50 feet for B1 Pile 14. A rebound zone exists between 70 and 80 feet for both test piles 14 and 5, as shown in Figure 3-8.  $N_{PD}$  for test pile 5 in B2 also increased to 87 blows/ft in the rebound zone, as shown in Figure 3-8b. Test pile 5 at B2 only exceeded the rebound limit of 0.25 in/blow at a depth of 20-35 ft and then became relatively constant at less than 0.25 in/blow at a depth of 35-80 ft. The corresponding  $N_{PD}$ , shown in Figure 3-8b, decreased to less than 50 blows/ft compared to that recorded at test pile 14 at B1.



Figure 3-7: Test piles, SPT boring, and CPTu sounding locations for SR 417 International Parkway I-4 Interchange

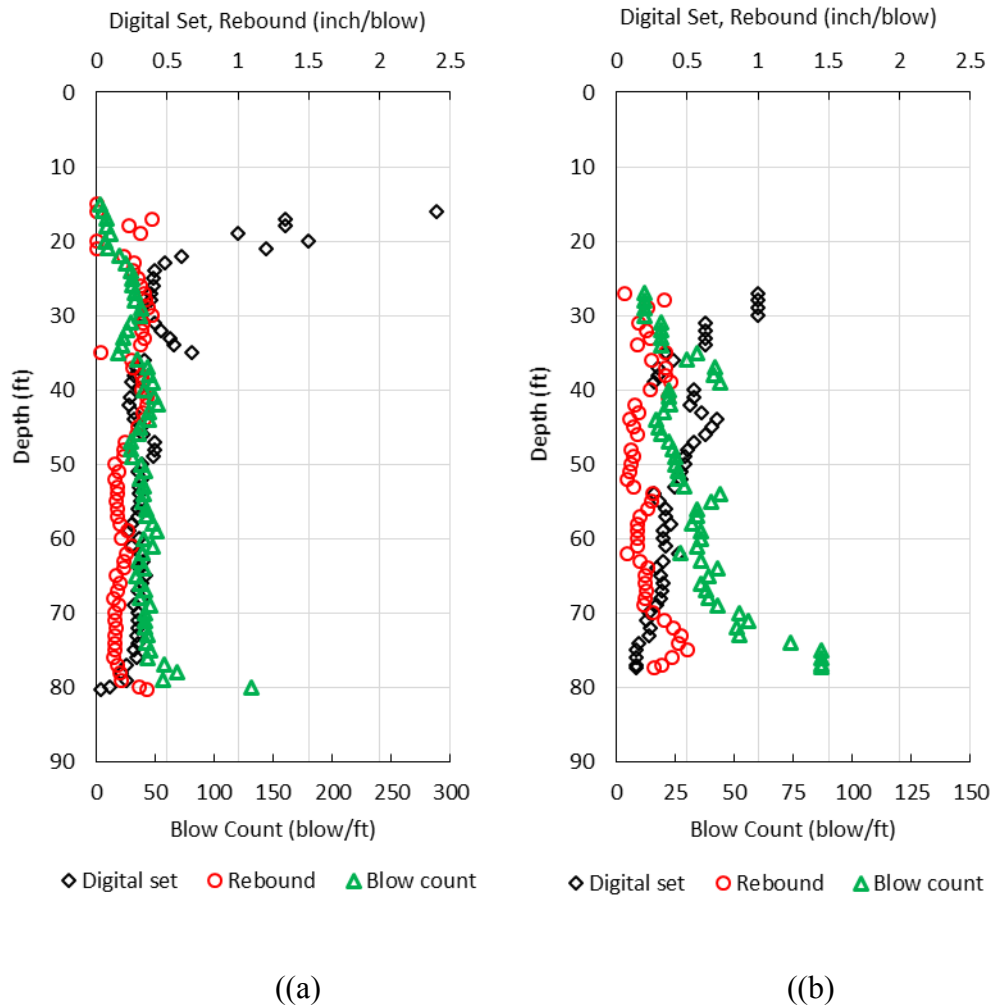


Figure 3-8: Digital set, pile rebound, and  $N_{PD}$  versus depth for depth for ((a) B1/pile 14 and ((b) B2/pile 5 at SR 417 International Parkway I-4 Interchange

### 3.2.2.3. SPT Data and General Soil Profile

Two SPT borings (i.e., SPT-B1 and SPT-B2) were performed at the State Road 417 International Parkway I-4 Interchange. General soil profile and the recorded  $N_{SPT}$  from SPT borings are presented graphically versus depth in Figure 3-9. Boring SPT-B1 was located 10 ft away from test pile 14 at bent 1(B1) while boring SPT-B2 was located 15 ft away from test pile 5 at bent 2 (B2). The GSE at both end bents was 72.3 ft. The SPT borings extended to a depth of 93 ft from the GSE. It can be noticed that cemented silty fine sand (SM) with trace phosphate and shell exists in the rebound zone (i.e., 70 ft to 80 ft). The average  $N_{SPT}$  is 50 blows/ft

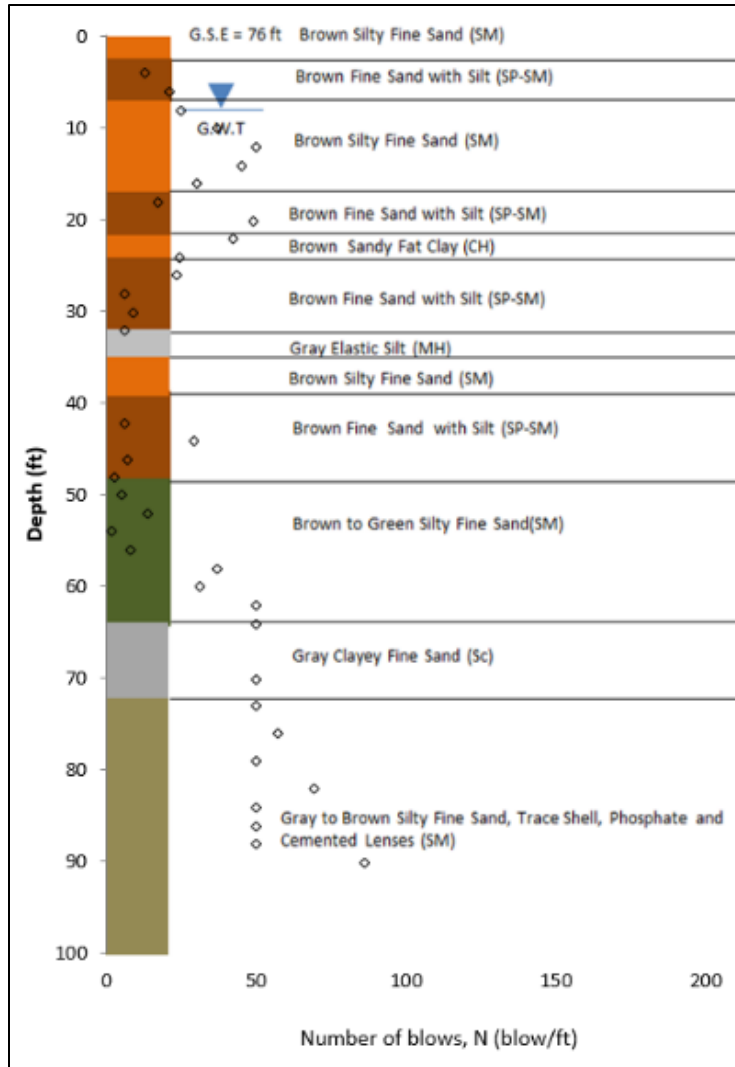


Figure 3-9: General soil profile with USCS classification and  $N_{SPT}$  from SPT borings SPT-B1 and SPT-B2 for SR 417 International Parkway I-4 Interchange

### 3.2.2.4. CPTu Data

Two CPTu soundings, CPT-1 and CPT-3, were conducted about 30 ft from the test piles at B1 and B2 respectively. The CPT soundings extended to a depth of 74 ft and 70 ft near B1 and B2 respectively. The data was presented versus depth as illustrated in Figure 3-10 and Figure 3-11. A thin rebound zone (70 ft to 75 ft), shown only in B2 Pile 5, was highlighted in the CPTu-1 profile in order to identify if there is any difference in the measured CPTu parameters (i.e.,  $q_c$ ,  $f_s$ , and  $u_2$ ) at the rebound zones. No rebound zones exist in B1/Pile 14; therefore, the data sounding CPT-3 was not highlighted.

Figure 3-10 contains data that show that  $q_c$  ranges from 50 tsf to 250 tsf for all depths. CPTu  $f_s$  increased and ranges from 0.5 tsf to 2 tsf in all depths. By inspecting the CPTu  $u_2$  profiles, shown in Figure 3-10 and Figure 3-11, we can see that the pore water pressure increased to a maximum value of 50 psi. State Road 417 International Parkway I-4 Interchange is classified as a non-rebound site.

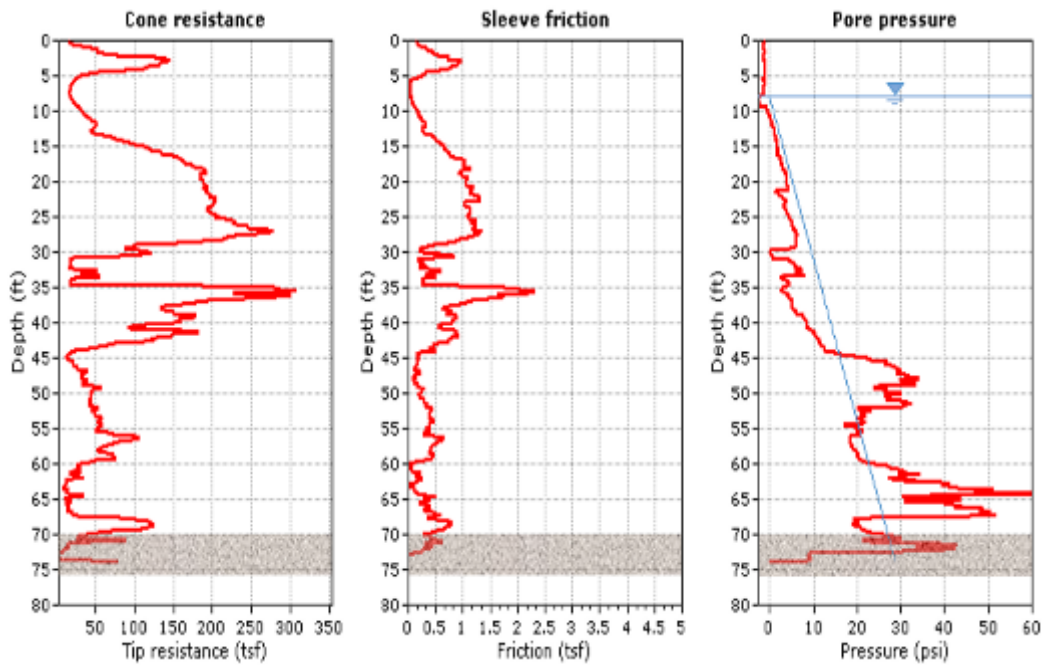


Figure 3-10: CPTu  $q_c$ ,  $f_s$ , and  $u_2$  versus depth from CPT-1 near B1/pile 14 at SR 417 International Parkway I-4 Interchange

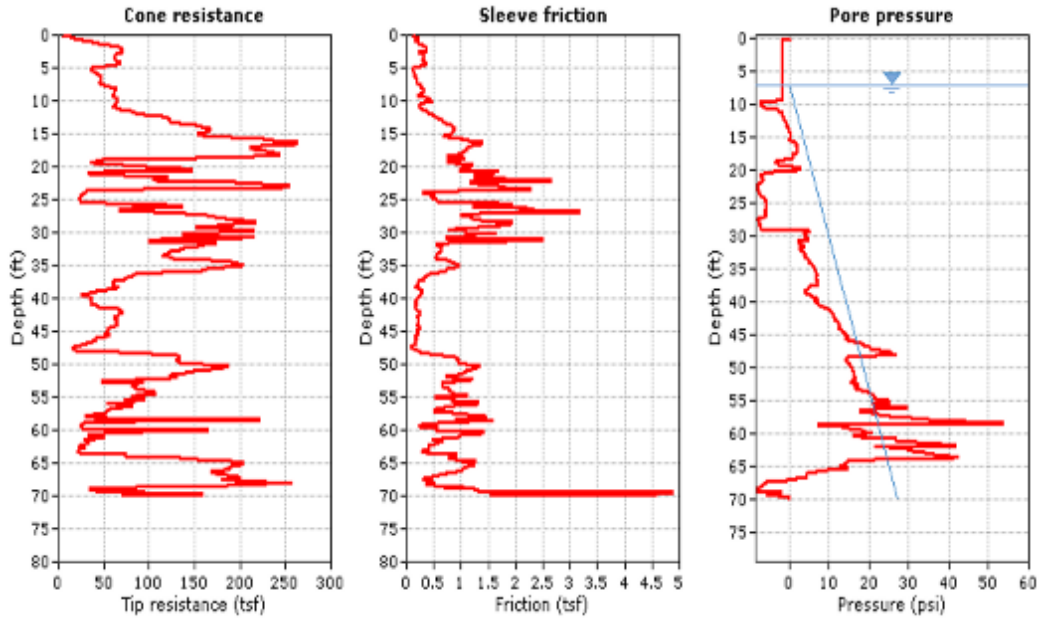


Figure 3-11: CPTu  $q_c$ ,  $f_s$ , and  $u_2$  versus depth from CPT-3 near B2/pile 5 at SR 417 International Parkway

### 3.2.3. State Road 50 over State Road 436

#### 3.2.3.1. General Description and Field Testing Locations

This site consists of the intersection of SR 50 and SR 436, and is located in Orlando, Orange County, Florida. The SR 50 Bridge extends over SR 436 from the west to the east of SR 436. The GSE of the site is 99 ft (NAVD88) and the GWT is located at 4 ft below the GSE. Twenty-four inch square PCPs 101 ft long were designed to support the SR50/SR436 overpass. Test pile 5 at the westbound lane of the overpass was instrumented with PDA. The test pile was placed in a predrilled hole to a depth of 32 ft from GSE before driving. A pile cushion, 14 inches thick, was used to drive the pile using an APE D62-42 single-acting diesel hammer with a ram weight of 13 kips and energy of 154 ft-kips (210 kJ). One SPT boring and CPT sounding were conducted 35 ft away from the test pile. Field-testing locations are shown in Figure 3-12.



Figure 3-12: Test piles, SPT boring, and CPTu sounding locations for SR50/SR436

### 3.2.3.2. PDA Data and Identification of HPR Zones

The PDA data is shown in Figure 3-13 for SR 50 over SR 436. Rebound increases from zero at 30 ft to between 0.5 and 0.75 inch/blow from 40 to 55 ft. Then it decreases to zero and remains relatively constant until a depth of about 68 ft, when it begins to increase to a maximum of about 1 inch near 75 ft before decreasing to about 0.3 inches at the end of the sounding.

Figure 3-13 indicates that the significant rebound zone with a maximum rebound of 1 inch/blow is located at a depth of 70-80 ft. In terms of the number of blows, Figure 3-13 shows that a minimum number of 4 blows/ft in the non-rebound zone and a maximum number of 300 blows/ft in the rebound zone were recorded. In terms of the digital set, a 2-inch maximum set was recorded between 32 ft and 70 ft and a minimum between zero and 0.35 inches between 70 ft and 80 ft, as can be seen in Figure 3-13. Therefore, the rebound zone at SR 50/ SR 436 is located at a depth of 70 ft to 80 ft.

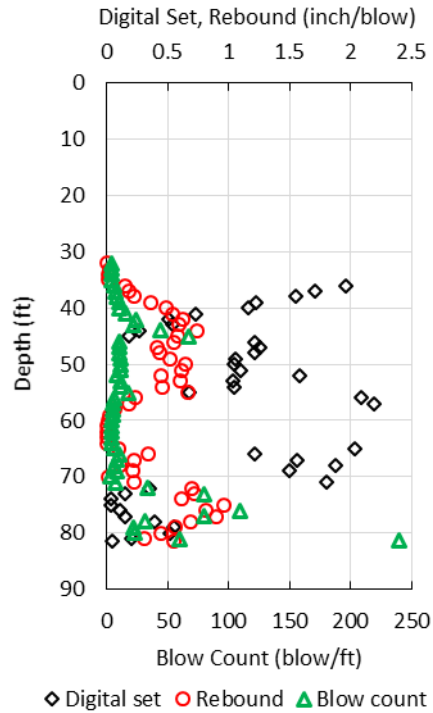


Figure 3-13: Digital set, pile rebound, and  $N_{PD}$  versus depth for pile 5 for the westbound side of SR 50 / SR 436

### 3.2.3.3. SPT Data and General Soil Profile

Standard penetration test boring TH-4B at SR 50/SR 436 was driven 30 ft away from test pile 5 located along the westbound side of the bridge. Figure 3-14 presents a general soil profile and  $N_{SPT}$  that were recorded during the SPT. The GSE for this boring was 99 ft. The SPT boring was predrilled to a depth of 10 ft and extended to a depth of 100 ft below GSE. The rebound zone (70 ft to 80 ft) is characterized by silty fine sand (SM) with trace clay and high plasticity clay (CH) with trace phosphate. The average  $N_{SPT}$  is 25 blows/ft for all depths other than the rebound depths where  $N_{SPT}$  suddenly increased from 15 blows/ft to 150 blows/ft.

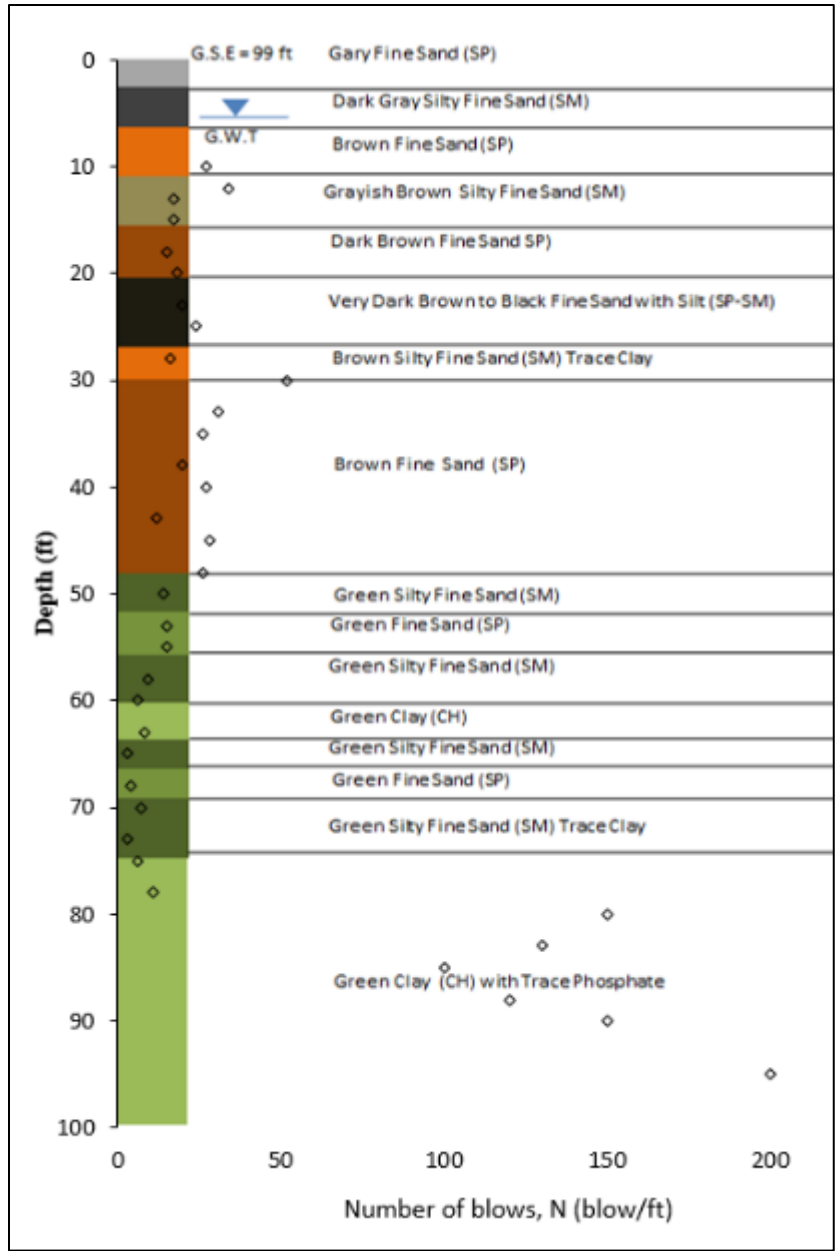


Figure 3-14: General soil profile with USCS classification and the actual  $N_{SPT}$  from SPT boring TH-4B near pile 5 at the westbound side of SR50/SR436

**3.1.1.1. CPTu Data**

A CPTu sounding, CPT-1, was conducted 35 ft away from test pile 5 in the westbound lane of SR 50/SR 436. The CPT sounding extended to a depth of 77 ft below GSE. The data was presented versus depth as illustrated in Figure 3-15. Using the PDA data, the rebound zone (i.e., 70 ft to 80 ft) was highlighted in the CPTu profiles in order to identify if there is any difference in the measured CPTu parameters (i.e.  $q_c$ ,  $f_s$ , and  $u_2$ ) in the rebound zone.

Figure 3-15 shows that  $q_c$  ranges from 30 to 100 tsf in the rebound zone, while it ranges from 50 tsf to 300 tsf in the non-rebound zones. The sleeve friction ( $f_s$ ) increased from 0.5 tsf to 2.5 tsf in the rebound zones, while it has an average of 1 tsf in the upper non-rebound zone (30 ft to 70 ft). However, a zone of high  $q_c$  and  $f_s$  is located at depth 10 ft to 30 ft. This zone was predrilled before pile driving; therefore, no information is available about pile rebound. Inspecting the  $u_2$  profile seen in Figure 3-15 shows a rapid increase in  $u_2$  within the rebound zones. The pore water pressure increased from 50 psi to 300 psi within a distance of about 5 ft.

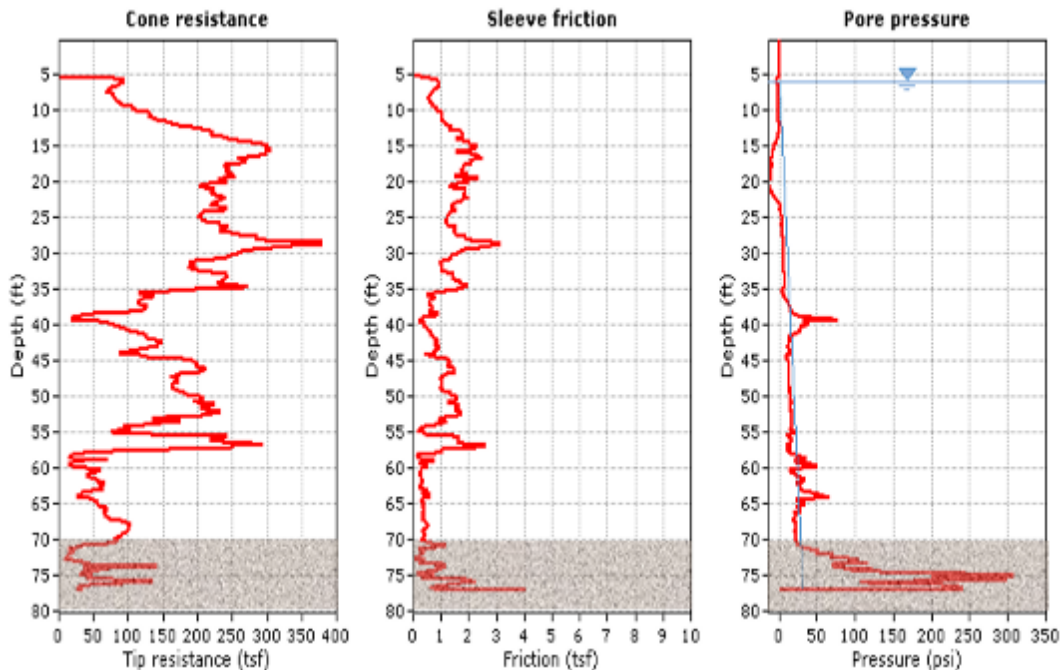


Figure 3-15: CPTu  $q_c$ ,  $f_s$ , and  $u_2$  versus depth from CPT-1 near pile 5 at the westbound side of SR 50 / SR436

### 3.2.4. I-4 / State Road 408 Interchange, Ramp B

#### 3.2.4.1. General Description and Field Testing Locations

The I-4/SR 408 interchange is located in downtown Orlando, Orange County, Florida. The GSE of the site is 106 ft (NAVD88) and the GWT is located at 5 ft to 10 ft below the GSE. SR 408 and ramp B extend over I-4. Ramp B consists of 16 piers with bridge span lengths varying from 139 ft to 263 ft. Pile 5 at the second pier of ramp B was driven as an instrumented test pile. The test pile was an 18-inch square PCP with a length of 97 ft. A Delmag D36-32

single-acting diesel hammer with a 9-inch plywood cushion was used to drive the pile into a 12-ft predrilled hole to a depth of 95 ft from GSE. An SPT boring and a CPT sounding were conducted 75 ft away from the test pile, as shown in Figure 3-16.

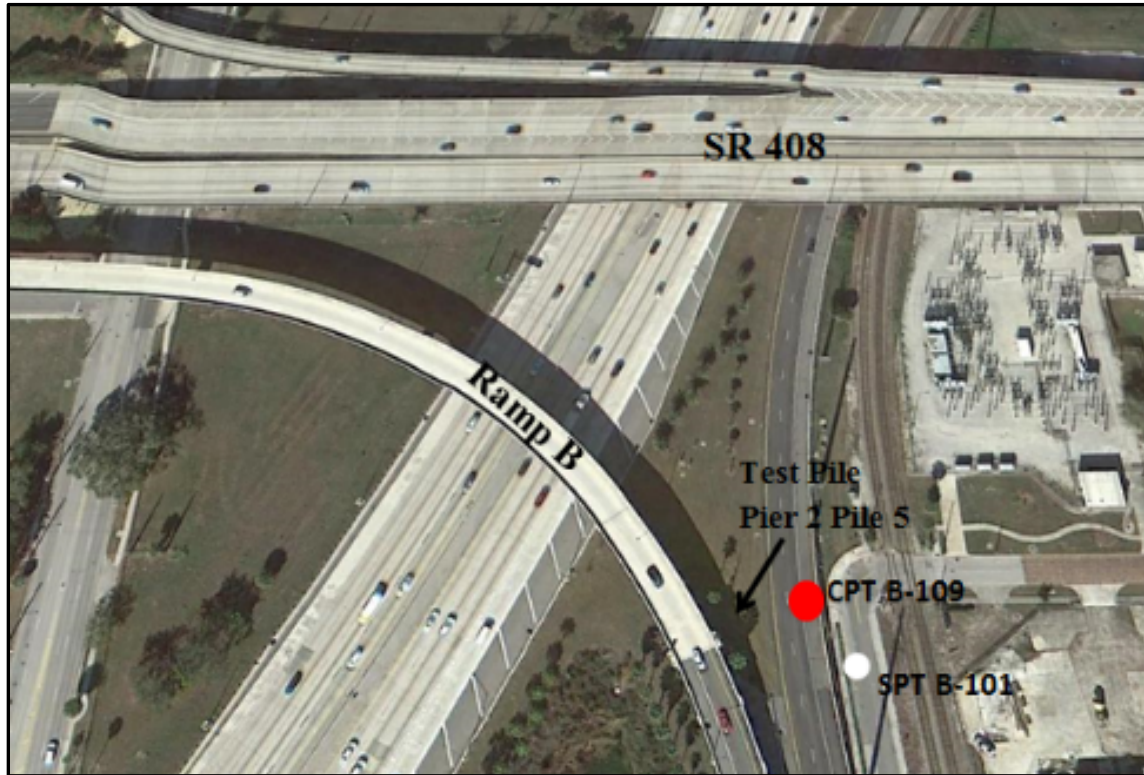


Figure 3-16: Test pile, SPT boring, and CPTu sounding locations for I-4/SR 408 (Ramp B)

#### 3.2.4.2. PDA Data and Identification of HPR Zones

An average rebound of 0.35 in/blow was recorded at depths ranging from 10 to 95 ft during driving of pile 5 at pier 2 for I-4/State Road 408 Ramp B with an average pile set of 0.25 in/blow, as can be seen in Figure 3-17. The average  $N_{PD}$  ranged from 25 to 50 blows/ft. This site was considered a non-rebound site.

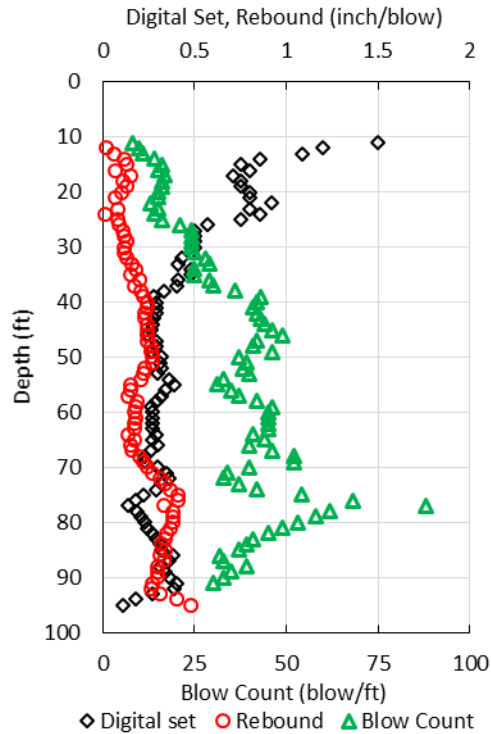


Figure 3-17: Digital set, pile rebound, and  $N_{PD}$  versus depth for pier 2/pile 5 at Ramp B of I-4 / SR 408

### 3.2.4.3. SPT Data and General Soil Profile

The SPT boring B-101 with a 103.3 ft GSE was driven at a distance of 20 ft away from the test pile 5 at the second pier of ramp B at the I-4/State Road 408. This boring was predrilled to a depth of 10 ft and extended approximately to a depth of 135 ft from the mentioned GSE.  $N_{SPT}$  was recorded and presented versus depth, as illustrated in Figure 3-18. The average  $N_{SPT}$  is 10 blows/ft at depth 10 ft to 70 ft and then is increased to an average of 20 blows/ft at depth 70 ft to 95 ft. The disturbed samples extracted during the test were classified according to the USCS and were used to develop the geotechnical profile shown in Figure 3-18.

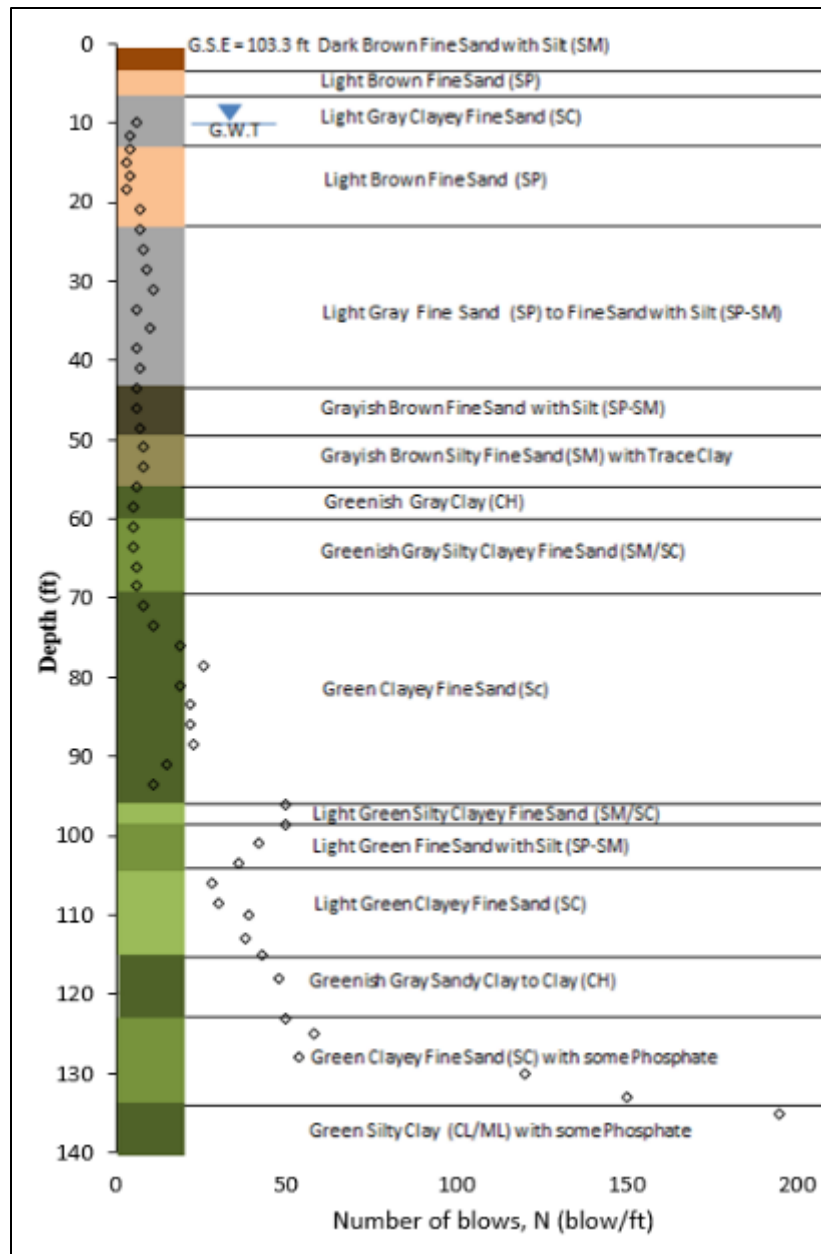


Figure 3-18: General soil profile with USCS classification and the actual number of blows (N) from SPT boring B-101 near pier 2/pile 5 at ramp B of I-4/SR 408

### 3.2.4.4. CPTu Data

A CPTu penetration test, CPT B-109, was conducted 75 ft from test pile 5 within the second pier of ramp B at I-4/SR 408. The CPT sounding extended to a depth of 92.5 ft below GSE. The data was presented versus depth as illustrated in Figure 3-19. There are no HPR zones highlighted because this site was considered a non-rebound site.

The plots in Figure 3-19 show that  $q_c$  ranges from 30 to 120 tsf, and  $f_s$  ranges from 0.25 tsf to 0.75 tsf. The  $u_2$  profile shows that it rapidly increased at 55 ft and remained above the hydrostatic pressures to the end of the sounding at 92.5 ft. Comparing this data to the PDA in Figure 3-17 shows that an increase in  $N_{PD}$  from 25 to 50 blows/ft also occurred from 55 ft to 92.5 ft, while the pile rebound averaged an acceptable 0.25 inch/blow.

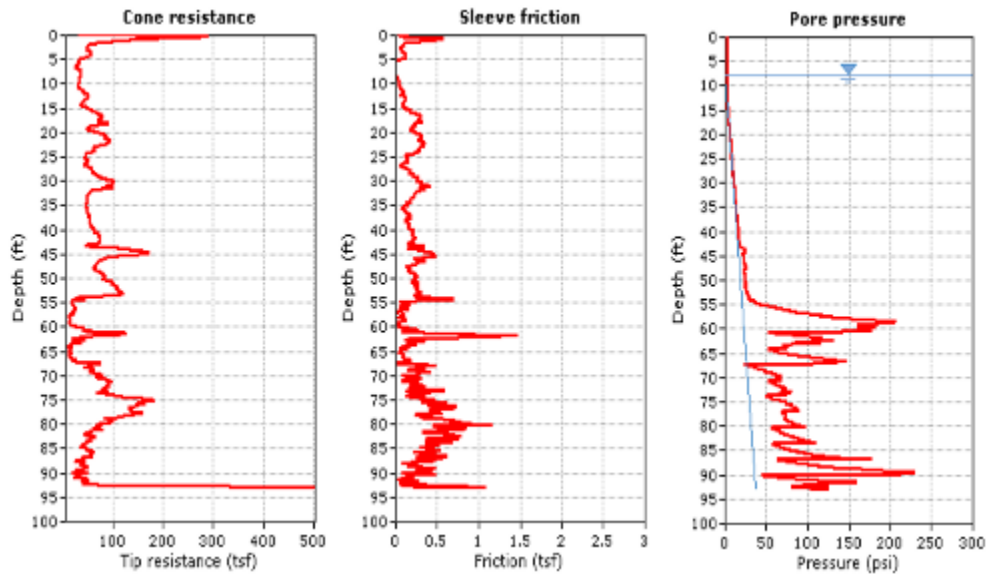


Figure 3-19: CPTu  $q_c$ ,  $f_s$ , and  $u_2$  versus depth from CPT B-109 near pier 2/pile 5 at ramp B of I-4/SR 408

### 3.2.5. Anderson Street Overpass

#### 3.2.5.1. General Description and Field Testing Locations

The Anderson street overpass is located at the intersection of Interstate 4 (I-4) and State Road 408 (SR408), in downtown Orlando, Orange County, Florida. The GSE is 104 ft (NAVD88) and the GWT is located at 6 ft to 8 ft from GSE. Six piers and two end bents support the bridge, which was constructed using 24-inch square PCPs, 124 ft in length. Two piles at pier 6, piles 5 and 6, were selected as test piles. The piles were installed in predrilled holes (10 ft and 30 ft respectively) and driven with a Delmag D62 single-acting diesel hammer with a rated energy of 90 ft-kips (122 kJ). Plywood cushions of 12 or 16 inches thick, respectively, were used during driving. An SPT boring and a CPTu sounding were conducted 100 ft from the test piles, as shown in Figure 3-20.



Figure 3-20: Test piles, SPT boring, and CPTu sounding locations for the Anderson Street overpass

### 3.2.5.2. PDA Data and Identification of HPR Zones

At the Anderson Street overpass, test piles 5 and 6 at pier 6 were driven with PDA sensors producing the data shown in Figure 3-21 (a) and (b), respectively. Rebound below 0.5 inches occurred from start of driving until 90 ft. The corresponding pile, set above 90 ft, ranged from 0.7 to 2 inches/blow. At 90 ft, the rebound increased significantly to values up to 1.5 inches with a decrease in the corresponding set to nearly zero inch/blow. Figure 3-21 shows that the non-rebound zone above 90 ft produced an average  $N_{PD}$  of about 20 blows/ft while the rebound zone below 90 ft had elevated  $N_{PD}$  values as high as 365 blows/ft.

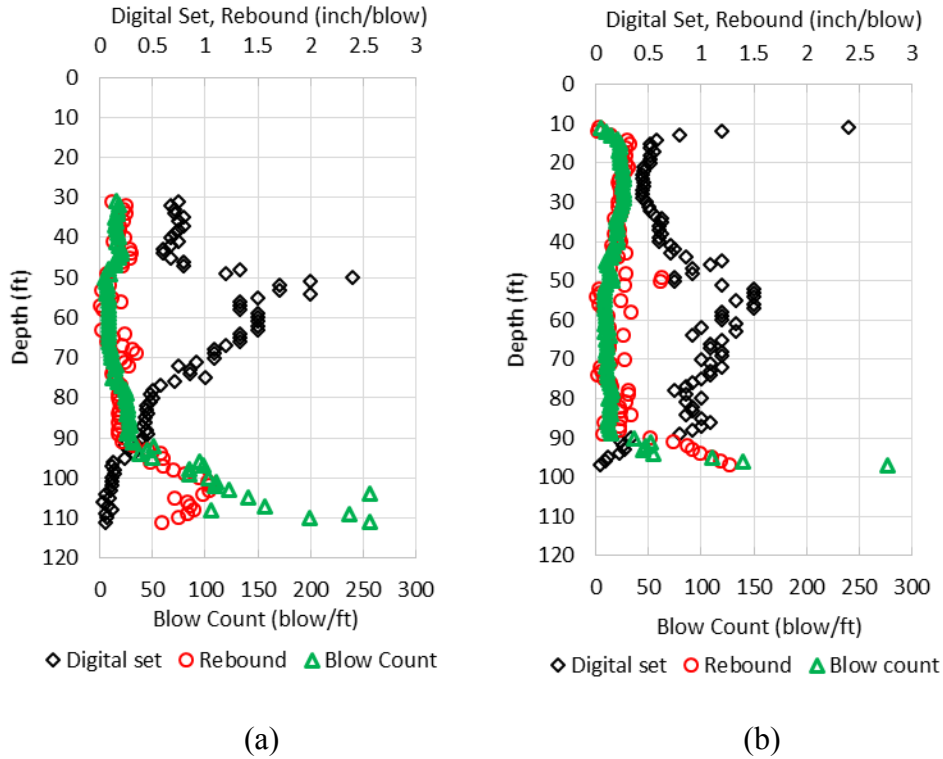


Figure 3-21: Digital set, pile rebound, and  $N_{PD}$  versus depth for (a) pier 6/pile 6 and (b) pier 6/pile 5 at the Anderson Street overpass

### 3.2.5.3. SPT Data and General Soil Profile

SPT P6-3 boring was driven 104 ft from GSE and was 40 ft from test piles 5 and 6 at pier 6 at the Anderson Street overpass. The predrilling depth for this boring was 7 ft and the test extended to a depth of approximately 120 ft from GSE.  $N_{SPT}$  was recorded and is presented versus depth in Figure 3-22.  $N_{SPT}$  at between 7 ft and 90 ft had an average of 10 blows/ft then increased to 40 blows/ft at a depth of more than 90 ft. The general soil profile was developed as shown in Figure 3-22. Three different soils, silty clayey fine sand (SM/SC), clayey fine sand (SC), and clay (CH), exist within the rebound zone (90 ft to 110 ft)

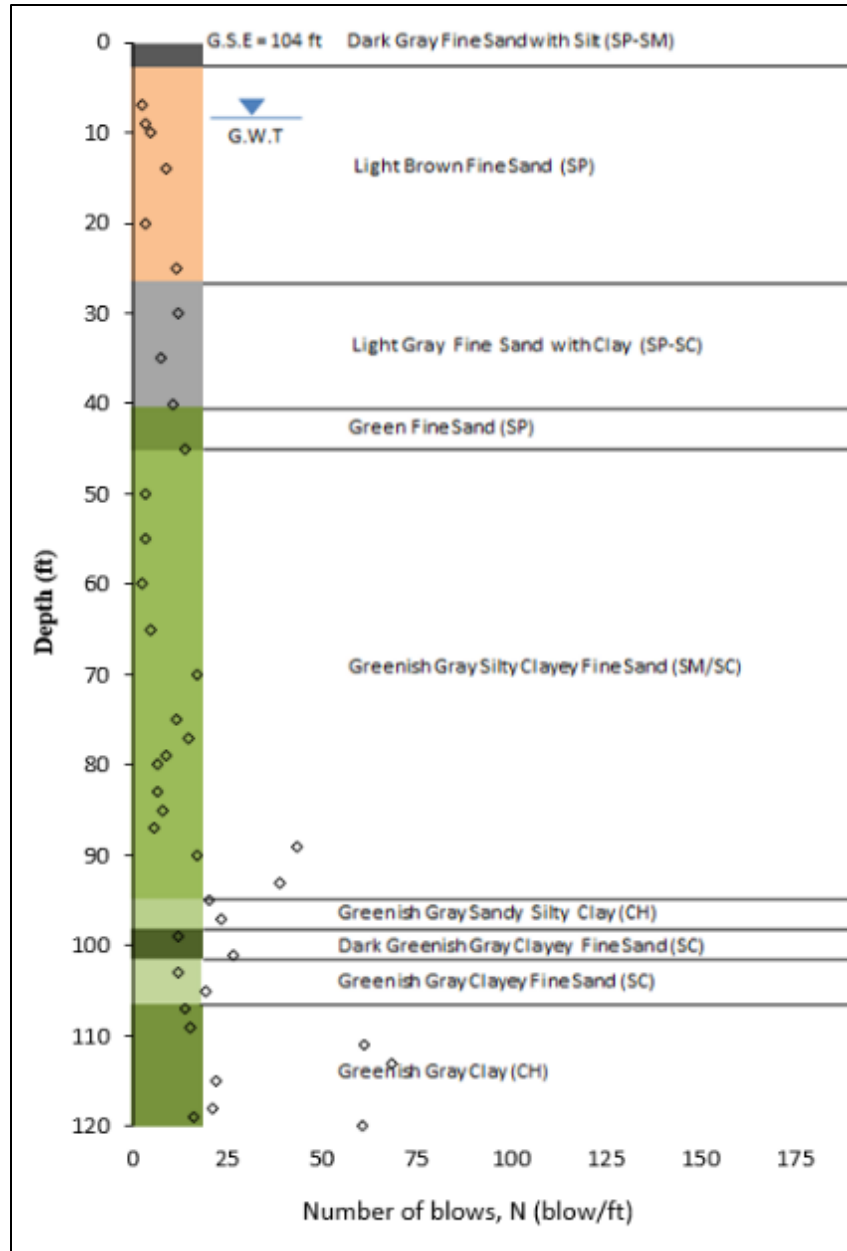


Figure 3-22: General soil profile with USCS classification and the actual  $N_{SPT}$  from SPT boring SPT P6-3 near pier 6 at the Anderson Street overpass

### 3.2.5.4. CPTu Data

The CPTu-5 sounding was conducted about 100 ft from pier 6 at the Anderson Street overpass. The CPTu sounding extended to a depth of 92 ft below GSE. The data collected was presented versus depth, as illustrated in Figure 3-23. By matching this data with the PDA presented in Figure 3-21, the rebound zone was identified at a depth of 90 ft to 110 ft. Therefore; no conclusion can be made in the rebound zone because the CPTu sounding was terminated at

the starting point of the rebound zone. However, the CPTu data were used and discussed as a non-rebound CPTu data.

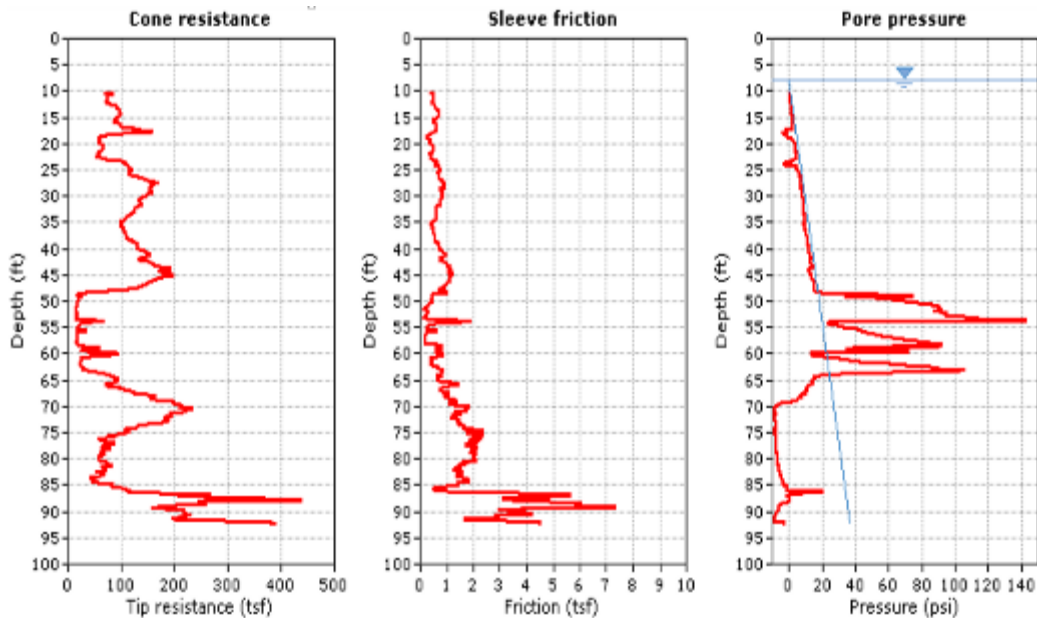


Figure 3-23: CPTu  $q_c$ ,  $f_s$ , and  $u_2$  versus depth from CPT-5 near pier 6 at the Anderson Street overpass

### 3.2.6. I-4 Widening Daytona

#### 3.2.6.1. General Description and Field Testing Locations

The I-4/Deer Wildlife crossing is located in Daytona, Volusia County, Florida. The approximate GSE is 42 ft (NAVD88) and the GWT is located at 7 ft below the GSE. The site consists of three end bents (EB-1, EB-2, and EB-3). PCPs were used to support the bridges at this site. Test pile 5, 24-inch square PCP, 115 ft long, was located at EB-3 and was driven with an APE D46-42 S single-acting diesel hammer with a rated energy of 114.11 ft-kips. The plywood pile cushion was 14 inches thick. The pile installation began with the predrilling process 33 ft below the GSE. The test pile was driven 63 ft through the soil, yielding a total pile penetration below the ground of 96 ft. An SPT boring and a CPT sounding were performed 56 ft from the test pile. The general site location and the approximate field-testing locations are shown in Figure 3-24.



Figure 3-24: Test piles, SPT boring, and CPTu sounding locations for I-4 Widening Daytona

### 3.2.6.2. PDA Data and Identification of HPR Zones

The I-4 Widening Daytona PDA data collection started at 45 ft, as can be seen in Figure 3-25. A high rebound zone was found from 80 to 90 ft where the rebound increases up to 0.5 inch/blow with a corresponding average set of up to 0.25 inch/blow. Below a depth of 90 ft, the rebound decreased to below 0.25 inch/blow. In Figure 3-25, a noticeable increase in  $N_{PD}$  occurred from an average of 35 blows/ft in the non-rebound zone up to 150 blows/ft in the rebound zone.

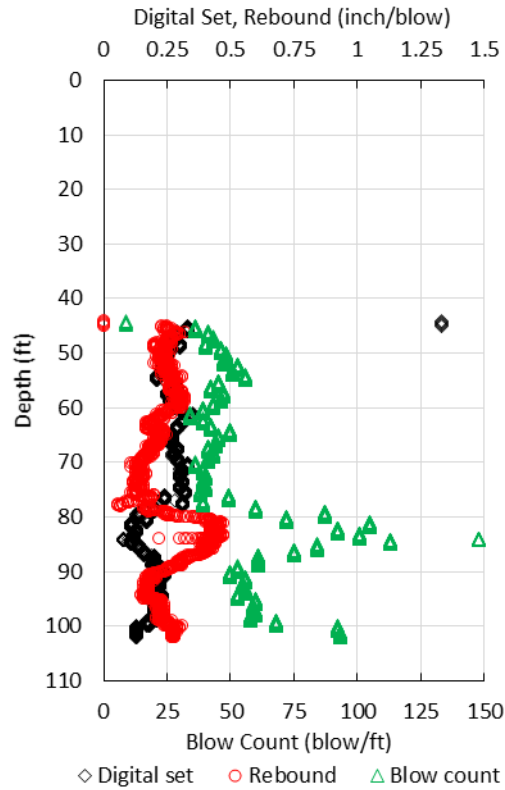


Figure 3-25: Digital set, pile rebound, and  $N_{PD}$  versus depth for EB3/pile 5 at I-4 Widening Daytona

### 3.2.6.3. SPT Data and General Soil Profile

Standard penetration test boring DC-1 at the I-4 Widening Daytona site was 56 ft from test pile 5, located at the third end bent of the bridge. The boring GSE was 109.6 ft. The SPT boring extended to a depth of 110 ft. Figure 3-26 presents the  $N_{SPT}$  versus depth. In the upper 62 ft, the average  $N_{SPT}$  was 12 blows/ft.  $N_{SPT}$  increased to values over 100 near 90 ft. The soil in the rebound zone (i.e., 80 to 90 ft) had  $N_{SPT}$  values increasing from 12 to 50 or higher and was classified as SM silty fine sand with trace shell.

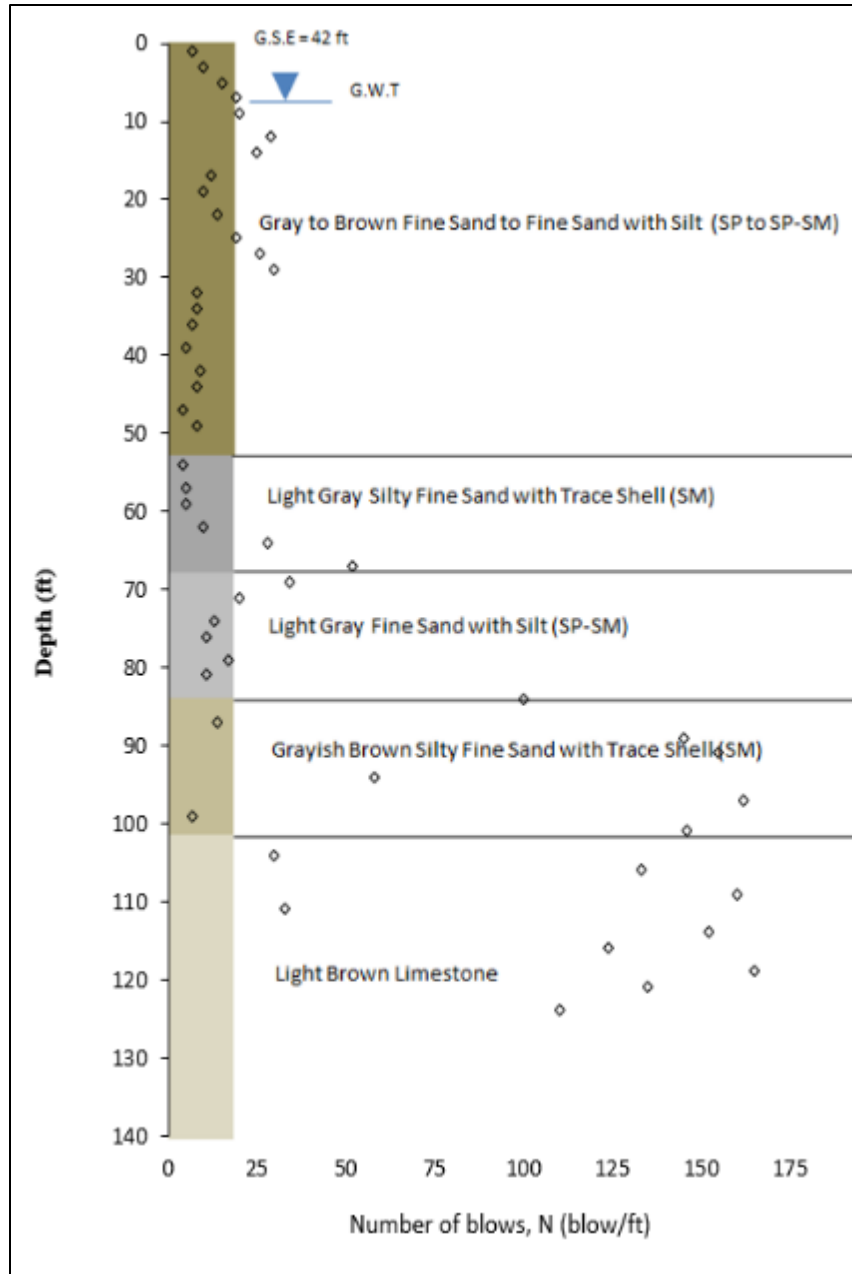


Figure 3-26: General soil profile with USCS classification and the actual  $N_{SPT}$  from SPT boring SPT DC-1 near EB3/pile 5 at I-4 Widening Daytona

#### 3.2.6.4. CPTu Data

A CPT sounding was conducted about 56 ft from the test pile 5 EB3 of location I-4 Widening Daytona. The CPT sounding extended to a depth of 71.5 ft below the GSE. The collected data was presented versus depth, as illustrated in Figure 3-27. By matching with the PDA presented in Figure 3-27, the rebound zone was identified at a depth of 80 ft. Therefore, no

conclusion can be made in the rebound zone because the CPT sounding was terminated before the start point of the rebound zone. However, the CPT data were used and discussed as a non-rebound CPT data.

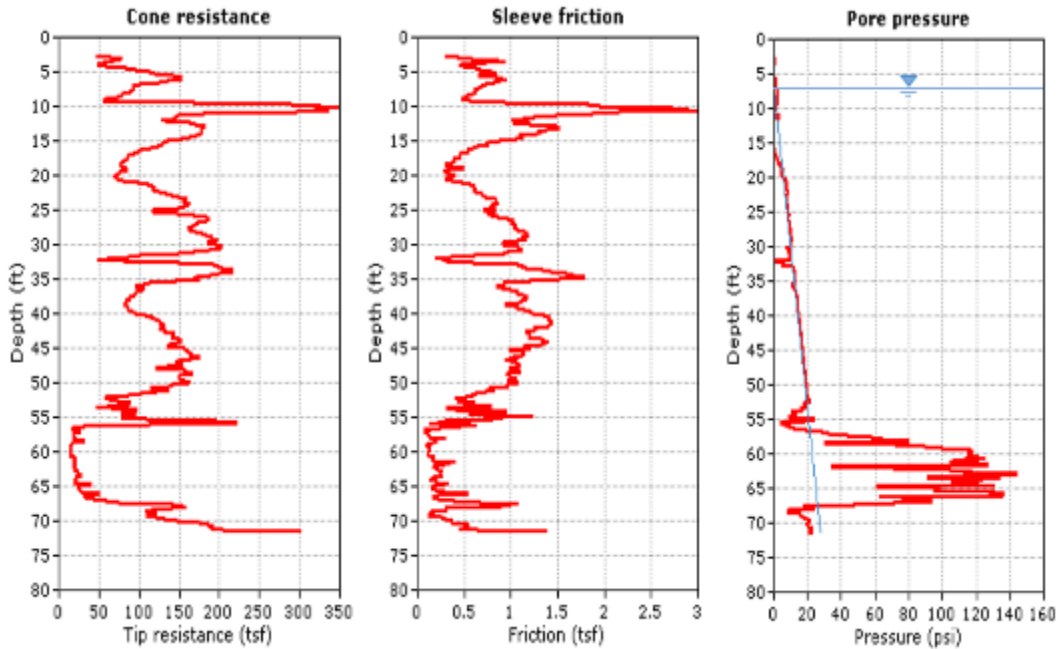


Figure 3-27: CPTu  $q_c$ ,  $f_s$ , and  $u_2$  versus depth near EB3/pile 5 at I-4 Widening Daytona

### 3.2.7. State Road 83 over Ramsey Branch Bridge

#### 3.2.7.1. General Description and File Testing Locations

Ramsey Branch Bridge is located north of the intersection of SR 83 (US 331) and Ramsey Branch Road in Walton County, Florida. The GSE at the site is 1 ft (NAVD 88) and the GWT is located at 1 ft below the GSE. The bridge consists of three middle bents and two end bents. The end bents EB1 and EB5 consist of four 24-inch square PCPs, while the middle bents (EB2, EB3, and EB4) consist of six 24-inch square PCPs. Pile 2 at end bent 5 was selected as a test pile for the analysis. Pile installation began with predrilling the soil to 33 ft below GSE followed by pile driving approximately 57 ft. An APE D50-42 S single-acting diesel hammer with a 15-inch thick plywood cushion was used for pile driving with a rated energy of 115.6 ft-kips. Two CPT tests, CPT-1 and CPT-2, and three SPT borings, B-1, B-2, and B-3, were conducted at the site. Figure 3-28 shows the overall view of the site and the field-testing locations.

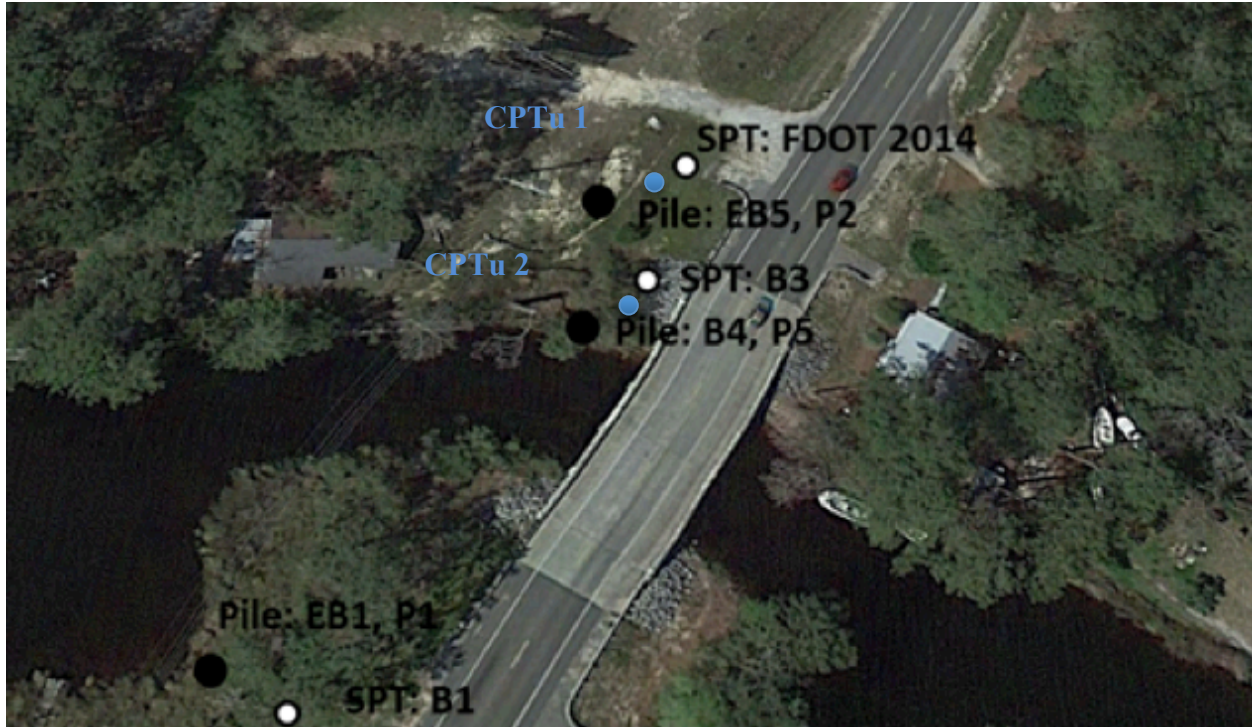


Figure 3-28: Test pile, SPT boring, and CPTu soundings locations for SR 83/Ramsey Branch Bridge

### 3.2.7.2. PDA and Identification of HPR Zones

The PDA data is shown in Figure 3-29 for the State Road 83 over Ramsey Branch Bridge. All the test depths produced a rebound greater than 0.25 inch/blow; therefore, the entire driving depth is the HPR zone. The maximum rebound of 1.3 inches/blow occurred at depths of 33 ft and 62 ft. The corresponding set was 1 to 0.15 inch/blow, respectively.  $N_{PD}$  of 100 and 150 blows/ft occurred at the depths 40 feet and 63 feet respectively. Figure 3-29 shows that the zone from 63 to 76 feet has HPR from about 0.3 to 1.5 inches/blow, with most of the values near 1 inch. Also the pile set remained below 0.15 inch/blow.  $N_{PD}$  increased from 12 to 150 blows/ft within this range. Therefore, the most critical HPR zone exists between 63 and 76 feet.

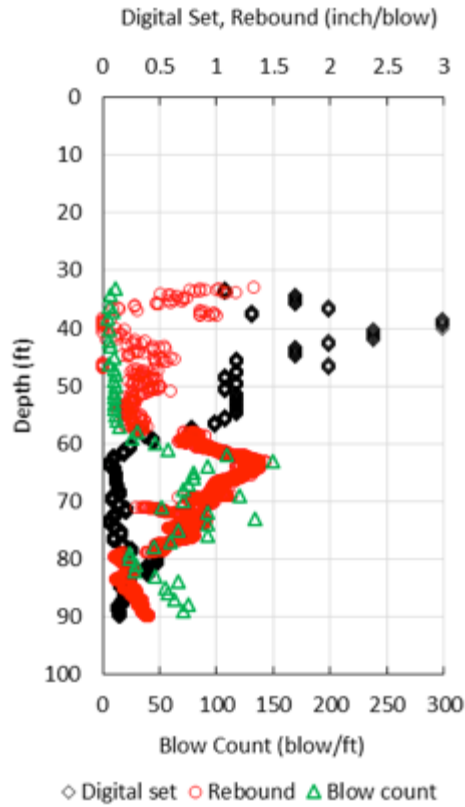


Figure 3-29: Digital set, pile rebound, and  $N_{PD}$  versus depth for EB5/pile 2 at SR 83/Ramsey Branch Bridge

### 3.2.7.3. SPT Data and General Soil Profile

The SPT boring B-3 with a 1.0 ft GSE was driven at a distance of 60 ft away from the test pile 2 at end bent 5 of the location State Road 83 over Ramsey Branch Bridge. This boring was drilled approximately to 100 ft from GSE.  $N_{SPT}$  was recorded and presented versus depth, as illustrated in Figure 3-30. The soil in the rebound zone (i.e., 63 to 76 ft) was classified as cemented clayey fine sand (SC).

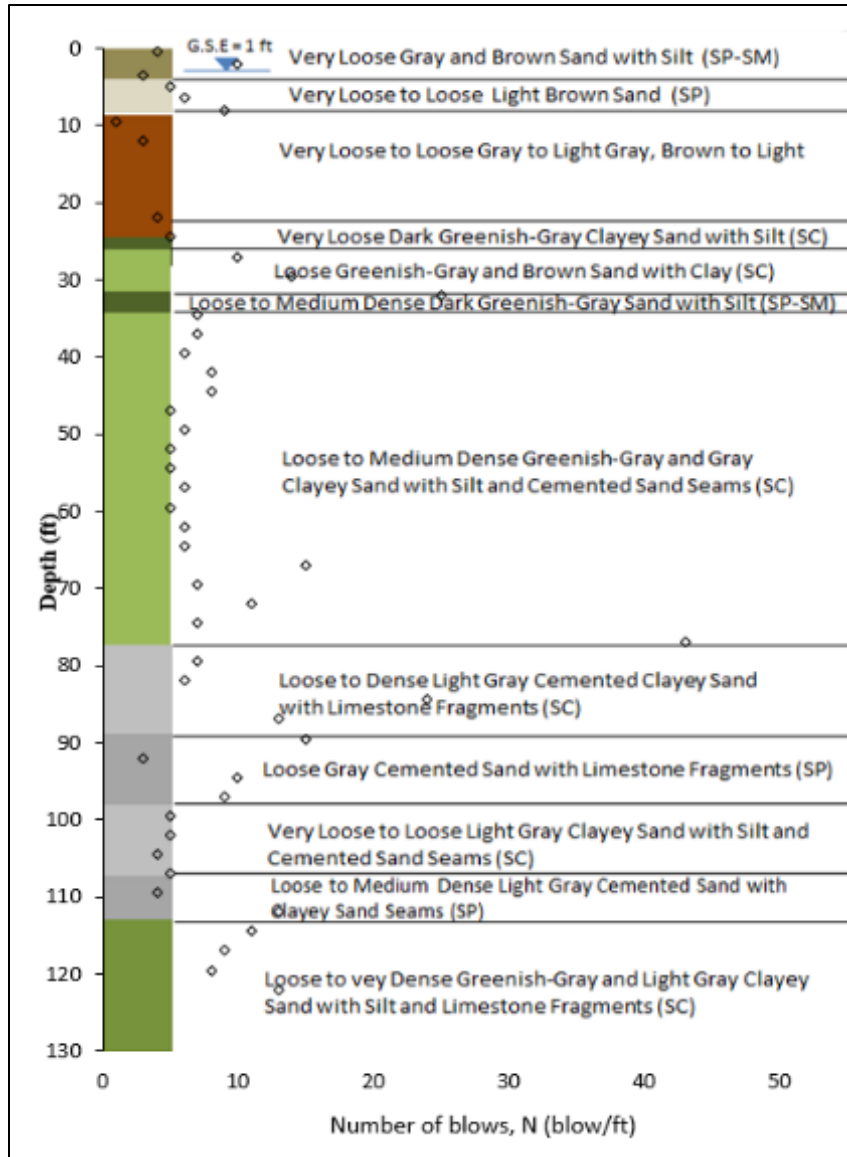


Figure 3-30: General soil profile with USCS classification and the actual  $N_{SPT}$  from SPT boring B-3 near EB5/pile 2 at SR 83/ Ramsey Branch Bridge

### 3.2.7.4. CPTu Data

Two CPT soundings, CPT-1 and CPT-2, were conducted about 28 ft north EB5/pile 2 at SR 83/Ramsey Branch Bridge. The soundings extended to an average depth of 77 ft. The data was presented versus depth as illustrated in Figure 3-31 and Figure 3-32. The rebound zones at all the test piles were highlighted in the CPT profiles in order to identify if there is any difference in the measured CPT parameters (i.e.,  $q_c$ ,  $f_s$ , and  $u_2$ ) at the rebound zones.

Figure 3-31 and Figure 3-32 show that the cone resistance had an average of 50 tsf at the zone from the GSE to 62 ft and then increased to an average of 250 tsf below 62ft. CPTu  $f_s$  fluctuated from 0.5 to 3.5 tsf through all depths. Inspecting the CPTu  $u_2$  profiles, shown in Figure 3-31 and Figure 3-32, shows that a significant increase in  $u_2$  started at 40 ft and ended near 74 ft. The pore water pressure increased from 1 psi to 570 psi within a vertical distance of about 5 ft.

### **3.2.8. Saint Johns Heritage Parkway, Brevard County, Florida**

#### **3.2.8.1. General Description and File Testing Locations**

The Saint Johns Heritage Parkway (Heritage Parkway) is located north of SR 514 Malabar Road, about 5 miles west of Interstate 95 in Brevard County, Florida. The GSE under the bridge is 17.12 ft (NAVD 88) and the GWT is located 15 ft below the GSE. The bridge consists of three middle bents and two end bents. The end bents EB1 and EB5 consist of seven 18-inch square PCPs while the middle bents (EB2, EB3, and EB4) consist of ten 18-inch square PCPs. Pile 5 at end bent 1 and pile 1 bent 3 were selected as a test piles. Pile installation began with predrilling the soil to 23 ft below the GSE with a 24 auger, followed by pile driving to elevation -90 ft. APE's D36-32 single-acting diesel hammer with a rated energy of 88.375 ft-kips with a 12 inch thick plywood cushion was used for pile driving. A series of CPTu tests and two SPT borings, TH-5, and TH-6, were conducted at the site (See Figure 3-33).

#### **3.2.8.2. PDA and Identification of HPR Zones**

At Heritage Parkway, the PDA results shown in Figure 3-34 indicate that a rebound greater than 0.25 inch/blow occurs between 32 and 50 ft; however, the maximum rebound is only about 0.5 inches. The remaining pile driving produced acceptable sets. This site is considered a rebound site with acceptable set.

#### **3.2.8.3. SPT Data and General Soil Profile**

At Heritage Parkway, the SPT results, shown in Figure 3-34, indicate an increase in  $N_{ES}$  at the same depths that rebound increased. The soils in this zone are cemented SM and SP-SM sands. FC values were in the 25% range.

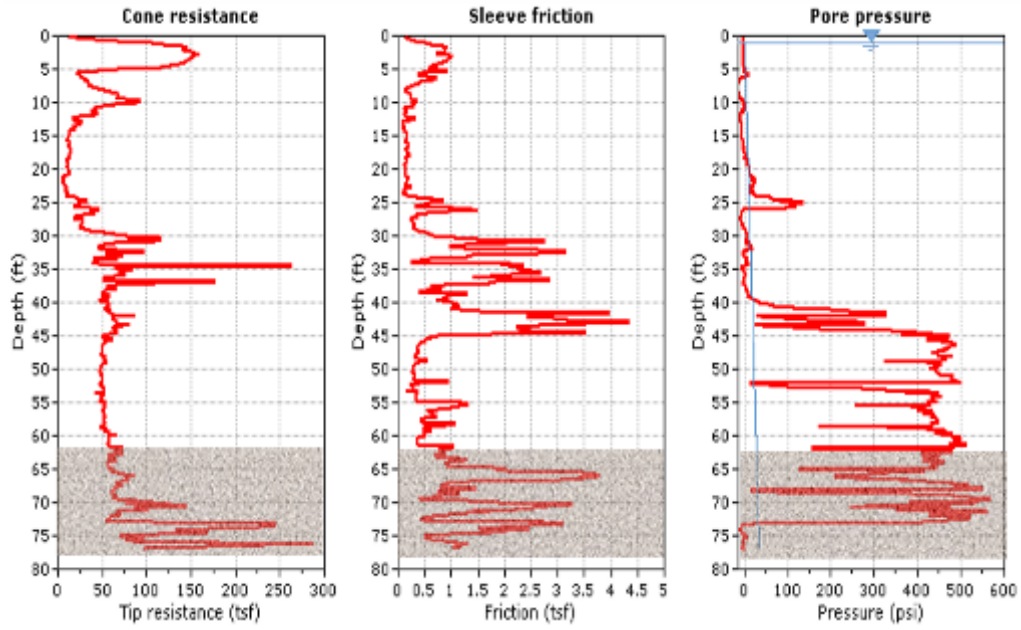


Figure 3-31: CPTu  $q_c$ ,  $f_s$ , and  $u_2$  versus depth from CPT-1 near EB5/pile 2 at SR 83/ Ramsey Branch Bridge

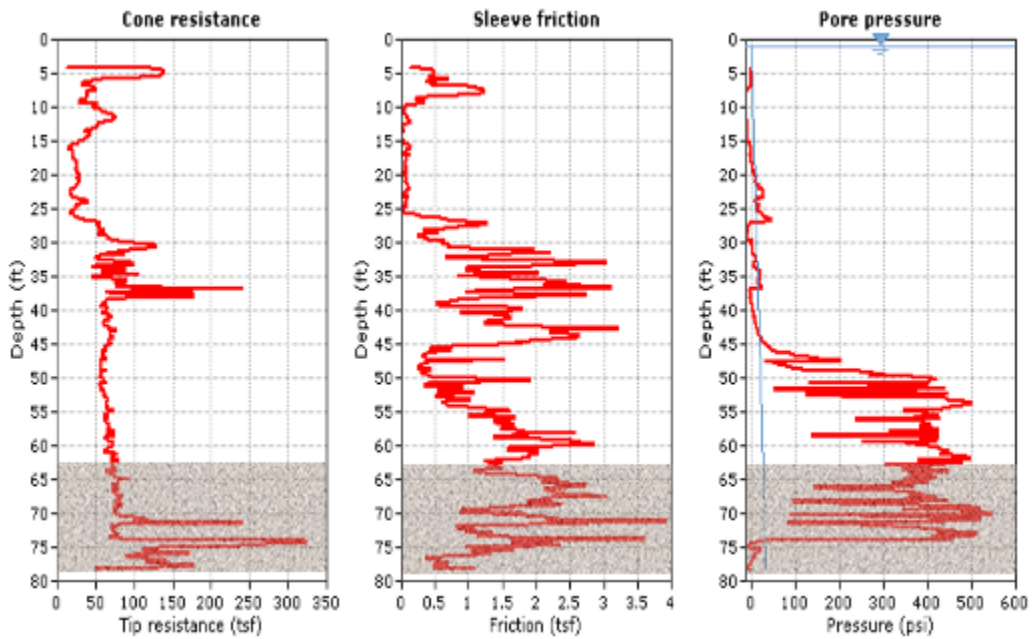


Figure 3-32: CPTu  $q_c$ ,  $f_s$ , and  $u_2$  versus depth from CPT-2 near EB5/pile 2 at SR 83/Ramsey Branch Bridge

### 3.2.8.4. CPTu Data

At Heritage Parkway, the CPTu testing was problematic. Gray sand with silt and abundant shell (Figure 3-34) prevented the CPTu cone from being advanced throughout the entire profile. Therefore, CPTu testing was attempted twice. The first time data was only obtained to a depth of about 35 feet, which was the beginning of the problematic layer of sand with silt and shell (Figure 3-34). The second attempt, which produced CPTu soundings to about 85 feet, was accomplished by predrilling through this shell layer to a depth of 55 feet before testing. As a result of the two-part CPTu testing, no data could be obtained in the rebound zone (i.e., between about 35 and 55 feet); therefore, this data was not included in the analyses. To construct CPTu data versus depth, the upper CPTu data was combined with the lower data. Figure 3-35 shows the combined  $q_c$ ,  $f_s$ , and PWP versus depth. A large increase in PWP occurs in the 60-foot zone; however, rebound did not increase in this same zone, as shown in Figure 3-34.

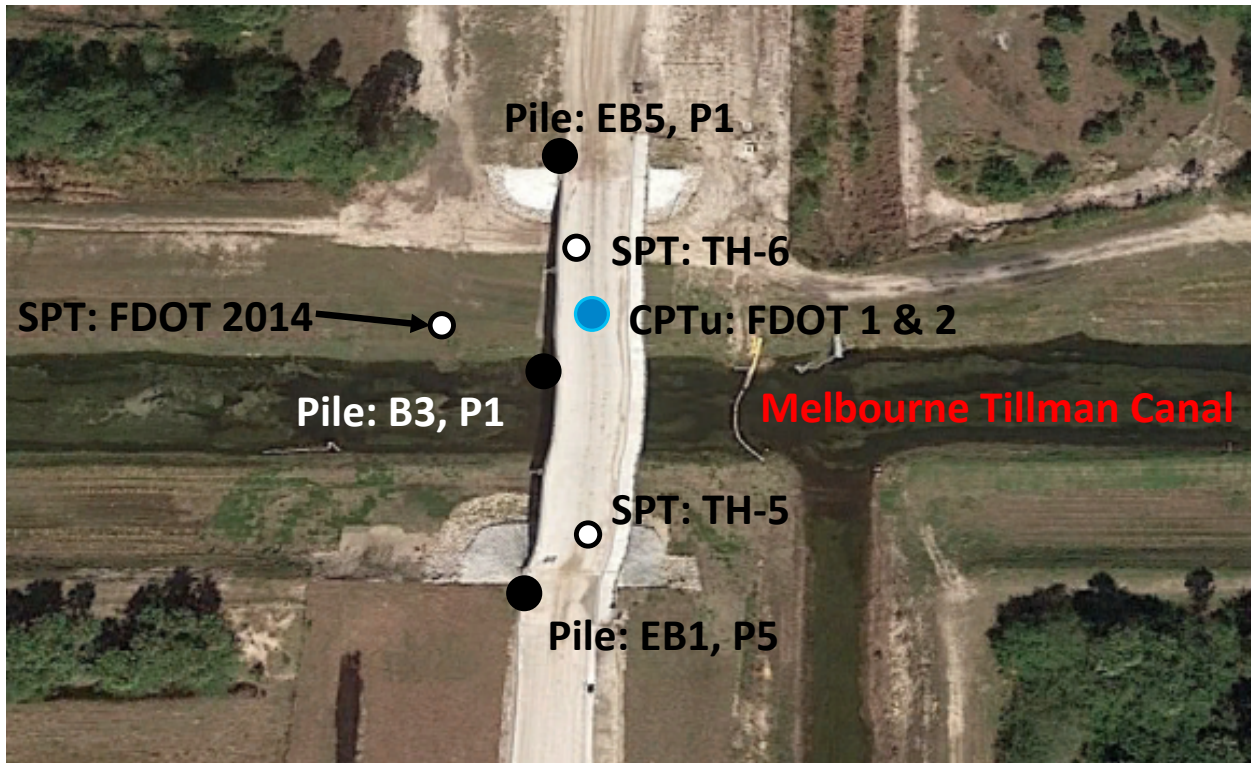


Figure 3-33: Site Location and test pile, SPT boring and CPTu sounding locations for Heritage Parkway, Brevard County, Florida

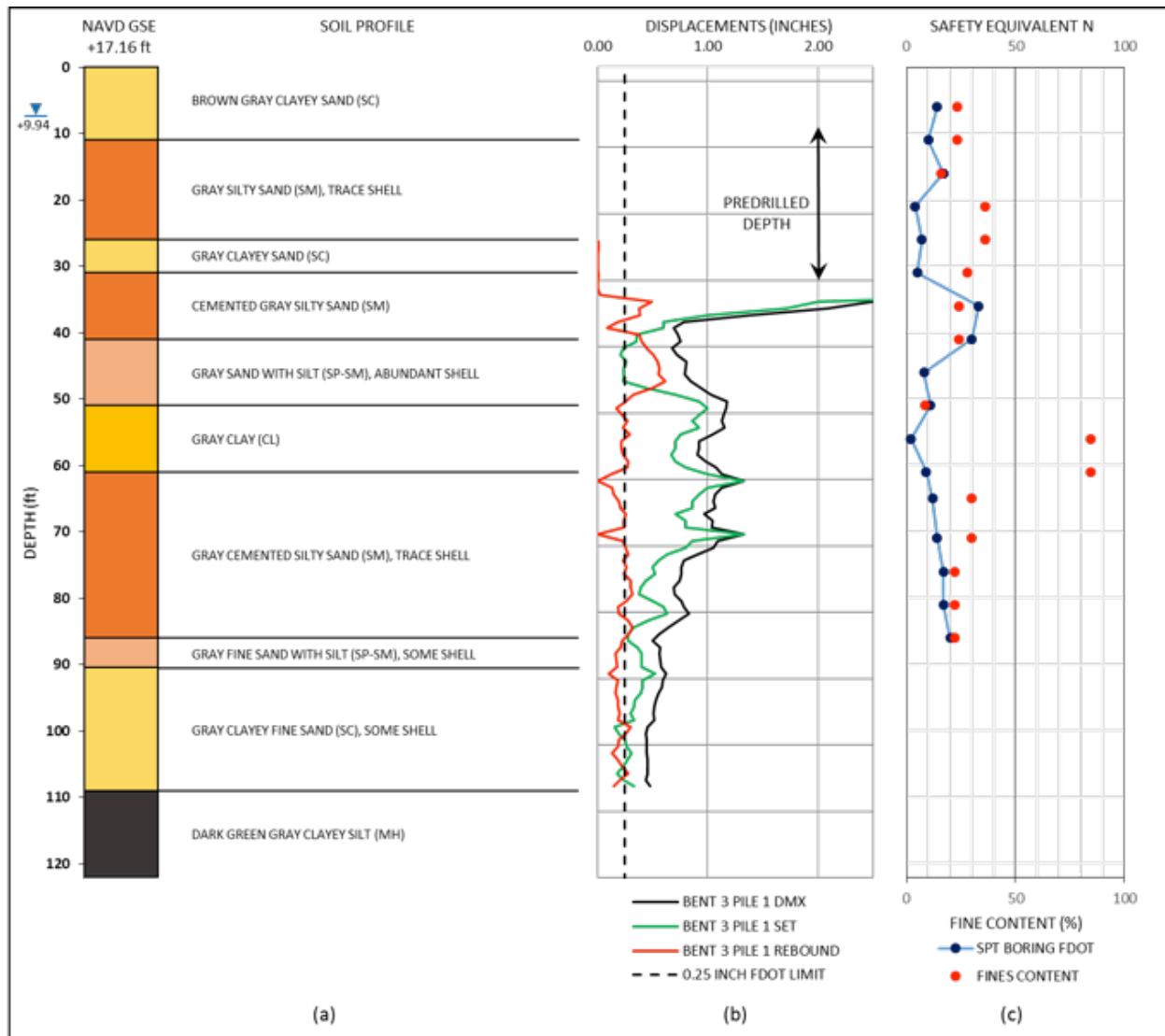


Figure 3-34: (a) FDOT and TH-6 soil profile, (b) PDA diagram, (c)  $N_{safe}$  and FC for Heritage Parkway test pile B3P1

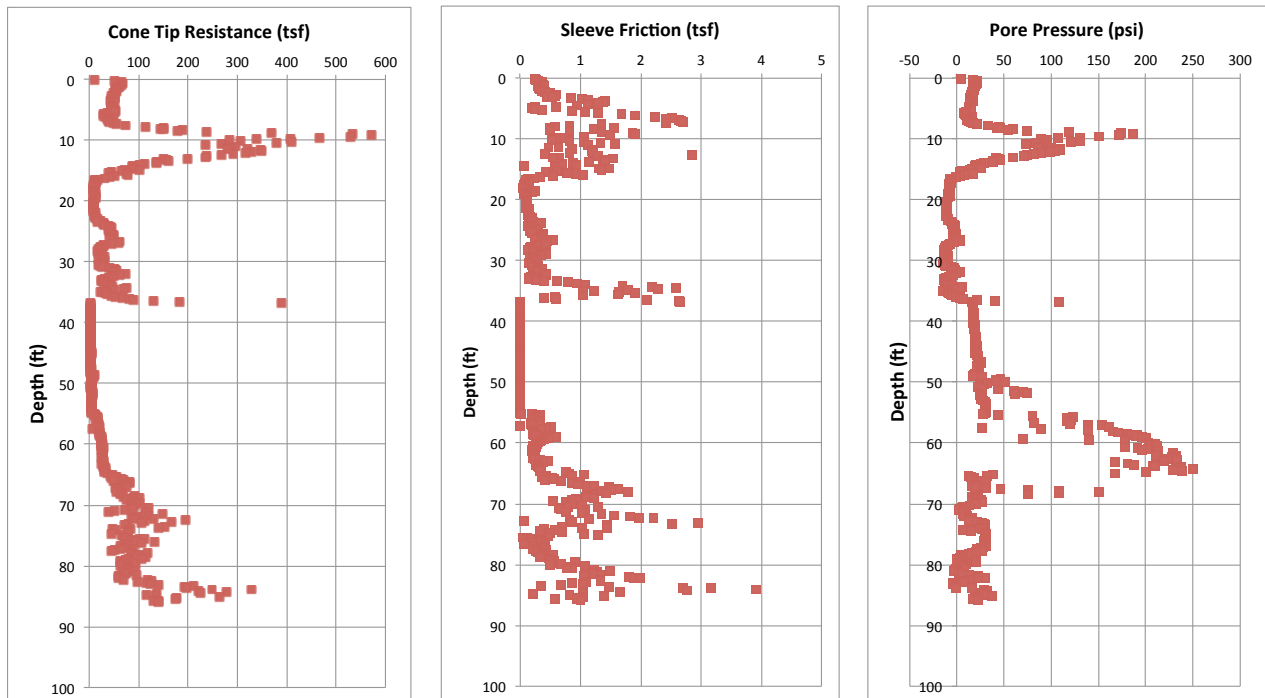


Figure 3-35: Combined CPTu Data from Heritage Parkway

### 3.2.9. I-10 Chaffee Road, Duval County, Florida

#### 3.2.9.1. General Description and File Testing Locations

The I-10 Chaffee Road Interchange is located west of downtown Jacksonville, about five miles west of Interstate 95 in Brevard County, Florida. The GSE of the site is 63.08 ft (NAVD 88) and the GWT is located 5 ft below GSE. The bridge consists of three middle bents and two end bents. The end bents EB1 and EB5 consist of four 18-inch square PCPs while the middle bents (EB2, EB3, and EB4) consist of six 18-inch square PCPs. Pile 5 at end bent 1 and pile 1 bent 3 were selected as a test piles. Pile installation began with predrilling the soil to 33 ft below the GSE followed by pile driving approximately 89 ft. A Pileco D35-22 single-acting diesel hammer with a 12-inch thick plywood cushion was used for pile driving. A CPT (note: no pore pressures were included test was attempted and only could be advanced 12 feet from GSE (Figure 3-36). One SPT boring was conducted at the site (Figure 3-36).



Figure 3-36: Site location, SPT boring and CPT sounding for I-10 Chaffee Road Interchange, Duval County, Florida

### 3.2.9.2. PDA and Identification of HPR Zones

At the I-10 Chaffee Road Interchange, the test depths below 45 feet produced a rebound greater than 0.25 inch/blow, with maximum rebounds near 2.0 inches/ blow. However, the iSet was large enough (i.e., between 2 to 4 inches) to allow the pile to penetrate adequately during installation. This site is considered an HPR with acceptable set.

### 3.2.9.3. SPT Data and General Soil Profile

The SPT boring with a 63.08 ft GSE was placed 60 ft away from the test pile 2 at end bent 5 of the I-10 Chaffee Road Interchange. This boring was extended to a depth of approximately 100 ft.  $N_{SPT}$  was recorded and is presented versus depth in Figure 3-37. The  $N_{SPT}$  values decreased to near zero in the HPR zone. The soils in the rebound zone (i.e., 45 to 80 ft) were mostly classified as clayey fine sand (SC) or sandy clay (CH). Limited FC data from indicate a very high value (i.e., 94% at 49.5 ft).

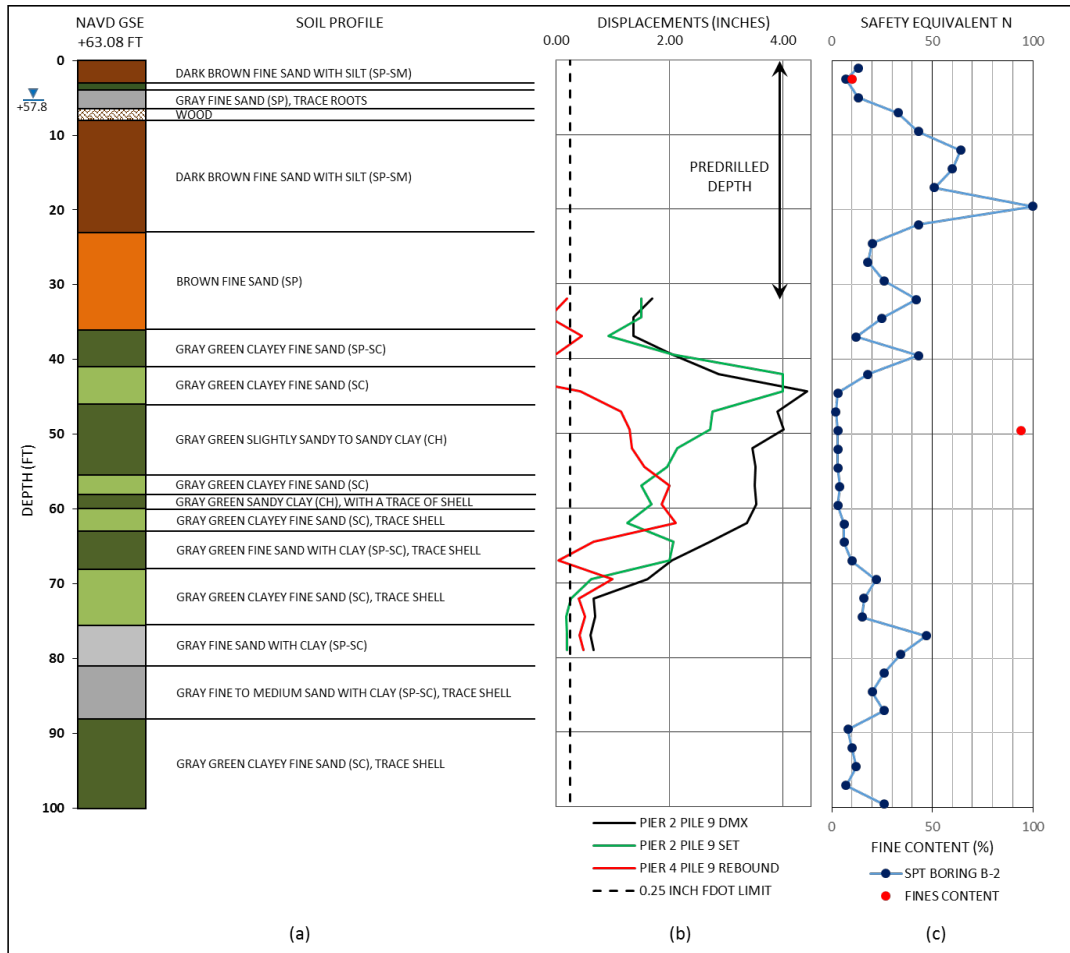


Figure 3-37: (a) Soil Profile, (b) PDA diagram, (c)  $N_{safe}$  and FC for I-10 Chaffee Road Interchange test pile B3 EB 1

### 3.2.9.4. CPTu Data

A CPT sounding was conducted to a depth of 12 feet. This testing did not produce enough data for further analysis and therefore is not included.

## 3.3. Summary of All Field Testing Results

The SPT data shows that seven major soil types were found at all the sites:

1. Clayey sand with and without trace shell (SC)
2. Silty sand soil with and without trace phosphate and shell (SM)
3. Clay (CH)
4. Poorly graded fine sand (SP)

5. Poorly graded fine sand with silt (SP-SM)
6. Fine sand with clay (SP-S(C))
7. Silty clayey fine sand (SM-S(C)).

All soils in the rebound zones are characterized as clayey fine sand (SC) or silty fine sand (SM) with trace phosphate and shell.

Measured CPT  $u_2$  profiles show an excellent relationship between measured pore pressure during CPT soundings and pile rebound. Generally, CPT pore water pressure was found to increase rapidly from low values up to 570 psi within a vertical distance of 5 ft to 10 ft. The rapid jump in pressure started at the same depth as the measured increase in soil rebound. The highlighted zones with HPR up to 1.5 inches/blow and blow counts from 100 to 300 blow/ft are characterized by elevated pore pressures up to 570 psi, which is noticeably higher than that in the zones of rebound less than 0.25 inch/blow and blow count less than 50 blow/ft.

The field-testing data is summarized in Table 3-2 for all locations. It shows some differences between the HPR and nonHPR data; with higher values in the rebound zone than nonHPR zone. Because the CPTu equipment could not penetrate the deeper strata, cone data could not be recorded in the rebound zones for two of the seven sites. Table 3-3 shows the overall average PDA, SPT, and CPT data for the HPR and nonHPR soils. It more clearly shows that the HPR soils produced higher average rebound,  $N_{PD}$ ,  $N_{SPT}$ ,  $q_c$ ,  $f_s$  and  $u_2$  values, and lower inspector sets.

Table 3-2: Summary of Field Testing Data for all Locations

Location Name	Depth (ft.)	PDA Data			SPT Data		CPT Data		
		Rebound (inch/blow)	Inspector Set (inch/blow)	N <sub>PD</sub> (blow/ft.)	N <sub>SPT</sub>	USCS Soil Type	Cone resistance q <sub>c</sub> (tsf)	Sleeve friction f <sub>s</sub> (tsf)	Pore pressure u <sub>2</sub> (psi)
I-4 / US-192 Interchange	40 – 65	≤ 0.25	0.25 to 0.5	ave. 50	ave. 20	SP, SP-SM	100-300	0.1 – 1	0 – 5
	65 – 100	0.25 to 0.9	≤ 0.25	70 – 300	> 25	SM*	50 – 100	1 – 4	300 – 550
SR 417 International Pkwy	40 – 70	0.15	0.35 to 0.75	18 – 40	ave. 10	SP-SM, SM	50 – 100	ave. 0.5	10 – 50
	30 – 40	0.25 to 0.4	≤ 0.32	50 – 87	ave. 10	SM	50 – 300	0.5 – 2.5	ave. 5
	70 – 80				ave. 50	SM, SC	50 – 100	ave. 0.5	20 – 40
SR50 / SR436	55 – 70	0.05	up to 3.5	ave. 10	5 – 10	SP	50 – 200	0.2 – 0.5	0 – 25
	40 – 55	0.5	≤ 0.27	25 – 45	ave. 20	SM	50 – 150	1 – 1.5	ave. 25
	70 – 80	1	0.04-0.24	50 – 300	ave. 15	SM*, CH*	50 – 100	0.5 – 3	75 – 300
I-4 / SR 408 Ramp B	12 – 75	≤ 0.25	up to 1.5	15 – 45	5 – 10	SP, SP-SM	ave. 100	ave. 0.25	0 – 100
	75 – 80	0.3 to 0.4	0.2 to 0.35	50 – 88	10 – 20	SC	30 – 100	0.25 – 0.75	50 – 100
Anderson Street Overpass	10 – 90	≤ 0.25	up to 2.5	ave. 15	3 – 10	SP, SP-SM, SP-SC	100 – 200	1 – 2	0 – 100
	90 – 110	up to 1.0	0.05 to 0.15	50 – 365	10 – 20	SC*	STAR	STAR	STAR
I-4 Widening Daytona	45 – 55	≤ 0.25	0.25 to 0.35	ave. 45	3 – 10	SP, SP-SM	50 – 200	0.5 – 1.5	0 – 20
	55 – 73				10 – 25	SP-SM, SM	25 – 100	0.25 – 1	60 – 140
	80 – 90	0.25 to 0.5	≤ 0.25	50 – 150	> 50	SM*	STAR	STAR	STAR
SR 83 / Ramsey Branch Bridge	40 – 60	0.25 to 0.5	1.25	ave. 15	ave. 5	SC	ave. 50	0.5 – 1.5	100 – 450
	30 – 40	up to 1.5	0.05 to 0.25	50 – 150	ave. 5	SC	50 – 150	1 – 4.5	ave. 450
	60 – 90				5 – 10	SC*	50 – 200	1 – 3.5	

\*Cemented soil with trace phosphate and/or shell STAR: Sounding terminated above rebound zone

Table 3-3: Average Results for NonHPR and HPR Sites

Site Type	Depth (ft.)	PDA Data			SPT Data	CPT Data		
		Rebound (inch/blow)	Inspector Set (inch/blow)	Driving Blows (blow/ft.)	N <sub>SPT</sub>	Point Resistance q <sub>c</sub> (tsf)	Sleeve Friction f <sub>s</sub> (tsf)	Pore Pressure u <sub>2</sub> (psi)
Ave NonHPR	37-70	0.21-0.24	1.2-1.3	27-33	8-13	66-156	0.4-1.0	21-111
Ave HPR	61-77	0.36-0.81	0.2-0.3	50-172	20-23	48-150	0.7-2.5	172-240

## 4. Analysis of CPTu Field Testing Data

The CPTu, SPT and laboratory data analysis is presented in the following chapters. The CPTu analysis is presented first, followed by the SPT and then the laboratory analyses. Table 4-1 is a summary of the sites tested using both SPT and CPTu equipment.

### 4.1. Overview of the CPTu Analysis

HPR analyses focused on developing relationships with soil properties using data from all possible sites. The analysis of the CPTu data was performed to characterize the soil behavior type (SBT) of soils at seven of the HPR sites (Table 4-1). The CPTu data was used to develop a soil stratigraphy for each site. The following six-geotechnical soil properties were estimated using existing CPTu correlations:

1. Soil density
2. Permeability
3. Relative density
4. State parameter ( $e_{\text{initial}} - e_{\text{critical}}$ )
5. Over-consolidation ratio
6. Undrained shear strength

After each property was calculated, it was plotted versus depth to develop a complete profile for each site and identify the differences in these soil properties in the rebound and non-rebound zones.

Table 4-1 SPT and CPTu Testing Sites

Number	Description	Testing	
		SPT	CPTu
1	I-4 / US-192 Interchange / Osceola County / Florida	✓	✓
2	State Road 417 International Parkway / Osceola County / Florida	✓	✓
3	State Road 50 and State Road 436 / Orange County / Florida	✓	✓
4	I-4 / State Road 408 Ramp B / Orange County / Florida	✓	✓
5	Anderson Street Overpass at I-4/SR-408 / Orange County / Florida	✓	✓
6	I-4 Widening Daytona / Volusia County / Florida	✓	✓
7	State Road 83 over Ramsey Branch Bridge / Walton County / Florida	✓	✓
8	Saint Johns Heritage Parkway/ Brevard County	✓	
9	I-10 Chaffee Road/Duval County Florida	✓	

## 4.2. Estimation of Soil Stratigraphy Using CPTu Data

Licensed geotechnical software, CPeT-IT v.1.6 (2014), was used to process the CPTu data. Gregg Drilling and Testing, Inc., developed this software in collaboration with Peter Robertson. The normalized soil behavior type index ( $I_c$ ) proposed by Robertson (1990) was used in the correlations for the six parameters. CPeT-IT software inputs the CPT results for each site and outputs depth profiles for cone tip ( $q_c$ ), sleeve friction ( $f_s$ ), cone pore water pressure measured directly behind the cone tip ( $u_2$ ), and soil type profiles in addition to the six soil properties listed above and along with normalized soil behavior type charts.

In order to use the SBT charts, the total and effective overburden stresses were calculated. Therefore, the soil density was first estimated based on the non-normalized CPTu data using the following Robertson and Cabal (2010) correlation:

$$\gamma/\gamma_w = 0.27 [\log R_f] + 0.36 [\log(q_t/p_a)] + 1.236 \quad \text{Equation 4-1}$$

where

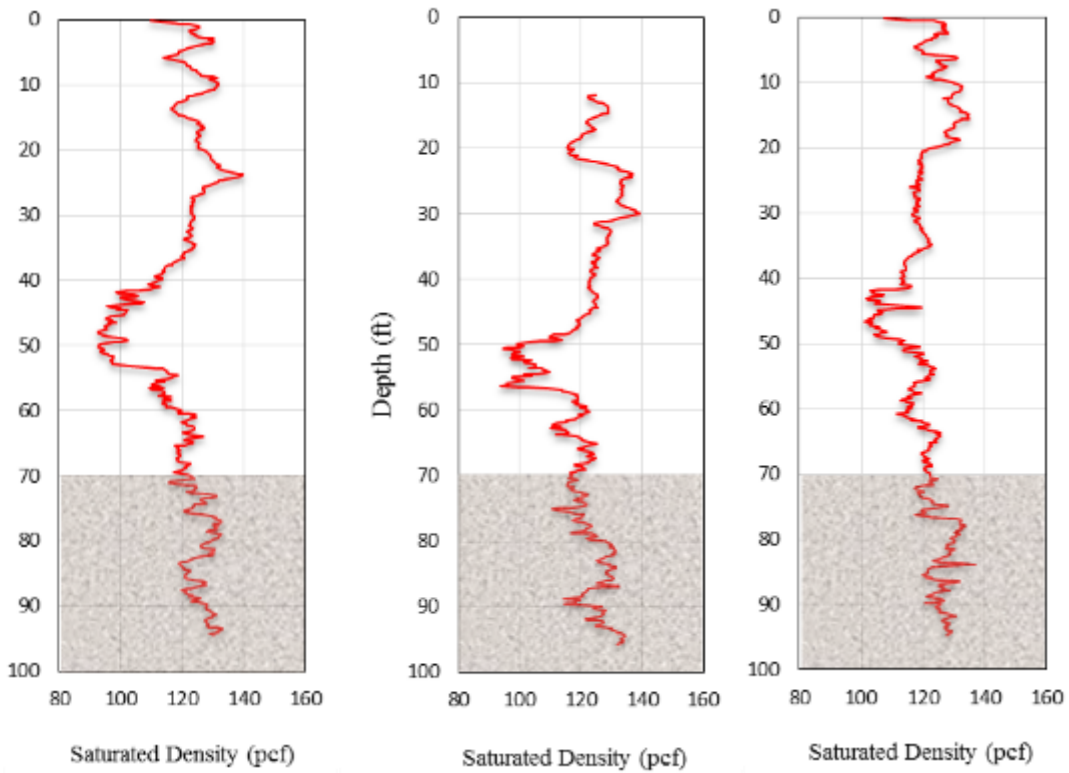
$R_f$  = measured cone friction ratio,  $R_f = (f_s/q_c) \times 100$

$q_t$  = corrected cone tip resistance for pore pressure =  $q_c + (1 - a_n)u_2$

$a_n$  = net area ratio for the cone, typical range between 0.70 and 0.85

$p_a$  = the atmospheric pressure in the same units of  $q_t$ .

The resulting estimated variation of soil density with depth for each of the seven sites is presented in Figure 4-1 to Figure 4-7. Using the associated PDA data, the rebound zones were highlighted in the density-depth distribution plots to better aid in the analysis. In general, a saturated soil density range between 80 and 130 lb/ft<sup>3</sup> exists throughout these profiles. A range from 115 to 130 lb/ft<sup>3</sup>, with an average soil density of 125 lb/ft<sup>3</sup>, exists in the rebound depths for all sites (Figure 4-1 to Figure 4-7). In order to verify the CPTu-based soil density in the rebound zones, the results were compared to the estimated soil density using SPT data. Using the SPT data, it was concluded that the number of blows in the rebound zones ranged from 15 to 35. For those N-values, the published saturated soil density ranges from 110 lb/ft<sup>3</sup> to 130 lb/ft<sup>3</sup>, with an average of 120 lb/ft<sup>3</sup> (Bowles, 1988). The CPTu saturated density of soils within the rebound zones is located in the upper limit of the published density range of 90-130 lb/ft<sup>3</sup> (Coduto, 2001).

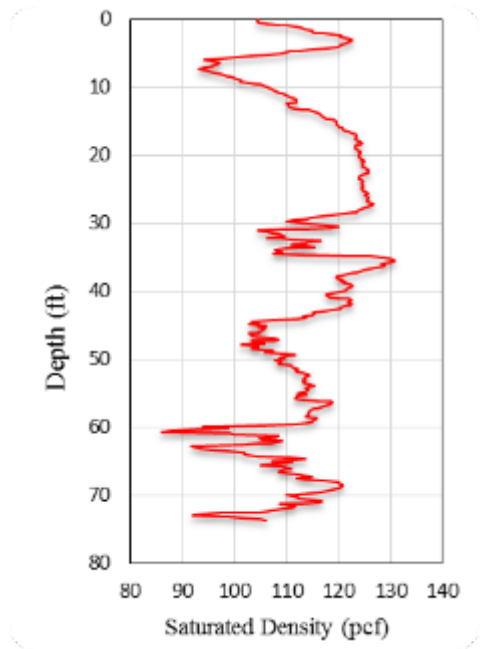


(a)

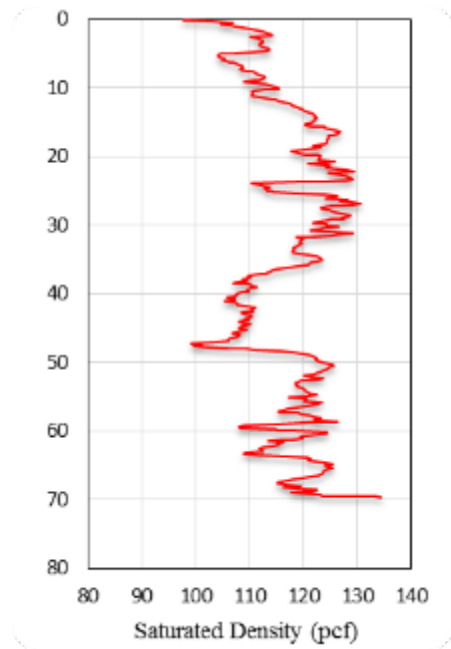
(b)

(c)

Figure 4-1: Saturated density versus depth for I-4/US 192 at (a) Pier 6/pile 16, (b) Pier 7/pile 10, and (c) Pier 8/pile 4 respectively with HPR zones shaded



(a)



(b)

Figure 4-2: Saturated density versus depth for SR 417 International Parkway at (a) B1/pile 14 (b) B2/pile 5

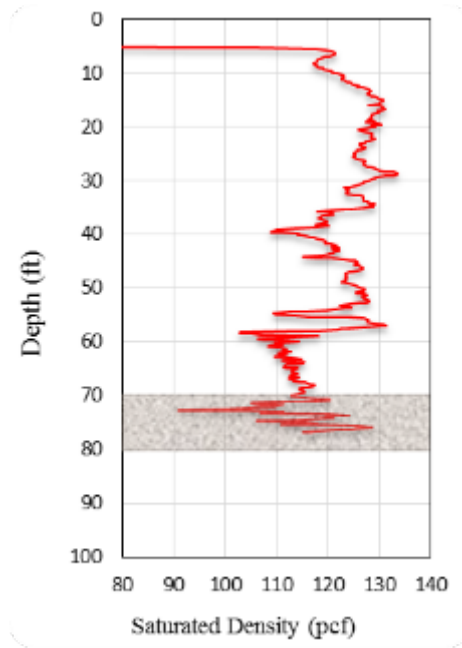


Figure 4-3: Saturated density versus depth for SR 50/SR436 at westbound/pile 5 with HPR zones shaded

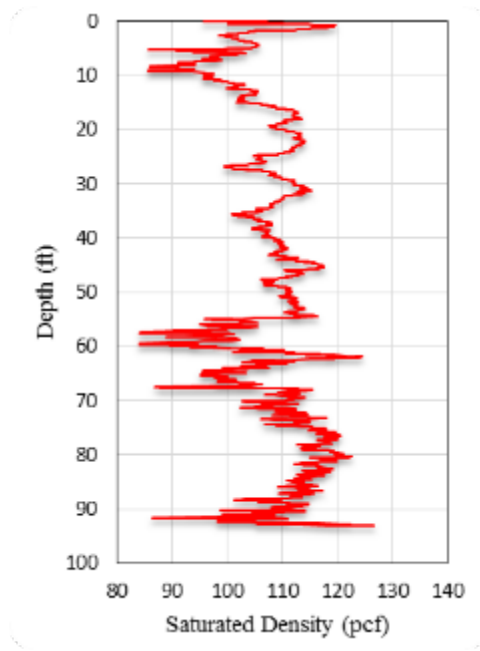


Figure 4-4: Saturated density versus depth for I-4/SR408 at pier 2/pile 5

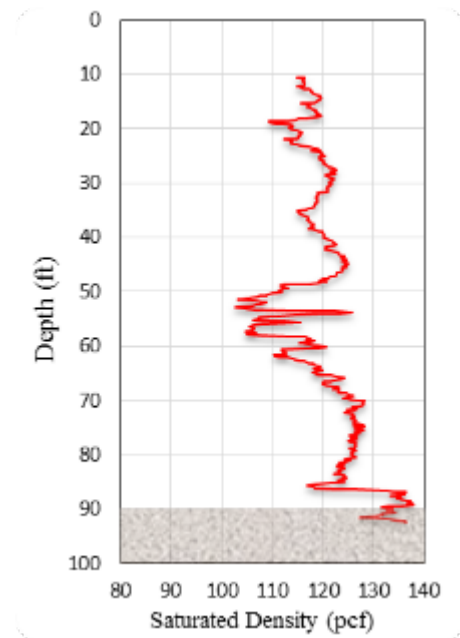


Figure 4-5: Saturated density versus depth for Anderson Street at pier 6/piles 5 and 6 with HPR zones shaded

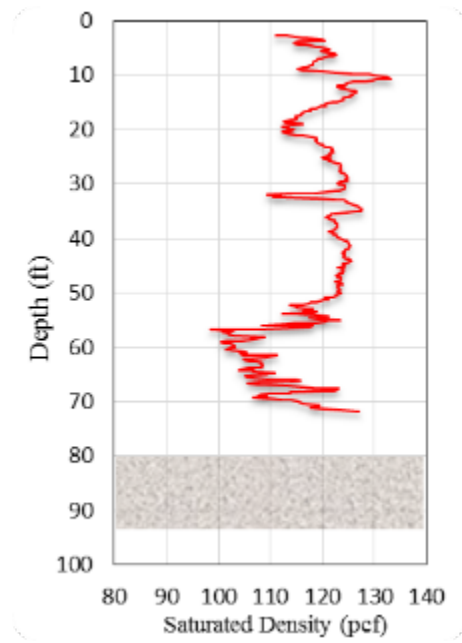


Figure 4-6: Saturated density versus depth for I-4 Widening Daytona at EB3/pile 5 with HPR zones shaded

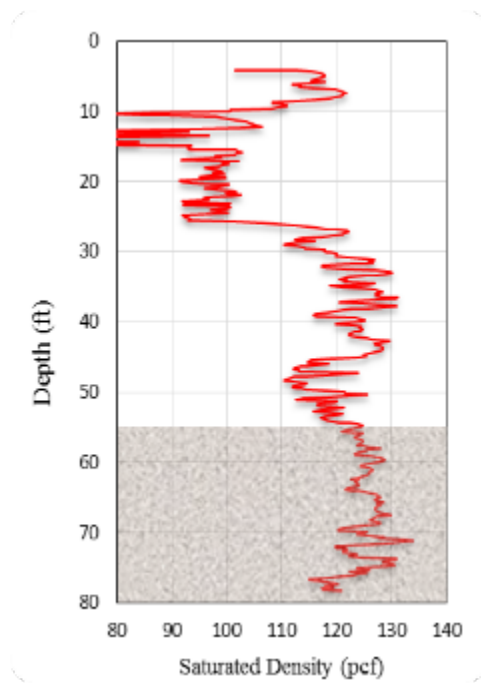


Figure 4-7: Saturated density versus depth for SR 83/Ramsey Branch Bridge at EB5/pile 2 with HPR zones shaded

Using the CPT-based soil density profiles, the total and effective overburden stresses were calculated and then used in CPeT-IT v.1.6 (2014) in order to produce normalized CPT information. The following profiles were produced:

- normalized soil behavior type index ( $I_c$ )
- normalized soil behavior type (SBTn) zone
- soil descriptions
- typical geotechnical sections.

These profiles for the seven sites are presented in Figure 4-8 to Figure 4-17. CPeT-IT v.1.6 (2014) produces color-coded SBTn zones to aid in visual representation. The  $I_c$  profiles represent the variation of soil behavior type. The  $I_c$  profiles illustrated in Figure 4-8 to Figure 4-17 show that all rebound zones have an  $I_c$  from 2.4 to 3.0. Based on Robertson's (1990) findings, this range classifies the soils as sand to silt/clay mixtures. The typical geotechnical sections for all sites presented in Figure 4-8 to Figure 4-17 show that the soils in the rebound zones classify as silty clay, clayey silt, sandy silt, and silty.

Comparing this result with the USCS-based soil classification, the soils in these zones were classified similarly as either silty sand (SM) or clayey sand (SC). This difference is likely to occur in the mixed soils region (i.e., sand-mixture and silt-mixture) (Robertson & Cabal 2015). Molle (2005) concludes that the differences between USCS-based and CPT-based soil types are related to soil classification criteria for each method. CPT-based soil classification depends on the cone response to the in-situ mechanical behavior, while the USCS-based classification depends on the grain size distribution and soil plasticity. He concludes that grain size and soil plasticity relate reasonably well."

Molle (2005) also concluded that soils with less than 50% fines may be classified as SM or SC, based on the USCS, and plasticity (soil with low plasticity classified as a silt whereas a soil with high plasticity classified as clay). When classifying with the CPT, if fines have a high clay content and high plasticity, the soil behavior may be more controlled by the clay and therefore CPT-based classification will predict a more clay-like behavior. If non-plastic fines exist, the sand will control the soil engineering behavior more and the CPT-based classification would predict a more sand-like soil type.

Based on the SBTn chart developed by Robertson (1990), it can be concluded that the mixed soils in the rebound zones contain a large percent of high plasticity fines, produce a clay-like behavior, and classify as clay to silty clay.

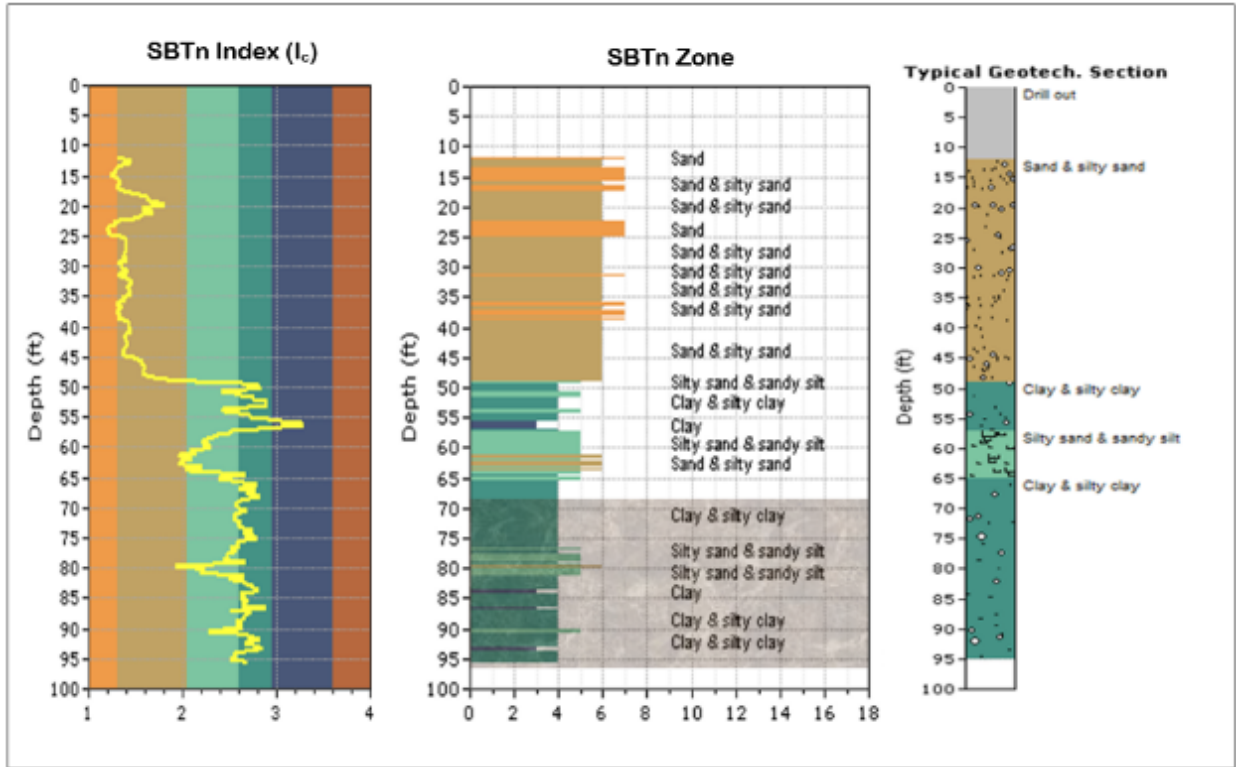


Figure 4-8: Normalized soil behavior type index and typical geotechnical section for I-4/US 192 at Pier 6/pile 16 with HPR zone shaded (GSE = 109.6 ft)

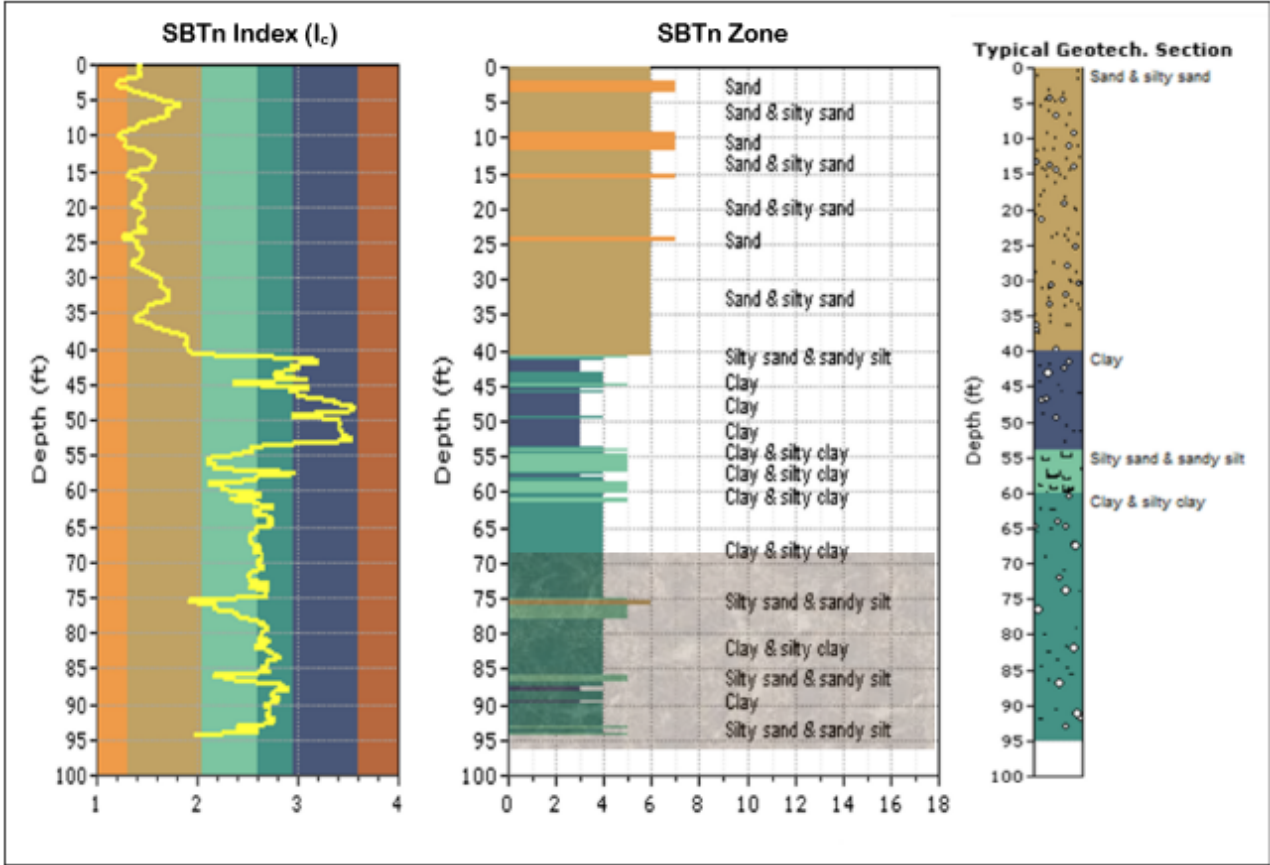


Figure 4-9: Normalized soil behavior type index and typical geotechnical section for I-4/US 192 at Pier 7/pile 10 with HPR zone shaded (GSE = 108.6 ft)

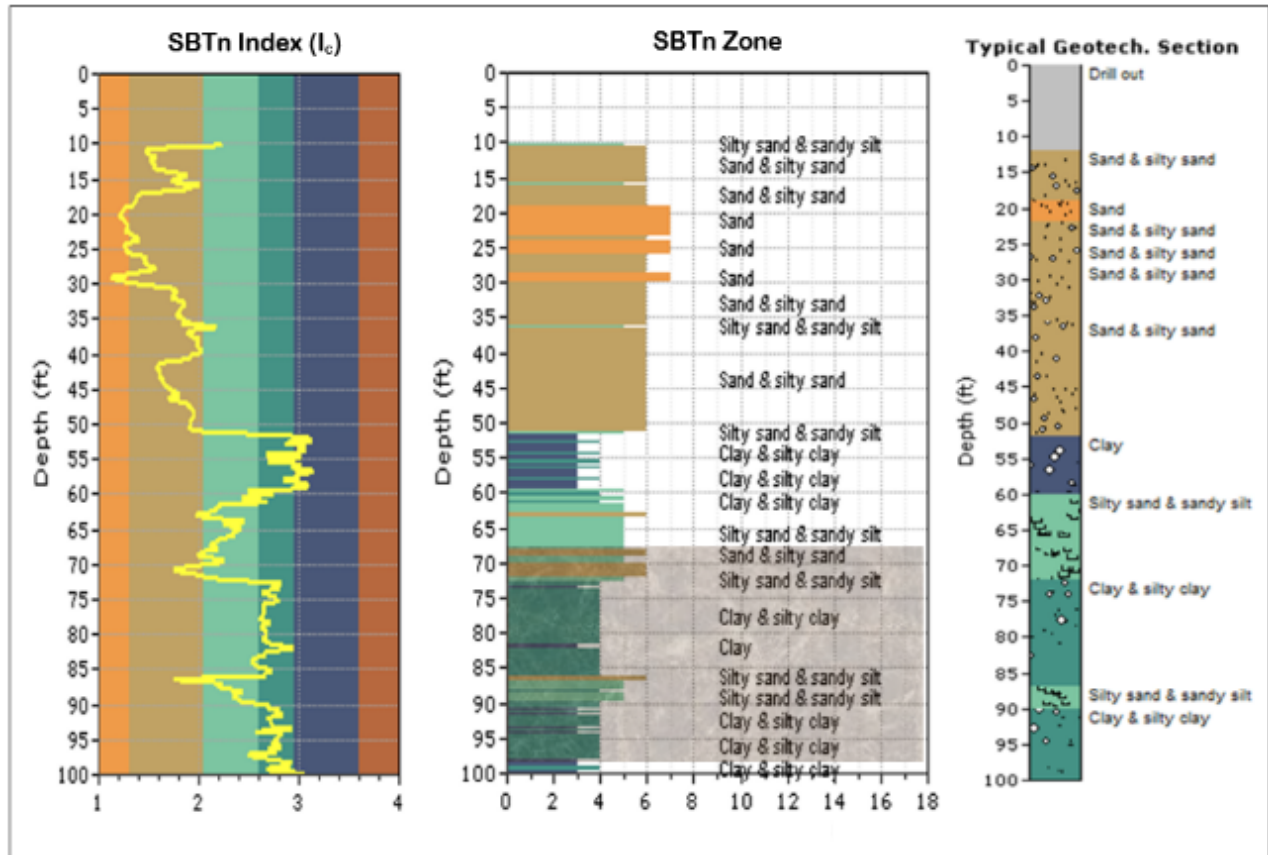


Figure 4-10: Normalized soil behavior type index and typical geotechnical section for I-4/US 192 at Pier 8/pile 4 with HPR zone shaded (GSE = 90.2 ft)

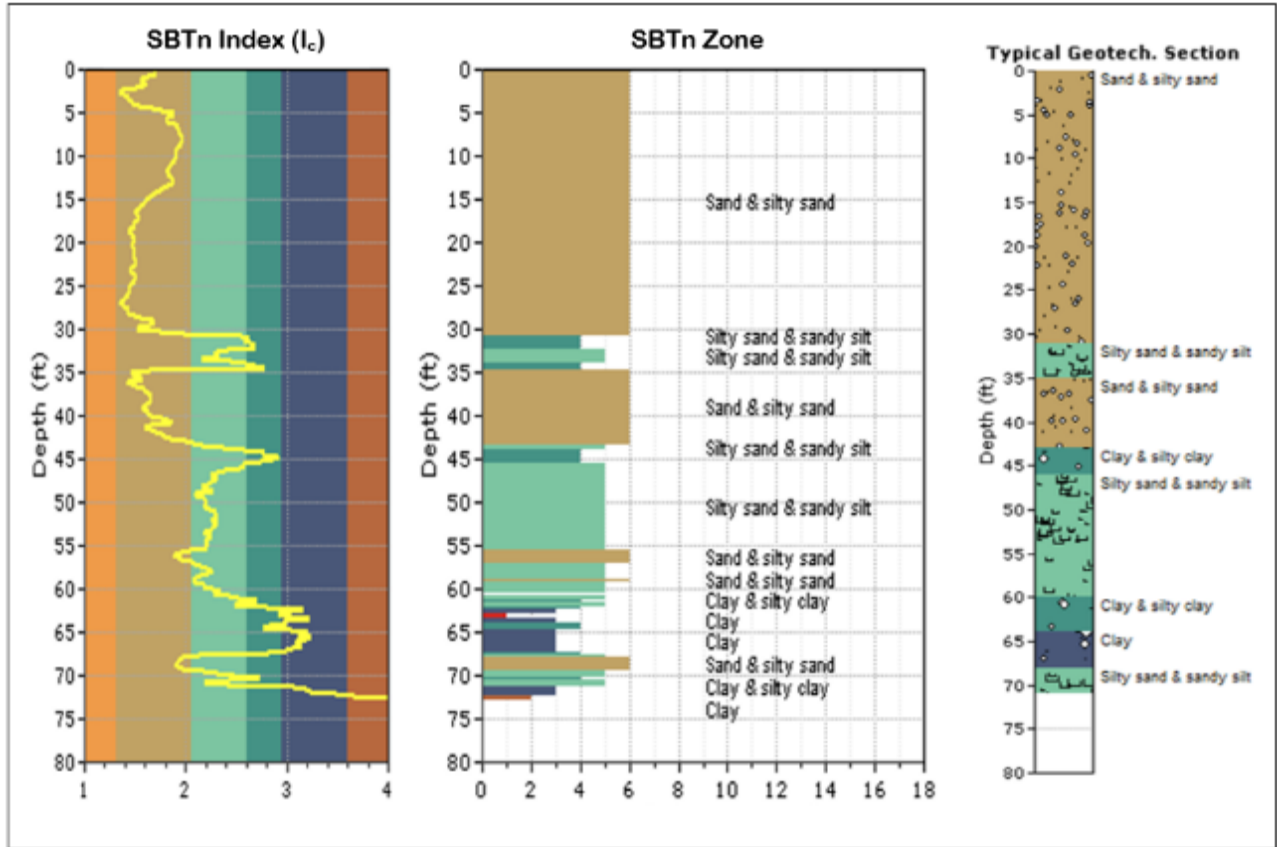


Figure 4-11: Normalized soil behavior type index and typical geotechnical section for SR 417 International Parkway at B1/pile 14 (GSE = 72.3 ft)

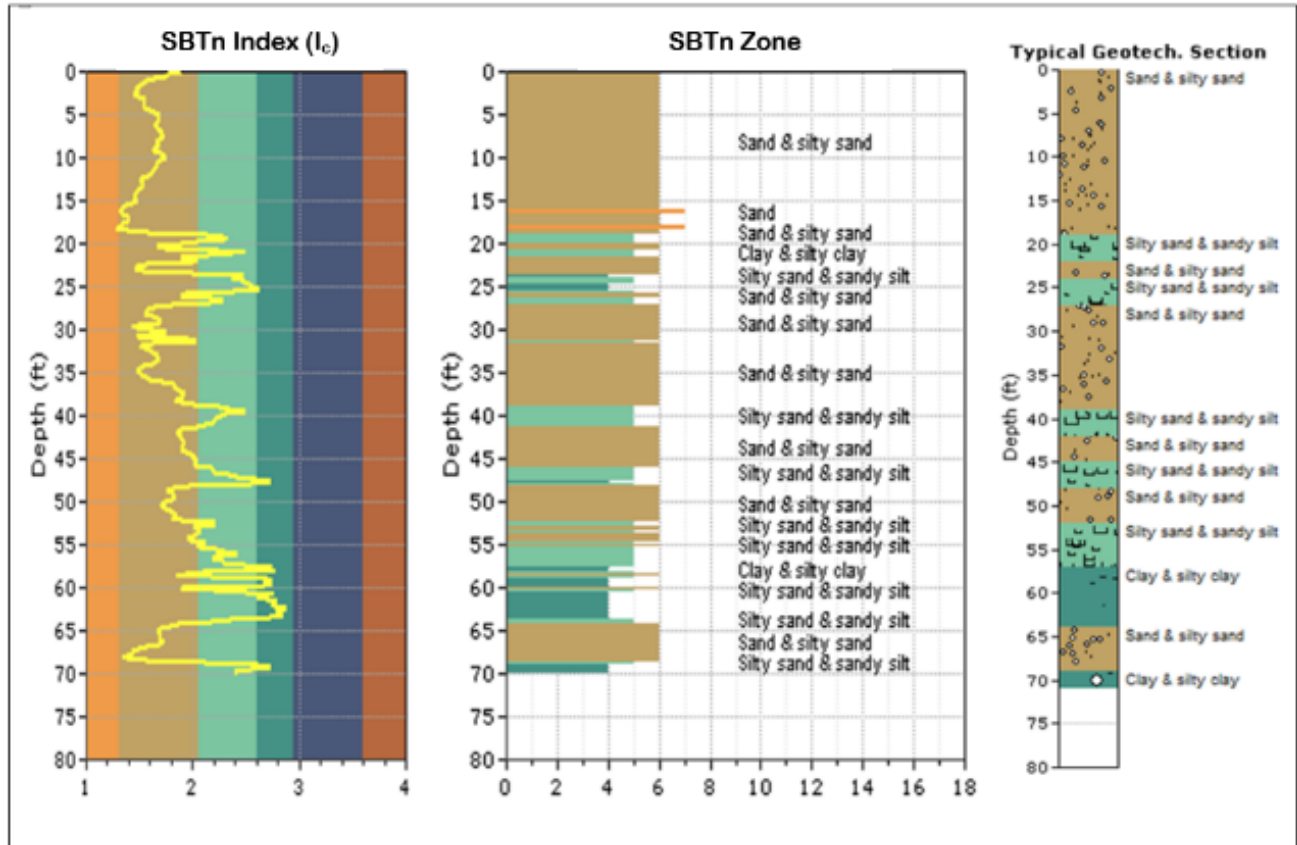


Figure 4-12: Normalized soil behavior type index and typical geotechnical section for SR 417 International Parkway at B2/pile 5 (GSE = 72.3 ft)

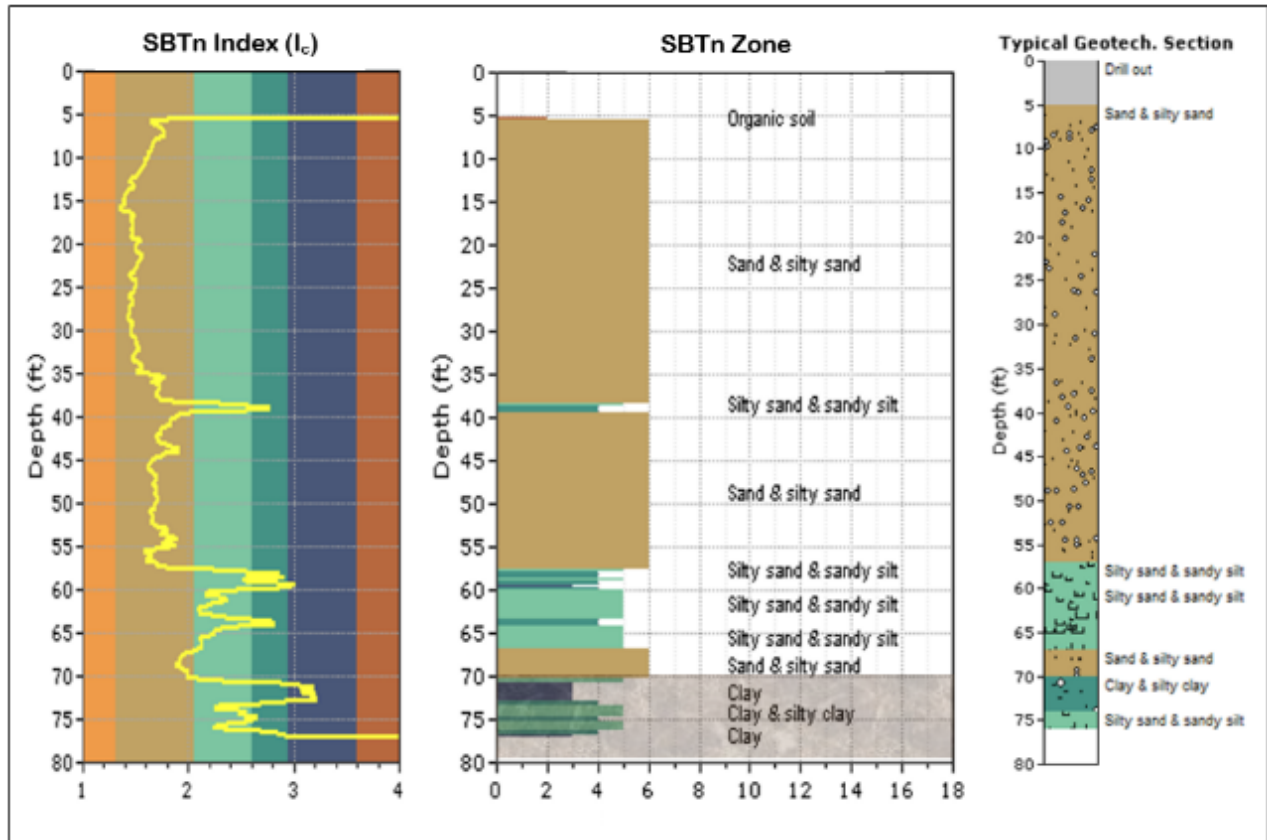


Figure 4-13: Normalized soil behavior type index and typical geotechnical section for SR 50/SR436 at west bound/pile 5 with HPR zone shaded (GSE = 99.0 ft)

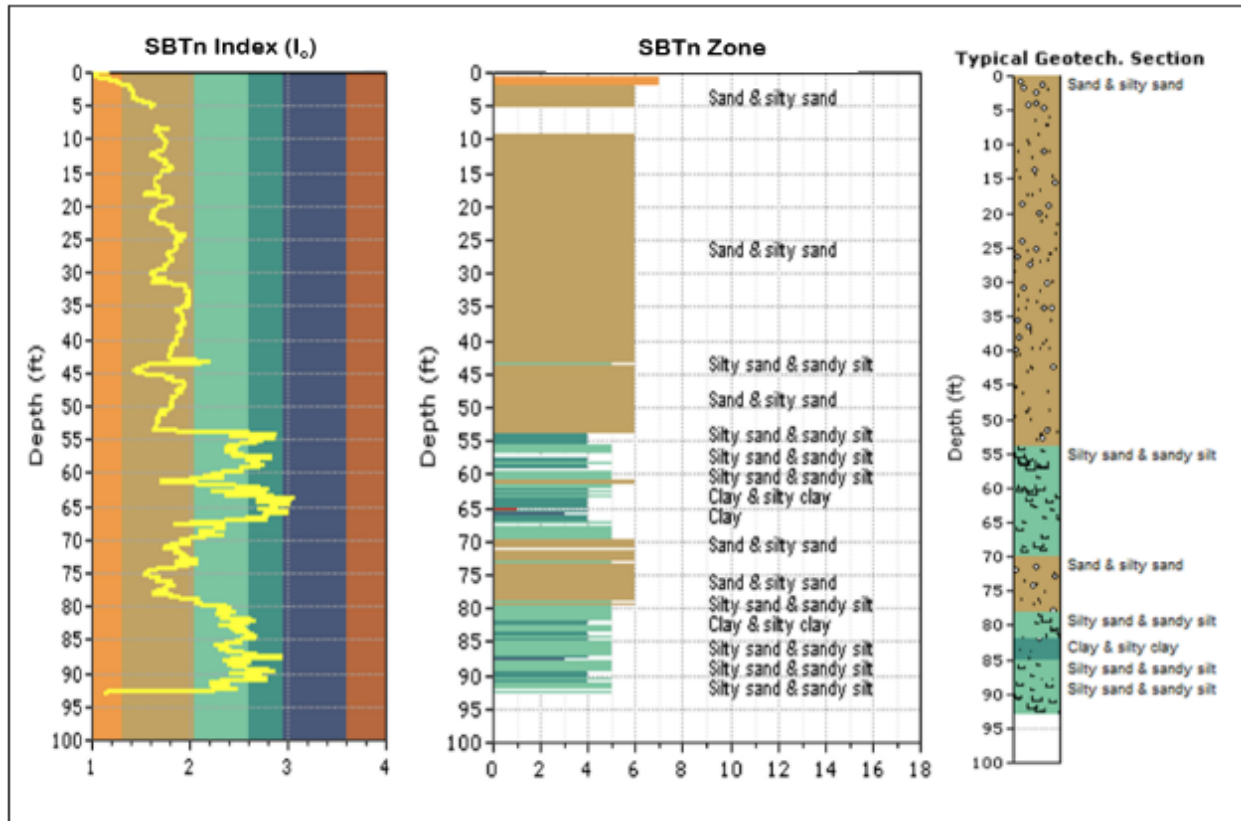


Figure 4-14: Normalized soil behavior type index and typical geotechnical section for I-4/SR408 at pier 2/pile 5 (GSE = 106 ft)

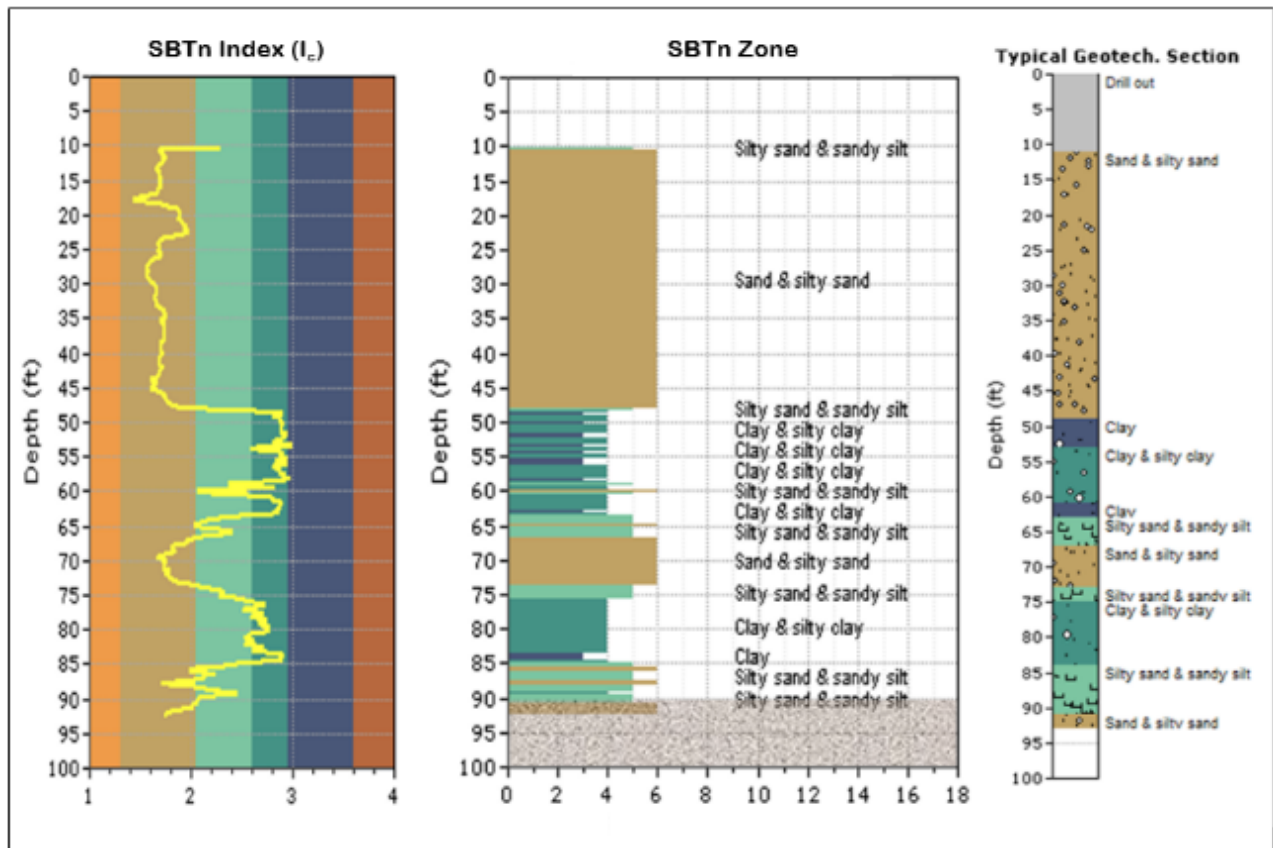


Figure 4-15: Normalized soil behavior index and typical geotechnical section for Anderson Street overpass at pier 6/pile 5, 6 with HPR zone shaded (GSE = 104 ft)

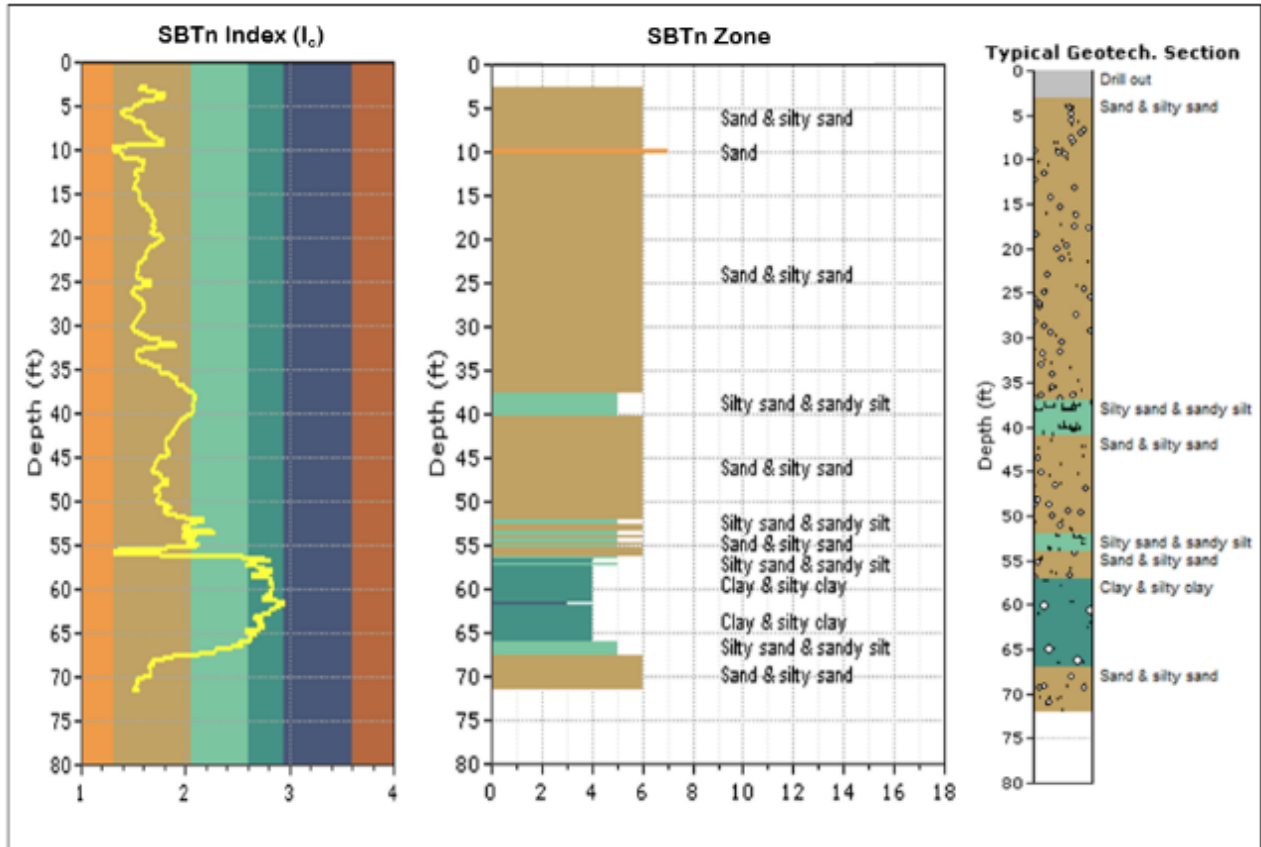


Figure 4-16: Normalized soil behavior type index and typical geotechnical section for I-4 Widening Daytona at EB3/pile 5 (GSE = 42.0 ft)

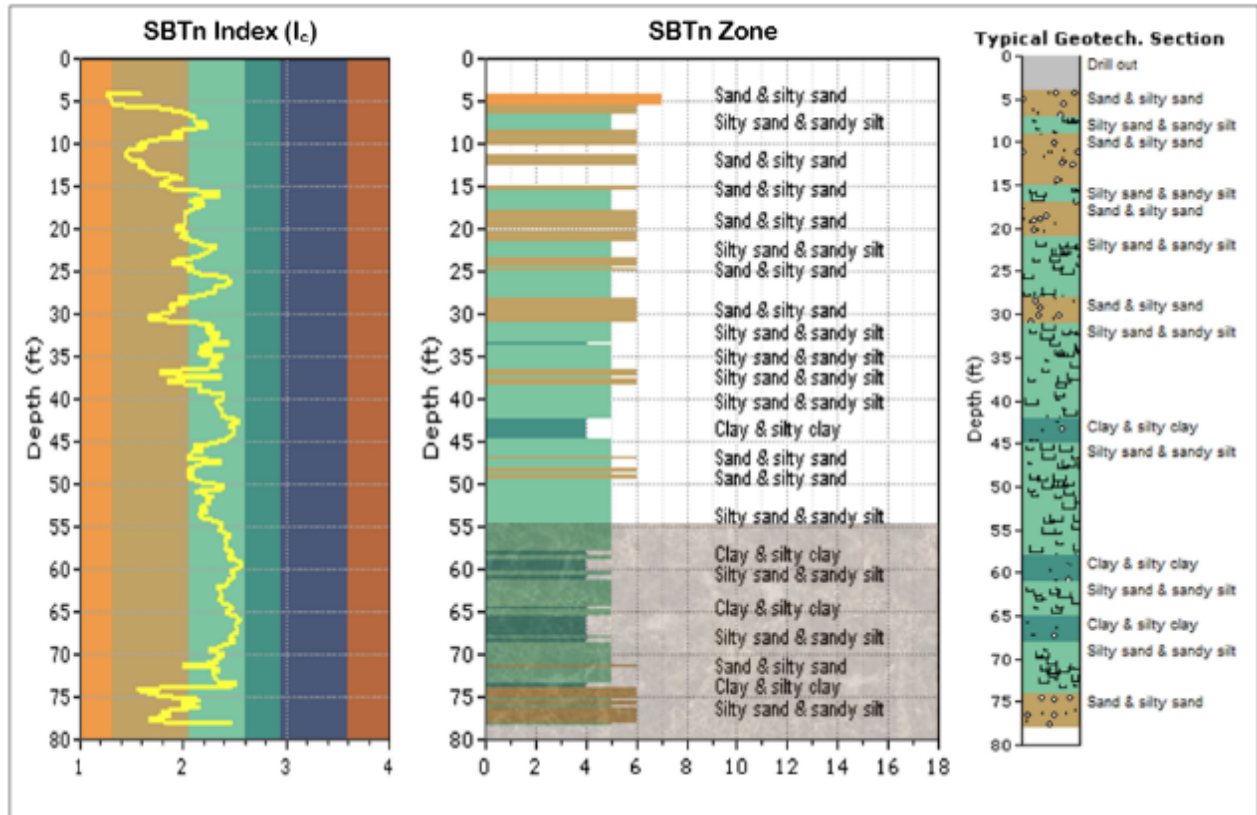


Figure 4-17: Normalized soil behavior type index and typical geotechnical section for SR 83 over Ramsey Branch Bridge at EB 5/pile 2 with HPR zone shaded (GSE = 1.0 ft)

### 4.3. Analysis of the Estimated Soil Properties

According to the CPT-based soil classifications, it can be concluded that both the rebound and non-rebound zones are silty sand, sandy silt, clay, and silty clay soils. Therefore, a unique soil type is not an indicator to predict the rebound problem. To determine if other parameters may be useful, estimated  $D_r$ ,  $\psi$  and OCR values were evaluated.

The state parameter ( $e_o - e_{cs}$ ) describes the behavior of dense and loose sand more precisely in terms of initial and critical void ratio (Bolton, 1986). The void ratio increases (i.e., soil expands) in dense sand while it decreases in loose sand (i.e., soil contracts). Therefore, dense soil is characterized by a negative state parameter whereas loose sand is characterized by a positive state parameter. Jefferies and Been (2006) suggested that soils with a state parameter less than -0.05 are dilative at large strains.

Figure 4-8 through Figure 4-17 show that some of the rebound zones are characterized by medium dense to dense silty sand to sandy silty soils with  $\psi$  ranging from -0.05 to -0.2. However, for the I-4 Widening in Daytona, medium to dense silty sand soil exists at a depth of 45 ft – 55 ft with  $\psi$  ranging from -0.1 to -0.13 where no rebound occurs. This location was predrilled to 40 ft before pile driving and therefore, no pile rebound was recorded. The other rebound zones are characterized by overconsolidated clay to silty clay soils with OCR ranging from 5 to 10. The soils in the rebound zones tend to dilate during the undrained loading due to the densification of the silty sand and sandy silt soils and overconsolidation of the silty clay and clay soils.

Some of the non-rebound zones presented in Figure 4-8 through Figure 4-17 are characterized by loose to medium dense soils with state parameters ranging from -0.05 to 0.15. Other non-rebound zones are characterized by normally consolidated to overconsolidated silty clay and clay soils with OCR ranging from 2 to 3. Therefore, the soils in the non-rebound zones tend to contract during pile driving. As a conclusion, the rebound zones are characterized by dilative soils whereas the non-rebound zones are characterized by contractive soils.

Soil dilation or contraction affects the generation of excess pore water pressures during pile driving and affects the shear strength of granular and cohesive soils (Das, 2008). Therefore,

the behavior of dilative and contractive soils in terms of pore water pressure generation and shear strength was studied and analyzed and is presented in the next section.

#### 4.4. Analysis of CPTu Pore Water Pressures

CPTu testing in saturated soils may produce excess pore water pressures in the vicinity of the cone sleeve and tip. These pore pressures occur in conjunction with (1) changes in the normal compressive stress ( $\Delta\sigma$ ), (2) the displacement of the soil particles and surrounding water, and (3) the shear stress ( $\Delta\tau$ ) due to the shear deformation of the soil adjacent to the cone. For penetration in saturated low permeability soils, these changes occur during undrained conditions (Burns & Mayne, 1998). Three additive components of pore water pressure exist when a cone penetrates any saturated soil deposit: hydrostatic pressures, normal compressive stress-induced, and shear stress-induced pore water pressure, as presented in the following equation:

$$u_m = u_0 + \Delta u_{\text{com}} + \Delta u_{\text{shear}} \quad \text{Equation 4-2}$$

where

$u_m$  = measured pore pressure during cone penetration

$u_0$  = hydrostatic pore water pressure

$\Delta u_{\text{com}}$  = compression-induced pore water pressure

$\Delta u_{\text{shear}}$  = shear-induced pore water pressure

These three components cannot be measured or distinguished separately during CPTu testing. However, approaches have been developed to estimate the compression-induced and the shear-induced pore water pressures. The hydrostatic pore pressure is the water density times the depth and is positive. The compression-induced pore water pressure models were developed according to cavity expansion theory. The principle of the expansion theory is that “the pressure required to produce a deep hole in an elastic-plastic medium is proportional to the required pressure of expanding a cavity of the same volume under the same conditions” (Gui & Jeng, 2009). Torstensson (1977) assumed that a plasticized spherical zone is generated around the cone tip due to the changes in the normal stresses during cone penetration. The radius of the cone and the rigidity index of the surrounding soil affect the size of the plasticized zone.

The shear-induced pore water pressure represents the final component. The zone of influence of the shear stress is limited to a thin layer along the cone sleeve (approximately 10 mm). Figure 4-18 shows the zones affected by cone penetration (Burns & Mayne, 1999).

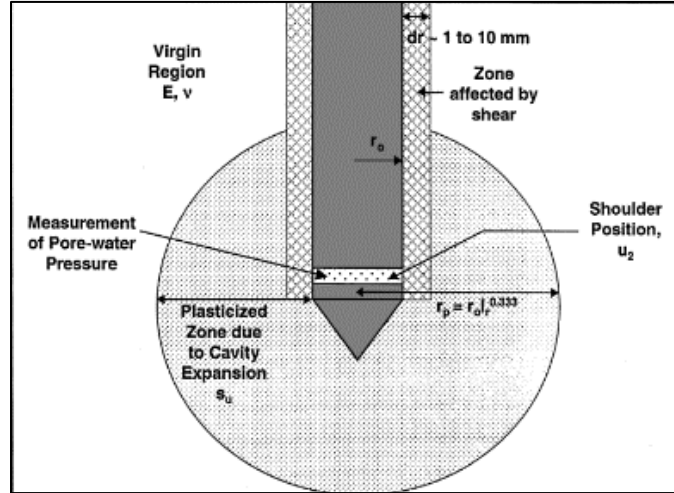


Figure 4-18: Zones affected by cone penetration (from Burns & Mayne, 1999)

Burns and Mayne (1999) developed two models to estimate both pore water pressure components induced due to penetration of a CPTu into clay soils. The equations for these models are:

$$\Delta u_{\text{compression}} = \frac{4}{3} \left[ \sigma'_{\text{vo}} \frac{M}{2} \left( \frac{\text{OCR}}{2} \right)^{0.8} \right] \ln I_r \quad \text{Equation 4-3}$$

$$\Delta u_{\text{shear}} = \sigma'_{\text{vo}} \left[ 1 - \left( \frac{\text{OCR}}{2} \right)^{0.8} \right] \quad \text{Equation 4-4}$$

where

$\sigma'_{\text{vo}}$  = effective overburden stress

$$M = \frac{6 \sin \phi'}{3 - \sin \phi'}$$

$\phi'$  = effective friction angle

OCR = over-consolidation ratio

$I_r$  = rigidity index =  $G/S_u$

$G$  = undrained shear modulus

$S_u$  = undrained shear strength

From Equation 4.3, it can be observed that the compression-induced pore water pressure is always positive and effectively increases as the effective stresses and OCR increase. As mentioned previously, the behavior of OCR soils is very similar to dense soils; therefore, the compression-induced pore water pressure increases with increasing the OCR of fines -grained soils or relative density of coarse-grained soils.

From Equation 4.4, the shear-induced component can be negative or positive depending on soil dilation or contraction under shear. Dilation of soil voids causes negative water pressures that draw the water into the pores. In contrast, the contractive soils have a tendency to compress when the shear stress is increased. As a result, the water in the soil pores increases in pressure (positive pressure) and attempts to flow out of these pores. Negative shear-induced pore water pressures are generated in dilative soils (i.e., fine-grained soils with OCR more than 4 or coarse-grained soils with medium to dense relative density). Positive shear-induced pore water pressures are generated in the contractive soils (i.e., fine-grained soils with OCR less than 4 or coarse-grained soils with loose relative density) (Burns & Mayne, 1999).

Since all rebound and non-rebound soils are assumed saturated and since they are below the water table, any pile-soil movements result in the generation of both shear-induced and compression-induced pore water pressures. The excess-shear induced pore pressures in the dilative soils in the rebound zones are negative. Contractive soils existing in the non-rebound zones generate positive shear-induced pore water pressures.

Data gathered during the CPTu for all the seven sites indicated that high positive pore water pressures (up to 570 psi) developed in the rebound zones. However, the pore water pressures at these zones show high positive values because the positive compression-induced pressures are much larger than the negative shear-induced pressures since the affected zone by compression is much larger than the zone affected by shear.

In conclusion, higher relative density or OCR occurred in the rebound zones than in the non-rebound zones at the seven sites. The soils at these rebound zones generates much higher compression-induced pore pressures and negative shear-induced pore pressures during cone penetration. The high total positive pore water pressures in the rebound zones measured during the CPTu does not indicate if the soil will contract or dilate unless the OCR (for fine soils) and

the relative density (for course soils) are estimated. The total pore water pressures induced during the CPTu have been used to predict the possibility of HPR (Jarushi et al., 2013).

#### 4.5. Evaluation of Existing Correlations between HPR and CPTu Pore Water Pressure

A recent statistical correlation developed by Jarushi et al. (2013) is shown in Figure 4-19. This correlation was based on 26 data points obtained by the analysis of PDA and CPTu data collected from eight sites described in Cosentino et al. (2012). Test piles at these eight sites were 24 in precast concrete piles driven with a single single-acting diesel hammers. As Figure 4-19 shows, pile rebound, measured in inch/blow, was found to correlate linearly with pore water pressure ( $u_2$ ) obtained from the CPTu test measured in tsf. The best coefficient of determination (i.e.,  $R^2$ ) obtained was 0.761. According to this correlation, high pile rebound (i.e.,  $> 0.25$  in) occurs only when pore water pressure obtained from the CPTu sounding exceeds about 5 tsf (70 psi).

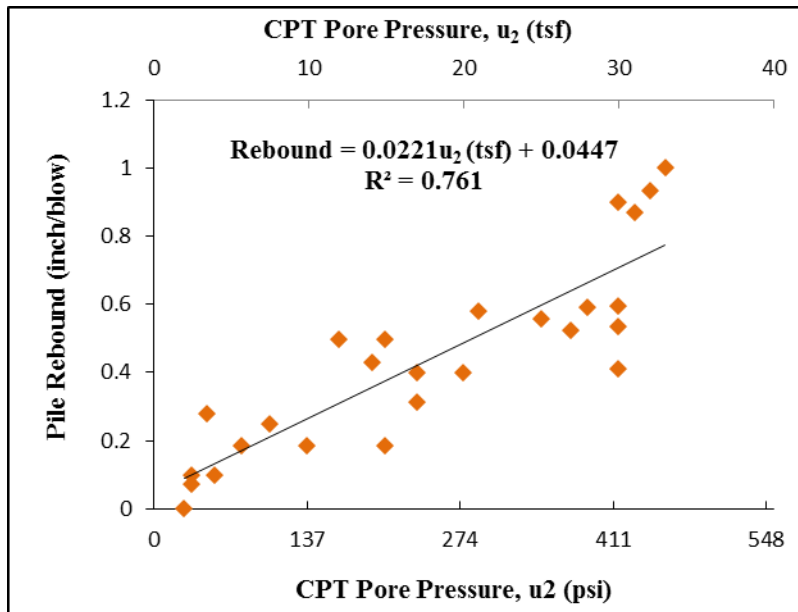


Figure 4-19: Pile rebound for 24 24-inch precast concrete piles versus CPTu  $u_2$  (Jarushi et al., 2013)

One of the main objectives of this research is to evaluate this correlation because it was based on so few (i.e., 26) data points. Using the extensive PDA and CPTu tests conducted in all of the study sites, CPTu pore water pressures and PDA rebound data were compared.

To reevaluate the correlation developed by Jarushi et al. (2013), several tasks had to be completed. First, the CPTu and PDA data from the sites were evaluated to determine if they could be matched based on elevation and depth. Once this step was completed, the second step was to determine one-foot averages from the matched CPTu and PDA data. To complete this step efficiently, a MatLAB program was developed and used. This coding produced a text file of CPTu and PDA data in one-foot intervals that could be imported into Excel; 6-inch intervals were also programmed but not used. Since both inspector and digital rebound were available, the data that was imported into Excel was used to generate plots of both digital and inspector rebound versus pore pressure for each site. These plots were evaluated and found to produce very low correlation coefficients between rebound and CPTu pore pressure, which therefore, did not support Jarushi et al.'s (2013) trends.

The  $R^2$  values from the digital rebound versus pore pressure plots were slightly higher than the  $R^2$  values from the inspector rebound versus pore pressure plots. These plots were combined to produce rebound versus CPTu for all the sites, which again produced very low correlation coefficients, as shown in Figure 4-20. This figure shows digital rebound versus CPTu pore pressure, which also has a slightly higher  $R^2$  than the inspector's rebound versus pore pressure plot. If nonlinear regressions were found, the  $R^2$  values were near 0.25, again indicating a poor correlation. This figure also shows a large scatter of data below 100 psi. When this data was excluded, low correlations still occurred. Correlations were also attempted using 0.5-inches instead of 0.25-inches of rebound as the cutoff between nonHPR and HPR, and the regression improved ( $R^2=0.482$ ), although there was a large gap in the data, as shown in Figure 4-21.

In summary, the original Jarushi et al. (2103) correlations were based on a very limited number of data points and are not valid. When one-foot averages were used and rebound versus CPTu pore pressure was compared for the study sites, very poor correlations were found regardless of whether they were linear or nonlinear.

Comparing the PDA rebound from the pile and  $u_2$  from CPTu is a problem involving several complex variables. First, there are most likely scaling effects between the 24-inch square PCPs (Area = 576 in<sup>2</sup>) and the 10-cm<sup>2</sup> (1.55 in<sup>2</sup>) cone. Note that the PCP area is over 370 times larger than the cone. Second, varying soil layer thicknesses affect two devices differently, as their zones of influence are also very different. Also, the insertion process from both devices is different, with the pile driving producing dynamic waves up and down the pile and the cone being pushed at a constant rate (2 cm/sec). Finally, the current FDOT definition of high rebound of 0.25 inches may need to be researched so that the dynamic pile capacity variations versus rebound are documented.

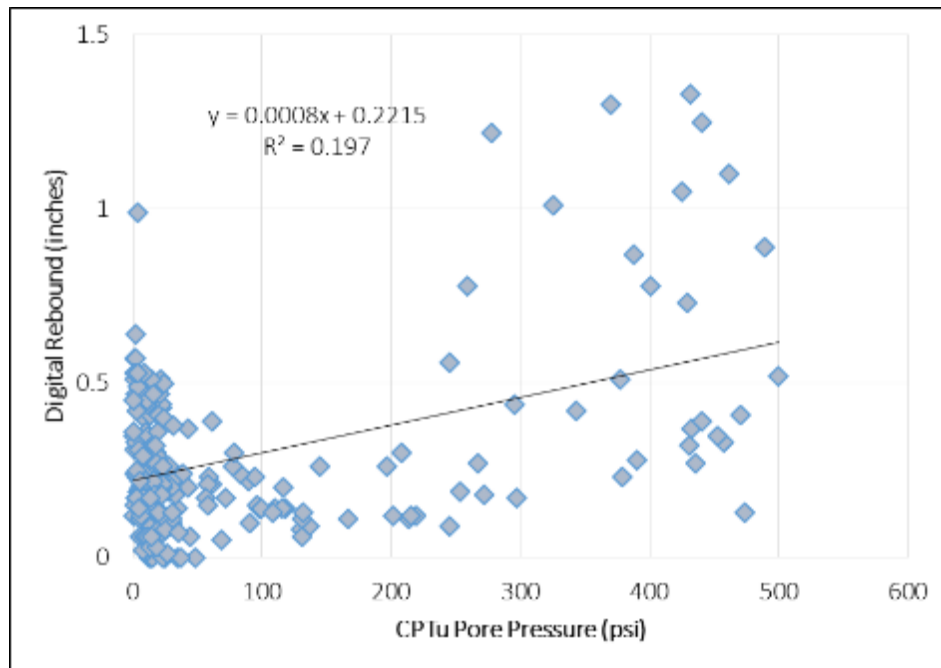


Figure 4-20: Digital Rebound versus CPTu pore pressure from six test sites

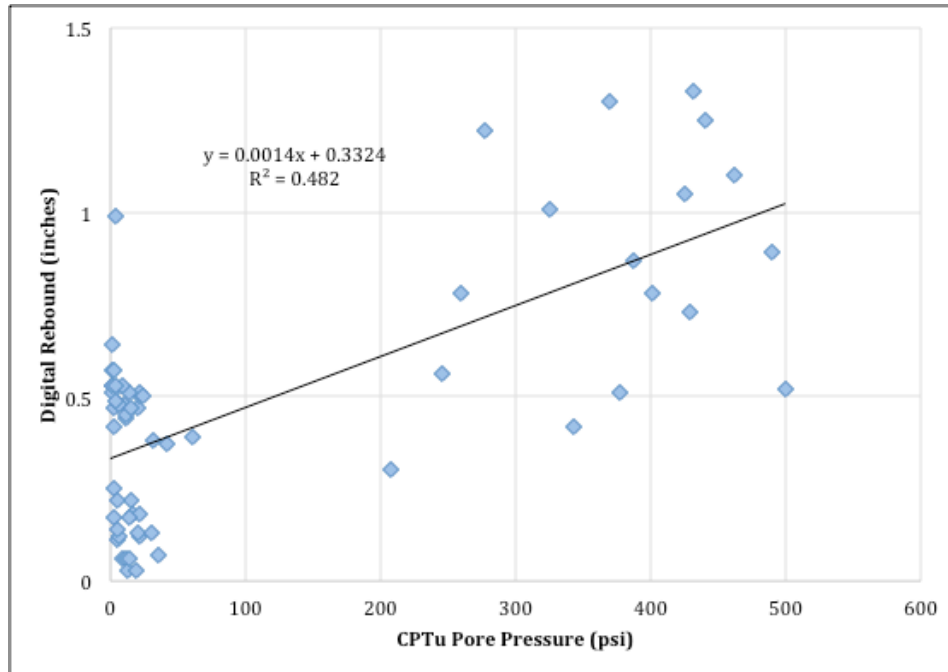


Figure 4-21: Digital Rebound versus CPTu pore pressure from six test sites with rebound > 0.5 inches

#### 4.6. Analysis of Soil Properties' Effect on the Induced Pore Water Pressures during Pile Driving

The pile performance during loading is directly influenced by the behavior of the surrounding soil during driving. Two categories of stress changes occur from pile driving: stresses along the pile shaft (shear stresses) and stresses at the pile tip (compressive stresses). Shear stresses develop during pile driving along the interface of the pile and soil due to the relative movement between the pile and the surrounding soil. Since pile-driving movement is downward, the shear stress direction is upward (Fellenius, 1984). This upward shear stress represents soil resistance to pile driving.

Soils respond to the stress changes; therefore, soil deformations occur adjacent to the pile shaft due to shear forces and at the pile tip due to compressive forces, as shown in Figure 4-22. Since soils are porous, the compressive and shear stresses during pile driving force water out of the voids. Due to the fast loading speed and low permeability coefficient of the soils in the rebound zones, water cannot flow out of the voids and the pore pressures cannot dissipate instantly. As a result, high pore water pressures generate along the pile shaft (i.e., shear induced)

and at the pile tip (i.e., compression induced). The effect of these two pore water pressure components on pile driving is discussed below.

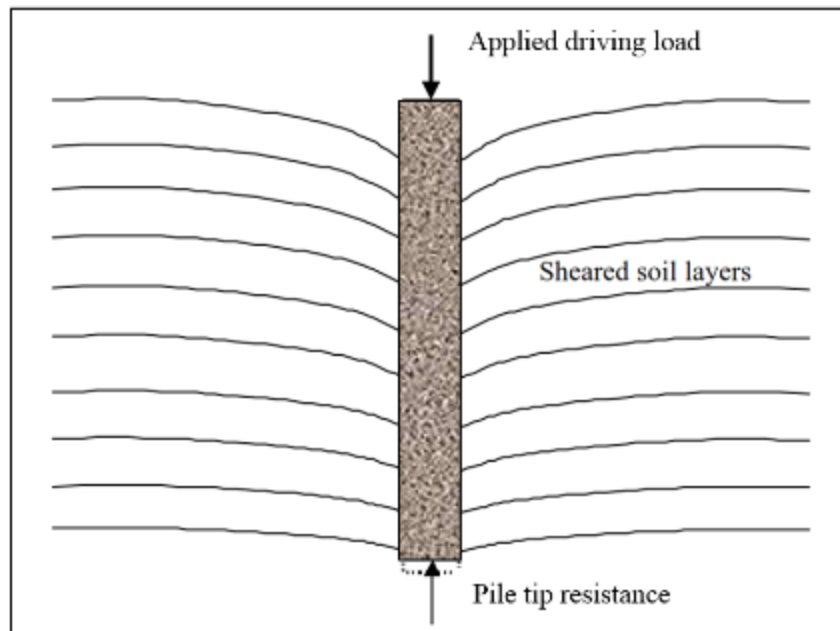


Figure 4-22: Soil layers deformations around a driven pile

#### 4.6.1. Shear-Induced Pore Water Pressure

The pore water pressure generated along the pile shaft or shear induced pore pressure can be negative or positive depending on soil density. The soils in the rebound zones were classified as dilative soils (i.e., tend to increase in volume). Soil heave occurs near a driven pile due to the volume changes during installation. As a result, negative pore water pressures occur along the pile shaft due to volume increase of the dilative soils existing in the rebound zones. The generated pore water pressure affects the soil shear strength along the pile shaft.

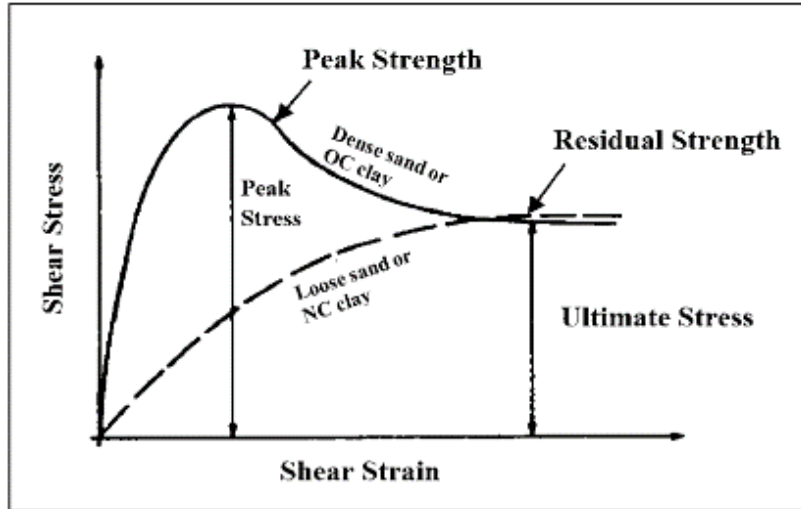


Figure 4-23: Typical shear stress versus shear strain for granular and cohesive soils (Das, 2008)

Lundgren (1979) developed the following relationships for the shear-induced pore water pressures at the soil-pile interface as a result of pile driving. They are used in the CPeT-IT software to determine the shear-induced pore water pressures developed along the pile shaft in overconsolidated and normally/lightly overconsolidated clays respectively.

$$\Delta u_{\text{shear}} = (A)S_u \quad \text{for OC clays} \quad \text{Equation 4-5}$$

$$\Delta u_{\text{shear}} = (B)S_u \quad \text{for NC clays} \quad \text{Equation 4-6}$$

where

A ranges from 5.5 to 7.5

B ranges from 1.5 to 3

$S_u$  is the undrained shear strength.

$S_u$  was estimated based on the CPT data using CPeT-IT to compare the results in the rebound and non-rebound zones. Profiles of the undrained shear strength versus depth for all the seven sites are presented in Figure 4-24 to Figure 4-30. CPeT-IT is programmed to estimate  $S_u$  at the zones where cohesive soil exists; therefore, missing data occurs at depths with cohesionless soils. The undrained shear strength in the rebound zones tends to be significantly higher than shear strength in the non-rebound zones. The undrained peak shear strength of the cohesive soil in the rebound zones ranges from 4 to 10 tsf and from 1 to 2 tsf in the non-rebound zones. The

increase in the undrained shear strength in the rebound zones may be related to the cementation and overconsolidation of soils at these zones (Mayne et al., 2009).

Soil consistency, which is soil ability to resist deformation and rupture, is related to the undrained shear strength. Soils with  $S_u$  greater than 2 tsf can be classified as hard (Geotechdata.info, 2013). Therefore, the cohesive soils in the rebound zones are characterized as hard.

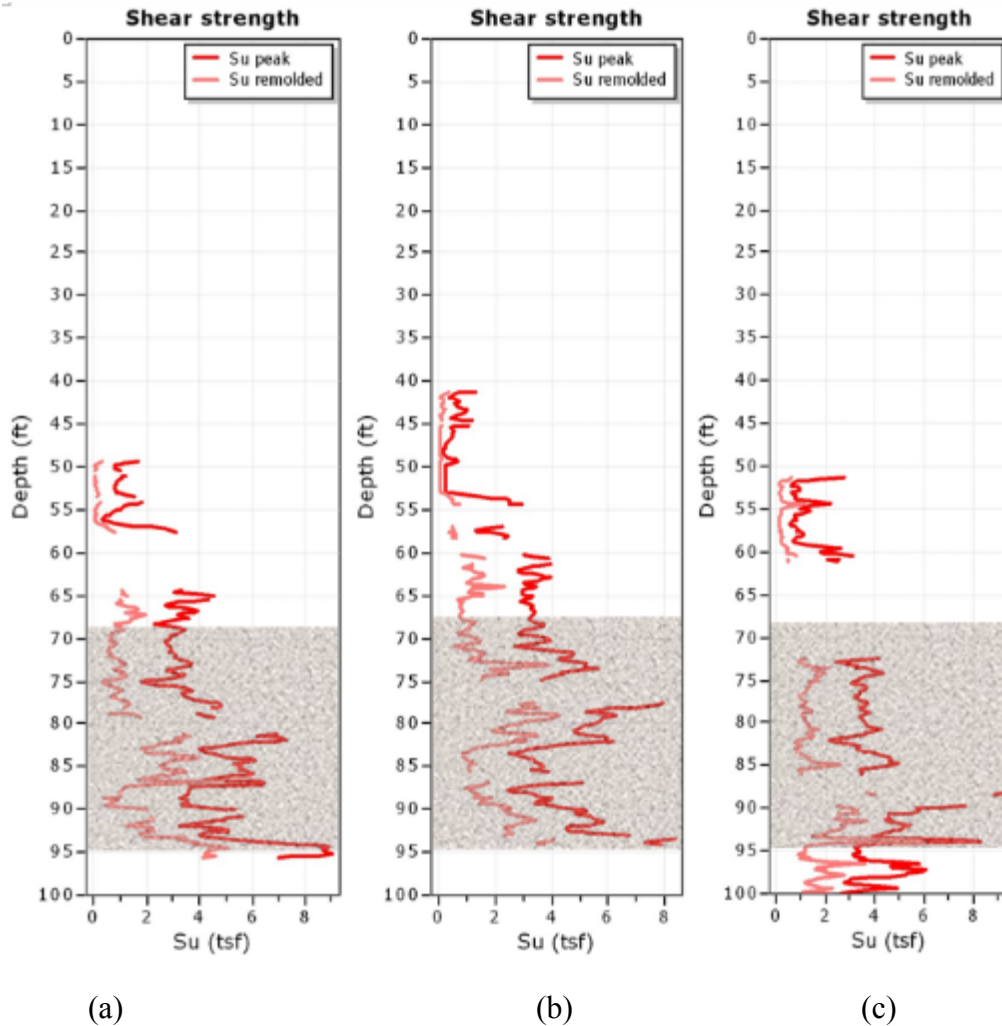


Figure 4-24: Undrained shear strength for I-4/US 192 at (a) pier 6/pile 16, (b) pier 7/pile 10, and (c) pier 8/pile 4 with HPR zones shaded

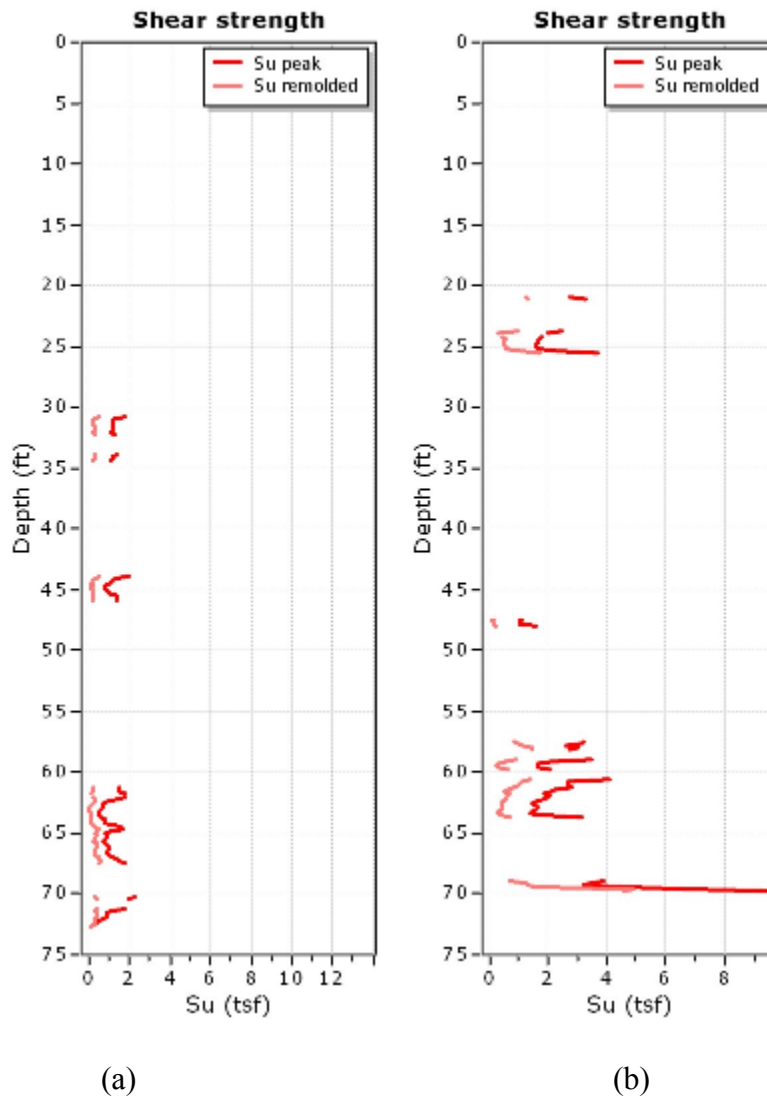


Figure 4-25: Undrained shear strength for SR 417 International Parkway at (a) B1/pile 14 and (b) B2/pile 5

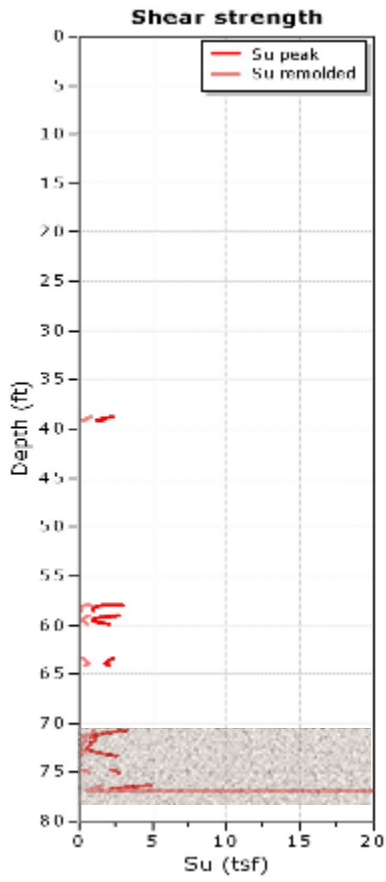


Figure 4-26: Undrained shear strength for SR 50/SR 436 at westbound/pile 5 with HPR zone shaded

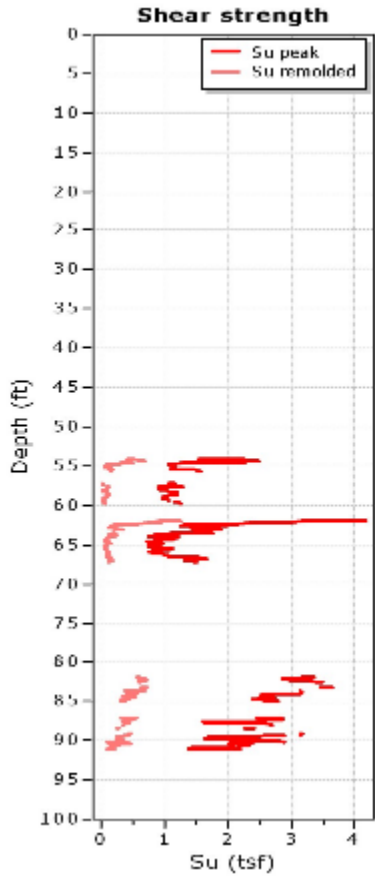


Figure 4-27: Undrained shear strength for I-4/SR 408 at pier 2/pile 5

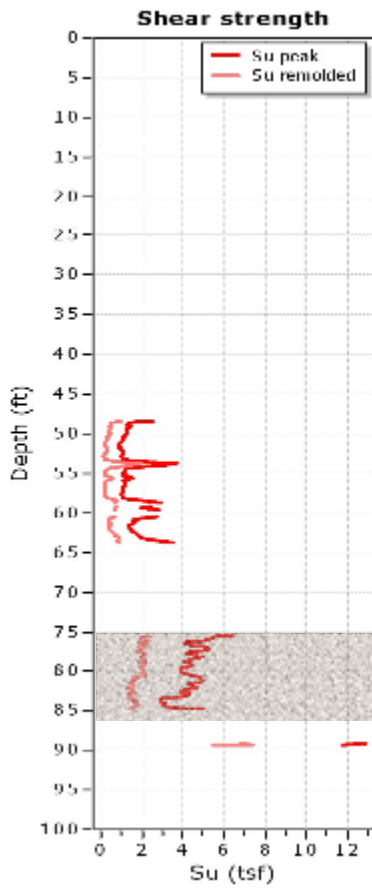


Figure 4-28: Undrained shear strength for Anderson Street at pier 6 with HPR zone shaded

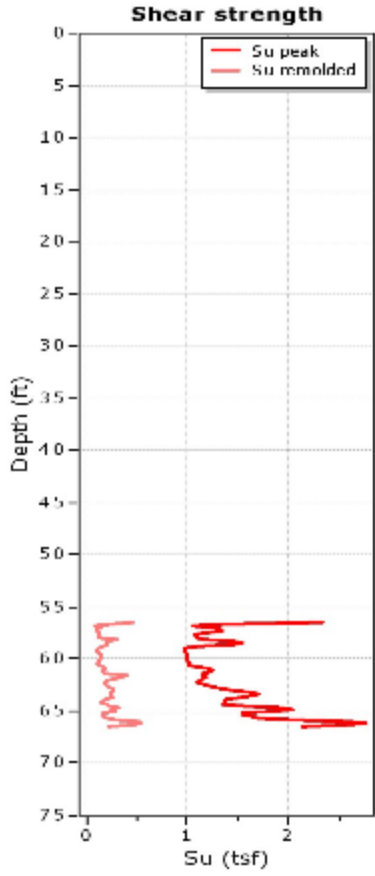


Figure 4-29: Undrained shear strength for I-4 Widening Daytona at EB3/pile 5

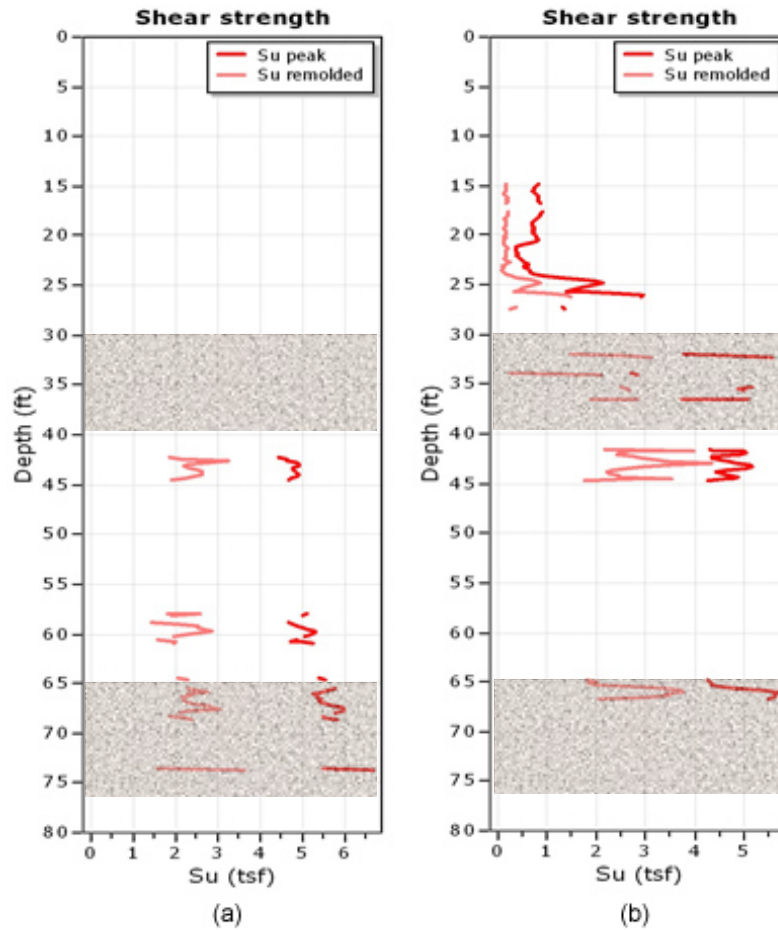


Figure 4-30: Undrained shear strength for SR 83/Ramsey Branch Bridge at EB 5/pile 2 with HPR zones shaded (a) CPT1, (b) CPT2

#### 4.6.2. Compression-Induced Pore Water Pressure

High excess pore water pressures may be generated during the installation of prestressed concrete piles due to the low permeability of soil and the rapid soil deformation by the hammer impact (Gui and Jeng, 2009). Bingjian (2011) found that driving piles in saturated soils creates a spherical cavity expansion at the pile tip due to pore water pressure and deformation. The influence of that sphere may expand up to 5 to 6 times the pile diameter. This region surrounding the pile is named a plastic zone. Maximum compression-induced excess pore water pressures are generated at the pile face and decrease with distance from the pile within the plastic zone and extend to the outer zone. The outer zone represents the elastic zone because reversible deformations occur beyond the plastic radius. The plastic and elastic zones around a driven pile are shown in Figure 4-31 (Wren, 2007).

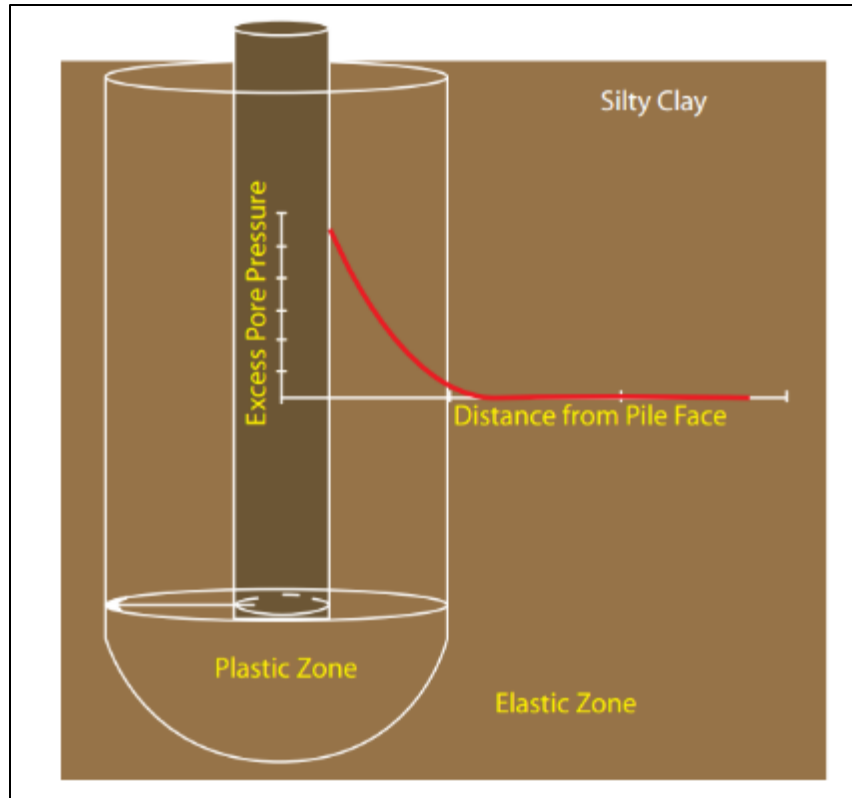


Figure 4-31: Plastic and elastic zones around single driven pile (Wren, 2007)

The radius of the plastic zone ( $R_p$ ) can be determined using Equation 4-7 and the excess of pore water pressure within the plastic zone can be determined using Equation 4-8 (Guihai et. al., 2011).

$$R_p = r_0 \left( G/S_u \right)^{1/2} \quad \text{Equation 4-7}$$

$$\Delta u = S_u \left[ 2 \ln \left( R_p/r \right) + 1.73A_f - 0.58 \right] \quad \text{Equation 4-8}$$

where

$r_0$  = radius of pile

$G$  = Shear modulus

$S_u$  = Undrained shear strength

$r$  = Distance from pile center

$A_f$  = Skempton's pore water pressure coefficient

The shear modulus and undrained shear strength were estimated using the CPT data. Skempton's Pore water pressure coefficient ( $A_f$ ) has a range of (0.5 to 1), (0 to 0.5), and (-0.5 to 0) for normally, lightly, and heavily consolidated clays respectively (Holtz & Kovacs, 1981). Since the maximum pore water pressures occur at the pile face within the plastic zone, Equation 4.10 was used to calculate the pore water pressure with  $r = r_o$ .

These equations were developed for clays or cohesive soils that have undrained shear strength ( $S_u$ ). Therefore, only three locations at site I-4/US 192 (piers 6, 7, and 8) were selected because the soil in the rebound zones was classified as clayey silty to silty clay according to the CPT-based classification. The maximum pore water pressures developed due to driving 24-inch prestressed concrete piles were estimated using Equation 4.11. The estimated maximum pore water pressures versus depth during driving for the three piers are shown in Figure 4-32. High pore water pressures (up to 870 psi) were developed in the rebound zones. The equivalent radius of a 24-inch square is 1.13 ft; therefore, the radius of the plastic zone in the rebound zones is approximately 23 ft. The estimated maximum pore water pressure due to pile driving (780 psi) is approximately equal to 1.6 times the measured CPT pore water pressure at the same depth.

These pressures represent upward extra resistance forces to pile driving and resist the downward pile movement. As the compression-induced pore water pressures increase, the resistance forces to pile driving increase. Therefore, the higher compression-induced pore water pressures, the more hammer blows are required to reach soil failure. Since the water is an incompressible fluid, pile bounce or rebound was observed or recorded. The generation and dissipation of the compression-induced pore water pressures is significantly affected by soil permeability. Since all the rebound zones have semi-impermeable to impermeable soils, the compression-induced pressures take a longer time to dissipate.

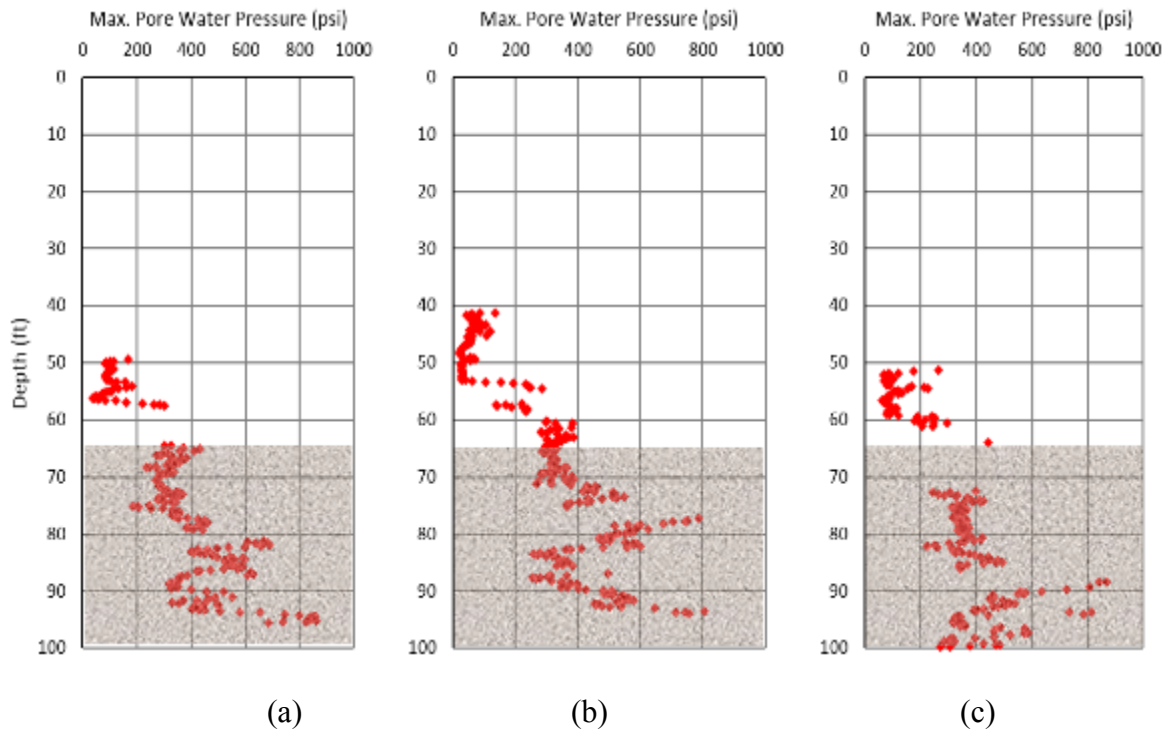


Figure 4-32: Gui and Jeng 's (2009) maximum compression-induced pore water pressure due to driving 24-inch prestressed concrete piles with HPR zones shaded for I-4/US 192 at (a) pier 6/pile 16, (b) pier 7/pile 10, and (c) pier 8/pile 4

## 4.7. Estimation and Analysis of Fines Content

FCs in percent were determined using the soil behavior type index,  $I_c$  for the soils at the seven CPTu sites. Initially,  $I_c$  was calculated from the CPTu data using Robertson's (1990) approach; then it was estimated according the approach proposed by Yi (2014). Yi's (2014) approach is presented below.

### 4.7.1. Validation of Yi's (2014) Equation

Laboratory FC values from field sampling were available and used for validating Yi's (2014) procedure. Some measured FC data was obtained from thin-walled tube samples and some was obtained from split spoon samples obtained during SPT borings. Laboratory sieve analysis was conducted on those samples and the resulting grain size distribution curves were then used for determining FC as the passing sieve #200. Measured and predicted FC values were compared using the same the sample depths. Based on 80 data points, Figure 4-33 shows a scatter plot of the predicted versus the measured FC. Each predicted FC data point was obtained by taking an average of six CPT readings over one-foot. This averaging ensured that the

measured and predicted data points were compared at the same depth. The 45° reference line helps to indicate how the predicted and measured data match with each other. The closer the data points to the 45° reference line, the better they match. There is excellent agreement between the measured and predicted FC because most of the data points are distributed on or very close to the 45° line.

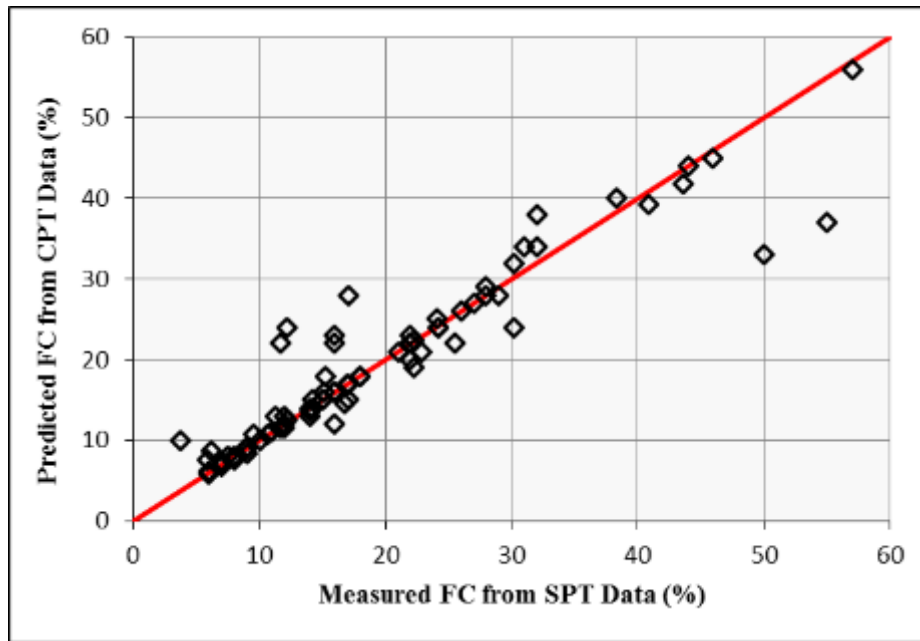


Figure 4-33: Verification of fines content estimation procedure based on 80 data points from all sites

#### 4.7.2. Profiles of Measured and CPTu Predicted Fines Content

After validating Yi's (2014) procedure, profiles of both predicted and measured fines content versus depth were developed for each site, as shown in Figure 4-34 to Figure 4-40. Using the PDA data, the rebound zones were highlighted to better aid in the analysis. Rebound zones in the Anderson Street overpass and I-4 Widening Daytona, respectively, are not highlighted since CPTu testing at these two locations was terminated at depths above the observed rebound depth.

Figure 4-34 to Figure 4-40 showed that HPR zones had a fines content range from 28% to 38%. Fines content has been used to evaluate soil liquefaction or strength loss. Sand-like soils with fines content less than 20% and more than 35% are susceptible to strength loss, while clay-like soils with fines content more than 20% are not susceptible to strength loss (Robertson & Cabal, 2009). The soils in the rebound zones were classified as clay-like soils based on CPT

data. Therefore, there is no possibility for the soils in the rebound zones to liquefy or lose strength during pile driving.

However, Figure 4-34 to Figure 4-40 showed nonrebound zones corresponding to such a fines content range. This clearly indicates that a fines content of this range is not the only factor that may cause the HPR problem. There should be other soil parameters, such as soil type, that interact and work together in producing excessive HPR. Figure 4-34 to Figure 4-40 represent the response of different soil types. Therefore, soil type and classification were investigated by separating the fines content for each soil type existing in all sites in this investigation.

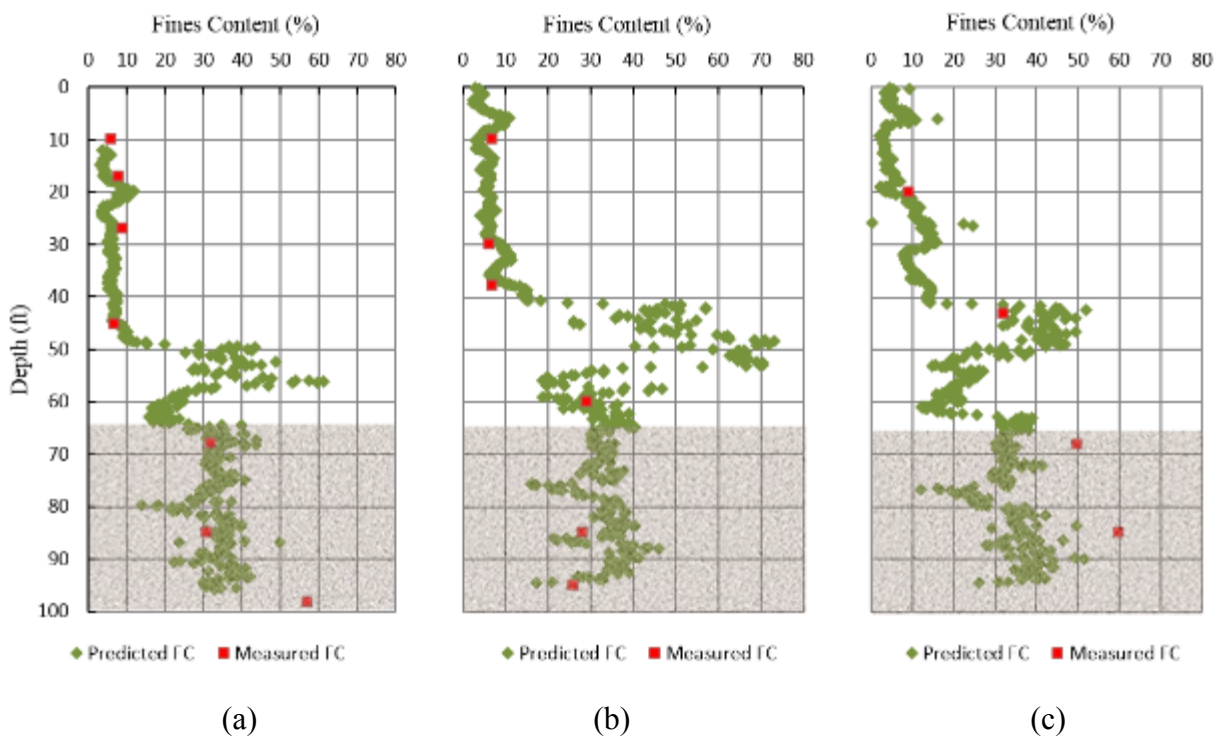


Figure 4-34: Predicted and measured fines content versus depth for I-4/US 192 at (a) Pier 6/pile 16 (b) Pier 7/pile 10 (c) Pier 8/pile 4 with HPR zones shaded

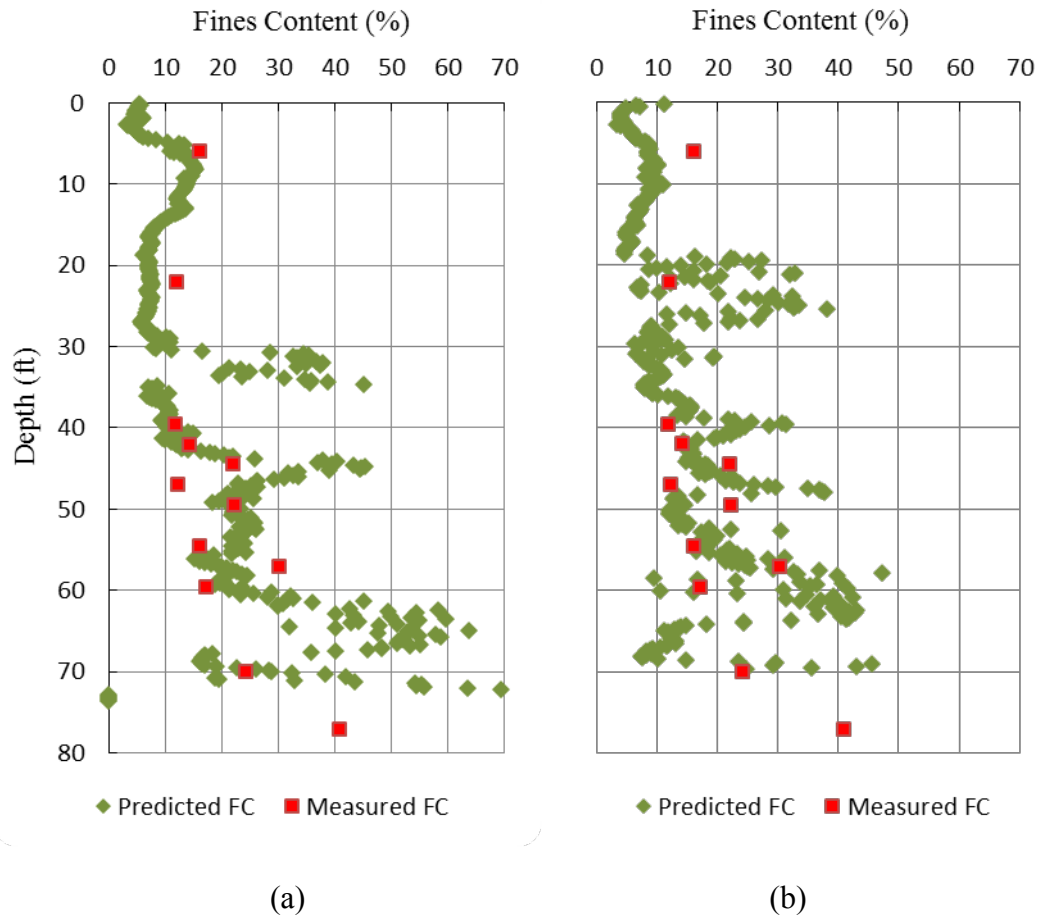


Figure 4-35: Predicted and measured fines content versus depth for SR 417 International Parkway at (a) B1/pile 14 (b) B2/pile 5

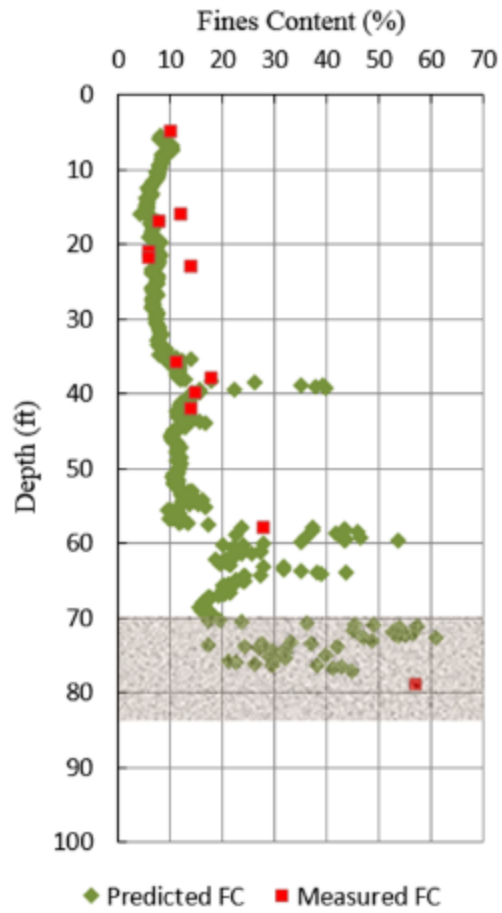


Figure 4-36 for Predicted and measured fines content versus depth for SR 50/SR 436 at westbound/pile 5 with HPR

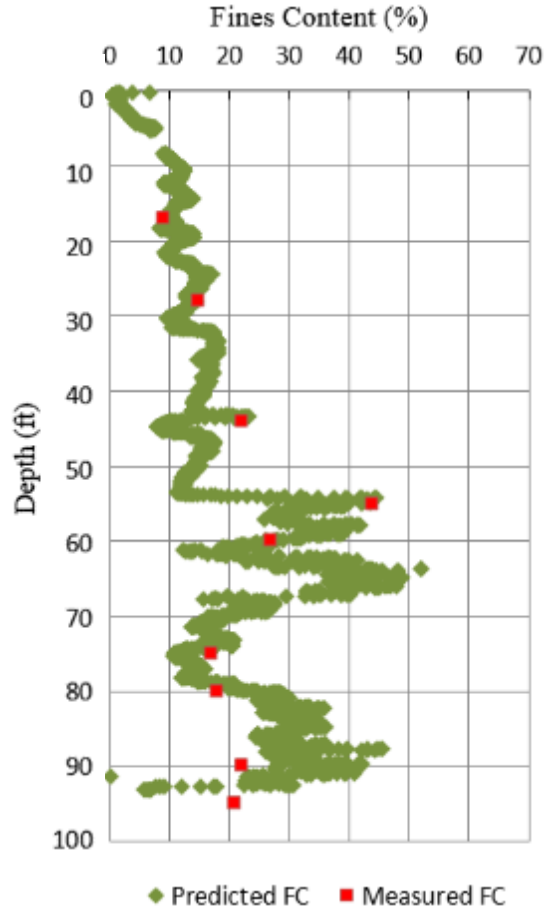


Figure 4-37 for Predicted and measured fines content versus depth for I-4/SR 408 at pier 2/pile 5

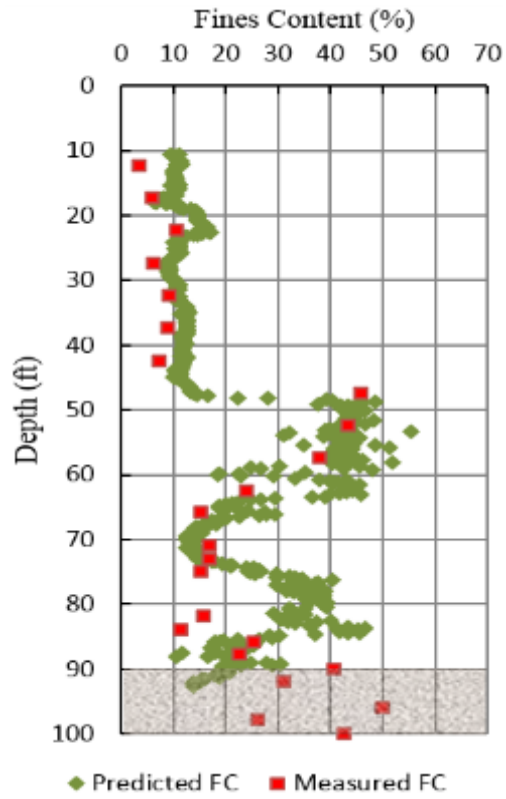


Figure 4-38 for Predicted and measured fines content versus depth for the Anderson Street overpass at pier 6/pile 5, 6 with HPR zone shaded

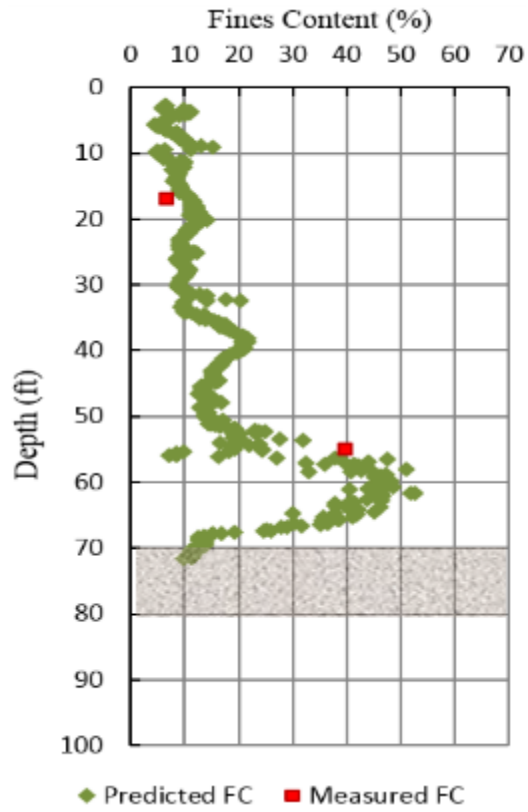


Figure 4-39 for Predicted and measured fines content versus depth for I-4 Widening Daytona at EB 3/pile 5 with HPR zone shaded

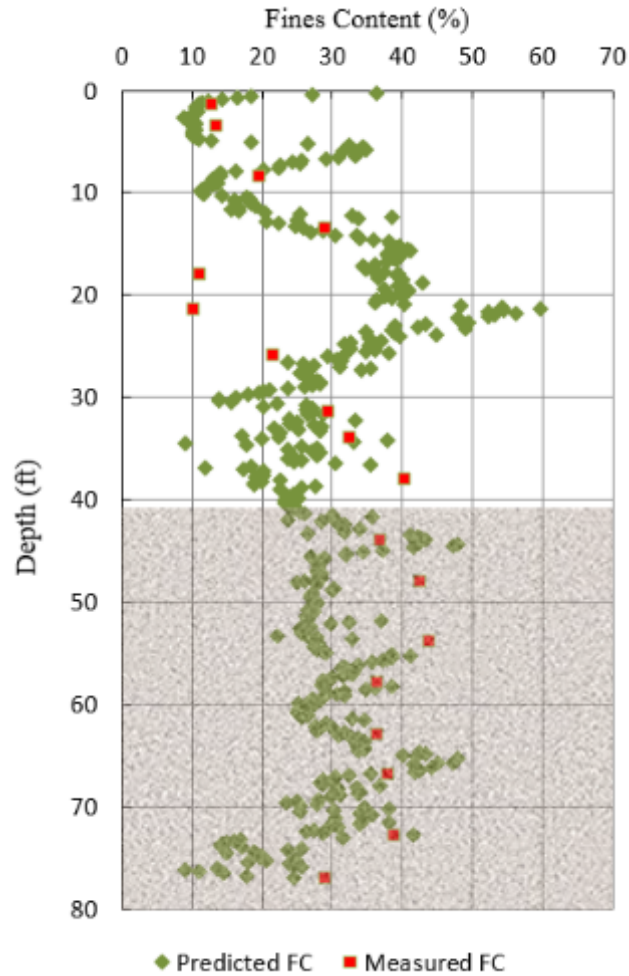


Figure 4-40: Predicted and measured fines content versus depth for SR 83 over Ramsey Branch Bridge at EB 5/pile 2 with HPR zone shaded

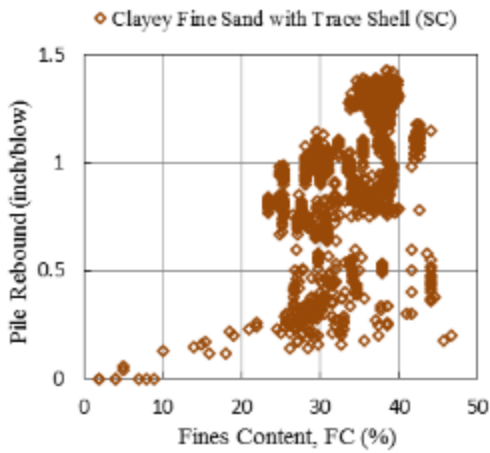
### 4.7.3. Effect of Fines Content on Pile Rebound

In order to assess the effect of fines content on pile rebound, estimated fines content from CPTu data was used and the soil types were divided into the following seven groups:

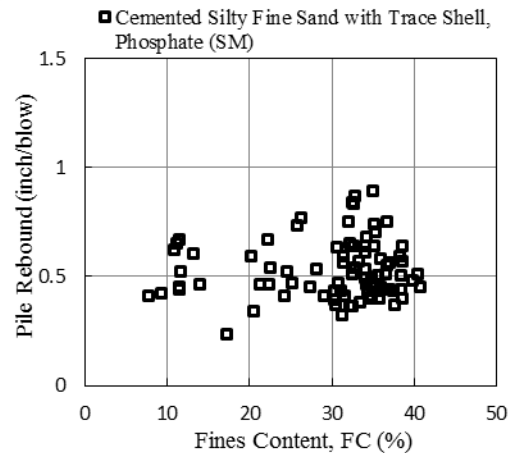
1. Clayey Fine Sand with Trace Shell (SC)
2. Cemented Silty Fine Sand with Trace Shell, Phosphate (SM)
3. Silty Fine Sand (SM)
4. Fine Sand with Clay (SP-SC)
5. Silty Clayey Fine Sand (SM-SC)
6. Poorly Graded Fine Sand (SP)
7. Poorly Graded Fine Sand with Silt (SP-SM)

Pile rebound data obtained from the PDA testing was plotted versus the CPTu fines content for seven soil types based on description and USCS type, as shown in Figure 4-41.

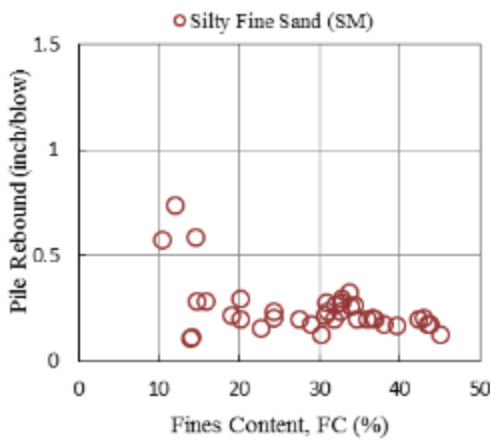
If all five parts of Figure 4-41 are reviewed, the largest increase in rebound occurs with the SC soils at FC values greater than about 23%. Figure 4-41(a) shows that clayey fine sand (SC) with trace shell produces pile rebound up to 1.4 inch/blow when the fines content nears 40%. There is a large range of rebound between 23 and 45% FC for the SC soils [Figure 4-41(a)]. Rebound in excess of 0.5 inches occurs with SM soils [Figure 4-41 (b) and (c)]. Rebound below 0.5 inches occurs with the other four soil types shown in Figure 4-41 (d) and (e).



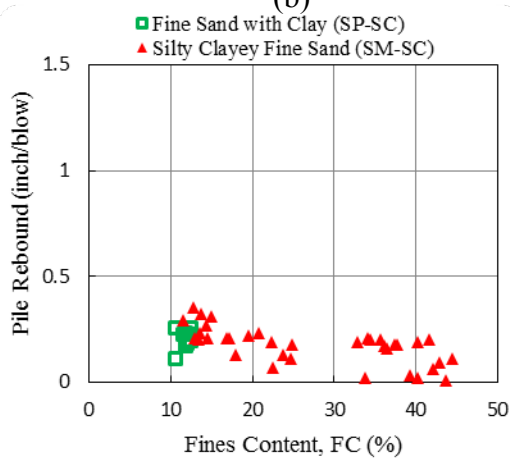
(a)



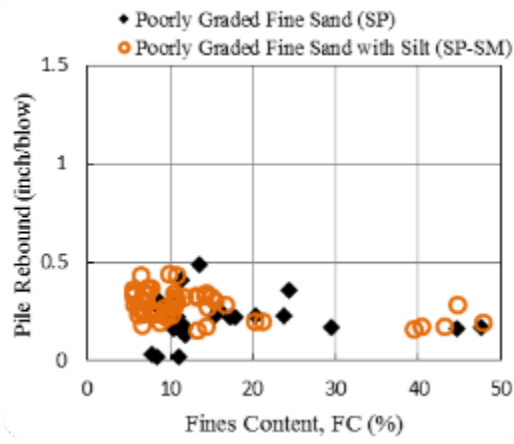
(b)



(c)



(d)



(e)

Figure 4-41: Pile rebound versus CPTu FC for different soil types

#### **4.8.4 Effect of Fines Content on CPT Pore Water Pressure**

The relationship of fines content and soil type with pore water pressure was also studied. Pore water pressure ( $u_2$ ) recorded during CPT soundings was plotted versus fines content for the same seven soils described in the previous figure (Figure 4-42). In all five plots, there is an increase in  $u_2$  as FC values pass the 20% level. The soils in Figure 4-42 (a) and (b), produce the highest pore water pressures at FC values over 20%. These two plots show  $u_2$  values over 500 psi. The higher values (550 to 580 psi) were the CPT soundings in SC with trace shell soils. These two plots show increasing pore pressure with FC although there is a large scatter of data. Figure 4-42 (c) shows pore pressures of up to 370 psi at FC values between 30 and 40%. CPTu pore water pressures less than 150 psi were observed for other soil types in Figure 4-42 (d) and (e) (SP, SP-SM, SP-SC, and SM-SC). In addition, there is no increase in  $u_2$  with FC in these plots.

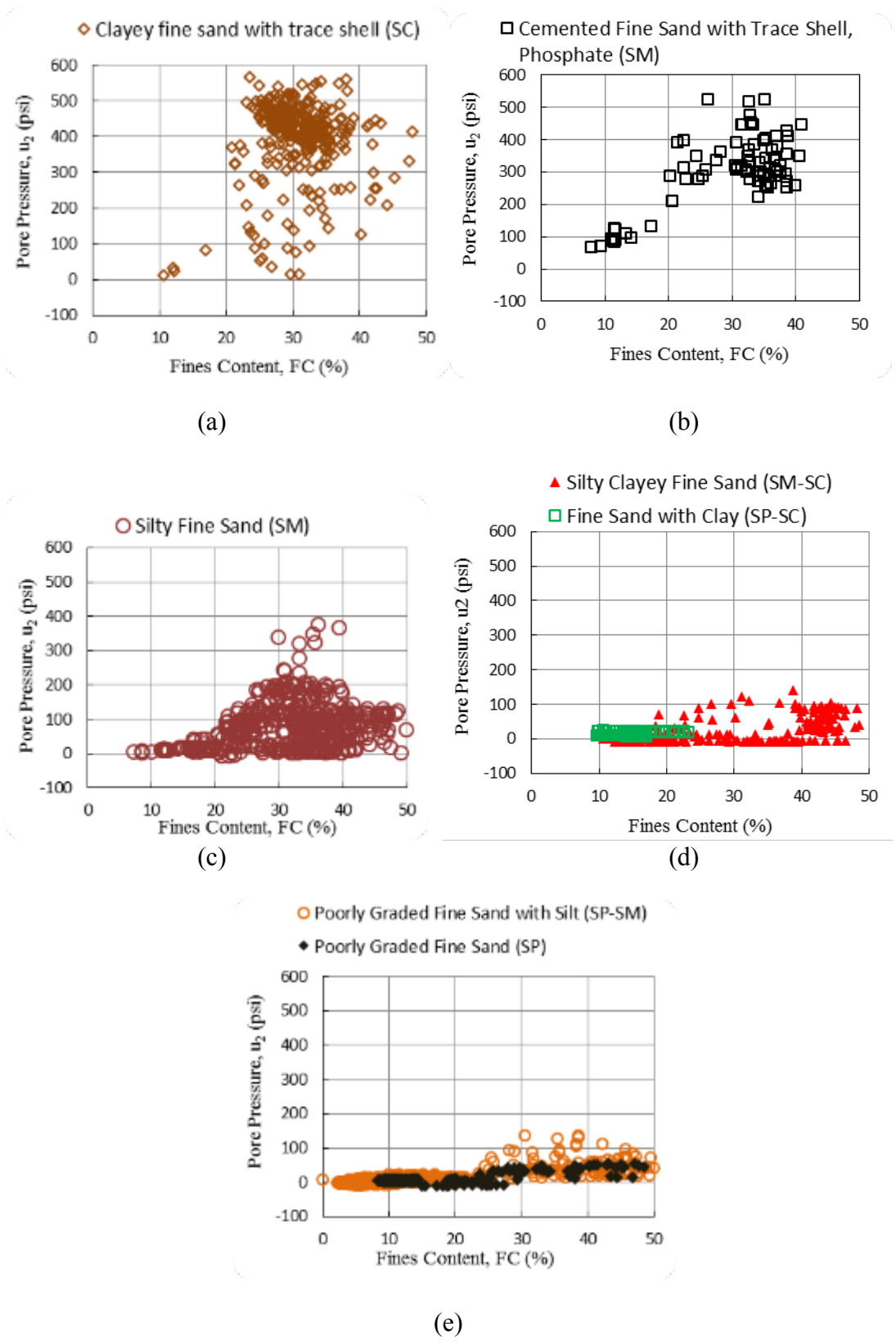


Figure 4-42: CPTu pore water pressure ( $u_2$ ) versus FC for different soil types

## 5. Analysis of SPT Data

### 5.1. Evaluation of Existing SPT and Fines Content Correlations

Cosentino et al. (2013) and Jarushi (2011) presented correlations based on limited data, shown in Figure 5.1, to predict pile rebound versus uncorrected N values and FC. Both plots show that higher rebound would occur if either N or FC were increased. In addition to these plots being developed from a limited number of points, the exact procedure used to determine these points and the very small number of N-values above thirty and FC over 40% prompted this new work.

In this study, over 1000 PDA data points from 25 PCP,s at 11 sites were evaluated to determine updated rebound correlations with N and FC. The names and associated testing performed for these sites are summarized in Table 5.1. All test sites previously reviewed by Cosentino et al. (2013) (i.e., Sites 6, 7 and 12) and sites 1, 4, 6, 7, and 12 evaluated by Jarushi (2011) were included. Five test piles were omitted from those originally reviewed because information such as GSE or location did not closely match SPT locations. These piles were replaced with other test piles that matched elevation and location more closely from the same site (Wisnom, 2015). Additionally, PDA analysis differed slightly from the previous studies where PDI plots were used to produce outputs averaged in one-foot increments. Analysis in this study utilized raw data that displayed all PDA parameters for every blow. To calculate rebound, the final inspector's set was subtracted from maximum displacement per blow ( $\text{Rebound} = \text{SET} - \text{DFN}$ ). This data was averaged over the one-foot intervals that matched the depths of the corresponding N values. Since FC values were taken sporadically throughout the test boring operations, they may be an average of two values that are five feet apart in depth or a single value that matched the PDA one-foot interval.

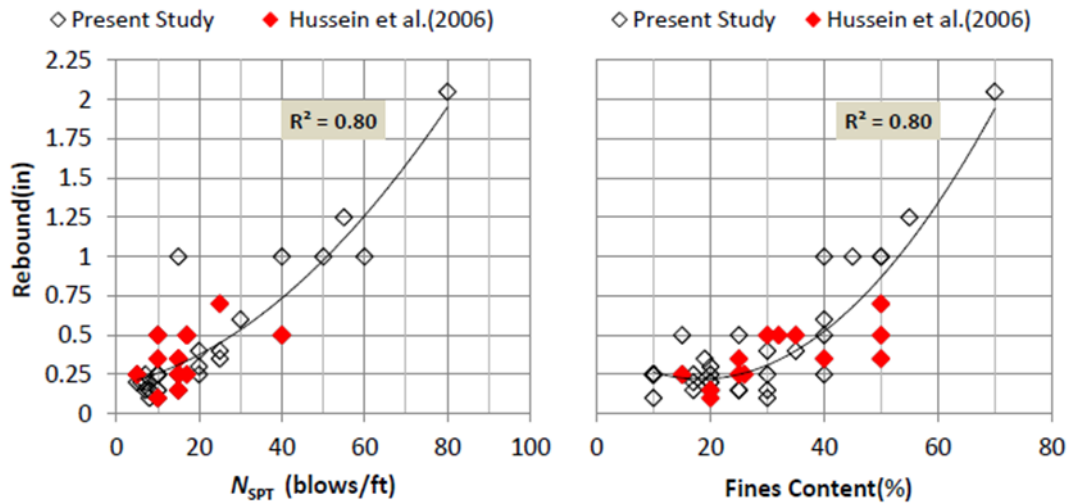


Figure 5-1: Rebound versus N and FC by Cosentino et al. (2011)

Table 5-1: List of High Pile Rebound Sites and Corresponding Testing

Number	Description	Testing			
		SPT	CPTu	DMT	Undisturbed
1	I-4 / US-192 Interchange / Osceola County / Florida.	✓	✓	⊗	✓
2	State Road 417 International Parkway / Osceola County / Florida.	✓	✓	⊗	✓
3	I-4 / Osceola Parkway / Osceola County / Florida.				✓
4	State Road 50 and State Road 436 / Orange County / Florida.	✓	✓		
5	I-4 / State Road 408 Ramp B / Orange County / Florida.	✓	✓		
6	Anderson Street Overpass at I-4/SR-408 / Orange County / Florida.	✓	✓		
7	I-4 John Young Parkway / Orange County / Florida	✓			
8	I-4 Widening Daytona / Volusia County / Florida.	✓	✓		
9	SR 528 over Indian River, Brevard County / Florida	✓			
10	Saint Johns Heritage Parkway, Brevard County / Florida	✓	✓	⊗	✓
11	I-10 Chaffee Road, Duval County / Florida	✓	⊗		✓
12	State Road 83 over Ramsey Branch Bridge / Walton County / Florida.	✓	✓		✓

- ✓ Indicates Testing Completed
- ⊗ Indicated Testing Attempted with Limited Results

### 5.1.1. Reevaluation of N versus Rebound

There are numerous corrections available for N that attempt to standardize the value. As part of this reevaluation, all the possible corrections were reviewed. Plots of rebound versus these N-values were evaluated for trends and the conclusion was that all corrections produce very similar plots. Although N was used in the original correlations,  $N_{ES}$ , which is the FDOT's

standard process for correcting  $N$ , was chosen. Re-evaluating the site data from Figure 5.1 produced the rebound versus  $N_{ES}$  plot shown in Figure 5.2. The scatter shown in this figure does not match the trend shown in Figure 5.1. In fact, Figure 5.2 shows the opposite trend as rebound generally decreases with an increase in  $N_{ES}$ . Rebound, magnitudes up to and greater than 1 inch, corresponded to  $N_{ES}$  values as low as 5, and the highest rebound measurements occurred when  $N_{ES}$  was less than 20. It is noted, however, that while rebound does appear to decrease at increasing  $N_{ES}$  values, it does not necessarily limit rebound to lower magnitudes, as an  $N_{ES}$  at refusal conditions corresponded to a rebound of 1.15 inches.

In summary, based on the larger number of PDA data points from 25 PCPs at 11 sites, there appears to be no correlation between rebound based on the inspector's set and SPT  $N$  values. The original  $N$ -rebound correlation was based on about 30 data points with only four above  $N$ -values of 40.

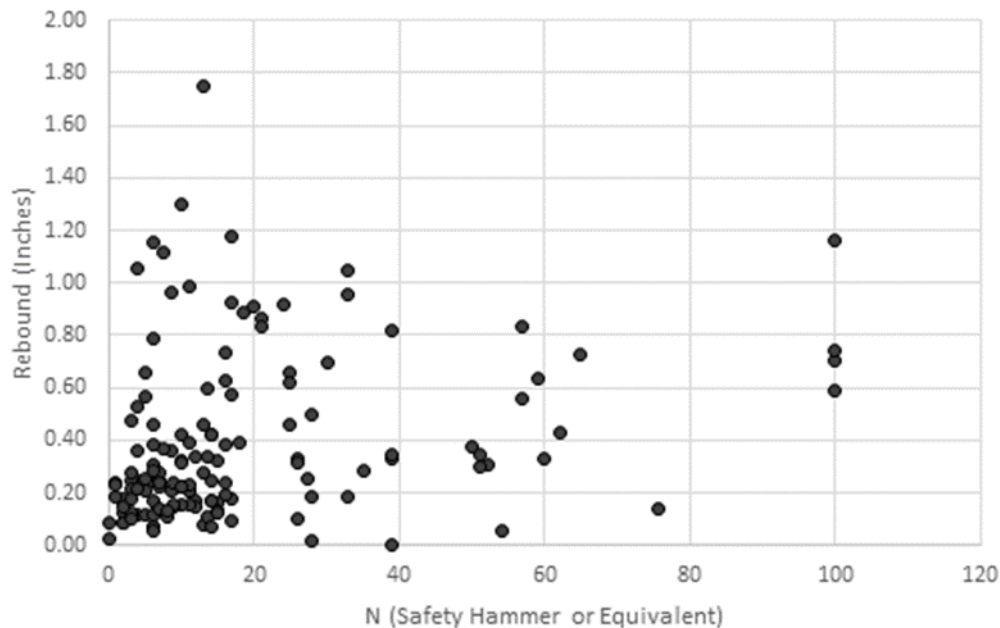


Figure 5-2: Current study rebound vs  $N_{ES}$  for sites reviewed by Cosentino et al. (2011) and Jarushi (2013)

### 5.1.2. FC versus Rebound

The nonlinear relationship between FC and rebound, shown in Figure 5.1, shows increasing rebound with an increase in FC to as high as 70%. Figure 5.3 was developed from the

same test piles used to develop Figure 5.2, and again does not lead to the conclusions originally proposed. It does, however, show a slight trend relating increased rebound magnitudes with increased FCs up to 33%, though further increases in FC produced rebound at lesser and varying magnitudes.

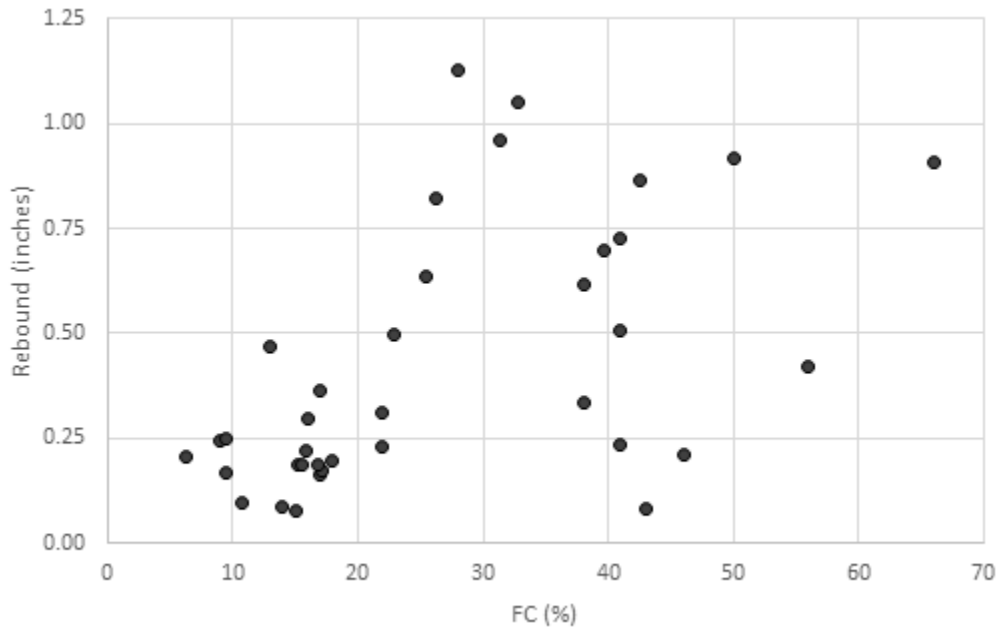


Figure 5.3: Current study rebound vs FC for sites reviewed by Cosentino et al. (2011)

Upon further review it was possible that Cosentino et al. (2011) presented only maximum or near maximum rebound magnitudes with their corresponding FCs. Several attempts were made to develop a plot similar to Figure 5.1. When revising Figure 5.3 to include only the FC data below 35%, a plot similar to Figure 5.1 was developed and produced a similar regression coefficient. Displaying what likely is a boundary condition for rebound potential, given FC up to 33%, Figure 5.4 does show strong agreement with a regression coefficient of 0.82. However, it does not exactly match Figure 5.1 where Cosentino et al. (2011) showed rebound increasing to FCs of approximately 70%.

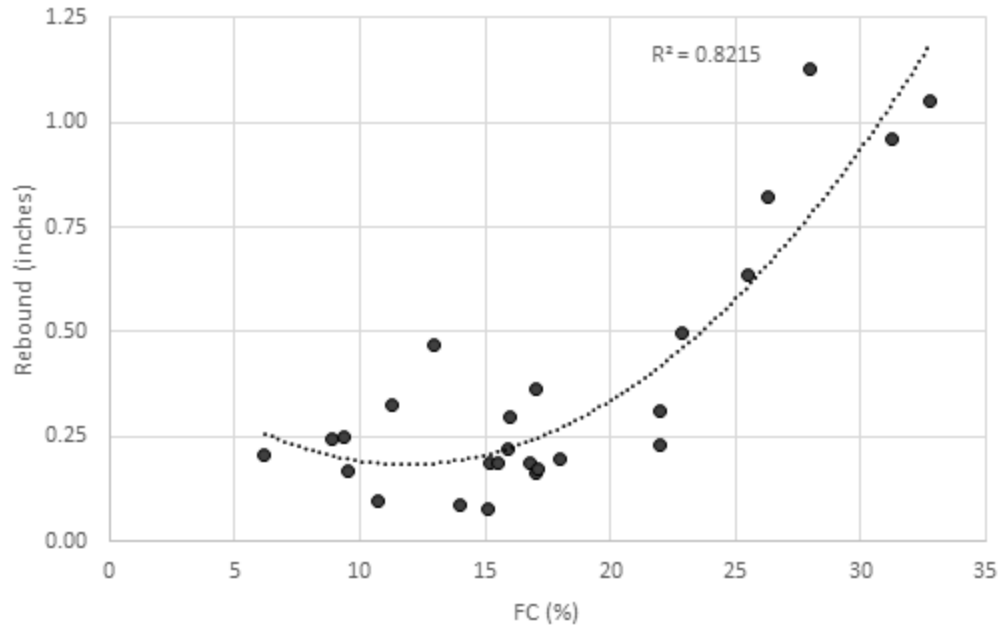


Figure 5.4: Minimum FC boundary with associated rebound (FC > 35% omitted)

In summary, there could be a relationship between rebound and FC up to FC values of about 35%. Once this threshold is exceeded, there does not seem to be any relationship.

## 5.2. Rebound versus Safety Hammer Equivalent SPT N Values

Rebound developed from PDA data and the inspector's set was evaluated for 25 test piles from 12 sites and was compared to SPT test results to develop correlations between  $N_{ES}$  and rebound. SPT N values were based on both safety and automatic hammer borings; therefore, all automatic hammer N values were converted to safety hammer equivalent by multiplying Nauto by 1.24 (FDOT, 2015).  $N_{ES}$  values were divided into three categories based on the USCS and FC. Categories included:

- sands with low fines (SP with FC < 12%)
- sands with fines (SP-SC and SP-SM with FC between 12% and 50%)
- high fines silts and clays (ML, MH or CL, CH with FC > 50%).

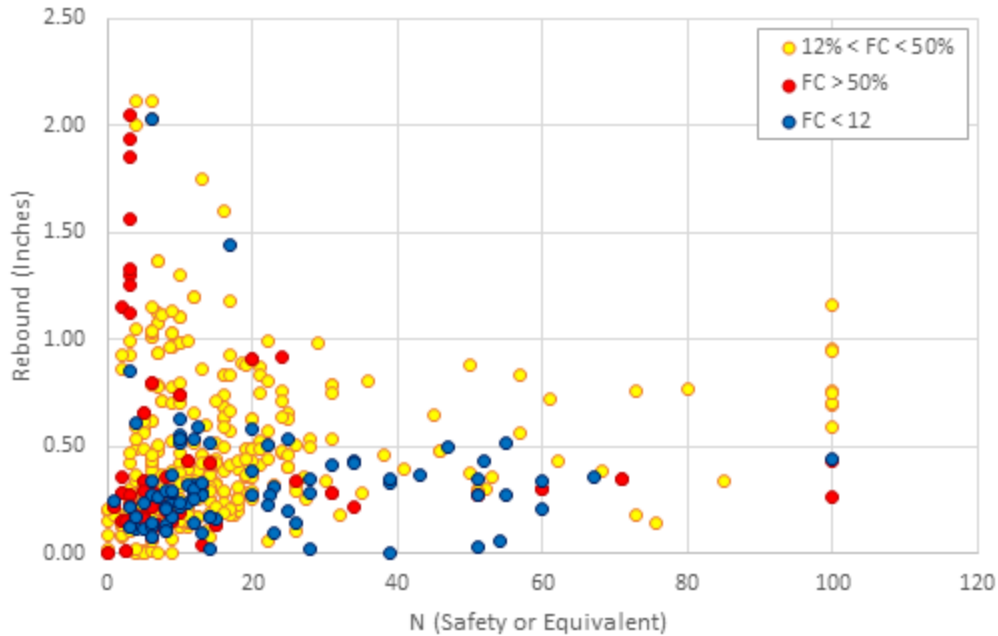


Figure 5.5: Rebound vs  $N_{ES}$  for all sites and soils

Figure 5.5 shows that generalizations can be made when comparing rebound displacements with each soil category, and that rebound maximums decrease as  $N_{ES}$  increases. The maximum rebound for all three soil types occurred when  $N_{ES}$  values were less than about 17 blows per foot. The highest measured rebound of over 2 inches occurred when  $N_{ES}$  was less than 6.

If the overall behavior of these three soil types versus  $N$  value is considered, when  $FC$  exceeds 50%, the blow counts are typically below 30. For  $12\% < FC < 50\%$ , the blow counts can vary from zero to 100, and for  $FC < 12\%$ , the blow counts are typically below 60.

After 20 blows per foot, rebound decreased to a somewhat constant value except for silty or clayey sands (SM with  $FC$  between 12 and 50%). These soils had rebound greater than 1 inch for all  $N_{ES}$  values up to SPT refusal. High fines soils (silts and clays) and sands with fines (SP-SC and SP-SM) appear to have HPR limiting  $N_{ES}$  values (24 and 20 respectively) and rebound did not exceed 0.50 inches once these were exceeded.

An SP-SC (P2P9 at Chaffee Road) and an SP-SM (B4P2 at Ramsey Branch) (See the points in blue with approximate coordinates of 6, 2.1 and 18, 1.45) were exceptions to the 0.50-inch rebound and had rebound greater than 1.40 inches. The Chaffee Road SP-SC soil is

sandwiched between CH/SC layers, which produced rebound in excess of 2 inches. Very limited FC data was available for most of the layers in this zone of soils and it is possible that the USCS symbol provided is reported incorrectly and may be CH. Rebound ceased after the pile penetrated this layer. It is possible that the influence of the soils above or the misidentified SP-SC layer resulted in this sand being identified for rebound. This phenomenon is also seen at Ramsey Branch where a thin SP-SC layer was sandwiched in between SC soils; it again is likely that any rebound was more influenced by the surrounding soils (rebound did decrease when the SP-SM layer was penetrated).

Rebound in excess of 2 inches occurred when  $N_{ES}$  was less than 6. Low fines sands generally do not produce rebounds greater than 1 inch, and at  $N_{ES}$  above 20, they produced rebound that did not exceed approximately 0.50 inches. Silts and clays (i.e.,  $FC > 50\%$ ) produced multiple instances of rebound greater than 1 inch when  $N_{ES}$  was less than 4, but did not exceed 0.35 inches at  $N_{ES}$  greater than 24 and/or as the soils became stiffer/harder. Sands with fines ( $12 < FC < 50\%$ ) showed the greatest potential for rebound as rebound magnitudes above 1 inch occur up to an  $N_{ES}$  of 18 and remain high, between 0.75 and 1 inch, as  $N_{ES}$  increased to refusal.

### **5.3. PDA Rebound versus SPT (N1)60 Values**

Correcting  $N_{60}$  to an equivalent vertical effective stress of 2000 psf can be seen in Figure 5.7. Low FC soils again display a low rebound maximum value of approximately 0.50 inches as (N1)60 increases above 25. Though the highest magnitude rebound occurred at low (N1)60 values for both low fines sands and sands with fines, there is a noticeable difference in silty and clayey sands as (N1)60 increased. Rebound had previously been limited to 1 inch, not considering refusal conditions, when  $N_{ES}$  or  $N_{60}$  increased above 20, but rebound greater than 1 inch can be seen throughout the range of (N1)60 values.

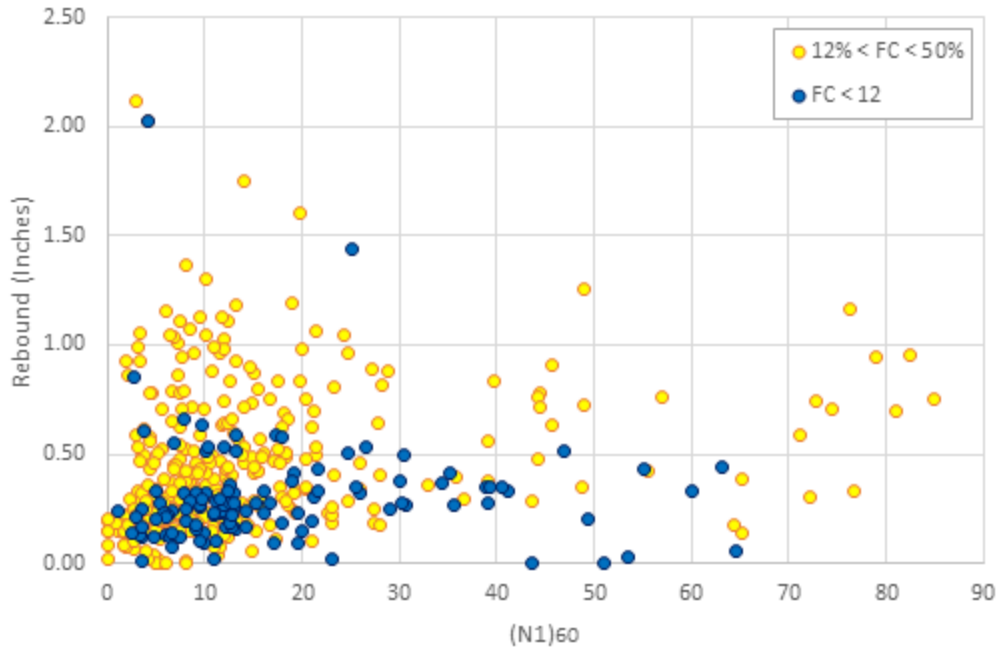


Figure 5.6: Rebound vs (N1)60 for sands

#### 5.4. PDA Rebound versus Fines Content

Construction drawings generally include two to five FC test results within the soil profile, occasionally including plasticity and water content data. This research produced complete FC profiles from 3 of the 11 sites. The remaining 8 sites produced two to three FCs. This data was combined; however, it should be noted that after all FC data was combined, 63% of the data was from Anderson Street, which may influence the results.

Though there is some scatter, Figure 5.8 shows a general trend of increasing rebound magnitudes with increasing FCs up to approximately 40%. As FC increases above 40%, there is a noticeable decrease in rebound magnitude though there are significantly fewer data points at higher FCs. A correlation could be made relating maximum rebound potential to FC, but the limited amount of data points, combined with the fact that a majority of soils analyzed were either SM or SC, results in the likelihood of too many unknowns. Silt or clay dominant sites would have to be included to provide higher FC data. FC and  $u_2$  showed some similar trends as those shown in Chapter 4. Therefore, it may be possible to use FC in lieu of CPTu data to identify rebound soils.

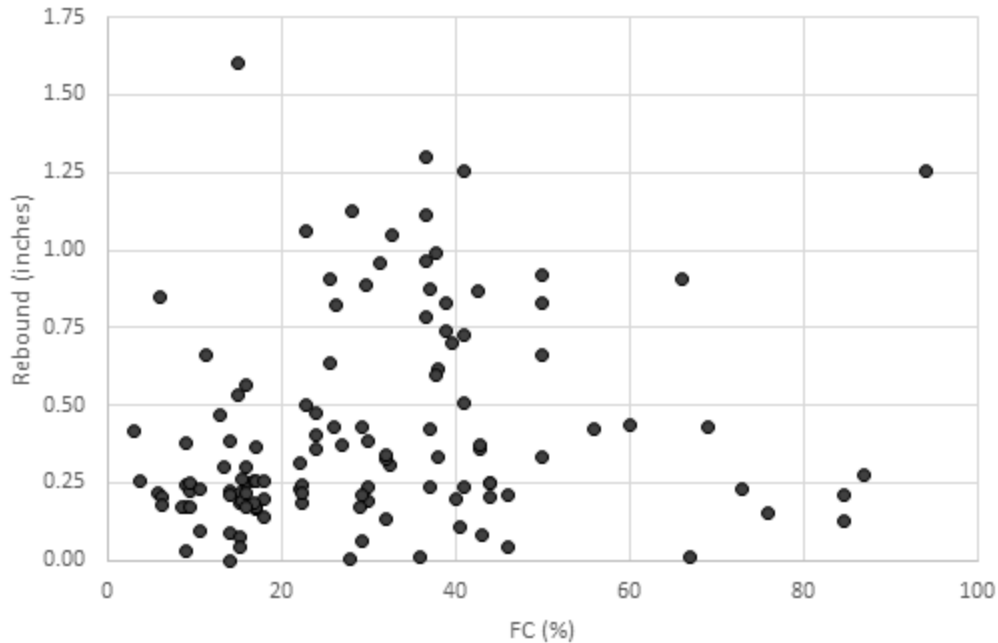


Figure 5.7: Rebound vs FC for all sites and soils

The data in Figure 5.9 displays frequency distributions of FC with 10% bins or increments based on rebound greater than and less than 0.50 inches. The rebound data shows an increasing likelihood of rebound  $> 0.50$  inches as FC increases up to 40%. The 30 to 40% FC bin had the highest number, with 13 of the 34 samples or 38% having FC in this range. At FCs greater than 40%, rebound over 0.50 inches occurs far less frequently and becomes almost nonexistent past an FC of 50%. It also shows that rebound less than 0.50 inches occurs more frequently at FCs between 10 and 20%, as 29 of the 91 samples or 32% were in this range. Within the 30 to 40% bin, 9 of the 91 samples were included or only 10%.

Table 5.2 is a summary of the FC occurrences from the histogram. It shows that in both the 30 to 40 and 40 to 50% bins, rebound is more likely than nonrebound; however, in the other ranges, it is less likely. There is about an equal probability of rebound and nonrebound in the 20 to 30% range. In summary, there seems to be some trend between FC in the 30 to 40% range and rebound greater than 0.50 inches as rebound was nearly four times more likely to occur for soils with these FCs. Additional FC data would help substantiate these trends.

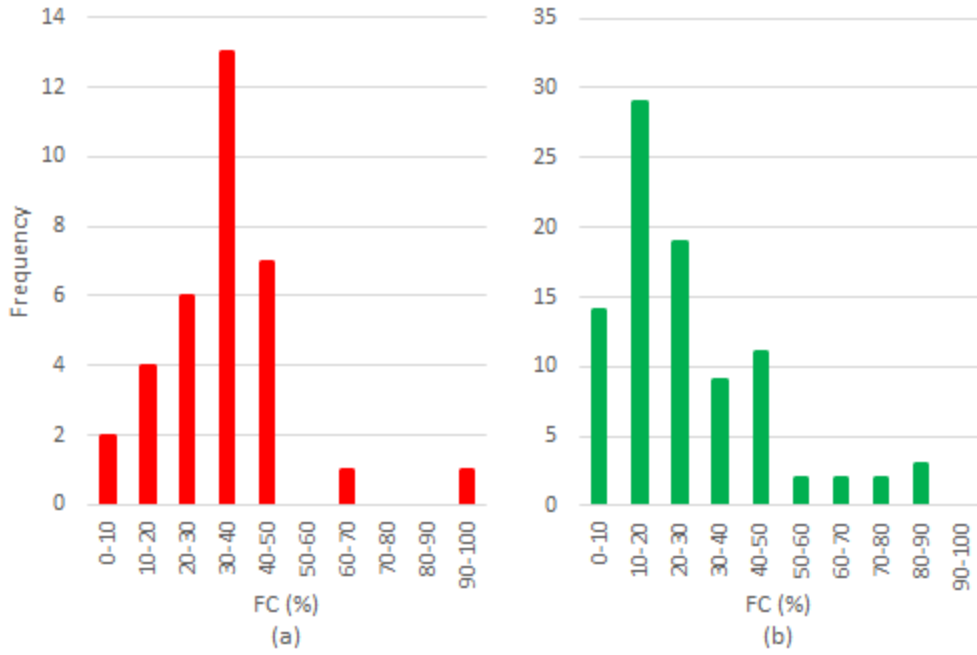


Figure 5.8: Frequency distribution of FC for (a) rebound > 0.50 inches and (b) rebound < 0.50 inches

Table 5.2 Percent FC Occurrences based on Rebound > and < 0.50 inches

FC % Frequency Bin	Percentages		
	Min	Max	Rebound
0	10	6%	15%
10	20	12%	32%
20	30	18%	21%
30	40	38%	10%
40	50	21%	12%
50	60	0%	2%
60	70	3%	2%
70	80	0%	2%
80	90	0%	3%
90	100	3%	0%
Total %		100%	100%

## **5.5. Predicting Contractive and Dilative Trends from N1(60) versus Rebound**

Based on work by Dekhn (2015), that indicates dilative and contractive behavior of HPR and nonHPR soils show some differences, SPT data that was used for this same purpose was investigated. Seed et al. (1985) considered liquefaction damage potential, which was redefined to reference contractive or dilative soil responses. Figure 5.10 is a frequency chart estimating the soil's contractive and dilative response based on (N1)60. Initial results on the P6P6 at Anderson Street data showed promising results, as all rebound zones directly related to dilative soils underneath the pile toe. Initial assumptions were that rebound was directly related to a dilative response.

Further analysis of other test piles did not show agreement with P6P6 and it was found that contractive soils were dominant in both rebound cases in Figure 5.10. Table 5.3 is a summary of the contractive, intermediate, and dilative potential from this N1(60) data. Note that contractive soil accounted for approximately 75% of soil responses when rebound did not exceed 0.50 inches. When rebound increased above 0.50 inches, contractive soils represented only about 50%. The SPT has a large variability associated with its results. When intermediate and dilative frequencies are added, there is about equal potential for rebound between contractive and this sum. When this same approach is used for the nonrebound soils, there is about a 70/30 split between contractive and the combination of intermediate and dilative soils.

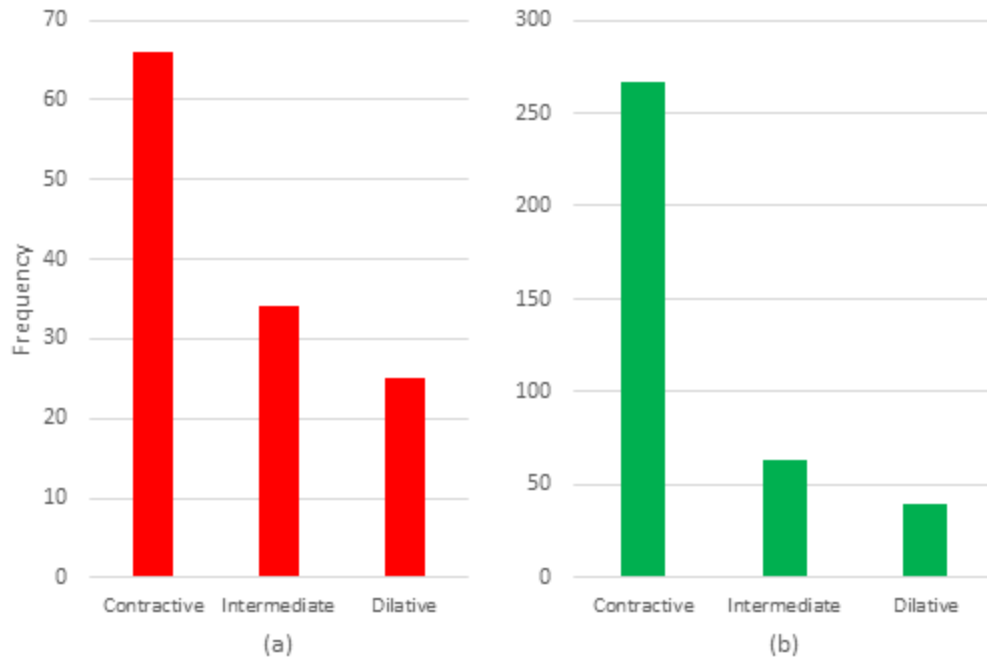


Figure 5.9: Soil predicted reaction to SPT equivalent (N1)60 after Wisnom (2015) for (a) Rebound > 0.50 inches and (b) Rebound < 0.50 inches

Table 5.3: Percent Liquefaction Potential Occurrences based on Rebound > and < 0.5 inches

Frequency Bin	Percentage	
	Rebound	NonRebound
Contractive	53%	72%
Intermediate	27%	18%
Dilative	20%	11%
Total	100%	100%

## **6. Analysis of Laboratory Data**

### **6.1. Analysis of Grain Size Properties for HPR and nonHPR Sites**

A series of laboratory tests were performed to determine the HPR and nonHPR soil properties. Based on exiting PDA data, samples were divided into two groups:

- (a) samples retrieved from HPR zones that produced more than 0.5 inches of rebound
- (b) samples retrieved from nonHPR zones considered as those that produced less than 0.25 inch rebound.

Based on the Unified Soil Classification System (USCS), these soils were then subdivided into cohesionless and cohesive groups.

In the following sections, factors such as sand content, silt content, clay content, fine content, particle size, void ratio, permeability, porosity, total unit weight, water content, and Atterberg limits were evaluated to determine possible HPR trends.

### **6.2. Evaluating HPR Trends from Grain Size and Classification Data**

The grain size properties from these soil samples are summarized and divided into two categories: cohesionless soils, shown in Table 6.1, and cohesive soils, shown in Table 6.2. Each table also distinguishes between the HPR and nonHPR soil data.

According to USCS, the majority of the soil samples from all sites, whether or not the samples were from high pile HPR zones, were identified as silty sands (SM), high plastic clays (CH), and low plastic clays (CL). According to AASHTO, the majority of these samples were either A-4 or A-2-4.

Figure 6.1 and Figure 6.2 show the grain size distributions for the HPR and nonHPR cohesionless soils. As shown in Table 6.1, fifteen samples were from soils where pile driving produced HPR great than 0.5 inch, while 11 samples were from soils where driving produced less than 0.2 inches of HPR.

Table 6.1: Physical Properties of Cohesionless Soil Samples

Site Name	Sample No.	Depth		GSE	D10	D30	D60	Cu	Cc	Sand	Silt	Clay	Fine	Classification	
		ft	ft	ft	mm	mm	mm			%	%	%	%	AASHTO	USCS
I-4/Osceola B1 Pier 2 Pile 8	S-1	75	76	89.2	0.004	0.049	0.118	30.4	5.2	56.0	36.1	7.9	44.0	A-4	SM
I-4/Osceola B1 Pier 2 Pile 8	S-2	75	76	89.2	0.002	0.033	0.065	38.2	9.9	35.8	54.1	10.1	64.2	A-4	ML
I-4/Osceola B1 Pier 2 Pile 8	S-3	80	81	89.2	0.007	0.085	0.185	27.8	5.8	74.2	19.7	6.1	25.8	A-2-4	SM
I-4/Osceola B1 Pier 2 Pile 8	S-4	85	87	89.2	0.063	0.130	0.230	3.7	1.2	87.8	5.4	6.8	12.2	A-2-4	SM
I-4 / US 192 Interchange Pier 6 Pile 4	S-5	80	82	95.0	0.005	0.069	0.110	24.4	9.6	66.2	26.8	7.0	33.8	A-2-4	SM
I-4 / US 192 Interchange Pier 6 Pile 4	S-6	80	82	95.0	0.004	0.074	0.110	31.4	14.2	69.1	24.0	6.8	30.8	A-2-4	SM
I-4 / US 192 Interchange Pier 7 Pile 10	S-7	70	72	89.2	0.002	0.075	0.110	61.1	28.4	56.3	34.4	9.3	43.7	A4	SM
I-4 / US 192 Interchange Pier 8 Pile 4	S-8	70	72	90.3	0.003	0.051	0.093	37.2	11.2	54.6	36.8	8.6	45.4	A-4	SM
I-4 / US 192 Interchange Pier 8 Pile 4	S-9	70	72	90.3	0.002	0.041	0.087	45.8	10.2	54.2	38.2	7.6	45.8	A4	SM
I-4 / US 192 Interchange Ramp BD End Bent 1 Pile 3	S-10	70	72	90.1	0.004	0.077	0.110	30.6	15.0	71.5	20.7	7.8	28.5	A-2-4	SM
I-4 / US 192 Interchange Ramp BD End Bent 1 Pile 3	S-11	70	72	90.1	0.002	0.075	0.130	81.3	27.0	70.0	19.4	10.6	30.0	A-2-4	SM
I-4 / US 192 Interchange Ramp BD End Bent 1 Pile 3	S-12	75	77	90.1	0.003	0.078	0.110	34.4	17.3	72.2	20.9	6.9	27.8	A-2-4	SM
I-4 / US 192 Interchange Ramp BD End Bent 1 Pile 3	S-13	75	77	90.1	0.002	0.075	0.110	57.9	26.9	70.0	20.4	9.6	30.0	A-2-4	SM
I-4 / US 192 Interchange West Bound End Bent 1 Pile 1	S-14	80	82	91.8	NA	0.071	0.103	NA	NA	75.6	15.9	8.4	24.3	A-2-4	SM
S.R. 83 Over Ramsey Branch Bridge End Bent 5 Pile 1	S-15	31	34	9.3	0.002	0.107	0.193	103.1	31.9	79.3	10.4	10.3	20.7	A-2-4	SM
SR 417 / International Parkway End Bent 1 Pile 14	S-16	42	44	68.5	0.0055	0.1	0.15	27.3	12.1	86.6	4.2	9.2	13.4	A-2-4	SM
SR 417 / International Parkway End Bent 1 Pile 14	S-17	57	58	68.5	0.00	0.08	0.12	60.0	28.0	75.5	15.2	9.4	24.6	A-2-4	SM
I-4 / US 192 Interchange Pier 6 Pile 4	S-18	60	62	95.0	0.0066	0.22	2	303.0	3.7	87.2	5.0	7.8	12.8	A-1-b	SM
I-4 / US 192 Interchange Pier 6 Pile 4	S-19	50	52	95.0	0.06	0.98	0.14	2.3	110.6	85.7	9.4	5.0	14.4	A-2-4	SM
I-4 / US 192 Interchange Pier 8 Pile 4	S-20	55	57	90.3	0.0035	0.12	0.235	67.1	17.5	76.3	15.8	7.9	23.7	A-2-4	SM
I-4 / US 192 Interchange Pier 8 Pile 4	S-21	55	57	90.3	0.01	0.17	0.31	37.3	11.2	86.4	6.9	6.7	13.6	A-2-4	SM
I-4 / US 192 Interchange Ramp BD End Bent 1 Pile 3	S-22	46	47	90.1	0.0041	0.13	0.28	68.3	14.7	74.5	19.6	5.9	25.5	A-2-4	SM
I-4 / US 192 Interchange South of Ramp BD End Bent 3 Pile 1	S-23	55	57	90.3	0.0016	0.096	0.18	112.5	32.0	75.7	13.9	10.4	24.3	A-2-4	SM
I-4 / US 192 Interchange South of Ramp BD End Bent 3 Pile 1	S-24	55	57	90.3	0.00	0.09	0.18	112.5	28.1	74.0	16.4	9.7	26.1	A-2-4	SM
I-4 / US 192 Interchange West Bound End Bent 1 Pile 1	S-25	50	52	91.8	0.00	0.12	0.21	100.0	32.7	79.5	11.5	9.0	20.5	A-2-4	SM
I-4 / US 192 Interchange West Bound End Bent 1 Pile 1	S-26	58	59	91.8	0.00	0.18	1.10	289.5	7.8	86.9	5.3	7.8	13.1	A-2-4	SM

Rebound > 0.5 in

Rebound < 0.22 in

USCS=Unified Soil Classification System; AASHTO = American Association of State Highway and Transportation Officials;

$$C_u = \frac{D_{60}}{D_{10}} ; C_c = \frac{D_{30}^2}{D_{60} \times D_{10}}$$

### 6.2.1. Cohesionless Soils

The cohesionless soils, where HPR was encountered, all classified as dense to very dense non-plastic silty sand (SM) according to USCS, but either A-4 or A-2-4 according to AASHTO. The results indicated that an average of 33% of the materials tested were finer than 0.075 mm (# 200 sieve). The average percentage of silt-size particles ( $< 2-7.5 \mu\text{m}$ ) was 25% and the average percentage of clay-sized particles ( $< 2 \mu\text{m}$ ) was 8.25%. These high HPR soils had an average void ratio of 1.1, an average  $D_{10}$  grain size of 0.007 mm, an average  $D_{30}$  grain size of 0.073 mm, and an average  $D_{60}$  grain size of 0.124 mm.

Cohesionless soils, where low to nonHPR was encountered, were also classified as very dense non-plastic silty sand SM according to USCS and A-2-4 (with one exception) according to AASHTO. A lower average of 19% of these soils was finer than 0.075 mm (# 200 sieve). The average percentage of silt-size particles ( $< 2-7.5\mu\text{m}$ ) was much lower at 11% and the average percentage of clay-sized particles ( $< 2\mu\text{m}$ ) was similar to the HPR soils at 8%. These silty sands have an average void ratio of 0.83, a slightly larger average  $D_{10}$  of 0.01 mm, an average  $D_{30}$  of 0.21 mm, which is three times that for HPR soils, and a larger average  $D_{60}$  of 0.45 mm, which was also three times larger than that for HPR soils.

In summary, for the cohesionless soils shown in Table 6.1, the silt content, plus  $D_{30}$  and  $D_{60}$ , are all higher in the HPR soils than in the nonHPR soils. The average silt content for the HPR soils is more than twice as high as for nonHPR soils, while both  $D_{30}$  and  $D_{60}$  are three times higher in the HPR soils than in the nonHPR soils. The USCS SM classification for HPR soils is consistent while the AASHTO classification for HPR soils varies from A-4, to A-2-4. The remaining classification parameters (i.e.,  $C_u$  and  $C_c$ ) were evaluated and no clear trends were observed.

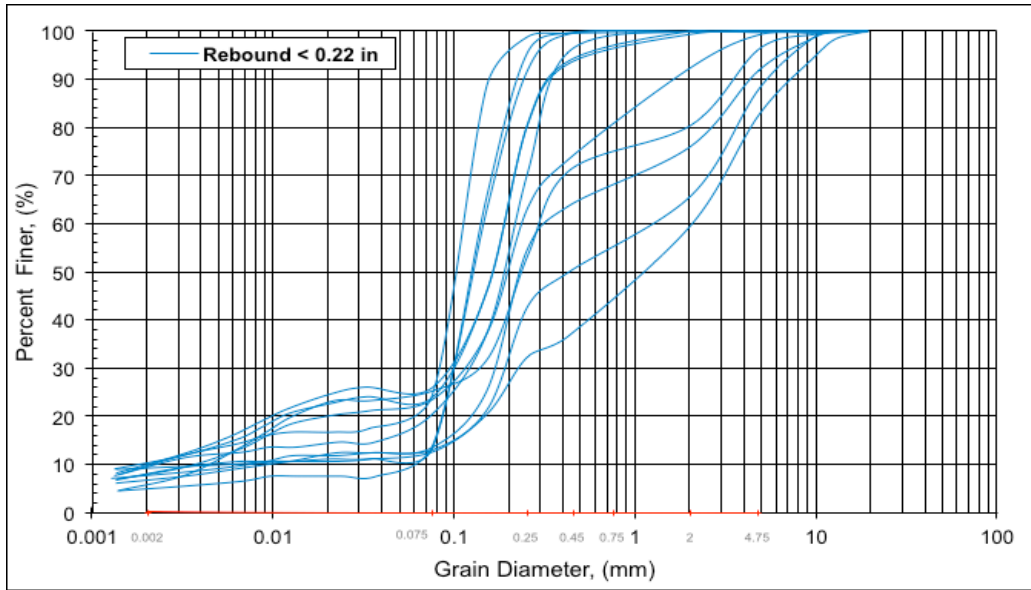


Figure 6.1: Grain size distribution curves for high pile HPR cohesionless soil

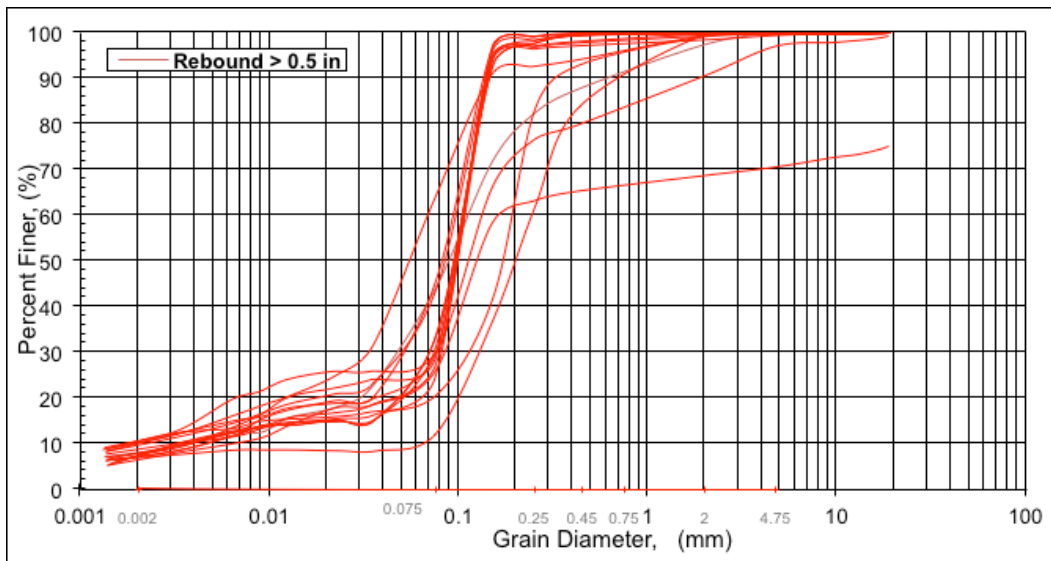


Figure 6.2: Grain size distribution curves for nonHPR cohesionless soils

### 6.2.2. Cohesive Soils

The grain size distributions for the HPR and nonHPR cohesive soils are shown in Figure 6.3 and Figure 6.4. Table 6.2 includes a summary of the key classification properties. Fifteen samples were from soils where pile driving produced HPR great than 0.5 inch, while eight samples were from soils where driving produced less than 0.2 inches of HPR.

Twelve out of 15 HPR samples classified as high plastic clay (CH) according to USCS with an average liquid limit (LL) of 63, a plastic limit (PL) of 23, and a plasticity index (PI) of 40. According to AASHTO, 13 of these 15 samples classified as A-7-6. The grain size for the HPR soils has an average of 76% of soils finer than 0.075 mm (# 200 sieve). The average percentage of clay-sized particles ( $< 2\mu\text{m}$ ) was 40.7%, while the percentage of silt-size particles ( $< 2-7.5\mu\text{m}$ ) was 35.9%. These high HPR soils have an average void ratio of 1.76, an average  $D_{30}$  of 0.04 mm, and an average  $D_{60}$  of 0.03 mm.

Based on USCS classifications, seven of the eight cohesive soils where low to nonHPR occurred were classified as low plasticity clay (CL). One sample was sandy clay (SC). According to AASHTO, half of these samples were A-7-6 and the other half was A-6. These soils had an average liquid limit (LL) of 41, a plastic limit (PL) of 18, and a plasticity index (PI) of 22. In terms of clay fraction ( $< 0.002$  mm), the results show that the average percentage of clay-sized particles ( $< 2\mu\text{m}$ ) was 24.5% while the percentage of silt-size particles ( $< 2-7.5\mu\text{m}$ ) was 54%. These low HPR soils have an average void ratio of 1.37, an average  $D_{30}$  of 0.04 mm, and an average  $D_{60}$  of 0.035 mm.

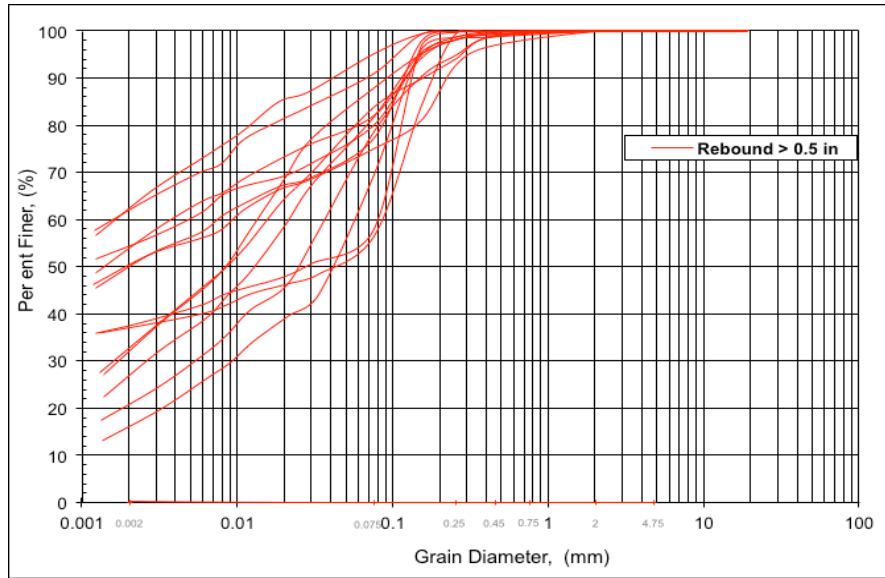


Figure 6.3: Grain size distribution curves for high pile HPR cohesive soils

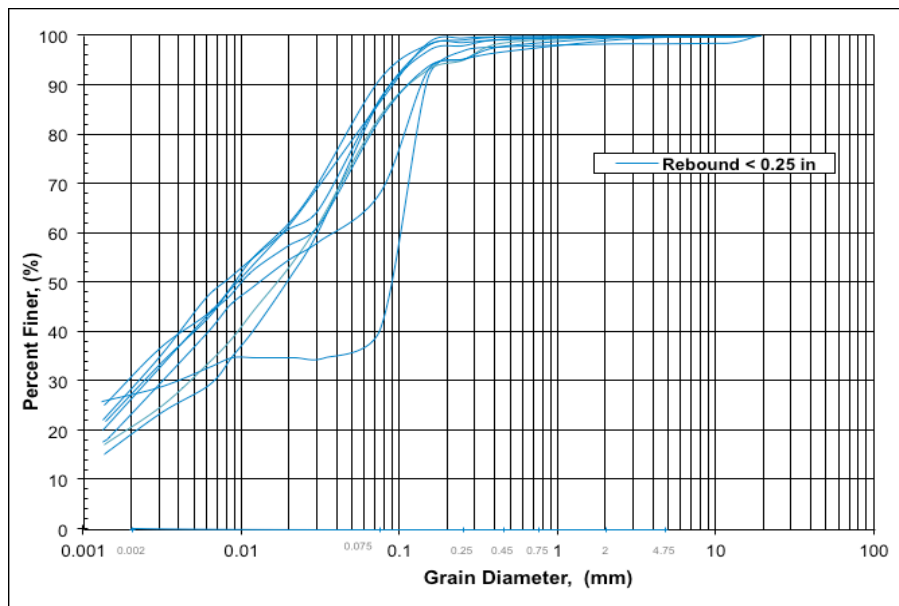


Figure 6.4: Grain size distribution curves for low to nonHPR cohesive soils

From Table 6.2, it can be concluded that Atterberg limits from cohesive HPR soils had an average plastic index nearly twice that encountered with cohesive nonHPR soils. As was the case for the cohesive soils, the remaining classification parameters were evaluated; however, no clear trends were observed.

## **6.3. Evaluating Silt Content Effects on Rebound**

Plots of silt content versus rebound were developed from the grain size data. The cohesionless data was evaluated separately from the cohesive data.

### **6.3.1. Cohesionless Soil**

The data in Figure 6.5 shows the influence of silt content on high pile HPR for all cohesionless samples. As can be seen, HPR did not begin to be clearly identified until the silt content reached 20%. Beyond this point, all soil samples experienced high pile HPR; below 20%, 11 samples produced no HPR and five produced HPR, although two additional samples had silt contents and HPR at just above 20%.

In summary, below 20% silt content, cohesionless soils may or may not produce high pile HPR; however, above 20%, all 10 samples produced HPR. It can be seen that the presence of the silts significantly affects high pile HPR.

### **6.3.2. Cohesive Soil**

The data in Figure 6.6 shows that the effect of silt content on HPR for the cohesive soils is different than for cohesionless soils. There is a distinct range over which the HPR changes, starting at 20% up to about 35%, from below 0.25 inches to greater than 0.75 inches. At silt contents greater than about 45%, HPR is approximately the same as HPR shown below 20%. Only one sample produced a silt content below 20% (14%) and HPR below 0.25 inches.

Table 6.2: Physical Properties of Cohesive Soil Samples

Site Name	Sample No.	Depth		GSE	Rebound		Ave. Rebound	D10	D30	D60	Sand	Silt	Clay	Fine	LL	PL	PI	Classification	
		ft	in		ft	in												AASHTO	USCS
Chaffee Road End Bent 1	S-27	47	49	62.34	0.34	1.26	0.80	⊗	⊗	0.085	43.1	19.9	37.0	56.9	51.0	16.0	35.0	A-7-6	CH
Chaffee Road End Bent 3	S-28	50	52	62.94	1.70	2.38	2.04	⊗	⊗	0.007	22.6	28.1	49.3	77.4	70.7	25.3	45.4	A-7-6	CH
Chaffee Road End Bent 3	S-29	50	52	62.94	1.70	2.38	2.04	⊗	⊗	0.007	22.6	28.1	49.3	77.4	70.7	25.3	45.4	A-7-6	CH
Chaffee Road End Bent 3	S-30	52	55	62.94	0.96	1.84	1.40	⊗	⊗	0.002	8.9	29.7	61.4	91.1	92.0	29.0	63.0	A-7-6	CH
Chaffee Road End Bent 3	S-31	52	55	62.94	0.96	1.84	1.40	⊗	⊗	0.002	4.9	33.8	61.3	95.1	91.0	30.0	61.0	A-7-5	CH
Chaffee Road End Bent 3	S-32	54	56	62.94	0.96	1.71	1.34	⊗	⊗	0.080	42.1	20.5	37.4	57.9	51.4	18.7	32.7	A-7-6	CH
Chaffee Road End Bent 3	S-33	54	56	62.94	0.96	1.71	1.34	⊗	⊗	0.080	42.1	20.2	37.4	57.6	51.4	18.7	32.7	A-7-6	CH
Chaffee Road End Bent 3	S-34	60	63	62.94	1.65	2.64	2.15	⊗	⊗	0.004	18.0	29.1	52.9	82.0	77.0	25.0	52.0	A-7-6	CH
Chaffee Road End Bent 3	S-35	60	63	62.94	1.65	2.64	2.15	⊗	⊗	0.005	19.8	26.2	54.0	80.2	79.0	24.0	55.0	A-7-6	CH
S.R. 83 Over Ramsey Branch Bridge End Bent 5 Pile 1	S-36	31	34	9.30	0.46	1.15	0.81	⊗	⊗	0.009	24.9	25.4	49.7	75.1	82.0	25.0	59.0	A-7-6	CH
SR 417 / International Parkway End Bent 2 Pile 5	S-37	55	57	68.50	0.00	0.10	0.05	⊗	0.004	0.10357	59.4	13.5	27.1	40.6	40.0	19.0	21.0	A-6	SC
Palm Bay Parkway Intermediate Bent 4 Pile 10	S-38	62	64	26.1	0.08	0.20	0.14	⊗	0.002	0.02	13.2	57.1	29.7	86.8	43.0	19.0	24.0	A-7-6	CL
Palm Bay Parkway Intermediate Bent 4 Pile 10	S-39	62	64	26.1	0.08	0.20	0.14	⊗	0.003	0.01742	8.7	65.1	26.2	91.3	44.0	19.0	25.0	A-7-6	CL
Palm Bay Parkway End Bent 5 Pile 1	S-40	57	59	24.86	0.32	0.11	0.22	⊗	0.006	0.03	12.7	68.8	18.5	87.3	44.0	21.0	24.0	A-7-6	CL
Palm bay Parkway End Bent 5 Pile 1	S-41	57	59	24.86	0.32	0.11	0.22	⊗	0.005	0.0281	16.1	63.8	20.1	83.9	43.0	21.0	23.0	A-7-6	CL
Palm bay Parkway End Bent 5 Pile 1	S-42	60	62	24.86	0.14	0.03	0.09	⊗	0.002	0.02	12.5	60.1	27.4	87.5	40.0	19.0	21.0	A-6	CL
Palm Bay Parkway End Bent 5 Pile 1	S-43	60	62	24.86	0.14	0.03	0.09	⊗	0.003	0.02621	16.8	58.0	25.2	83.2	37.0	14.0	23.0	A-6	CL
Palm Bay Parkway End Bent 5 Pile 1	S-44	65	67	24.86	0.09	0.26	0.18	⊗	0.004	0.03829	31.7	46.0	22.3	68.3	37.0	18.0	19.0	A-6	CL

USCS=Unified Soil Classification System; AASHTO = American Association of State Highway and Transportation Officials;

$$C_u = \frac{D_{60}}{D_{10}}, \quad C_c = \frac{D_{30}^2}{D_{60} \times D_{10}}$$

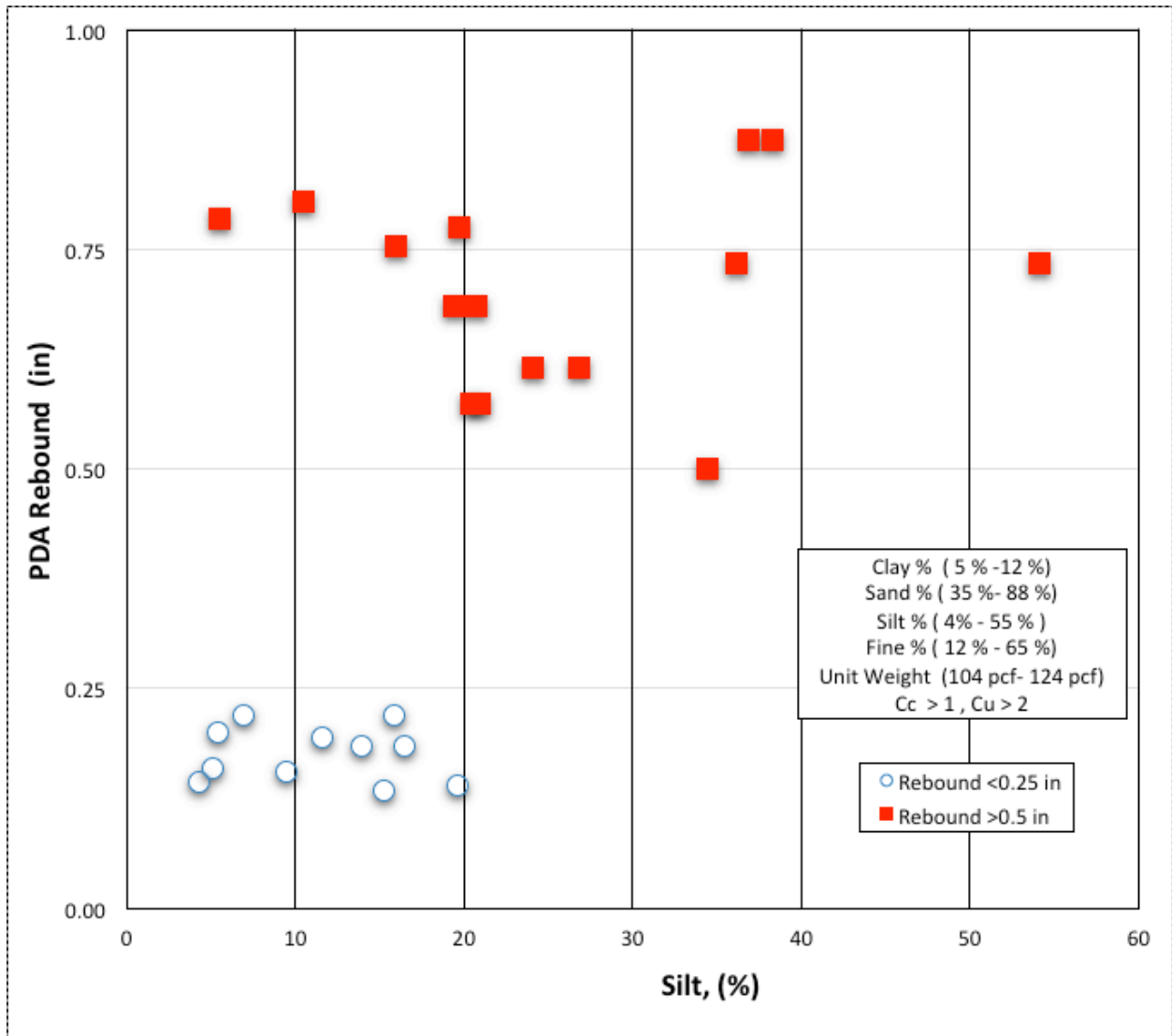


Figure 6.5: Silt content (%) vs. PDA HPR (in) – cohesionless soils (SM) from all sites

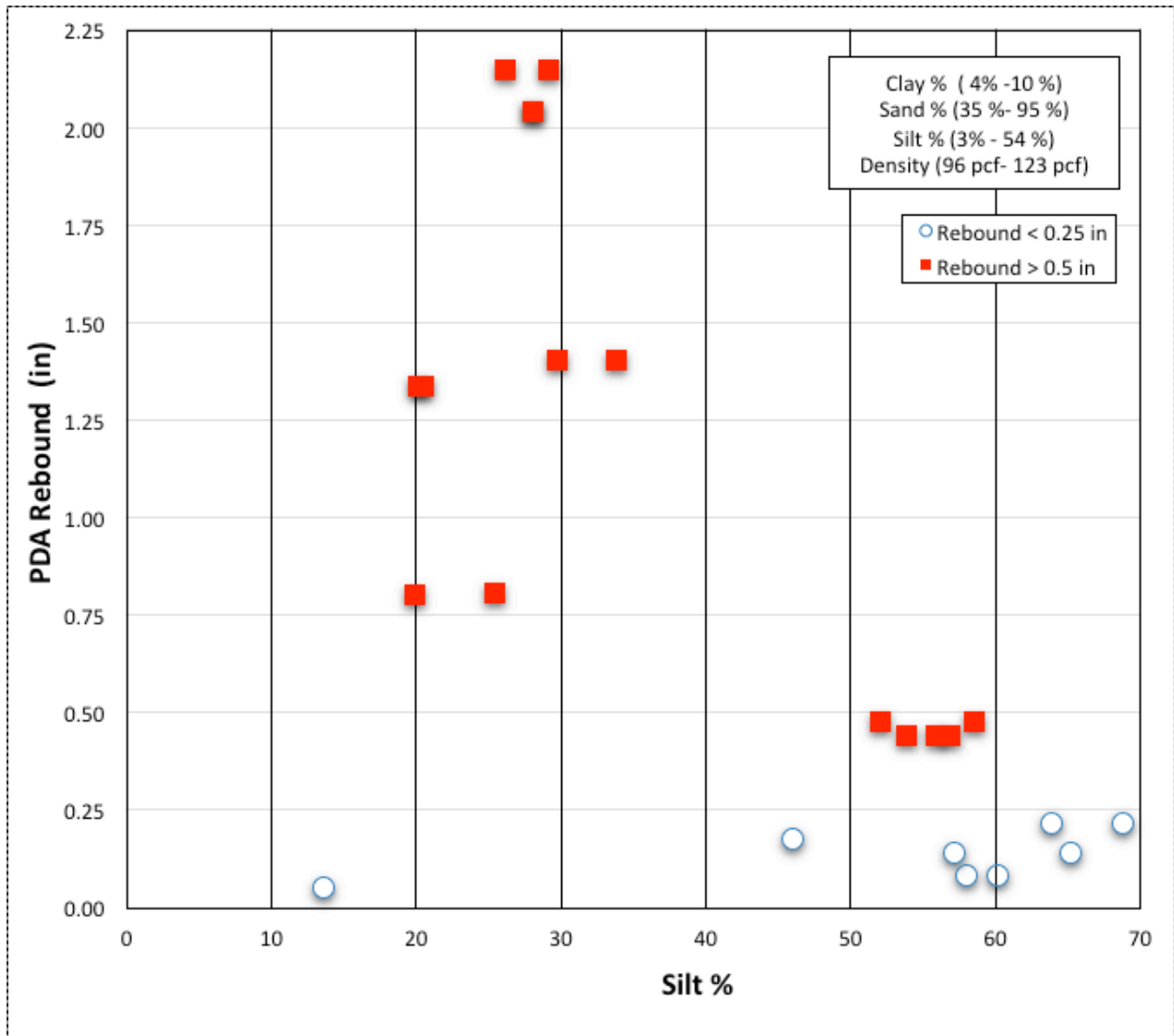


Figure 6.6: Silt content (%) vs. PDA HPR (in) – cohesive soils (CH, CL) from all sites

## 6.4. Evaluating Clay Content Effects on HPR and NonHPR Soils

Plots of clay content versus HPR were developed from the grain size information. The cohesionless data was evaluated separately from the cohesive data.

### 6.4.1. Cohesionless Soil

The data in Figure 6.7 shows that the clay content in the cohesionless soils had no effect on high pile HPR. The clay content for both HPR and nonHPR soils was between 5 to 11%.

Therefore the clay content may not be an effective index for predicting whether or not high pile HPR would occur during driving in cohesionless soils. Additional data would be helpful in clarifying this finding.

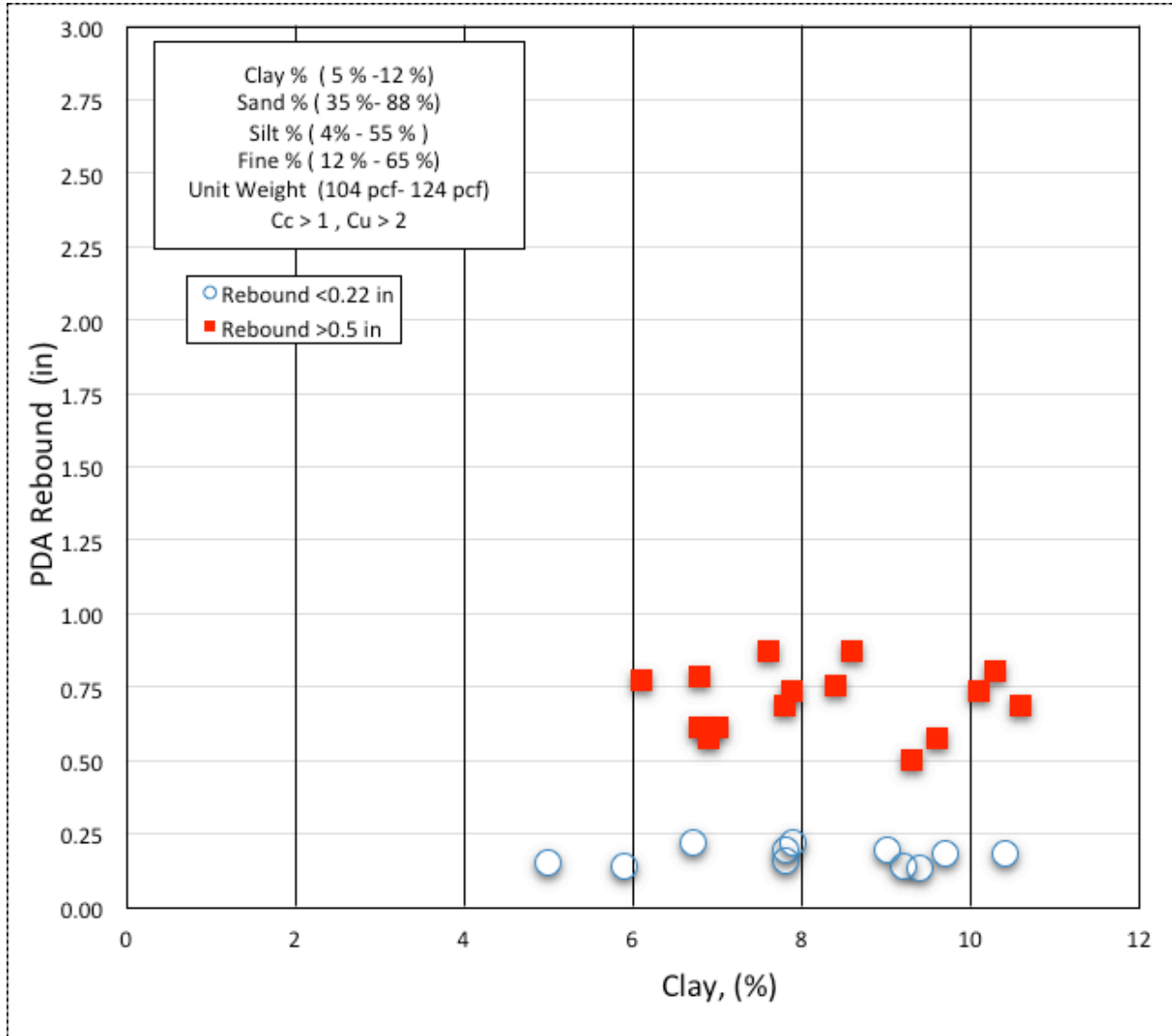


Figure 6.7: Clay Content (%) vs. PDA HPR (in) – cohesionless soils (SM) from all sites

### 6.4.2. Cohesive Soils

Figure 6.8 shows clay content versus PDA HPR for the cohesive soils. Cohesive soils with clay content less than about 30% produced HPR below 0.25 inches, while cohesive soils with clay contents above about 35% produced HPR.

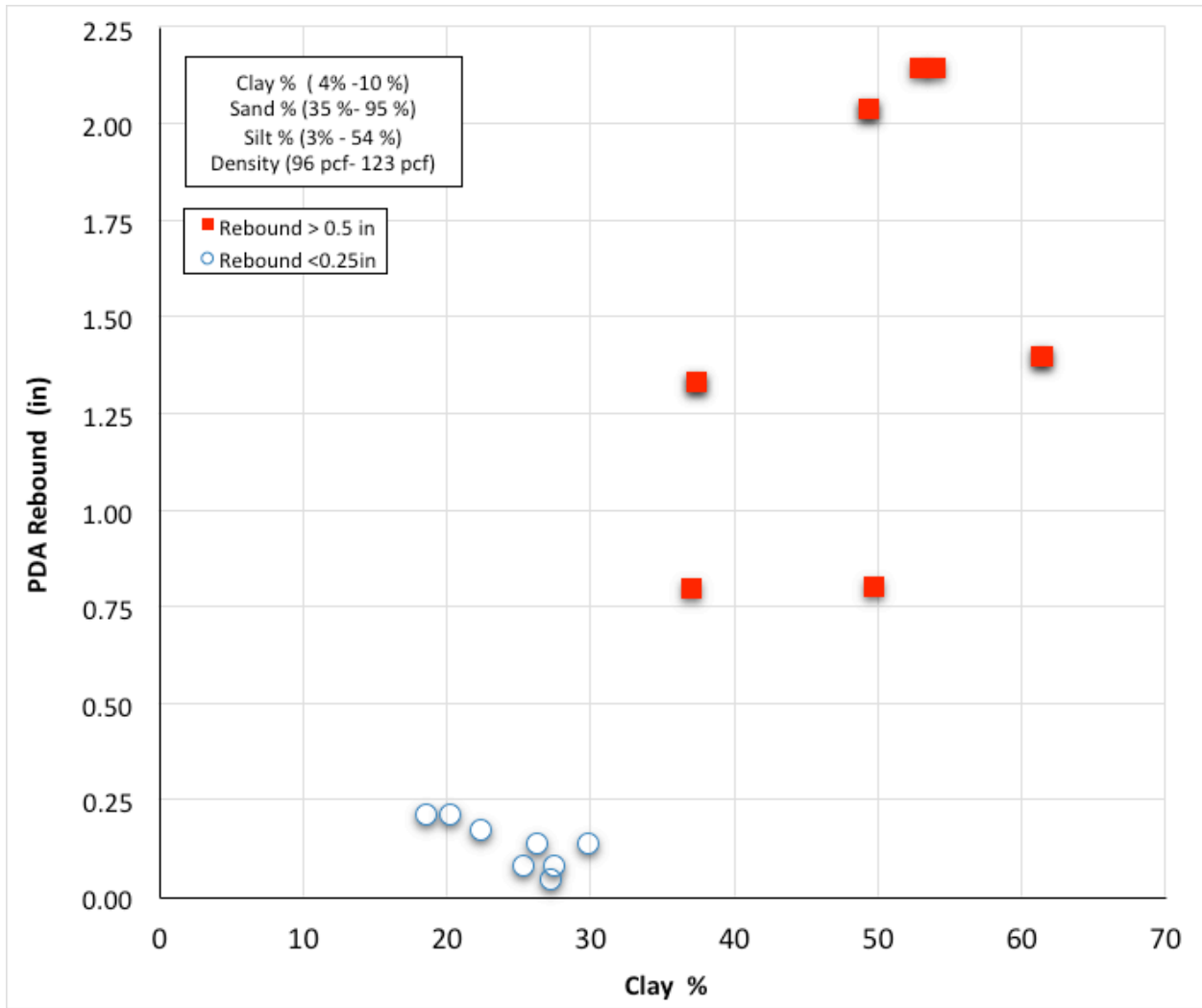


Figure 6.8: Clay content (%) vs. PDA HPR (in) – cohesive soils (CH, CL) from all sites

## **6.5. Evaluating Sand Content Effects on HPR and NonHPR Soils**

Plots of sand content versus HPR were developed from the grain size information. The cohesionless data was evaluated separately from the cohesive data.

### **6.5.1. Cohesionless Soils**

The data in Figure 6.9 shows the sand content and corresponding PDA HPR for all cohesionless specimens retrieved from HPR and nonHPR sites. The specimens that produced HPR less than 0.25 inches have a sand content greater than 74%. High pile HPR specimens were found to have sand contents between 35% and 87%.

Between 35% and 74% sand content, all specimens were found to produce high pile HPR. In summary, cohesionless soils with sand contents below 74% are more likely to produce HPR.

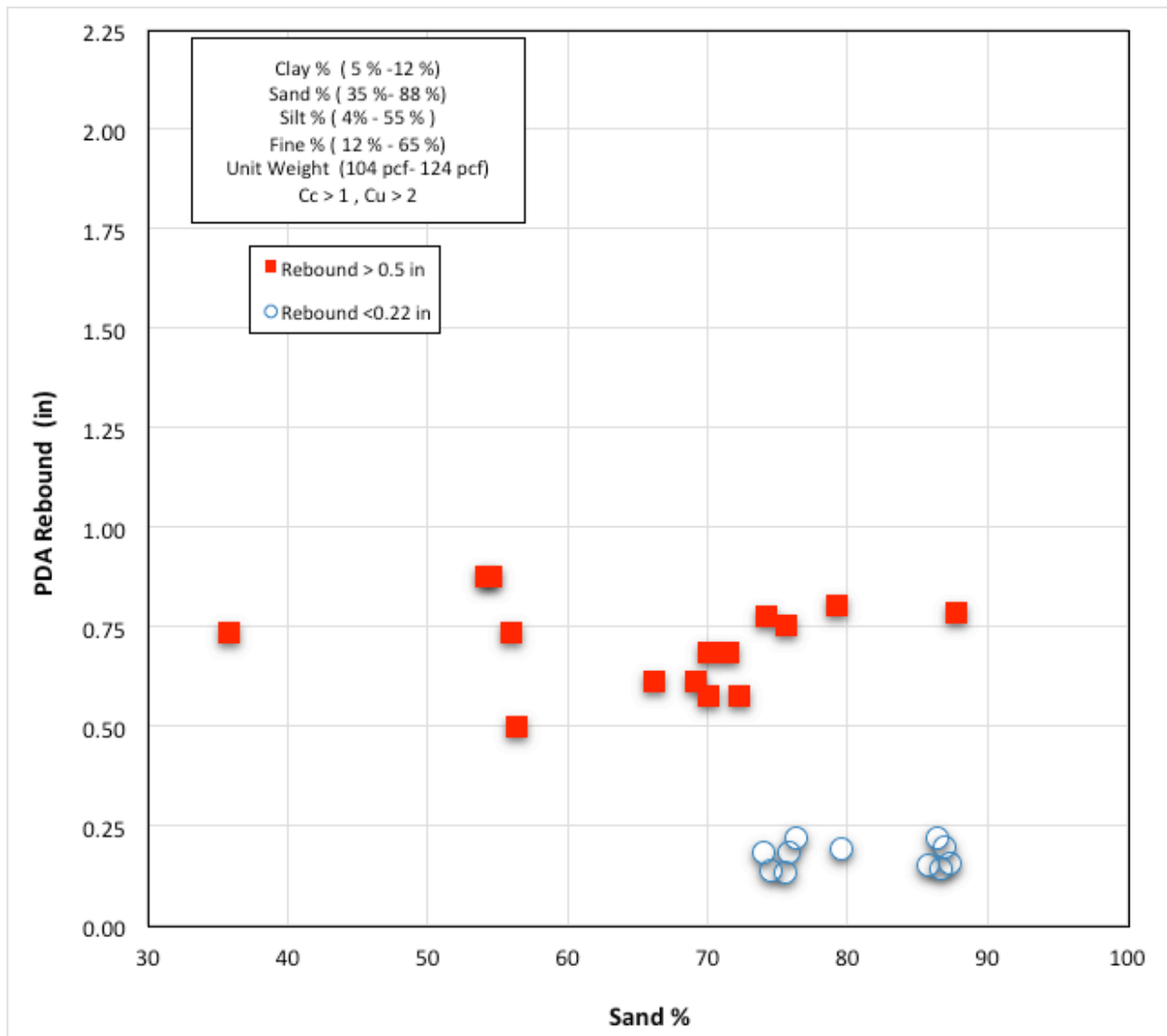


Figure 6.9: Sand Content (%) vs. PDA HPR (in) – cohesionless soils (SM) from all sites

### 6.5.2. Cohesive Soils

The large scatter of data shown in Figure 6.10 indicates no clear trend from cohesive soils for identifying high pile HPR. There is a very slight decrease in rebound as sand content increases above 25%. Overall, the data shows an excessive scatter, which implies that HPR in cohesive soils does not depend on sand content.

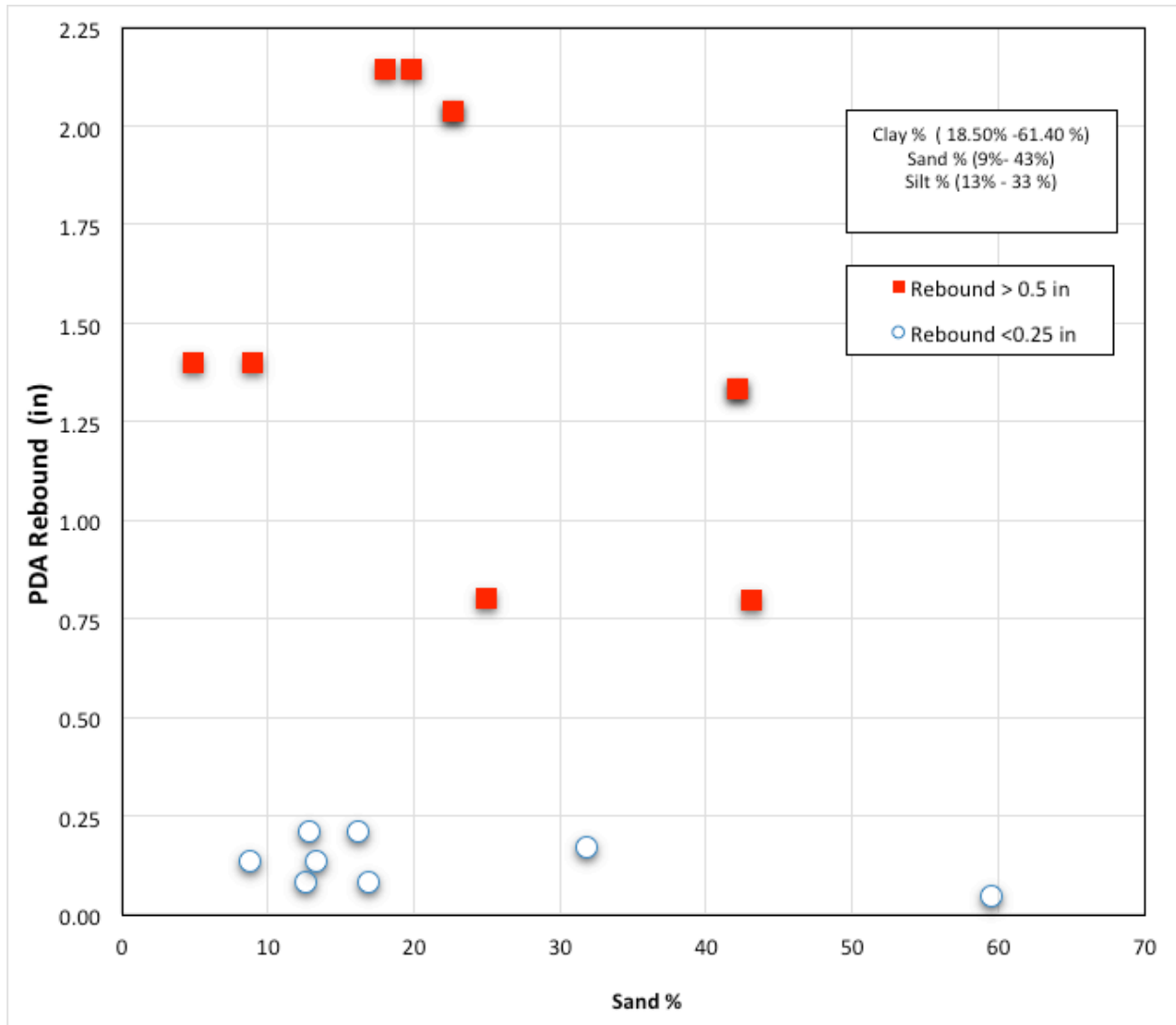


Figure 6.10: Sand content (%) vs. PDA HPR (in) – cohesive soils (CH, CL) from all sites

## 6.6. Evaluating Silt Content versus Sand Content for HPR and NonHPR Soils

Plots of sand content versus silt content were developed from the grain size information. The cohesionless data was evaluated separately from the cohesive data.

### 6.6.1. Cohesionless Soils

The data in Figure 6.11 shows the influence of silt and sand content on high and no pile HPR specimens from all sites. The results indicate that below about 70% sand and above about 20% silt, HPRs greater than 0.5 inches occur. At percentages outside this range, there is a

mixture between HPR and nonHPR behavior, with nonHPR being prevalent. This plot indicates that the variation of silt and sand in cohesionless soils significantly affects high pile HPR.

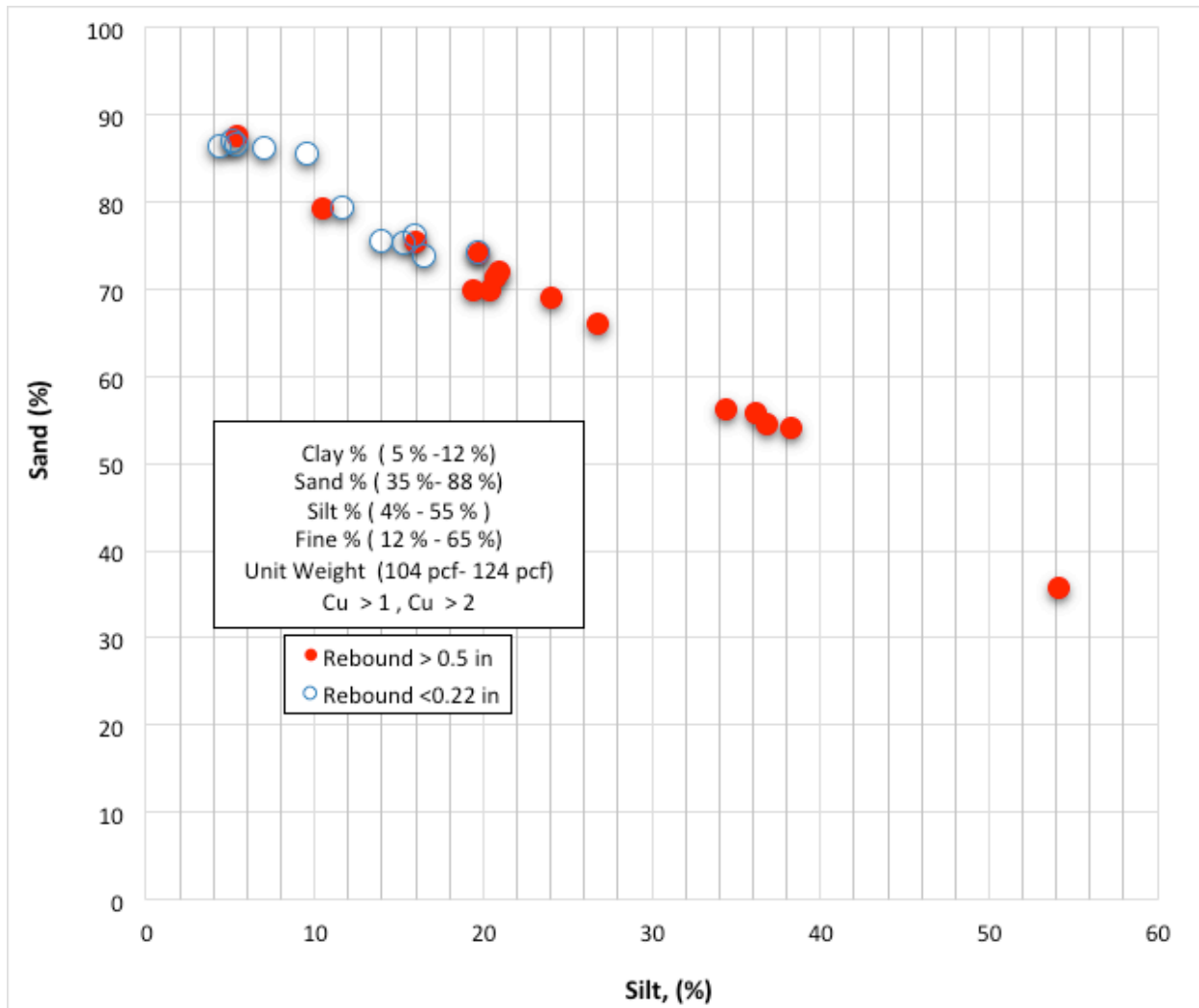


Figure 6.11: Silt content (%) vs. sand content (%) – cohesionless soils (SM) from all sites

### 6.6.2. Cohesive Soils

The results in Figure 6.12 show that HPR and nonHPR soils plot along two distinct lines, which also display high regression (i.e.,  $R^2 > 0.94$ ) coefficients. Additional data might further clarify boundaries for these lines. Due to the relatively low number of data points, no equations were included for the lines. The nonHPR percentages plot farther up or higher on each axis. Also of note is that the high HPR data points only exist between 20 and 34% silt.

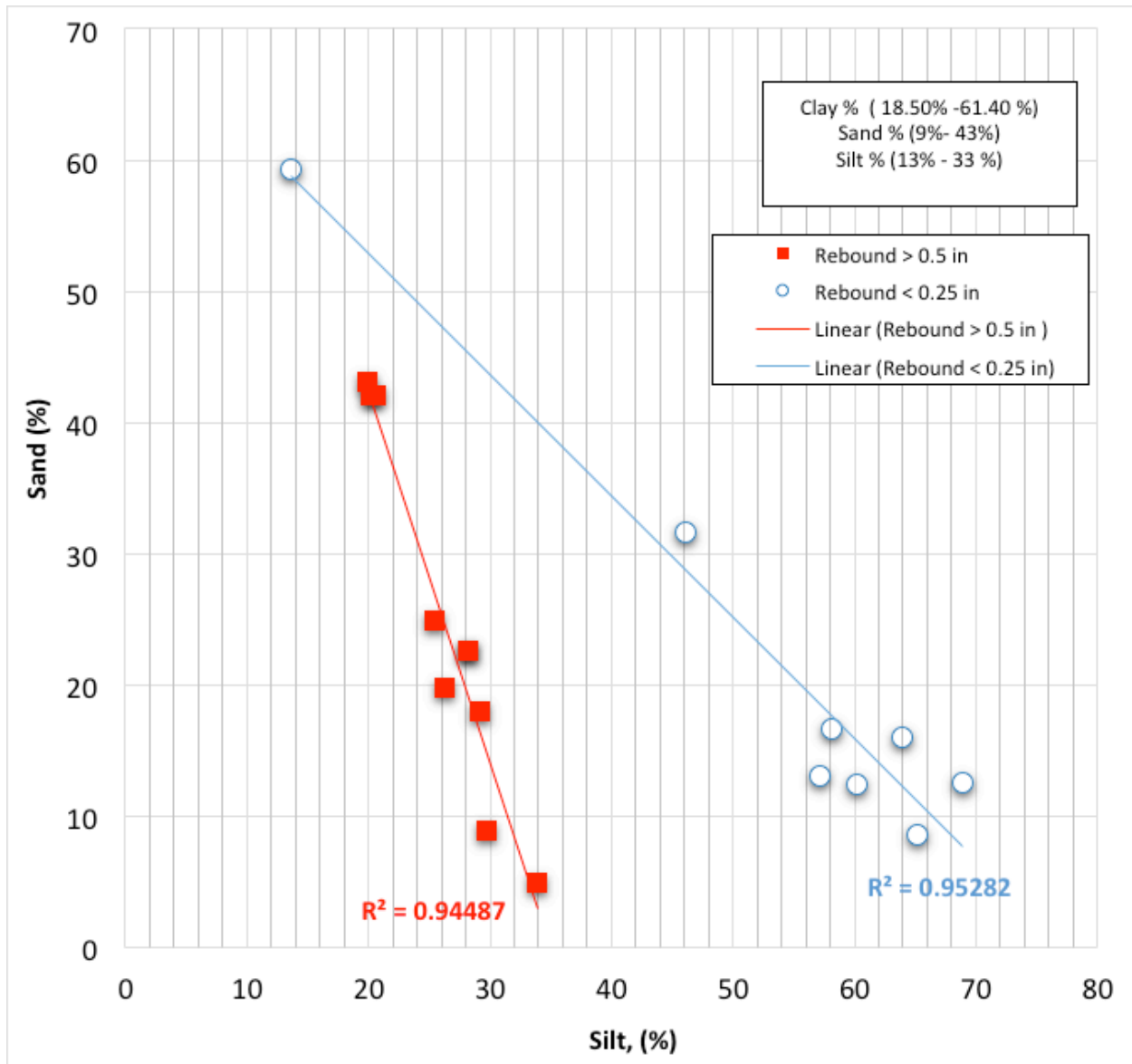


Figure 6.12: Silt Content (%) vs. Sand Content (%) – Cohesive soils (CH, CL) from all sites.

## 6.7. Evaluating Silt Content versus Clay Content for HPR and NonHPR Soils

### 6.7.1. Cohesionless Soils

Figure 6.13 is a semi-log plot of silt content versus clay content for the cohesionless soils. As has been shown in previous figures, when the silt content exceeds 20%, an HPR of 0.5 inches or more occurs. There are no visible thresholds associated with the clay content, which ranges

from 5% to 11%. It appears from this log-log plot that the HPR of cohesionless soils is more dependent upon silt content than on clay content.

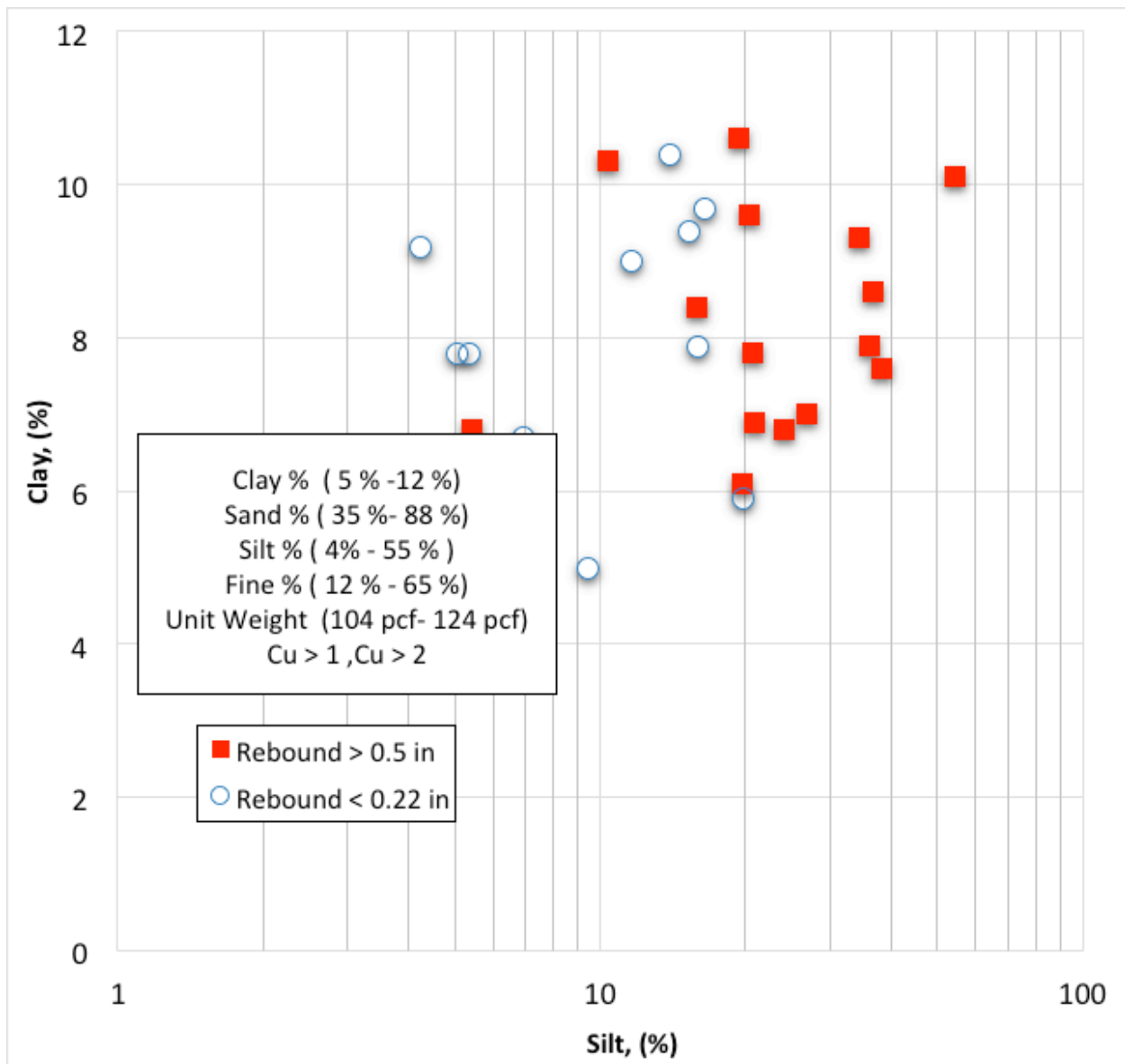


Figure 6.13: Silt content (%) vs. clay content – cohesionless soils (SM) from all sites

### 6.7.2. Cohesive Soils

A semi-log plot of log of silt content versus clay content was developed, as shown in Figure 6.14. When compared to Figure 6.13, Figure 6.14 shows the influence of silt content and clay content on high pile HPR in cohesive soils to be more significant than they are for cohesionless soils. The data in Figure 6.14 indicates that HPR was encountered in a clear zone

between clay and silt contents, with data points from 37%, 19% to 61%, and 34%. Specimens with clay contents above 37% produced high pile HPR. However, all specimens with clay contents below 30% produced no HPR.

In summary, clay content plays a significant role in identifying HPR in cohesive soils when it is above 37% and the silt content is between 20 and about 40%. More data is needed to verify these findings.

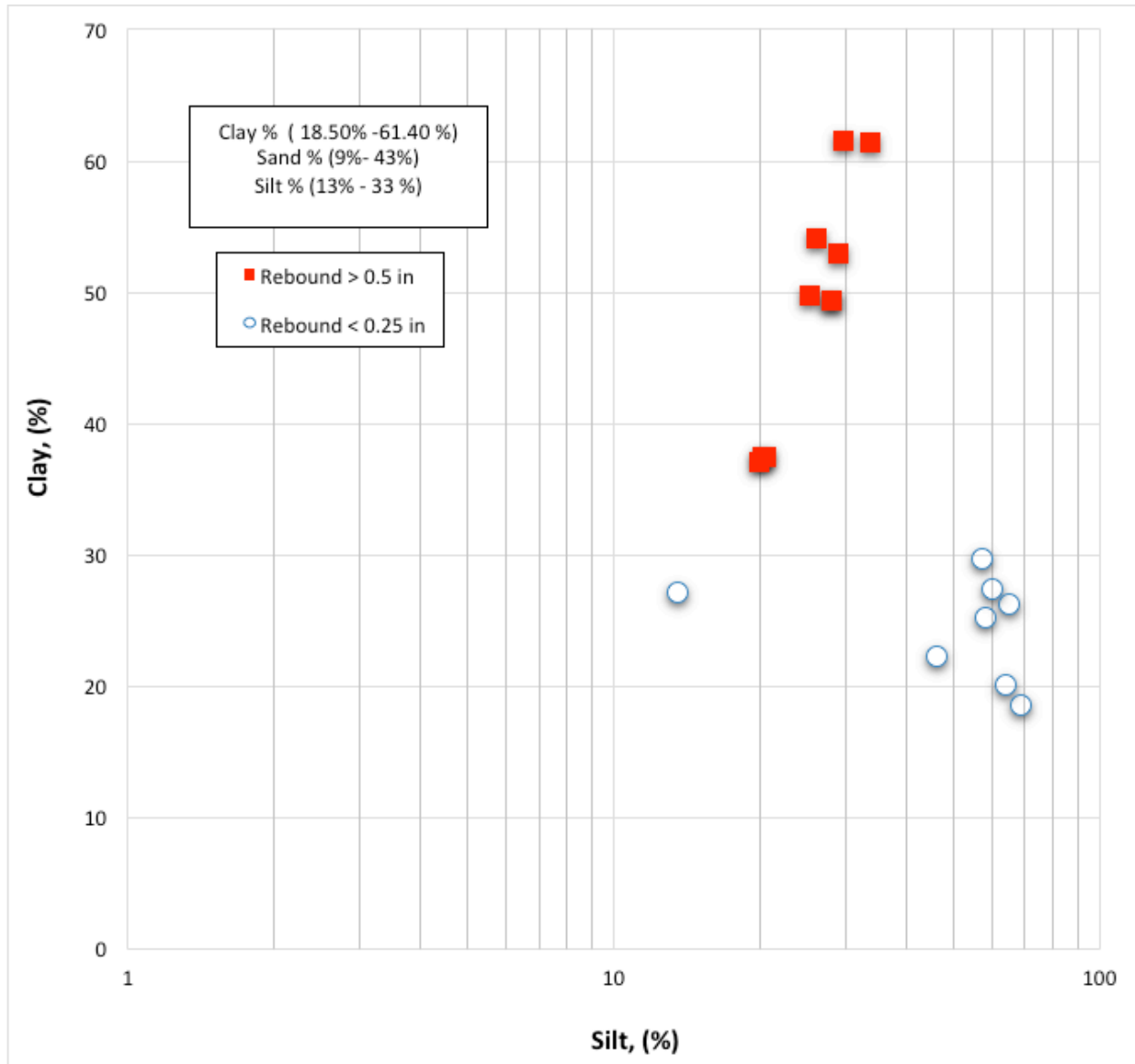


Figure 6.14: Silt content (%) vs. clay content – cohesive soils (CH, CL) from all sites

## 6.8. Evaluation of the Silt Content and Grain Size Distribution Factors $D_{10}$ , $D_{30}$ , $D_{60}$ on HPR and nonHPR Soils

### 6.8.1. Cohesionless Soils

As the semi-log data shown in Figure 6.15 indicates,  $D_{10}$  does not change with the silt content of cohesionless (SM) HPR soils. In conclusion, based on this data,  $D_{10}$  is not an indicator of HPR.

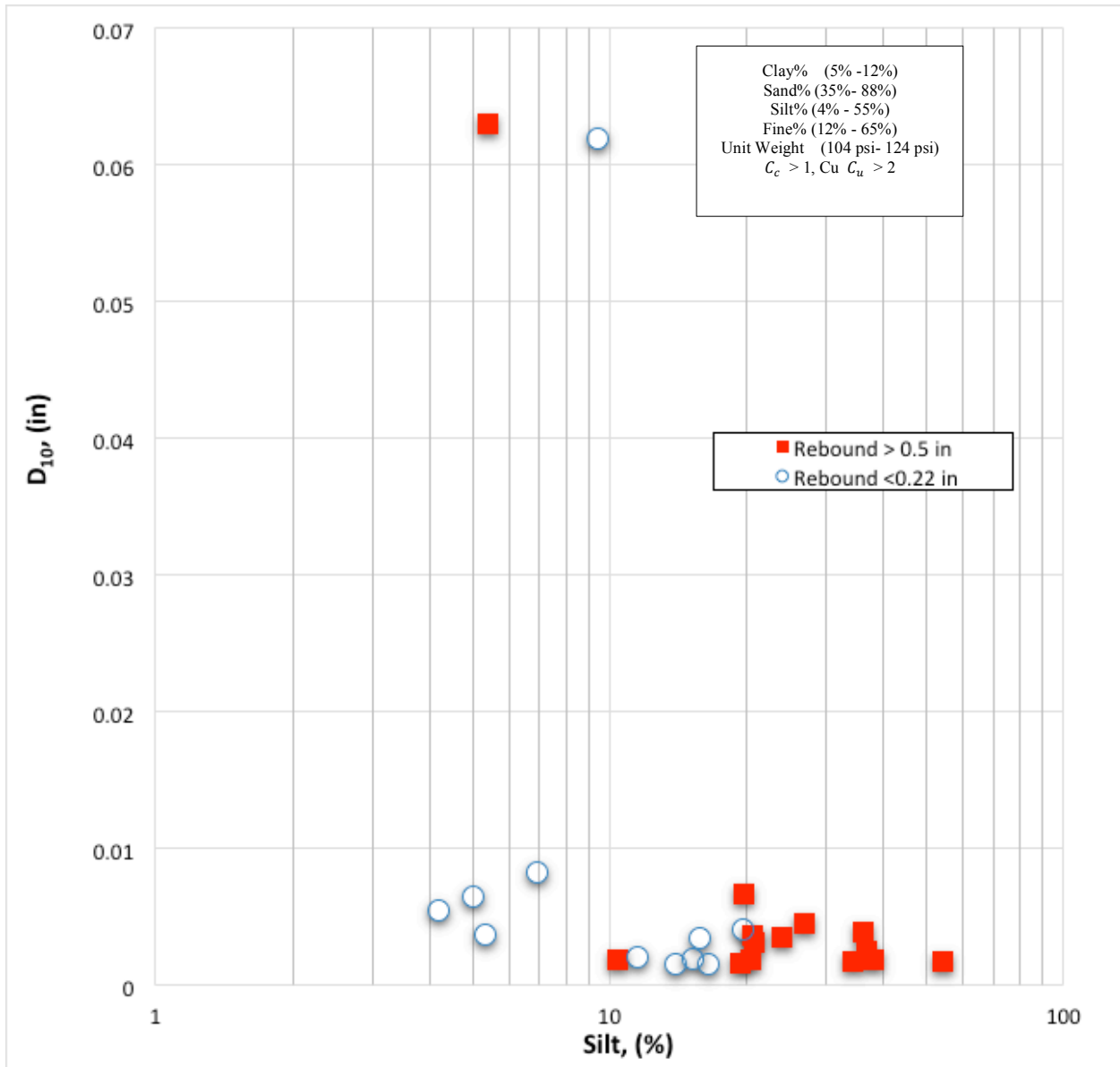


Figure 6.15: Silt content (%) vs.  $D_{10}$  content – cohesionless soils (SM) from all sites

As the semi-log data in Figure 6.16 indicates,  $D_{30}$  does not change with the silt content of cohesionless (SM) HPR soils. In conclusion, based on this data,  $D_{30}$  is not an indicator of HPR.

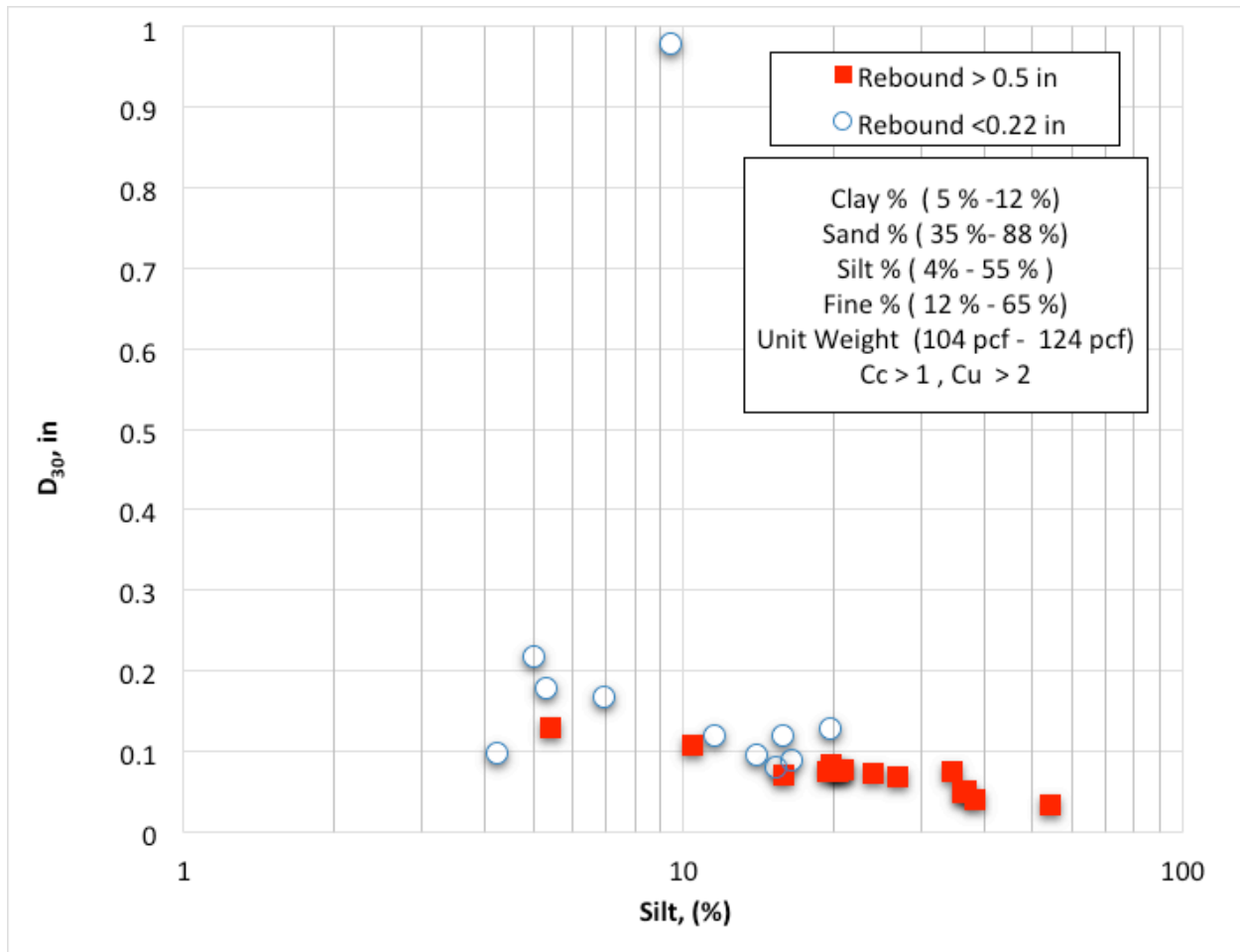


Figure 6.16: Silt content (%) vs.  $D_{30}$  content – cohesionless soils (SM) from all sites

As the semi-log data shown in Figure 6.17 indicate,  $D_{60}$  does not change with the silt content of cohesionless (SM) HPR soils. In conclusion, based on this data,  $D_{60}$  is not an indicator of HPR.

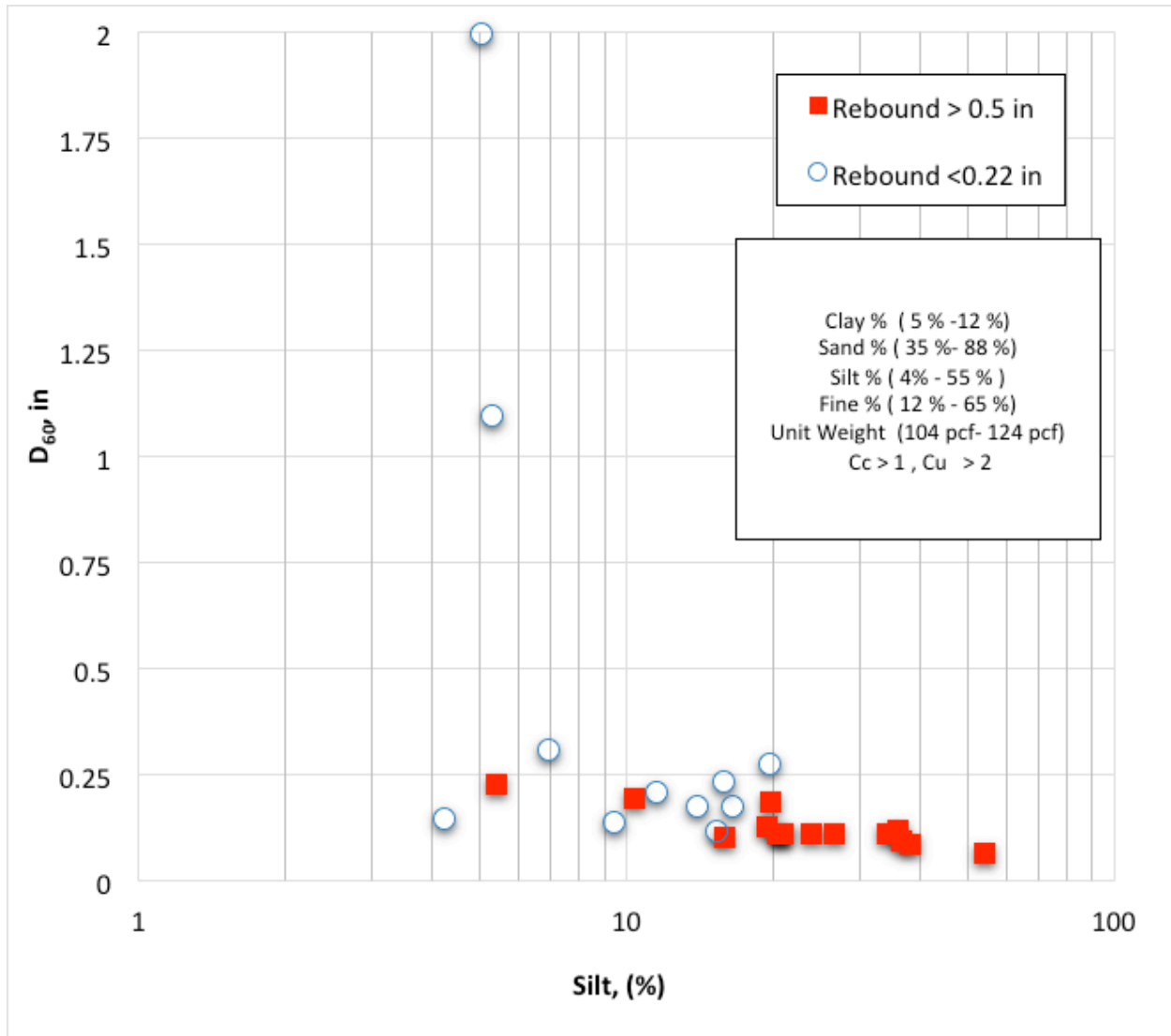


Figure 6.17: Silt content (%) vs.  $D_{60}$  content – cohesionless soils (SM) from all sites

### 6.8.2. Cohesive Soils

There is no  $D_{10}$  data from the soils evaluated and there is no HPR data for the soils with grain sizes through  $D_{30}$ ; therefore these plots are not shown. When  $D_{60}$  is plotted versus clay content, as shown in Figure 6.18, the data indicate that  $D_{60}$  for HPR soils lies in distinct ranges. The upper range, which consists of only two data points, corresponds to  $D_{60}$  near 0.08 and the clay content around 37%. The lower range, consisting of five points, corresponds to  $D_{60}$  values below 0.01 and clay contents equal to or greater than 50%. In conclusion, there is a possible trend between  $D_{60}$  and clay content; however, more data is needed to substantiate this finding.

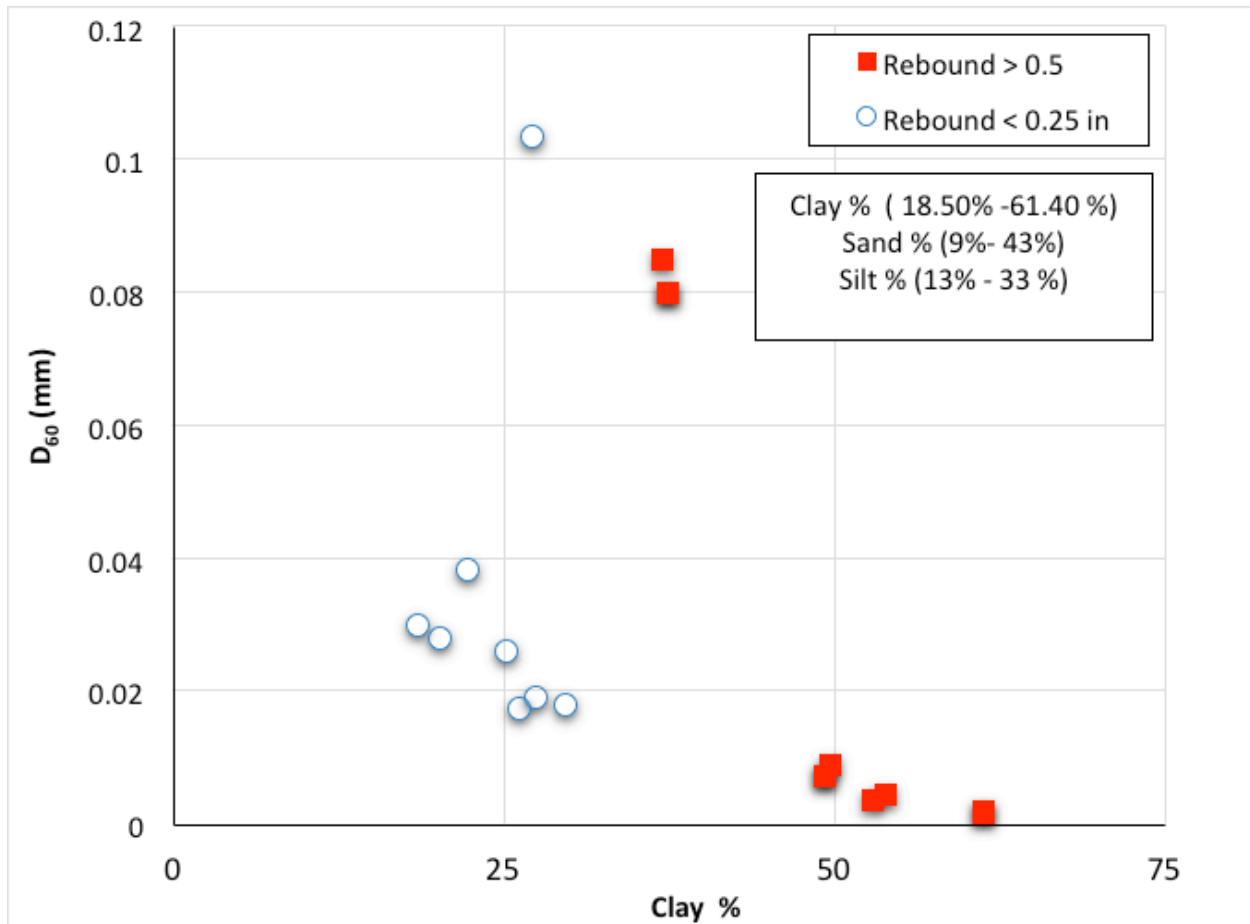


Figure 6.18: Clay content (%) vs. D<sub>60</sub> content – cohesive soils (CH, CL) from all sites

## 6.9. Evaluation of Fine Content versus Silt Content for HPR and NonHPR Soils

### 6.9.1. Cohesionless Soil

The data in Figure 6.11 shows the influence of silt and sand content on high and no pile HPR specimens from all sites. The results indicate that HPR greater than 0.5 inches occurs in soils below approximately 70% sand and above approximately 20% silt. At percentages outside this range, there is a mixture between HPR and nonHPR behavior, with nonHPR being prevalent. This plot indicates that the variation of silt and sand in cohesionless soils significantly affects high pile HPR.

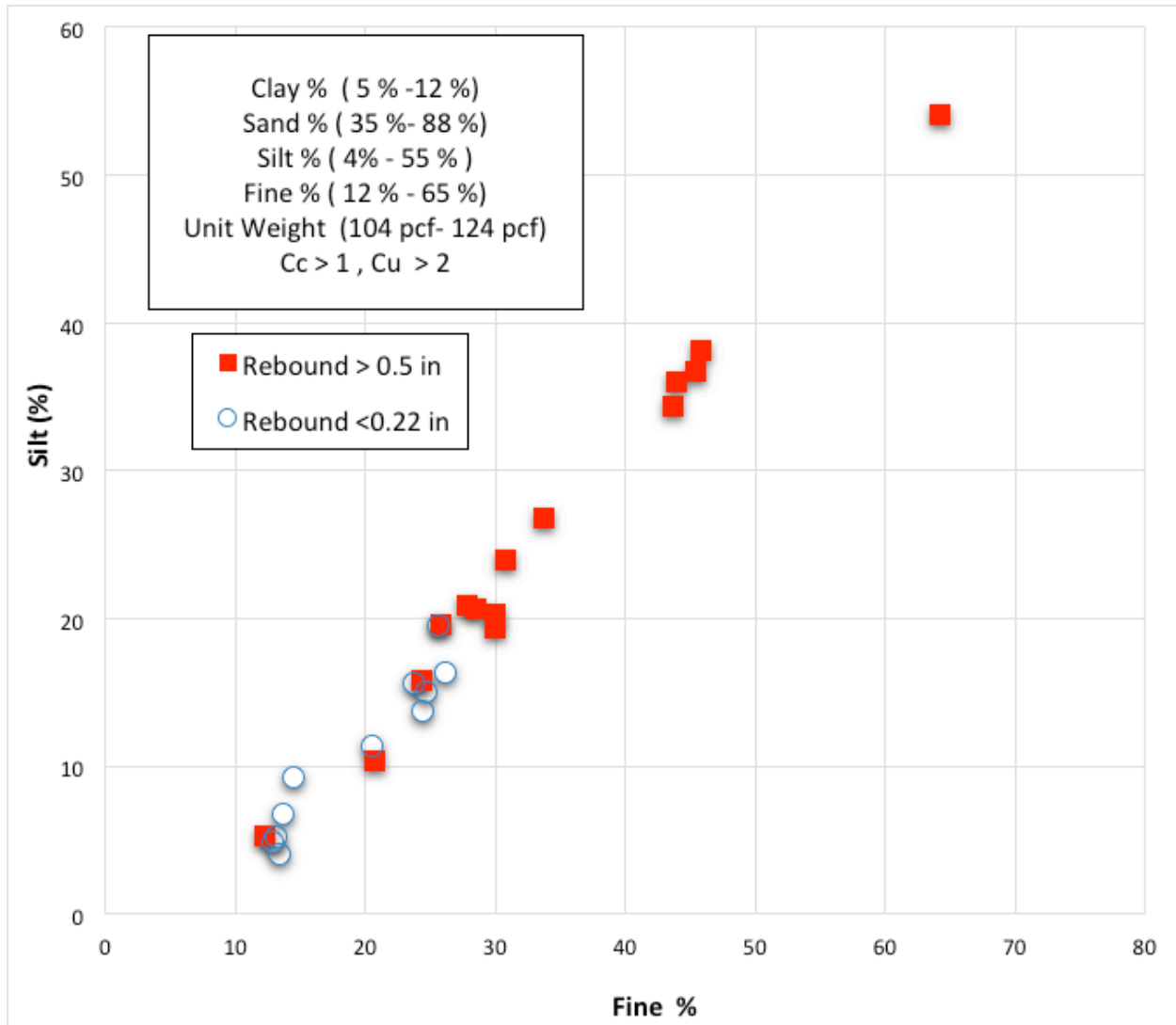


Figure 6.19: Silt content (%) vs. fines content (%) – cohesionless soils (SM) from all sites

### 6.9.2. Cohesive Soils

As was the case when silt was compared to sand content (See Figure 6.12), the results in Figure 6.20 show that HPR and nonHPR soils plot along two distinct lines, which also display high regression (i.e.,  $R^2 > 0.95$ ) coefficients. Additional data might further clarify boundaries for these lines. Due to the relatively low number of data points, no equations were included for the lines. The nonHPR percentages plot farther up or higher on each axis. Also of note is that the high HPR data points only exist between 20 and 34% silt, while the nonHPR points extend from 13 to 69% silt.

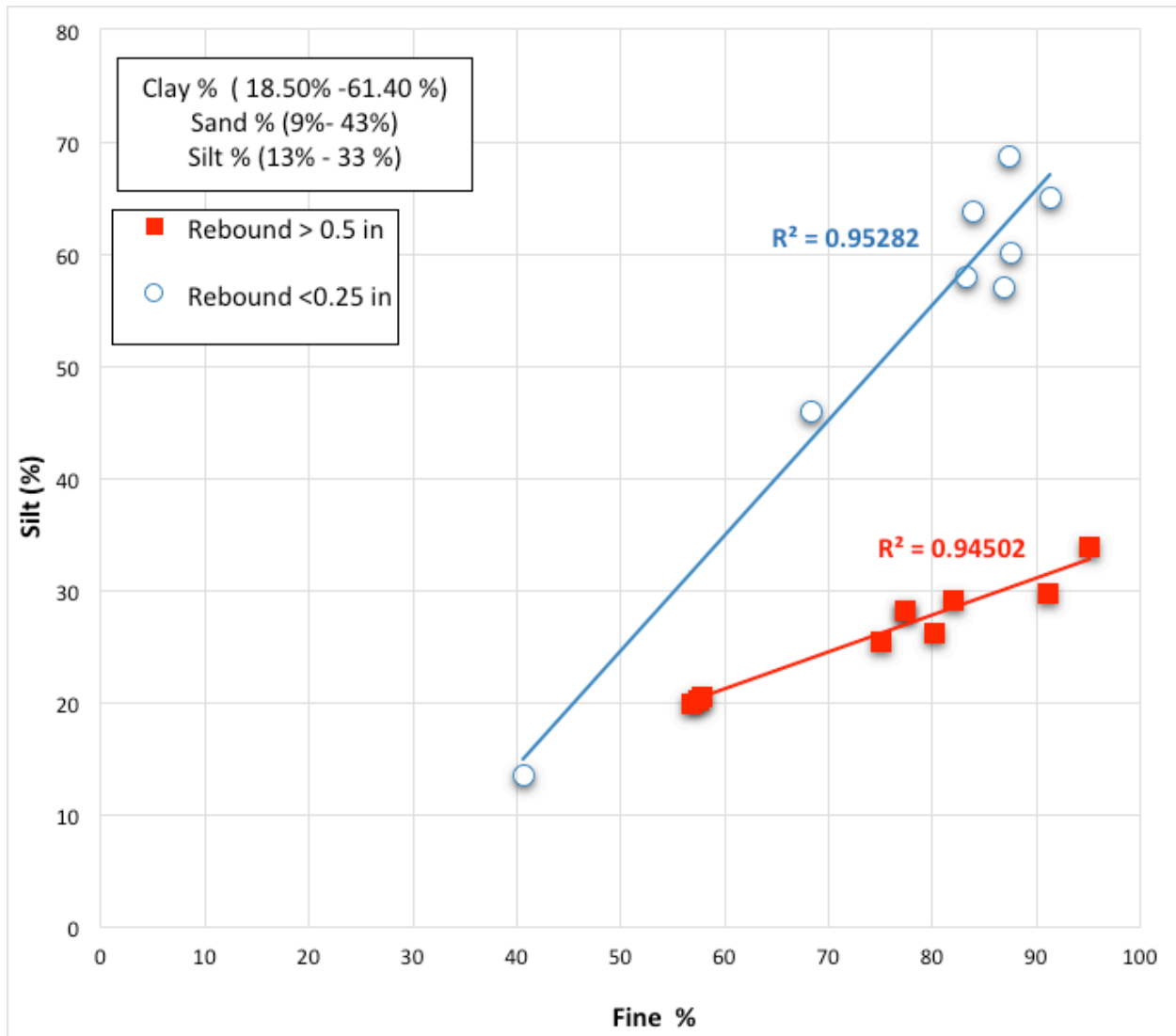


Figure 6.20: Silt content (%) vs. fines content (%) – cohesive soils (CH, CL) from all sites

### 6.10. Evaluation the Effect of Clay Content and Plasticity Index on HPR and nonHPR in Cohesive Soils

The data from the selected cohesive soils were used in order to determine the combined effects of clay content and plasticity index (PI) on the HPR and nonHPR cohesive soils. Based on the result shown in Figure 6.21, there is a clear trend showing that HPR soils have PIs greater than about 30% with clay contents in excess of 37%, while nonHPR cohesive soils have PIs less than about 26% and clay contents below 30%.

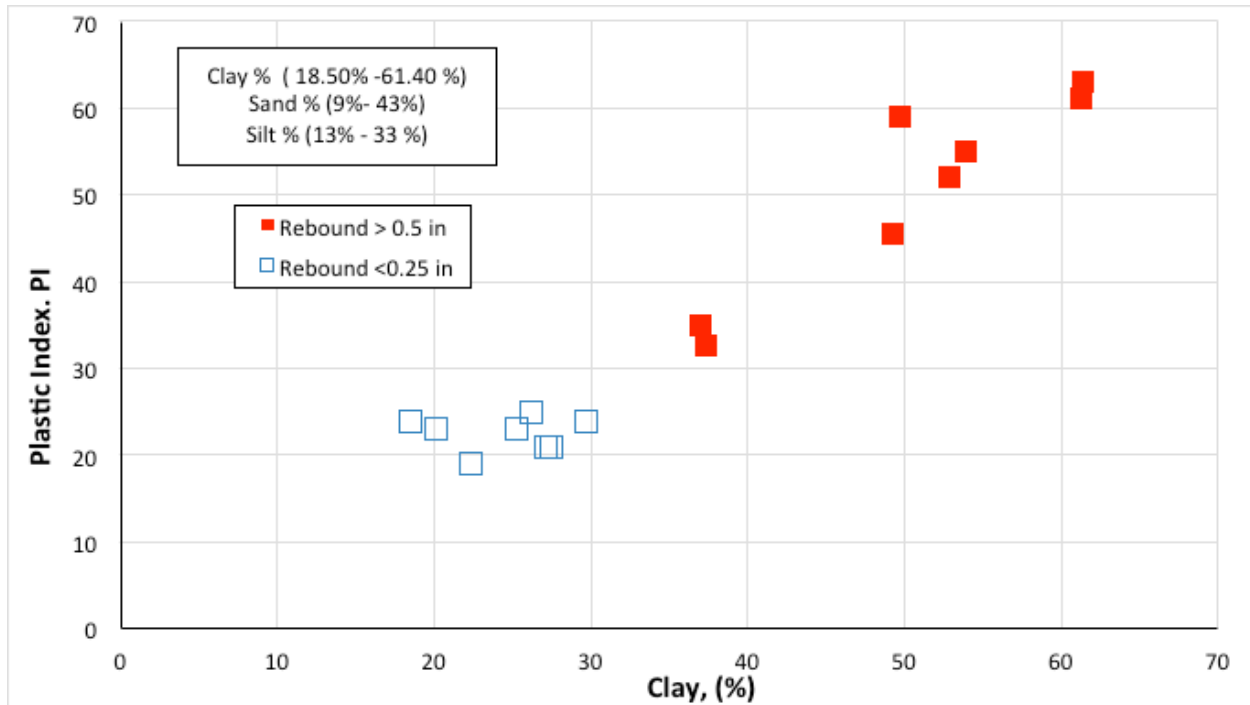


Figure 6.21: Clay content (%) versus Plastic Index (PI)

### 6.11. Evaluation the Effect of Plasticity Index and Liquid Limit on HPR and nonHPR in Cohesive Soils

The combined effects of liquid limit and PI on the HPR and nonHPR cohesive soils were evaluated, as shown in Figure 6.22. There is a clear trend showing HPR soils have PIs greater than 30% and LL greater than 50%, while nonHPR soils have PIs less than 24 and LL less than 45. The PI of the HPR soils is clearly higher than the PI for the nonHPR soils.

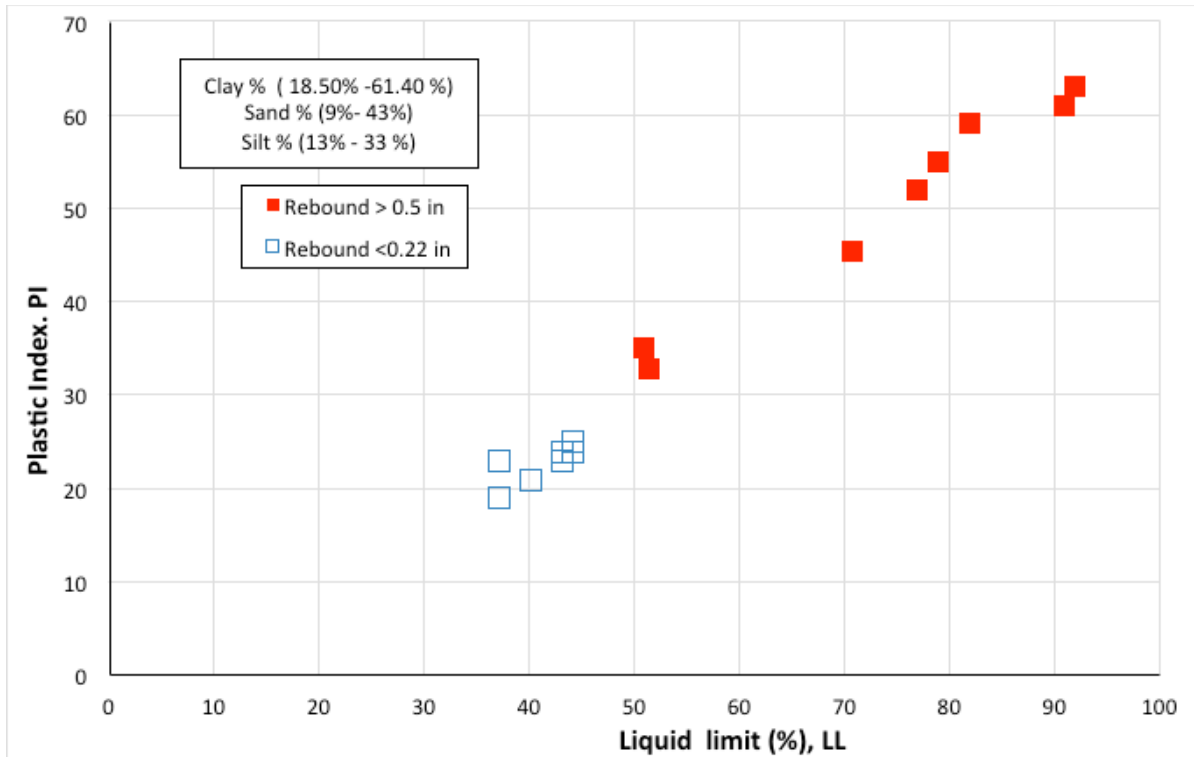


Figure 6.22: Liquid limit (LL) versus Plastic Index, (PI) for cohesive (CL, CH) soils

## 6.12. Evaluating Silt Content versus Permeability for HPR and NonHPR Soils

### 6.12.1. Cohesionless Soils

The 16 data points in Figure 6.23 indicate that the permeability of cohesionless HPR soils is lower than the permeability of nonHPR soils. In general, the permeability of the HPR soils was one or two orders of magnitude lower than the nonHPR soils. Specifically, the HPR soils have permeabilities below  $5 \times 10^{-6}$ , while the nonHPR values were larger than  $1.2 \times 10^{-5}$ .

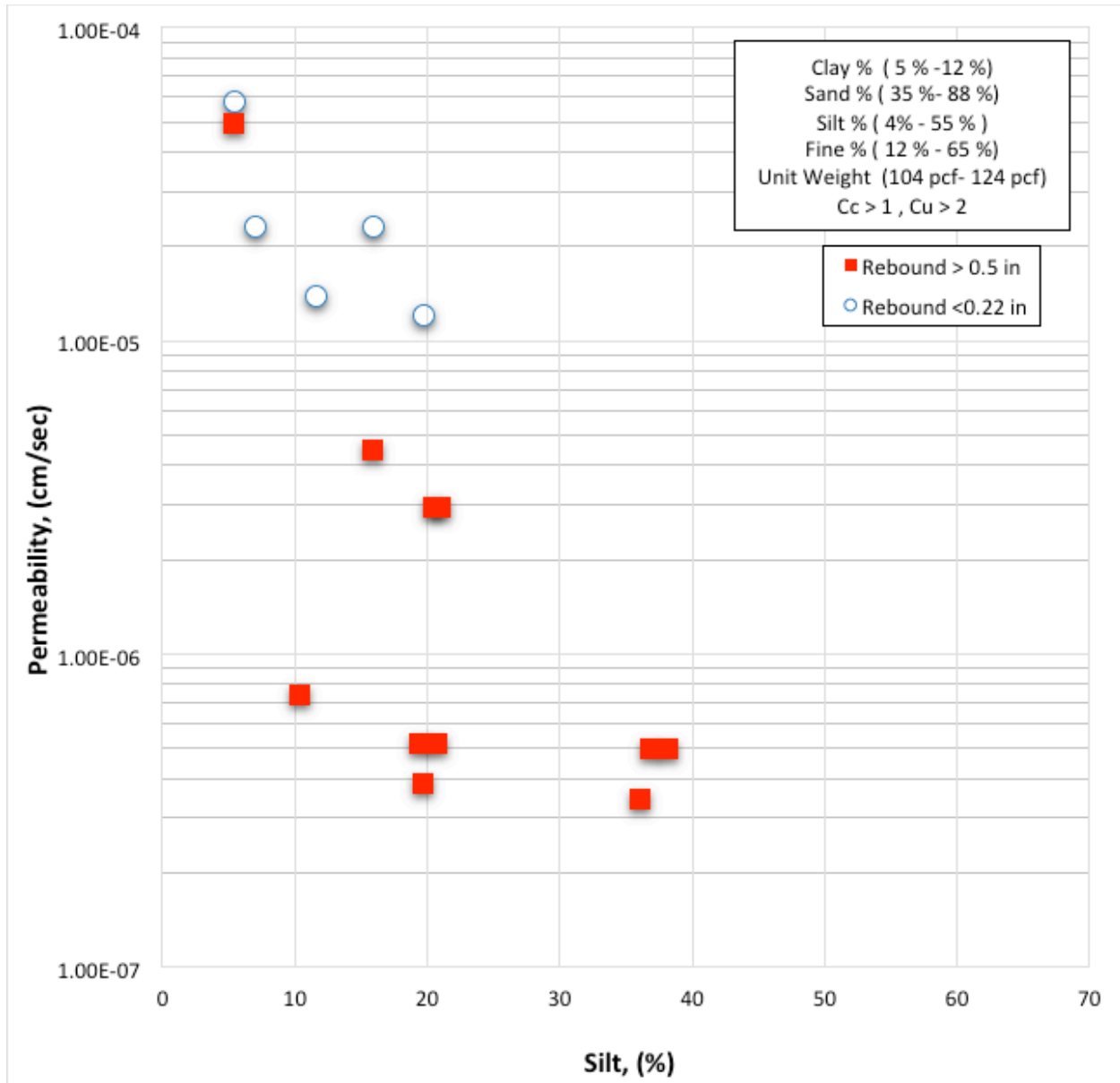


Figure 6.23: Permeability vs. silt content – cohesionless soils (SM) from all sites

### 6.12.2. Cohesive Soils

The data in Figure 6.24 indicate that the permeability of the cohesive HPR and soils is generally one order of magnitude lower than the nonHPR cohesive soils. There are only nine data points on this graph, and one HPR data point has a much higher permeability than the other four.

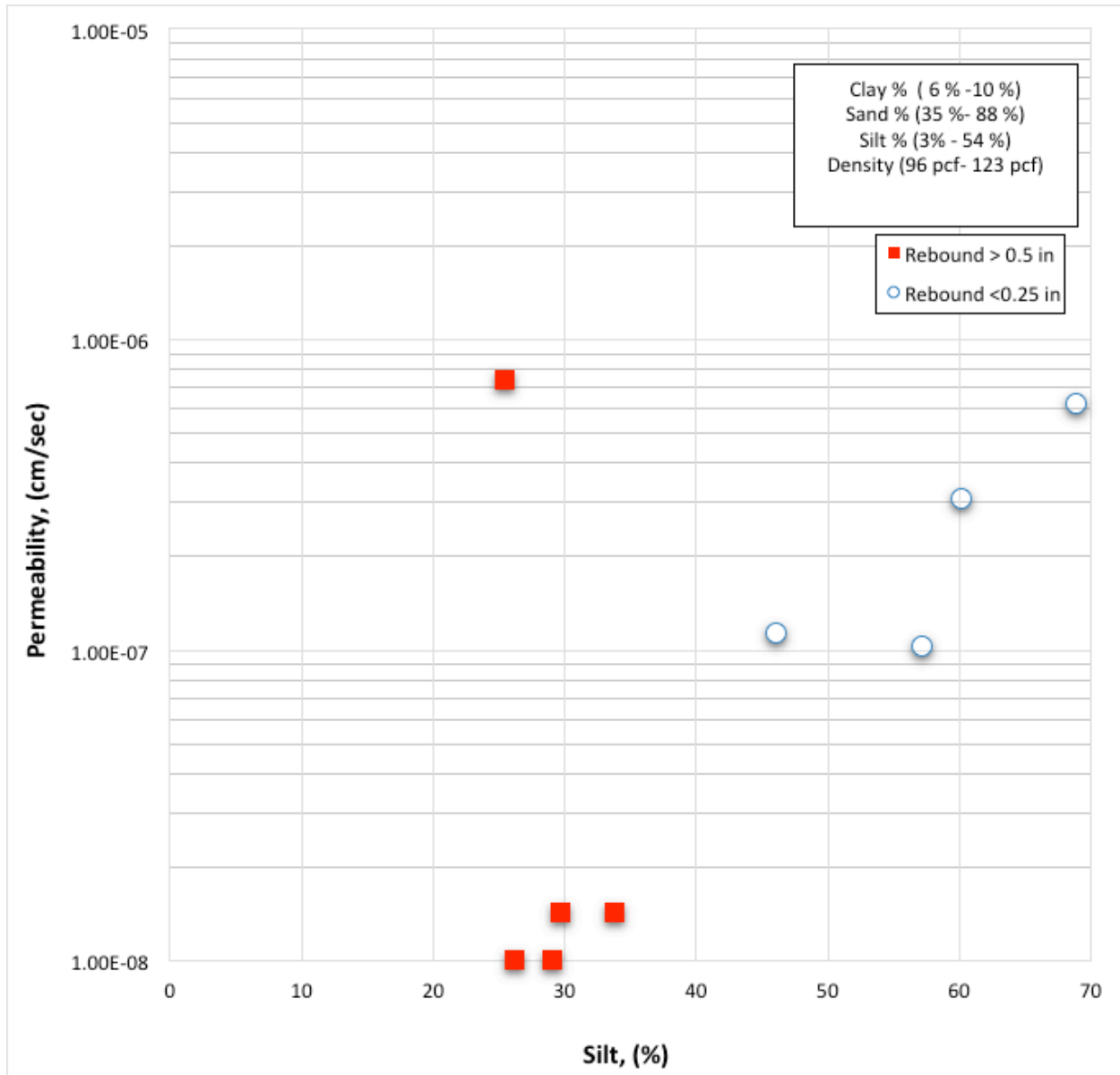


Figure 6.24: Permeability vs. Silt content – Cohesive soils (CH, CL) from all sites

## 6.13. Evaluation of the Silt Content versus Unit Weight on HPR and NonHPR Soils

### 6.13.1. Cohesionless Soil

The data in Figure 6.25 show that the HPR soils possess lower dry unit weights than the nonHPR soils. The dry unit weights for the nonHPR soils range from 111 to 123 pcf, while for HPR soils, it ranged from 104 to 121 pcf.

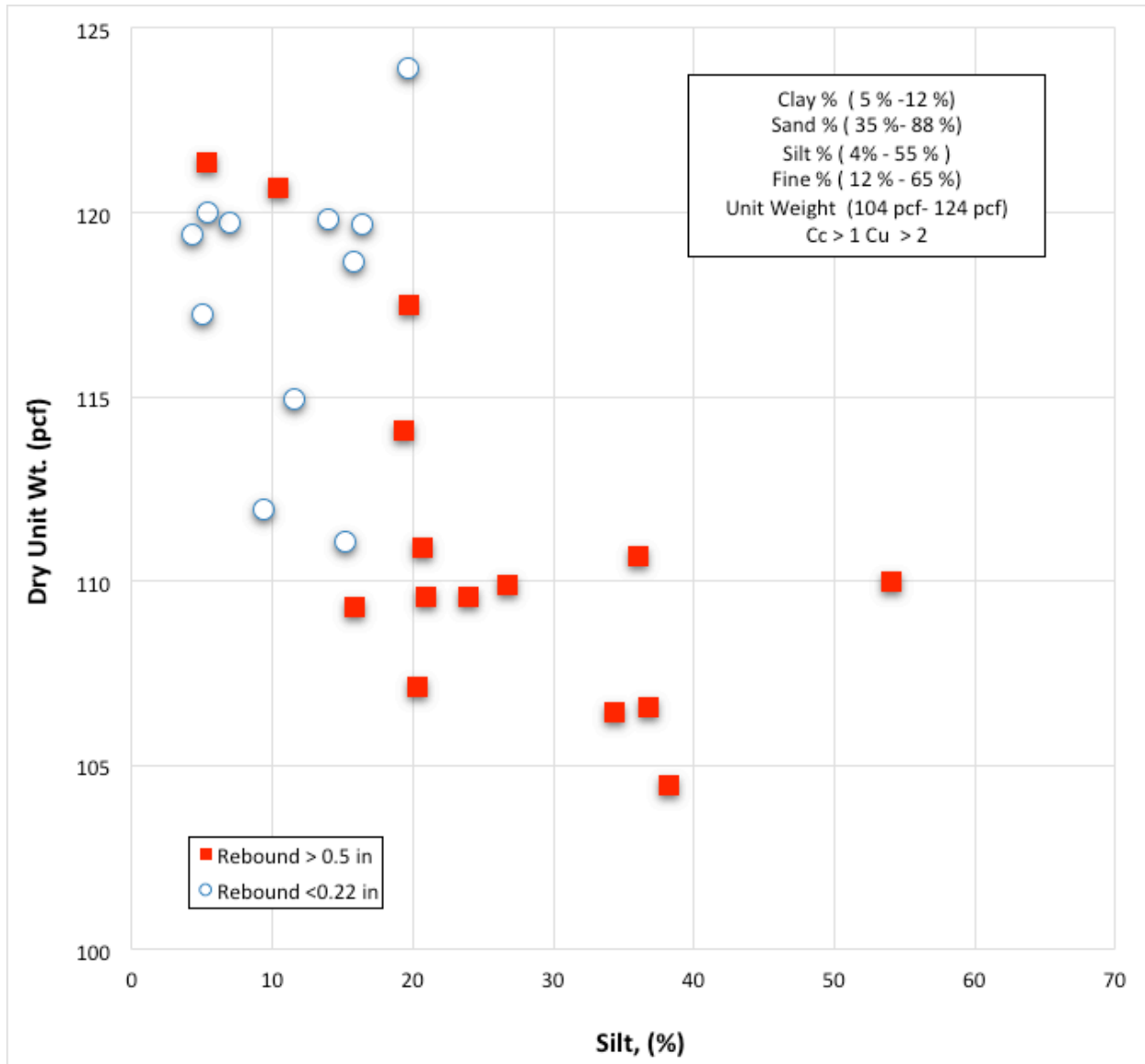


Figure 6.25: Dry unit weight vs. silt content – cohesionless soils (SM) from all sites

### 6.13.1. Cohesive Soils

The data in Figure 6.26 show that both the HPR and nonHPR cohesive soils have relatively low dry unit weights. There are only 17 data points, so making a clear conclusion is difficult. However, there seems to be a trend that the HPR soils have lower dry unit weights than the nonHPR soils, since five of the HPR densities are below the density of water or 62.4 pcf, while the nonHPR densities range from 64 to 83 pcf.

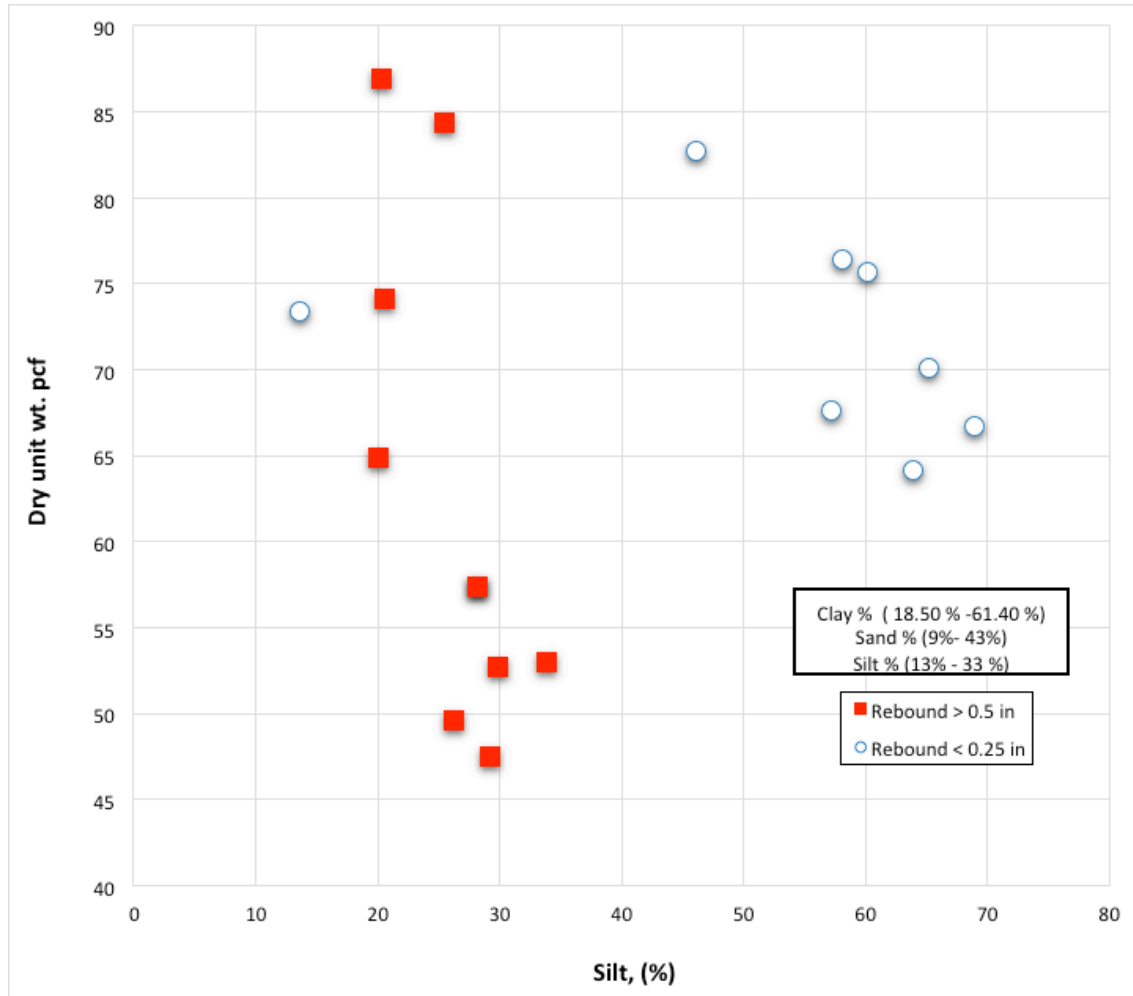


Figure 6.26: Dry unit weight vs. silt content – cohesive soils (CH, CL) from all sites

## 6.14. HPR Behavior during Cyclic Loading

Following the preliminary index testing, a complete cyclic testing program was performed on all undisturbed thin-walled tube samples. The experimental study included 30 cyclic undrained triaxial tests on samples from six sites that had fines contents varying from 12 to 95%. Each specimen was subjected to a series of cyclic loads in order to evaluate the behavior of soils subjected to high pile HPR. Prior to the cyclic testing, 30 consolidated undrained tests were conducted to determine the maximum deviator stress at failure for each sample. The applied cyclic load was selected as a percentage of the maximum CU deviator stress of each retrieved sample.

The results were divided into two categories based on their soil types: cohesionless soils and cohesive soils. Factors such as axial strain, pore water pressure, number of cycles, and time and cyclic stress ratios were evaluated.

### **6.14.1. The Effect of Number of Cycles on Axial Strain for HPR and NonHPR Soils**

#### **6.14.1.1. Cohesionless Soils**

The response from cyclic loading of 30 specimens was plotted in terms of number of cycles required to generate 1, 2.5, 5, and 15% axial strains, as shown in Figure 6.27. The data shows that after 1% strain, HPR soils reached the chosen strains at a higher number of cycles than the NonHPR soils. For example, the number of cycles ranged from 1000 to 8500 to produce 1% axial strain in both HPR and nonHPR soils. Above 1% axial strain, nonHPR soils reached the strains at a lower number of cycles than the HPR soils. For example, to reach 2.5% strain, at least 3000 cycles were required for HPR soils, while nonHPR soils only required 1000 cycles.

#### **6.14.1.2. Cohesive Soils**

The response from cyclic loading of 20 cohesive specimens were plotted in terms of number of cycles needed to generate 0.42, 1, 2.5, 5, and 15% axial strains (See Figure 6.28). The 0.42 failure strain is considered an anomaly and was not used in determining trends from this data. The data shows a similar trend to the cohesionless soils in that after 1% strain, HPR soils reached the chosen strains at a higher number of cycles than the NonHPR soils. For example, to produce 1% axial strain for both HPR and nonHPR soils, the number of cycles ranged from 2500 to 8500. Above 1% axial strain, the nonHPR soils reached the strains at lower cycles than the HPR soils. At 2.5% strains, at least 5400 cycles were required for HPR soils, while nonHPR soils only needed 3750 cycles.

In conclusion, the HPR soils required many more (two to three times) cycles to produce the 2.5, 5, 10, and 15% strains than the nonHPR soils and are therefore termed more resilient.

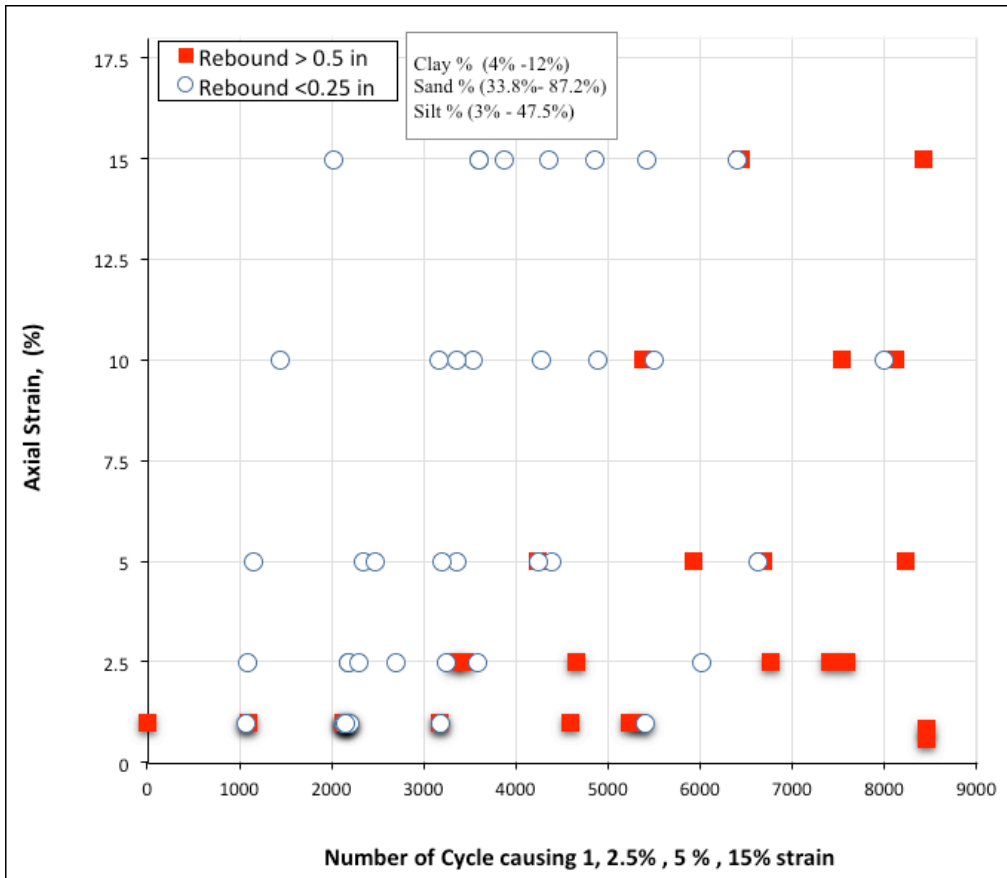


Figure 6.27: Number of cycles required to achieve 1%, 2.5%, 5%, 10%, and 15% strain for cohesionless soils susceptible to HPR and nonHPR

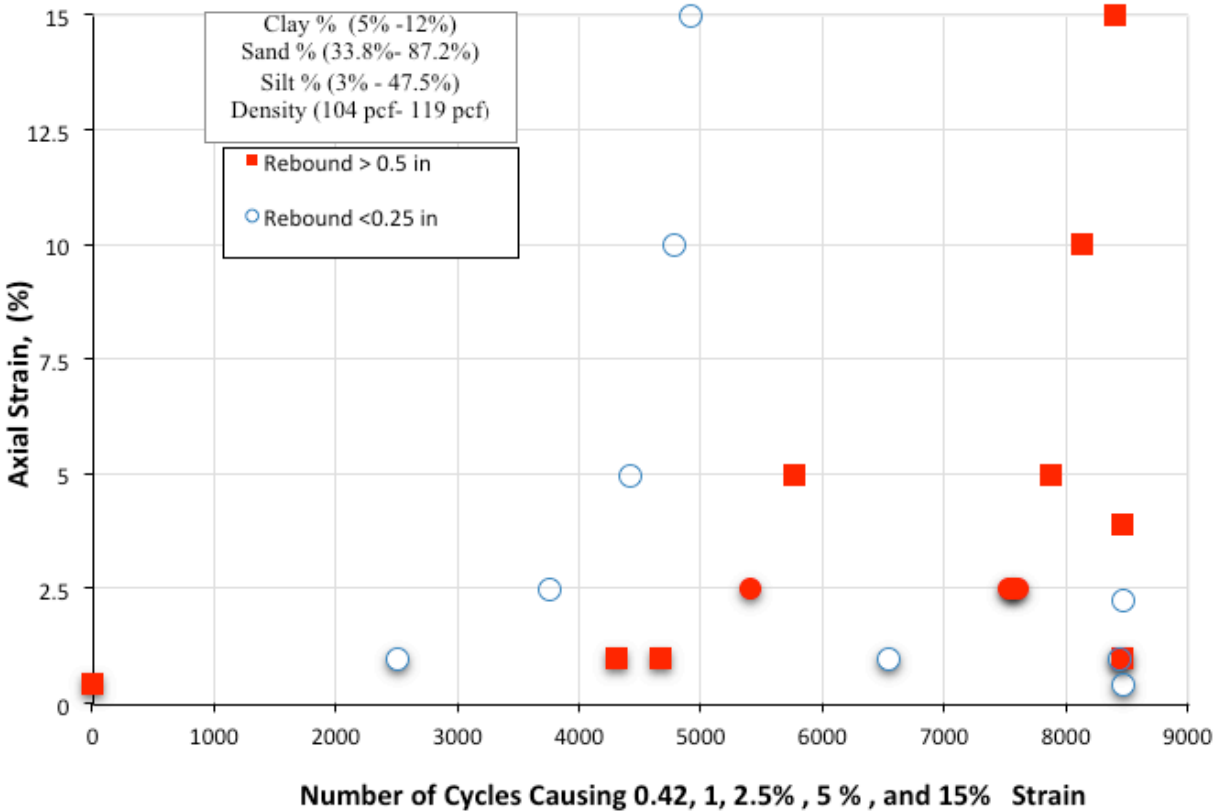


Figure 6.28: Number of cycles required to achieve 1%, 2.5%, 5%, 10%, and 15% strain for cohesive soils susceptible to HPR and nonHPR

### 6.14.2. Evaluation of Failure Strain and Pore Water Pressure during Cyclic Loading

The number of cycles required to produce failure from cyclic loading was evaluated in terms of failure strain and pore water pressure ratio ( $\Delta u/\sigma_3'$ ). HPR and nonHPR data were plotted with failure strain and  $\Delta u/\sigma_3'$  data versus number of cycles to failure.

#### 6.14.2.1. Failure Strain versus Number of Cycles to Failure

The data in Figure 6.29 show that the number of cycles to failure for the nonHPR cohesionless soils ranges from 2000 to 8000 and occurs when the failure strains are at least 10% and mostly 15%. The number of cycles to failure for the HPR cohesionless soils ranges from 5200 to 8500 but occurs over a much larger range (i.e., 1 to 15%) of failure strains than the nonHPR soils. In summary, the cyclic failure strains for cohesionless nonHPR soils are typically high compared to the cyclic failure strains of cohesionless HPR soils. This testing result would

indicate that pile driving through cohesionless HPR soils would require more hammer blows than pile driving through cohesionless nonHPR soils.

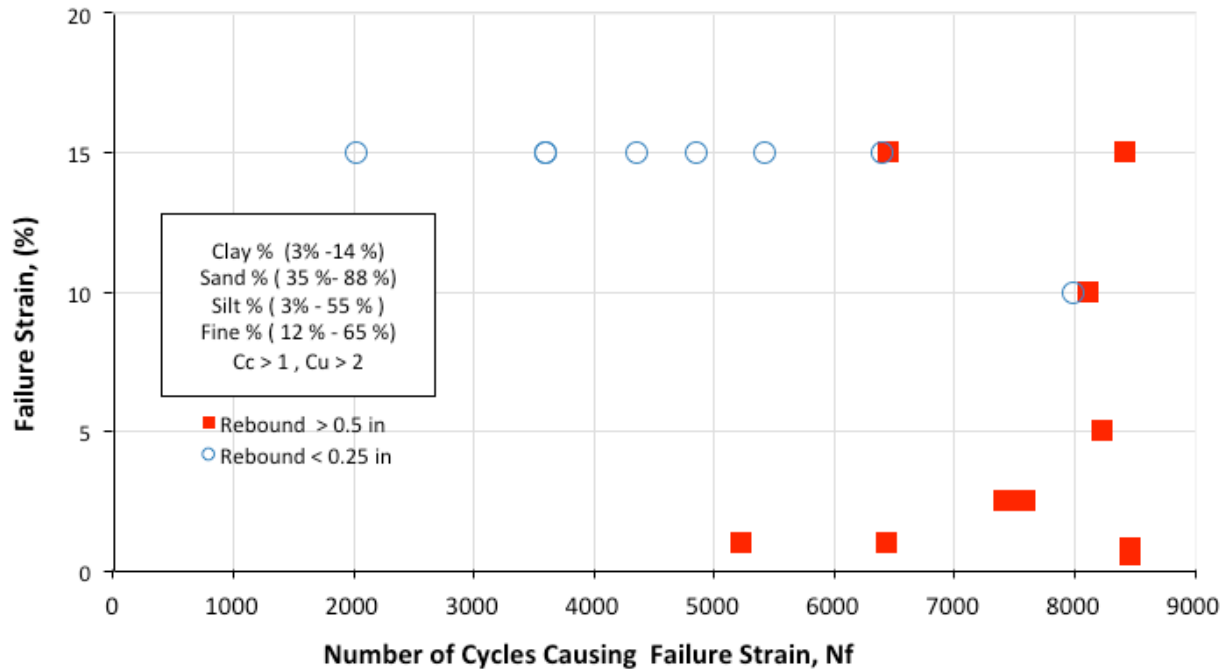


Figure 6.29: Cyclic triaxial failure strain versus number of cycles from cyclic triaxial tests performed on cohesionless HPR and nonHPR soils

#### 6.14.2.2. Pore Water Pressure Ratio versus Number of Cycles to Failure

The data in Figure 6.30 shows that the  $\Delta u/\sigma_3'$  for nonHPR soils ranged from 0.82 to 0.97, while for HPR soils, it ranged from 0.34 to 0.89. This lower range indicates that the HPR soils take more time to produce increases in pore pressures than the nonHPR soils. The same trend as the previous cyclic figures displayed is also shown here, in that the number of cycles to failure for the nonHPR soils is lower than for the HPR soils. Only two of the 10 HPR soils had failure ratios in excess of 0.8, while all of the nonHPR soils had failure ratios larger than 0.8. HPR specimens appeared to have lower pore water pressure ratios at failure than nonHPR specimens.

The results also show that nonHPR specimens approached a  $\Delta u/\sigma_3'$  ratio equal to 1 at failure, which caused them to lose shear strength. This failure was clearly observed in their large

axial strain of the nonHPR specimens during the cyclic loading. As the number of cycles to failure increases past 4000, the pore pressure ratio at failure decreases.

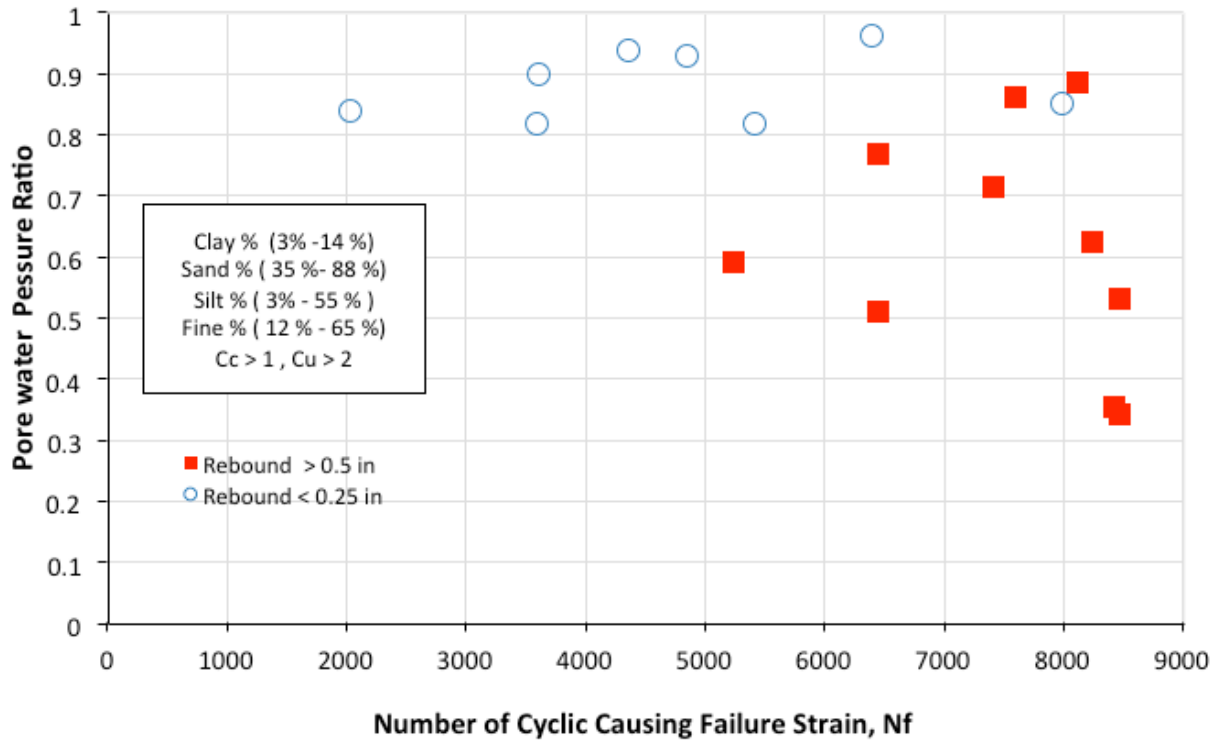


Figure 6.30: Pore water pressure ratio versus number of cyclic loadings from cyclic triaxial tests on HPR and nonHPR cohesionless soils.

### 6.15. Soil Behavior Chart Trends

The deviator stress at failure from cyclic triaxial data was plotted versus the cone tip resistance from CPTu tests at the same elevation as the samples. The data is shown in Figure 6.31. A linear regression was performed on the data producing the equation and  $R^2$  values shown in the plot. Although there is an increasing linear trend, the regression coefficient is low ( $R^2 = 0.47$ ). In summary, it may be possible to predict cone tip resistance based on deviator stress at failure from cyclic triaxial tests.

There is published evidence that Soil Behavior Charts (SBTs) can be used to distinguish between HPR and nonHPR soils (Dekhn, 2015). To plot the lab data on Robertson’s 2012 SBT chart, the regression equation from Figure 6.31 was used for each cyclic triaxial sample. At each point, the deviator stress at failure was used and a predicted cone tip resistance was determined.

The friction ratio obtained from CPTu testing at the same location and elevation was used as the x-coordinate so that the data could be placed on Robertson's 2012 SBT chart.

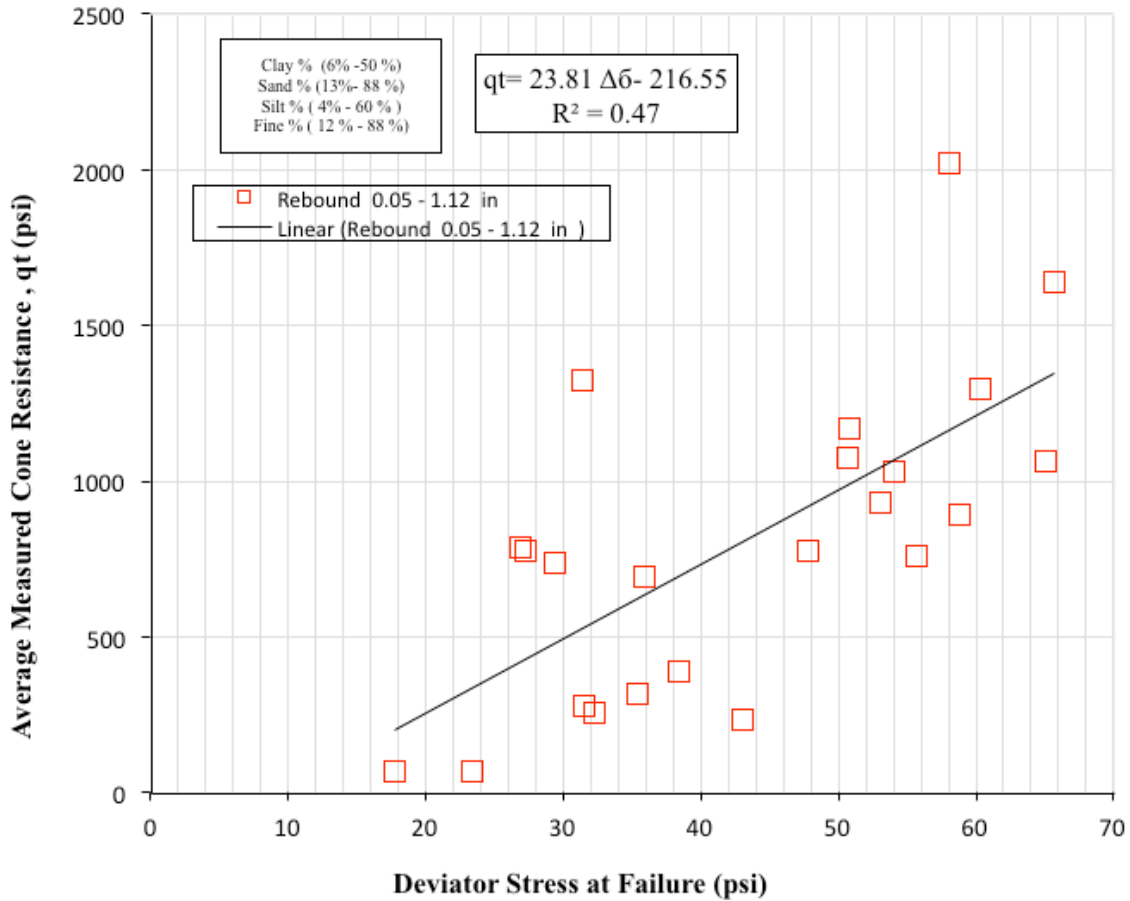


Figure 6.31 Averaged CPTu cone tip resistance near thin-walled tube sample versus cyclic triaxial deviator stress at failure from corresponding sample

Figure 6.32 shows that the HPR soils produce data points in the dilative zones of soil types 3, 4, and 5. One of the 12 HPR soils plots in the contractive zone. It also shows that nonHPR soils mostly plot in the contractive zones for soil types 5 and 6. Three of the nine nonHPR data points are near the contractive-dilative boundary.

A second SBT chart was developed using the actual data in Figure 6.31. Instead of using the regression equation to predict cone resistance, the measured CPTu cone tip and friction ratio near the cyclic triaxial sample was used for each data point. Figure 6.33 is the SBT chart and it shows similar trends as the previous figure. The HPR soils plot in the dilative areas and the nonHPR soils plot in the contractive areas. The main difference between this figure and the

previous one is that the HPR dilative soils are mainly in zones 4 and 5 and plot very near the soil behavior index of 2.6. A second difference is that the one HPR sample that plotted in the contractive zone in the first SBT chart plotted on the boundary between the contractive and dilative zones.

In summary, the HPR soils mainly plot in dilative zones 4 and 5 and the regression equation produces more scatter within the SBT chart.

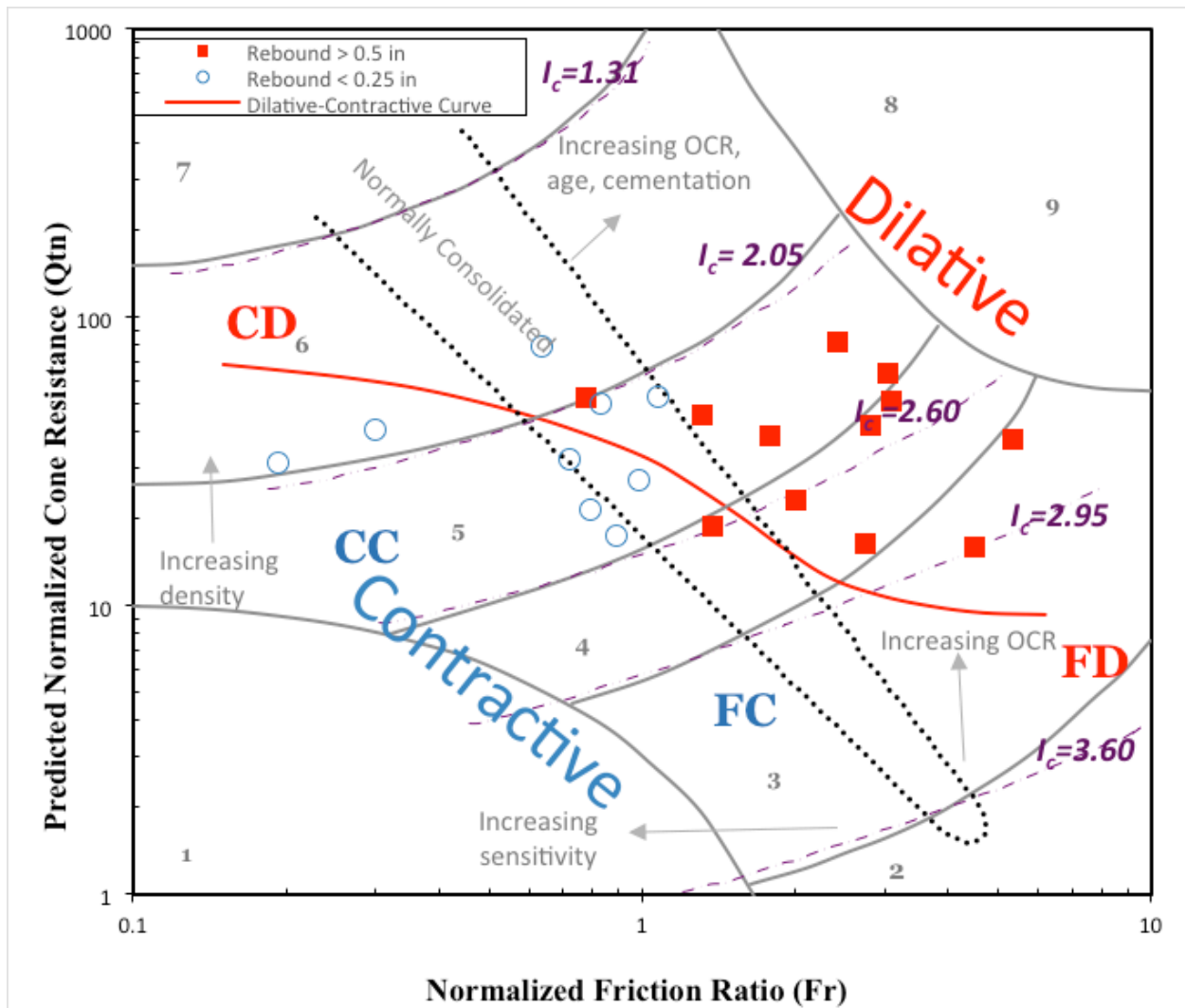


Figure 6.32: Estimated soil behavior based on regression equation from HPR and nonHPR laboratory samples on Robertson's (2012) updated normalized cone resistance versus friction ratio SBT chart

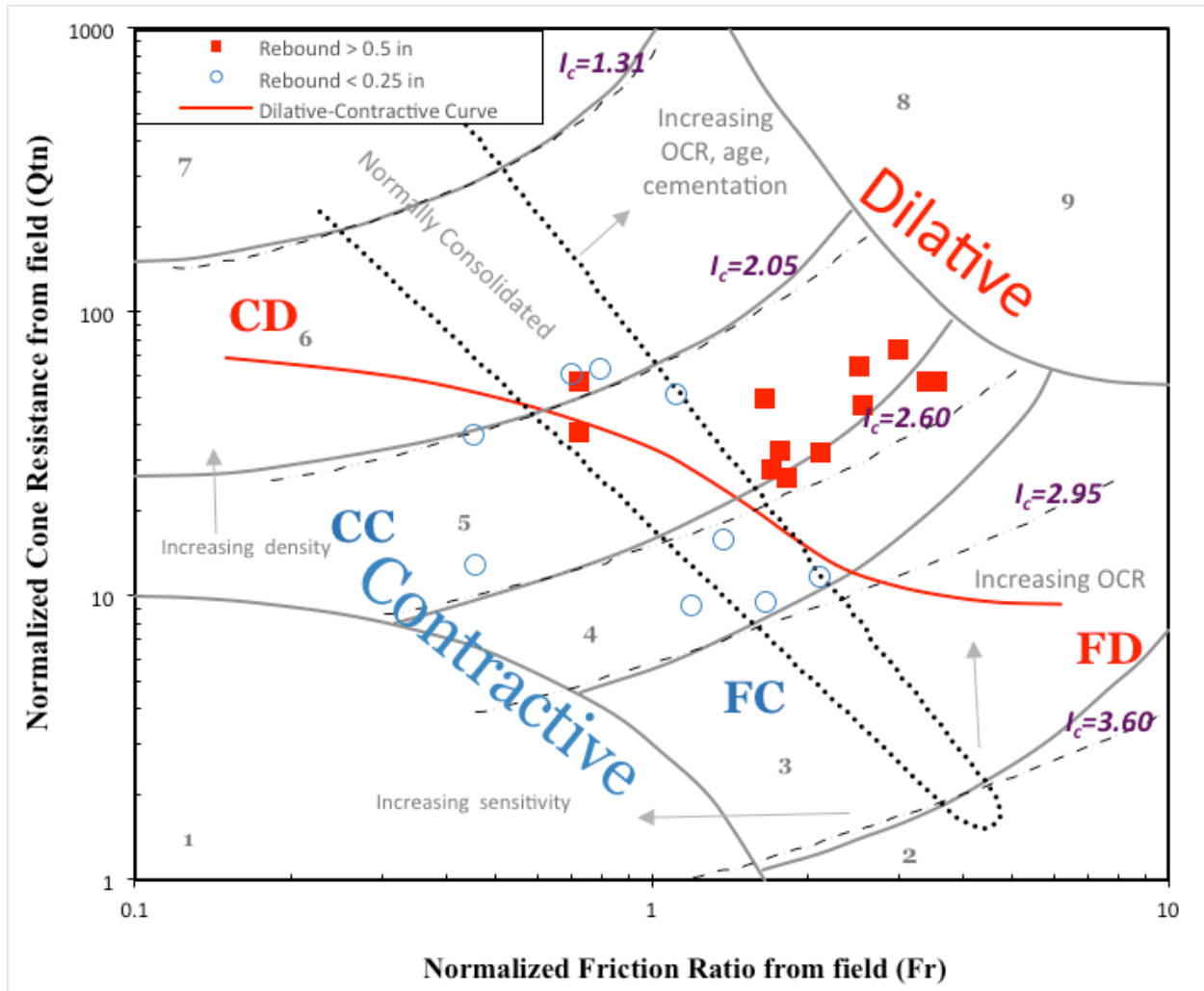


Figure 6.33: Estimated soil behavior based on CPT results matched to HPR and nonHPR laboratory sample elevations on Robertson's (2012) updated normalized cone resistance versus friction ratio SBT chart

## **7. Analysis of Soil Behavior Type**

Soil behavior type (SBT) charts have been used for many years to help engineers understand the soil types encountered during CPT testing. Robertson developed a well-known SBT chart in 1986. SBT charts can be based on just point and friction data or point, friction, and pore pressure data.

### **7.1. Basic Approach**

The CPT data for all the seven sites (See Table 4.1) were analyzed to determine the relationship between soil type and HPR. CPeT-IT software charts developed by Robertson (1990), Robertson (2012), Schneider et al. (2008), and Eslami and Fellenius (1997) were used. CPTu data for the HPR and nonHPR zones was placed on each of these charts.

### **7.2. Soil Behavior Type Classification (Robertson, 1990)**

#### **7.2.1. Normalized Cone Resistance versus Normalized Friction Ratio**

Two normalized soil behavior charts originally developed by Robertson (1990) were used to classify soils in the HPR and nonHPR zones at the seven sites. In the first chart, the normalized cone tip resistance ( $Q_{tn}$ ) is plotted versus the normalized friction ratio ( $F_r$ ). Figure 7.1 shows data from HPR soils while Figure 7.2 shows the data for the nonHPR soils. Both the Wroth (1984) and Houlsby (1988) normalization processes, which require normalizing using overburden pressures, were used for  $Q_{tn}$  and  $F_r$ , respectively.

The majority of the normalized CPT data points for HPR soils in Figure 7.1 are closely clustered above the left-most portion of the normally consolidated area in Zones 3 and 4 with some located in Zone 5. Figure 7.1 also shows that approximately 90% of the data points are located in the region of increasing OCR age or cementation (i.e., the upper right region). This figure shows that  $F_r$  ranges from 0.4 to 10 (i.e., the right half of the chart) while  $Q_t$  ranges from 3 to 40. In summary, Figure 7.1 indicates that the soils in the HPR zones are classified as overconsolidated fine-grained soil (clayey silt to silty clay) or cemented coarse-grained soil (silty sand to sandy silt).

Although there is a large scatter of data, the majority of the data points for the nonHPR zones are located in Zones 4, 5, and 6 as shown in Figure 7.2. Some of these points are also located in Zones 1 and 3. Approximately 95% of the data in Zones 4 and 5 are located on and below the normally consolidated region (i.e., decreasing of OCR or cementation). The soil in the nonHPR zones classifies as clean sand, uncemented silty sand, or underconsolidated/normally consolidated clayey silt. The majority of the data points in Figure 7.2 are located in the left half, with  $F_r$  ranging from 0.1 to 4 and  $Q_{tn}$  ranging from 2 to 400.

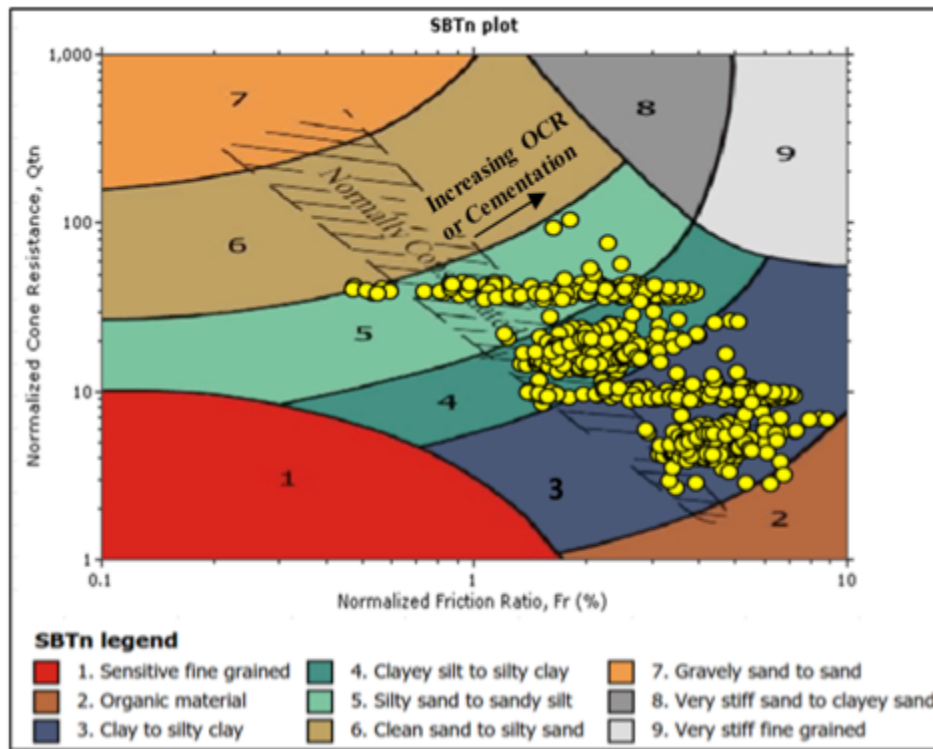


Figure 7.1: HPR data overlaid on Robertson's (1990) normalized cone resistance versus normalized friction ratio SBT chart with the normally consolidated zone shown

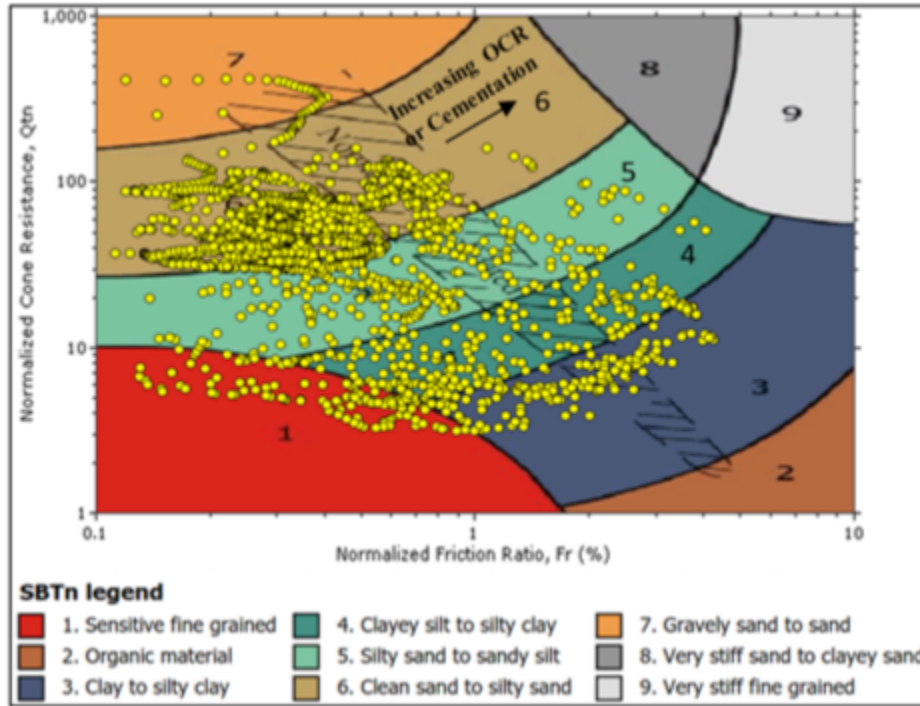


Figure 7.2: NonHPR data overlaid on Robertson’s (1990) normalized cone resistance versus normalized friction ratio SBT chart with the normally consolidated zone shown.

In summary, Figure 7.1 shows that the HPR soils are overconsolidated fine-grained soil (clayey silt to silty clay) or cemented coarse-grained soil (silty sand to sandy silt). Figure 7.2 has a large scatter of data; however, there is a large group of data indicating that these soils are clean sand, uncemented silty sand, or underconsolidated/normally consolidated clayey silt.

### 7.2.2. Cone Resistance versus Pore Pressure Ratio

SBT charts can be improved if pore pressure data is also normalized and added (Robertson, 2009). Normalization of pore pressures requires separation of pore pressures that are a function of soil response and those existing in the ground prior to the penetration. Measured penetration pore pressure during CPT testing ( $u_2$ ) represents the sum of the in situ or hydrostatic pore pressure ( $u_0$ ) and the excess pore pressure ( $\Delta u_2$ ) (Schneider et al., 2008). The pore pressure normalization formula suggested by Wroth (1984) is:

$$B_q = \frac{\Delta u}{q_t - \sigma_{v0}} = \frac{u_2 - u_0}{q_t - \sigma_{v0}} \quad \text{Equation 7-1}$$

where

$B_q$  = Pore pressure ratio

$u_2$  = pore pressure measured at the cone shoulder

$u_0$  = in situ pore pressure

$q_t$  = cone resistance corrected for pore water pressure at cone shoulder

$\sigma_{v0}$  = total overburden stress

Robertson's (1990) SBT chart accounts for pore pressure and soil type as  $B_q$  is plotted versus  $q_t$ . The data points from the HPR soils were superimposed on Figure 7.3 and nonHPR zones on Figure 7.4. The data points in Figure 7.3 are mainly located in Zones 3, 4, 5, and 6 in the direction of OCR or cementation increase. Therefore, the soil in the HPR zones can be classified as cemented silty clay to silty sand. This finding is similar to the previous conclusion (Figure 7.1) with respect to soil type.

The majority of the data points in Figure 7.3 are located on the right side of the classification chart (i.e., positive  $B_q$ ).  $B_q$  for these point ranges from 0.2 to 0.9 corresponding to a corrected tip resistance range of 1 tsf to 5.5 tsf. Figure 7.4 presents  $B_q$  versus  $q_t$  chart for nonHPR zones. The data points are located longitudinally on the upper part of the chart with a range of cone resistance ( $q_t$ ) from 1 tsf up to 70 tsf.  $B_q$  is low and ranges from -0.05 to 0.22.

Based on the results shown in all four figures (i.e., Figure 7.1, Figure 7.2, Figure 7.3, and Figure 7.4) the HPR and nonHPR soils may overlay in Zones 4 and 5. The data in the HPR zones lies above the normally consolidated region and high pore pressure ratios, while for the nonHPR zones, the data lie on and below that region with low pore pressure ratios. These findings agree with the estimated soil properties discussed in Chapter 4. A summary of the data overlaid on Robertson's (1990) charts in terms of HPR and nonHPR is presented in Table 7-1.

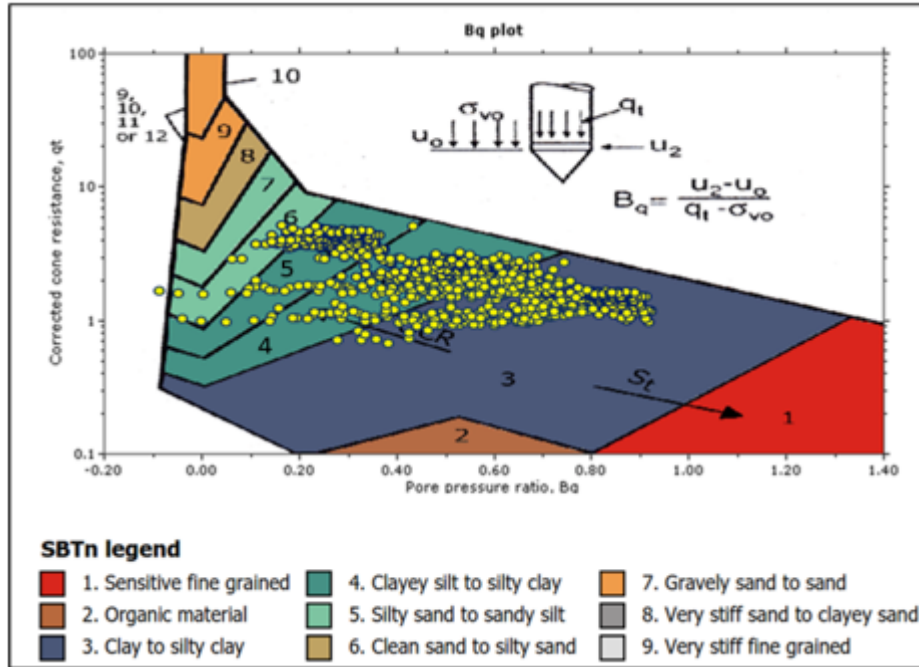


Figure 7.3: HPR data overlaid on Robertson's (1990) cone resistance versus pore pressure ratio SBT chart

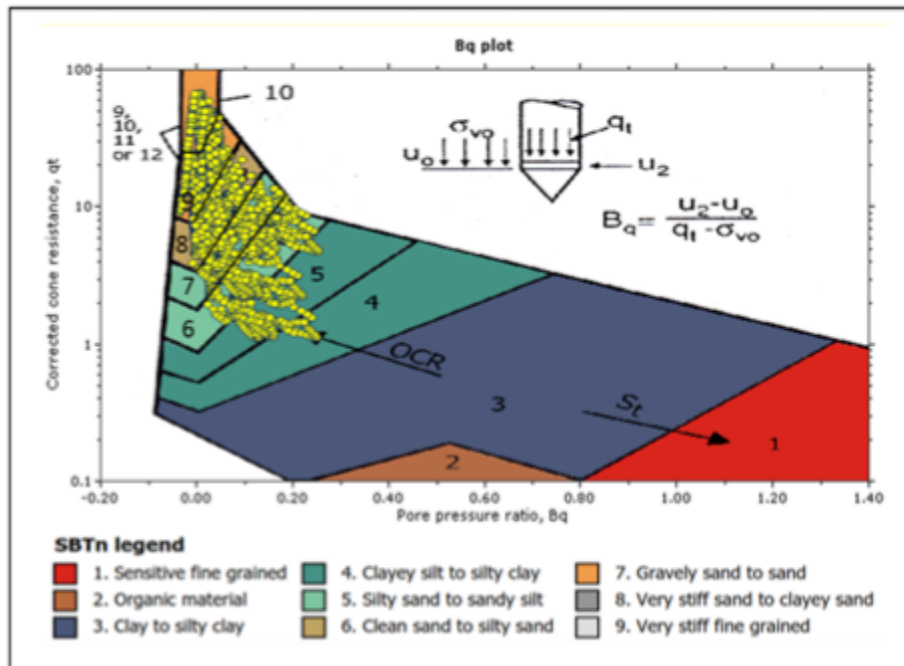


Figure 7.4: NonHPR data overlaid on Robertson's (1990) cone resistance versus pore pressure ratio SBT chart

Table 7-1: Ranges from Robertson's (1990) Soil Behavior Type Classification Charts for HPR and NonHPR Zones at All Sites

Zone	SBTn Zone	Normalized cone resistance ( $Q_{tn}$ )	Normalized friction ratio ( $F_r$ %)	Pore pressure ratio ( $B_q$ )	Corrected cone resistance, $q_t$ (tsf)
HPR	3,4,5	3 – 40	0.4 – 10	0.2 – 0.9	1 – 5.5
NonHPR	1,4,5,6,7	2 – 400	0.1 – 4	-0.05 – 2.2	1 – 70

### 7.3. Soil Behavior Type Classification (Robertson, 2012)

Robertson (2012) modified his original (1990) SBT chart and added a line that accounts for soil dilation and contraction. Two regions were identified on this chart based on the state parameter ( $\psi$ ) and OCR. Coarse-grained soils with  $\psi$  less than -0.05 and fine-grained soils with an OCR greater than 4 are dilative at typical pile driving strains and CPT testing. Robertson (2012) also divided each region into three sub-regions based on drainage: undrained, transitional, and drained. The undrained region included fine-grained soils while the drained region included coarse-grained soils. The transitional region represents mixed soils (i.e., coarse and fine). Therefore, four major groups of soil behavior were identified on this chart: fine dilative (**FD**), coarse dilative (**CD**), fine contractive (**FC**), and coarse contractive (**CC**).

The normalized CPT data for the HPR and nonHPR zones from the seven sites were superimposed onto the updated SBT chart (Robertson, 2012) (Figure 7.5 and Figure 7.6). The data shown in Figure 7.5 indicates that the HPR soils plot in the fine to mixed grained (i.e., transitional) dilative soil zones. A large portion of the HPR data is located within the **FD** zone (i.e., fine grained soils with high OCR). Some of the HPR data plots in the transitional or mixed zone (i.e., medium to dense sandy mixed soil). As shown in Figure 7.6, the nonHPR soils plot in the fine, transitional or mixed grained, and coarse contractive soil zones. The majority of the nonHPR CPT data is located in the **CC** zone (i.e., loose sandy soils). The remaining portion of

the nonHPR zone data is located in fine and mixed grained zone (i.e., normally consolidated fine soil and loose mixed soil).

Based on the data presented in Figure 7.5 and Figure 7.6, it can be concluded that the HPR soils plot in the **FD** zone whereas the nonHPR soils plot in the **FC** and **CC** zones. However, the transitional or mixed grained zone may include both the HPR and nonHPR soils depending on the state parameter or OCR of the mixed soil.

In conclusion, this SBT chart indicates that HPR soils generally plot as overconsolidated fine grained or dense mixed grained while the nonHPR soils generally plot as normally consolidated fine grained or loose mixed/coarse grained. Using these charts may be simpler and less costly, since CPTu testing is not required.

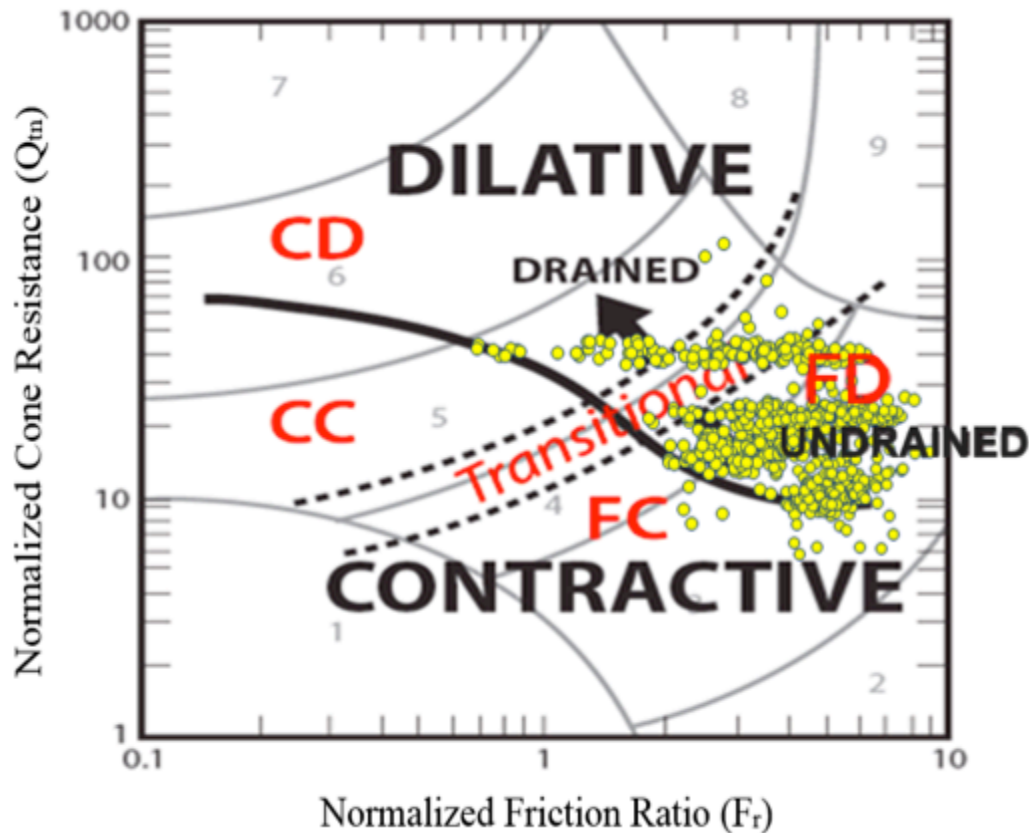


Figure 7.5: HPR data overlaid on Robertson's (2012) updated normalized cone resistance versus friction ratio SBT chart

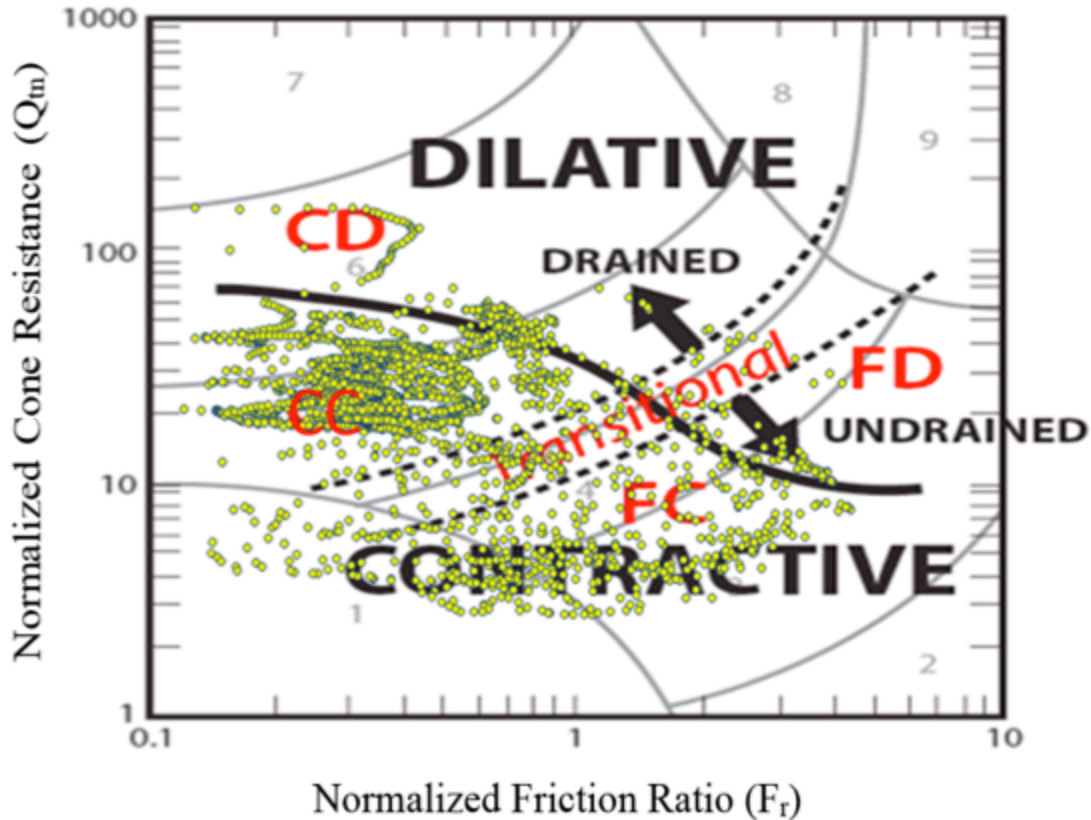


Figure 7.6: NonHPR data overlaid on Robertson's (2012) updated normalized cone resistance versus friction ratio SBT chart

#### 7.4. Soil Classification Using Schneider et al. (2008)

The soil classification chart developed by Schneider et al. (2008) was used to analyze the CPT data from all sites. This chart was proposed for classifying soil using normalized CPT data from the corrected tip resistance ( $q_t$ ) and  $u_2$ . The cone tip resistance was normalized by dividing by the vertical effective stress,  $\sigma'_{v0}$ , (Wroth, 1984), while  $u_2$  was normalized using:

$$\text{Normalized pore water pressure} = \frac{\Delta u_2}{\sigma'_{v0}} = \frac{u_2 - u_0}{\sigma'_{v0}} \quad \text{Equation 7-2}$$

where

$u_2$  = pore pressure measured at cone shoulder

$u_0$  = in situ pore pressure

$\sigma'_{v0}$  = effective overburden stress.

The normalized CPT data for the HPR and nonHPR zones were plotted on a semi-log  $Q$  versus  $\Delta u_2 / \sigma'_{v0}$  chart, as illustrated in Figure 7.7 and Figure 7.8 respectively. Figure 7.7 shows

that most HPR data lies within the silts and low rigidity index (Ir) clays (i.e., Zone 1a) and some lies in the clay zone (i.e., Zone 1b). The normalized pore water pressure ranges from 2 up to 10 for the data in Zone 1a and 1 to 5 for the data in Zone 1b.

The soil classification chart in Figure 7.8 indicates that most of the nonHPR data falls in Zone 2, essentially drained sands, and a small fraction in Zone 3, transitional and silt soils. The data in Figure 7.8 has very low negative and positive normalized pore water pressures and very high tip resistance.

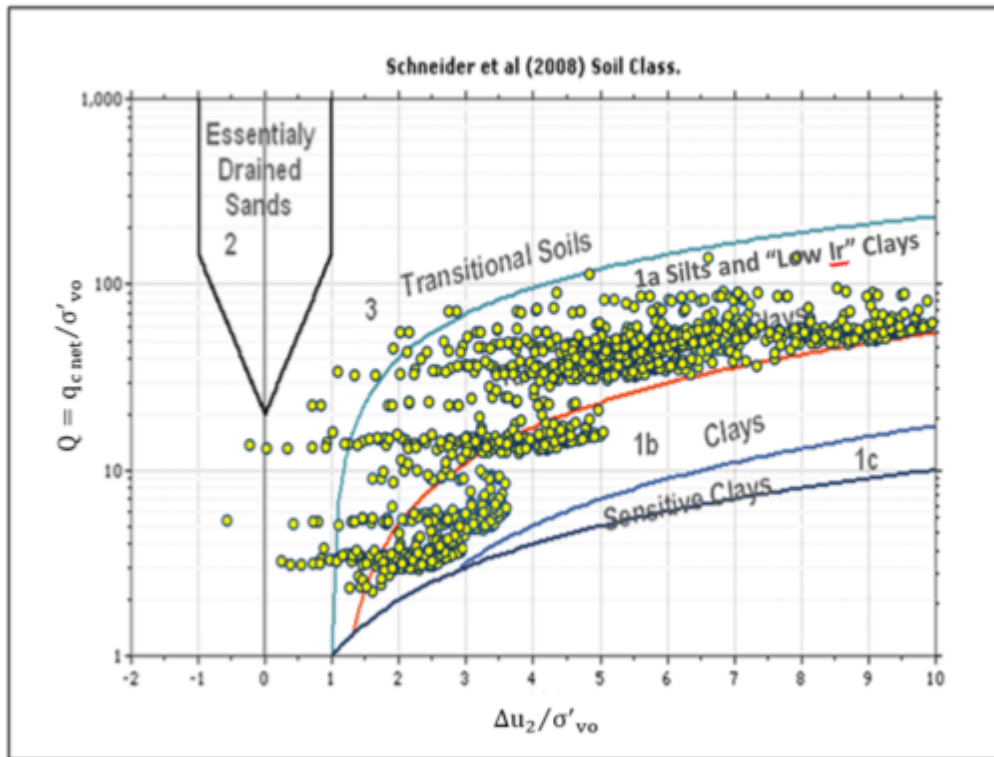


Figure 7.7: HPR data overlaid on Schneider et al.'s (2008) SBT chart

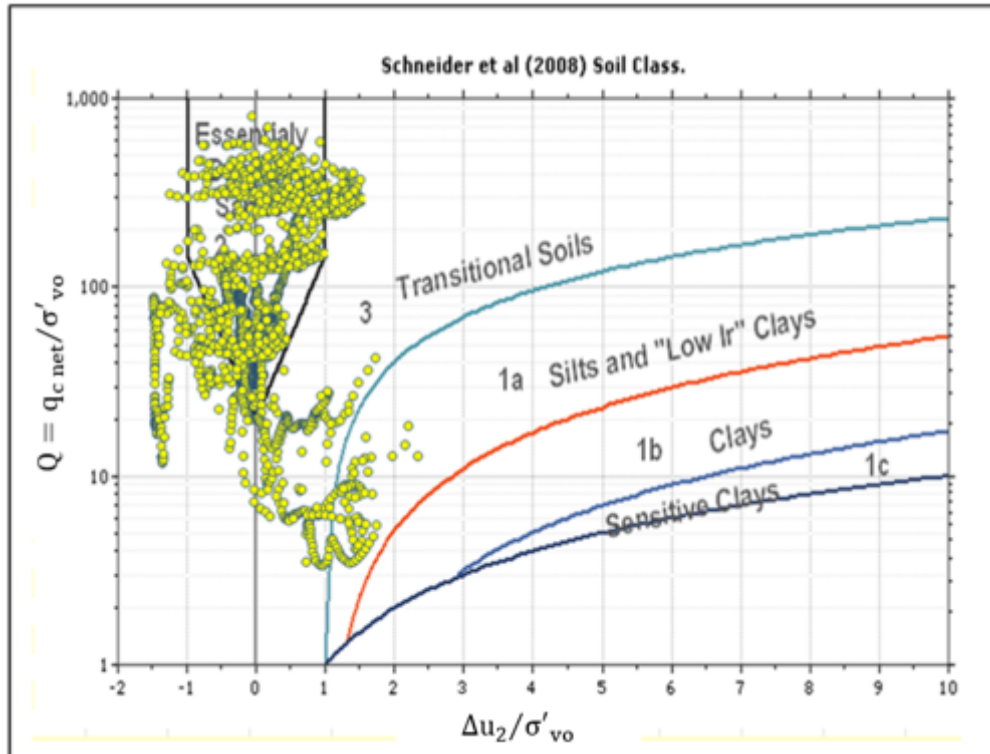


Figure 7.8: NonHPR data overlaid on Schneider et al.'s (2008) SBT chart

## 7.5. Soil Classification Using Eslami and Fellenius (1997)

Most of the referenced soil profiling methods use cone resistance plotted against the friction ratio. However, the friction ratio includes the cone resistance. This manner of data presentation violates the principle of not plotting a variable against itself. Eslami and Fellenius (1997) developed a soil profiling method to classify the soil using CPT data. This classification method depends on the CPT parameters measured directly during the test (i.e.,  $q_t$  or  $q_c$ ,  $f_s$ , and  $u_2$ ). Therefore, it can be developed directly during the CPT sounding because the normalization by division with effective overburden stress is not required.

The classification procedure is accomplished using a log-log plot of  $f_s$  versus the effective cone resistance ( $q_E$ ), determined by:

$$q_E = q_t - u_2 \quad \text{Equation 7-3}$$

where

$q_t$  = cone resistance corrected for pore water pressure on cone shoulder

$u_2$  = pore water pressure measured at cone shoulder

HPR and nonHPR CPT data from all sites was superimposed on Eslami and Fellenius' (1997) SBT chart, as shown in Figure 7.9 and Figure 7.10. Figure 7.9 indicates that the soil at the HPR zones can be classified as silty sand to silty clay. The data points have  $f_s$  ranging from 50 kPa to 700 kPa and  $q_E$  ranging from 1 MPa to 10 MPa.

Figure 7.10 represents the classification of the soils in the nonHPR zones. There is significantly more scatter in this data. The soil can be classified as sand to sandy silt with a low fraction in the sensitive – collapsible clay and/or silt – zone. The majority of the data has  $f_s$  ranging from 2.0 kPa to 80 kPa and  $q_E$  ranging from 0.4 MPa to 40 MPa. It can be concluded that the HPR data tends to have high  $f_s$  and low  $q_E$  while the data at the nonHPR zones has low  $f_s$  and from low to high  $q_E$ .

## 7.6. Summary of Soil Behavior Type Classification

The soil behavior type (SBT) charts can identify the HPR and nonHPR soils. Based on all SBT charts discussed earlier, the HPR soils are silty clay to clayey silt or silty sand to sandy silt. These soil types also exist in the nonHPR zones in addition to the sandy soil. Although the same soils exist in both HPR and nonHPR zones, there are other soil properties that identify the HPR and nonHPR soils in addition to the soil type. The HPR soils have higher CPT pore water pressure ( $u_2$ ), higher sleeve friction, lower tip resistance, and are located in the zone of increasing OCR/cementation. In contrast, the nonHPR soils have low CPT pore water pressure ( $u_2$ ), low sleeve friction, high tip resistance, and are located in and/or below the normally consolidated zone. The HPR soils are fine undrained dilative (FD) soils while the nonHPR soils are coarse and fine drained contractive (**FC** and **CC**) soils.

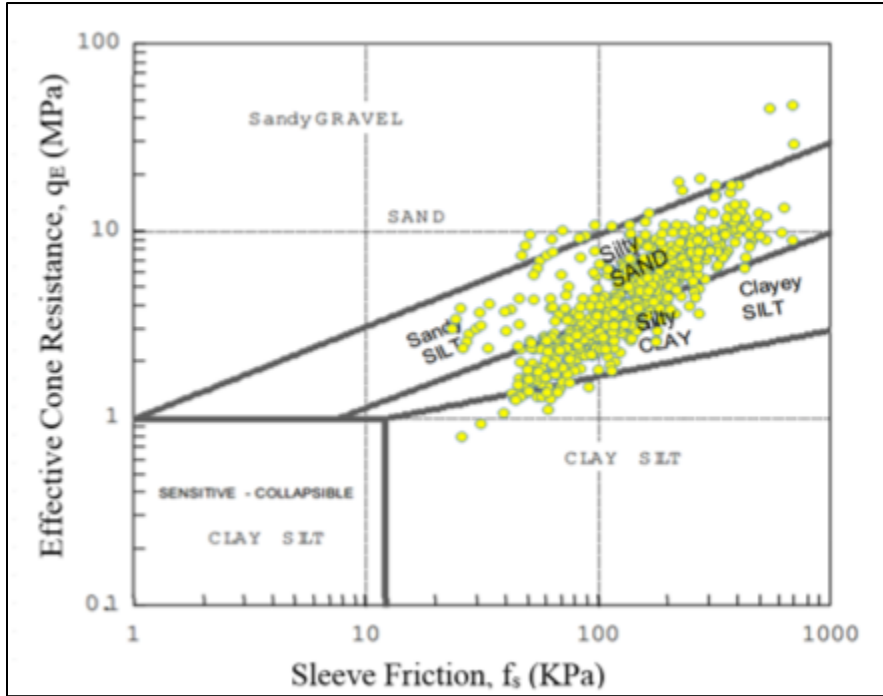


Figure 7.9: HPR data overlaid on Eslami and Fellenius' (1997) SBT chart

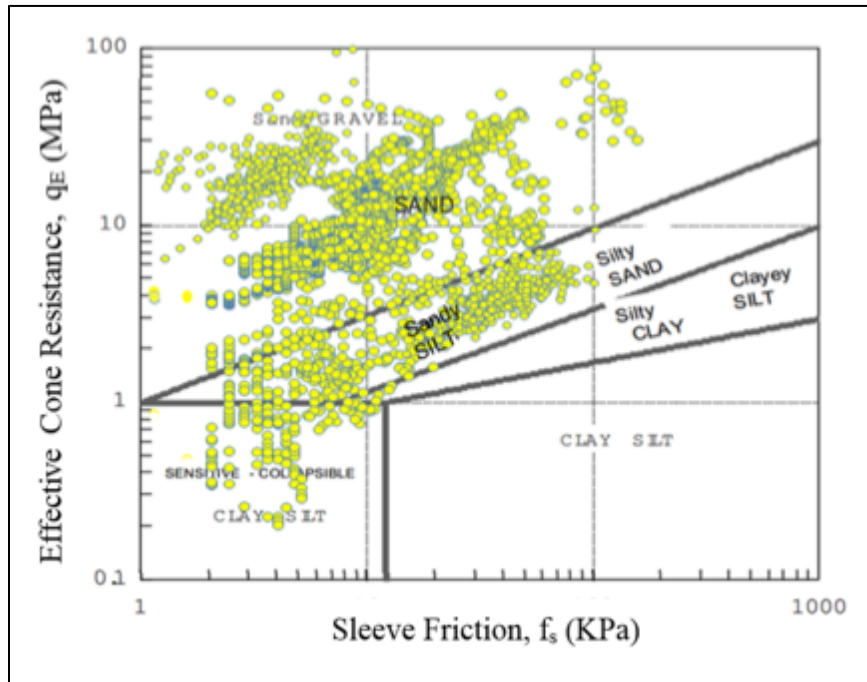


Figure 7.10: NonHPR data overlaid on Eslami and Fellenius' (1997) SBT chart

## **8. Conclusions and Recommendations**

Pile rebound that occurred during installation of 18- or 24-inch square PCPs from 11 sites was evaluated. The sites were located in central Florida, western Jacksonville, and the Florida Panhandle near Destin. All piles were driven with open-ended diesel hammers into soils in the Hawthorn formation. These conclusions are based solely on the data from these sites. Diesel hammers' impact velocities, which are much higher than the velocities from hydraulic or air/steam hammers, may be one of many causes for the excessive rebound. The effects of hammer impact velocity were not evaluated during this research.

Many of the conclusions and recommendations from this work were based on rebound greater than or equal to 0.5-inches and non-rebound still below 0.25-inches due to clearer and more distinct trends at these limits. They are not intended to replace FDOT Specification 455-5.10.3 for use as maximum specification limits and should produce conservative results.

### **8.1. Conclusions**

#### **8.1.1. Re-evaluations of Correlations**

The main objective of this research was to re-evaluate the rebound versus N and fines content correlations published by Cosentino et al. (2013) and Jarushi (2011), which were based on limited data.

Based on the large number of PDA data points from 25 PCPs at 11 sites, there appears to be a very poor correlation between rebound based on the inspectors' set and SPT N values. The original N-rebound correlation was based on about 30 data points with only four above N-values of 40.

Based on several evaluations of rebound versus FC, there could be a relationship between these variables up to FC values of about 35%; however, beyond this threshold, there is no clear relationship.

#### **8.1.2. Grain Size Trends**

A successful evaluation of numerous grain size distribution parameters shows that rebound may be a function of certain grain sizes. The classification findings for the rebound sites

are consistent with the description of the soils in the Hawthorn Formation. The findings indicate that engineers could inexpensively locate HPR soils and zones in properly completed soil borings.

The following conclusions are based on the results from 44 thin-walled tube samples retrieved from six sites.

1. There was no clear tendency in USCS or AASHTO classifications as both classified as SM or A-4/A-2-4. These soils could be either HPR or nonHPR.
2. The Atterberg limits PI and clay content clearly showed differences between HPR and nonHPR soils, with higher PIs and clay content in the HPR soils than in the nonHPR soils. The Atterberg limits of the HPR cohesive soils tested produced an average plastic index nearly twice that of the soils that displayed low to nonHPR problems.
3. The presence of the silt significantly affects HPR. Below 20% silt content in cohesionless soils, HPR may not be clearly identified; however, above 20%, all ten cohesionless samples produced HPR. For cohesive soils, HPR was evident for all samples, with between about 20 and 35% silt; however, with silt contents greater than about 50%, HPR occurred about half of the time. It was also noted that the average silt content for the HPR soils is more than twice as high as for nonHPR soils, while both  $D_{30}$  and  $D_{60}$  are three times higher in the HPR soils than in the nonHPR soils.
4. The clay content of cohesionless soils may not be an effective index for predicting HPR. Cohesive soils with clay contents less than about 30% produced nonHPR, while cohesive soils with clay contents above about 35% produced HPR.
5. Cohesionless soils with sand contents below 74% all produced HPR. HPR in cohesive soils does not depend on their sand content.

The reevaluation of rebound versus  $N_{ES}$  (i.e., the FDOT standard correction process using 1.24) was performed by dividing the soils into three groups: (a) FC below 12%, (b) FC between 12 and 50%, and (c) FC above 50%. Soils with less than 50% fines, which are sands, and the soils with more than 50% fines, which are silts and clays of low or high plasticity, produced the following conclusions:

1. Sands with FC less than 12% generally do not produce rebound greater than 1 inch, and at  $N_{ES}$  above 20, produced rebound less than 0.50 inches.
2. Silts and clays (i.e.,  $FC > 50\%$ ) produced multiple instances of rebound greater than 1 inch when  $N_{ES}$  was less than 4, but rebound did not exceed 0.35 inches at  $N_{ES}$  greater than 24 *and/or as the soils became stiffer/harder*.
3. Sands with 12 to 50% fines showed the greatest potential for rebound as rebound above 1 inch occurred up to an  $N_{ES}$  of 18. They remained high, between 0.75 and 1 inch, as  $N_{ES}$  increased to refusal.

Numerous N-value correction techniques were attempted to determine how they might affect the rebound versus N relationships. Regardless of the technique used, the same three trends, discussed above, were shown.

A histogram with a frequency of rebound greater than and less than 0.5 inches based on FC, categorized in 10% FC increments, shows that FCs between 30 and 40% produce the highest probability (nearly 40%) of rebound in excess of 0.5 inches. However, these FCs produce only 10% probability of rebound of less than 0.5 inches. This indicates that FC in the 30 to 40% range could be an indicator of rebound greater than 0.5 inches.

### **8.1.3. Permeability and Density Trends**

In general, the permeability coefficient of the HPR soils was one or two orders of magnitude lower (i.e., slower flow) than the nonHPR soils. Specifically, cohesionless HPR soils have permeabilities slower than  $5 \times 10^{-6}$  (i.e.,  $10^{-7}$ ,  $10^{-8}$ ), while cohesionless nonHPR soils have permeabilities faster than  $1.2 \times 10^{-5}$  cm/s (i.e.,  $10^{-4}$ ,  $10^{-3}$ ). The permeability of the cohesive HPR soils is based on very limited data and may be on the order of  $10^{-8}$  cm/s or one order of magnitude slower than the nonHPR cohesive soils ( $10^{-7}$  cm/s).

The lower end of the range of dry unit weights of the HPR soils (104 pcf) is about 10% lower than the lower end of the range of dry unit weights of the nonHPR soils (111 pcf).

### **8.1.4. Cyclic Triaxial Trends**

Basic triaxial testing did not show any variations in failure stresses between the HPR and nonHPR soils. This finding matches the original problem statement associated with HPR, in that

conventional geotechnical testing did not show and differences between HPR and nonHPR soils. The loading rate during these tests is much slower than the pile-driving, CPTu penetration or cyclic triaxial rates, clearly indicating that this phenomenon is related to the rate of loading of these soils.

HPR cohesionless soils required about two to three times more cycles to produce 1, 2.5, 5, 10, and 15% strains than the nonHPR soils and are therefore considered twice to three times as resilient. This finding suggests that pile driving in these cohesionless resilient soils would also require more hammer blows during installation. These same soils have also been termed liquefaction resistant, and CPT SBT charts, along with SPT N values related to contractive and dilative behavior, lead to this same trend.

The cyclic failure strains for nonHPR soils are typically higher (*with nearly all failing at 15% strain*) than the cyclic failure strains of HPR soils (*which mostly failed in the 1 to 5% range*).

During cyclic loading HPR specimens have lower pore water pressure ratios ( $\Delta u/\sigma_3'$ ) at failure than nonHPR specimens, indicating that the HPR soils take longer to produce increases in pore pressures than the nonHPR soils. This finding matches what we see in the field that the displacement piles do not penetrate the HPR soils.

### **8.1.5. CPTu Trends**

1. There are consistent trends indicating that increased CPTu pore pressures in fine silty sands with clays correlate to HPR for large diameter PCPs.
2. The CPT pore water pressures ( $u_2$ ) may be linearly correlated to the pile rebound.
3. The pore water pressures during CPTu testing over a 5 to 10 pile diameters (relatively thick layer) are very high with values in the 300 to 550 psi range when cemented SM and SC soils are encountered.
4. CPTu predicted undrained shear strengths for HPR soils are higher than those from nonHPR soils, which matches the trend of difficult driving with displacement piles in HPR soils.

### 8.1.6. SBT Chart Trends

1. HPR and nonHPR soils plot in distinct regions on SBT charts.
2. The rebound soils are cemented silty fine sand (SM) with trace phosphate and shell or cemented clayey fine sand (SC) with fines.
3. CPT data from rebound soils typically plotted in the dilative zones of the Robertson (2012) SBT chart, while non-rebound soils typically plotted in its contractive zones.
4. Most SBT charts give an indication of type and behavior of rebound and nonrebound soils. Placing the CPTu data on these charts and determining which soils would potentially produce HPR is a time-consuming operation.
  - a. Robertson's (1990) Tip and Sleeve SBT chart shows some slight trends that the HPR soils plot in Zones 3, 4, and 5 to the right of the normally consolidated soils; however, the nonHPR soils may plot more to the left of the normally consolidated soils in Zones 1 and 3 through 7.
  - b. Robertson's (1990) Tip and Pore Pressure SBT chart indicates rebound when the pore pressure ratio  $B_q$  is greater than 0.2 and no rebound when it is less than 0.2.
  - c. Islami and Fellenius' (1997) SBT chart shows HPR soils plot in the silty clay, silty sand, and sandy silt ranges
  - d. Based on the CPTu data and the laboratory testing data, the Robertson's (2012) SBT chart shows HPR soils as dilative within zones 3, 4, and 5 and contractive soils within zones 1 and 3 through 6 within the contractive areas.
  - e. Schneider et al.'s (2008) SBT chart indicates HPR soils plot in zones 1 a and b, plus 3 when the ratio  $\Delta u_2/\sigma'_{v0}$  exceeds 1, and that nonHPR soils plot in zones 2 and 3 when this ratio is below 1.
5. FC between 25% and 40% likely results in liquefaction resistant soils.
6. Medium dense to very dense silty sands have a dilative response, produced rebound, and may lead to refusal.

7. Soft to very stiff clays can produce rebound in excess of 2 inches. Rebound reduces as clays become harder.

## 8.2. Recommendations

Based on the findings from this research, the following decision tree was developed to help geotechnical engineers determine whether rebound is a concern. These charts are based on limited data and the engineer is cautioned that they are very preliminary and that rebound may occur even when these charts lead engineers to believe that it may not.

The decision tree rebound criterion is based on FDOT Specification 455-5.10.3 is 0.25 inches and should result in conservative predictions of rebound problems. The existing methods used to determine rebound to accuracies of ¼-inch are limited and an improved approach for measuring it in the field would benefit FDOT.

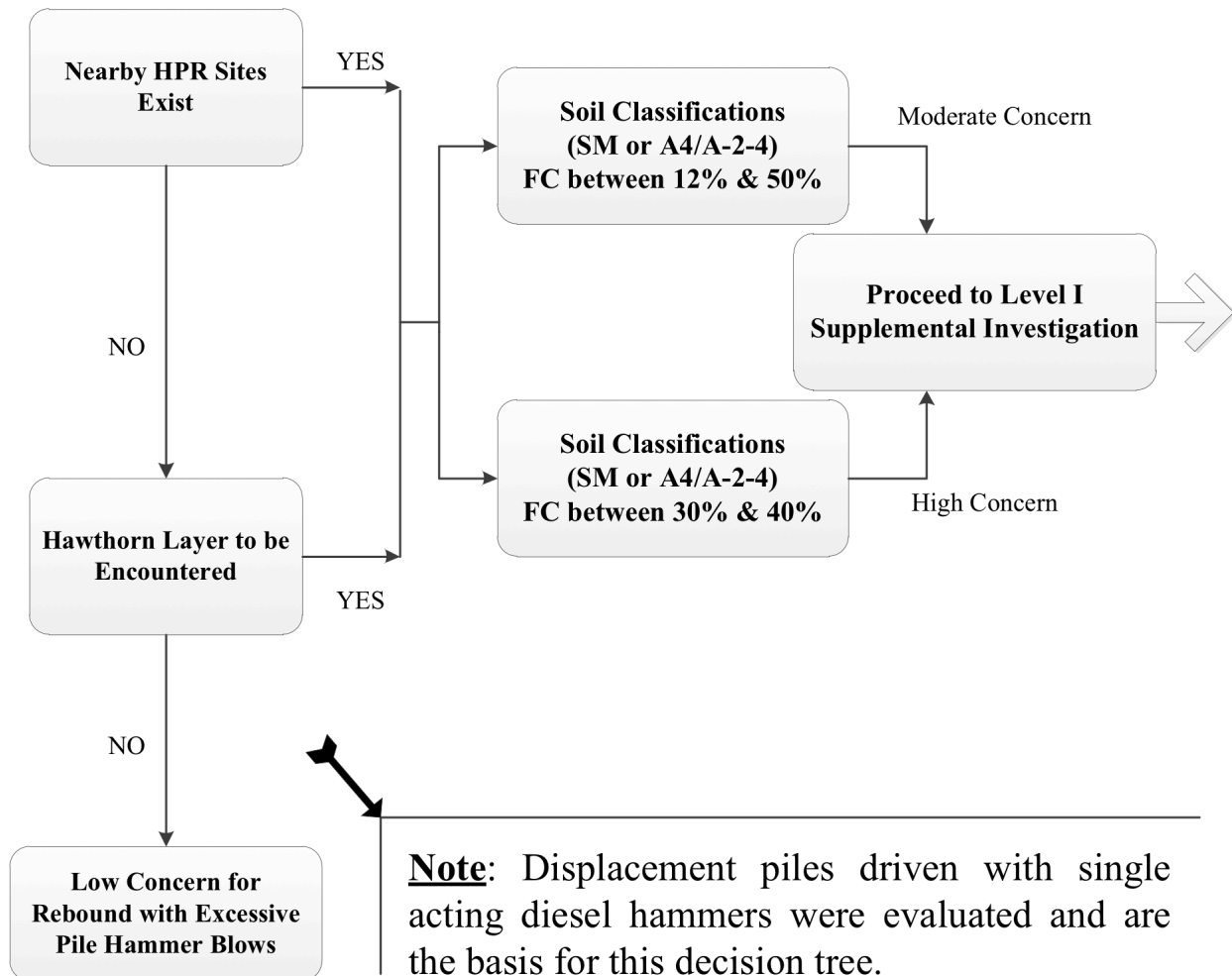
Three levels are presented:

1. Level I should be used to guide the geotechnical engineer through basic design phase information needed to guide them to a point where they can identify problem HPR sites. It includes basic knowledge of the geologic conditions from the Hawthorn layer, the locations of other HPR sites, and the intended use of displacement piles driven with open-ended (i.e., single acting) diesel hammers. Also, from the design phase, the engineer should know some FCs, although they may not be from the critical layers.
2. Level II guides the geotechnical engineer through a supplemental laboratory testing investigation that should seriously be consider. It includes a complete grain size analysis with hydrometer and Atterberg limits from SPT samples on cohesive soils from critical layers within the soil profile. There is a separate decision tree for the cohesive and cohesionless soils based on FCs, percent clay and silt, and Atterberg limits. Based on the data retrieved to date, the decision matrix leads the engineer to a level of concern believed to be either high or moderate for HPR problems. FDOT should consider processes that allow additional data to be added to the existing plots, especially grain size and limits data.

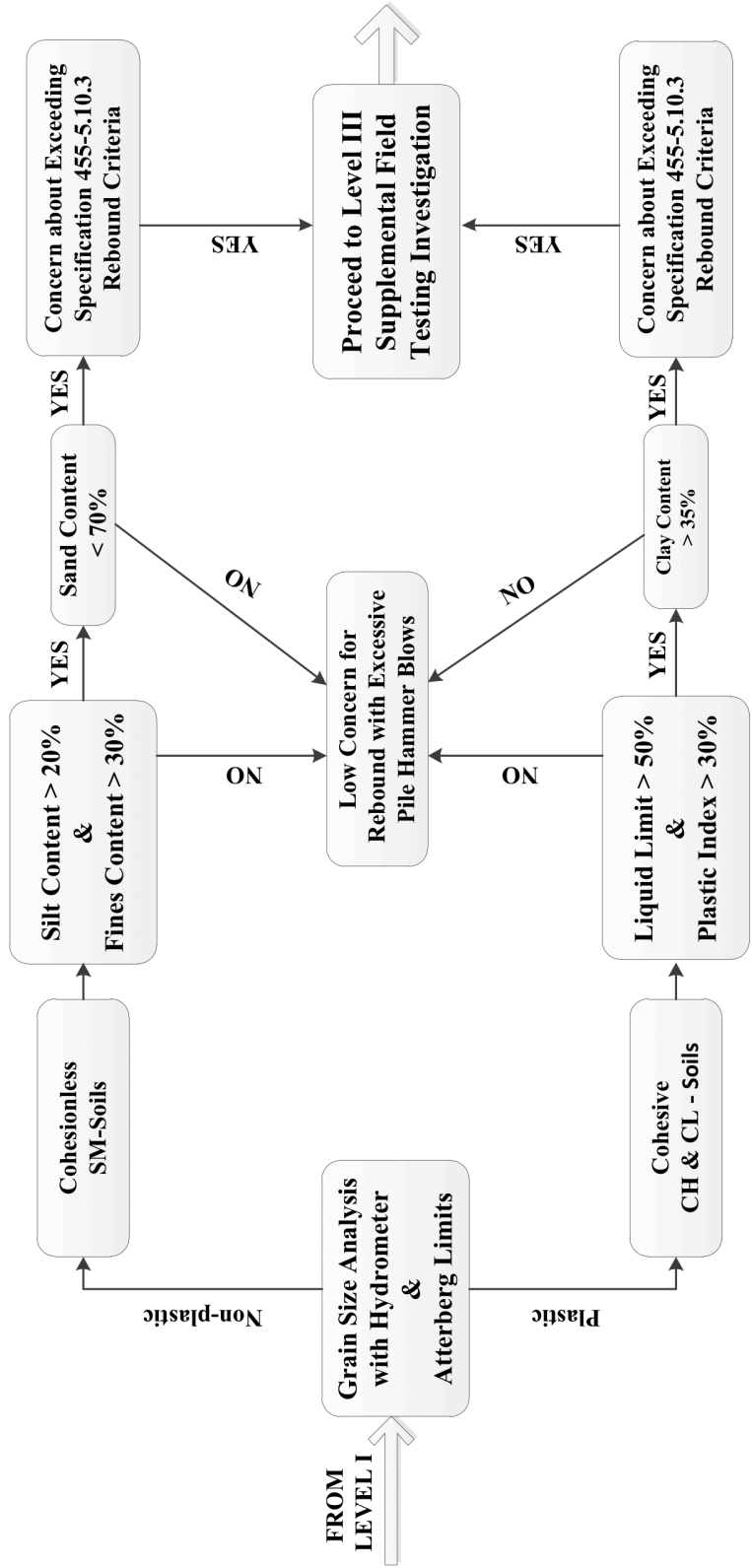
3. The level III supplemental field-testing investigation, if desired, should focus on permeability so that the differences between the HPR and nonHPR soils can be evaluated. This level would require thin-walled tube sampling and triaxial permeability testing. Also CPTu testing could be performed to show pore pressures possibly in excess of 100 psi in the HPR soils. Finally, the resilient behavior shown from the stress-level cyclic triaxial testing, conducted as described in this report, is noted on the third level decision tree so that engineers know that pile driving in these soils would be more difficult.

# High Pile Rebound Decision Tree

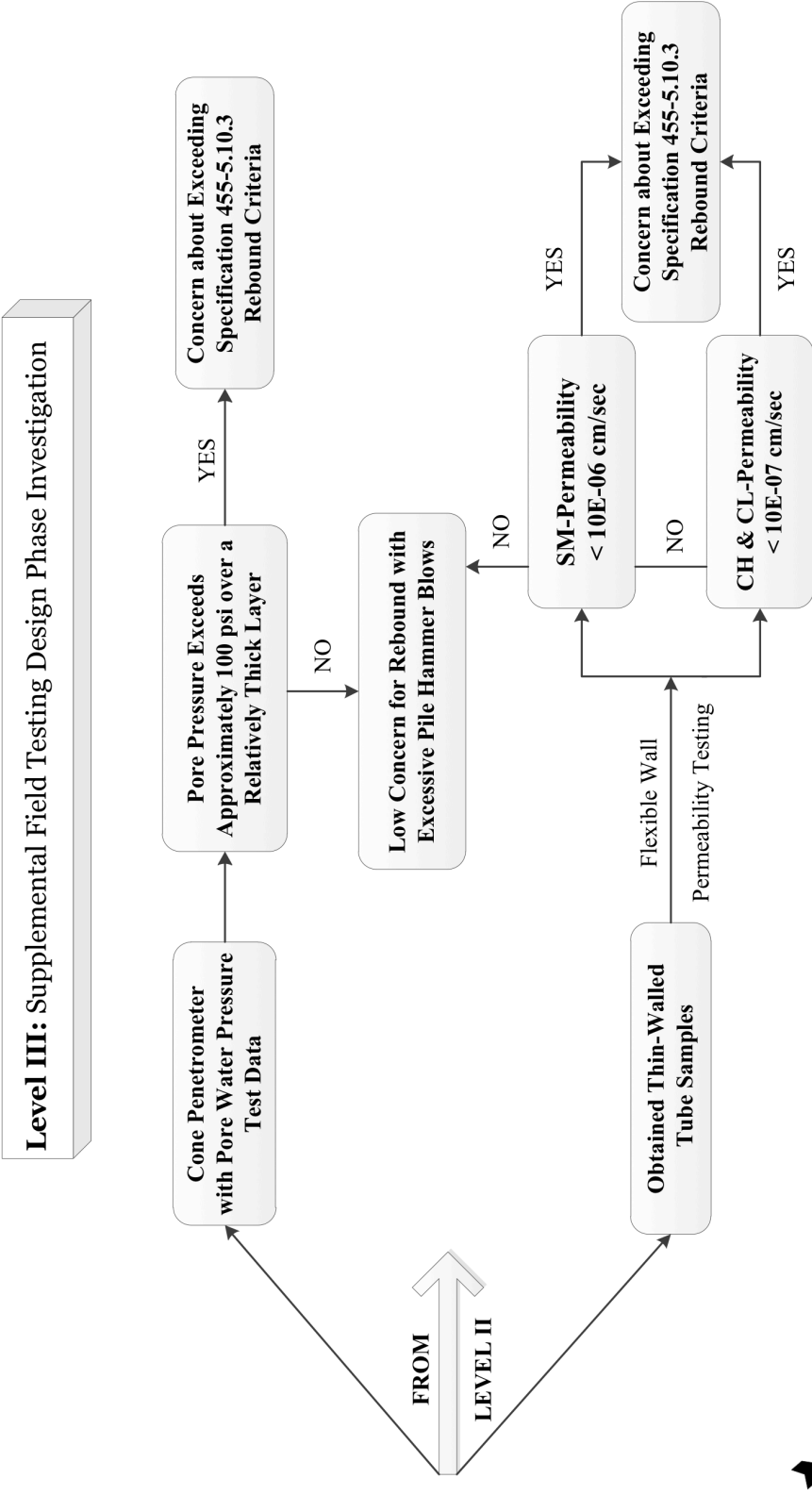
## Level I: Basic Design Phase Information



**Level II: Supplemental Laboratory Testing Design Phase Investigation**



LL & PI above A line



**Note** that stress-level cyclic triaxial testing with 1000 cycles each at stress levels at 20, 40, 60, and 80% of the failure stress from triaxial tests conducted in accordance with ASTM D4767 indicated that HRP soils required two to three times more cycles to attain 2.5, 5, 10, and 15% strain levels than nonHRP soils and are termed more resilient, which matches the phenomenon that occurs during driving in these soils.

Existing correlations between SPT N values and CPT qc values should be investigated to determine how these correlations can be used and if they possibly could lead to SPT data being used on the SBT charts that do not include pore water pressure data.

Permeability correlations between; a) ASTM D 5084 triaxial permeability testing, b) CPTu –k correlations and c) CPTu dissipation testing should be performed in the rebound soils from the existing sites. The CPTu and lab data are already available for many of the sites evaluated to date.

A multivariable regression analysis should be performed that incorporates the SPT N-values, fines content, silt content, clay content, and possibly the  $D_{10}$ ,  $D_{30}$  and  $D_{60}$  values as variables. These findings could be used to validate the decision tree.

Using rebound of 0.5 inches or more produced clearer findings than using 0.25-inches and should be investigated when more precise field measurements become available. The current problems with double integrating the PDA accelerations to determine a digital set should be addressed by considering fixed laser systems mounted possibly on the driving templates or the ground surface not affected by pile driving vibrations.

## 9. References

- Arab, A., & Belkhatir, M. (2012). "Fines content and cyclic preloading effect on liquefaction potential of silty sand." *Acta Polytechnica Hungarica*, 9(4), 47. (pp. 1785-8860).
- American Society for Testing and Materials (ASTM). (2011). "standard test method for Penetration Test and Split-Barrel Sampling of Soils." D1586, West Conshohocken, PA.
- American Society for Testing and Materials (ASTM). (2005). "Standard test method for mechanical cone penetration tests of soil." D3441, West Conshohocken, PA.
- American Society for Testing and Materials (ASTM). (2007). "Standard test method for performing electronic friction cone and piezocone penetration testing of soils." D5778-95, West Conshohocken, PA.
- Authier, J., & Fellenius, B. H. (1980). "Quake values determined from dynamic measurements." In *1st International Conference on the Application of Stress-Wave Theory on Piles*, Stockholm, 1980, (pp. 197- 216).
- Awad, N. A. (1957). *Soil behaviour under repeated vertical and horizontal stresses* (Unpublished Master's Thesis). McMaster University, Canada, 274
- Bandini, P., & Sathiskumar, S. (2009). "Effects of silt content and void ratio on the saturated hydraulic conductivity and compressibility of Sand-Silt Mixtures." *Journal of Geotechnical and Geoenvironmental Engineering, ASCE*, 135(12), 1976-1980.
- Bazaraa, A.R.S. (1967). "Use of the standard penetration test for estimating settlement of shallow foundations on sands." Ph.D. Thesis, University of Illinois.
- Belkhatir, M., Schanz, T., & Arab, A. (2013). "Effect of fines content and void ratio on the saturated hydraulic conductivity and undrained shear strength of sand-silt mixtures." *Environmental Earth Sciences*, 70(6), 2469-2479.

- Bingjian, Z. (2011). "Study of the pore water pressure variation rule in saturated soft soil caused by prestressed concrete pile penetration." *Electric Technology and Civil Engineering*, 756-759.
- Bolton, M. D. (1984). Strength and dilatancy of sands. *Cambridge University, Engineering Department, (Technical Report) CUED/D-Soils*.
- Boulanger R. W., & Idriss, I. M. (2006). "Liquefaction susceptibility criteria for silts and clays." *Journal of Geotechnical and Geoenvironmental Engineering*, 132(11), pp. 1413-1426.
- Boulanger, R. W., & Idriss, I. M. (2007). "Evaluation of cyclic softening in silts and clays." *Journal of Geotechnical and Geoenvironmental Engineering*, 133(6), pp. 641-652.
- Idriss, I. M., and Boulanger, R. W. (2008). "Soil liquefaction during earthquake." EERI *Publication MNO-12*, Earthquake Engineering Research Institute.
- Bowles, J. E. (1977). *Foundation analysis and design, 2nd Ed.* New York, NY: McGraw Hill, Inc.
- Bowles, J. E. (1988). *Foundation analysis and design, 4th Ed.* New York, NY: McGraw Hill, Inc.
- Bray, J. D., Sancio, R. B., Riemer, M. F., & Durgunoglu, T. (2004). "Liquefaction susceptibility of fine-grained soils." In *11th Int. Conf. on Soil Dynamics and Earthquake Engineering and 3rd Int. Conf. on Earthquake Geotechnical Engineering, 1*, 655–662.
- Hettiarachchi, H and Brown, T. (2009). "Use of the SPT Blow Counts to Estimate Shear Strength Properties of Soils: Energy Balance Approach." *Journal of Geotechnical and Geoenvironmental Engineering*, ASCE, pp. 830-834
- Bum-Jae, Y., Oh, S., Han, S., & Lee S. (2002). "Visual measurement of pile penetration and

- rebound movement using a high-speed line-scan camera.” In *IEEE International Conference on Robotics and Automation: ICRA '02*, Washington, DC, 11-12 May 2002, 4307- 4312.
- Burns, S. E., & Mayne, P. W. (1998). “Monotonic and dilatatory pore-pressure decay during piezocone tests in clay.” *Canadian Geotechnical Journal*, 35(6), 1063-1073.
- Burns, S. E., & Mayne, P. W. (1999). “Pore pressure dissipation behavior surrounding driven piles and cone penetrometers.” *Transp. Res. Rec.*, (1675), 17-23.
- California Department of Transportation -CDOT. (2014). “Geotechnical design manual soil.”
- Cetin, K. O., & Ozan, C. (2009). “CPT-based probabilistic soil characterization and classification.” *J.Geotech.Geoenviron.Eng.*, 135(1), 84-107.
- Chen, B. S., & Mayne, P. W. (1996). “Statistical relationships between piezocone measurements and stress history of clays.” *Canadian Geotechnical Journal*, 33(3), 488-498.
- Chen, R., Hu, Y., & Chen, Y. (2001). “Determining driving resistance with rebound of pile-top during pile driving.” *Journal of Zhejiang University (SCIENCE)*, 2(2), 179-185.
- CPeT-IT v.1.4 (2014). Geologismiki geotechnical software for reducing cone penetrometer data, Retrieved from [www.geologismiki.gr](http://www.geologismiki.gr).
- Coduto, D. P. (2001). *Foundation design principles and practice, 2<sup>nd</sup> Ed.* New Jersey: Prentice Hall, Inc.
- Cosentino, P., Kalajian, E., Misilo, T., Chin Fong, Y., Davis, K., Jarushi F., Bleakley A., Hussein M. H., & Bates, Z. (2010). Design phase identification of high pile rebound soils. *Rep. No. FL/DOT/BDK81 977-01*, Florida Department of Transportation

- Cosentino, P. et al. (2011) Cosentino, P., Kalajian, E., Jarushi, F. (2011). "Using fines content and uncorrected SPT blow counts of soils to predict high pile rebound," *Journal of the Transportation Research Board*, No. 13-2880, pp. 47-55.
- Das, B. (2008). *Advanced soil mechanics, 3<sup>rd</sup> Ed.* New York: Taylor and Francis.
- Das, B. M. (2014). *Principles of foundation engineering, 8<sup>th</sup> Ed.*, Cengage Learning, Massachusetts.
- Dash, H.K., & Sitharam, T. G. (2009). "Undrained cyclic pore water pressure response of sand-silt mixtures: Effect of nonplastic fines and other parameters." *Geotechnical and Geological Engineering*. 27(4), pp. 502-517.
- DeAlba, P., Seed, H. B., and Chan, C. K. (1976). "Sand liquefaction in large-scale simple shear tests." *Journal of Geotechnical Engineering Division, ASCE. Vol.102, No.GT9*, pp. 909-927.
- Dekhn, H. (2015). *Engineering properties of pile rebound soils based on cone penetration testing* (Unpublished Doctoral dissertation). Florida Institute of Technology, Melbourne FL.
- Dowell, G.R., & Bolton, M. D. (2000). "Effect of particle size distribution on pile tip resistance in calcareous sand in the geotechnical centrifuge." *Granular Matter*, 2(4), 179-187.
- Eigenbrod, K. D., & Issigonis, T. (1996). "Pore-water pressures in soft to firm clay during driving of piles into underlying dense sand." *Canadian Geotechnical Journal*, (33), 209-218.
- Eslami, A., & Fellenius, B. H. (1997). "Pile capacity by direct CPT and CPTu methods applied to 102 case histories." *Canadian Geotechnical Journal*, 34(6), 886-904.

- Florida Department of Transportation- FDOT. (2015). Standard Specification for Road and Bridges Section 455..
- Fellenius, B. H. (1984). "Negative skin friction and settlement of piles." Proceedings of the 2<sup>nd</sup> International Seminar, Pile Foundations, Nanyang Technological Institute, Singapore.
- Fellenius, B. H., & Eslami, A. (2000). "Soil profiles interpreted from CPTu data." *Geotechnical*. In "Year 2000 Geotechs:" *Geotechnical Engineering Conference*, Asian Institute of Technology, Bangkok, Thailand, November 27-30, 2000 (pp. 18).
- Finn, W. D. L. (1982). "Soil liquefaction studies in the people's republic of China," *Soil Mechanics, Transient of Cyclic Loads: Constitutive Relations and Numerical Treatment.*, pp. 609-626
- Frost, M. W., Fleming, P. R., & Rogers, C.D.F. ( 2004). "Cyclic triaxial tests on clay subgrades for analytical pavement design." *Journal of the Transportation Engineering Division, ASCE. 130(3)*, 378-386.
- Gerwick, B. C. (2004). "Pile installation in difficult soils." *Journal of Geotechnical and Geotechnical and Geoenvironmental Engineering, ASCE, 130(5)*, 454-460.
- Gibbs, H.J. and Holts, W.G. (1957). "Research on determining the density of sands by spoon penetration testing." Proceedings of the 4<sup>th</sup> International Conference on Soil Mechanics and Foundation Engineering, Vol. 1, 35-39.
- Gui, M.W., & Jeng, D.S. (2009). "Application of cavity expansion theory in predicting centrifuge cone penetration resistance." *Open Civil Engineering Journal*, 3, 1-6.
- Guo, T., & Prakash, S. (1999). "Liquefaction of silts and silt-clay mixtures." *Journal of Geotechnical and Geoenvironmental Engineering, 125(8)*, 706-710.
- Hattori, A., & Nishiwaki S. (1974). "Measurements of the dynamic behavior of concrete piles

- during driving operations using a He-Cd laser.” *Optics and Laser Technology*, 6, 273-275.
- Hazirbaba, K. (2005) Pore Pressure Generation Characteristics of Sands and Silty Sands: A Strain Approach. PhD Thesis, The University of Texas Austin, Austin.
- Hoenstine, R W. (1984). Biostratigraphy of selected cores of the Hawthorn Formation in Northeast and East-Central Florida. *Report of Investigation No. 93. Tallahassee, Florida: Bureau of Geology Division of Resource Management.*
- Holtz, R. D., & Kovacs, W. D. (1981). *An Introduction to Geotechnical Engineering*, New Jersey: Prentice Hall, Inc.
- Houlsby, G. T. (1988). “Piezocone penetration test.” In *Geotechnology Conference on Penetration Testing in U.K.*, Birmingham, July 6-8, (pp. 141–146).
- Holubec, I., & D'Appolonia, E. (1972). “Effect of particle shape on the Engineering Properties of Granular Soils.” *ASTM Special Technical Publication*, 304-318.
- Hussein, M., Woerner, W., & Sharp, M. (2006). “Pile drivability and bearing capacity in high-rebound soils.” *Geo-congress*, 1-4.
- Hussein, M. H., Woerner, W. A., Sharp, M., & Hwang, C. (2006). “Pile driveability and bearing capacity in high-rebound soils.” *GeoCongress*, 63.
- Idriss, I. M., & Boulanger, R. W. (2008). “Soil liquefaction during earthquake.” *EERI Publication MNO-12*, Earthquake Engineering Research Institute.
- Ishihara, K. (1996). *Soil behavior in earthquake*. Oxford: Geotechnical Clarendon Press.
- Jamiolkowski, M., Presti, D., & Manassero, M. (2003). “Evaluation of relative density and shear

- strength of sands from CPT and DMT.” In *Soil Behavior and Soft Ground Construction: Proceeding of the Symposium*, Geo-Institute, Cambridge, Massachusetts, October 5-6, 2001, 119, 201-238.
- Cosentino, P., Kalajian, E., Jarushi, F. (2011). “Using fines content and uncorrected SPT blow counts of soils to predict high pile rebound,” *Journal of the Transportation Research Board*, No. 13-2880, pp. 47-55.
- Jarushi, F. (2013). *Evaluating geotechnical engineering properties associated with high pile Rebound* (Unpublished Master’s Thesis). Florida Institute of Technology, Melbourne, FL.
- Jefferies, M.G. & Been, K. (2006). *Soil Liquefaction a critical state approach*. New York: Taylor and Francis.
- Kishida, H. (1969). “Characteristics of Liquefied Sands during Mino-Owarim Tohnankai, and Fukui Earthquakes.” *Soils and Foundations*, 9(1), pp. 75-92
- Koester, J.P. (1994) “The influence of fine type and content on cyclic strength.” *Ground Failures under Seismic Conditions*, Geotechnical Special Publication No. 44, ASCE, pp. 17-33.
- Koester, J.P. (2013). “Effects of fines type and content on liquefaction potential of low-to-medium plasticity fine-grained soils.” In *1993 Nat. Earthquake Conference*, Vicksburg, MS, (1993): 20180-6199.
- Koizumi, Y. (1966). “Change in Density of Sand Subsoil caused by the Niigata Earthquake.” *Soil and Found*, Tokyo, Japan, 8(2), pp. 38-44.
- Kulhawy, F.H., & Mayne, P.W. (1990). *Manual on estimating soil properties for Foundation Design*. Project No.1493-6, New York: Cornell University.
- Likins, Garland E. (1983). “Pile installation difficulties in soils with large quakes.” In G.G.

Globe, (Ed.), In *Symposium 6 at the 1983 ASCE Convention*, Philadelphia, PA, 18 May 1983.

ASCE Geotechnical Engineering Division.

Lee, K. L., and Seed, H. B. (1967). "Cyclic stresses causing liquefaction of sand." *Journal of Soil Mechanics and Foundation Division, ASCE, Vol. 93, No. SM1, Proc Paper 5058, Jan, (47-70)*.

Liao, C. and Whitman, R. (1986). "Overburden correction factors for SPT in sand." *Journal of Geotechnical Engineering, ASCE. (373-377)*.

Lundgren, R. (1979). "Behavior of deep foundations." ASTM Special Technical Publication, No. STP 670.

Lunne, T., Robertson, P.K., & Powell, J.J. (1997). *Cone penetration testing in geotechnical practice*. E & FN Spon Routledge.

Mayne, P. W. (2002). "Flow properties from Piezocone Dissipation Tests." In *Soil Mechanics: Interpretation of In-Situ Tests*, Georgia Institute of Technology, Georgia, USA, 2002, pp. 1-8.

Mayne, P. W. (2007). "Cone Penetration Testing." Georgia Institute of Technology, A Synthesis of Highway Practice - 368, *Transportation Research Board (TRB)*, Washington, D.C.

Mayne, P. W. (2007). "Cone penetration testing State-of-Practice." Transportation Research Board, *NCHRP Project 20-05 - Topic 37-14*, Washington, DC.

Kulhawy, F.H., and Mayne, P.W. (1990). "Manual on estimating soil properties for foundation Design." *Project No. 1493-6*, Cornell University, New York.

Mayne, P. W., Peuchen, J., & Bouwmeester, D. (2010). "Soil unit weight estimation from CPTs." In *2nd International Symposium on Cone Penetration Testing - CPT'10*, Huntington Beach, California, 2, pp. 1-8.

- McDowell, G. R., & Bolton, M. D. (2000). "Effect of particle size distribution on Pile Tip Resistance in Calcareous Sand in the Geotechnical Centrifuge." *Springer-Verlag, Granular Matter* (2), 179-187.
- Mes, J. M., & McDermott, R. J. (1976). "Pile driveability is unpredictable in sand or silt." *Petroleum Engineer* 2(2), 76-92.
- Molle, J. (2005). *The accuracy of the interpretation of CPT based Soil Classification Methods in soft soils* (Unpublished Master's Thesis). Delf University of Technology.
- Murrell, K. L. Canivan, G. J., & Camp, W. M. (2008). "High and low strain testing of bouncing piles." In The 33rd Annual and 11th International Conference on Deep Foundations, 18(20).
- Moses, G. G., & Rao., S. N. (2003). "Degradation in cemented marine clay subjected to cyclic compressive loading marine." *Georesourses and Geotechnology*, 21, 37-62.
- Nishiwaki, A., & Hattori, S. (1974). "Measurements of the Dynamic Behavior of Concrete Piles during Driving Operations using A He-Cd Laser." *Opt.Laser Technol.*, 6(6), 273-275.
- Okur, V., Altun, S., & Ansal, A. (2008). "The variation of pore water pressure related with failure in fine-grained soils under Uniform Cyclic Loadings." *American Society of Civil Engineers*, 149-156.
- Oliveira, J. R., Nunes, P. R., Silva, M. R. (2013). "Field Apparatus for Measurement of Elastic Rebound and Final Set for Driven Pile Capacity Estimation." *Geotechnical Testing Journal*, ASTM, 34(2) pp. 1-5.
- Oliveira, J. R. M. S., Nunes, P. R. R. L., Silva, M. R. L., Cabral, D. A., Ferreira, A. C. G., Carneiro, L. A. V., and Giraldo, M. T. M. R. (2011). "Field apparatus for measurement of elastic rebound and final set for driven pile capacity estimation." *Geotech Test J* 34(2).

- Osipov V.I., Gratchev I.B., Sassa K. (2005). "The mechanism of liquefaction of clayey soils (M124)". In K. Sassa, H. Fukoka, F. Wang, & G. Wang (Eds.), *Landslides* (pp. 127-131). Springer Berlin Heidelberg.
- Peck, R. B. and Bazarra, A. R. (1969). "Discussion of Settlement of Spread Footings on Sand." *Journal of Soil Mechanics and Foundations Division: Proceedings of ASCE*. Vol. 95, No. 3, pp. 905-909
- Polito, C. P. (1999). *The effects of non-plastic and plastic fines on the liquefaction of sandy soils* (Unpublished Doctoral dissertation). Virginia Polytechnic Institute and State University, 274.
- Poulos, H. G., & Davis, E. H. (1980). *Pile Foundation Analysis and Design*. New York: Wiley
- Puppala, A. J., Chomtid, S., & Wattanasanticharoen, E. (2004). "Plastic deformation potentials of sandy clay from repeated Load Triaxial Test." *Geotechnical Special Publication (0895-0563) 126(1)*, 938.
- Putri, E. E., Rao, N., & Mannan, M. A. (2012). "Threshold stress of the soil subgrade evaluation for highway formations." *World Academy of Science, Engineering and Technology*, 68.
- Rausche, F., Goble, G.G., & Likins, G.E. (1985). "Dynamic determination of pile capacity." *Journal of Geotechnical Engineering, ASCE*, 111(3), 123-134.
- Regan, J. E., & Higgins III, K. A. (2009). "Use of dynamic measurements to drive high capacity concrete piles in Washington's Potomac Formation." In *Contemporary Topics in Deep Foundations - 2009 International Foundation Congress and Equipment Expo*, ASCE, Orlando, FL, United States, p. 271-278.
- Ren-peng, C., Shi-fang, W., & Yun-min C. (2003). "Study on pile drivability with One Dimensional Wave Propagation Theory." *Journal of Zhejiang University*, 683-693

- Ren-peng, C., Ya-yuan, H., & Yun-min, C. (2000). "Determining driving resistance with rebound of pile-top during pile driving." *Journal of Zhejiang University*, 179-185
- Robertson, P. K., & Campanella, R. G. (1983). "Interpretation of cone penetration tests part I (sand) and part II (clay)." *Canadian Geotechnical Journal*, 20(4), 1-83.
- Robertson, P. K., Campanella, R. G., Gillespie, D., & Greig, J. (1986). "Use of Piezometer Cone Data." *Use of In Situ Tests in Geotechnical Engineering*, ASCE (Geotechnical Special Publ 6), Blacksburg, VA, USA, 1263-1280.
- Robertson, P. K., Campanella, R. G., & Gillespie, D. (1989). Use of Piezometer Cone Data, *Situ '86 use of in-Situ Testing in Geotechnical Engineering*, (pp. 1263-1280). Reston, VA: Specialty Publication.
- Robertson, P. K., Woeller, D. J., & Gillespie, D. (1990). "Evaluation of excess pore pressures and drainage conditions around driven piles using the Cone Penetration Test with Pore Pressure Measurements." *Canadian Geotechnical Journal*, 27(2), 249-254.
- Robertson, P. K. (1990). "Soil classification using the cone penetration test." *Canadian Geotechnical Journal*, 27(1), 151-158.
- Robertson, P. K., & Wride, C. E. (1998). "Evaluating cyclic liquefaction potential using the Cone Penetration Test." *Canadian Geotechnical Journal*, 35(3), 442-459.
- Robertson, P.K. and Wride, C.E. (1998). "Cyclic liquefaction and its evaluation based on the CPT." *Canadian Geotechnical Journal*, 35(3): 442-459
- Robertson, P. K. (2009). "Interpretation of cone penetration tests - A unified approach." *Canadian Geotechnical Journal*, 46(11), 1337-1355.
- Robertson, P. K. (2010). "Estimating in-situ soil permeability from CPT & CPTu." 2<sup>nd</sup>

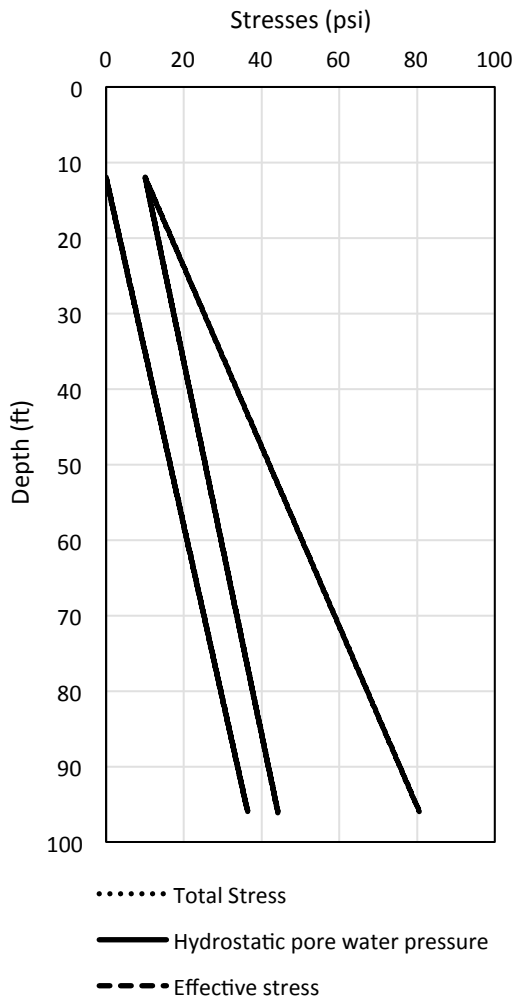
- International Symposium on Cone Penetration Testing-CPT'10*, Huntington Beach, California, 2: Equipment and Procedures, pp. 2-51.
- Robertson, P. K. (2010). "Estimating in-situ state parameter and friction angle in sandy soils from the CPT." In *2<sup>nd</sup> International Symposium on Cone Penetration Testing, CPT'10*, Huntington Beach, CA, USA.
- Robertson, P. K. (2010). "Soil behavior type from the CPT: an update." *2<sup>nd</sup> International Symposium on Cone Penetration Testing - CPT'10*, Huntington Beach, California, 2, pp. 1-8.
- Robertson, P. K. (2012). "Interpretation of in-situ tests – some insights." Mitchell Lecture ISC'4 Brazil, pp. 1-22.
- Robertson, P. K., & Cabal, K. L. (2010). "Estimating Soil Unit Weight from CPT." *2<sup>nd</sup> International Symposium on Cone Penetration Testing - CPT'10*, Huntington Beach, California, pp. 1-8.
- Robertson, P. K., & Cabal, K.L. (2015). "Guide to cone penetration testing for geotechnical Engineering-6th ed." Gregg Drilling & Testing, Inc., Signal Hill, California, pp. 138.
- Sandoval-Shannon, J.A. (1989). *Liquefaction and settlement characteristics of silt soils* (Unpublished Doctoral dissertation). University of Missouri.
- Schmertmann, J. H. (1975). "Measurement of insitu shear strength, insitu measurement of soil properties." Proceedings of Specialty Conference, ASCE, vol. 2. pp. 57-138.
- Schmertmann, J. H. (1978). "Use the SPT to measure dynamic soil properties?—Yes, But...!" Dynamic Geotechnical Testing, ASTM STP 654, American Society for Testing and Materials. (341-355).
- Schneider, J. A., Randolph, M. F., Mayne, P. W., & Ramsey, N. R. (2008). "Analysis of factors

- influencing soil classification using normalized piezocone tip resistance and pore pressure parameters.” *Journal of the Geotechnical Engineering Division. ASCE*, 134(11), pp. 1569-1586.
- Scott, T. (1990). The lithostratigraphy of the Hawthorn Group of peninsular Florida. Open File Report 36. Tallahassee: Florida Geological Survey.
- Scott, T., & MacGill, P.L. (1981). The Hawthorn Formation of Central Florida. Tallahassee: Published for the Bureau of Geology, Division of Resource Management in cooperation with United States Bureau of Mines
- Seed, H. B. (1979). “Soil liquefaction and cyclic mobility evaluation for level ground during earthquake.” *Journal of the Geotechnical Engineering Division. ASCE*, 105(2), pp. 201-255.
- Seed, H. B., Idriss, I. M., and Arango, I. (1983). “Evaluation of liquefaction potential using field performance data.” *Journal of the Geotechnical Engineering Division. ASCE*, 109(3), pp. 458-482.
- Seed, H.B., Tokimatsu, K., Harder, L. F., Chung, R. (1985). “Influence of SPT Procedures in Soil Liquefaction Resistance Evaluations.” *J. Geotech. Engrg. ASCE*, 111(12), pp. 1425-1445.
- Seed, H.B., Martin, P.P. and Lysmer, J. (1975b), “The generation and dissipation of pore water pressures during soil liquefaction,” UCB/EERC, Report No. 75-26, EERC and Department of Civil Engineering, Berkeley, California.
- Shahin, M. A., Loh, R. B., & Nikraz, H. R. (2011). “Some observations on the behavior of soft clay under undrained cyclic loading.” *Journal of Geo Engineering*, 6(2), 109-112.

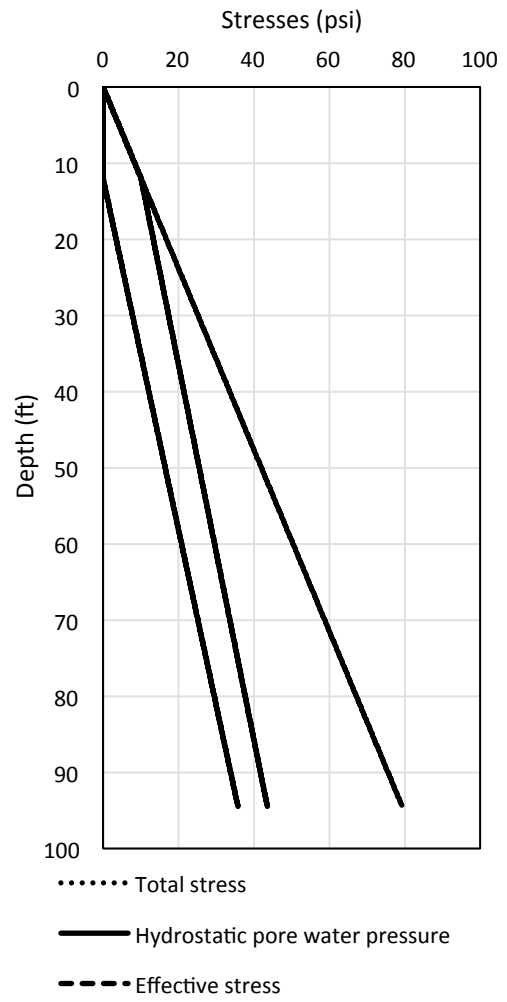
- Skempton, A. W. (1986). "Standard penetration test procedures and the effects of overburden pressure, relative density, particle size, aging and overconsolidation." *Geotechnique*, 36(3), 425-447.
- Smith, E.A.L. (1960). "Pile driving analysis by the wave equation." American Society of Civil Engineers, ASCE, *Journal of Soil Mechanics and Foundation Engineering*, SM4, 86 (1960): p. 35-61.
- Stevens, F. R. (2012). "The effect of grain shape on pile capacity in sand." In *Offshore Technology Conference*, Houston, Texas, 30 April-3 May 2012.
- Tokimatsu, K. and Yoshimi, Y. (1983) "Empirical correlation of soil liquefaction based on SPT N-value and fines content." *Soils and Foundations, Japanese Society of Soil Mechanics and Foundation Engineering*, Vol. 23, No. 4, pp. 56-74
- Torstenssen, B. A. (1977). "The pore pressure probe." Nordisk Mote, Bergmekanikk, Oslo, Norway.
- Wilson, N. E., & Greenwood J. R. (1974). "Pore pressures and strains after repeated loading of saturated clay." *Canadian Geotechnical Journal*, 11(2), 269.
- Wisnom, F. B. (2105). *Reevaluating properties of pile rebound soils based on Standard Penetration Testing* (Unpublished Master's Thesis). Florida Institute of Technology, Melbourne, FL.
- Wren, J. (2007). "The Great Chicago Flood. Analysis of Chicago's Second Great Disaster'." *Structure Magazine*, 38.
- Wroth, C. P. (1984). "Interpretation of In Situ Soil Tests." *Geotechnique*, 34(4), 449-489.
- Yi, F. (2014). "Estimating soil fines contents from CPT Data. Proceedings from CPT '14": *3rd International Symposium on Cone Penetration Testing*, Las Vegas, Nevada, pp. 3-22.

Ziaie-Moayed, R. (2006). "Evaluation of the fine contents of silty sands using CPTU results." In *The Geological Society of London, IAEG 2006* (pp.1-5).

## **Appendix A CPTu Effective Stress Profiles**

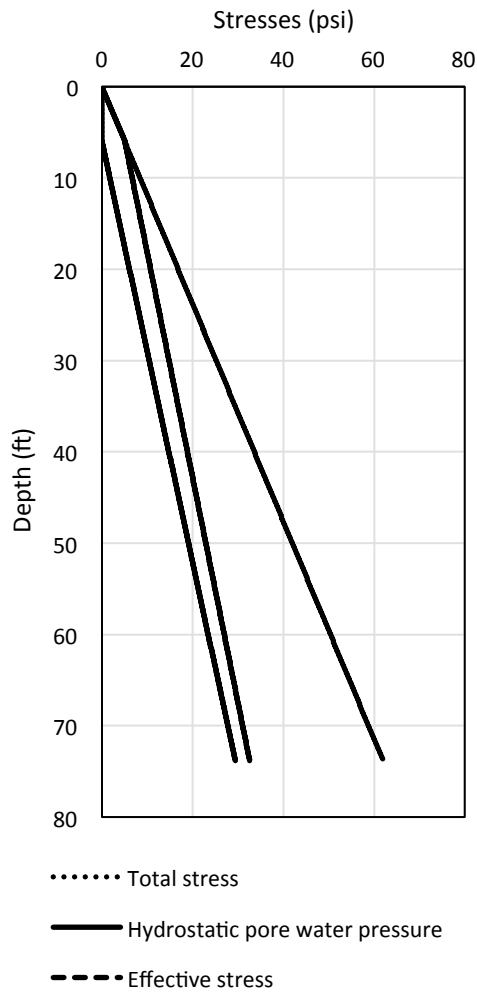


(a)

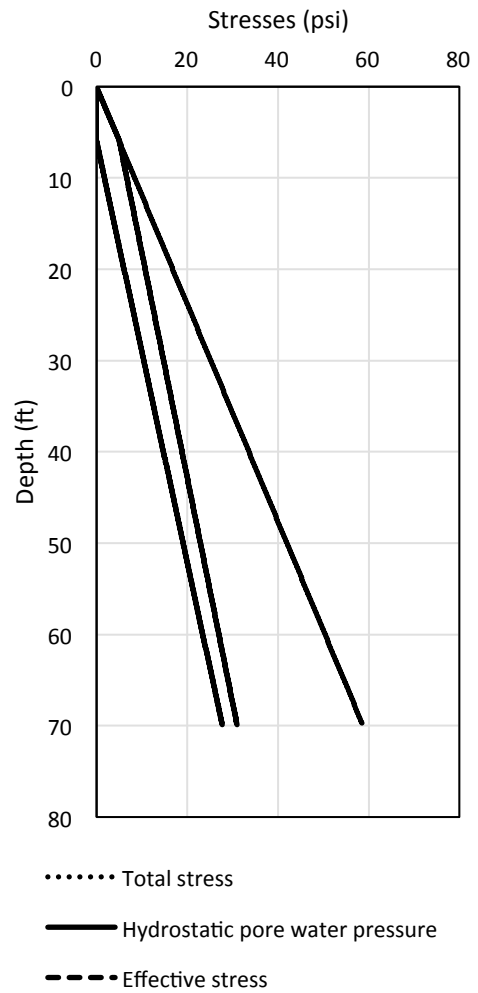


(b)

Figure A-1 Total stress, hydrostatic pore water pressure, and effective stress versus depth for I-4 / US 192 at (a) pier 6 / pile 16 and (b) pier 7 / pile 10



(a)



(b)

Figure A-2 Total stress, hydrostatic pore water pressure, and effective stress versus depth for SR 417 International Parkway at (a) B1 / pile 14 and (b) B2 / pile 5

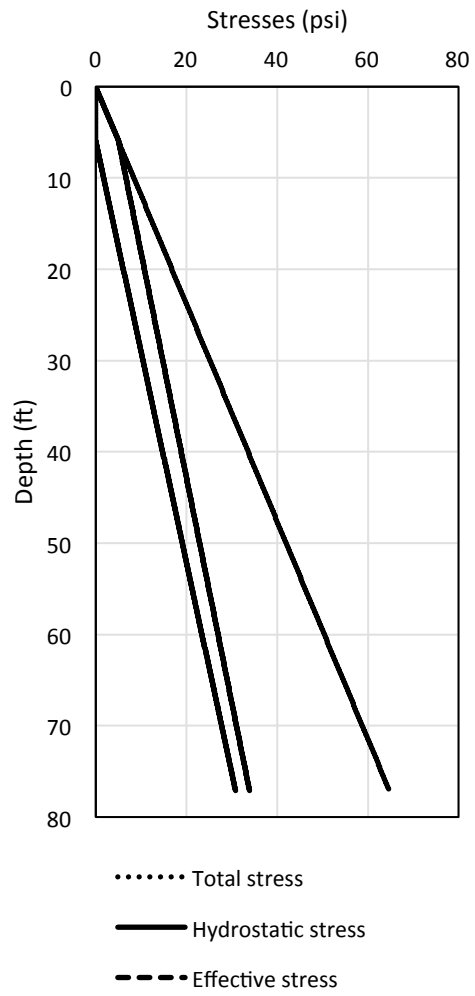


Figure A-3 Total stress, hydrostatic pore water pressure, and effective stress versus depth for SR 50 / SR 436 at west bound / pile 5

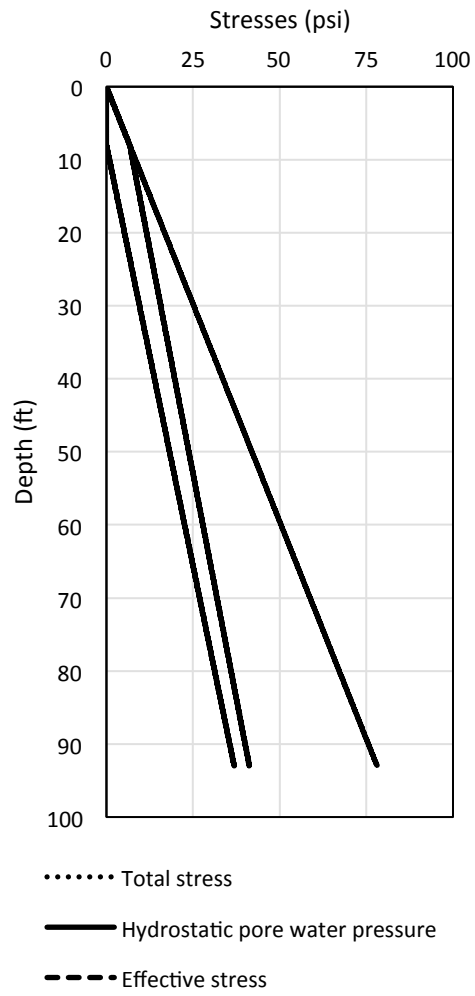


Figure A-4 Total stress, hydrostatic pore water pressure, and effective stress versus depth for I-4 / SR 408 at pier 2 / pile 5

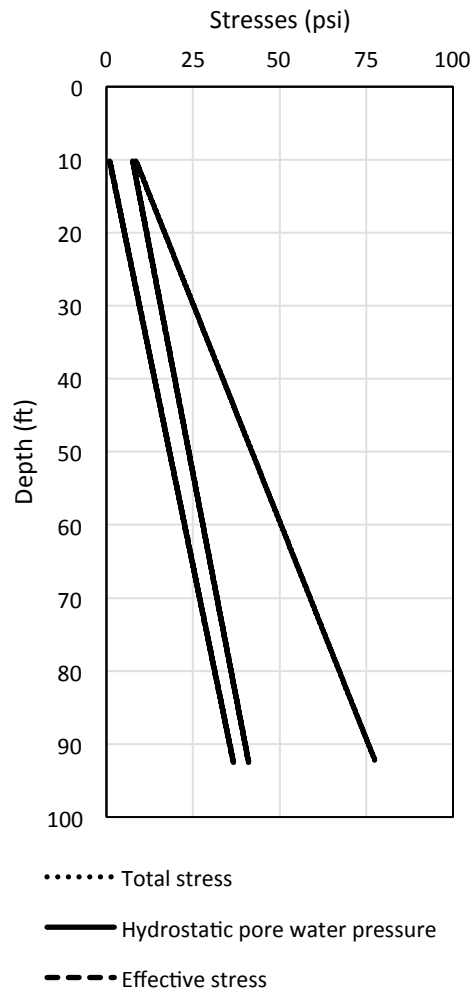


Figure A-5 Total stress, hydrostatic pore water pressure, and effective stress versus depth for Anderson Street at pier 6 / pile 5, 6

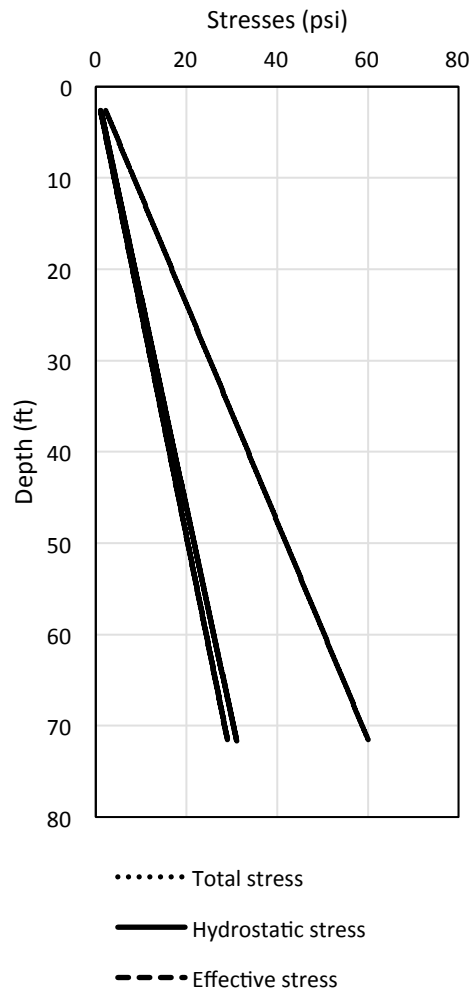


Figure A-6 Total stress, hydrostatic pore water pressure, and effective stress versus depth for I-4 Widening Daytona at EB3 / pile 5

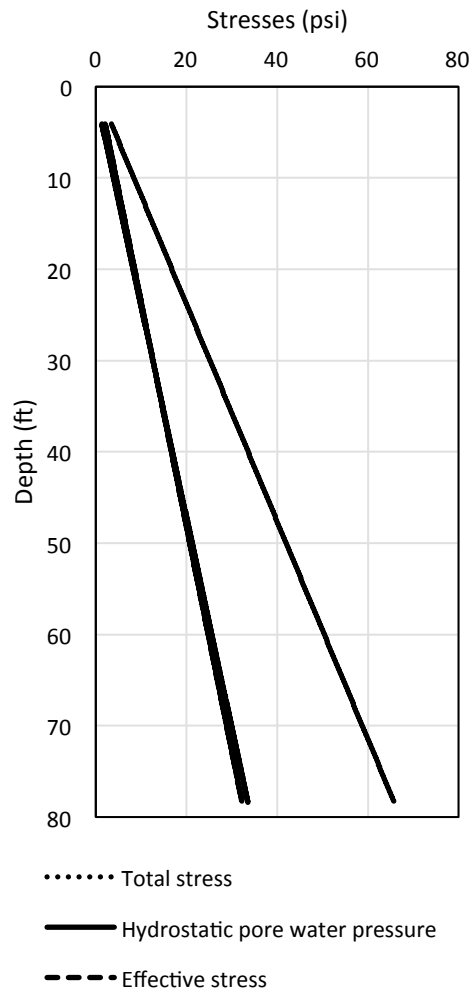


Figure A-7 Total stress, hydrostatic pore water pressure, and effective stress versus depth for SR 83/Ramsey Branch Bridge at EB 5 / pile 2

## **Appendix B SPT Correlations**

## B.1. Test Pile PDA Data Correlated to SPT Samples

### B.1.1. A.1. I-4 / US-192 Interchange

#### B.1.1.1. Test Pile EB1P3 (Ramp BD)

Elevation	Depth	SPT B-27	FMX	bl/ft	DMX	DFN	iSET	Rebound	SFT	EBR	CSX	TSX	FVP	Jc
feet	feet	N <sub>safe</sub>	kips		inches	inches	inches	inches	kips	kips	ksi	ksi		
70.15	19.36	54	681	12	1.05	0.85	1.00	0.05	0	184	1.2	0.7	0.99	0.8
67.56	21.94	39	1012	17	0.72	0.34	0.71	0.00	2	352	1.8	0.9	1	0.8
65.11	24.39	39	1066	41	0.62	0.22	0.29	0.33	0	426	1.8	0.8	1	0.8
62.63	26.87	60	999	52	0.57	0.20	0.23	0.33	0	395	1.7	0.6	1	0.8
60.12	29.38	39	1005	44	0.62	0.27	0.27	0.35	0	389	1.7	0.7	1	0.8
57.64	31.86	13	936	37	0.60	0.25	0.33	0.28	0	336	1.6	0.6	1	0.8
55.13	34.37	3	899	35	0.56	0.42	0.34	0.22	198	161	1.6	0.6	1	0.8
52.62	36.88	WH	909	24	0.58	0.50	0.50	0.08	261	96	1.6	0.6	1	0.8
50.11	39.39	3	956	29	0.51	0.39	0.41	0.10	350	94	1.7	0.5	1	0.8
47.63	41.87	WH	1000	25	0.51	0.39	0.49	0.02	402	71	1.7	0.6	1	0.8
45.13	44.37	7	1043	38	0.46	0.35	0.32	0.14	440	78	1.8	0.7	1	0.8
42.63	46.87	12	1127	39	0.45	0.33	0.31	0.14	437	112	1.9	0.9	1	0.8
40.12	49.38	11	1169	38	0.47	0.42	0.32	0.15	365	156	2.0	0.9	1	0.8
37.62	51.88	10	1165	40	0.45	0.38	0.30	0.15	306	171	2.0	1.0	1	0.8
35.11	54.39	7	1202	36	0.61	0.61	0.34	0.27	278	179	2.1	1.1	1	0.8
32.63	56.87	9	1222	38	0.47	0.37	0.32	0.15	315	223	2.1	0.7	1	0.8
30.12	59.38	10	1235	37	0.55	0.47	0.32	0.23	260	222	2.1	0.9	1	0.8
27.60	61.90	17	1078	56	0.79	0.32	0.22	0.57	41	297	1.9	1.0	1	0.8
25.11	64.39	17	991	76	1.08	0.24	0.16	0.92	5	268	1.7	1.0	1	0.8
22.53	66.97	20	1007	313	0.95	0.11	0.04	0.91	9	243	1.7	1.1	1	0.8
20.13	69.37	25	1080	128	0.75	0.22	0.09	0.66	78	292	1.9	1.0	1	0.8
17.64	71.86	16	1195	74	0.79	0.29	0.16	0.63	111	310	2.1	1.1	1	0.8
15.17	74.33	25	1105	219	0.68	0.12	0.05	0.62	67	262	1.9	1.1	1	0.8
12.65	76.85	25	1375	56	0.68	0.25	0.21	0.46	199	436	2.4	0.8	1	0.8
10.12	79.38	14	1288	49	0.66	0.10	0.24	0.42	183	399	2.2	0.7	1	0.8
7.62	81.88	16	1263	45	0.65	0.16	0.27	0.39	200	378	2.2	0.6	1	0.8
5.12	84.38	18	1278	44	0.66	0.22	0.27	0.39	212	374	2.2	0.7	1	0.8
2.59	86.91	14	1346	55	0.64	0.15	0.22	0.42	220	383	2.3	0.7	1	0.8
0.11	89.39	43	1458	103	0.46	0.17	0.12	0.34	335	608	2.5	0.5	1	0.8

### B.1.1.2. Test Pile P7P10 (Ramp CA)

Elevation	Depth	SPT B-40	FMX	bl/ft	DMX	DFN	iSET	Rebound	SFT	EBR	CSX	TSX	FVP	Jc
feet	feet	N <sub>safe</sub>	kips		inches	inches	inches	inches	kips	kips	ksi	ksi		
63.60	25.60	50/3	1331	73	0.60	0.25	0.16	0.44	77	819	2.31	0.50	1	0
61.10	28.10	31	1430	55	0.63	0.27	0.22	0.42	89	766	2.48	0.75	1	0
58.60	30.60	67	1565	40	0.65	0.35	0.30	0.35	102	760	2.71	1.11	1	0
56.10	33.10	20	1511	36	0.60	0.19	0.33	0.27	259	563	2.62	1.16	1	0
53.59	35.61	10	1388	37	0.56	0.51	0.33	0.23	517	295	2.41	1.09	1	0
51.10	38.10	3	1405	41	0.46	0.36	0.29	0.17	646	205	2.44	1.10	1	0
48.62	40.58	1	1368	53	0.40	0.34	0.23	0.17	776	119	2.37	0.95	1	0
46.10	43.10	2	1385	50	0.39	0.31	0.24	0.15	808	96	2.41	0.99	1	0
43.59	45.61	0	1330	57	0.36	0.27	0.21	0.15	808	60	2.31	0.96	1	0
41.10	48.10	9	1434	52	0.40	0.31	0.23	0.17	845	174	2.49	1.04	1	0
38.60	50.60	10	1571	42	0.48	0.37	0.28	0.20	802	310	2.73	1.16	1	0
36.10	53.10	9	1291	50	0.40	0.29	0.24	0.16	750	186	2.24	0.87	1	0
33.61	55.59	8	1060	64	0.40	0.30	0.19	0.21	778	2	1.84	0.50	1	0
31.10	58.10	10	1049	47	0.45	0.33	0.26	0.20	659	40	1.82	0.61	1	0
28.60	60.60	10	1103	47	0.51	0.32	0.26	0.25	631	73	1.91	0.68	1	0
26.10	63.10	23	1164	50	0.56	0.35	0.24	0.32	500	200	2.02	0.81	1	0
23.60	65.61	14	1190	50	0.61	0.34	0.24	0.37	267	398	2.08	1.03	1	0
21.10	68.10	17	1232	50	0.65	0.37	0.24	0.41	165	517	2.14	1.18	1	0
16.10	73.10	25	1008	135	0.49	0.19	0.09	0.40	261	369	1.75	0.64	1	0
13.56	75.64	28	1172	128	0.63	0.26	0.09	0.53	232	389	2.03	0.81	1	0
11.10	78.10	24	1234	120	0.74	0.25	0.10	0.64	130	474	2.14	1.21	1	0
8.60	80.60	28	1194	109	0.61	0.21	0.11	0.50	245	416	2.07	0.95	1	0
6.10	83.10	21	1305	71	0.65	0.36	0.17	0.49	253	489	2.27	1.15	1	0
3.57	85.63	14	1335	65	0.61	0.31	0.18	0.43	241	555	2.32	1.21	1	0
1.10	88.10	21	1352	71	0.58	0.29	0.17	0.41	254	613	2.35	1.21	1	0
-1.40	90.60	20	1371	86	0.57	0.28	0.14	0.43	260	645	2.38	1.19	1	0
-3.90	93.10	15	1326	81	0.56	0.29	0.15	0.41	272	580	2.30	1.08	1	0
-6.25	95.45	11	1372	171	0.46	0.31	0.07	0.39	352	682	2.39	0.72	1	0

### B.1.1.3. Test Pile P8P4 (Ramp CA)

Elevation	Depth	SPT B-41	FMX	bl/ft	DMX	DFN	iSET	Rebound	SFT	EBR	CSX	TSX	FVP	Jc
feet	feet	N <sub>safe</sub>	kips		inches	inches	inches	inches	kips	kips	ksi	ksi		
70.02	20.82	51	966	17	0.72	0.26	0.69	0.03	0	271	1.7	1.0	1	0.5
67.71	23.13	13	1119	24	0.78	0.41	0.50	0.27	0	347	2.0	1.1	1	0.5
65.19	25.65	12	1134	31	0.68	0.37	0.39	0.30	1	376	2.0	0.9	1	0.5
62.70	28.14	9	1109	40	0.59	0.27	0.30	0.29	3	407	1.9	0.8	1	0.5
60.21	30.63	13	1080	48	0.58	0.25	0.25	0.33	2	430	1.9	0.6	1	0.5
57.70	33.14	23	1078	45	0.57	0.22	0.27	0.31	24	433	1.9	0.6	1	0.5
55.22	35.62	6	1075	43	0.56	0.31	0.28	0.27	139	345	1.9	0.6	1	0.5
52.70	38.14	4	1077	32	0.54	0.42	0.38	0.17	342	138	1.9	0.7	1	0.5
50.20	40.64	2	1104	30	0.55	0.42	0.40	0.16	381	91	1.9	0.8	1	0.5
47.71	43.13	2	1158	30	0.53	0.40	0.40	0.13	462	78	2.0	0.9	1	0.5
45.19	45.65	2	1192	31	0.53	0.39	0.38	0.15	422	99	2.1	1.0	1	0.5
42.71	48.13	1	1237	36	0.51	0.35	0.33	0.18	517	65	2.1	1.0	1	0.5
40.21	50.63	0	1308	39	0.51	0.35	0.31	0.21	522	103	2.3	1.1	1	0.5
37.71	53.13	10	1333	37	0.53	0.34	0.33	0.20	418	158	2.3	1.1	1	0.5
35.20	55.64	7	1376	35	0.55	0.37	0.34	0.20	398	167	2.4	1.2	1	0.5
32.71	58.13	8	1388	37	0.54	0.39	0.33	0.21	398	184	2.4	1.1	1	0.5
30.20	60.64	12	1427	38	0.58	0.36	0.32	0.27	349	235	2.5	1.1	1	0.5
25.19	65.65	16	1211	48	0.89	0.31	0.25	0.64	42	351	2.1	1.1	1	0.5
22.72	68.12	17	1096	49	0.91	0.21	0.24	0.66	38	321	1.9	1.1	1	0.5
20.21	70.63	17	1152	97	0.95	0.17	0.12	0.83	53	339	2.0	1.1	1	0.5
17.69	73.15	20	1306	99	1.02	0.17	0.12	0.90	61	394	2.3	1.2	1	0.5
15.22	75.62	22	1220	155	0.65	0.19	0.08	0.57	103	333	2.1	1.1	1	0.5
12.71	78.13	26	1163	73	0.67	0.09	0.16	0.58	141	315	2.0	0.9	1	0.5
10.14	80.70	24	1326	90	0.89	0.23	0.13	0.75	155	329	2.3	1.3	1	0.5
7.76	83.08	22	1223	92	0.57	0.26	0.13	0.44	279	274	2.1	0.8	1	0.5
5.20	85.64	18	1240	80	0.58	0.27	0.15	0.43	286	272	2.2	0.8	1	0.5
2.71	88.13	14	1263	54	0.63	0.33	0.22	0.41	327	249	2.2	0.9	1	0.5
0.20	90.64	19	1320	61	0.64	0.30	0.20	0.44	345	279	2.3	0.8	1	0.5
-1.84	92.68	19	1391	86	0.51	0.21	0.14	0.37	349	561	2.4	0.4	1	0.5

### B.1.1.4. Test Pile P2P8 (Ramp D2)

Elevation	Depth	SPT B-41	FMX	bl/ft	DMX	DFN	iSET	Rebound	SFT	EBR	CSX	TSX	FVP	Jc
feet	feet	N <sub>safe</sub>	kips		inches	inches	inches	inches	kips	kips	ksi	ksi		
43.81	47.99	31	311	43	0.18	0.00	0.28	-0.10	192	42	0.5	0.1	1.20	0.8
41.80	50.00	51	1199	39	0.57	0.10	0.31	0.27	159	300	2.1	0.7	1.10	0.8
39.29	52.51	3	1167	41	0.52	0.40	0.29	0.23	329	217	2.0	0.7	1.10	0.8
36.78	55.02	18	1250	47	0.51	0.39	0.26	0.26	427	229	2.2	0.6	1.10	0.8
34.30	57.50	18	1198	44	0.58	0.50	0.27	0.31	423	192	2.1	0.5	1.10	0.8
31.81	59.99	6	1164	39	0.56	0.52	0.31	0.25	463	132	2.0	0.6	1.10	0.8
29.30	62.50	14	1156	36	0.64	0.62	0.33	0.31	341	206	2.0	0.6	1.10	0.8
26.82	64.98	9	1150	28	0.65	0.59	0.43	0.22	196	288	2.0	0.6	1.10	0.8
24.31	67.49	13	1154	25	0.79	0.57	0.48	0.31	73	343	2.0	0.7	1.10	0.8
21.75	70.05	13	1043	35	0.76	0.26	0.34	0.42	68	351	1.8	0.7	1.10	0.8
19.30	72.50	11	1141	38	0.65	0.27	0.32	0.33	120	352	2.0	0.7	1.10	0.8
16.77	75.03	16	1092	72	0.76	0.26	0.17	0.59	99	334	1.9	0.8	1.10	0.8
14.30	77.50	24	1118	76	0.87	0.16	0.16	0.71	107	283	1.9	1.0	1.10	0.8
11.76	80.04	50	1206	130	0.97	0.08	0.09	0.88	114	214	2.1	1.1	1.10	0.8
9.30	82.50	21	1006	150	0.82	0.13	0.08	0.74	65	282	1.7	0.9	1	0.8
6.85	84.95	19	1054	108	0.99	0.16	0.11	0.88	68	268	1.8	0.9	1	0.8
4.31	87.49	13	1045	100	0.99	0.18	0.12	0.86	68	272	1.8	0.9	1	0.8
1.83	89.97	12	1206	78	0.81	0.28	0.15	0.65	61	346	2.1	1.1	1	0.8

## B.1.2. SR-417 and International Parkway

### B.1.2.1. Test Pile EB1P14

Elevation feet	Depth feet	SPT B-1 N <sub>safe</sub>	FMX kips	bl/ft	DMX inches	DFN inches	iSET inches	Rebound inches	SFT kips	EBR kips	CSX ksi	TSX ksi	FVP	Jc
66.50	5.77	39	579	3	4.00	4.00	4.00	0.00	0	0	1.00	0.75	1	0.4
64.77	7.505	23	786	8	1.92	1.60	1.60	0.32	18	48	1.20	0.90	1	0.4
62.78	9.495	11	1040	11	1.42	1.09	1.09	0.33	27	147	1.30	0.85	1	0.4
59.80	12.47	7	769	16	0.87	0.73	0.73	0.14	24	170	1.40	0.95	1	0.4
57.30	14.975	13	936	29	0.66	0.41	0.41	0.26	22	261	1.50	1.00	1	0.4
54.81	17.465	17	1076	31	0.71	0.38	0.39	0.33	32	289	1.75	1.20	1	0.4
52.30	19.97	30	1212	38	0.70	0.32	0.32	0.38	41	370	1.80	1.20	1	0.4
49.80	22.475	13	1270	27	0.77	0.44	0.44	0.32	29	322	1.80	1.20	1	0.4
47.30	24.97	13	1153	21	0.83	0.56	0.57	0.26	31	248	1.85	1.30	1	0.4
44.80	27.475	33	1089	41	0.55	0.30	0.30	0.25	62	335	1.85	1.30	1	0.4
42.30	29.975	14	1259	46	0.58	0.26	0.26	0.32	92	407	1.85	1.30	1	0.4
39.80	32.47	8	1405	52	0.59	0.23	0.23	0.35	138	477	1.10	0.60	1	0.4
37.31	34.965	26	1476	43	0.61	0.28	0.28	0.33	181	443	1.45	0.90	1	0.4
34.80	37.475	13	1461	31	0.61	0.38	0.38	0.23	241	332	1.25	0.70	1	0.4
32.31	39.96	10	1463	31	0.58	0.38	0.38	0.20	495	152	0.85	0.40	1	0.4
29.80	42.475	7	1331	39	0.45	0.31	0.31	0.14	701	66	0.50	0.20	1	0.4
27.31	44.96	0	1358	40	0.45	0.30	0.30	0.14	785	31	1.95	1.20	1	0.4
24.80	47.47	3	1396	41	0.44	0.29	0.29	0.15	830	39	1.70	1.05	1	0.4
22.30	49.97	4	1500	48	0.46	0.24	0.25	0.21	782	152	1.45	0.85	1	0.4
19.80	52.47	4	1494	42	0.51	0.29	0.29	0.23	567	184	1.60	0.90	1	0.4
17.31	54.96	25	1451	39	0.49	0.30	0.31	0.18	550	154	1.50	0.80	1	0.4
14.81	57.46	13	1389	40	0.46	0.30	0.30	0.16	527	117	1.60	0.90	1	0.4
12.30	59.97	4	1341	44	0.43	0.27	0.27	0.16	519	114	1.50	0.80	1	0.4
9.81	62.465	7	1333	41	0.42	0.29	0.29	0.13	510	107	1.55	0.85	1	0.4
7.30	64.975	4	1324	42	0.41	0.28	0.29	0.13	513	99	1.55	0.85	1	0.4
4.80	67.47	3	1336	53	0.38	0.23	0.23	0.15	550	114	1.70	0.95	1	0.4
2.30	69.97	34	1542	72	0.38	0.17	0.17	0.22	560	461	1.55	0.85	1	0.4

### B.1.2.2. Test Pile EB2P5

Elevation	Depth	SPT B-2	FMX	bl/ft	DMX	DFN	iSET	Rebound	SFT	EBR	CSX	TSX	FVP	Jc
feet	feet	N <sub>safe</sub>	kips		inches	inches	inches	inches	kips	kips	ksi	ksi		
49.82	22.48	20	1130	12	1.34	1.23	1.00	0.34	0	187	2.0	1.3	0.99	0.4
47.31	24.99	13	668	16	0.81	0.31	0.77	0.04	0	155	1.2	0.7	0.90	0.4
44.79	27.51	24	832	19	0.86	0.33	0.63	0.23	0	183	1.4	0.9	0.90	0.4
42.29	30.01	32	928	31	0.65	0.49	0.38	0.27	0	302	1.6	0.9	0.94	0.4
39.80	32.50	19	983	42	0.64	0.53	0.29	0.35	1	374	1.7	0.9	0.98	0.4
37.32	34.98	24	1139	22	0.88	0.70	0.55	0.33	0	271	2.0	1.2	0.94	0.4
34.80	37.50	3	923	19	0.76	0.66	0.62	0.15	16	224	1.6	1.0	0.99	0.4
32.29	40.01	3	1016	19	0.78	0.70	0.65	0.14	87	183	1.8	1.2	1	0.4
29.81	42.49	3	948	24	0.60	0.58	0.50	0.10	180	134	1.6	1.0	1	0.4
27.29	45.02	2	926	26	0.55	0.52	0.47	0.09	227	98	1.6	1.0	1	0.4
24.79	47.51	18	1021	32	0.53	0.39	0.38	0.15	222	161	1.8	0.9	1	0.4
22.30	50.00	8	1019	36	0.57	0.37	0.33	0.23	93	216	1.8	0.9	1	0.4
19.80	52.50	3	961	32	0.51	0.33	0.37	0.14	157	173	1.7	0.9	1	0.4
17.31	54.99	5	987	35	0.48	0.38	0.34	0.14	314	95	1.7	1.0	1	0.4
14.80	57.50	4	1047	38	0.50	0.40	0.32	0.18	338	103	1.8	1.0	1	0.4
12.30	60.00	8	1081	37	0.52	0.38	0.32	0.20	343	122	1.9	1.0	1	0.4
9.80	62.50	10	1079	39	0.50	0.31	0.30	0.19	408	93	1.9	1.0	1	0.4
7.30	65.00	24	1227	55	0.52	0.29	0.22	0.30	325	305	2.1	0.8	1	0.4
4.80	67.50	19	1400	55	0.68	0.30	0.22	0.46	109	542	2.4	1.2	0.93	0.4
2.30	70.00	50/5	1250	86	0.57	0.20	0.14	0.43	125	479	2.2	1.1	1	0.4
0.19	72.11	50/4	1443	86	0.40	0.07	0.14	0.26	213	1725	2.5	0.8	1	0.4

### B.1.3. SR-50 and SR-436

#### B.1.3.1. Test Pile EB4P10

Elevation	Depth	SPT TH-4B	FMX	bl/ft	DMX	DFN	iSET	Rebound	SFT	EBR	CSX	TSX	FVP	Jc
feet	feet	N <sub>safe</sub>	kips		inches	inches	inches	inches	kips	kips	ksi	ksi		
71.94	26.86	15	771	3	3.21	3.17	4.00	-0.79	0	0	1.2	0.5	0.97	0.3
69.41	29.39	49	775	5	1.75	1.40	2.40	-0.65	0	86	1.3	0.9	0.98	0.3
67.00	31.80	31	614	9	1.00	0.46	1.32	-0.32	0	120	1.0	0.7	1	0.3
64.52	34.27	26	634	9	1.11	0.51	1.35	-0.24	0	126	1.1	0.7	1	0.3
62.02	36.77	20	460	6	1.18	0.54	2.00	-0.82	0	54	0.7	0.5	0.92	0.3
59.44	39.36	27	535	10	0.98	0.34	1.24	-0.26	0	128	1.1	0.7	0.97	0.3
56.97	41.82	12	738	11	1.00	0.55	1.07	-0.07	0	202	1.3	0.8	1	0.3
54.50	44.30	28	757	15	0.79	0.42	0.78	0.02	1	179	1.3	0.8	1	0.3
52.02	46.78	26	813	17	0.82	0.41	0.72	0.10	1	222	1.4	0.9	1	0.3
49.51	49.29	14	842	16	0.82	0.44	0.75	0.07	1	230	1.5	0.9	1	0.3
46.99	51.81	15	778	21	0.71	0.31	0.58	0.13	2	231	1.3	0.8	1	0.3
44.47	54.32	15	802	24	0.63	0.33	0.51	0.13	12	221	1.4	0.9	1	0.3
42.00	56.80	9	986	23	0.68	0.43	0.52	0.15	76	244	1.7	1.0	1	0.3
39.48	59.32	6	928	21	0.64	0.46	0.58	0.06	165	136	1.6	1.0	1	0.3
37.01	61.79	8	1004	25	0.61	0.38	0.48	0.13	217	159	1.8	1.1	1	0.3
34.45	64.34	3	920	34	0.53	0.25	0.35	0.18	234	171	1.6	0.9	1	0.3
31.99	66.80	4	1016	40	0.52	0.19	0.30	0.22	273	221	1.8	0.9	1	0.3
29.50	69.30	7	1049	33	0.60	0.24	0.37	0.23	223	196	1.8	1.1	1	0.3
26.99	71.81	3	1106	35	0.62	0.25	0.34	0.27	143	308	1.9	1.1	1	0.3
24.53	74.26	6	1183	38	0.60	0.23	0.31	0.29	165	314	2.1	1.1	1	0.3
21.97	76.82	7	1218	39	0.55	0.23	0.31	0.24	250	301	2.1	1.1	1	0.3

### B.1.3.2. Test Pile P3P10 (EB)

Elevation	Depth	SPT TH-3B	FMX	bl/ft	DMX	DFN	iSET	Rebound	SFT	EBR	CSX	TSX	FVP	Jc
feet	feet	N <sub>safe</sub>	kips		inches	inches	inches	inches	kips	kips	ksi	ksi		
60.62	32.74	9	731	4	3.00	3.00	3.00	0.00	0	0	1.3	0.8	0.90	0.5
58.53	34.83	7	593	3	3.47	3.47	3.47	0.00	0	0	1.0	0.6	0.90	0.5
55.92	37.43	14	649	7	1.68	1.66	1.66	0.02	1	110	1.1	0.6	0.91	0.5
53.47	39.88	13	700	14	0.97	0.88	0.88	0.09	0	194	1.2	0.6	0.99	0.5
51.02	42.33	26	803	14	0.98	0.83	0.83	0.14	0	209	1.4	0.8	1	0.5
48.52	44.84	23	802	13	0.99	0.89	0.89	0.09	0	202	1.4	0.8	1	0.5
45.98	47.38	22	904	22	0.78	0.55	0.55	0.23	13	247	1.6	0.8	1	0.5
43.49	49.87	55	986	24	0.77	0.49	0.49	0.27	16	257	1.7	0.8	1	0.5
40.96	52.40	8	1058	27	0.65	0.44	0.44	0.21	88	276	1.8	0.8	1	0.5
38.49	54.86	7	1123	35	0.58	0.34	0.34	0.24	279	218	1.9	0.8	1.02	0.5
35.98	57.38	8	1160	33	0.57	0.36	0.36	0.20	453	113	2.0	0.9	1.07	0.5
33.50	59.86	12	1200	49	0.50	0.24	0.24	0.25	566	152	2.1	0.7	1.05	0.5
31.01	62.35	5	1265	40	0.59	0.30	0.30	0.29	449	194	2.2	0.9	1	0.5
28.50	64.85	6	1287	26	0.68	0.47	0.47	0.22	419	136	2.2	1.1	1	0.5
25.97	67.38	51	1405	38	0.58	0.31	0.31	0.27	542	225	2.4	0.9	1	0.5
23.49	69.86	71	1461	39	0.66	0.31	0.31	0.35	244	359	2.5	1.1	1	0.5
20.92	72.43	60	1368	44	0.57	0.27	0.28	0.30	214	407	2.4	1.0	1	0.5

### B.1.4. Heritage Parkway

#### B.1.4.1. Test Pile EB1P1

Elevation	Depth	SPT TH-5	FMX	bl/ft	DMX	DFN	iSET	Rebound	SFT	EBR	CSX	TSX	FVP	Jc
feet	feet	N <sub>safe</sub>	kips		inches	inches	inches	inches	kips	kips	ksi	ksi		
0.55	21.45	6	569	15	1.25	0.80	0.80	0.45	0	155	1.8	0.8	1	0.53
-4.88	26.88	WH	468	1	12.00	12.00	12.00	0.00	0	0	1.4	0.9	1	0.53
-9.63	31.63	5	549	2	6.00	6.00	6.00	0.00	0	0	1.7	1.1	1	0.53
-14.88	36.88	5	389	1	12.01	12.01	12.00	0.01	0	-1	1.2	0.7	0.90	0.53
-19.46	41.46	15	409	6	2.42	2.00	2.00	0.42	0	0	1.3	0.6	0.90	0.53
-24.53	46.53	20	664	20	0.97	0.59	0.59	0.38	8	256	2.1	0.8	1	0.53
-29.48	51.48	20	834	34	0.94	0.35	0.35	0.58	36	395	2.6	0.7	1	0.53
-34.55	56.55	2	794	9	1.61	1.33	1.33	0.28	45	151	2.4	1.4	1	0.53
-39.50	61.50	2	617	13	1.08	0.93	0.93	0.15	75	116	1.9	1.0	1	0.53
-44.51	66.51	5	655	12	1.17	1.00	1.00	0.17	40	136	2.0	1.0	1	0.53
-49.50	71.50	9	666	13	1.15	0.93	0.93	0.23	36	141	2.1	1.1	1	0.53
-54.49	76.49	11	686	14	1.19	0.85	0.85	0.34	16	169	2.1	1.1	1	0.53
-59.53	81.53	20	887	20	0.89	0.60	0.60	0.29	93	244	2.7	1.1	1	0.53
-64.52	86.52	16	793	18	0.96	0.66	0.67	0.29	57	166	2.5	1.2	1	0.53
-69.50	91.50	14	897	29	0.70	0.41	0.41	0.29	156	226	2.8	0.9	1.10	0.53
-74.48	96.48	10	926	26	0.69	0.46	0.46	0.23	219	173	2.9	1.0	1	0.53
-79.57	101.57	5	990	42	0.57	0.32	0.28	0.29	425	243	3.1	0.7	1	0.53
-84.50	106.50	17	963	38	0.52	0.45	0.31	0.21	306	165	3.0	0.8	1	0.53
-89.44	111.44	31	1003	60	0.48	0.33	0.20	0.28	269	317	3.1	0.3	1	0.53

### B.1.4.2. Test Pile B3P1

Elevation	Depth	SPT FDOT	FMX	bl/ft	DMX	DFN	iSET	Rebound	SFT	EBR	CSX	TSX	FVP	Jc
feet	feet	N <sub>safe</sub>	kips		inches	inches	inches	inches	kips	kips	ksi	ksi		
-9.25	18.25	6	281	1	12.01	12.01	12.00	0.01	0	-1	0.9	0.3	1	0.54
-13.75	22.75	4	429	1	12.01	12.01	12.00	0.00	0	-1	1.3	0.8	0.90	0.54
-18.89	27.89	27	493	7	1.98	1.62	1.62	0.36	0	70	1.5	0.8	0.94	0.54
-23.85	32.85	25	597	36	0.74	0.34	0.34	0.40	6	331	1.8	0.5	1	0.54
-28.85	37.85	6	750	50	0.79	0.24	0.24	0.55	18	413	2.3	0.5	1	0.54
-33.88	42.88	9	689	12	1.16	0.99	0.99	0.17	20	174	2.1	1.1	1	0.54
-38.84	47.84	1	673	17	0.92	0.70	0.71	0.21	50	168	2.1	1.0	1	0.54
-43.83	52.83	7	670	12	1.13	1.00	1.00	0.13	19	144	2.1	1.1	1	0.54
-47.86	56.86	10	688	14	1.05	0.86	0.86	0.19	25	154	2.1	1.1	1	0.54
-53.86	62.86	11	723	14	1.09	0.86	0.86	0.24	14	168	2.2	1.2	1	0.54
-58.84	67.84	14	778	23	0.76	0.51	0.51	0.25	80	215	2.4	0.9	1	0.54
-63.83	72.83	14	797	20	0.79	0.60	0.60	0.18	86	175	2.5	1.0	1	0.54
-68.83	77.83	16	801	42	0.50	0.28	0.29	0.22	208	258	2.5	0.5	1	0.54

### B.1.4.3. Test Pile EB5P1

Elevation	Depth	SPT TH-6	FMX	bl/ft	DMX	DFN	iSET	Rebound	SFT	EBR	CSX	TSX	FVP	Jc
feet	feet	N <sub>safe</sub>	kips		inches	inches	inches	inches	kips	kips	ksi	ksi		
-4.89	25.69	2	313	1	12.01	12.01	12.00	0.01	0	0	1.0	0.4	1	0.6
-9.52	30.32	6	536	4	3.23	3.00	3.00	0.23	0	19	1.7	1.0	1	0.6
-14.89	35.69	5	541	1	12.00	12.00	12.00	0.00	0	0	1.7	1.2	1	0.6
-19.58	40.38	20	501	5	2.85	2.22	2.22	0.62	0	38	1.5	0.9	0.87	0.6
-24.52	45.32	12	552	32	0.77	0.38	0.38	0.39	1	285	1.7	0.4	0.99	0.6
-29.51	50.31	46	583	67	0.65	0.18	0.18	0.47	17	403	1.8	0.3	1	0.6
-34.49	55.29	2	521	15	0.95	0.80	0.80	0.15	44	131	1.6	0.7	1	0.6
-39.51	60.31	5	547	13	1.09	0.93	0.93	0.16	41	113	1.7	0.8	1	0.6
-44.50	65.30	4	546	14	1.01	0.86	0.86	0.15	37	128	1.7	0.8	1	0.6
-49.47	70.27	11	577	18	0.86	0.67	0.67	0.18	65	151	1.8	0.8	1	0.6
-54.50	75.30	16	612	19	0.82	0.62	0.62	0.19	63	169	1.9	0.8	1	0.6
-59.51	80.31	20	675	29	0.66	0.41	0.41	0.26	131	208	2.1	0.6	1	0.6
-64.49	85.29	12	741	26	0.72	0.46	0.46	0.25	129	200	2.3	0.8	1	0.6
-69.50	90.30	22	807	41	0.57	0.29	0.29	0.27	200	310	2.5	0.4	1	0.6
-74.50	95.30	12	828	32	0.55	0.37	0.38	0.17	379	144	2.6	0.6	1	0.6
-79.51	100.31	17	848	40	0.48	0.29	0.30	0.18	436	194	2.6	0.3	1	0.6

## B.1.5. Anderson Street Overpass

### B.1.5.1. Test Pile P6P5

Elevation	Depth	SPT P6-4	FMX	bl/ft	DMX	DFN	iSET	Rebound	SFT	EBR	CSX	TSX	FVP	Jc
feet	feet	N <sub>safe</sub>	kips		inches	inches	inches	inches	kips	kips	ksi	ksi		
86.88	17.70	8	875	23	0.78	0.44	0.52	0.26	0	287	1.5	0.5	0.90	0.55
81.88	22.70	5	891	27	0.66	0.36	0.44	0.22	10	260	1.6	0.5	1	0.55
76.87	27.71	17	894	27	0.68	0.26	0.45	0.23	99	217	1.6	0.5	0.94	0.55
71.90	32.68	11	877	19	0.81	0.36	0.63	0.18	80	256	1.5	0.5	1	0.55
66.88	37.70	12	875	20	0.82	0.52	0.60	0.22	7	300	1.5	0.5	0.98	0.55
61.90	42.69	14	814	13	1.08	0.87	0.91	0.17	0	197	1.4	0.5	0.91	0.55
56.83	47.75	18	950	16	1.34	1.11	0.75	0.59	103	191	1.7	1.1	1	0.55
51.89	52.69	5	1034	8	1.52	1.31	1.48	0.04	92	222	1.8	1.2	1	0.55
46.88	57.70	3	986	10	1.26	1.05	1.20	0.06	142	206	1.7	1.0	1	0.55
41.88	62.70	2	1027	12	1.18	0.88	0.96	0.21	139	251	1.8	1.0	1	0.55
36.88	67.70	4	1034	10	1.18	1.00	1.16	0.01	130	297	1.8	1.0	1	0.55
33.40	71.18	13	1036	11	1.17	0.99	1.13	0.04	128	318	1.8	1.0	1	0.55
28.37	76.21	17	1047	15	1.04	0.74	0.78	0.26	108	373	1.8	1.0	1	0.55
26.40	78.18	33	1042	13	1.20	0.95	0.95	0.25	58	391	1.8	1.0	1	0.55
24.38	80.20	28	1002	13	1.12	0.68	0.90	0.22	46	395	1.7	0.9	1	0.55
21.40	83.18	16	1003	13	1.21	0.74	0.95	0.26	23	396	1.7	1.0	1	0.55
18.35	86.23	9	996	13	1.20	0.82	0.94	0.25	17	389	1.7	0.9	1	0.55
15.34	89.24	10	1022	47	0.92	0.24	0.25	0.66	1	442	1.8	0.8	1	0.55
13.39	91.19	59	995	45	1.17	0.33	0.27	0.91	1	402	1.7	0.9	1	0.55
11.31	93.27	28	997	93	1.19	0.24	0.13	1.06	1	389	1.7	0.9	1	0.55
9.32	95.27	65	1025	245	1.30	0.13	0.05	1.25	11	337	1.8	1.0	1	0.55

### B.1.5.2. Test Pile P6P6

Elevation	Depth	SPT P6-4	FMX	bl/ft	DMX	DFN	iSET	Rebound	SFT	EBR	CSX	TSX	FVP	Jc
feet	feet	N <sub>safe</sub>	kips		inches	inches	inches	inches	kips	kips	ksi	ksi		
76.70	26.18	17	926	17	0.85	0.42	0.75	0.10	67	220	1.6	1.0	1	0.6
71.86	31.02	11	930	17	0.97	0.69	0.77	0.21	43	196	1.6	1.0	1	0.6
66.89	35.99	12	936	18	0.89	0.37	0.72	0.17	82	195	1.6	1.0	1	0.6
61.90	40.98	14	900	17	1.00	0.67	0.75	0.24	0	234	1.6	1.0	0.99	0.6
56.84	46.05	18	846	7	1.56	1.43	2.13	-0.57	3	119	1.5	1.1	1	0.6
51.86	51.02	5	842	10	1.60	1.45	1.39	0.21	6	114	1.5	1.1	1	0.6
46.89	55.99	3	822	9	1.44	1.28	1.50	-0.07	26	99	1.4	1.0	1	0.6
41.86	61.02	2	843	10	1.42	1.28	1.33	0.09	23	113	1.5	1.0	1	0.6
36.86	66.02	4	868	14	1.22	1.17	0.97	0.25	45	133	1.5	1.0	1	0.6
33.40	69.48	13	857	15	0.96	0.88	0.88	0.08	81	132	1.5	1.0	1	0.6
28.40	74.48	17	921	26	0.66	0.25	0.48	0.17	187	153	1.6	0.9	1	0.6
26.38	76.50	33	929	26	0.66	0.20	0.47	0.19	189	161	1.6	0.9	1	0.6
24.38	78.50	28	934	28	0.63	0.19	0.44	0.19	200	161	1.6	0.9	1	0.6
21.38	81.50	16	958	29	0.62	0.20	0.43	0.19	222	150	1.7	0.9	1	0.6
17.38	85.50	9	1015	31	0.62	0.21	0.40	0.22	244	152	1.8	0.9	1	0.6
15.39	87.49	10	1047	51	0.57	0.15	0.25	0.32	196	349	1.8	0.6	1	0.6
13.35	89.53	59	1135	41	0.94	0.42	0.30	0.64	46	364	2.0	1.0	1	0.6
11.38	91.50	28	1103	97	0.63	0.22	0.13	0.50	187	371	1.9	0.6	0.98	0.6
9.38	93.50	65	1217	86	0.87	0.23	0.14	0.73	118	372	2.1	0.9	0.99	0.6
7.37	95.51	33	1169	105	1.08	0.04	0.12	0.96	88	335	2.0	1.1	1	0.6
5.37	97.51	33	1209	113	1.16	0.13	0.11	1.05	82	302	2.1	1.2	1	0.6
3.42	99.46	24	1124	235	0.97	0.12	0.05	0.92	81	294	1.9	1.1	1	0.6
1.43	101.45	39	1106	326	0.85	0.05	0.03	0.82	119	293	1.9	1.0	1	0.6
-0.70	103.58	21	1289	133	0.96	0.22	0.09	0.87	118	316	2.2	1.2	1	0.6
-2.64	105.52	30	1196	213	0.76	0.03	0.06	0.70	155	264	2.1	1.2	1	0.6

## B.1.6. I-4 Widening Daytona

### B.1.6.1. Test Pile EB3-1, P5

Elevation	Depth	SPT DC-1	FMX	bl/ft	DMX	DFN	iSET	Rebound	SFT	EBR	CSX	TSX	FVP	Jc
feet	feet	N <sub>safe</sub>	kips		inches	inches	inches	inches	kips	kips	ksi	ksi		
7.36	38.82	10	1041	13	1.01	0.90	0.90	0.11	51	360	1.8	0.7	1	0.5
5.00	41.18	9	1025	42	0.55	0.28	0.28	0.27	71	351	1.8	0.7	1	0.5
2.50	43.68	6	1006	46	0.50	0.26	0.26	0.24	116	347	1.7	0.6	1	0.5
-0.01	46.19	11	1009	50	0.48	0.24	0.24	0.24	126	358	1.7	0.5	1	0.5
-2.48	48.66	15	1055	55	0.50	0.22	0.22	0.28	134	359	1.8	0.6	1	0.5
-5.02	51.20	11	1160	45	0.55	0.27	0.27	0.28	180	340	2.0	0.7	1	0.5
-7.50	53.68	10	1247	42	0.58	0.28	0.28	0.29	267	263	2.2	0.9	1	0.5
-10.01	56.19	5	1219	37	0.53	0.32	0.32	0.21	412	172	2.1	0.9	1	0.5
-12.49	58.67	10	1225	49	0.47	0.24	0.24	0.23	531	149	2.1	0.8	1	0.5
-14.99	61.17	0	1242	42	0.48	0.28	0.28	0.20	643	89	2.2	0.9	1	0.5
-17.49	63.67	5	1264	41	0.45	0.30	0.30	0.15	778	19	2.2	1.0	1	0.5
-20.01	66.19	6	1298	40	0.45	0.30	0.30	0.15	810	15	2.2	1.0	1	0.5
-22.51	68.69	6	1306	40	0.45	0.30	0.30	0.15	798	24	2.3	1.0	1	0.5
-24.98	71.16	12	1315	42	0.41	0.28	0.28	0.13	803	63	2.3	1.0	1	0.5
-27.49	73.67	35	1358	83	0.42	0.14	0.14	0.28	624	371	2.4	0.8	1	0.5
-29.99	76.17	64	1446	98	0.56	0.12	0.12	0.43	155	753	2.5	1.0	1	0.5
-32.47	78.65	42	1310	108	0.53	0.11	0.11	0.42	181	675	2.3	0.4	1	0.5
-34.97	81.15	25	1240	65	0.54	0.18	0.18	0.35	245	481	2.2	0.4	1	0.5
-37.50	83.68	16	1175	52	0.48	0.23	0.23	0.24	545	232	2.0	0.4	1	0.5
-39.99	86.17	14	1202	55	0.39	0.22	0.22	0.17	797	120	2.1	0.4	1	0.5
-42.52	88.70	21	1286	54	0.40	0.22	0.22	0.17	681	252	2.2	0.4	1	0.5
-45.00	91.18	14	1397	60	0.43	0.20	0.20	0.23	484	457	2.4	0.4	1	0.5
-47.53	93.71	100	1461	71	0.43	0.17	0.17	0.26	350	811	2.5	0.5	1	0.5
-49.66	95.84	17	1518	92	0.41	0.13	0.13	0.28	372	954	2.6	0.4	1	0.5

## B.1.7. SR-83 over Ramsey Branch

### B.1.7.1. Test Pile EB1P1

Elevation	Depth	SPT B-1	FMX	bl/ft	DMX	DFN	iSET	Rebound	SFT	EBR	CSX	TSX	FVP	Jc
feet	feet	N <sub>safe</sub>	kips		inches	inches	inches	inches	kips	kips	ksi	ksi		
-48.56	50.01	5	1061	13	1.17	0.91	0.91	0.27	11	179	1.83	1.17	1	0.7
-51.00	52.45	5	1049	16	1.08	0.76	0.76	0.32	24	163	1.81	1.15	1	0.7
-53.54	54.99	5	1079	19	1.04	0.62	0.62	0.41	17	209	1.87	1.26	1	0.7
-56.00	57.45	5	1056	30	1.02	0.40	0.40	0.62	37	169	1.84	1.15	1	0.7
-58.55	60.00	6	1089	45	0.98	0.26	0.26	0.72	47	205	1.89	1.09	1	0.7
-61.00	62.45	13	1126	63	0.87	0.19	0.19	0.68	75	266	1.96	0.98	1	0.7
-63.47	64.92	13	1123	118	0.93	0.10	0.10	0.83	68	287	1.95	1.00	1	0.7
-65.99	67.44	10	1261	68	0.77	0.17	0.18	0.59	84	390	2.19	1.03	1	0.7
-68.48	69.93	12	1358	42	0.71	0.28	0.28	0.42	185	349	2.35	1.03	1	0.7
-71.00	72.45	6	1345	50	0.54	0.24	0.24	0.30	345	389	2.34	0.60	1	0.7
-73.46	74.91	4	1344	58	0.42	0.20	0.21	0.22	600	332	2.34	0.45	1	0.7
-76.00	77.45	5	1505	74	0.47	0.16	0.16	0.30	740	297	2.61	0.62	1	0.7
-78.48	79.93	55	1521	67	0.57	0.18	0.18	0.39	652	271	2.64	0.83	1	0.7
-80.52	81.97	20	1521	50	0.64	0.24	0.24	0.40	644	233	2.65	1.00	1	0.7

### B.1.7.2. Test Pile P4P5

Elevation	Depth	SPT B-3	FMX	bl/ft	DMX	DFN	iSET	Rebound	SFT	EBR	CSX	TSX	FVP	Jc
feet	feet	N <sub>safe</sub>	kips		inches	inches	inches	inches	kips	kips	ksi	ksi		
-23.45	23.45	6	925	4	4.04	4.04	3.00	1.04	2	0	1.6	1.0	1	0.5
-26.00	26.00	12	975	15	1.98	1.66	0.79	1.19	3	35	1.7	1.1	1	0.5
-28.42	28.42	17	866	20	2.04	1.40	0.60	1.44	4	6	1.5	1.0	0.99	0.5
-30.95	30.95	31	893	4	3.78	3.78	3.00	0.78	0	0	1.6	1.1	1	0.5
-33.51	33.51	9	879	8	2.59	2.37	1.56	1.03	1	0	1.5	1.1	1	0.5
-36.03	36.03	9	969	7	2.77	2.61	1.81	0.97	6	0	1.7	1.1	1	0.5
-38.47	38.47	7	974	16	1.85	1.70	0.73	1.13	14	53	1.7	1.1	1	0.5
-40.94	40.94	10	1001	10	2.29	2.16	1.18	1.11	4	38	1.7	1.1	1	0.5
-43.53	43.53	10	974	7	2.69	2.69	1.71	0.98	0	19	1.7	1.0	1	0.5
-46.00	46.00	6	936	8	2.59	2.59	1.58	1.01	0	32	1.6	1.0	1	0.5
-48.51	48.51	7	978	13	2.00	2.00	0.92	1.08	0	98	1.7	1.0	1	0.5
-50.99	50.99	6	1075	20	1.05	0.60	0.60	0.45	14	240	1.9	1.1	1	0.5
-53.60	53.60	6	987	52	1.26	0.23	0.23	1.03	3	224	1.7	1.1	1	0.5
-55.95	55.95	7	1005	155	1.44	0.08	0.08	1.36	4	228	1.7	1.1	1	0.5
-58.47	58.47	6	1068	160	1.12	0.08	0.07	1.04	56	184	1.9	1.1	1	0.5
-61.01	61.01	7	1018	171	1.01	0.07	0.07	0.94	53	213	1.8	1.0	1	0.5
-63.50	63.50	7	1147	34	0.83	0.35	0.35	0.48	57	337	2.0	1.1	1	0.5
-66.01	66.01	19	1080	40	0.78	0.30	0.30	0.49	118	255	1.9	0.9	1	0.5
-68.50	68.50	9	1049	38	0.60	0.32	0.32	0.29	136	327	1.8	0.6	1	0.5
-70.99	70.99	14	1089	40	0.56	0.30	0.30	0.25	198	310	1.9	0.5	1	0.5
-73.51	73.51	9	1188	50	0.53	0.24	0.24	0.29	238	440	2.1	0.5	1	0.5
-76.02	76.02	53	1252	81	0.50	0.15	0.15	0.35	236	606	2.2	0.4	1	0.5
-78.49	78.49	9	1291	59	0.59	0.20	0.20	0.39	178	433	2.2	0.8	1	0.5
-80.99	80.99	7	1326	42	0.65	0.28	0.29	0.36	157	335	2.3	0.9	1	0.5
-83.51	83.51	30	1321	32	0.71	0.37	0.37	0.34	150	312	2.3	1.1	1	0.5
-86.02	86.02	16	1177	36	0.61	0.33	0.33	0.28	124	265	2.0	0.9	1	0.5
-88.49	88.49	19	1187	41	0.58	0.29	0.30	0.28	145	255	2.1	0.9	1	0.5
-91.01	91.01	4	1197	38	0.62	0.31	0.31	0.31	135	287	2.1	1.0	1	0.5
-93.50	93.50	12	1245	41	0.61	0.29	0.29	0.32	166	292	2.2	1.0	1	0.5
-96.00	96.00	11	1258	38	0.64	0.32	0.32	0.32	153	328	2.2	1.1	1	0.5
-98.50	98.50	6	1251	44	0.60	0.27	0.27	0.33	140	332	2.2	0.9	1	0.5
-101.00	101.00	6	1262	42	0.62	0.28	0.28	0.34	149	345	2.2	1.0	1	0.5
-103.51	103.51	5	1255	40	0.60	0.30	0.30	0.29	260	274	2.2	0.9	1	0.5
-106.00	106.00	6	1497	71	0.37	0.17	0.17	0.20	539	229	2.6	0.8	1	0.5

### B.1.7.3. Test Pile EB5P2

Elevation	Depth	SPT FDOT	FMX	bl/ft	DMX	DFN	iSET	Rebound	SFT	EBR	CSX	TSX	FVP	Jc
feet	feet	N <sub>safe</sub>	kips		inches	inches	inches	inches	kips	kips	ksi	ksi		
-22.69	30.09	19	999	10	2.04	1.13	1.15	0.89	0	101	1.7	1.0	1	0.41
-25.18	32.58	52	967	6	2.18	1.86	1.88	0.30	0	72	1.7	1.0	1	0.41
-27.63	35.03	21	967	4	3.00	2.98	3.00	0.00	0	0	1.7	1.0	1	0.41
-30.20	37.60	14	887	5	2.51	2.38	2.40	0.11	0	0	1.5	0.9	0.98	0.41
-32.71	40.11	10	926	7	2.13	1.69	1.71	0.42	0	52	1.6	0.9	0.99	0.41
-35.13	42.53	16	967	8	1.84	1.58	1.60	0.24	0	94	1.7	1.0	1	0.41
-37.73	45.13	9	962	11	1.47	1.09	1.11	0.36	0	136	1.7	0.9	1	0.41
-40.21	47.61	7	990	10	1.53	1.14	1.16	0.37	0	118	1.7	0.9	1	0.41
-42.70	50.10	9	993	10	1.40	1.18	1.20	0.20	0	162	1.7	0.9	1	0.41
-45.21	52.61	6	998	12	1.28	1.01	1.03	0.25	1	180	1.7	0.9	1	0.41
-47.69	55.09	6	979	29	1.19	0.39	0.41	0.78	2	259	1.7	0.9	1	0.41
-50.22	57.62	9	967	54	1.19	0.20	0.22	0.97	7	272	1.7	0.9	1	0.41
-52.67	60.07	10	913	138	1.39	0.07	0.09	1.30	3	295	1.6	0.9	1	0.41
-55.20	62.60	7	1095	80	1.26	0.12	0.15	1.11	35	361	1.9	1.0	1	0.41
-57.74	65.14	11	1254	80	1.14	0.13	0.15	0.99	249	281	2.2	1.2	1	0.41
-60.17	67.57	14	1249	58	0.81	0.18	0.21	0.60	357	273	2.2	1.0	1	0.41
-62.67	70.07	21	1123	126	0.93	0.07	0.10	0.83	165	312	2.0	1.0	1	0.41
-65.23	72.63	16	1122	85	0.88	0.11	0.14	0.74	179	245	2.0	0.9	1	0.41
-67.65	75.05	62	1164	41	0.72	0.27	0.29	0.43	207	357	2.0	0.9	1	0.41
-70.22	77.62	11	1190	28	0.65	0.42	0.44	0.21	248	311	2.1	0.7	1	0.41
-72.73	80.13	76	1295	50	0.38	0.21	0.24	0.14	572	288	2.3	0.4	1	0.41
-75.21	82.61	27	1428	56	0.47	0.18	0.21	0.26	450	442	2.5	0.5	1	0.41
-77.69	85.09	15	1406	74	0.49	0.14	0.16	0.33	390	466	2.4	0.5	1	0.41

## B.1.8. SR-528 over Indian River

### B.1.8.1. Test Pile P4P7

Elevation	Depth	SPT TB-4	FMX	bl/ft	DMX	DFN	iSET	Rebound	SFT	EBR	CSX	TSX	FVP	Jc
feet	feet	N <sub>safe</sub>	kips		inches	inches	inches	inches	kips	kips	ksi	ksi		
-20.78	25.28	22	922	31	0.89	0.79	0.39	0.50	0	560	1.4	0.2	0.9	0.5
-23.01	27.51	25	879	34	0.89	0.74	0.35	0.53	0	575	1.4	0.2	0.9	0.5
-25.51	30.01	10	783	37	0.84	0.69	0.33	0.51	0	577	1.2	0.2	0.9	0.5
-28.00	32.50	10	804	41	0.83	0.42	0.29	0.54	5	604	1.2	0.2	0.9	0.5
-30.50	35.00	12	932	36	0.87	0.55	0.34	0.53	4	596	1.4	0.3	0.9	0.5
-33.01	37.51	10	1065	41	0.92	0.67	0.29	0.63	9	597	1.7	0.4	0.9	0.5
-35.45	39.95	14	1163	22	1.05	0.88	0.54	0.52	14	489	1.8	0.6	0.9	0.5
-37.98	42.48	28	1201	14	1.19	0.95	0.85	0.35	24	336	1.9	0.9	0.9	0.5
-40.60	45.10	4	1225	22	1.04	0.93	0.55	0.49	21	541	1.9	0.7	0.9	0.5
-43.00	47.50	5	1298	45	0.85	0.56	0.27	0.58	33	659	2.0	0.5	0.9	0.5
-45.48	49.98	55	1335	25	1.00	0.68	0.49	0.51	36	558	2.1	0.8	0.9	0.5
-47.98	52.48	60	1343	12	1.18	0.99	0.97	0.20	47	391	2.1	1.1	0.9	0.5
-50.48	54.98	6	828	22	0.74	0.46	0.55	0.19	52	261	1.3	0.5	0.9	0.5
-53.00	57.50	6	834	24	0.71	0.41	0.50	0.20	67	269	1.3	0.5	0.9	0.5
-55.51	60.01	5	841	26	0.69	0.39	0.47	0.22	67	299	1.3	0.5	0.9	0.5
-58.00	62.50	6	851	22	0.74	0.39	0.55	0.19	82	254	1.3	0.6	0.9	0.5
-60.50	65.00	15	855	22	0.77	0.49	0.55	0.22	96	217	1.3	0.7	0.9	0.5
-63.01	67.51	15	860	41	0.61	0.25	0.29	0.32	86	405	1.3	0.6	0.9	0.5
-65.52	70.02	20	1401	35	0.83	0.19	0.35	0.48	173	701	2.2	1.0	0.9	0.5
-68.01	72.51	22	1418	43	0.79	0.11	0.28	0.51	181	825	2.2	1.0	0.9	0.5
-70.51	75.01	24	1411	44	0.74	0.16	0.27	0.47	194	831	2.2	0.8	0.9	0.5
-73.00	77.50	26	1403	40	0.80	0.11	0.30	0.50	185	739	2.2	0.9	0.9	0.5
-75.46	79.96	31	1385	30	0.92	0.57	0.39	0.53	163	568	2.1	1.1	0.9	0.5
-77.99	82.49	38	992	31	0.85	0.19	0.38	0.46	125	431	1.5	0.3	0.9	0.5
-80.48	84.98	12	944	23	1.06	0.46	0.53	0.53	84	241	1.5	0.4	0.9	0.5
-83.00	87.50	15	881	24	1.21	0.42	0.50	0.71	55	251	1.4	0.4	0.9	0.5
-85.52	90.02	31	803	28	1.18	0.29	0.43	0.75	124	217	1.2	0.3	0.9	0.5
-88.00	92.50	36	789	30	1.21	0.27	0.40	0.81	151	170	1.2	0.3	0.9	0.5
-90.48	94.98	7	838	25	1.27	0.35	0.49	0.78	132	160	1.3	0.4	0.9	0.5
-93.00	97.50	7	909	22	1.33	0.35	0.55	0.78	88	193	1.4	0.5	0.9	0.5
-95.51	100.01	9	969	19	1.32	0.56	0.62	0.70	85	186	1.5	0.6	0.9	0.5
-98.01	102.51	9	1042	33	0.88	0.45	0.36	0.52	83	483	1.6	0.4	0.9	0.5
-100.56	105.06	45	1153	54	0.86	0.63	0.22	0.64	196	511	1.8	0.5	0.9	0.5
-102.85	107.35	73	1337	389	0.79	-0.06	0.03	0.76	451	399	2.1	0.9	0.9	0.5

### B.1.8.2. Test Pile P9P3

Elevation	Depth	SPT TB-5	FMX	bl/ft	DMX	DFN	iSET	Rebound	SFT	EBR	CSX	TSX	FVP	Jc
feet	feet	N <sub>safe</sub>	kips		inches	inches	inches	inches	kips	kips	ksi	ksi		
-34.62	34.62	3	810	31	0.59	0.48	0.39	0.20	92	292	1.3	0.6	0.90	0.5
-37.01	37.01	4	817	31	0.60	0.45	0.39	0.22	96	290	1.3	0.7	0.91	0.5
-39.50	39.50	7	830	27	0.61	0.46	0.45	0.16	96	268	1.3	0.6	0.91	0.5
-42.00	42.00	11	832	22	0.67	0.58	0.54	0.12	94	217	1.3	0.7	0.91	0.5
-44.52	44.52	18	833	30	0.62	0.45	0.40	0.23	89	300	1.3	0.7	0.92	0.5
-46.97	46.97	5	825	18	0.80	0.64	0.67	0.12	90	172	1.3	0.7	0.94	0.5
-49.48	49.48	4	826	10	1.19	1.02	1.18	0.02	77	86	1.3	0.9	0.95	0.5
-52.00	52.00	11	832	12	1.12	0.87	0.97	0.14	80	110	1.3	0.9	0.98	0.5
-54.51	54.51	7	832	13	1.09	0.77	0.93	0.16	89	111	1.3	0.9	1	0.5
-56.99	56.99	7	832	14	1.11	0.74	0.88	0.23	97	100	1.3	0.9	0.99	0.5
-59.52	59.52	7	834	22	0.78	0.37	0.54	0.24	95	217	1.3	0.8	0.99	0.5
-62.00	62.00	85	941	59	0.54	0.02	0.20	0.33	168	504	1.5	0.6	0.97	0.5
-64.50	64.50	41	1225	54	0.61	0.23	0.22	0.39	197	690	1.9	0.6	0.90	0.5
-66.96	66.96	24	1271	46	0.74	0.49	0.26	0.48	178	600	2.0	1.0	0.90	0.5
-69.49	69.49	22	1291	29	0.92	0.43	0.41	0.51	129	456	2.0	1.3	0.90	0.5
-71.99	71.99	19	872	55	0.64	0.25	0.22	0.42	99	358	1.4	0.9	0.90	0.5
-74.50	74.50	10	876	39	0.68	0.16	0.31	0.38	111	239	1.4	0.9	0.92	0.5
-76.99	76.99	10	868	36	0.66	0.25	0.33	0.33	128	222	1.3	0.8	0.95	0.5
-79.50	79.50	3	890	31	0.68	0.25	0.38	0.30	148	189	1.4	0.9	0.96	0.5
-81.98	81.98	4	902	33	0.69	0.26	0.36	0.34	160	194	1.4	0.9	0.97	0.5
-84.48	84.48	4	907	28	0.72	0.32	0.43	0.29	179	149	1.4	1.0	0.98	0.5
-87.00	87.00	3	897	28	0.66	0.39	0.43	0.23	190	148	1.4	0.9	0.99	0.5
-89.50	89.50	5	909	31	0.65	0.34	0.39	0.26	195	172	1.4	0.9	0.99	0.5
-92.04	92.04	6	913	32	0.66	0.30	0.37	0.28	188	160	1.4	0.9	0.98	0.5
-94.51	94.51	7	918	84	0.65	-0.02	0.14	0.51	150	360	1.4	1.0	0.95	0.5
-97.06	97.06	61	1328	125	0.81	0.09	0.10	0.72	229	418	2.1	1.1	0.90	0.5
-99.06	99.06	80	1310	200	0.82	0.02	0.06	0.76	252	334	2.0	1.1	0.90	0.5

### B.1.8.3. Test Pile P20P6

Elevation	Depth	SPT TB-11	FMX	bl/ft	DMX	DFN	iSET	Rebound	SFT	EBR	CSX	TSX	FVP	Jc
feet	feet	N <sub>safe</sub>	kips		inches	inches	inches	inches	kips	kips	ksi	ksi		
-26.99	18.99	14	804	7	1.61	0.48	1.63	-0.03	64	90	1.2	0.9	0.90	0.5
-29.77	21.77	11	751	1	4.42	4.42	12.00	-7.58	0	0	1.2	1.1	0.90	0.5
-31.77	23.77	11	862	2	2.56	2.40	6.00	-3.44	9	14	1.3	1.2	0.90	0.5
-34.51	26.51	9	808	4	1.49	1.10	2.88	-1.39	132	39	1.3	1.0	0.90	0.5
-36.96	28.96	7	801	3	3.70	3.70	3.50	0.20	58	9	1.3	1.1	0.90	0.5
-39.50	31.50	10	876	4	2.38	1.99	2.80	-0.42	96	87	1.3	1.1	0.90	0.5
-41.98	33.98	8	833	6	1.75	1.30	2.12	-0.37	76	51	1.3	1.1	0.90	0.5
-44.52	36.52	12	832	6	1.44	1.07	2.00	-0.56	91	88	1.3	1.1	0.90	0.5
-47.00	39.00	18	860	9	1.55	1.16	1.29	0.26	97	123	1.3	1.0	0.90	0.5
-49.47	41.47	11	843	5	1.88	1.49	2.40	-0.52	78	81	1.3	1.1	0.90	0.5
-52.04	44.04	9	856	6	1.85	1.79	2.08	-0.23	54	45	1.3	1.1	0.90	0.5
-54.49	46.49	7	862	7	1.68	1.53	1.75	-0.07	55	60	1.3	1.0	0.90	0.5
-56.99	48.99	6	868	7	1.52	1.35	1.63	-0.11	53	65	1.3	1.0	0.90	0.5
-59.54	51.54	6	871	9	1.41	1.18	1.30	0.11	50	80	1.3	1.0	0.90	0.5
-62.02	54.02	73	884	28	0.60	0.25	0.43	0.17	60	389	1.4	0.7	0.90	0.5
-64.93	56.93	51	894	35	0.63	-0.17	0.34	0.29	63	452	1.4	0.8	0.90	0.5
-66.98	58.98	21	877	21	1.08	0.30	0.56	0.52	41	247	1.4	1.0	0.90	0.5
-69.53	61.53	9	873	24	1.28	-0.06	0.50	0.78	50	190	1.4	1.0	0.90	0.5
-72.01	64.01	13	881	42	0.75	0.15	0.29	0.46	66	326	1.4	0.8	0.90	0.5
-74.47	66.47	20	893	45	0.75	0.18	0.26	0.48	80	262	1.4	0.8	0.90	0.5
-77.00	69.00	10	889	36	1.13	0.61	0.34	0.79	76	140	1.4	1.0	0.90	0.5
-79.51	71.51	10	885	58	0.91	0.26	0.21	0.70	93	193	1.4	0.9	0.90	0.5
-82.00	74.00	5	872	86	0.63	0.05	0.14	0.49	84	399	1.4	0.6	0.90	0.5
-84.50	76.50	12	868	39	0.82	0.22	0.31	0.51	120	162	1.3	0.8	0.90	0.5
-87.00	79.00	10	867	37	0.87	0.23	0.32	0.55	129	138	1.3	0.9	0.90	0.5
-89.52	81.52	5	870	40	0.92	0.30	0.30	0.62	130	121	1.3	0.9	0.90	0.5
-92.00	84.00	4	868	41	0.88	-0.07	0.29	0.59	156	118	1.3	0.8	0.91	0.5
-94.54	86.54	5	868	40	0.62	0.25	0.30	0.32	181	146	1.3	0.7	0.90	0.5
-97.00	89.00	6	957	120	0.53	0.22	0.10	0.43	490	309	1.5	0.4	0.90	0.5
-99.51	91.51	22	1330	42	1.08	0.37	0.28	0.80	383	188	2.1	1.3	0.90	0.5
-102.05	94.05	29	1350	118	1.08	0.28	0.10	0.98	350	290	2.1	1.2	0.90	0.5

## B.1.9. I-10 and Chaffee Road Overpass

### B.1.9.1. Test Pile P2P9

Elevation	Depth	SPT B-2	FMX	bl/ft	DMX	DFN	iSET	Rebound	SFT	EBR	CSX	TSX	FVP	Jc
feet	feet	N <sub>safe</sub>	kips		inches	inches	inches	inches	kips	kips	ksi	ksi		
28.61	34.47	25	646	8	1.70	1.03	1.50	0.20	0	191	2.0	0.8	1	0.6
26.03	37.05	12	769	10	1.29	0.55	1.15	0.14	19	257	2.4	1.0	1	0.6
23.60	39.48	43	766	10	1.53	0.63	1.16	0.37	13	217	2.4	1.1	1	0.6
21.07	42.01	18	751	6	2.07	1.34	1.88	0.19	4	129	2.3	1.1	1	0.6
18.72	44.36	3	728	3	2.92	2.67	4.00	-1.08	0	35	2.2	1.1	1	0.6
16.05	47.03	2	706	3	4.36	4.35	4.00	0.36	0	0	2.2	1.1	1	0.6
13.65	49.43	3	716	5	3.77	3.76	2.52	1.25	0	0	2.2	1.2	1	0.6
11.02	52.06	3	697	6	3.89	3.87	1.95	1.94	0	0	2.2	1.1	1	0.6
8.65	54.43	3	699	5	3.45	3.40	2.32	1.13	0	0	2.1	1.1	1	0.6
6.01	57.07	4	675	8	3.61	3.61	1.49	2.11	0	0	2.1	1.0	1	0.6
3.61	59.47	3	669	8	3.55	3.54	1.50	2.05	0	0	2.1	1.0	1	0.6
1.01	62.07	6	670	9	3.34	3.15	1.32	2.03	0	0	2.1	1.0	1	0.6
-1.45	64.53	6	646	9	3.35	3.08	1.32	2.03	0	0	2.0	0.9	1	0.6
-3.95	67.03	10	679	6	2.55	2.10	2.00	0.55	0	153	2.1	0.9	1	0.6
-6.45	69.53	22	678	6	2.05	1.45	2.00	0.05	0	181	2.1	0.9	1	0.6
-8.97	72.05	16	639	24	1.01	0.40	0.51	0.50	28	201	2.0	0.5	1	0.6
-11.44	74.52	15	656	73	0.60	0.17	0.16	0.44	91	341	2.0	0.2	1	0.6
-13.92	77.00	47	847	65	0.68	0.13	0.18	0.50	139	414	2.6	0.4	1.01	0.6
-16.42	79.50	34	960	70	0.60	0.15	0.17	0.43	238	436	3.0	0.4	1.03	0.6

## B.1.10. I-4 and John Young Parkway

### B.1.10.1. Test Pile P2P1 (Ramp A)

Elevation	Depth	SPT FB-11	FMX	bl/ft	DMX	DFN	iSET	Rebound	SFT	EBR	CSX	TSX	FVP	Jc
feet	feet	N <sub>safe</sub>	kips		inches	inches	inches	inches	kips	kips	ksi	ksi		
75.53	19.95	7	364	3	3.20	3.10	4.00	-0.80	0	0	0.6	0.2	0.67	0.5
73.07	22.41	9	516	4	3.36	3.23	3.00	0.36	0	0	0.9	0.5	0.93	0.5
70.57	24.91	9	786	4	4.13	4.07	3.00	1.13	0	0	1.4	0.9	1	0.5
68.07	27.41	16	633	4	4.60	4.59	3.00	1.60	0	0	1.1	0.6	0.90	0.5
65.57	29.91	6	641	4	3.80	3.74	3.00	0.80	0	0	1.1	0.7	0.90	0.5
63.07	32.41	5	700	4	3.34	3.24	3.00	0.34	0	0	1.2	0.8	0.90	0.5
60.59	34.88	5	911	5	1.95	1.46	2.40	-0.45	0	87	1.6	1.0	1	0.5
58.07	37.41	6	827	4	3.14	3.00	3.00	0.14	0	0	1.5	1.0	1	0.5
55.57	39.91	3	765	4	3.93	3.88	3.00	0.93	0	0	1.3	0.9	1	0.5
53.07	42.41	3	710	4	3.99	3.96	3.00	0.99	0	0	1.2	0.8	1	0.5
50.59	44.88	2	698	5	3.26	3.13	2.40	0.86	0	0	1.2	0.7	0.94	0.5
48.07	47.41	2	875	4	1.71	1.19	3.00	-1.29	0	127	1.5	1.0	1	0.5
45.57	49.91	2	950	4	2.03	1.60	3.00	-0.98	0	94	1.7	1.1	1	0.5
43.00	52.47	7	908	5	2.57	2.34	2.64	-0.07	0	4	1.6	1.0	1	0.5
40.57	54.91	6	883	4	2.67	2.47	3.00	-0.33	0	0	1.5	1.0	1	0.5
38.07	57.41	4	878	4	2.74	2.57	3.00	-0.26	0	0	1.5	1.0	1	0.5
35.57	59.91	5	860	4	2.99	2.86	3.00	-0.01	0	0	1.5	1.0	1	0.5
33.07	62.41	3	844	4	2.89	2.76	3.00	-0.11	0	0	1.5	0.9	1	0.5
30.59	64.88	4	838	5	3.00	2.90	2.40	0.60	0	0	1.5	0.9	1	0.5
27.94	67.53	3	826	6	2.85	2.73	2.00	0.85	0	0	1.5	0.9	1	0.5
25.24	70.24	32	1169	18	0.83	0.29	0.66	0.18	3	553	2.0	0.9	1	0.5
22.94	72.54	50/5	1288	77	0.91	0.20	0.16	0.75	58	458	2.2	1.2	1	0.5
20.49	74.99	77/9	1433	137	1.04	0.17	0.09	0.96	65	530	2.5	1.1	1	0.5

### B.1.10.2. Test Pile P9P12 (Ramp A)

Elevation	Depth	SPT FB-3	FMX	bl/ft	DMX	DFN	iSET	Rebound	SFT	EBR	CSX	TSX	FVP	Jc
feet	feet	N <sub>safe</sub>	kips		inches	inches	inches	inches	kips	kips	ksi	ksi		
77.83	18.37	16	765	2	3.05	2.80	5.33	-2.28	0	0	1.30	0.90	1	0.4
75.50	20.71	9	767	3	4.07	4.05	4.00	0.07	0	0	1.30	0.90	1	0.4
72.83	23.37	6	615	3	4.36	4.36	4.50	-0.14	0	0	1.08	0.63	0.93	0.4
70.27	25.93	9	548	3	4.36	4.36	4.67	-0.31	0	0	0.97	0.50	0.90	0.4
67.83	28.37	5	673	2	4.59	4.59	6.00	-1.41	0	0	1.17	0.73	1	0.4
65.33	30.87	5	620	2	4.56	4.56	6.00	-1.44	0	0	1.10	0.67	0.90	0.4
62.83	33.37	10	612	4	3.74	3.72	3.00	0.74	0	0	1.06	0.64	0.90	0.4
60.44	35.77	11	740	4	3.68	3.65	3.25	0.43	0	0	1.28	0.83	1	0.4
57.83	38.37	15	715	4	3.17	3.10	3.20	-0.03	0	0	1.22	0.80	1	0.4
55.33	40.87	2	674	5	3.33	3.30	2.40	0.93	0	0	1.18	0.70	1	0.4
52.83	43.37	3	660	3	4.61	4.61	4.50	0.11	0	0	1.13	0.70	1	0.4
50.33	45.87	2	633	3	4.08	4.08	4.00	0.08	0	0	1.10	0.67	1	0.4
47.83	48.37	4	640	3	3.55	3.55	4.00	-0.45	0	0	1.10	0.63	1	0.4
45.33	50.87	3	633	3	3.19	3.16	4.00	-0.81	0	0	1.13	0.63	1	0.4
42.83	53.37	2	663	3	3.24	3.22	3.75	-0.51	0	0	1.18	0.70	1	0.4
40.44	55.77	3	660	4	2.97	2.89	3.25	-0.28	0	0	1.15	0.70	0.98	0.4
37.83	58.37	3	625	4	2.78	2.66	2.88	-0.10	0	0	1.08	0.64	0.92	0.4
35.33	60.87	2	627	3	2.98	2.89	4.00	-1.02	0	0	1.10	0.63	0.90	0.4
32.83	63.37	6	712	4	3.17	3.11	3.00	0.17	0	0	1.24	0.78	1	0.4
30.33	65.87	4	800	4	3.19	3.15	3.00	0.19	0	0	1.40	0.90	1	0.4
27.83	68.37	6	864	3	3.62	3.57	3.60	0.02	0	0	1.50	1.00	1	0.4
25.31	70.89	11	926	5	2.50	2.23	2.36	0.14	0	25	1.60	1.03	1	0.4
22.81	73.39	72/11	1149	57	0.91	0.16	0.21	0.70	43	427	1.99	1.19	1	0.4
20.58	75.62	86/11	1351.1	240	1.00	0.06	0.05	0.95	66	431	2.36	1.25	1	0.4

### B.1.10.3. Test Pile P10P14 (Ramp A)

Elevation	Depth	SPT FB-4	FMX	bl/ft	DMX	DFN	iSET	Rebound	SFT	EBR	CSX	TSX	FVP	Jc
feet	feet	N <sub>safe</sub>	kips		inches	inches	inches	inches	kips	kips	ksi	ksi		
78.38	17.42	18	783	5	1.60	0.95	2.40	-0.80	0	132	1.3	0.6	0.96	0.4
75.73	20.07	27	958	4	1.87	1.33	3.00	-1.13	0	164	1.4	0.8	1	0.4
73.31	22.49	38	828	3	3.59	3.54	3.67	-0.08	0	134	1.4	0.8	1	0.4
70.89	24.91	13	621	5	4.30	4.30	2.55	1.75	0	139	1.4	0.8	1	0.4
68.35	27.45	6	571	4	3.31	3.26	3.00	0.31	0	166	1.5	0.9	1	0.4
65.98	29.82	3	712	5	2.87	2.70	2.40	0.47	0	0	1.6	1.0	1	0.4
63.35	32.45	4	723	4	3.21	3.10	2.85	0.36	0	0	0.8	0.5	0.88	0.4
61.04	34.76	6	740	4	3.27	3.18	3.20	0.07	0	0	0.9	0.4	0.83	0.4
58.38	37.42	6	680	5	3.55	3.49	2.40	1.15	0	0	1.2	0.7	0.90	0.4
56.08	39.72	6	654	5	3.02	2.86	2.63	0.39	0	0	1.3	0.8	0.90	0.4
53.31	42.49	4	629	3	2.97	2.81	4.00	-1.03	0	0	1.3	0.8	0.90	0.4
50.98	44.82	4	644	3	3.00	2.85	4.00	-1.00	0	0	1.2	0.7	0.90	0.4
48.35	47.45	2	646	4	2.77	2.56	3.00	-0.24	0	0	1.2	0.7	0.90	0.4
45.85	49.95	5	628	4	2.55	2.30	3.00	-0.46	0	0	1.1	0.6	0.90	0.4
43.14	52.66	6	761	3	3.05	2.88	4.00	-0.95	0	0	1.1	0.6	0.90	0.4
41.04	54.76	5	786	4	3.03	2.83	3.20	-0.17	0	0	1.1	0.6	0.90	0.4
38.38	57.42	3	818	4	2.97	2.80	2.72	0.25	0	0	1.1	0.6	0.90	0.4
35.95	59.85	5	808	4	3.32	3.21	2.76	0.56	0	0	1.2	0.7	0.90	0.4
33.31	62.49	5	797	3	3.30	3.19	4.00	-0.70	0	0	1.4	0.9	0.90	0.4
30.85	64.95	2	810	4	3.09	2.97	3.00	0.09	0	0	1.4	0.9	0.90	0.4
28.38	67.42	5	799	5	3.06	2.91	2.40	0.66	0	0	1.4	0.9	0.90	0.4
25.98	69.82	4	801	5	3.45	3.39	2.40	1.05	0	0	1.4	0.8	0.90	0.4
23.35	72.45	6	800	4	3.46	3.40	3.00	0.46	0	0	1.4	0.9	0.90	0.4
20.85	74.95	4	820	4	3.53	3.48	3.00	0.53	0	0	1.4	0.9	0.90	0.4
18.38	77.42	17	828	5	3.44	3.35	2.26	1.18	0	0	1.4	0.8	0.90	0.4
15.93	79.87	82/9	898	8	2.74	2.47	1.58	1.16	0	0	1.4	0.8	0.91	0.4
13.36	82.44	50/5	1086	18	1.39	0.51	0.68	0.71	0	0	1.5	0.9	0.97	0.4
10.86	84.94	90/11	1056	52	0.98	0.39	0.23	0.75	26	305	1.9	1.1	1	0.4
8.41	87.39	50/5	1151	84	0.73	0.24	0.14	0.59	61	369	1.9	1.0	1	0.4
5.84	89.96	57	1322	112	0.94	0.18	0.11	0.84	73	365	2.3	1.1	1	0.4
3.32	92.48	57	1445	64	0.75	0.42	0.19	0.56	100	543	2.6	1.2	1	0.4

## B.1.11. I-4 and SR-406 Intersection

### B.1.11.1. Test Pile P2P5 (Ramp B5)

Elevation	Depth	SPT B-110	FMX	b/ft	DMX	DFN	iSET	Rebound	SFT	EBR	CSX	TSX	FVP	Jc
feet	feet	N <sub>safe</sub>	kips		inches	inches	inches	inches	kips	kips	ksi	ksi		
91.85	11.45	4	557	9	1.23	0.83	1.29	-0.06	-	-	-	-	1	-
90.25	13.05	5	630	12	1.09	0.67	1.00	0.10	-	-	-	-	1	-
88.86	14.44	6	612	16	0.90	0.50	0.77	0.13	-	-	-	-	1	-
86.35	16.95	7	643	17	0.86	0.34	0.72	0.14	-	-	-	-	1	-
83.83	19.47	6	667	15	0.90	0.45	0.79	0.11	-	-	-	-	1	-
81.39	21.91	8	643	14	0.88	0.51	0.89	-0.01	-	-	-	-	1	-
78.83	24.47	3	650	15	0.85	0.48	0.78	0.07	-	-	-	-	1	-
76.34	26.96	3	522	24	0.60	0.34	0.50	0.10	-	-	-	-	1	-
73.84	29.46	2	522	24	0.62	0.28	0.50	0.12	-	-	-	-	1	-
71.25	32.05	2	514	28	0.54	0.00	0.42	0.12	-	-	-	-	1	-
68.80	34.50	10	563	25	0.64	0.21	0.48	0.16	-	-	-	-	1	-
66.29	37.01	11	564	33	0.56	-0.05	0.37	0.19	-	-	-	-	1	-
63.78	39.52	1	595	42	0.53	-0.10	0.29	0.24	-	-	-	-	1	-
61.26	42.04	7	599	42	0.52	-0.09	0.28	0.23	-	-	-	-	1	-
58.81	44.49	5	612	46	0.50	-0.07	0.26	0.24	-	-	-	-	1	-
56.34	46.96	1	628	41	0.55	0.13	0.29	0.26	-	-	-	-	1	-
53.80	49.50	1	672	38	0.58	-0.02	0.31	0.27	-	-	-	-	1	-
51.32	51.98	2	639	39	0.54	0.14	0.31	0.23	-	-	-	-	1	-
48.85	54.45	6	721	31	0.55	0.21	0.38	0.16	-	-	-	-	1	-
46.29	57.01	14	762	39	0.45	0.11	0.31	0.15	-	-	-	-	1	-
43.84	59.46	15	778	45	0.44	0.10	0.27	0.17	-	-	-	-	1	-
41.29	62.01	14	771	44	0.44	0.14	0.27	0.17	-	-	-	-	1	-
38.80	64.50	9	771	44	0.44	0.20	0.27	0.17	-	-	-	-	1	-
36.28	67.02	10	808	49	0.42	0.10	0.25	0.18	-	-	-	-	1	-
33.85	69.45	11	706	42	0.53	0.08	0.29	0.25	-	-	-	-	1	-
31.28	72.02	12	778	35	0.66	0.09	0.34	0.32	-	-	-	-	1	-
28.80	74.50	50	780	54	0.63	-0.02	0.22	0.40	-	-	-	-	1	-
26.33	76.97	51	901	75	0.52	-0.14	0.16	0.36	-	-	-	-	1	-
23.79	79.51	26	972	53	0.61	-0.03	0.23	0.38	-	-	-	-	1	-
21.29	82.01	26	986	43	0.63	0.02	0.28	0.35	-	-	-	-	1	-
18.83	84.48	51	990	38	0.66	0.09	0.32	0.34	-	-	-	-	1	-
16.31	86.99	35	942	36	0.65	0.08	0.34	0.31	-	-	-	-	1	-
13.88	89.42	13	936	34	0.66	0.12	0.36	0.30	-	-	-	-	1	-
11.28	92.02	16	899	36	0.62	-0.02	0.33	0.29	-	-	-	-	1	-
8.77	94.53	84	894	108	0.59	-0.22	0.11	0.48	-	-	-	-	1	-

## B.2. SPT Borings and Soil Correlations

### B.2.1. I-4 / US-192 Interchange

#### B.2.1.1. SPT B-27 (EB1P3, Ramp BD)

Depth (ft)	Elevation (ft)	USCS	FC actual/estimate	B-27 Nsafe	SPT N60	SPT Ntrip	SPT (N1)60	SPT (N1)60t	SPT (N1)trip	SPT (N1)60ta	u psf	$\sigma'_{vo}$ (avg) psf	Rebound inch
0	90.12	SP-SM					-						
1.5	88.62	PT		20	15	12	30	30	23	30	0	150	
3.5	86.62	SM	12	10	8	6	15	15	12	20	17	355	
5.5	84.62	PT	54	3	2	2	5	5	4	14	142	415	
7.5	82.62	SM	12	11	8	7	16	18	14	23	267	505	
9.5	80.62	SP-SM	8.5	2	2	1	3	3	2	7	392	577	
12.5	77.62	SP-SM	8.5	15	11	10	19	21	16	25	579	736	
15	75.12	SP-SM	8.5	34	29	22	43	43	33	47	735	900	
17.5	72.62	SP-SM	8.5	43	37	28	50	50	38	54	891	1079	
20	70.12	SP-SM	8.5	54	51	39	65	65	50	69	1047	1260	0.05
22.5	67.62	SP	0	39	37	28	44	44	34	44	1203	1442	0.00
25	65.12	SP	0	39	37	28	41	41	32	41	1359	1623	0.33
27.5	62.62	SP-SM	8.5	60	57	44	60	60	46	64	1515	1805	0.33
30	60.12	SP-SM	8.5	39	39	30	39	39	30	43	1671	1976	0.35
32.5	57.62	SP-SM	8.5	13	13	11	13	14	11	18	1827	2125	0.28
35	55.12	SP-SM	8.5	3	3	3	3	3	2	7	1983	2214	0.22
37.5	52.62	SM	43	WH	WH	WH	0	0	0	8	2139	2245	0.08
40	50.12	SM	12	3	3	3	3	3	2	8	2295	2294	0.10
42.5	47.62	SM	12	WH	WH	WH	0	0	0	5	2451	2320	0.02
45	45.12	SM	12	7	7	6	6	7	5	12	2607	2399	0.14
47.5	42.62	SM	12	12	12	10	11	12	9	17	2763	2513	0.14
50	40.12	SM	12	11	11	9	10	11	8	16	2919	2632	0.15
52.5	37.62	SM	12	10	10	9	9	9	7	15	3075	2751	0.15
55	35.12	SM	12	7	7	6	6	7	5	12	3231	2850	0.27
57.5	32.62	SM	12	9	9	8	7	8	6	13	3387	2954	0.15
60	30.12	SM	12	10	10	9	8	9	7	14	3543	3061	0.23
62.5	27.62	SM	12	17	17	15	13	15	12	20	3699	3187	0.57
65	25.12	SM	12	17	17	15	13	15	11	20	3855	3319	0.92
67.5	22.62	CL	66	20	20	17	15	-	-	-	4011	3480	0.91
70	20.12	SM	12	25	25	21	19	21	16	26	4167	3619	0.66
72.5	17.62	SM	12	16	16	14	12	13	10	18	4323	3741	0.63
75	15.12	SM	12	25	25	21	18	20	15	25	4479	3870	0.62
77.5	12.62	SM	12	25	25	21	18	20	15	25	4635	4001	0.46
80	10.12	CL	56	14	14	12	10	-	-	-	4791	4153	0.42
82.5	7.62	SM	12	16	16	14	11	12	9	17	4947	4279	0.39
85	5.12	SM	12	18	18	15	12	13	10	19	5103	4398	0.39
87.5	2.62	SM	12	14	14	12	9	10	8	16	5259	4517	0.42
90	0.12	GWL		43	43	33	28	28	22	28	5415	4696	0.34
92.5	-2.38	GWL		58	58	45	37	37	29	37	5571	4900	
95	-4.88	GWL		18	18	15	11	13	10	13	5727	5077	
97.5	-7.38	GWL		22	22	19	14	15	12	15	5883	5256	
100	-9.88	GWL		23	23	20	14	15	12	15	6039	5437	
102.5	-12.38	GWL		35	35	27	21	21	16	21	6195	5619	
105	-14.88	GWL		25	25	21	15	16	13	16	6351	5800	
107.5	-17.38	GWL		18	18	15	10	12	9	12	6507	5972	
110	-19.88	GWL		28	28	24	16	18	14	18	6663	6151	
112.5	-22.38	GWL		32	32	27	18	20	15	20	6819	6332	
115	-24.88	GWL		11	11	9	6	7	5	7	6975	6484	

Depth (ft)	Elevation (ft)	USCS	Rebound inch	Liquefaction Soil Response	Terzaghi Dr	Schmertmann Φ'	Hatanaka Φ'	Peck Φ'	Mayne OCR	Hera Cu (psf)	Hettiarachchi Cu (psf)	CDOT Qu (psf)
0	90.12	SP-SM										
1.5	88.62	PT		Intermediate	71%	46	41	31				
3.5	86.62	SM		Intermediate	50%	38	35	29				
5.5	84.62	PT		Contractive	27%	27	29	28				
7.5	82.62	SM		Intermediate	52%	38	37	30				
9.5	80.62	SP-SM		Contractive	22%	23	27	28				
12.5	77.62	SP-SM		Intermediate	56%	40	38	30				
15	75.12	SP-SM		Dilative	85%	48	46	35				
17.5	72.62	SP-SM		Dilative	91%	49	48	37				
20	70.12	SP-SM	0.05	Dilative	104%	52	52	41				
22.5	67.62	SP	0.00	Dilative	85%	48	46	37				
25	65.12	SP	0.33	Dilative	83%	47	45	37				
27.5	62.62	SP-SM	0.33	Dilative	100%	51	50	42				
30	60.12	SP-SM	0.35	Dilative	81%	47	45	38				
32.5	57.62	SP-SM	0.28	Contractive	46%	36	35	31				
35	55.12	SP-SM	0.22	Contractive	22%	24	27	28				
37.5	52.62	SM	0.08	Contractive	0%	0	20	27				
40	50.12	SM	0.10	Contractive	22%	23	27	28				
42.5	47.62	SM	0.02	Contractive	0%	0	20	27				
45	45.12	SM	0.14	Contractive	33%	30	30	29				
47.5	42.62	SM	0.14	Contractive	42%	34	34	31				
50	40.12	SM	0.15	Contractive	40%	33	33	30				
52.5	37.62	SM	0.15	Contractive	38%	32	32	30				
55	35.12	SM	0.27	Contractive	31%	29	30	29				
57.5	32.62	SM	0.15	Contractive	35%	31	31	30				
60	30.12	SM	0.23	Contractive	37%	31	32	30				
62.5	27.62	SM	0.57	Intermediate	47%	36	35	32				
65	25.12	SM	0.92	Contractive	47%	36	35	32				
67.5	22.62	CL	0.91	-					5.217	966	1640	3790
70	20.12	SM	0.66	Intermediate	56%	39	38	34				
72.5	17.62	SM	0.63	Contractive	44%	34	34	32				
75	15.12	SM	0.62	Intermediate	55%	38	38	34				
77.5	12.62	SM	0.46	Intermediate	54%	38	37	34				
80	10.12	CL	0.42	-					3.613	747	1148	2429
82.5	7.62	SM	0.39	Contractive	43%	33	34	32				
85	5.12	SM	0.39	Contractive	45%	34	34	32				
87.5	2.62	SM	0.42	Contractive	39%	32	33	31				
90	0.12	GWL	0.34	Intermediate								
92.5	-2.38	GWL		Dilative								
95	-4.88	GWL		Contractive								
97.5	-7.38	GWL		Contractive								
100	-9.88	GWL		Contractive								
102.5	-12.38	GWL		Intermediate								
105	-14.88	GWL		Contractive								
107.5	-17.38	GWL		Contractive								
110	-19.88	GWL		Contractive								
112.5	-22.38	GWL		Contractive								
115	-24.88	GWL		Contractive								

### B.2.1.2. SPT B-40 (P7P10, Ramp CA)

Depth (ft)	Elevation (ft)	USCS	FC actual/estimate	B-40 Nsafe	SPT N60	SPT Ntrip	SPT (N1)60	SPT (N1)60t	SPT (N1)trip	SPT (N1)60ta	u psf	$\sigma'_{vo}$ (avg) psf	Rebound inch
0	108.6												
1.5	107.1	SP-SM	8.5	4	3	2	6	6	5	10	0	143	
3.5	105.1	SP-SM	8.5	12	9	7	18	18	14	22	0	410	
5.5	103.1	SP-SM	8.5	44	33	25	56	56	43	60	0	705	
7.5	101.1	SP-SM	8.5	76	57	44	80	80	62	84	0	1005	
9.5	99.1	SM	17	27	20	16	25	25	20	31	0	1275	
12.5	96.1	SM	12	6	5	3	5	5	4	10	0	1583	
15	93.6	SM	12	19	16	12	17	17	13	22	0	1913	
17.5	91.1	SP-SM	8.5	33	28	22	26	26	20	30	0	2283	
20	88.6	SM	12	27	26	20	22	22	17	28	0	2633	
22.5	86.1	SM	12	16	15	13	13	14	11	19	156	2822	
25	83.6	SM	12	80	76	58	62	62	47	67	312	3048	
27.5	81.1	SM	12	69	66	50	51	51	39	56	468	3282	
30	78.6	SP-SM	6	66	66	51	50	50	38	51	624	3529	
32.5	76.1	SM	12	95/10	95/10	95/10	73	73	73	78	780	3765	
35	73.6	SP-SM	8.5	72	72	55	51	51	39	55	936	4012	
37.5	71.1	SP-SM	8.5	81/11.5	81/11.5	81/11.5	69	69	69	73	1092	4261	
40	68.6	SP-SM	8.5	50/4.5	50/4.5	50/4.5	67	67	67	71	1248	4510	
42.5	66.1	SP-SM	8.5	50/4.5	50/4.5	50/4.5	65	65	65	69	1404	4759	
45	63.6	SP-SM	8.5	50/3	50/3	50/3	63	63	63	67	1560	5008	0.44
47.5	61.1	SP	3	31	31	26	19	21	16	21	1716	5232	0.42
50	58.6	SP	0	67	67	52	40	40	31	40	1872	5476	0.35
52.5	56.1	SP	0	20	20	17	12	13	10	13	2028	5687	0.27
55	53.6	SP-SM	8.5	10	10	9	6	6	5	10	2184	5854	0.23
57.5	51.1	SM	12	3	3	3	2	2	1	7	2340	5950	0.17
60	48.6	SM	29	1	1	1	1	1	0	8	2496	6022	0.17
62.5	46.1	SM	12	2	2	2	1	1	1	6	2652	6091	0.15
65	43.6	SM	12	WH	WH	WH	0	0	0	5	2808	6147	0.15
67.5	41.1	SM	12	9	9	8	5	6	4	11	2964	6264	0.17
70	38.6	SM	12	10	10	9	6	6	5	11	3120	6405	0.20
72.5	36.1	SM	12	9	9	8	5	6	4	11	3276	6537	0.16
75	33.6	SM	12	8	8	7	4	5	4	10	3432	6653	0.21
77.5	31.1	SM	12	10	10	9	5	6	5	11	3588	6780	0.20
80	28.6	SM	12	10	10	9	5	6	5	11	3744	6909	0.25
82.5	26.1	SM	12	23	23	20	12	14	10	19	3900	7075	0.32
85	23.6	SM	27	14	14	12	7	8	6	15	4056	7237	0.37
87.5	21.1	SM	12	17	17	15	9	10	8	15	4212	7408	0.41
92.5	16.1	SM	12	25	25	21	13	14	11	19	4524	7726	0.40
95	13.6	SM	12	28	28	24	14	16	12	21	4680	7915	0.53
97.5	11.1	SM	12	24	24	21	12	13	10	18	4836	8092	0.64
100	8.6	SM	12	28	28	24	14	15	12	20	4992	8278	0.50
102.5	6.1	SM	12	21	21	18	10	11	9	17	5148	8455	0.49
105	3.6	SM	26	14	14	12	7	7	6	14	5304	8616	0.43
107.5	1.1	SM	12	21	21	18	10	11	9	16	5460	8788	0.41
110	-1.4	SM	12	20	20	17	9	10	8	16	5616	8962	0.43
112.5	-3.9	TSWLS		15	15	13	7	8	6	8	5772	9173	0.41
115	-6.4	TWL		11	11	9	5	6	4	6	5928	9380	0.39
117.5	-8.9	TWL		6	6	5	3	3	2	3	6084	9559	
120	-11.4	TWL		50/3	50/3	50/3	45	45	45	45	6240	9833	
122.5	-13.9	TWL		12	12	10	5	6	5	6	6396	10052	
125	-16.4	TWL		12	12	10	5	6	5	6	6552	10256	
127.5	-18.9	TWL		38	38	32	17	18	14	18	6708	10497	
130	-21.4	TWL		50/2	50/2	50/2	43	43	43	43	6864	10771	

Depth (ft)	Elevation (ft)	USCS	Rebound inch	Liquefaction Soil Response	Terzaghi Dr	Schmertmann Φ'	Hatanaka Φ'	Peck Φ'	Mayne OCR	Hera Cu (psf)	Hettiarachchi Cu (psf)	CDOT Qu (psf)
0	108.6											
1.5	107.1	SP-SM		Contractive	32%	31	30	28				
3.5	105.1	SP-SM		Intermediate	55%	39	37	30				
5.5	103.1	SP-SM		Dilative	96%	50	49	36				
7.5	101.1	SP-SM		Dilative	116%	54	55	42				
9.5	99.1	SM		Dilative	65%	43	40	33				
12.5	96.1	SM		Contractive	29%	28	29	28				
15	93.6	SM		Intermediate	52%	39	36	32				
17.5	91.1	SP-SM		Dilative	66%	43	40	35				
20	88.6	SM		Intermediate	61%	41	39	34				
22.5	86.1	SM		Contractive	46%	36	35	32				
25	83.6	SM		Dilative	101%	50	51	47				
27.5	81.1	SM		Dilative	92%	49	48	44				
30	78.6	SP-SM		Dilative	91%	48	48	45				
32.5	76.1	SM		Dilative	110%	52	58	52				
35	73.6	SP-SM		Dilative	92%	48	48	46				
37.5	71.1	SP-SM		Dilative	107%	51	57	52				
40	68.6	SP-SM		Dilative	105%	50	56	52				
42.5	66.1	SP-SM		Dilative	104%	50	56	52				
45	63.6	SP-SM	0.44	Dilative	103%	49	56	52				
47.5	61.1	SP	0.42	Intermediate	57%	38	38	36				
50	58.6	SP	0.35	Dilative	82%	45	45	45				
52.5	56.1	SP	0.27	Contractive	44%	33	34	33				
55	53.6	SP-SM	0.23	Contractive	31%	27	30	30				
57.5	51.1	SM	0.17	Contractive	17%	19	25	28				
60	48.6	SM	0.17	Contractive	10%	13	23	27				
62.5	46.1	SM	0.15	Contractive	14%	16	24	28				
65	43.6	SM	0.15	Contractive	0%	0	20	27				
67.5	41.1	SM	0.17	Contractive	29%	26	29	30				
70	38.6	SM	0.20	Contractive	31%	27	30	30				
72.5	36.1	SM	0.16	Contractive	29%	26	29	30				
75	33.6	SM	0.21	Contractive	27%	25	29	29				
77.5	31.1	SM	0.20	Contractive	30%	26	30	30				
80	28.6	SM	0.25	Contractive	30%	26	30	30				
82.5	26.1	SM	0.32	Contractive	45%	33	34	34				
85	23.6	SM	0.37	Contractive	35%	28	31	31				
87.5	21.1	SM	0.41	Contractive	38%	30	32	32				
92.5	16.1	SM	0.40	Contractive	46%	33	35	34				
95	13.6	SM	0.53	Intermediate	48%	34	36	35				
97.5	11.1	SM	0.64	Contractive	45%	32	34	34				
100	8.6	SM	0.50	Intermediate	48%	33	35	35				
102.5	6.1	SM	0.49	Contractive	41%	31	33	33				
105	3.6	SM	0.43	Contractive	34%	27	31	31				
107.5	1.1	SM	0.41	Contractive	41%	30	33	33				
110	-1.4	SM	0.43	Contractive	40%	30	33	33				
112.5	-3.9	TSWLS	0.41	Contractive								
115	-6.4	TWL	0.39	Contractive								
117.5	-8.9	TWL		Contractive								
120	-11.4	TWL		Dilative								
122.5	-13.9	TWL		Contractive								
125	-16.4	TWL		Contractive								
127.5	-18.9	TWL		Contractive								
130	-21.4	TWL		Dilative								

### B.2.1.3. SPT B-41 (P8P4, Ramp CA)

Depth (ft)	Elevation (ft)	USCS	FC actual/estimate	B-41 Nsafe	SPT N60	SPT Ntrip	SPT (N1)60	SPT (N1)60t	SPT (N1)trip	SPT (N1)60ta	u psf	$\sigma'_{vo}$ (avg) psf	Rebound inch
0	90.2												
1.5	88.7	SP	0	HA							0	174	
3.5	86.7	SP-SM	8.5	HA							0	409	
5.5	84.7	SP-SM	8.5	HA							50	616	
7.5	82.7	SP-SM	8.5	22	17	13	27	27	21	31	175	745	
9.5	80.7	SP-SM	8.5	46	35	27	52	52	40	56	300	884	
12.5	77.7	SP-SM	8.5	59	44	34	60	60	46	64	487	1102	
15	75.2	SP-SM	8.5	50/5.5	50/5.5	50/5.5	106	106	106	110	643	1283	
17.5	72.7	SP-SM	8.5	69	59	45	69	69	53	73	799	1465	
20	70.2	SP-SM	9	51	48	37	53	53	41	57	955	1646	0.03
22.5	67.7	SP-SM	8.5	13	12	11	13	14	11	18	1111	1798	0.27
25	65.2	SP-SM	8.5	12	11	10	12	13	10	17	1267	1942	0.30
27.5	62.7	SP-SM	8.5	9	9	7	8	9	7	13	1423	2066	0.29
30	60.2	SP-SM	8.5	13	13	11	12	14	11	18	1579	2195	0.33
32.5	57.7	SP	0	23	23	18	21	21	16	21	1735	2346	0.31
35	55.2	SP	0	6	6	5	5	6	5	6	1891	2463	0.27
37.5	52.7	SP-SM	8.5	4	4	4	4	4	4	8	2047	2549	0.17
40	50.2	SM	12	2	2	2	2	2	1	7	2203	2601	0.16
42.5	47.7	SM	32	2	2	2	2	2	2	9	2359	2645	0.13
45	45.2	SM	12	2	2	2	2	2	1	7	2515	2689	0.15
47.5	42.7	SM	12	1	1	1	1	1	1	6	2671	2723	0.18
50	40.2	SM	12	WR	WR	WR	0	0	0	5	2827	2744	0.21
52.5	37.7	SM	12	10	10	9	8	9	7	15	2983	2833	0.20
55	35.2	SM	12	7	7	6	6	6	5	12	3139	2930	0.20
57.5	32.7	SM	12	8	8	7	6	7	6	12	3295	3034	0.21
60	30.2	SM	12	12	12	10	10	11	8	16	3451	3150	0.27
65	25.2	SM	12	16	16	14	12	14	11	19	3763	3388	0.64
67.5	22.7	SM	50	17	17	15	13	14	11	23	3919	3517	0.66
70	20.2	SM	50	17	17	15	13	14	11	23	4075	3649	0.83
72.5	17.7	SM	12	20	20	17	15	16	12	21	4231	3780	0.90
75	15.2	SM	12	22	22	19	16	17	13	23	4387	3912	0.57
77.5	12.7	SM	12	26	26	22	18	20	16	26	4543	4043	0.29
80	10.2	SM	12	24	24	21	17	18	14	24	4699	4175	0.75
82.5	7.7	SM	12	22	22	19	15	17	13	22	4855	4306	0.44
85	5.2	SM	60	18	18	15	12	13	10	23	5011	4428	0.43
87.5	2.7	SM	12	14	14	12	9	10	8	16	5167	4547	0.41
90	0.2	SM	12	19	19	16	12	14	11	19	5323	4676	0.44
92.5	-2.3	SM	12	19	19	16	12	14	10	19	5479	4797	0.37
95	-4.8	TSWL		56	56	43	35	35	27	35	5635	4986	
97.5	-7.3	TWL		13	13	11	8	9	7	9	5791	5163	
100	-9.8	TSWL		24	24	21	15	16	13	16	5947	5342	
102.5	-12.3	TSWL		20	20	17	12	13	10	13	6103	5513	
105	-14.8	TSWL		56	56	43	33	33	26	33	6259	5702	
107.5	-17.3	TSWL		11	11	9	6	7	5	7	6415	5866	
110	-19.8	TWL		12	12	10	7	8	6	8	6571	6023	
112.5	-22.3	TSWL		24	24	21	14	15	12	15	6727	6199	

Depth (ft)	Elevation (ft)	USCS	Rebound inch	Liquefaction Soil Response	Terzaghi Dr	Schmertmann Φ'	Hatanaka Φ'	Peck Φ'	Mayne OCR	Hera Cu (psf)	Hettiarachchi Cu (psf)	CDOT Qu (psf)
0	90.2											
1.5	88.7	SP		Contractive								
3.5	86.7	SP-SM		Contractive								
5.5	84.7	SP-SM		Contractive								
7.5	82.7	SP-SM		Dilative	67%	43	40	32				
9.5	80.7	SP-SM		Dilative	93%	50	48	37				
12.5	77.7	SP-SM		Dilative	100%	51	50	39				
15	75.2	SP-SM		Dilative	133%	58	66	52				
17.5	72.7	SP-SM		Dilative	107%	52	52	43				
20	70.2	SP-SM	0.03	Dilative	94%	50	49	40				
22.5	67.7	SP-SM	0.27	Contractive	47%	36	35	31				
25	65.2	SP-SM	0.30	Contractive	44%	35	34	30				
27.5	62.7	SP-SM	0.29	Contractive	37%	32	32	30				
30	60.2	SP-SM	0.33	Contractive	45%	36	35	31				
32.5	57.7	SP	0.31	Intermediate	59%	41	38	34				
35	55.2	SP	0.27	Contractive	30%	28	30	29				
37.5	52.7	SP-SM	0.17	Contractive	24%	25	29	28				
40	50.2	SM	0.16	Contractive	17%	20	25	28				
42.5	47.7	SM	0.13	Contractive	17%	20	26	28				
45	45.2	SM	0.15	Contractive	17%	20	25	28				
47.5	42.7	SM	0.18	Contractive	12%	16	24	27				
50	40.2	SM	0.21	Contractive	0%	0	20	27				
52.5	37.7	SM	0.20	Contractive	37%	32	32	30				
55	35.2	SM	0.20	Contractive	31%	29	30	29				
57.5	32.7	SM	0.21	Contractive	33%	29	31	29				
60	30.2	SM	0.27	Contractive	40%	33	33	31				
65	25.2	SM	0.64	Contractive	45%	35	34	32				
67.5	22.7	SM	0.66	Intermediate	46%	35	35	32				
70	20.2	SM	0.83	Intermediate	46%	35	35	32				
72.5	17.7	SM	0.90	Intermediate	49%	36	36	33				
75	15.2	SM	0.57	Intermediate	51%	37	36	33				
77.5	12.7	SM	0.29	Intermediate	55%	38	38	35				
80	10.2	SM	0.75	Intermediate	53%	37	37	34				
82.5	7.7	SM	0.44	Intermediate	50%	36	36	33				
85	5.2	SM	0.43	Intermediate	45%	34	34	32				
87.5	2.7	SM	0.41	Contractive	39%	32	33	31				
90	0.2	SM	0.44	Contractive	46%	34	35	33				
92.5	-2.3	SM	0.37	Contractive	45%	34	34	33				
95	-4.8	TSWL		Dilative								
97.5	-7.3	TWL		Contractive								
100	-9.8	TSWL		Contractive								
102.5	-12.3	TSWL		Contractive								
105	-14.8	TSWL		Dilative								
107.5	-17.3	TSWL		Contractive								
110	-19.8	TWL		Contractive								
112.5	-22.3	TSWL		Contractive								

### B.2.1.4. SPT B-46 (P2P8, Ramp D2)

Depth	Elevation	USCS	FC	B-46	SPT	SPT	SPT	SPT	SPT	SPT	u	$\sigma'_{vo}$ (avg)	Rebound
(ft)	(ft)		actual/estimate	Nsafe	N60	Ntrip	(N1)60	(N1)60t	(N1)trip	(N1)60ta	psf	psf	inch
0	91.8												
1.5	90.3	SP-SM	8.5	HA	5	4	10	10	8	14	0	158	
3.5	88.3	SP-SM	8.5	HA	5	4	10	10	8	14	0	420	
5.5	86.3	SM	12	HA	5	4	9	10	8	15	56	636	
7.5	84.3	SM	12	6	5	4	7	8	6	13	181	777	
9.5	82.3	SM	17	12	9	8	13	15	11	20	306	934	
12.5	79.3	SM	12	12	9	8	12	13	10	18	493	1135	
15	76.8	SM	12	10	10	9	12	14	11	19	649	1309	
17.5	74.3	SM	12	10	10	9	12	13	10	18	805	1483	
20	71.8	SM	29	8	8	6	8	9	7	16	961	1644	
22.5	69.3	SP	5	17	16	14	17	19	14	19	1117	1853	
25	66.8	SP	5	20	19	16	19	21	16	21	1273	2072	
27.5	64.3	SP	5	25	24	18	22	22	17	22	1429	2291	
30	61.8	SP	5	29	29	22	26	26	20	26	1585	2523	
32.5	59.3	SP	5	28	28	22	24	24	18	24	1741	2744	
35	56.8	SP-SM	8.5	10	10	9	8	9	7	13	1897	2926	
37.5	54.3	SP-SM	8.5	23	23	20	18	20	16	24	2053	3125	
40	51.8	SP-SM	8	16	16	14	12	14	11	17	2209	3316	
42.5	49.3	SP-SM	8.5	12	12	10	9	10	8	14	2365	3505	
45	46.8	SP-SM	8.5	16	16	14	12	13	10	17	2521	3694	
47.5	44.3	SP-SM	8.5	31	31	24	22	22	17	26	2677	3896	-0.10
50	41.8	SP-SM	8.5	51	51	39	36	36	27	40	2833	4125	0.27
52.5	39.3	ML	73	3	3	3	2	-	-	-	2989	4234	0.23
55	36.8	SM	12	18	18	15	12	13	10	19	3145	4393	0.26
57.5	34.3	SM	12	18	18	15	12	13	10	18	3301	4567	0.31
60	31.8	SC	44	6	6	5	4	4	3	13	3457	4691	0.25
62.5	29.3	SM	12	14	14	12	9	10	8	15	3613	4855	0.31
65	26.8	SM	12	9	9	8	6	6	5	12	3769	5004	0.22
67.5	24.3	SM	12	13	13	11	8	9	7	14	3925	5160	0.31
70	21.8	SM	12	13	13	11	8	9	7	14	4081	5319	0.42
72.5	19.3	SM	12	11	11	9	7	7	6	13	4237	5478	0.33
75	16.8	SM	12	16	16	14	10	11	8	16	4393	5650	0.59
77.5	14.3	SM	12	24	24	21	14	16	12	21	4549	5836	0.71
80	11.8	SM	12	50	50	38	29	29	22	34	4705	6038	0.88
82.5	9.3	SM	12	21	21	18	12	13	10	18	4861	6217	0.74
85	6.8	SM	37	19	19	16	11	12	9	20	5017	6391	0.88
87.5	4.3	SM	12	13	13	11	7	8	6	13	5173	6552	0.86
90	1.8	SM	12	12	12	10	7	7	6	12	5329	6711	0.65
92.5	-0.7	SM	12	22	22	19	12	13	10	18	5485	6883	
95	-3.2	SM	12	16	16	14	9	9	7	15	5641	7057	
97.5	-5.7	SM	12	50/2	100	77	52	52	40	58	5797	7281	
100	-8.2	TSWL		53/6	100	77	51	51	40	51	5953	7565	
102.5	-10.7	TSWL		50/2.5	100	77	50	50	39	50	6109	7859	
105	-13.2	TSWL		26	26	22	13	14	11	14	6265	8103	
107.5	-15.7	TSWL		25	25	21	12	14	10	14	6421	8337	
110	-18.2	TSWL		17	17	15	8	9	7	9	6577	8571	
112.5	-20.7	TSWL		50	50	38	24	24	18	24	6733	8817	
115	-23.2	TSWL		18	18	15	8	9	7	9	6889	9054	
117.5	-25.7	TWL		14	14	12	7	7	6	7	7045	9275	
120	-28.2	TWL		16	16	14	7	8	6	8	7201	9494	

Depth (ft)	Elevation (ft)	USCS	Rebound inch	Liquefaction Soil Response	Terzaghi Dr	Schmertmann Φ'	Hatanaka Φ'	Peck Φ'	Mayne OCR	Hera Cu (psf)	Hettiarachchi Cu (psf)	CDOT Qu (psf)
0	91.8											
1.5	90.3	SP-SM		Contractive	41%	35	32	29				
3.5	88.3	SP-SM		Contractive	41%	34	32	29				
5.5	86.3	SM		Contractive	38%	33	32	29				
7.5	84.3	SM		Contractive	35%	31	31	28				
9.5	82.3	SM		Intermediate	47%	37	35	30				
12.5	79.3	SM		Contractive	45%	36	34	30				
15	76.8	SM		Contractive	45%	36	35	30				
17.5	74.3	SM		Contractive	44%	35	34	30				
20	71.8	SM		Contractive	37%	32	32	29				
22.5	69.3	SP		Contractive	53%	39	37	32				
25	66.8	SP		Intermediate	56%	40	38	33				
27.5	64.3	SP		Intermediate	61%	41	38	34				
30	61.8	SP		Intermediate	66%	42	40	35				
32.5	59.3	SP		Intermediate	63%	42	39	35				
35	56.8	SP-SM		Contractive	37%	32	32	30				
37.5	54.3	SP-SM		Intermediate	55%	39	38	34				
40	51.8	SP-SM		Contractive	46%	35	35	32				
42.5	49.3	SP-SM		Contractive	39%	32	32	31				
45	46.8	SP-SM		Contractive	44%	34	34	32				
47.5	44.3	SP-SM	-0.10	Intermediate	61%	40	38	36				
50	41.8	SP-SM	0.27	Dilative	77%	44	43	41				
52.5	39.3	ML	0.23	-					1.233	247	246	515
55	36.8	SM	0.26	Contractive	45%	34	34	32				
57.5	34.3	SM	0.31	Contractive	45%	34	34	32				
60	31.8	SC	0.25	Contractive	26%	25	28	29				
62.5	29.3	SM	0.31	Contractive	39%	31	32	31				
65	26.8	SM	0.22	Contractive	31%	27	30	30				
67.5	24.3	SM	0.31	Contractive	37%	30	32	31				
70	21.8	SM	0.42	Contractive	36%	30	32	31				
72.5	19.3	SM	0.33	Contractive	33%	28	31	30				
75	16.8	SM	0.59	Contractive	40%	31	33	32				
77.5	14.3	SM	0.71	Intermediate	48%	35	35	34				
80	11.8	SM	0.88	Dilative	69%	41	41	41				
82.5	9.3	SM	0.74	Contractive	45%	33	34	33				
85	6.8	SM	0.88	Contractive	42%	32	33	33				
87.5	4.3	SM	0.86	Contractive	35%	28	31	31				
90	1.8	SM	0.65	Contractive	33%	28	31	31				
92.5	-0.7	SM		Contractive	44%	33	34	33				
95	-3.2	SM		Contractive	38%	30	32	32				
97.5	-5.7	SM		Dilative	93%	46	48	52				
100	-8.2	TSWL		Dilative								
102.5	-10.7	TSWL		Dilative								
105	-13.2	TSWL		Contractive								
107.5	-15.7	TSWL		Contractive								
110	-18.2	TSWL		Contractive								
112.5	-20.7	TSWL		Intermediate								
115	-23.2	TSWL		Contractive								
117.5	-25.7	TWL		Contractive								
120	-28.2	TWL		Contractive								

## B.2.2. SR-417 and International Parkway

### B.2.2.1. SPT B-1 (EB1P14)

Depth (ft)	Elevation (ft)	USCS	FC actual/estimate	B-1 N <sub>safe</sub>	SPT N <sub>60</sub>	SPT N <sub>trip</sub>	SPT (N1) <sub>60</sub>	SPT (N1) <sub>60t</sub>	SPT (N1) <sub>trip</sub>	SPT (N1) <sub>60ta</sub>	u psf	σ' <sub>vo</sub> (avg) psf	Rebound inch
0.0	72.3	-	-	-	-	-	-	-	-	-	-	-	-
1.5	70.8	SP	0	20	15	12	30	30	23	30	0	173	
3.5	68.8	SP	0	29	22	17	44	44	33	44	0	418	
5.5	66.8	SP	0	39	29	22	51	51	39	51	0	668	0.00
7.5	64.8	SP	0	23	17	13	26	26	20	26	0	903	0.32
9.5	62.8	SC	12	11	8	7	11	11	9	16	0	1110	0.33
12.5	59.8	SM	12	7	5	4	6	7	5	12	137	1273	0.14
15.0	57.3	SP-SM	8.5	13	11	9	13	14	11	18	293	1407	0.26
17.5	54.8	SP-SM	8.5	17	14	12	16	18	14	22	449	1551	0.33
20.0	52.3	SP-SM	8.5	30	29	22	30	30	23	34	605	1705	0.38
22.5	49.8	CH	50	13	12	11	12	-	-	-	761	1871	0.32
25.0	47.3	SP-SM	8.5	13	12	11	12	13	10	17	917	2010	0.26
27.5	44.8	SP-SM	8.5	33	31	24	29	29	22	33	1073	2162	0.25
30.0	42.3	SP-SM	8.5	14	14	12	13	14	11	18	1229	2308	0.32
32.5	39.8	CH	50	8	8	7	7	-	-	-	1385	2452	0.35
35.0	37.3	CH	50	26	26	20	22	-	-	-	1541	2616	0.33
37.5	34.8	SP-SM	8.5	13	13	11	11	12	9	16	1697	2755	0.23
40.0	32.3	SP-SM	8.5	10	10	9	8	9	7	13	1853	2877	0.20
42.5	29.8	SM	12	7	7	6	6	7	5	12	2009	2976	0.14
45.0	27.3	SM	12	WH	WH	WH	0	0	0	5	2165	3010	0.14
47.5	24.8	SM	12	3	3	3	2	2	2	7	2321	3049	0.15
50.0	22.3	SM	12	4	4	3	3	3	3	9	2477	3103	0.21
52.5	19.8	SM	12	4	4	3	3	3	3	9	2633	3159	0.23
55.0	17.3	SP-SM	8.5	25	25	21	18	20	15	24	2789	3286	0.18
57.5	14.8	SP-SM	8.5	13	13	11	9	10	8	14	2945	3420	0.16
60.0	12.3	SM	12	4	4	3	3	3	3	9	3101	3491	0.16
62.5	9.8	CH	50	7	7	6	5	-	-	-	3257	3608	0.13
65.0	7.3	CH	50	4	4	3	3	-	-	-	3413	3739	0.13
67.5	4.8	CH	50	3	3	3	2	-	-	-	3569	3861	0.15
70.0	2.3	ML	50	34	34	26	22	-	-	-	3725	3990	0.22
72.5	-0.2	ML	50	36	36	28	23	-	-	-	3881	4131	
75.0	-2.7	ML	50	50/2	50/2	50/2	64	-	-	-	4037	4295	
77.5	-5.2	ML	50	50/0	50/0	50/0	63	-	-	-	4193	4464	
80.0	-7.7	SP	0	63/10	63/10	63/10	62	69	62	69	4349	4643	
82.5	-10.2	SP	0	50/0	50/0	50/0	61	68	61	68	4505	4825	
85.0	-12.7	ML	50	50/3	50/3	50/3	60	-	-	-	4661	4996	
87.5	-15.2	ML	50	50/3	50/3	50/3	59	-	-	-	4817	5165	
90.0	-17.7	SP	0	50/5	50/5	50/5	58	64	58	64	4973	5344	
92.5	-20.2	ML	50	50/6	50/6	50/6	57	-	-	-	5129	5516	
95.0	-22.7	ML	50	50/1	50/1	50/1	56	-	-	-	5285	5685	

Depth (ft)	Elevation (ft)	USCS	Rebound inch	Liquefaction Soil Response	Terzaghi Dr	Schmertmann Φ'	Hatanaka Φ'	Peck Φ'	Mayne OCR	Hera Cu (psf)	Hettiarachchi Cu (psf)	CDOT Qu (psf)
0.0	72.3	-										
1.5	70.8	SP		Intermediate	71%	46	41	31				
3.5	68.8	SP		Dilative	85%	48	46	33				
5.5	66.8	SP	0.00	Dilative	92%	49	48	35				
7.5	64.8	SP	0.32	Intermediate	66%	43	40	32				
9.5	62.8	SC	0.33	Contractive	43%	35	34	30				
12.5	59.8	SM	0.14	Contractive	32%	30	30	29				
15.0	57.3	SP-SM	0.26	Contractive	47%	37	35	30				
17.5	54.8	SP-SM	0.33	Intermediate	52%	39	37	31				
20.0	52.3	SP-SM	0.38	Dilative	71%	45	41	35				
22.5	49.8	CH	0.32	-					5.739	683	1013	3000
25.0	47.3	SP-SM	0.26	Contractive	45%	36	34	31				
27.5	44.8	SP-SM	0.25	Dilative	70%	44	41	36				
30.0	42.3	SP-SM	0.32	Contractive	47%	36	35	31				
32.5	39.8	CH	0.35	-					3.532	500	656	1750
35.0	37.3	CH	0.33	-					7.609	1082	2132	5500
37.5	34.8	SP-SM	0.23	Contractive	43%	34	34	31				
40.0	32.3	SP-SM	0.20	Contractive	37%	32	32	30				
42.5	29.8	SM	0.14	Contractive	32%	28	30	29				
45.0	27.3	SM	0.14	Contractive	0%	0	20	27				
47.5	24.8	SM	0.15	Contractive	18%	22	26	28				
50.0	22.3	SM	0.21	Contractive	22%	24	27	28				
52.5	19.8	SM	0.23	Contractive	22%	24	27	28				
55.0	17.3	SP-SM	0.18	Intermediate	55%	39	38	34				
57.5	14.8	SP-SM	0.16	Contractive	39%	33	32	31				
60.0	12.3	SM	0.16	Contractive	22%	23	27	28				
62.5	9.8	CH	0.13	-					2.469	454	574	1250
65.0	7.3	CH	0.13	-					1.638	303	328	750
67.5	4.8	CH	0.15	-					1.314	247	246	500
70.0	2.3	ML	0.22	-					6.844	1312	2788	5500
72.5	-0.2	ML		-					6.950	1368	2952	5750
75.0	-2.7	ML		-					13.679	3447	8200	16000
77.5	-5.2	ML		-					13.320	3447	8200	15750
80.0	-7.7	SP		Dilative	102%	50	55	52				
82.5	-10.2	SP		Dilative	101%	50	55	52				
85.0	-12.7	ML		-					12.326	3447	8200	15000
87.5	-15.2	ML		-					12.047	3447	8200	14750
90.0	-17.7	SP		Dilative	98%	49	54	52				
92.5	-20.2	ML		-					11.514	3447	8200	14250
95.0	-22.7	ML		-					11.277	3447	8200	14000

### B.2.2.2. SPT B-2 (EB2P5)

Depth	Elevation	USCS	FC	B-2	SPT	SPT	SPT	SPT	SPT	SPT	u	$\sigma'_{vo}$ (avg)	Rebound
(ft)	(ft)		actual/estimate	Nsafe	N60	Ntrip	(N1)60	(N1)60t	(N1)trip	(N1)60ta	psf	psf	inch
0.0	72.3	-	-	-	-	-	-	-	-	-	-	-	-
1.5	70.8	SP-SM	8.5	10	9	7	15	15	12	19	0	158	
3.5	68.8	SP-SM	8.5	13	12	9	20	20	15	24	0	375	
5.5	66.8	SP-SM	8.5	15	14	11	21	21	16	25	0	595	
7.5	64.8	SM	12	11	10	8	13	13	10	18	0	808	
9.5	62.8	SM	12	7	6	5	7	7	6	13	6	996	
12.5	59.8	SP-SM	8.5	12	11	9	12	13	10	17	193	1144	
15.0	57.3	SP-SM	8.5	18	18	15	19	21	16	25	349	1286	
17.5	54.8	SM	12	22	22	17	22	22	17	27	505	1430	
20.0	52.3	CH	50	17	19	16	18	-	-	-	661	1594	
22.5	49.8	SM	12	20	23	18	20	20	16	26	817	1733	0.34
25.0	47.3	CH	50	13	15	13	13	-	-	-	973	1894	0.04
27.5	44.8	SM	12	24	27	21	23	23	17	28	1129	2033	0.23
30.0	42.3	SP-SM	8.5	32	38	29	31	31	24	35	1285	2185	0.27
32.5	39.8	SC	12	19	23	20	18	20	15	25	1441	2321	0.35
35.0	37.3	SP-SM	8.5	24	29	22	22	22	17	26	1597	2473	0.33
37.5	34.8	SM	12	3	4	3	3	3	2	8	1753	2549	0.15
40.0	32.3	SM	12	3	4	3	3	3	2	8	1909	2606	0.14
42.5	29.8	SM	12	3	4	3	3	3	2	8	2065	2662	0.10
45.0	27.3	SM	12	2	2	2	2	2	1	7	2221	2709	0.09
47.5	24.8	SM	12	18	22	19	15	17	13	22	2377	2823	0.15
50.0	22.3	SM	12	8	10	9	7	7	6	13	2533	2934	0.23
52.5	19.8	SP-SM	8.5	3	4	3	2	3	2	7	2689	3006	0.14
55.0	17.3	SM	12	5	6	5	4	4	3	10	2845	3073	0.14
57.5	14.8	CH	50	4	5	4	3	-	-	-	3001	3192	0.18
60.0	12.3	ML	50	8	10	9	6	-	-	-	3157	3294	0.20
62.5	9.8	CH	50	10	12	10	8	-	-	-	3313	3428	0.19
65.0	7.3	SM	12	24	29	25	18	20	15	25	3469	3562	0.30
67.5	4.8	SM	12	19	23	20	14	16	12	21	3625	3693	0.46
70.0	2.3	ML	50	50/5	50/5	50/5	72	-	-	-	3781	3855	0.43
72.5	-0.2	ML	50	50/4	50/4	50/4	71	-	-	-	3937	4024	0.26
75.0	-2.7	ML	50	50/0	50/0	50/0	69	-	-	-	4093	4193	
77.5	-5.2	ML	50	50/1	50/1	50/1	68	-	-	-	4249	4362	
80.0	-7.7	ML	50	50/0	50/0	50/0	66	-	-	-	4405	4531	
82.5	-10.2	ML	50	50/3	50/3	50/3	65	-	-	-	4561	4700	
85.0	-12.7	ML	50	65	78	65	42	-	-	-	4717	4859	
87.5	-15.2	ML	50	50/1	50/1	50/1	63	-	-	-	4873	5025	
90.0	-17.7	ML	50	66/11	66/11	66/11	62	-	-	-	5029	5194	

Depth (ft)	Elevation (ft)	USCS	Rebound inch	Liquefaction Soil Response	Terzaghi Dr	Schmertmann Φ'	Hatanaka Φ'	Peck Φ'	Mayne OCR	Hera Cu (psf)	Hettiarachchi Cu (psf)	CDOT Qu (psf)
0.0	72.3	-										
1.5	70.8	SP-SM		Contractive	50%	41	35	30				
3.5	68.8	SP-SM		Intermediate	57%	42	37	31				
5.5	66.8	SP-SM		Intermediate	59%	42	38	31				
7.5	64.8	SM		Contractive	47%	38	34	30				
9.5	62.8	SM		Contractive	35%	33	31	29				
12.5	59.8	SP-SM		Contractive	45%	38	34	30				
15.0	57.3	SP-SM		Intermediate	56%	42	38	32				
17.5	54.8	SM		Intermediate	61%	43	38	33				
20.0	52.3	CH		-					8.626	931	1558	4523.174
22.5	49.8	SM	0.34	Intermediate	58%	42	38	34				
25.0	47.3	CH	0.04	-					6.507	785	1230	3172.671
27.5	44.8	SM	0.23	Intermediate	61%	43	39	35				
30.0	42.3	SP-SM	0.27	Dilative	71%	46	42	38				
32.5	39.8	SC	0.35	Intermediate	54%	41	37	34				
35.0	37.3	SP-SM	0.33	Intermediate	60%	43	38	35				
37.5	34.8	SM	0.15	Contractive	21%	25	27	28				
40.0	32.3	SM	0.14	Contractive	21%	25	27	28				
42.5	29.8	SM	0.10	Contractive	21%	25	27	28				
45.0	27.3	SM	0.09	Contractive	17%	20	25	28				
47.5	24.8	SM	0.15	Intermediate	50%	39	36	33				
50.0	22.3	SM	0.23	Contractive	33%	32	31	30				
52.5	19.8	SP-SM	0.14	Contractive	20%	24	26	28				
55.0	17.3	SM	0.14	Contractive	26%	27	28	29				
57.5	14.8	CH	0.18	-					2.130	356	410	791.521
60.0	12.3	ML	0.20	-				30	3.361			
62.5	9.8	CH	0.19	-					3.708	669	984	1909.619
65.0	7.3	SM	0.30	Intermediate	55%	40	38	35				
67.5	4.8	SM	0.46	Intermediate	48%	38	35	34				
70.0	2.3	ML	0.43	-					14.738	3447	8200	25000
72.5	-0.2	ML	0.26	-					14.308	3447	8200	25000
75.0	-2.7	ML		-					13.908	3447	8200	25000
77.5	-5.2	ML		-					13.535	3447	8200	25000
80.0	-7.7	ML		-					13.185	3447	8200	25000
82.5	-10.2	ML		-					12.856	3447	8200	25000
85.0	-12.7	ML		-					12.565	3447	8200	25000
87.5	-15.2	ML		-					12.277	3447	8200	25000
90.0	-17.7	ML		-					12.000	3447	8200	25000

## B.2.3. SR-50 and SR-436

### B.2.3.1. SPT TH-4B (EB4P10)

Depth (ft)	Elevation (ft)	USCS	FC actual/estimate	TH-4B Nsafe	SPT N60	SPT Ntrip	SPT (N1)60	SPT (N1)60t	SPT (N1)trip	SPT (N1)60ta	u psf	$\sigma'_{vo}$ (avg) psf	Rebound inch
0.0	99.0	-											
7.0	92.0	SM	12	11	8	7	15	17	13	22	219	586	
8.5	90.5	SM	12	11	8	7	14	16	12	21	313	665	
10.0	89.0	SP	0	27	20	15	32	32	25	32	406	759	
11.5	87.5	SP	0	34	26	20	40	40	31	40	500	865	
13.0	86.0	SP-SM	8	17	14	11	20	20	15	23	594	959	
15.0	84.0	SP-SM	8	17	14	12	19	21	16	24	719	1074	
17.0	82.0	SM	12	15	13	11	17	19	15	24	844	1181	
19.5	79.5	SP	0	18	15	13	18	20	15	20	1000	1333	
22.0	77.0	SP	0	20	19	15	22	22	17	22	1156	1489	
24.5	74.5	SP	0	24	23	18	25	25	19	25	1313	1655	
27.0	72.0	SP	0	16	15	13	16	18	14	18	1469	1814	-0.79
29.5	69.5	SP	0	52	49	38	49	49	38	49	1625	2000	-0.65
32.0	67.0	SP	0	31	31	24	30	30	23	30	1781	2174	-0.32
34.5	64.5	SP	7	26	26	20	24	24	18	26	1938	2333	-0.24
37.0	62.0	SP	0	20	20	17	18	20	15	20	2094	2489	-0.82
39.5	59.5	SP	0	27	27	21	23	23	18	23	2250	2645	-0.26
42.0	57.0	SM	12	12	12	10	10	11	9	16	2406	2771	-0.07
44.5	54.5	SP	0	28	28	22	23	23	18	23	2563	2920	0.02
47.0	52.0	SM	12	26	26	20	21	21	16	26	2719	3056	0.10
49.5	49.5	SM	12	14	14	12	11	12	9	17	2875	3178	0.07
52.0	47.0	SM	12	15	15	13	12	13	10	19	3031	3296	0.13
54.5	44.5	CH	50	15	15	13	11	-	-	-	3188	3445	0.13
57.0	42.0	CH	50	9	9	8	7	-	-	-	3344	3591	0.15
59.5	39.5	SM	12	6	6	5	4	4	3	10	3500	3675	0.06
62.0	37.0	SP	0	8	8	7	6	7	5	7	3656	3784	0.13
64.5	34.5	SM	12	3	3	3	2	2	2	7	3813	3843	0.18
67.0	32.0	SM	12	4	4	3	3	3	3	9	3969	3896	0.22
69.5	29.5	SM	12	7	7	6	5	6	4	11	4125	3973	0.23
72.0	27.0	CH	50	3	3	3	2	-	-	-	4281	4074	0.27
74.5	24.5	CH	50	6	6	5	4	-	-	-	4438	4200	0.29
77.0	22.0	CH	50	7	7	6	5	-	-	-	4594	4331	0.24
79.5	19.5	CH	50	50/3	50/3	50/3	67	-	-	-	4750	4493	
82.0	17.0	CH	50	50/4	50/4	50/4	66	-	-	-	4906	4661	
84.5	14.5	CH	50	50/5.5	50/5.5	50/5.5	64	-	-	-	5063	4830	
87.0	12.0	CH	50	50/3	50/3	50/3	63	-	-	-	5219	4999	
89.5	9.5	CH	50	50/5	50/5	50/5	62	-	-	-	5375	5168	
92.0	7.0	CH	50	50/1	50/1	50/1	61	-	-	-	5531	5336	
94.5	4.5	CH	50	50/4	50/4	50/4	60	-	-	-	5688	5505	

Depth (ft)	Elevation (ft)	USCS	Rebound inch	Liquefaction Soil Response	Terzaghi Dr	Schmertmann Φ'	Hatanaka Φ'	Peck Φ'	Mayne OCR	Hera Cu (psf)	Hettiarachchi Cu (psf)	CDOT Qu (psf)
0.0	99.0	-										
7.0	92.0	SM		Intermediate								
8.5	90.5	SM		Intermediate								
10.0	89.0	SP		Dilative								
11.5	87.5	SP		Dilative	82%	47	45	35				
13.0	86.0	SP-SM		Intermediate	58%	41	38	31				
15.0	84.0	SP-SM		Intermediate	56%	40	38	31				
17.0	82.0	SM		Intermediate	53%	39	37	31				
19.5	79.5	SP		Contractive	55%	40	38	31				
22.0	77.0	SP		Intermediate	61%	41	38	33				
24.5	74.5	SP		Intermediate	65%	43	40	34				
27.0	72.0	SP	-0.79	Contractive	52%	38	37	31				
29.5	69.5	SP	-0.65	Dilative	90%	49	47	41				
32.0	67.0	SP	-0.32	Intermediate	71%	44	41	36				
34.5	64.5	SP	-0.24	Intermediate	63%	42	39	35				
37.0	62.0	SP	-0.82	Contractive	55%	39	38	33				
39.5	59.5	SP	-0.26	Intermediate	62%	41	39	35				
42.0	57.0	SM	-0.07	Contractive	41%	34	33	31				
44.5	54.5	SP	0.02	Intermediate	62%	41	39	35				
47.0	52.0	SM	0.10	Intermediate	59%	40	38	35				
49.5	49.5	SM	0.07	Contractive	43%	34	34	31				
52.0	47.0	SM	0.13	Contractive	45%	34	34	31				
54.5	44.5	CH	0.13	-					4.309	785	1230	2750
57.0	42.0	CH	0.15	-					2.945	544	738	1750
59.5	39.5	SM	0.06	Contractive	26%	26	28	29				
62.0	37.0	SP	0.13	Contractive	32%	28	30	29				
64.5	34.5	SM	0.18	Contractive	18%	21	26	28				
67.0	32.0	SM	0.22	Contractive	22%	23	27	28				
69.5	29.5	SM	0.23	Contractive	29%	27	29	29				
72.0	27.0	CH	0.27	-					1.267	247	246	500
74.5	24.5	CH	0.29	-					1.999	406	492	1000
77.0	22.0	CH	0.24	-					2.177	454	574	1250
79.5	19.5	CH		-					13.262	3447	8200	16750
82.0	17.0	CH		-					12.930	3447	8200	16500
84.5	14.5	CH		-					12.617	3447	8200	16000
87.0	12.0	CH		-					12.322	3447	8200	15750
89.5	9.5	CH		-					12.043	3447	8200	15500
92.0	7.0	CH		-					11.779	3447	8200	15250
94.5	4.5	CH		-					11.529	3447	8200	15000

### B.2.3.2. SPT TH-3B (P3P10, EB)

Depth	Elevation	USCS	FC	TH-3B	SPT	SPT	SPT	SPT	SPT	SPT	u	$\sigma'_{vo}$ (avg)	Rebound
(ft)	(ft)		actual/estimate	Nsafe	N60	Ntrip	(N1)60	(N1)60t	(N1)trip	(N1)60ta	psf	psf	inch
0.0	98.0	-											
7.0	91.0	SP	0	7	5	4	9	10	8	10	193	682	
8.5	89.5	SP	0	7	5	4	8	9	7	9	287	775	
10.0	88.0	SP	0	14	11	9	16	18	14	18	381	874	
11.5	86.5	SP	0	15	11	10	16	18	14	18	474	976	
13.0	85.0	SP	0	26	22	17	30	30	23	30	568	1078	
15.0	83.0	SP	0	18	15	12	20	20	15	20	693	1214	
17.0	81.0	SP-SM	6	12	10	9	12	13	10	14	817	1349	
19.5	78.5	SP-SM	8.5	19	16	14	19	21	16	25	973	1519	
22.0	76.0	SP	0	25	24	18	26	26	20	26	1129	1695	
24.5	73.5	SP	0	34	32	25	33	33	25	33	1285	1872	
27.0	71.0	SP	0	38	36	28	36	36	28	36	1441	2049	
29.5	68.5	SP	0	44	42	32	40	40	31	40	1597	2227	
32.0	66.0	SP	0	33	33	25	30	30	23	30	1753	2404	
34.5	63.5	SP	0	30	30	23	26	26	20	26	1909	2579	
37.0	61.0	SM	12	9	9	8	8	9	7	14	2065	2745	0.00
39.5	58.5	SM/SC	14	7	7	6	6	7	5	12	2221	2900	0.00
42.0	56.0	SP	0	14	14	12	11	12	9	12	2377	3065	0.02
44.5	53.5	SP	0	13	13	11	10	11	9	11	2533	3234	0.09
47.0	51.0	SP	0	26	26	20	20	20	15	20	2689	3407	0.14
49.5	48.5	SP-SM	8.5	23	23	20	17	19	15	23	2845	3581	0.09
52.0	46.0	SP-SM	8.5	22	22	19	16	18	14	22	3001	3755	0.23
54.5	43.5	SP-SM	8.5	55	55	42	39	39	30	43	3157	3940	0.27
57.0	41.0	SP-SM	8.5	8	8	7	6	7	5	11	3313	4107	0.21
59.5	38.5	SC	12	7	7	6	5	6	4	11	3469	4259	0.24
62.0	36.0	SP-SM	8.5	8	8	7	5	6	4	10	3625	4418	0.20
64.5	33.5	SP-SM	8.5	12	12	10	8	9	7	13	3781	4585	0.25
67.0	31.0	CH	50	5	5	4	3	-	-	-	3937	4678	0.29
69.5	28.5	CH	50	6	6	5	4	-	-	-	4093	4758	0.22
72.0	26.0	CH	50	51	51	39	33	-	-	-	4249	4900	0.27
74.5	23.5	CH	50	71	71	55	45	-	-	-	4405	5056	0.35
77.0	21.0	CH	50	60	60	46	37	-	-	-	4561	5213	0.30
79.5	18.5	CH	50	50/4	50/4	50/4	61	-	-	-	4717	5369	
82.0	16.0	CH	50	50/1	50/1	50/1	60	-	-	-	4873	5526	
84.5	13.5	SST	50	50/0	50/0	50/0	59	59	59	68	5029	5732	

Depth (ft)	Elevation (ft)	USCS	Rebound inch	Liquefaction Soil Response	Terzaghi Dr	Schmertmann Φ'	Hatanaka Φ'	Peck Φ'	Mayne OCR	Hera Cu (psf)	Hettiarachchi Cu (psf)	CDOT Qu (psf)
0.0	98.0	-										
7.0	91.0	SP		Contractive								
8.5	89.5	SP		Contractive								
10.0	88.0	SP		Contractive								
11.5	86.5	SP		Contractive	52%	38	37	30				
13.0	85.0	SP		Intermediate	71%	45	41	33				
15.0	83.0	SP		Contractive	58%	40	38	32				
17.0	81.0	SP-SM		Contractive	45%	36	34	30				
19.5	78.5	SP-SM		Intermediate	56%	40	38	32				
22.0	76.0	SP		Intermediate	66%	43	40	34				
24.5	73.5	SP		Dilative	74%	45	43	36				
27.0	71.0	SP		Dilative	77%	46	44	37				
29.5	68.5	SP		Dilative	82%	47	45	39				
32.0	66.0	SP		Intermediate	71%	44	41	36				
34.5	63.5	SP		Intermediate	66%	43	40	36				
37.0	61.0	SM	0.00	Contractive	37%	31	32	30				
39.5	58.5	SM/SC	0.00	Contractive	32%	29	30	29				
42.0	56.0	SP	0.02	Contractive	43%	34	34	31				
44.5	53.5	SP	0.09	Contractive	41%	33	33	31				
47.0	51.0	SP	0.14	Contractive	58%	39	38	35				
49.5	48.5	SP-SM	0.09	Intermediate	53%	38	37	34				
52.0	46.0	SP-SM	0.23	Intermediate	52%	37	37	33				
54.5	43.5	SP-SM	0.27	Dilative	81%	46	44	42				
57.0	41.0	SP-SM	0.21	Contractive	32%	28	30	29				
59.5	38.5	SC	0.24	Contractive	29%	26	29	29				
62.0	36.0	SP-SM	0.20	Contractive	29%	27	29	29				
64.5	33.5	SP-SM	0.25	Contractive	37%	30	32	31				
67.0	31.0	CH	0.29	-					1.637	356	410	750
69.5	28.5	CH	0.22	-					1.835	406	492	1000
72.0	26.0	CH	0.27	-					7.856	1757	4182	8250
74.5	23.5	CH	0.35	-					9.655	2230	5822	11250
77.0	21.0	CH	0.30	-					8.419	1976	4920	9250
79.5	18.5	CH		-					11.730	3447	8200	15250
82.0	16.0	CH		-					11.500	3447	8200	15000
84.5	13.5	SST		Dilative								

## B.2.4. Heritage Parkway

### B.2.4.1. SPT TH-5 (EB1P1)

Depth (ft)	Elevation (ft)	USCS	FC actual/estimate	TH-5 Nsafe	SPT N60	SPT Ntrip	SPT (N1)60	SPT (N1)60t	SPT (N1)trip	SPT (N1)60ta	u psf	$\sigma'_{vo}$ (avg) psf	Rebound inch
0.0	25.0	-	-	-	-	-	-	-	-	-	-	-	-
1.0	24.0	SC	12	5	4	3	8	8	6	13	0	95	
2.5	22.5	SP	0	12	9	7	18	18	14	18	0	253	
4.0	21.0	SP	0	13	10	7	20	20	15	20	0	423	
5.5	19.5	SC	12	16	12	9	22	22	17	27	0	585	
7.0	18.0	SC	12	17	13	10	21	21	16	26	0	743	
8.5	16.5	SC	12	20	15	12	22	22	17	27	0	900	
10.0	15.0	SP	0	18	14	10	18	18	14	18	0	1068	
14.5	10.5	SC	12	9	9	8	10	11	9	16	0	1525	
19.5	5.5	SP	0	33	34	26	35	35	27	35	281	1902	
24.5	0.5	SM	12	6	7	6	7	8	6	13	593	2130	0.45
29.5	-4.5	CH	50	WH	WH	WH	0	-	-	-	905	2320	0.00
34.5	-9.5	SM	12	5	6	5	5	6	4	11	1217	2486	0.00
39.5	-14.5	SC	12	5	6	5	5	6	4	11	1529	2649	0.01
44.5	-19.5	SC	12	15	18	15	15	17	13	22	1841	2902	0.42
49.5	-24.5	SP-SM	9	20	24	21	19	21	16	25	2153	3187	0.38
54.5	-29.5	SP-SM	8.5	20	24	21	18	20	15	24	2465	3475	0.58
59.5	-34.5	CH	50	2	3	3	2	-	-	-	2777	3718	0.28
64.5	-39.5	CH	76	2	3	3	2	-	-	-	3089	3956	0.15
69.5	-44.5	CH	50	5	6	5	4	-	-	-	3401	4217	0.17
74.5	-49.5	SM/SC	12	9	11	9	7	8	6	13	3713	4435	0.23
79.5	-54.5	SM/SC	12	11	14	12	9	10	8	15	4025	4670	0.34
84.5	-59.5	SM/SC	12	20	24	21	15	17	13	22	4337	4931	0.29
89.5	-64.5	SM/SC	12	16	20	17	12	13	10	19	4649	5171	0.29
94.5	-69.5	SM/SC	12	14	17	14	10	11	9	16	4961	5409	0.29
99.5	-74.5	SM/SC	12	10	12	10	7	8	6	13	5273	5625	0.23
104.5	-79.5	SM/SC	12	5	6	5	4	4	3	10	5585	5748	0.29
109.5	-84.5	SM/SC	12	17	21	18	12	13	10	19	5897	5973	0.21
114.5	-89.5	MH	87	31	38	29	21	-	-	-	6209	6234	0.28
119.5	-94.5	MH	50	9	11	9	6	-	-	-	6521	6429	
124.5	-99.5	MH	50	7	9	8	5	-	-	-	6833	6595	
129.5	-104.5	SC	12	10	12	10	7	8	6	13	7145	6803	
134.5	-109.5	SC	12	10	12	10	6	7	5	12	7457	6993	
139.5	-114.5	SC	12	12	15	13	8	9	7	14	7769	7204	
144.5	-119.5	SC	12	24	29	24	15	17	13	22	8081	7462	
149.5	-124.5	SC	12	20	24	21	12	13	10	19	8393	7702	

Depth (ft)	Elevation (ft)	USCS	Rebound inch	Liquefaction Soil Response	Terzaghi Dr	Schmertmann Φ'	Hatanaka Φ'	Peck Φ'	Mayne OCR	Hera Cu (psf)	Hettiarachchi Cu (psf)	CDOT Qu (psf)
0.0	25.0	-										
1.0	24.0	SC		Contractive	35%	33	31	28				
2.5	22.5	SP		Contractive	55%	40	37	30				
4.0	21.0	SP		Contractive	57%	40	37	30				
5.5	19.5	SC		Intermediate	61%	41	38	31				
7.0	18.0	SC		Intermediate	59%	41	38	31				
8.5	16.5	SC		Intermediate	61%	42	38	31				
10.0	15.0	SP		Contractive	55%	40	37	31				
14.5	10.5	SC		Contractive	41%	34	33	30				
19.5	5.5	SP		Dilatative	76%	46	43	37				
24.5	0.5	SM	0.45	Contractive	34%	30	31	29				
29.5	-4.5	CH	0.00	-					NA	NA	NA	NA
34.5	-9.5	SM	0.00	Contractive	29%	28	29	29				
39.5	-14.5	SC	0.01	Contractive	29%	28	29	29				
44.5	-19.5	SC	0.42	Intermediate	50%	37	36	32				
49.5	-24.5	SP-SM	0.38	Intermediate	56%	39	38	34				
54.5	-29.5	SP-SM	0.58	Intermediate	55%	38	38	34	5.921	1102	1968	4500
59.5	-34.5	CH	0.28	-					1.349	247	246	500
64.5	-39.5	CH	0.15	-					1.292	247	246	500
69.5	-44.5	CH	0.17	-					1.994	406	492	1000
74.5	-49.5	SM/SC	0.23	Contractive	34%	29	31	30				
79.5	-54.5	SM/SC	0.34	Contractive	39%	31	32	31				
84.5	-59.5	SM/SC	0.29	Intermediate	50%	36	36	34				
89.5	-64.5	SM/SC	0.29	Contractive	45%	34	34	33				
94.5	-69.5	SM/SC	0.29	Contractive	41%	32	33	32				
99.5	-74.5	SM/SC	0.23	Contractive	34%	29	31	31				
104.5	-79.5	SM/SC	0.29	Contractive	26%	23	28	29				
109.5	-84.5	SM/SC	0.21	Contractive	45%	33	34	33				
114.5	-89.5	MH	0.28	-					5.384	1408	3075	5250
119.5	-94.5	MH		-					2.193	608	861	1500
124.5	-99.5	MH		-					1.937	544	738	1250
129.5	-104.5	SC		Contractive	34%	28	31	31				
134.5	-109.5	SC		Contractive	32%	27	30	31				
139.5	-114.5	SC		Contractive	37%	29	32	31				
144.5	-119.5	SC		Intermediate	50%	34	36	35				
149.5	-124.5	SC		Contractive	45%	33	34	34				

### B.2.4.2. SPT FDOT (B3P1)

Depth	Elevation	USCS	FC	FDOT	SPT	SPT	SPT	SPT	SPT	SPT	u	$\sigma'_{vo}$ (avg)	Rebound
(ft)	(ft)		actual/estimate	Nsafe	N60	Ntrip	(N1)60	(N1)60t	(N1)trip	(N1)60ta	psf	psf	inch
0	17.16	-	-	-	-	-	-	-	-	-	-	-	-
6	11.16	SC	<b>23.17</b>	15	14	11	25	25	19	31	0	1466	
11	6.16	SC	<b>23.17</b>	11	10	9	15	17	13	23	240	1686	
16	1.16	SM	<b>15.73</b>	16	17	13	22	22	17	28	552	1967	
21	-3.84	SM	<b>35.95</b>	4	4	3	5	6	4	13	864	2232	
26	-8.84	SM	<b>35.95</b>	6	7	6	8	9	7	16	1176	2518	0.01
31	-13.84	SC	<b>27.85</b>	4	5	4	5	6	4	12	1488	2806	0.00
36	-18.84	SM	<b>24.01</b>	27	33	25	33	33	25	39	1800	3094	0.36
41	-23.84	SM	<b>24.01</b>	25	30	23	28	28	22	34	2112	3269	0.40
46	-28.84	-		6	8	7	7	8	6	8	2424	3387	0.29
51	-33.84	SP-SM	<b>8.59</b>	9	11	9	9	10	8	14	2736	3478	0.17
56	-38.84	CL	<b>84.7</b>	1	2	2	2	-	-	-	3048	3633	0.21
61	-43.84	CL	<b>84.7</b>	7	9	8	7	-	-	-	3360	3792	0.13
65	-47.84	SM	<b>29.98</b>	10	12	10	9	10	8	17	3609	4053	0.19
71	-53.84	SM	<b>29.98</b>	11	14	12	10	11	9	18	3984	4165	0.24
76	-58.84	SM	<b>22.24</b>	14	17	15	12	13	10	20	4296	4273	0.25
81	-63.84	SM	<b>22.24</b>	14	17	15	12	13	10	20	4608	4431	0.18
86	-68.84	SM	<b>22.24</b>	16	20	17	13	14	11	21	4920	4606	0.22

Depth	Elevation	USCS	Rebound	Liquefaction	Terzaghi	Schmertmann	Hatanaka	Peck	Mayne	Hera	Hettiarachchi	CDOT
(ft)	(ft)		inch	Soil Response	Dr	$\Phi'$	$\Phi'$	$\Phi'$	OCR	Cu (psf)	Cu (psf)	Qu (psf)
0	17.16	-										
6	11.16	SC		Dilative	65%	39	40	31				
11	6.16	SC		Intermediate	50%	35	36	30				
16	1.16	SM		Intermediate	61%	39	38	32				
21	-3.84	SM		Contractive	29%	26	29	28				
26	-8.84	SM	0.01	Contractive	37%	29	32	29				
31	-13.84	SC	0.00	Contractive	29%	26	29	29				
36	-18.84	SM	0.36	Dilative	74%	42	43	36				
41	-23.84	SM	0.40	Dilative	68%	41	41	36				
46	-28.84	-	0.29	Contractive	34%	29	31	29				
51	-33.84	SP-SM	0.17	Contractive	39%	31	32	30				
56	-38.84	CL	0.21	-					1.036	184	164	500
61	-43.84	CL	0.13	-					2.837	544	738	1750
65	-47.84	SM	0.19	Contractive	39%	31	32	31				
71	-53.84	SM	0.24	Contractive	41%	32	33	31				
76	-58.84	SM	0.25	Contractive	45%	34	34	32				
81	-63.84	SM	0.18	Contractive	45%	34	34	32				
86	-68.84	SM	0.22	Intermediate	47%	35	35	33				

### B.2.4.3. SPT TH-6 (EB5P1)

Depth	Elevation	USCS	FC	TH-6	SPT	SPT	SPT	SPT	SPT	SPT	u	$\sigma'_{vo}$ (avg)	Rebound
(ft)	(ft)		actual/estimate	Nsafe	N60	Ntrip	(N1)60	(N1)60t	(N1)trip	(N1)60ta	psf	psf	inch
0	20	SC	12	-	-		-						
1	19	SC	12	7	5	4	11	11	8	16	0	100	
2.5	17.5	SC	12	16	12	9	24	24	18	29	0	255	
4	16	SC	12	22	17	13	33	33	25	38	0	418	
5.5	14.5	SC	12	24	18	14	33	33	26	39	0	583	
7	13	SC	12	16	12	10	20	22	17	27	0	743	
8.5	11.5	SC	12	23	17	13	26	26	20	31	0	900	
10	10	SC	12	22	17	13	23	23	17	28	0	1058	
14.5	5.5	SP	0	40	41	31	49	49	38	49	281	1389	
19.5	0.5	SP-SM	8.5	10	10	9	11	12	10	16	593	1665	
24.5	-4.5	CH	67	2	3	2	3	-	-	-	905	1928	0.01
29.5	-9.5	SM	14	6	7	6	7	8	6	13	1217	2146	0.23
34.5	-14.5	SC	12	5	6	5	6	6	5	11	1529	2336	0.00
39.5	-19.5	SC	12	20	24	18	21	21	16	26	1841	2592	0.62
44.5	-24.5	SC	14	12	15	13	13	14	11	19	2153	2855	0.39
49.5	-29.5	SC	12	46	56	43	44	44	34	49	2465	3163	0.47
54.5	-34.5	CH	50	2	3	3	2	-	-	-	2777	3408	0.15
59.5	-39.5	CH	50	5	6	5	4	-	-	-	3089	3669	0.16
64.5	-44.5	CH	50	4	5	4	3	-	-	-	3401	3932	0.15
69.5	-49.5	SM/SC	12	11	14	12	9	10	8	16	3713	4172	0.18
74.5	-54.5	SM/SC	12	16	20	17	13	15	11	20	4025	4433	0.19
79.5	-59.5	SM/SC	12	20	24	21	16	17	13	23	4337	4696	0.26
84.5	-64.5	SM	12	12	15	13	10	11	8	16	4649	4936	0.25
89.5	-69.5	SP-SM	8.5	22	27	23	17	19	14	23	4961	5219	0.27
94.5	-74.5	SC	12	12	15	13	9	10	8	15	5273	5462	0.17
99.5	-79.5	SC	12	17	21	18	12	14	11	19	5585	5700	0.18
104.5	-84.5	SC	12	6	8	6	4	5	4	10	5897	5848	
109.5	-89.5	SC	12	52	63	48	36	36	28	41	6209	6144	
114.5	-94.5	MH	97	6	8	6	4	-	-	-	6521	6299	
119.5	-99.5	MH	50	10	12	10	7	-	-	-	6833	6505	
124.5	-104.5	MH	50	10	12	10	7	-	-	-	7145	6718	

Depth (ft)	Elevation (ft)	USCS	Rebound inch	Liquefaction Soil Response	Terzaghi Dr	Schmertmann Φ'	Hatanaka Φ'	Peck Φ'	Mayne OCR	Hera Cu (psf)	Hettiarachchi Cu (psf)	CDOT Qu (psf)
0	20	SC										
1	19	SC		Contractive	42%	36	33	29	23.954	342	431	2625
2.5	17.5	SC		Intermediate	63%	43	39	31	22.214	620	984	6000
4	16	SC		Dilative	74%	45	43	32	19.697	780	1353	8250
5.5	14.5	SC		Dilative	75%	45	43	32	16.626	830	1476	8338
7	13	SC		Intermediate	57%	40	38	31	10.637	669	984	4924
8.5	11.5	SC		Dilative	65%	43	40	32	11.963	805	1415	6429
10	10	SC		Intermediate	61%	42	39	32	10.382	780	1353	5673
14.5	5.5	SP		Dilative	90%	49	47	38				
19.5	0.5	SP-SM		Contractive	43%	35	34	30				
24.5	-4.5	CH	0.01	-					2.047	238	234	726
29.5	-9.5	SM	0.23	Contractive	34%	30	31	29				
34.5	-14.5	SC	0.00	Contractive	30%	29	30	29	2.995	406	492	1388
39.5	-19.5	SC	0.62	Intermediate	59%		38	34	7.247	1021	1968	5271
44.5	-24.5	SC	0.39	Contractive	46%	35	35	31	4.905	785	1230	3139
49.5	-29.5	SC	0.47	Dilative	86%	47	46	42	11.258	1868	4551	11034
54.5	-34.5	CH	0.15	-					1.432	247	246	575
59.5	-39.5	CH	0.16	-					2.195	406	492	1108
64.5	-44.5	CH	0.15	-					1.716	330	369	802
69.5	-49.5	SM/SC	0.18	Contractive	39%	32	33	31				
74.5	-54.5	SM/SC	0.19	Contractive	47%	35	35	33				
79.5	-59.5	SM/SC	0.26	Intermediate	51%	36	36	34				
84.5	-64.5	SM	0.25	Contractive	40%	32	33	31				
89.5	-69.5	SP-SM	0.27	Intermediate	53%	37	37	35				
94.5	-74.5	SC	0.17	Contractive	39%	31	32	31	3.137	785	1230	2269
99.5	-79.5	SC	0.18	Contractive	46%	34	35	33	3.840	1001	1722	3110
104.5	-84.5	SC		Contractive	27%	25	29	29	1.856	477	615	1096
109.5	-89.5	SC		Dilative	77%	43	44	44	7.775	2046	5166	8986
114.5	-94.5	MH		-					1.764	477	615	1057
119.5	-99.5	MH		-					2.385	669	984	1663
124.5	-104.5	MH		-					2.332	669	984	1637

## B.2.5. Anderson Street Overpass

### B.2.5.1. SPT P6-4 (P6P5)

Depth (ft)	Elevation (ft)	USCS	FC actual/estimate	P6-4 Nsafe	SPT N60	SPT Ntrip	SPT (N1)60	SPT (N1)60t	SPT (N1)trip	SPT (N1)60ta	u psf	$\sigma'_{vo}$ (avg) psf	Rebound inch
0.0	102.88	-	-	-	-	-	-	-	-	-	-	-	-
16	86.88	SP	3.7	8	8	7	10	11	8	11	351	1466	0.26
20	82.88	SP-SM	5.9	5	6	5	6	7	5	8	663	1686	0.22
26	76.88	SP-SM	10.7	17	19	17	20	22	17	27	975	1967	0.23
31	71.88	SP-SM	6.2	11	13	11	12	14	11	15	1287	2232	0.18
36	66.88	SP-SM	9.5	12	14	12	13	14	11	19	1599	2518	0.22
41	61.88	SP-SM	8.90	14	17	14	14	16	12	20	1911	2806	0.17
46	56.88	SP-SM	7.5	18	22	18	17	19	15	22	2223	3094	0.59
51	51.88	SM	46	5	6	5	5	5	4	14	2535	3269	0.04
56	46.88	SM	29.2	3	4	3	3	3	2	10	2847	3387	0.06
61	41.88	SM	14	2	2	2	2	2	2	7	3159	3478	0.21
66	36.88	SP-SM	9.4	4	5	4	4	4	3	8	3471	3633	0.01
69.5	33.38	SM	15.1	13	16	13	11	13	10	18	3689	3792	0.04
74.5	28.38	SM	17.1	17	20	17	14	16	12	22	4001	4053	0.26
76.5	26.38	SM	16.8	33	40	30	27	27	21	33	4126	4165	0.25
78.5	24.38	SM	15.2	28	34	26	23	23	18	29	4251	4273	0.22
81.5	21.38	SM	15.5	16	19	16	13	14	11	20	4438	4431	0.26
85.5	17.38	SM	15.9	9	11	9	7	8	6	13	4687	4606	0.25
87.5	15.38	SP-SM	11.3	10	12	10	8	9	7	14	4812	4699	0.66
89.5	13.38	SM	25.5	59	71	54	46	46	35	52	4937	4824	0.91
91.5	11.38	SM	22.9	28	34	26	21	21	16	28	5062	4937	1.06
93.5	9.38	SM	40.9	65	78	60	49	49	38	57	5187	5065	1.25
95.5	7.38	SM	31.3	33	40	30	25	25	19	32	5311	5185	
97.5	5.38	SM	32.8	33	40	30	24	24	19	32	5436	5292	
99.5	3.38	CL	50	24	29	25	17	-	-	-	5561	5420	
101.5	1.38	SM	26.3	39	47	36	28	28	22	35	5686	5540	
103.5	-0.62	SC	42.6	21	25	22	15	17	13	25	5811	5648	
105.5	-2.62	SM	39.7	30	36	28	21	21	16	29	5935	5753	
107.5	-4.62	MH	74.1	13	16	13	9	-	-	-	6060	5851	
109.5	-6.62	SM	25.6	27	32	28	19	21	16	27	6185	5954	
111.5	-8.62	SM	27.6	24	29	25	17	18	14	25	6310	6059	
113.5	-10.62	SM	31.2	40	48	37	27	27	21	34	6435	6172	
115.5	-12.62	SM	21	28	34	29	19	21	16	27	6559	6279	
117.5	-14.62	SM	38.6	35	42	32	24	24	18	31	6684	6384	
119.5	-16.62	SM	32.1	9	11	9	6	7	5	14	6809	6467	

Depth (ft)	Elevation (ft)	USCS	Rebound inch	Liquefaction Soil Response	Terzaghi Dr	Schmertmann Φ'	Hatanaka Φ'	Peck Φ'	Mayne OCR	Hera Cu (psf)	Hettiarachchi Cu (psf)	CDOT Qu (psf)
0.0	102.88	-										
16	86.88	SP	0.26	Contractive	40%	34	33	30				
20	82.88	SP-SM	0.22	Contractive	32%	30	30	29				
26	76.88	SP-SM	0.23	Intermediate	57%	40	38	33				
31	71.88	SP-SM	0.18	Contractive	46%	36	35	31				
36	66.88	SP-SM	0.22	Contractive	46%	36	35	31				
41	61.88	SP-SM	0.17	Contractive	49%	37	36	32				
46	56.88	SP-SM	0.59	Intermediate	54%	38	37	33				
51	51.88	SM	0.04	Contractive	28%	27	29	29				
56	46.88	SM	0.06	Contractive	21%	23	27	28				
61	41.88	SM	0.21	Contractive	17%	20	26	28				
66	36.88	SP-SM	0.01	Contractive	24%	24	28	29				
69.5	33.38	SM	0.04	Contractive	43%	34	34	32				
74.5	28.38	SM	0.26	Intermediate	49%	36	36	33				
76.5	26.38	SM	0.25	Dilative	68%	42	41	38				
78.5	24.38	SM	0.22	Intermediate	62%	40	39	37				
81.5	21.38	SM	0.26	Contractive	46%	35	35	33				
85.5	17.38	SM	0.25	Contractive	34%	29	31	30				
87.5	15.38	SP-SM	0.66	Contractive	36%	30	32	31				
89.5	13.38	SM	0.91	Dilative	87%	46	46	46				
91.5	11.38	SM	1.06	Intermediate	60%	39	38	37				
93.5	9.38	SM	1.25	Dilative	90%	47	47	47				
95.5	7.38	SM		Dilative	64%	40	39	38				
97.5	5.38	SM		Dilative	64%	40	39	38				
99.5	3.38	CL		-					4.943	1256	2362	4374
101.5	1.38	SM		Dilative	68%	41	41	40				
103.5	-0.62	SC		Intermediate	50%	35	36	34				
105.5	-2.62	SM		Intermediate	59%	38	38	37				
107.5	-4.62	MH		-					3.073	808	1279	2280
109.5	-6.62	SM		Intermediate	56%	37	38	36				
111.5	-8.62	SM		Intermediate	53%	36	37	35				
113.5	-10.62	SM		Dilative	67%	41	41	40				
115.5	-12.62	SM		Intermediate	56%	37	38	37				
117.5	-14.62	SM		Dilative	63%	39	39	39				
119.5	-16.62	SM		Contractive	32%	27	30	30				

### B.2.5.2. B.5.2. SPT P6-4 (P6P6)

Depth	Elevation	USCS	FC	P6-4	SPT	SPT	SPT	SPT	SPT	SPT	u	$\sigma'_{vo}$ (avg)	Rebound
(ft)	(ft)		actual/estimate	Nsafe	N60	Ntrip	(N1)60	(N1)60t	(N1)trip	(N1)60ta	psf	psf	inch
0.0	102.88	-	-	-	-	-	-	-	-	-	-	-	-
16	86.88	SP	<b>3.7</b>	8	8	7	10	11	8	11	351	1466	
20	82.88	SP-SM	<b>5.9</b>	5	6	5	6	7	5	8	663	1686	
26	76.88	SP-SM	<b>10.7</b>	17	19	17	20	22	17	27	975	1967	0.10
31	71.88	SP-SM	<b>6.2</b>	11	13	11	12	14	11	15	1287	2232	0.21
36	66.88	SP-SM	<b>9.5</b>	12	14	12	13	14	11	19	1599	2518	0.17
41	61.88	SP-SM	<b>8.90</b>	14	17	14	14	16	12	20	1911	2806	0.24
46	56.88	SP-SM	<b>7.5</b>	18	22	18	17	19	15	22	2223	3094	-0.57
51	51.88	SM	<b>46</b>	5	6	5	5	5	4	14	2535	3269	0.21
56	46.88	SM	<b>29.2</b>	3	4	3	3	3	2	10	2847	3387	-0.07
61	41.88	SM	<b>14</b>	2	2	2	2	2	2	7	3159	3478	0.09
66	36.88	SP-SM	<b>9.4</b>	4	5	4	4	4	3	8	3471	3633	0.25
69.5	33.38	SM	<b>15.1</b>	13	16	13	11	13	10	18	3689	3792	0.08
74.5	28.38	SM	<b>17.1</b>	17	20	17	14	16	12	22	4001	4053	0.17
76.5	26.38	SM	<b>16.8</b>	33	40	30	27	27	21	33	4126	4165	0.19
78.5	24.38	SM	<b>15.2</b>	28	34	26	23	23	18	29	4251	4273	0.19
81.5	21.38	SM	<b>15.5</b>	16	19	16	13	14	11	20	4438	4431	0.19
85.5	17.38	SM	<b>15.9</b>	9	11	9	7	8	6	13	4687	4606	0.22
87.5	15.38	SP-SM	<b>11.3</b>	10	12	10	8	9	7	14	4812	4699	0.32
89.5	13.38	SM	<b>25.5</b>	59	71	54	46	46	35	52	4937	4824	0.64
91.5	11.38	SM	<b>22.9</b>	28	34	26	21	21	16	28	5062	4937	0.50
93.5	9.38	SM	<b>40.9</b>	65	78	60	49	49	38	57	5187	5065	0.73
95.5	7.38	SM	<b>31.3</b>	33	40	30	25	25	19	32	5311	5185	0.96
97.5	5.38	SM	<b>32.8</b>	33	40	30	24	24	19	32	5436	5292	1.05
99.5	3.38	CL	<b>50</b>	24	29	25	17	-	-	-	5561	5420	0.92
101.5	1.38	SM	<b>26.3</b>	39	47	36	28	28	22	35	5686	5540	0.82
103.5	-0.62	SC	<b>42.6</b>	21	25	22	15	17	13	25	5811	5648	0.87
105.5	-2.62	SM	<b>39.7</b>	30	36	28	21	21	16	29	5935	5753	0.70
107.5	-4.62	MH	<b>74.1</b>	13	16	13	9	-	-	-	6060	5851	
109.5	-6.62	SM	<b>25.6</b>	27	32	28	19	21	16	27	6185	5954	
111.5	-8.62	SM	<b>27.6</b>	24	29	25	17	18	14	25	6310	6059	
113.5	-10.62	SM	<b>31.2</b>	40	48	37	27	27	21	34	6435	6172	
115.5	-12.62	SM	<b>21</b>	28	34	29	19	21	16	27	6559	6279	
117.5	-14.62	SM	<b>38.6</b>	35	42	32	24	24	18	31	6684	6384	
119.5	-16.62	SM	<b>32.1</b>	9	11	9	6	7	5	14	6809	6467	

Depth (ft)	Elevation (ft)	USCS	Rebound inch	Liquefaction Soil Response	Terzaghi Dr	Schmertmann Φ'	Hatanaka Φ'	Peck Φ'	Mayne OCR	Hera Cu (psf)	Hettiarachchi Cu (psf)	CDOT Qu (psf)
0.0	102.88	-										
16	86.88	SP		Contractive	40%	34	33	30				
20	82.88	SP-SM		Contractive	32%	30	30	29				
26	76.88	SP-SM	0.10	Intermediate	57%	40	38	33				
31	71.88	SP-SM	0.21	Contractive	46%	36	35	31				
36	66.88	SP-SM	0.17	Contractive	46%	36	35	31				
41	61.88	SP-SM	0.24	Contractive	49%	37	36	32				
46	56.88	SP-SM	-0.57	Intermediate	54%	38	37	33				
51	51.88	SM	0.21	Contractive	28%	27	29	29				
56	46.88	SM	-0.07	Contractive	21%	23	27	28				
61	41.88	SM	0.09	Contractive	17%	20	26	28				
66	36.88	SP-SM	0.25	Contractive	24%	24	28	29				
69.5	33.38	SM	0.08	Contractive	43%	34	34	32				
74.5	28.38	SM	0.17	Intermediate	49%	36	36	33				
76.5	26.38	SM	0.19	Dilative	68%	42	41	38				
78.5	24.38	SM	0.19	Intermediate	62%	40	39	37				
81.5	21.38	SM	0.19	Contractive	46%	35	35	33				
85.5	17.38	SM	0.22	Contractive	34%	29	31	30				
87.5	15.38	SP-SM	0.32	Contractive	36%	30	32	31				
89.5	13.38	SM	0.64	Dilative	87%	46	46	46				
91.5	11.38	SM	0.50	Intermediate	60%	39	38	37				
93.5	9.38	SM	0.73	Dilative	90%	47	47	47				
95.5	7.38	SM	0.96	Dilative	64%	40	39	38				
97.5	5.38	SM	1.05	Dilative	64%	40	39	38				
99.5	3.38	CL	0.92	-					4.943	1256	2362	4374
101.5	1.38	SM	0.82	Dilative	68%	41	41	40				
103.5	-0.62	SC	0.87	Intermediate	50%	35	36	34				
105.5	-2.62	SM	0.70	Intermediate	59%	38	38	37				
107.5	-4.62	MH		-					3.073	808	1279	2280
109.5	-6.62	SM		Intermediate	56%	37	38	36				
111.5	-8.62	SM		Intermediate	53%	36	37	35				
113.5	-10.62	SM		Dilative	67%	41	41	40				
115.5	-12.62	SM		Intermediate	56%	37	38	37				
117.5	-14.62	SM		Dilative	63%	39	39	39				
119.5	-16.62	SM		Contractive	32%	27	30	30				

## B.2.6. I-4 Widening Daytona

### B.2.6.1. SPT DC-1 (EB3-1, P5)

Depth (ft)	Elevation (ft)	USCS	FC actual/estimate	DC-1 Nsafe	SPT N60	SPT Ntrip	SPT (N1)60	SPT (N1)60t	SPT (N1)trip	SPT (N1)60ta	u psf	$\sigma'_{vo}$ (avg) psf	Rebound inch
0.0	42.0	-	-	-	-	-	-	-	-	-	-	-	-
1.0	41.0	SP X SP-SM	5	7	8	6	16	16	12	16	0	108	
3.0	39.0	SP X SP-SM	5	10	11	8	23	23	17	23	12	314	
5.0	37.0	SP X SP-SM	5	15	17	13	34	34	26	34	137	431	
7.0	35.0	SP X SP-SM	5	19	21	16	40	40	31	40	262	564	
9.0	33.0	SP X SP-SM	5	20	23	18	38	38	29	38	387	699	
12.0	30.0	SP X SP-SM	5	29	33	25	48	48	37	48	574	915	
14.5	27.5	SP X SP-SM	5	25	32	25	43	43	33	43	730	1086	
17.0	25.0	SP X SP-SM	5	12	15	13	19	22	17	22	886	1235	
19.5	22.5	SP X SP-SM	7	10	13	11	15	17	13	19	1042	1379	
22.0	20.0	SP X SP-SM	5	14	20	15	23	23	18	23	1198	1523	
24.5	17.5	SP X SP-SM	5	19	27	21	30	30	23	30	1354	1677	
27.0	15.0	SP X SP-SM	5	26	37	28	39	39	30	39	1510	1844	
29.5	12.5	SP X SP-SM	5	30	43	33	43	43	33	43	1666	2013	
32.0	10.0	SP X SP-SM	5	8	12	10	12	13	10	13	1822	2152	
34.5	7.5	SP X SP-SM	5	8	12	10	11	12	10	12	1978	2283	0.11
37.0	5.0	SP X SP-SM	5	7	11	9	10	11	8	11	2134	2415	0.27
39.5	2.5	SP X SP-SM	5	5	8	7	7	7	6	7	2290	2536	0.24
42.0	0.0	SP X SP-SM	5	9	14	12	12	13	10	13	2446	2665	0.24
44.5	-2.5	SP X SP-SM	5	12	18	15	15	17	13	17	2602	2807	0.28
47.0	-5.0	SP X SP-SM	5	9	14	12	11	12	10	12	2758	2941	0.28
49.5	-7.5	SP X SP-SM	5	8	12	10	10	11	8	11	2914	3072	0.29
52.0	-10.0	SM	12	4	6	5	5	5	4	11	3070	3164	0.21
54.5	-12.5	SM	12	8	12	10	9	10	8	16	3226	3275	0.23
57.0	-15.0	SM	40	WH	WH	WH	0	0	0	8	3382	3314	0.20
59.5	-17.5	SM	12	4	6	5	5	5	4	10	3538	3383	0.15
62.0	-20.0	SM	12	5	8	7	6	6	5	12	3694	3475	0.15
64.5	-22.5	SM	12	5	8	7	6	6	5	11	3850	3569	0.15
67.0	-25.0	SC	12	10	15	13	11	12	9	17	4006	3683	0.13
69.5	-27.5	SP-SM	8.5	28	42	32	30	30	23	34	4162	3832	0.28
72.0	-30.0	SP-SM	8.5	52	78	60	55	55	42	59	4318	4008	0.43
74.5	-32.5	SP-SM	8.5	34	51	39	35	35	27	39	4474	4180	0.42
77.0	-35.0	SM	12	20	30	23	20	20	16	26	4630	4319	0.35
79.5	-37.5	SM	12	13	20	17	13	15	11	20	4786	4450	0.28
82.0	-40.0	SM	16	11	17	15	11	12	9	18	4942	4572	0.17
84.5	-42.5	SM	12	17	26	22	17	18	14	24	5098	4701	0.17
87.0	-45.0	SM	12	11	17	15	11	12	9	17	5254	4822	0.23
89.5	-47.5	LBWLS		50/6	50/6	50/6	63	63	63	63	5410	5021	0.27
92.0	-50.0	LBWLS		14	21	18	13	14	11	14	5566	5200	0.28
94.5	-52.5	LBWLS		50/1	50/1	50/1	61	61	61	61	5722	5409	
97	-55	LBWLS		50/0	50/0	50/0	60	60	60	60	5878	5628	
99.5	-57.5	LBWLS		50/1	50/1	50/1	58	58	58	58	6034	5847	
102	-60	LBWLS		50/0	50/0	50/0	57	57	57	57	6190	6066	
104.5	-62.5	LBWLS		7	11	9	6	7	5	7	6346	6225	
107	-65	LBWLS		50/1	50/1	50/1	56	56	56	56	6502	6429	
109.5	-67.5	LBWLS		30	45	35	25	25	19	25	6658	6628	
112	-70	LBWLS		50/1	50/1	50/1	54	54	54	54	6814	6842	
114.5	-72.5	LBWLS		50/1	50/1	50/1	53	53	53	53	6970	7061	
117	-75	LBWLS		33	50	38	26	26	20	26	7126	7260	

Depth (ft)	Elevation (ft)	USCS	Rebound inch	Liquefaction Soil Response	Terzaghi Dr	Schmertmann Φ'	Hatanaka Φ'	Peck Φ'	Mayne OCR	Hera Cu (psf)	Hettiarachchi Cu (psf)	CDOT Qu (psf)
0.0	42.0	-										
1.0	41.0	SP X SP-SM		Contractive	51%	40	36	29				
3.0	39.0	SP X SP-SM		Intermediate	61%	42	39	30				
5.0	37.0	SP X SP-SM		Dilative	75%	45	43	32				
7.0	35.0	SP X SP-SM		Dilative	82%	47	45	33				
9.0	33.0	SP X SP-SM		Dilative	80%	47	44	34				
12.0	30.0	SP X SP-SM		Dilative	90%	49	47	36				
14.5	27.5	SP X SP-SM		Dilative	85%	48	46	36				
17.0	25.0	SP X SP-SM		Intermediate	57%	40	38	31				
19.5	22.5	SP X SP-SM		Contractive	51%	38	36	31				
22.0	20.0	SP X SP-SM		Intermediate	62%	42	39	33				
24.5	17.5	SP X SP-SM		Intermediate	70%	44	41	35				
27.0	15.0	SP X SP-SM		Dilative	80%	47	44	37				
29.5	12.5	SP X SP-SM		Dilative	84%	48	46	39				
32.0	10.0	SP X SP-SM		Contractive	44%	35	34	31				
34.5	7.5	SP X SP-SM	0.11	Contractive	43%	35	34	31				
37.0	5.0	SP X SP-SM	0.27	Contractive	40%	34	33	30				
39.5	2.5	SP X SP-SM	0.24	Contractive	33%	31	31	29				
42.0	0.0	SP X SP-SM	0.24	Contractive	44%	35	34	31				
44.5	-2.5	SP X SP-SM	0.28	Contractive	50%	37	36	32				
47.0	-5.0	SP X SP-SM	0.28	Contractive	43%	35	34	31				
49.5	-7.5	SP X SP-SM	0.29	Contractive	40%	33	33	31				
52.0	-10.0	SM	0.21	Contractive	28%	27	29	29				
54.5	-12.5	SM	0.23	Contractive	40%	32	33	31				
57.0	-15.0	SM	0.20	Contractive	0%	0	20	27				
59.5	-17.5	SM	0.15	Contractive	28%	26	29	29				
62.0	-20.0	SM	0.15	Contractive	31%	29	30	29				
64.5	-22.5	SM	0.15	Contractive	31%	28	30	29				
67.0	-25.0	SC	0.13	Contractive	43%	34	34	31				
69.5	-27.5	SP-SM	0.28	Dilative	71%	43	42	39				
72.0	-30.0	SP-SM	0.43	Dilative	96%	49	49	47				
74.5	-32.5	SP-SM	0.42	Dilative	77%	44	43	41				
77.0	-35.0	SM	0.35	Intermediate	58%	39	38	36				
79.5	-37.5	SM	0.28	Contractive	47%	35	35	33				
82.0	-40.0	SM	0.17	Contractive	43%	33	34	32				
84.5	-42.5	SM	0.17	Intermediate	53%	37	37	35				
87.0	-45.0	SM	0.23	Contractive	42%	33	33	32				
89.5	-47.5	LBWLS	0.27	Dilative								
92.0	-50.0	LBWLS	0.28	Contractive								
94.5	-52.5	LBWLS		Dilative								
97	-55	LBWLS		Dilative								
99.5	-57.5	LBWLS		Dilative								
102	-60	LBWLS		Dilative								
104.5	-62.5	LBWLS		Contractive								
107	-65	LBWLS		Dilative								
109.5	-67.5	LBWLS		Intermediate								
112	-70	LBWLS		Dilative								
114.5	-72.5	LBWLS		Dilative								
117	-75	LBWLS		Intermediate								

## B.2.7. SR-83 over Ramsey Branch

### B.2.7.1. SPT B-1 (EB1P1)

Depth (ft)	Elevation (ft)	USCS	FC actual/estimate	B-1 Nsaf	SPT N60	SPT Ntrip	SPT (N1)60	SPT (N1)60t	SPT (N1)trip	SPT (N1)60ta	u psf	$\sigma'_{vo}$ (avg) psf	Rebound inch	Liquefaction Soil Response
0	3.5													
0.5	3	SP	0	2	2	2	5	5	3	5	0	48		Contractive
2	1.5	SC	12	5	5	4	9	9	8	9	31	174		Contractive
3.5	0	PT		2	2	2	-	-	-	-	125	230		-
5	-1.5	PT	6.4	1	1	1	-	-	-	-	218	264		-
6.5	-3	PT		WH	WH	WH	-	-	-	-	312	281		-
8	-4.5	PT		WH	WH	WH	-	-	-	-	406	292		-
9.5	-6	SP-SM	8.5	2	2	2	5	5	4	9	499	333		Contractive
12	-8.5	SC	12	WH	WH	WH	0	0	0	5	655	367		Contractive
14.5	-11	SC	16.6	WH	WH	WH	0	0	0	6	811	386		Contractive
17	-13.5	SC	12	WH	WH	WH	0	0	0	5	967	405		Contractive
19.5	-16	SC	12	WH	WH	WH	0	0	0	5	1123	424		Contractive
22	-18.5	SC	12	WH	WH	WH	0	0	0	5	1279	443		Contractive
24.5	-21	SC	12	WH	WH	WH	0	0	0	5	1435	462		Contractive
27	-23.5	SM	31.3	2	3	2	5	6	5	13	1591	541		Contractive
29.5	-26	SC	12	7	9	7	15	16	13	22	1747	665		Intermediate
32	-28.5	SC	12	11	14	10	21	21	16	27	1903	797		Intermediate
34.5	-31	SC	12	6	8	6	11	12	9	17	2059	918		Contractive
37	-33.5	SC	12	10	12	10	17	18	14	24	2215	1047		Intermediate
39.5	-36	SC	12	10	12	10	16	17	13	23	2371	1179		Intermediate
42	-38.5	SC	12	7	9	8	11	12	10	18	2527	1300		Contractive
44.5	-41	SC	12	7	9	8	11	12	9	17	2683	1419		Contractive
47	-43.5	SC	30.7	6	8	6	9	10	7	17	2839	1538		Contractive
49.5	-46	SC	12	6	8	6	8	9	7	14	2995	1657		Contractive
52	-48.5	SC	12	6	8	6	8	9	7	14	3151	1766	0.27	Contractive
54.5	-51	SC	12	6	8	6	8	9	7	14	3307	1873	0.32	Contractive
57	-53.5	SC	12	6	8	6	8	8	6	14	3463	1979	0.41	Contractive
59.5	-56	SC	12	6	8	6	7	8	6	13	3619	2086	0.62	Contractive
62	-58.5	SC	12	7	9	8	9	10	7	15	3775	2202	0.72	Contractive
64.5	-61	SC	12	16	20	17	18	20	15	25	3931	2331	0.68	Intermediate
67	-63.5	SC	12	16	20	17	18	20	15	25	4087	2463	0.83	Intermediate
69.5	-66	SP	0	12	15	13	13	15	11	15	4243	2614	0.59	Contractive
72	-68.5	SC	12	15	18	15	15	17	13	22	4399	2751	0.42	Intermediate
74.5	-71	SM	12	7	9	8	8	8	6	14	4555	2862	0.30	Contractive
77	-73.5	SM	12	5	6	5	5	5	4	11	4711	2949	0.22	Contractive
79.5	-76	SM	13.4	6	8	6	6	7	5	12	4867	3040	0.30	Contractive
82	-78.5	SM	12	68	83	63	65	65	50	70	5023	3194	0.39	Dilative
84.5	-81	SM	12	25	30	23	23	23	18	28	5179	3333	0.40	Intermediate
87	-83.5	SM	12	5	6	5	5	5	4	10	5335	3425		Contractive
89.5	-86	SM	12	6	8	6	6	6	5	11	5491	3516		Contractive
92	-88.5	SC	12	10	12	10	9	10	8	15	5647	3630		Contractive
94.5	-91	SC	12	6	8	6	5	6	5	11	5803	3729		Contractive
97	-93.5	SP	0	7	9	8	6	7	6	7	5959	3853		Contractive
99.5	-96	SP	0	9	11	9	7	8	6	8	6115	3985		Contractive
102	-98.5	SP	0	9	11	9	7	8	6	8	6271	4116		Contractive
104.5	-101	SP	0	7	9	8	6	7	5	7	6427	4238		Contractive
107	-103.5	SP	0	9	11	9	7	8	6	8	6583	4367		Contractive
109.5	-106	SP	0	15	18	15	12	13	10	13	6739	4508		Contractive
112	-108.5	SM	12	11	14	12	9	10	8	15	6895	4632		Contractive
114.5	-111	SM	21.2	11	14	12	9	10	7	16	7051	4751		Contractive

Depth (ft)	Elevation (ft)	USCS	Rebound inch	Liquefaction Soil Response	Terzaghi Dr	Schmertmann Φ'	Hatanaka Φ'	Peck Φ'	Mayne OCR	Hera Cu (psf)	Hettiarachchi Cu (psf)	CDOT Qu (psf)
0	3.5											
0.5	3	SP		Contractive	27%	29	28	28				
2	1.5	SC		Contractive	39%	34	32	28				
3.5	0	PT		-								
5	-1.5	PT		-								
6.5	-3	PT		-								
8	-4.5	PT		-								
9.5	-6	SP-SM		Contractive	27%	27	29	28				
12	-8.5	SC		Contractive	0%	0	20	27				
14.5	-11	SC		Contractive	0%	0	20	27				
17	-13.5	SC		Contractive	0%	0	20	27				
19.5	-16	SC		Contractive	0%	0	20	27				
22	-18.5	SC		Contractive	0%	0	20	27				
24.5	-21	SC		Contractive	0%	0	20	27				
27	-23.5	SM		Contractive	30%	28	30	28				
29.5	-26	SC		Intermediate	50%	37	36	30				
32	-28.5	SC		Intermediate	60%	41	38	31				
34.5	-31	SC		Contractive	43%	35	34	29				
37	-33.5	SC		Intermediate	53%	39	37	31				
39.5	-36	SC		Intermediate	51%	38	36	31				
42	-38.5	SC		Contractive	43%	35	34	30				
44.5	-41	SC		Contractive	42%	35	34	30				
47	-43.5	SC		Contractive	38%	33	32	29				
49.5	-46	SC		Contractive	37%	32	32	29				
52	-48.5	SC	0.27	Contractive	36%	32	32	29				
54.5	-51	SC	0.32	Contractive	36%	32	32	29				
57	-53.5	SC	0.41	Contractive	35%	31	31	29				
59.5	-56	SC	0.62	Contractive	35%	31	31	29				
62	-58.5	SC	0.72	Contractive	38%	32	32	30				
64.5	-61	SC	0.68	Intermediate	55%	39	38	33				
67	-63.5	SC	0.83	Intermediate	54%	39	37	33				
69.5	-66	SP	0.59	Contractive	47%	36	35	31				
72	-68.5	SC	0.42	Intermediate	51%	37	36	32				
74.5	-71	SM	0.30	Contractive	35%	31	31	30				
77	-73.5	SM	0.22	Contractive	29%	27	29	29				
79.5	-76	SM	0.30	Contractive	32%	29	30	29				
82	-78.5	SM	0.39	Dilative	104%	51	52	48				
84.5	-81	SM	0.40	Intermediate	62%	41	39	36				
87	-83.5	SM		Contractive	28%	26	29	29				
89.5	-86	SM		Contractive	31%	28	30	29				
92	-88.5	SC		Contractive	39%	32	32	31				
94.5	-91	SC		Contractive	30%	28	30	29				
97	-93.5	SP		Contractive	33%	29	31	30				
99.5	-96	SP		Contractive	35%	30	31	30				
102	-98.5	SP		Contractive	35%	30	31	30				
104.5	-101	SP		Contractive	32%	28	30	30				
107	-103.5	SP		Contractive	34%	29	31	30				
109.5	-106	SP		Contractive	45%	34	34	32				
112	-108.5	SM		Contractive	38%	31	32	31				
114.5	-111	SM		Contractive	38%	31	32	31				
117	-113.5	SM		Contractive	44%	33	34	32				
119.5	-116	SP		Dilative	102%	49	55	52				

**B.2.7.2. B.7.2. SPT B-2 (P4P5)**

Depth (ft)	Elevation (ft)	USCS	FC actual/estimate	B-2 Nsafe	SPT N60	SPT Ntrip	SPT (N1)60	SPT (N1)60t	SPT (N1)trip	SPT (N1)60ta	u psf	$\sigma'_{vo}$ (avg) psf	Rebound inch
0	1												
0.5	0.5	SP-SM	8.5	5	5	4	9	9	7	9	0	51	
2	-1	SP	0	12	11	8	23	23	17	27	62	165	
3.5	-2.5	SP	0	4	3	3	7	8	6	8	156	249	
5	-4	SC	12	6	6	5	11	13	10	18	250	323	
6.5	-5.5	SP-SC	8.5	7	7	6	14	15	12	19	343	404	
8	-7	SP-SC	8.5	11	10	8	20	20	16	24	437	491	
9.5	-8.5	SP-SC	8.5	1	1	1	2	2	2	6	530	545	
12	-11	SP-SC	8.7	4	3	3	6	7	5	11	686	642	
14.5	-13.5	SP-SC	8.5	WH	WH	WH	0	0	0	4	842	694	
17	-16	SP-SC	8.5	WH	WH	WH	0	0	0	4	998	732	
19.5	-18.5	SP-SC	8.5	WH	WH	WH	0	0	0	4	1154	769	
22	-21	SC	12	5	6	5	9	10	7	15	1310	872	
24.5	-23.5	SC	12	6	7	6	10	11	9	16	1466	991	1.04
27	-26	SC	12	12	14	12	19	21	16	26	1622	1120	1.19
29.5	-28.5	SP-SM	8.5	17	20	15	25	25	19	29	1778	1272	1.44
32	-31	SC	12	31	38	29	44	44	34	50	1934	1428	0.78
34.5	-33.5	SC	12	9	11	9	12	13	10	18	2090	1555	1.03
37	-36	SC	12	9	11	9	11	13	10	18	2246	1674	0.97
39.5	-38.5	SC	28	7	9	8	10	11	8	17	2402	1793	1.13
42	-41	SC	12	10	12	10	12	14	10	19	2558	1912	1.11
44.5	-43.5	SC	12	10	12	10	12	13	10	18	2714	2031	0.98
47	-46	SC	12	6	8	7	7	8	6	13	2870	2140	1.01
49.5	-48.5	SC	12	7	9	8	8	9	7	15	3026	2246	1.08
52	-51	SC	12	6	8	7	7	8	6	13	3182	2353	0.45
54.5	-53.5	SC	12	6	8	7	7	8	6	13	3338	2459	1.03
57	-56	SC	12	7	9	8	8	9	7	14	3494	2566	1.36
59.5	-58.5	SC	12	6	8	7	7	7	6	12	3650	2662	1.04
62	-61	SC	12	7	9	8	8	9	7	14	3806	2766	0.94
64.5	-63.5	SC	12	7	9	8	8	8	6	14	3962	2873	0.48
67	-66	SC	12	19	23	20	18	20	16	26	4118	2999	0.49
69.5	-68.5	SC	12	9	11	9	8	9	7	15	4274	3111	0.29
72	-71	SC	12	14	17	15	13	14	11	20	4430	3237	0.25
74.5	-73.5	SC	12	9	11	9	8	9	7	14	4586	3349	0.29
77	-76	SC	12	53	65	50	49	49	37	54	4742	3505	0.35
79.5	-78.5	SC	12	9	11	9	8	9	7	14	4898	3624	0.39
82	-81	SC	17	7	9	8	7	7	6	13	5054	3731	0.36
84.5	-83.5	SC	12	30	36	28	26	26	20	31	5210	3867	0.34
87	-86	SC	12	16	20	17	14	15	12	21	5366	4001	0.28
89.5	-88.5	SC	12	19	23	20	16	17	13	23	5522	4133	0.28
92	-91	SC	12	4	5	4	3	3	3	9	5678	4204	0.31
94.5	-93.5	SP	0	12	15	13	10	11	9	11	5834	4331	0.32
97	-96	SP	0	11	14	12	9	10	8	10	5990	4475	0.32
99.5	-98.5	SP	0	6	8	7	5	6	4	6	6146	4589	0.33
102	-101	SC	12	6	8	7	5	5	4	11	6302	4675	0.34
104.5	-103.5	SC	12	5	6	5	4	4	3	10	6458	4747	0.29
107	-106	SC	12	6	8	7	5	5	4	11	6614	4826	0.20
109.5	-108.5	SC	12	5	6	5	4	4	3	9	6770	4897	
112	-111	SP	0	16	20	17	12	14	11	14	6926	5026	
114.5	-113.5	SP	0	14	17	15	10	11	9	11	7082	5170	
117	-116	SP	0	11	14	12	8	9	7	9	7238	5314	
119.5	-118.5	SC	12	10	12	10	7	8	6	13	7394	5428	
122	-121	SC	12	16	20	17	12	13	10	18	7550	5545	
124.5	-123.5	SC	14.3	50/6	50/6	50/6	59	59	59	65	7706	5704	
127	-126	SC	12	50/6	50/6	50/6	58	58	58	64	7862	5873	
129.5	-128.5	SC	12	50/5.5	50/5.5	50/5.5	58	58	58	63	8018	6042	

Depth (ft)	Elevation (ft)	USCS	Rebound inch	Liquefaction Soil Response	Terzaghi Dr	Schmertmann Φ'	Hatanaka Φ'	Peck Φ'	Mayne OCR	Hera Cu (psf)	Hettiarachchi Cu (psf)	CDOT Qu (psf)
0	1											
0.5	0.5	SP-SM		Contractive	39%	36	32	29				
2	-1	SP		Intermediate	61%	43	39	30				
3.5	-2.5	SP		Contractive	34%	30	31	28				
5	-4	SC		Contractive	43%	36	34	29				
6.5	-5.5	SP-SC		Contractive	47%	37	35	29				
8	-7	SP-SC		Intermediate	58%	40	38	30				
9.5	-8.5	SP-SC		Contractive	19%	21	26	27				
12	-11	SP-SC		Contractive	32%	0	30	27				
14.5	-13.5	SP-SC		Contractive	0%	0	20	27				
17	-16	SP-SC		Contractive	0%	0	20	27				
19.5	-18.5	SP-SC		Contractive	0%	0	20	27				
22	-21	SC		Contractive	38%	0	32	27				
24.5	-23.5	SC	1.04	Contractive	41%	0	33	27				
27	-26	SC	1.19	Intermediate	56%	40	38	31				
29.5	-28.5	SP-SM	1.44	Intermediate	65%	43	40	33				
32	-31	SC	0.78	Dilative	86%	48	46	38				
34.5	-33.5	SC	1.03	Contractive	45%	36	34	30				
37	-36	SC	0.97	Contractive	44%	36	34	30				
39.5	-38.5	SC	1.13	Contractive	40%	33	33	30				
42	-41	SC	1.11	Contractive	45%	36	34	31				
44.5	-43.5	SC	0.98	Contractive	45%	35	34	31				
47	-46	SC	1.01	Contractive	35%	31	31	29				
49.5	-48.5	SC	1.08	Contractive	38%	32	32	30				
52	-51	SC	0.45	Contractive	34%	31	31	29				
54.5	-53.5	SC	1.03	Contractive	34%	31	31	29				
57	-56	SC	1.36	Contractive	36%	31	32	30				
59.5	-58.5	SC	1.04	Contractive	33%	30	31	29				
62	-61	SC	0.94	Contractive	36%	31	31	30				
64.5	-63.5	SC	0.48	Contractive	35%	31	31	30				
67	-66	SC	0.49	Intermediate	55%	39	38	34				
69.5	-68.5	SC	0.29	Contractive	37%	32	32	30				
72	-71	SC	0.25	Contractive	46%	36	35	32				
74.5	-73.5	SC	0.29	Contractive	37%	32	32	30				
77	-76	SC	0.35	Dilative	90%	48	47	44				
79.5	-78.5	SC	0.39	Contractive	36%	31	32	30				
82	-81	SC	0.36	Contractive	33%	29	31	30				
84.5	-83.5	SC	0.34	Dilative	66%	42	40	37				
87	-86	SC	0.28	Intermediate	48%	36	35	33				
89.5	-88.5	SC	0.28	Intermediate	51%	37	36	34				
92	-91	SC	0.31	Contractive	23%	24	27	29				
94.5	-93.5	SP	0.32	Contractive	41%	33	33	31				
97	-96	SP	0.32	Contractive	39%	32	32	31				
99.5	-98.5	SP	0.33	Contractive	29%	27	29	29				
102	-101	SC	0.34	Contractive	29%	27	29	29				
104.5	-103.5	SC	0.29	Contractive	25%	25	28	29				
107	-106	SC	0.20	Contractive	28%	27	29	29				
109.5	-108.5	SC		Contractive	25%	24	28	29				
112	-111	SP		Contractive	45%	34	35	33				
114.5	-113.5	SP		Contractive	41%	32	33	32				
117	-116	SP		Contractive	37%	31	32	31				
119.5	-118.5	SC		Contractive	35%	49	31	52				
122	-121	SC		Contractive	44%	49	34	52				
124.5	-123.5	SC		Dilative	99%	48	54	52				
127	-126	SC		Dilative	99%	48	54	52				
129.5	-128.5	SC		Dilative	98%	48	54	52				

### B.2.7.3. B.7.3. SPT FDOT (EB5P2)

Depth	Elevation	USCS	FC	FDOT	SPT	SPT	SPT	SPT	SPT	SPT	u	$\sigma'_{vo}$ (avg)	Rebound
(ft)	(ft)		actual/estimate	Nsafe	N60	Ntrip	(N1)60	(N1)60t	(N1)trip	(N1)60ta	psf	psf	inch
0	9.3												
1	8.3	SM	<b>13</b>	10	9	7	18	18	14	18	0	125	
3	6.3	SM	<b>13.4</b>	21	19	15	38	38	29	44	0	375	
5	4.3	SM	<b>13.4</b>	14	12	10	24	24	18	29	62	548	
7	2.3	SM	<b>19.5</b>	6	6	5	10	11	8	17	187	645	
9	0.3	SM	<b>19.5</b>	5	5	4	7	8	6	14	312	733	
12	-2.7	SM	<b>29.1</b>	WH	WH	WH	0	0	0	7	499	773	
14.5	-5.2	SM	<b>29.1</b>	2	3	2	4	4	3	11	655	832	
17	-7.7	SM	<b>10.9</b>	WH	WH	WH	0	0	0	5	811	861	
19.5	-10.2	SM	<b>10.9</b>	WH	WH	WH	0	0	0	5	967	880	
22	-12.7	SP-SM	<b>10.3</b>	WH	WH	WH	0	0	0	5	1123	919	
24.5	-15.2	SM	<b>21.6</b>	2	3	2	4	5	3	11	1279	983	
27	-17.7	SM	<b>21.6</b>	5	6	5	8	9	7	15	1435	1082	
29.5	-20.2	SM	<b>29.6</b>	20	23	18	29	29	22	36	1591	1219	
32	-22.7	SM	<b>29.6</b>	19	23	17	27	27	21	34	1747	1363	0.89
34.5	-25.2	SM	<b>32.4</b>	52	63	48	72	72	55	79	1903	1527	0.30
37	-27.7	SM	<b>40.4</b>	21	26	20	28	28	21	36	2059	1676	0.00
39.5	-30.2	SM	<b>40.4</b>	14	17	14	17	19	15	27	2215	1810	0.11
42	-32.7	SM	<b>37</b>	10	12	10	12	14	10	21	2371	1931	0.42
44.5	-35.2	SM	<b>37</b>	16	20	17	19	21	16	29	2527	2060	0.24
47	-37.7	SM	<b>42.7</b>	9	11	9	10	11	9	19	2683	2182	0.36
49.5	-40.2	SM	<b>42.7</b>	7	9	8	8	9	7	18	2839	2301	0.37
52	-42.7	SM	<b>43.9</b>	9	11	9	10	11	8	19	2995	2420	0.20
54.5	-45.2	SM	<b>43.9</b>	6	8	6	7	7	6	16	3151	2529	0.25
57	-47.7	SM	<b>36.6</b>	6	8	6	7	7	6	15	3307	2635	0.78
59.5	-50.2	SM	<b>36.6</b>	9	11	9	9	10	8	18	3463	2752	0.97
62	-52.7	SM	<b>36.5</b>	10	12	10	10	11	9	19	3619	2871	1.30
64.5	-55.2	SM	<b>36.5</b>	7	9	8	7	8	6	16	3775	2980	1.11
67	-57.7	SM	<b>37.8</b>	11	14	12	11	12	9	20	3931	3096	0.99
69.5	-60.2	SM	<b>37.8</b>	14	17	14	13	14	11	22	4087	3225	0.60
72	-62.7	SM	<b>38.9</b>	21	26	22	20	22	17	30	4243	3357	0.83
74.5	-65.2	SM	<b>38.9</b>	16	20	17	15	16	13	24	4399	3488	0.74
77	-67.7	SM	<b>29.2</b>	62	75	58	56	56	43	62	4555	3650	0.43
79.5	-70.2	SM	<b>29.2</b>	11	14	12	10	11	8	18	4711	3779	0.21
82	-72.7	SM	<b>17.9</b>	76	92	70	65	65	50	71	4867	3938	0.14
84.5	-75.2	SM	<b>17.9</b>	27	33	25	23	23	18	29	5023	4077	0.26
87	-77.7	SM	<b>32</b>	15	18	15	12	14	11	21	5179	4198	0.33
89.5	-80.2	SM	<b>32</b>	14	17	14	11	12	10	20	5335	4317	

Depth (ft)	Elevation (ft)	USCS	Rebound inch	Liquefaction Soil Response	Terzaghi Dr	Schmertmann Φ'	Hatanaka Φ'	Peck Φ'	Mayne OCR	Hera Cu (psf)	Hettiarachchi Cu (psf)	CDOT Qu (psf)
0	9.3											
1	8.3	SM		Contractive	55%	41	37	30				
3	6.3	SM		Dilative	80%	47	44	33				
5	4.3	SM		Intermediate	63%	41	39	31				
7	2.3	SM		Contractive	41%	34	33	29				
9	0.3	SM		Contractive	35%	31	31	28				
12	-2.7	SM		Contractive	0%	0	20	27				
14.5	-5.2	SM		Contractive	26%	26	28	28				
17	-7.7	SM		Contractive	0%	0	20	27				
19.5	-10.2	SM		Contractive	0%	0	20	27				
22	-12.7	SP-SM		Contractive	0%	0	20	27				
24.5	-15.2	SM		Contractive	26%	0	28	27				
27	-17.7	SM		Contractive	36%	0	32	27				
29.5	-20.2	SM		Dilative	70%	0	41	27				
32	-22.7	SM	0.89	Dilative	67%	44	40	34				
34.5	-25.2	SM	0.30	Dilative	110%	53	53	44				
37	-27.7	SM	0.00	Dilative	68%	44	41	34				
39.5	-30.2	SM	0.11	Intermediate	54%	39	37	32				
42	-32.7	SM	0.42	Intermediate	45%	36	34	31				
44.5	-35.2	SM	0.24	Intermediate	57%	40	38	33				
47	-37.7	SM	0.36	Contractive	41%	34	33	30				
49.5	-40.2	SM	0.37	Contractive	37%	32	32	30				
52	-42.7	SM	0.20	Contractive	40%	33	33	30				
54.5	-45.2	SM	0.25	Contractive	33%	30	31	29				
57	-47.7	SM	0.78	Contractive	33%	30	31	29				
59.5	-50.2	SM	0.97	Contractive	39%	32	32	30				
62	-52.7	SM	1.30	Contractive	41%	33	33	31				
64.5	-55.2	SM	1.11	Contractive	35%	31	31	30				
67	-57.7	SM	0.99	Contractive	43%	34	34	31				
69.5	-60.2	SM	0.60	Intermediate	47%	35	35	32				
72	-62.7	SM	0.83	Intermediate	57%	39	38	34				
74.5	-65.2	SM	0.74	Intermediate	50%	36	36	33				
77	-67.7	SM	0.43	Dilative	96%	49	49	47				
79.5	-70.2	SM	0.21	Contractive	40%	33	33	31				
82	-72.7	SM	0.14	Dilative	104%	50	52	50				
84.5	-75.2	SM	0.26	Intermediate	62%	40	39	36				
87	-77.7	SM	0.33	Intermediate	46%	34	35	32				
89.5	-80.2	SM		Contractive	43%	33	34	32				

## B.2.8. SR-528 over Indian River

### B.2.8.1. SPT TB-4 (P4P7)

Depth (ft)	Elevation (ft)	USCS	FC actual/estimate	TB-4 Nsafe	SPT N60	SPT Ntrip	SPT (N1)60	SPT (N1)60t	SPT (N1)trip	SPT (N1)60ta	u psf	$\sigma'_{vo}$ (avg) psf	Rebound inch
0	4												
7	-3	SP	0	5	4	3	7	8	6	8	250	525	
8.5	-4.5	SP	0	2	2	1	3	3	2	3	343	589	
12	-8	SM	12	3	2	2	4	4	3	9	562	691	
14.5	-10.5	CL	50	2	2	1	3	-	-	-	718	810	
17	-13	CL	50	4	3	3	5	-	-	-	874	941	
19.5	-15.5	SP	0	20	17	13	23	23	18	23	1030	1093	
22	-18	SP	0	23	22	17	28	28	21	28	1186	1259	
24.5	-20.5	SP	0	22	21	16	25	25	19	25	1342	1428	0.50
27	-23	SP	0	25	24	18	27	27	20	27	1498	1597	0.53
29.5	-25.5	SP-SM	8.5	10	10	8	10	11	9	15	1654	1736	0.51
32	-28	SP-SM	8.5	10	10	9	10	11	9	15	1810	1868	0.54
34.5	-30.5	SP-SM	8.5	12	12	10	12	13	10	17	1966	1999	0.53
37	-33	SP-SM	8.5	10	10	9	10	11	8	15	2122	2131	0.63
39.5	-35.5	SP-SM	8.5	14	14	12	13	15	11	19	2278	2272	0.52
42	-38	SP-SM	8.5	28	28	22	25	25	20	29	2434	2426	0.35
44.5	-40.5	SC	12	4	4	3	4	4	3	9	2590	2513	0.49
47	-43	SC	12	5	5	4	4	5	4	10	2746	2582	0.58
49.5	-45.5	SP	0	55	55	42	47	47	36	47	2902	2751	0.51
52	-48	SP	0	60	60	46	49	49	38	49	3058	2945	0.20
54.5	-50.5	SM	12	6	6	5	5	5	4	11	3214	3049	0.19
57	-53	SM	12	6	6	5	5	5	4	11	3370	3130	0.20
59.5	-55.5	SM	12	5	5	4	4	4	3	10	3526	3202	0.22
62	-58	SM	12	6	6	5	5	5	4	10	3682	3281	0.19
64.5	-60.5	SM	12	15	15	13	12	13	10	18	3838	3392	0.22
67	-63	SM	12	15	15	13	11	13	10	18	3994	3511	0.32
69.5	-65.5	SM	12	20	20	17	15	16	13	22	4150	3640	0.48
72	-68	SM	12	22	22	19	16	18	14	23	4306	3772	0.51
74.5	-70.5	SM	12	24	24	21	17	19	15	24	4462	3903	0.47
77	-73	SM	12	26	26	22	18	20	16	26	4618	4035	0.50
79.5	-75.5	SM	12	31	31	24	21	21	17	27	4774	4166	0.53
82	-78	SM	12	38	38	29	26	26	20	31	4930	4308	0.46
84.5	-80.5	SM	12	12	12	10	8	9	7	14	5086	4422	0.53
87	-83	SM	12	15	15	13	10	11	9	16	5242	4538	0.71
89.5	-85.5	SM	12	31	31	24	20	20	16	25	5398	4667	0.75
92	-88	SM	12	36	36	28	23	23	18	28	5554	4799	0.81
94.5	-90.5	SC	12	7	7	6	4	5	4	10	5710	4890	0.78
97	-93	SC	12	7	7	6	4	5	4	10	5866	4962	0.78
99.5	-95.5	SC	12	9	9	8	6	6	5	11	6022	5051	0.70
102	-98	SC	12	9	9	8	6	6	5	11	6178	5145	0.52
104.5	-100.5	SM	12	45	45	35	28	28	21	33	6334	5279	0.64
107	-103	SM	12	73	73	56	44	44	34	49	6490	5443	0.76
109.5	-105.5	SM	12	50/1	100	77	60	60	46	65	6646	5612	
112	-108	CH	50	50/2	100	77	59	-	-	-	6802	5781	
114.5	-110.5	CH	92	50/2	100	77	58	-	-	-	6958	5950	
117	-113	LBSL		50/1	100	77	57	57	44	57	7114	6159	
119.5	-115.5	LBSL		50/0	100	77	56	56	43	56	7270	6378	
122	-118	LBSL		50/0	100	77	55	55	42	55	7426	6597	
124.5	-120.5	LBSL		50/1	100	77	54	54	42	54	7582	6816	
127	-123	LBSL		50/0	100	77	53	53	41	53	7738	7035	
129.5	-125.5	LBSL		50/1	100	77	53	53	40	53	7894	7254	
132	-128	LBSL		50/1	100	77	52	52	40	52	8050	7473	
134.5	-130.5	LBSL		50/0	100	77	51	51	39	51	8206	7692	

Depth (ft)	Elevation (ft)	USCS	Rebound inch	Liquefaction Soil Response	Terzaghi Dr	Schmertmann Φ'	Hatanaka Φ'	Peck Φ'	Mayne OCR	Hera Cu (psf)	Hettiarachchi Cu (psf)	CDOT Qu (psf)
0	4											
7	-3	SP		Contractive	35%	31	31	28				
8.5	-4.5	SP		Contractive	21%	23	27	28				
12	-8	SM		Contractive	25%	26	28	28				
14.5	-10.5	CL		-					2.606	164	139	667.8643
17	-13	CL		-					3.788	270	279	1238.93
19.5	-15.5	SP		Intermediate	62%	42	39	32				
22	-18	SP		Intermediate	68%	44	41	33				
24.5	-20.5	SP	0.50	Intermediate	64%	0	40	27				
27	-23	SP	0.53	Intermediate	67%	0	40	27				
29.5	-25.5	SP-SM	0.51	Contractive	41%	0	33	27				
32	-28	SP-SM	0.54	Contractive	42%	0	33	27				
34.5	-30.5	SP-SM	0.53	Contractive	45%	0	34	27				
37	-33	SP-SM	0.63	Contractive	40%	0	33	27				
39.5	-35.5	SP-SM	0.52	Contractive	47%	36	35	31				
42	-38	SP-SM	0.35	Intermediate	65%	42	40	35				
44.5	-40.5	SC	0.49	Contractive	24%	25	28	28				
47	-43	SC	0.58	Contractive	27%	27	29	29				
49.5	-45.5	SP	0.51	Dilative	88%	48	47	42				
52	-48	SP	0.20	Dilative	91%	48	48	43				
54.5	-50.5	SM	0.19	Contractive	28%	27	29	29				
57	-53	SM	0.20	Contractive	28%	27	29	29				
59.5	-55.5	SM	0.22	Contractive	26%	25	28	29				
62	-58	SM	0.19	Contractive	28%	27	29	29				
64.5	-60.5	SM	0.22	Contractive	44%	34	34	31				
67	-63	SM	0.32	Contractive	43%	34	34	31				
69.5	-65.5	SM	0.48	Intermediate	50%	36	36	33				
72	-68	SM	0.51	Intermediate	52%	37	37	33				
74.5	-70.5	SM	0.47	Intermediate	54%	38	37	34				
77	-73	SM	0.50	Intermediate	55%	38	38	35				
79.5	-75.5	SM	0.53	Intermediate	60%	40	38	36				
82	-78	SM	0.46	Dilative	66%	41	40	38				
84.5	-80.5	SM	0.53	Contractive	37%	30	32	31				
87	-83	SM	0.71	Contractive	41%	32	33	31				
89.5	-85.5	SM	0.75	Intermediate	58%	39	38	36				
92	-88	SM	0.81	Intermediate	62%	40	39	37				
94.5	-90.5	SC	0.78	Contractive	27%	25	29	29				
97	-93	SC	0.78	Contractive	27%	25	29	29				
99.5	-95.5	SC	0.70	Contractive	31%	27	30	30				
102	-98	SC	0.52	Contractive	31%	27	30	30				
104.5	-100.5	SM	0.64	Dilative	68%	41	41	40				
107	-103	SM	0.76	Dilative	86%	46	46	46				
109.5	-105.5	SM		Dilative	100%	49	50	52				
112	-108	CH		-					11.147	2854	8200	14704.74
114.5	-110.5	CH		-					10.928	2854	8200	14494.4
117	-113	LBSL		Dilative								
119.5	-115.5	LBSL		Dilative								
122	-118	LBSL		Dilative								
124.5	-120.5	LBSL		Dilative								
127	-123	LBSL		Dilative								
129.5	-125.5	LBSL		Dilative								
132	-128	LBSL		Dilative								
134.5	-130.5	LBSL		Dilative								

### B.2.8.2. B.8.2. SPT TB-5 (P9P3)

Depth (ft)	Elevation (ft)	USCS	FC actual/estimate	TB-5 Nsafe	SPT N60	SPT Ntrip	SPT (N1)60	SPT (N1)60t	SPT (N1)trip	SPT (N1)60ta	u psf	$\sigma'_{vo}$ (avg) psf	Rebound inch
0	-7.5												
1	-8.5	SP	0	4	3	3	6	7	5	7	534	47	
2.5	-10	SP	0	5	4	3	8	8	6	8	629	123	
4	-11.5	SP	0	3	2	2	5	5	4	5	723	191	
5.5	-13	SP	0	2	2	1	3	4	3	4	817	249	
7	-14.5	SM	12	2	2	1	3	4	3	9	911	290	
9.5	-17	SM	42	WR	WR	WR	0	0	0	8	1068	315	
12	-19.5	SP	0	30	26	20	51	51	39	51	1226	473	
14.5	-22	SP	0	38	36	28	63	63	48	63	1383	666	
17	-24.5	SP	0	17	16	12	25	25	19	25	1540	839	
19.5	-27	SP	0	14	13	11	19	21	16	21	1697	997	
22	-29.5	SP-SM	8.5	7	7	6	9	10	8	14	1854	1132	
24.5	-32	SM	12	4	4	3	5	6	4	11	2011	1223	
27	-34.5	SM	12	3	3	3	4	4	3	9	2168	1293	0.20
29.5	-37	SM	12	4	4	3	5	5	4	11	2325	1371	0.22
32	-39.5	SM	12	7	7	6	8	9	7	14	2483	1471	0.16
34.5	-42	SM	12	11	11	9	12	14	11	19	2640	1587	0.12
37	-44.5	SM	12	18	18	15	19	22	17	27	2797	1715	0.23
39.5	-47	SM	12	5	5	4	5	6	4	11	2954	1805	0.12
42	-49.5	SM	12	4	4	3	4	5	4	10	3111	1875	0.02
44.5	-52	SM	12	11	11	9	11	12	9	17	3268	1983	0.14
47	-54.5	SM	12	7	7	6	7	8	6	13	3425	2091	0.16
49.5	-57	SM	12	7	7	6	7	7	6	13	3582	2196	0.23
52	-59.5	SM	12	7	7	6	7	7	6	12	3740	2302	0.24
54.5	-62	SM	12	85	85	65	77	77	59	82	3897	2457	0.33
57	-64.5	SM	12	41	41	32	36	36	28	41	4054	2615	0.39
59.5	-67	SM	12	24	24	18	20	20	16	26	4211	2750	0.48
62	-69.5	SM	12	22	22	19	18	20	16	26	4368	2881	0.51
64.5	-72	SM	12	19	19	16	15	17	13	22	4525	3011	0.42
67	-74.5	SM	12	10	10	9	8	9	7	14	4682	3122	0.38
69.5	-77	SM	12	10	10	9	8	9	7	14	4839	3227	0.33
72	-79.5	SM	12	3	3	3	2	3	2	8	4997	3282	0.30
74.5	-82	SM	38	4	4	3	3	3	3	11	5154	3335	0.34
77	-84.5	SC	12	4	4	3	3	3	3	9	5311	3391	0.29
79.5	-87	SC	41	3	3	3	2	3	2	11	5468	3436	0.23
82	-89.5	SC	12	5	5	4	4	4	3	9	5625	3499	0.26
84.5	-92	SC	12	6	6	5	4	5	4	10	5782	3567	0.28
87	-94.5	SC	41	7	7	6	5	6	4	14	5939	3645	0.51
89.5	-97	SM	12	61	61	47	44	44	34	50	6096	3785	0.72
92	-99.5	SM	12	80	80	62	57	57	44	62	6254	3950	0.76
94.5	-102	SM	12	69	69	53	48	48	37	53	6411	4118	
97	-104.5	SC	12	36	36	28	25	25	19	30	6568	4266	
99.5	-107	SC	12	24	24	21	16	18	14	23	6725	4399	
102	-109.5	SC	12	28	28	24	19	21	16	26	6882	4529	
104.5	-112	LBSL		50/0	50/0	50/0	65	65	65	65	7039	4730	
107	-114.5	LBSL		50/0	50/0	50/0	64	64	64	64	7196	4948	
109.5	-117	LBSL		50/1	50/1	50/1	62	62	62	62	7353	5165	
112	-119.5	LBSL		50/1	50/1	50/1	61	61	61	61	7511	5383	
114.5	-122	LBSL		50/1	50/1	50/1	60	60	60	60	7668	5601	
117	-124.5	LBSL		50/2	50/2	50/2	59	59	59	59	7825	5819	
119.5	-127	LBSL		50/1	50/1	50/1	58	58	58	58	7982	6037	
122	-129.5	LBSL		50/0	50/0	50/0	57	57	57	57	8139	6255	
124.5	-132	LBSL		50/0	50/0	50/0	56	56	56	56	8296	6473	
127	-134.5	LBSL		50/1	50/1	50/1	55	55	55	55	8453	6691	
129.5	-137	LBSL		50/4	50/4	50/4	54	54	54	54	8610	6908	

Depth (ft)	Elevation (ft)	USCS	Rebound inch	Liquefaction Soil Response	Terzaghi Dr	Schmertmann Φ'	Hatanaka Φ'	Peck Φ'	Mayne OCR	Hera Cu (psf)	Hettiarachchi Cu (psf)	CDOT Qu (psf)
0	-7.5											
1	-8.5	SP		Contractive	32%	31	30	28				
2.5	-10	SP		Contractive	35%	33	31	28				
4	-11.5	SP		Contractive	27%	28	29	28				
5.5	-13	SP		Contractive	24%	26	28	28				
7	-14.5	SM		Contractive	24%	25	28	28				
9.5	-17	SM		Contractive	0%	0	20	27				
12	-19.5	SP		Dilative	92%	49	48	34				
14.5	-22	SP		Dilative	102%	51	51	37				
17	-24.5	SP		Intermediate	64%	43	40	32				
19.5	-27	SP		Intermediate	56%	40	38	31				
22	-29.5	SP-SM		Contractive	38%	33	32	29				
24.5	-32	SM		Contractive	29%	28	29	28				
27	-34.5	SM	0.20	Contractive	25%	26	28	28				
29.5	-37	SM	0.22	Contractive	28%	28	29	28				
32	-39.5	SM	0.16	Contractive	37%	32	32	29				
34.5	-42	SM	0.12	Contractive	45%	36	35	30				
37	-44.5	SM	0.23	Intermediate	57%	40	38	32				
39.5	-47	SM	0.12	Contractive	30%	28	29	29				
42	-49.5	SM	0.02	Contractive	26%	26	28	28				
44.5	-52	SM	0.14	Contractive	43%	35	34	30				
47	-54.5	SM	0.16	Contractive	34%	30	31	29				
49.5	-57	SM	0.23	Contractive	33%	30	31	29				
52	-59.5	SM	0.24	Contractive	33%	30	31	29				
54.5	-62	SM	0.33	Dilative	113%	53	54	49				
57	-64.5	SM	0.39	Dilative	77%	46	43	38				
59.5	-67	SM	0.48	Intermediate	58%	40	38	34				
62	-69.5	SM	0.51	Intermediate	55%	39	38	33				
64.5	-72	SM	0.42	Intermediate	51%	37	36	33				
67	-74.5	SM	0.38	Contractive	37%	31	32	30				
69.5	-77	SM	0.33	Contractive	36%	31	32	30				
72	-79.5	SM	0.30	Contractive	20%	22	26	28				
74.5	-82	SM	0.34	Contractive	23%	24	27	28				
77	-84.5	SC	0.29	Contractive	23%	23	27	28				
79.5	-87	SC	0.23	Contractive	20%	21	26	28				
82	-89.5	SC	0.26	Contractive	25%	25	28	29				
84.5	-92	SC	0.28	Contractive	27%	26	29	29				
87	-94.5	SC	0.51	Contractive	29%	27	29	29				
89.5	-97	SM	0.72	Dilative	86%	47	46	43				
92	-99.5	SM	0.76	Dilative	97%	49	50	48				
94.5	-102	SM		Dilative	90%	47	47	45				
97	-104.5	SC		Intermediate	64%	41	39	37				
99.5	-107	SC		Intermediate	52%	37	37	34				
102	-109.5	SC		Intermediate	56%	38	38	35				
104.5	-112	LBSL		Dilative								
107	-114.5	LBSL		Dilative								
109.5	-117	LBSL		Dilative								
112	-119.5	LBSL		Dilative								
114.5	-122	LBSL		Dilative								
117	-124.5	LBSL		Dilative								
119.5	-127	LBSL		Dilative								
122	-129.5	LBSL		Dilative								
124.5	-132	LBSL		Dilative								
127	-134.5	LBSL		Dilative								
129.5	-137	LBSL		Dilative								

### B.2.8.3. B.8.3. SPT TB-11 (P20P6)

Depth (ft)	Elevation (ft)	USCS	FC actual/estimate	TB-11 Nsafe	SPT N60	SPT Ntrip	SPT (N1)60	SPT (N1)60t	SPT (N1)trip	SPT (N1)60ta	u psf	$\sigma'_{vo}$ (avg) psf	Rebound inch
0	-8												
1	-9	SM	12	9	7	6	14	15	12	15	566	52	
2.5	-10.5	SM	12	7	5	4	11	12	9	17	660	125	
4	-12	SM	12	3	2	2	5	5	4	10	754	181	
5.5	-13.5	SM	42	3	2	2	5	5	4	13	848	229	
9	-17	CH	50	9	7	6	14	-	-	-	1068	447	
11.5	-19.5	SM	12	11	8	7	15	17	13	22	1226	585	
14	-22	CH	50	3	3	2	4	-	-	-	1383	715	
16.5	-24.5	OL	50	3	3	2	4	-	-	-	1540	795	
19	-27	SM	20	14	12	10	18	20	15	26	1697	913	-0.03
21.5	-29.5	SM	12	11	10	9	14	16	12	21	1854	1044	-7.58
24	-32	ML	50	11	10	9	14	-	-	-	2011	1174	-3.44
26.5	-34.5	SM	12	9	9	7	11	12	9	17	2168	1294	-1.39
29	-37	SM	18	7	7	6	8	9	7	15	2325	1402	0.20
31.5	-39.5	SM	13	10	10	9	11	13	10	18	2483	1518	0.47
34	-42	SM	12	8	8	7	9	10	8	15	2640	1636	-0.37
36.5	-44.5	SM	12	12	12	10	13	14	11	19	2797	1763	-0.56
39	-47	SM	12	18	18	15	18	21	16	26	2954	1894	0.26
41.5	-49.5	SM	12	11	11	9	11	12	9	17	3111	2014	-0.52
44	-52	SM	12	9	9	8	9	10	7	15	3268	2132	-0.23
46.5	-54.5	SM	12	7	7	6	7	7	6	13	3425	2240	-0.07
49	-57	SM	12	6	6	5	6	6	5	11	3582	2335	-0.11
51.5	-59.5	SM	12	6	6	5	5	6	5	11	3740	2418	0.11
54	-62	SM	12	73	73	56	64	64	50	70	3897	2569	0.17
56.5	-64.5	SM	12	51	51	39	44	44	34	49	4054	2726	0.29
59	-67	SM	12	21	21	18	18	20	15	25	4211	2862	0.52
61.5	-69.5	SM	12	9	9	8	7	8	6	13	4368	2972	0.78
64	-72	SM	12	13	13	11	10	12	9	17	4525	3088	0.46
66.5	-74.5	SM	12	20	20	17	16	18	14	23	4682	3205	0.48
69	-77	SM	12	10	10	9	8	9	7	14	4839	3313	0.79
71.5	-79.5	SM	12	10	10	9	8	8	7	14	4997	3419	0.70
74	-82	SM	12	5	5	4	4	4	3	9	5154	3494	0.49
76.5	-84.5	SM	12	12	12	10	9	10	8	15	5311	3602	0.51
79	-87	SM	12	10	10	9	7	8	6	13	5468	3710	0.55
81.5	-89.5	SM	38	5	5	4	4	4	3	12	5625	3785	0.62
84	-92	SM	12	4	4	3	3	3	2	8	5782	3843	0.59
86.5	-94.5	SM	12	5	5	4	4	4	3	9	5939	3908	0.32
89	-97	SM	12	6	6	5	4	5	4	10	6096	3976	0.43
91.5	-99.5	SM	12	22	22	19	15	17	13	22	6254	4094	0.80
94	-102	SM	12	29	29	25	20	22	17	27	6411	4225	0.98
96.5	-104.5	CL	50	34	34	26	23	-	-	-	6568	4385	
99	-107	CL	50	33	33	25	22	-	-	-	6725	4553	
101.5	-109.5	SC	12	50/5	50/5	50/5	65	65	65	70	6882	4721	
104	-112	SC	12	50/6	50/6	50/6	64	64	64	69	7039	4889	
106.5	-114.5	SC	32	50/5	50/5	50/5	63	63	63	70	7196	5056	
109	-117	SC	12	50/4	50/4	50/4	62	62	62	67	7353	5224	
111.5	-119.5	LS		70	70	54	43	43	33	43	7511	5422	
114	-122	LS		50/5	50/5	50/5	60	60	60	60	7668	5638	
116.5	-124.5	LS		50/0	50/0	50/0	58	58	58	58	7825	5855	
119	-127	LS		50/1	50/1	50/1	57	57	57	57	7982	6073	
121.5	-129.5	LS		50/2	50/2	50/2	56	56	56	56	8139	6291	

Depth (ft)	Elevation (ft)	USCS	Rebound inch	Liquefaction Soil Response	Terzaghi Dr	Schmertmann Φ'	Hatanaka Φ'	Peck Φ'	Mayne OCR	Hera Cu (psf)	Hettiarachchi Cu (psf)	CDOT Qu (psf)
0	-8											
1	-9	SM		Contractive	47%	39	35	29				
2.5	-10.5	SM		Contractive	42%	36	33	29				
4	-12	SM		Contractive	27%	28	29	28				
5.5	-13.5	SM		Contractive	27%	28	29	28				
9	-17	CH		-					10.153	442	554	3375
11.5	-19.5	SM		Intermediate	50%	37	36	30				
14	-22	CH		-					3.755	219	209	1066
16.5	-24.5	OL		-					3.489	219	209	1011
19	-27	SM	-0.03	Intermediate	54%	39	37	31				
21.5	-29.5	SM	-7.58	Intermediate	49%	37	36	30				
24	-32	ML	-3.44	-					7.052	606	857	3410
26.5	-34.5	SM	-1.39	Contractive	42%	35	33	30				
29	-37	SM	0.20	Contractive	36%	32	32	29				
31.5	-39.5	SM	0.47	Contractive	44%	35	34	30				
34	-42	SM	-0.37	Contractive	38%	33	32	29				
36.5	-44.5	SM	-0.56	Contractive	46%	36	35	31				
39	-47	SM	0.26	Intermediate	56%	40	38	32				
41.5	-49.5	SM	-0.52	Contractive	43%	35	34	30				
44	-52	SM	-0.23	Contractive	38%	33	32	30				
46.5	-54.5	SM	-0.07	Contractive	33%	30	31	29				
49	-57	SM	-0.11	Contractive	30%	29	30	29				
51.5	-59.5	SM	0.11	Contractive	30%	28	30	29				
54	-62	SM	0.17	Dilative	104%	51	51	46				
56.5	-64.5	SM	0.29	Dilative	85%	47	46	41				
59	-67	SM	0.52	Intermediate	54%	38	37	33				
61.5	-69.5	SM	0.78	Contractive	35%	31	31	30				
64	-72	SM	0.46	Contractive	42%	34	33	31				
66.5	-74.5	SM	0.48	Intermediate	51%	37	36	33				
69	-77	SM	0.79	Contractive	36%	31	32	30				
71.5	-79.5	SM	0.70	Contractive	36%	31	31	30				
74	-82	SM	0.49	Contractive	25%	25	28	29				
76.5	-84.5	SM	0.51	Contractive	39%	32	32	31				
79	-87	SM	0.55	Contractive	35%	30	31	30				
81.5	-89.5	SM	0.62	Contractive	25%	24	28	29				
84	-92	SM	0.59	Contractive	22%	23	27	28				
86.5	-94.5	SM	0.32	Contractive	24%	24	28	29				
89	-97	SM	0.43	Contractive	27%	26	29	29				
91.5	-99.5	SM	0.80	Intermediate	51%	36	36	33				
94	-102	SM	0.98	Intermediate	58%	39	38	35				
96.5	-104.5	CL		-					6.413	1312	2788	5741
99	-107	CL		-					6.122	1285	2706	5468
101.5	-109.5	SC		Dilative	104%	50	56	52				
104	-112	SC		Dilative	103%	50	56	52				
106.5	-114.5	SC		Dilative	102%	49	55	52				
109	-117	SC		Dilative	102%	49	55	52				
111.5	-119.5	LS		Dilative	84%	49	46	52				
114	-122	LS		Dilative	100%	49	55	52				
116.5	-124.5	LS		Dilative	99%	48	54	52				
119	-127	LS		Dilative	98%	48	54	52				
121.5	-129.5	LS		Dilative	97%	48	54	52				

## B.2.9. I-10 and Chaffee Road Overpass

### B.2.9.1. SPT B-2 (P2P9)

Depth (ft)	Elevation (ft)	USCS	FC actual/estimate	B-2 Nsafe	SPT N60	SPT Ntrip	SPT (N1)60	SPT (N1)60t	SPT (N1)trip	SPT (N1)60ta	u psf	$\sigma'_{vo}$ (avg) psf	Rebound inch
0	63.08			-	-		-						
1	62.08	SP-SM	10	13	10	7	18	18	14	18	0	581	
2.5	60.58	SM	12	7	5	4	9	9	7	14	0	736	
5	58.08	SP-SM	8.5	13	10	7	14	14	11	18	0	996	
7	56.08	WOOD		33	25	19	35	35	27	35	107	1017	
9.5	53.58	SP-SM	8.5	43	32	25	43	43	33	47	263	1146	
12	51.08	SP-SM	8.5	64	64	49	59	59	45	63	419	1325	
14.5	48.58	SP-SM	8.5	60	51	39	59	59	45	63	575	1506	
17	46.08	SP-SM	8.5	51	43	33	47	47	36	51	731	1688	
19.5	43.58	SP-SM	8.5	86/10.5	86/10.5	86/10.5	103	103	103	107	887	1869	
22	41.08	SP-SM	8.5	43	41	31	40	40	31	44	1043	2041	
24.5	38.58	SP	0	20	19	16	18	20	15	20	1199	2200	
27	36.08	SP	0	18	17	15	16	18	13	18	1355	2356	
29.5	33.58	SP	0	26	25	19	22	22	17	22	1511	2513	
32	31.08	SP	0	42	42	32	36	36	28	36	1667	2689	0.19
34.5	28.58	SP	0	25	25	19	21	21	16	21	1823	2851	-0.13
37	26.08	SP-SC	8.5	12	12	10	10	11	8	15	1979	2987	0.45
39.5	23.58	SP-SC	8.5	43	43	33	34	34	26	38	2135	3139	-0.01
42	21.08	SC	12	18	18	15	14	16	12	21	2291	3275	-1.14
44.5	18.58	SC	12	3	3	3	2	3	2	8	2447	3337	0.42
47	16.08	CH	50	2	2	2	2	-	-	-	2603	3441	1.15
49.5	13.58	CH	94	3	3	3	2	-	-	-	2759	3560	1.30
52	11.08	CH	50	3	3	3	2	-	-	-	2915	3679	1.33
54.5	8.58	CH	50	3	3	3	2	-	-	-	3071	3798	1.56
57	6.08	SC	12	4	4	3	3	3	2	8	3227	3867	2.00
59.5	3.58	CH	50	3	3	3	2	-	-	-	3383	3973	1.85
62	1.08	SC	12	6	6	5	4	5	4	10	3539	4052	2.11
64.5	-1.42	SP-SC	8.5	6	6	5	4	5	4	9	3695	4131	0.66
67	-3.92	SP-SC	8.5	10	10	9	7	8	6	12	3851	4243	0.04
69.5	-6.42	SC	12	22	22	19	15	17	13	22	4007	4372	0.99
72	-8.92	SC	12	16	16	14	11	12	9	17	4163	4493	0.39
74.5	-11.42	SC	12	15	15	13	10	11	8	16	4319	4612	0.51
77	-13.92	SP-SC	8.5	47	47	36	30	30	23	34	4475	4761	0.41
79.5	-16.42	SP-SC	8.5	34	34	26	22	22	17	26	4631	4908	0.48
82	-18.92	SP-SC	8.5	26	26	22	16	18	14	22	4787	5052	
84.5	-21.42	SP-SC	8.5	20	20	17	12	14	11	18	4943	5186	
87	-23.92	SP-SC	8.5	26	26	22	16	18	14	22	5099	5327	
89.5	-26.42	SC	12	8	8	7	5	5	4	11	5255	5421	
92	-28.92	SC	12	10	10	9	6	7	5	12	5411	5513	
94.5	-31.42	SC	12	12	12	10	7	8	6	13	5567	5617	
97	-33.92	SC	12	7	7	6	4	5	4	10	5723	5693	
99.5	-36.42	SC	12	26	26	22	15	17	13	22	5879	5812	

Depth (ft)	Elevation (ft)	USCS	Rebound inch	Liquefaction Soil Response	Terzaghi Dr	Schmertmann Φ'	Hatanaka Φ'	Peck Φ'	Mayne OCR	Hera Cu (psf)	Hettiarachchi Cu (psf)	CDOT Qu (psf)
0	63.08											
1	62.08	SP-SM		Contractive	55%	39	37	30				
2.5	60.58	SM		Contractive	38%	33	32	29				
5	58.08	SP-SM		Contractive	48%	37	35	30				
7	56.08	WOOD		Dilative	76%	46	43	34				
9.5	53.58	SP-SM		Dilative	84%	48	46	36				
12	51.08	SP-SM		Dilative	99%	54	50	44				
14.5	48.58	SP-SM		Dilative	99%	51	50	41				
17	46.08	SP-SM		Dilative	89%	49	47	39				
19.5	43.58	SP-SM		Dilative	131%	56	65	52				
22	41.08	SP-SM		Dilative	82%	47	45	38				
24.5	38.58	SP		Intermediate	55%	39	38	33				
27	36.08	SP		Contractive	51%	38	36	32				
29.5	33.58	SP		Intermediate	61%		38	34				
32	31.08	SP	0.19	Dilative	78%	46	44	39				
34.5	28.58	SP	-0.13	Intermediate	59%	40	38	34				
37	26.08	SP-SC	0.45	Contractive	40%	33	33	31				
39.5	23.58	SP-SC	-0.01	Dilative	76%	45	43	39				
42	21.08	SC	-1.14	Intermediate	48%	36	36	32				
44.5	18.58	SC	0.42	Contractive	20%	22	26	28				
47	16.08	CH	1.15	-					1.076	184	164	381
49.5	13.58	CH	1.30	-					1.390	247	246	562
52	11.08	CH	1.33	-					1.359	247	246	553
54.5	8.58	CH	1.56	-					1.329	247	246	544
57	6.08	SC	2.00	Contractive	22%	23	27	28				
59.5	3.58	CH	1.85	-					1.289	247	246	532
62	1.08	SC	2.11	Contractive	27%	25	28	29				
64.5	-1.42	SP-SC	0.66	Contractive	26%	25	28	29				
67	-3.92	SP-SC	0.04	Contractive	34%	29	31	30				
69.5	-6.42	SC	0.99	Intermediate	50%	36	36	33				
72	-8.92	SC	0.39	Contractive	42%	33	34	32				
74.5	-11.42	SC	0.51	Contractive	41%	32	33	31				
77	-13.92	SP-SC	0.41	Dilative	71%	43	42	40				
79.5	-16.42	SP-SC	0.48	Intermediate	60%	39	38	37				
82	-18.92	SP-SC		Intermediate	52%	36	37	35				
84.5	-21.42	SP-SC		Contractive	45%	34	35	33				
87	-23.92	SP-SC		Intermediate	52%	36	37	35				
89.5	-26.42	SC		Contractive	28%	26	29	29				
92	-28.92	SC		Contractive	32%	28	30	30				
94.5	-31.42	SC		Contractive	35%	29	31	31				
97	-33.92	SC		Contractive	26%	25	28	29				
99.5	-36.42	SC		Intermediate	50%	35	36	35				

## B.2.10. I-4 and John Young Parkway

### B.2.10.1. SPT FB-11 (P2P1, Ramp A)

Depth (ft)	Elevation (ft)	USCS	FC actual/estimate	FB-11 Nsafe	SPT N60	SPT Ntrip	SPT (N1)60	SPT (N1)60t	SPT (N1)trip	SPT (N1)60ta	u psf	$\sigma'_{vo}$ (avg) psf	Rebound inch
0	93												
2	91	PT	99	WH	WH	WH	0	0	0	0	125	35	
4	89	SP-SM	8.5	8	6	5	12	13	10	27	250	123	
6	87	SP-SM	8.5	6	5	4	9	10	8	14	374	228	
8	85	SM	12	6	5	4	9	10	8	15	499	326	
10	83	SM	12	10	8	6	15	17	13	22	624	429	
12.5	80.5	SC	12	6	5	4	9	10	7	15	780	540	
15	78	SP-SM	8.5	8	7	6	12	13	10	17	936	667	
17.5	75.5	SP-SM	8.5	7	6	5	9	10	8	14	1092	798	-0.80
20	73	SP-SM	8.5	9	9	7	13	14	11	18	1248	930	0.36
22.5	70.5	SM	12	9	9	7	12	13	10	18	1404	1051	1.13
25	68	SM	15	16	15	13	20	22	17	27	1560	1180	1.60
27.5	65.5	CH	50	6	6	5	7	-	-	-	1716	1322	0.80
30	63	CH	50	5	5	4	6	-	-	-	1872	1466	0.34
32.5	60.5	SC	12	5	5	4	6	6	5	11	2028	1570	-0.45
35	58	SP-SM	8.5	6	6	5	7	7	6	11	2184	1664	0.14
37.5	55.5	SC	12	3	3	3	3	4	3	9	2340	1728	0.93
40	53	SM	12	3	3	3	3	4	3	9	2496	1784	0.99
42.5	50.5	SC	12	2	2	2	2	2	2	8	2652	1831	0.86
45	48	SC	12	2	2	2	2	2	2	7	2808	1875	-1.29
47.5	45.5	SM	12	2	2	2	2	2	2	7	2964	1919	-0.98
50	43	SM	12	7	7	6	7	8	6	13	3120	2013	-0.07
52.5	40.5	SM	12	6	6	5	6	6	5	12	3276	2109	-0.33
55	38	SM	12	4	4	3	4	4	3	9	3432	2183	-0.26
57.5	35.5	SM	12	5	5	4	5	5	4	10	3588	2262	-0.01
60	33	SM	12	3	3	3	3	3	2	8	3744	2324	-0.11
62.5	30.5	SP-SM	8.5	4	4	3	4	4	3	8	3900	2400	0.60
65	28	SP-SM	6	3	3	3	3	3	2	4	4056	2477	0.85
67.5	25.5	SM	12	32	32	25	28	28	22	33	4212	2607	0.18
70	23	SM	12	50/5	50/5	50/5	85	85	85	90	4368	2771	0.75
72.5	20.5	SC	12	77/9	77/9	77/9	82	82	82	88	4524	2940	0.96
75	18	SC	12	81/10	81/10	81/10	80	80	80	85	4680	3109	
77.5	15.5	SC	12	81/11	81/11	81/11	78	78	78	83	4836	3278	
80	13	SC	12	50/5.5	50/5.5	50/5.5	76	76	76	81	4992	3447	
82.5	10.5	SC	12	91/11	91/11	91/11	74	74	74	80	5148	3616	
85	8	SC	12	62	4	3	45	45	35	50	5304	3785	

Depth (ft)	Elevation (ft)	USCS	Rebound inch	Liquefaction Soil Response	Terzaghi Dr	Schmertmann Φ'	Hatanaka Φ'	Peck Φ'	Mayne OCR	Hera Cu (psf)	Hettiarachchi Cu (psf)	CDOT Qu (psf)
0	93											
2	91	PT		Contractive	0%	0	20	27				
4	89	SP-SM		Intermediate	45%	37	34	29				
6	87	SP-SM		Contractive	39%	34	32	28				
8	85	SM		Contractive	39%	33	32	28				
10	83	SM		Intermediate	50%	37	36	29				
12.5	80.5	SC		Contractive	38%	32	32	28				
15	78	SP-SM		Contractive	44%	35	34	29				
17.5	75.5	SP-SM	-0.80	Contractive	40%	33	33	29				
20	73	SP-SM	0.36	Contractive	46%	36	35	30				
22.5	70.5	SM	1.13	Contractive	44%	36	34	30				
25	68	SM	1.60	Intermediate	57%	40	38	32				
27.5	65.5	CH	0.80	-					4.281	391	467	1753
30	63	CH	0.34	-					3.643	356	410	1460
32.5	60.5	SC	-0.45	Contractive	31%	29	30	29				
35	58	SP-SM	0.14	Contractive	33%	30	31	29				
37.5	55.5	SC	0.93	Contractive	23%	25	27	28				
40	53	SM	0.99	Contractive	23%	24	27	28				
42.5	50.5	SC	0.86	Contractive	19%	22	26	28				
45	48	SC	-1.29	Contractive	19%	21	26	28				
47.5	45.5	SM	-0.98	Contractive	18%	21	26	28				
50	43	SM	-0.07	Contractive	34%	31	31	29				
52.5	40.5	SM	-0.33	Contractive	31%	29	30	29				
55	38	SM	-0.26	Contractive	25%	26	28	28				
57.5	35.5	SM	-0.01	Contractive	28%	27	29	29				
60	33	SM	-0.11	Contractive	22%	23	27	28				
62.5	30.5	SP-SM	0.60	Contractive	25%	25	28	28				
65	28	SP-SM	0.85	Contractive	21%	23	27	28				
67.5	25.5	SM	0.18	Dilative	68%	43	41	36				
70	23	SM	0.75	Dilative	119%	54	61	52				
72.5	20.5	SC	0.96	Dilative	117%	53	61	52				
75	18	SC		Dilative	116%	53	60	52				
77.5	15.5	SC		Dilative	114%	53	60	52				
80	13	SC		Dilative	113%	52	59	52				
82.5	10.5	SC		Dilative	111%	52	59	52				
85	8	SC		Dilative	87%	23	46	28				

### B.2.10.2. B.10.2. SPT FB-3 (P9P12, Ramp A)

Depth (ft)	Elevation (ft)	USCS	FC actual/estimate	FB-3 Nsafe	SPT N60	SPT Ntrip	SPT (N1)60	SPT (N1)60t	SPT (N1)trip	SPT (N1)60ta	u psf	$\sigma'_{vo}$ (avg) psf	Rebound inch
0	95.82	-											
1	94.32	PT	<b>20</b>	HA							0	120	
2.5	92.82	PT		HA							0	240	
4	91.32	SP-SM	8.5	HA							80	301	
5.5	89.82	SM	12	HA							173	354	
7	88.32	SM	12	6	5	4	9	10	8	15	267	418	
8.5	86.82	SP-SM	8.5	12	9	8	18	20	15	24	361	500	
10	85.32	SP-SM	8.5	12	9	8	17	18	14	22	454	586	
12.5	82.82	SM	12	15	13	10	21	21	16	26	610	720	
15	80.32	SM	<b>17</b>	19	16	12	25	25	19	30	766	852	
17.5	77.82	SP-SM	8.5	16	14	12	19	21	16	25	922	993	-2.28
20	75.32	SM	12	9	9	7	11	13	10	18	1078	1117	0.07
22.5	72.82	SM	12	6	6	5	7	8	6	13	1234	1226	-0.14
25	70.32	SC	12	9	9	7	10	12	9	17	1390	1343	-0.31
27.5	67.82	CH	50	5	5	4	6	-	-	-	1546	1472	-1.41
30	65.32	SM	12	5	5	4	6	6	5	11	1702	1573	-1.44
32.5	62.82	CH	50	10	10	9	11	-	-	-	1858	1717	0.74
35	60.32	CH	<b>69</b>	11	11	9	11	-	-	-	2014	1874	0.43
37.5	57.82	SC	12	15	15	13	15	17	13	22	2170	2010	-0.03
40	55.32	SM	12	2	2	2	2	2	2	7	2326	2072	0.93
42.5	52.82	SM	12	3	3	3	3	3	2	8	2482	2126	0.11
45	50.32	SM	12	2	2	2	2	2	2	7	2638	2172	0.08
47.5	47.82	CL	50	4	4	3	4	-	-	-	2794	2286	-0.45
50	45.32	SM	12	3	3	3	3	3	2	8	2950	2358	-0.81
52.5	42.82	SM	12	2	2	2	2	2	2	7	3106	2404	-0.51
55	40.32	SM	12	3	3	3	3	3	2	8	3262	2458	-0.28
57.5	37.82	SM	12	3	3	3	3	3	2	8	3418	2515	-0.10
60	35.32	SM	<b>12</b>	2	2	2	2	2	2	7	3574	2561	-1.02
62.5	32.82	SM	12	6	6	5	5	6	4	11	3730	2635	0.17
65	30.32	SC	12	4	4	3	3	4	3	9	3886	2697	0.19
67.5	27.82	SC	12	6	6	5	5	6	4	11	4042	2773	0.02
70	25.32	SM	12	11	11	9	9	10	8	15	4198	2885	0.14
72.5	22.82	SM	12	72/11	72/11	72/11	81	81	81	86	4354	3044	0.70
75	20.32	SM	12	86/11	86/11	86/11	79	79	79	84	4510	3213	0.95
77.5	17.82	SM	12	50/5	50/5	50/5	77	77	77	82	4666	3382	
80	15.32	SM	12	50/5.5	50/5.5	50/5.5	75	75	75	80	4822	3551	
82.5	12.82	SM	12	50/5	50/5	50/5	73	73	73	79	4978	3720	
85	10.32	SM	<b>49</b>	50/4	50/4	50/4	72	72	72	81	5134	3889	
87.5	7.82	SM	12	50/3	50/3	50/3	70	70	70	75	5290	4058	
90	5.32	SM	12	50/2	50/2	50/2	69	69	69	74	5446	4227	
92.5	2.82	SM	12	36	36	28	24	24	19	30	5602	4366	
95	0.82	SM	12	50/1	50/1	50/1	67	67	67	72	5727	4493	

Depth (ft)	Elevation (ft)	USCS	Rebound inch	Liquefaction Soil Response	Terzaghi Dr	Schmertmann Φ'	Hatanaka Φ'	Peck Φ'	Mayne OCR	Hera Cu (psf)	Hettiarachchi Cu (psf)	CDOT Qu (psf)
0	95.82	-										
1	94.32	PT										
2.5	92.82	PT										
4	91.32	SP-SM										
5.5	89.82	SM										
7	88.32	SM		Contractive	39%	33	32	28				
8.5	86.82	SP-SM		Intermediate	55%	39	38	30				
10	85.32	SP-SM		Intermediate	53%	38	37	30				
12.5	82.82	SM		Intermediate	60%	41	38	31				
15	80.32	SM		Dilative	64%	43	40	32				
17.5	77.82	SP-SM	-2.28	Intermediate	57%	40	38	31				
20	75.32	SM	0.07	Contractive	44%	35	34	30				
22.5	72.82	SM	-0.14	Contractive	35%	31	31	29				
25	70.32	SC	-0.31	Contractive	42%	34	33	30				
27.5	67.82	CH	-1.41	-					3.506	343	390	1384
30	65.32	SM	-1.44	Contractive	31%	29	30	29				
32.5	62.82	CH	0.74	-					5.265	587	820	2698
35	60.32	CH	0.43	-					5.294	628	902	2841
37.5	57.82	SC	-0.03	Intermediate	50%	38	36	31				
40	55.32	SM	0.93	Contractive	18%	21	26	28				
42.5	52.82	SM	0.11	Contractive	22%	24	27	28				
45	50.32	SM	0.08	Contractive	18%	21	26	28				
47.5	47.82	CL	-0.45	-					2.299	303	328	935
50	45.32	SM	-0.81	Contractive	21%	23	27	28				
52.5	42.82	SM	-0.51	Contractive	17%	20	26	28				
55	40.32	SM	-0.28	Contractive	21%	23	27	28				
57.5	37.82	SM	-0.10	Contractive	21%	23	27	28				
60	35.32	SM	-1.02	Contractive	17%	20	25	28				
62.5	32.82	SM	0.17	Contractive	30%	28	29	29				
65	30.32	SC	0.19	Contractive	24%	25	28	28				
67.5	27.82	SC	0.02	Contractive	29%	28	29	29				
70	25.32	SM	0.14	Contractive	39%	32	33	30				
72.5	22.82	SM	0.70	Dilative	116%	53	60	52				
75	20.32	SM	0.95	Dilative	115%	53	60	52				
77.5	17.82	SM		Dilative	113%	52	59	52				
80	15.32	SM		Dilative	112%	52	59	52				
82.5	12.82	SM		Dilative	111%	52	58	52				
85	10.32	SM		Dilative	109%	51	58	52				
87.5	7.82	SM		Dilative	108%	51	57	52				
90	5.32	SM		Dilative	107%	51	57	52				
92.5	2.82	SM		Intermediate	64%	41	39	37				
95	0.82	SM		Dilative	105%	50	57	52				

**B.2.10.3. B.10.3. SPT FB-4 (P10P14, Ramp A)**

Depth (ft)	Elevation (ft)	USCS	FC actual/estimate	B-27 Nsafe	SPT N60	SPT Ntrip	SPT (N1)60	SPT (N1)60t	SPT (N1)trip	SPT (N1)60ta	u psf	$\sigma'_{vo}$ (avg) psf	Rebound inch
0	95.9												
1	94.9	SP-SM		HA							0	105	
2.5	93.4	SP-SM		HA							0	261	
4	91.9	SM		HA							81	354	
5.5	90.4	SM		HA							175	444	
7	88.9	SP-SM	8.5	8	6	5	12	13	10	17	268	526	
8.5	87.4	SP-SM	5	13	10	8	18	20	15	20	362	610	
10	85.9	SP-SM	8.5	16	12	9	20	20	16	24	456	696	
12.5	83.4	SP	0	24	18	14	27	27	21	27	612	860	
15	80.9	SM	12	18	15	12	22	22	17	27	768	999	
17.5	78.4	SM	12	18	15	12	20	20	16	26	924	1131	-0.80
20	75.9	SM	15	27	26	20	32	32	25	38	1080	1272	-1.13
22.5	73.4	SM	12	38	36	28	43	43	33	48	1236	1426	-0.08
25	70.9	SM	12	13	12	11	14	16	12	21	1392	1563	1.75
27.5	68.4	SM	12	6	6	5	6	7	5	12	1548	1664	0.31
30	65.9	SM	24	3	3	3	3	4	3	10	1704	1728	0.47
32.5	63.4	SM	12	4	4	3	4	5	4	10	1860	1795	0.36
35	60.9	CH	50	6	6	5	6	-	-	-	2016	1924	0.07
37.5	58.4	SC	12	6	6	5	6	7	5	12	2172	2028	1.15
40	55.9	SC	30	6	6	5	6	6	5	13	2328	2122	0.39
42.5	53.4	SC	12	4	4	3	4	4	3	9	2484	2196	-1.03
45	50.9	SM	12	4	4	3	4	4	3	9	2640	2265	-1.00
47.5	48.4	SM	12	2	2	2	2	2	2	7	2796	2314	-0.24
50	45.9	CL	54	5	5	4	5	-	-	-	2952	2428	-0.46
52.5	43.4	SM	12	6	6	5	5	6	5	11	3108	2519	-0.95
55	40.9	SM	12	5	5	4	4	5	4	10	3264	2591	-0.17
57.5	38.4	SM	12	3	3	3	3	3	2	8	3420	2650	0.25
60	35.9	SM	16	5	5	4	4	5	4	10	3576	2716	0.56
62.5	33.4	SM	12	5	5	4	4	5	4	10	3732	2785	-0.70
65	30.9	SM	12	2	2	2	2	2	1	7	3888	2834	0.09
67.5	28.4	CL	50	5	5	4	4	-	-	-	4044	2948	0.66
70	25.9	SM	12	4	4	3	3	4	3	9	4200	3020	1.05
72.5	23.4	SM	12	6	6	5	5	5	4	11	4356	3096	0.46
75	20.9	SM	15	4	4	3	3	4	3	9	4512	3158	0.53
77.5	18.4	SM	12	17	17	15	13	15	11	20	4668	3274	1.18
80	15.9	SM	12	82/9	82/9	82/9	76	76	76	81	4824	3436	1.16
82.5	13.4	SM	12	50/5	50/5	50/5	74	74	74	80	4980	3605	0.71
85	10.9	SM	12	90/11	90/11	90/11	73	73	73	78	5136	3774	0.75
87.5	8.4	SM	12	50/5	50/5	50/5	71	71	71	76	5292	3943	0.59
90	5.9	SM	12	57	57	57	40	40	40	45	5448	4102	0.84
92.5	3.4	SM	12	57	57	44	39	39	30	44	5604	4258	0.56
95	0.9	SM	12	65	65	65	44	44	44	49	5760	4415	
97.5	-1.6	SM	12	50/5	50/5	50/5	66	66	66	71	5916	4581	
100	-4.1	SM	12	50/0	50/0	50/0	65	65	65	70	6072	4750	

Depth (ft)	Elevation (ft)	USCS	Rebound inch	Liquefaction Soil Response	Terzaghi Dr	Schmertmann Φ'	Hatanaka Φ'	Peck Φ'	Mayne OCR	Hera Cu (psf)	Hettiarachchi Cu (psf)	CDOT Qu (psf)
0	95.9											
1	94.9	SP-SM										
2.5	93.4	SP-SM										
4	91.9	SM										
5.5	90.4	SM										
7	88.9	SP-SM		Contractive	44%	35	34	29				
8.5	87.4	SP-SM		Contractive	54%	39	37	30				
10	85.9	SP-SM		Intermediate	58%	40	38	31				
12.5	83.4	SP		Intermediate	68%	44	41	32				
15	80.9	SM		Intermediate	60%	41	38	32				
17.5	78.4	SM	-0.80	Intermediate	58%	41	38	32				
20	75.9	SM	-1.13	Dilative	73%	45	42	34				
22.5	73.4	SM	-0.08	Dilative	84%	48	46	37				
25	70.9	SM	1.75	Intermediate	48%	37	35	31				
27.5	68.4	SM	0.31	Contractive	32%	30	30	29				
30	65.9	SM	0.47	Contractive	23%	25	27	28				
32.5	63.4	SM	0.36	Contractive	27%	27	28	28				
35	60.9	CH	0.07	-					3.424	406	492	1529
37.5	58.4	SC	1.15	Contractive	32%	29	30	29				
40	55.9	SC	0.39	Contractive	31%	29	30	29				
42.5	53.4	SC	-1.03	Contractive	25%	26	28	28				
45	50.9	SM	-1.00	Contractive	25%	26	28	28				
47.5	48.4	SM	-0.24	Contractive	18%	21	26	28				
50	45.9	CL	-0.46	-					2.572	356	410	1134
52.5	43.4	SM	-0.95	Contractive	30%	28	30	29				
55	40.9	SM	-0.17	Contractive	27%	27	29	29				
57.5	38.4	SM	0.25	Contractive	21%	23	27	28				
60	35.9	SM	0.56	Contractive	27%	26	29	29				
62.5	33.4	SM	-0.70	Contractive	27%	26	29	29				
65	30.9	SM	0.09	Contractive	17%	20	25	28				
67.5	28.4	CL	0.66	-					2.250	356	410	1029
70	25.9	SM	1.05	Contractive	23%	24	27	28				
72.5	23.4	SM	0.46	Contractive	28%	27	29	29				
75	20.9	SM	0.53	Contractive	23%	24	27	28				
77.5	18.4	SM	1.18	Contractive	47%	36	35	32				
80	15.9	SM	1.16	Dilative	113%	52	59	52				
82.5	13.4	SM	0.71	Dilative	111%	52	59	52				
85	10.9	SM	0.75	Dilative	110%	52	58	52				
87.5	8.4	SM	0.59	Dilative	109%	51	58	52				
90	5.9	SM	0.84	Dilative	81%	46	48	42				
92.5	3.4	SM	0.56	Dilative	81%	45	45	42				
95	0.9	SM		Dilative	85%	46	50	44				
97.5	-1.6	SM		Dilative	105%	50	56	52				
100	-4.1	SM		Dilative	104%	50	56	52				

## B.2.11. I-4 and SR-408 Intersection

### B.2.11.1. SPT B-110 (P2P5, Ramp B5)

Depth (ft)	Elevation (ft)	USCS	FC actual/estimate	B-110 Nsafe	SPT N60	SPT Ntrip	SPT (N1)60	SPT (N1)60t	SPT (N1)trip	SPT (N1)60ta	u psf	$\sigma'_{vo}$ (avg) psf	Rebound inch
0.0	103.3	SC	12										
2.0	101.3	SP-SM	8.5	5	4	3	8	8	6	12	0	200	
3.5	99.8	SP-SM	8.5	4	3	2	6	6	5	10	0	345	
8.5	94.8	SC	12	2	2	1	3	3	2	8	0	708	0.13
10.0	93.3	SC	12	6	5	4	7	8	6	13	87	760	0.12
11.5	91.8	SP-SC	8.5	4	3	3	5	5	4	9	181	819	0.12
13.0	90.3	SP-SC	8.5	5	4	4	6	7	5	11	275	880	0.12
14.5	88.8	SP-SC	8.5	6	5	4	7	8	6	12	368	949	0.12
17.0	86.3	SP-SC	8.5	7	6	5	8	9	7	13	524	1068	-0.05
19.5	83.8	SP-SC	8.5	6	5	4	7	7	6	11	680	1177	0.07
22.0	81.3	SP-SC	8.5	8	8	6	9	10	8	14	836	1304	0.11
24.5	78.8	SP-SC	8.5	3	3	2	3	4	3	8	992	1385	0.12
27.0	76.3	SP-SC	8.5	3	3	2	3	4	3	8	1148	1454	0.13
29.5	73.8	SC	17	2	2	2	2	2	2	8	1304	1503	0.16
32.0	71.3	SC	12	2	2	2	2	3	2	8	1460	1547	0.18
34.5	68.8	SP	0	10	10	9	11	12	9	12	1616	1671	0.22
37.0	66.3	SP	0	11	11	9	12	13	10	13	1772	1815	0.23
39.5	63.8	SP	0	1	1	1	1	1	1	1	1928	1899	0.24
42.0	61.3	SC	12	7	7	6	7	8	6	13	2084	1998	0.25
44.5	58.8	SC	12	5	5	4	5	5	4	11	2240	2085	0.26
47.0	56.3	SC	22	1	1	1	1	1	1	7	2396	2126	0.23
49.5	53.8	SC	12	1	1	1	1	1	1	6	2552	2158	0.19
52.0	51.3	SC	12	2	2	2	2	2	2	7	2708	2199	0.15
54.5	48.8	SC	12	6	6	5	6	6	5	11	2864	2283	0.17
57.0	46.3	SP-SC	8.5	14	14	12	13	14	11	18	3020	2417	0.17
59.5	43.8	SP-SC	8.5	15	15	13	13	15	11	19	3176	2561	0.16
62.0	41.3	SP-SC	8.5	14	14	12	12	13	10	17	3332	2695	0.17
64.5	38.8	SC	12	9	9	8	8	8	6	14	3488	2807	0.24
67.0	36.3	SC	22	10	10	9	8	9	7	15	3644	2913	0.31
69.5	33.8	SC	12	11	11	9	9	10	8	15	3800	3030	0.39
72.0	31.3	SC	12	12	12	10	10	11	8	16	3956	3139	0.34
74.5	28.8	SC	12	50	50	38	39	39	30	44	4112	3285	0.38
77.0	26.3	SP-SC	8.5	51	51	39	39	39	30	43	4268	3452	0.35
79.5	23.8	SC	12	26	26	22	19	22	17	27	4424	3591	0.33
82.0	21.3	SC	12	26	26	22	19	21	16	26	4580	3722	0.32
84.5	18.8	SC	16	51	51	39	37	37	28	42	4736	3874	0.30
87.0	16.3	SC	12	35	35	27	25	25	19	30	4892	4020	0.29
89.5	13.8	SC	12	13	13	11	9	10	8	15	5048	4144	0.46
92.0	11.3	SC	12	16	16	14	11	12	9	17	5204	4263	
94.5	8.8	SC	12	84	84	65	56	56	43	62	5360	4422	
97	6.3	SC	12	50/5.5	50/5.5	50/5.5	66	66	66	71	5516	4591	
99.5	3.8	SC	12	56	56	43	36	36	28	42	5672	4750	
102	1.3	SC	12	53	53	41	34	34	26	39	5828	4897	
104.5	-1.2	SC	12	53	53	41	33	33	26	39	5984	5041	
107	-3.7	SC	12	20	20	17	12	14	11	19	6140	5165	
109.5	-6.2	SC	22	17	17	15	10	12	9	18	6296	5284	
112	-8.7	SC	12	18	18	15	11	12	9	17	6452	5403	
114.5	-11.2	SC	12	22	22	19	13	15	11	20	6608	5532	

Depth (ft)	Elevation (ft)	USCS	Rebound inch	Liquefaction Soil Response	Terzaghi Dr	Schmertmann Φ'	Hatanaka Φ'	Peck Φ'	Mayne OCR	Hera Cu (psf)	Hettiarachchi Cu (psf)	CDOT Qu (psf)
0.0	103.3	SC										
2.0	101.3	SP-SM		High	35%	32	31	28				
3.5	99.8	SP-SM		Contractive	32%	30	30	28				
8.5	94.8	SC	0.13	Contractive	21%	23	26	28				
10.0	93.3	SC	0.12	Contractive	35%	31	31	28				
11.5	91.8	SP-SC	0.12	Contractive	28%	27	29	28				
13.0	90.3	SP-SC	0.12	Contractive	33%	30	30	28				
14.5	88.8	SP-SC	0.12	Contractive	35%	31	31	29				
17.0	86.3	SP-SC	-0.05	Contractive	37%	32	32	29				
19.5	83.8	SP-SC	0.07	Contractive	33%	31	31	29				
22.0	81.3	SP-SC	0.11	Contractive	40%	34	33	29				
24.5	78.8	SP-SC	0.12	Contractive	24%	25	28	28				
27.0	76.3	SP-SC	0.13	Contractive	24%	25	28	28				
29.5	73.8	SC	0.16	Contractive	19%	22	26	28				
32.0	71.3	SC	0.18	Contractive	19%	22	26	28				
34.5	68.8	SP	0.22	Contractive	43%	35	34	30				
37.0	66.3	SP	0.23	Contractive	44%	35	34	30				
39.5	63.8	SP	0.24	Contractive	13%	17	24	27				
42.0	61.3	SC	0.25	Contractive	34%	31	31	29				
44.5	58.8	SC	0.26	Contractive	29%	28	29	29				
47.0	56.3	SC	0.23	Contractive	13%	17	24	27				
49.5	53.8	SC	0.19	Contractive	13%	17	24	27				
52.0	51.3	SC	0.15	Contractive	18%	21	26	28				
54.5	48.8	SC	0.17	Contractive	31%	29	30	29				
57.0	46.3	SP-SC	0.17	Contractive	46%	36	35	31				
59.5	43.8	SP-SC	0.16	Contractive	47%	36	35	31				
62.0	41.3	SP-SC	0.17	Contractive	45%	35	34	31				
64.5	38.8	SC	0.24	Contractive	36%	31	31	30				
67.0	36.3	SC	0.31	Contractive	37%	32	32	30				
69.5	33.8	SC	0.39	Contractive	39%	32	32	30				
72.0	31.3	SC	0.34	Contractive	40%	33	33	31				
74.5	28.8	SC	0.38	Dilative	81%	46	44	41				
77.0	26.3	SP-SC	0.35	Dilative	80%	46	44	41				
79.5	23.8	SC	0.33	Intermediate	57%	39	38	35				
82.0	21.3	SC	0.32	Intermediate	56%	39	38	35				
84.5	18.8	SC	0.30	Dilative	78%	45	44	41				
87.0	16.3	SC	0.29	Intermediate	64%	41	39	37				
89.5	13.8	SC	0.46	Contractive	39%	32	32	31				
92.0	11.3	SC		Contractive	43%	33	34	32				
94.5	8.8	SC		Dilative	97%	49	49	48				
97	6.3	SC		Dilative	105%	50	56	52				
99.5	3.8	SC		Dilative	78%	44	44	42				
102	1.3	SC		Dilative	75%	43	43	41				
104.5	-1.2	SC		Dilative	75%	43	43	41				
107	-3.7	SC		Contractive	46%	34	35	33				
109.5	-6.2	SC		Contractive	42%	32	33	32				
112	-8.7	SC		Contractive	43%	33	34	32				
114.5	-11.2	SC		Contractive	47%	34	35	33				

## B.3. C. SPT Soil Borings

### B.3.1. Typical SPT Driving Specifications

#### **GENERAL NOTES**

STANDARD PENETRATION TEST BORINGS WERE PERFORMED IN ACCORDANCE WITH ASTM D-1586. STANDARD PENETRATION RESISTANCES ARE SHOWN ON THE BORINGS AT THE TEST DEPTHS IN BLOWS PER FOOT UNLESS OTHERWISE NOTED.

SUBSURFACE CONDITIONS SHOWN ON THE BORINGS REPRESENT THE CONDITIONS ENCOUNTERED AT THE BORING LOCATIONS. ACTUAL CONDITIONS BETWEEN BORINGS MAY VARY FROM THOSE SHOWN. UNIFIED SOIL CLASSIFICATIONS SHOWN ON THE BORINGS ARE BASED ON VISUAL EXAMINATION AND THE LABORATORY TESTING SHOWN.

GROUND SURFACE ELEVATIONS AT THE BORING LOCATIONS WERE ESTIMATED FROM ROADWAY CROSS SECTIONS PROVIDED BY HDR AND SHOULD BE CONSIDERED APPROXIMATE.

BASED ON A REVIEW OF THE U.S. GEOLOGICAL SURVEY MAP ENTITLED "POTENTIOMETRIC SURFACE OF THE UPPER FLORIDAN AQUIFER IN THE ST. JOHNS RIVER WATER MANAGEMENT DISTRICT AND VICINITY, FLORIDA, SEPTEMBER 2007" FOR THE PROJECT AREA, THE APPROXIMATE ELEVATION OF THE ARTESIAN HEAD IS ESTIMATED TO BE +25 FT. MGD, THE CONTRACTOR SHALL BE PREPARED TO HANDLE ARTESIAN HEAD LEVELS UP TO +25 FT. MGD.

SPLIT SPOON SAMPLER:  
INSIDE DIAMETER: 1.375 IN.  
OUTSIDE DIAMETER: 2.0 IN.  
AVERAGE HAMMER DROP: 30 IN.  
HAMMER WEIGHT: 140 LBS.  
HAMMER TYPE: SAFETY (MANUAL)

ENVIRONMENTAL CLASSIFICATION:  
SUPERSTRUCTURE: SLIGHTLY AGGRESSIVE  
SUBSTRUCTURE: STEEL: EXTREMELY AGGRESSIVE (pH=4.6)  
CONCRETE: EXTREMELY AGGRESSIVE (pH=4.6)

### B.3.2. Typical Engineering Classification

#### ENGINEERING CLASSIFICATION

GRANULAR MATERIALS		
Relative Density	Safety Hammer SPT N-Value (Blows/Foot)	Automatic Hammer SPT N-Value (Blows/Foot)
VERY LOOSE	Less than 4	Less than 3
LOOSE	4 - 10	3 - 7
MEDIUM DENSE	10 - 30	7 - 21
DENSE	30 - 50	21 - 35
VERY DENSE	Greater than 50	Greater than 35

SILTS AND CLAYS		
Consistency	Safety Hammer SPT N-Value (Blows/Foot)	Automatic Hammer SPT N-Value (Blows/Foot)
VERY SOFT	Less than 2	Less than 1
SOFT	2 - 4	1 - 3
FIRM	4 - 8	3 - 6
STIFF	8 - 15	6 - 11
VERY STIFF	15 - 30	11 - 21
HARD	Greater than 30	Greater than 21

#### ENVIRONMENTAL CLASSIFICATION

**SUBSTRUCTURE: Extremely Aggressive**  
(soil pH < 5.0)

**SUPERSTRUCTURE: Slightly Aggressive**

### B.3.3. Typical Soil Profile Legend

#### LEGEND

	SAND		SILTY SAND
	CLAYEY SAND		CLAY
	SHELLY SAND		LIMESTONE

(SP) UNIFIED SOIL CLASSIFICATION GROUP SYMBOL

▼ ENCOUNTERED GROUNDWATER LEVEL  
5-30-12 DATE NOTED

▽ ESTIMATED NORMAL SEASONAL HIGH GROUNDWATER LEVEL

W=0	NATURAL MOISTURE CONTENT (%)
-200=0	FINES PASSING No. 200 SIEVE (%)
LL=0	LIQUID LIMIT (%)
PI=0	PLASTICITY INDEX
NP	NON-PLASTIC

N STANDARD PENETRATION RESISTANCE IN BLOWS PER FOOT UNLESS OTHERWISE NOTED

50/6" NUMBER OF BLOWS REQUIRED (50) TO ADVANCE SAMPLING SPOON (6) INCHES

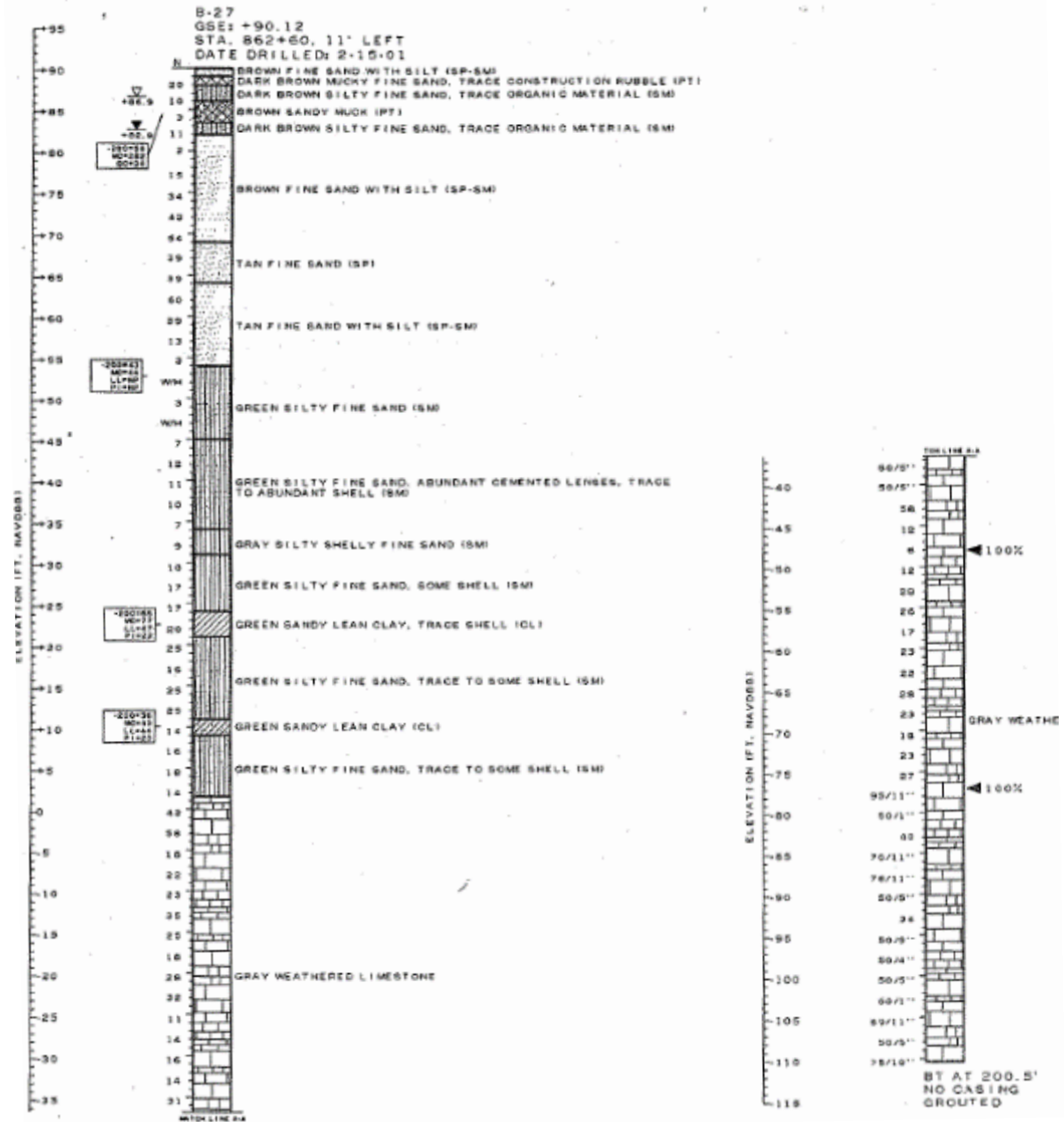
WR WEIGHT OF ROD SUFFICIENT TO ADVANCE SAMPLE SPOON

WH WEIGHT OF ROD AND HAMMER SUFFICIENT TO ADVANCE SAMPLE SPOON

### B.3.4. SPT Soil Boring Profiles

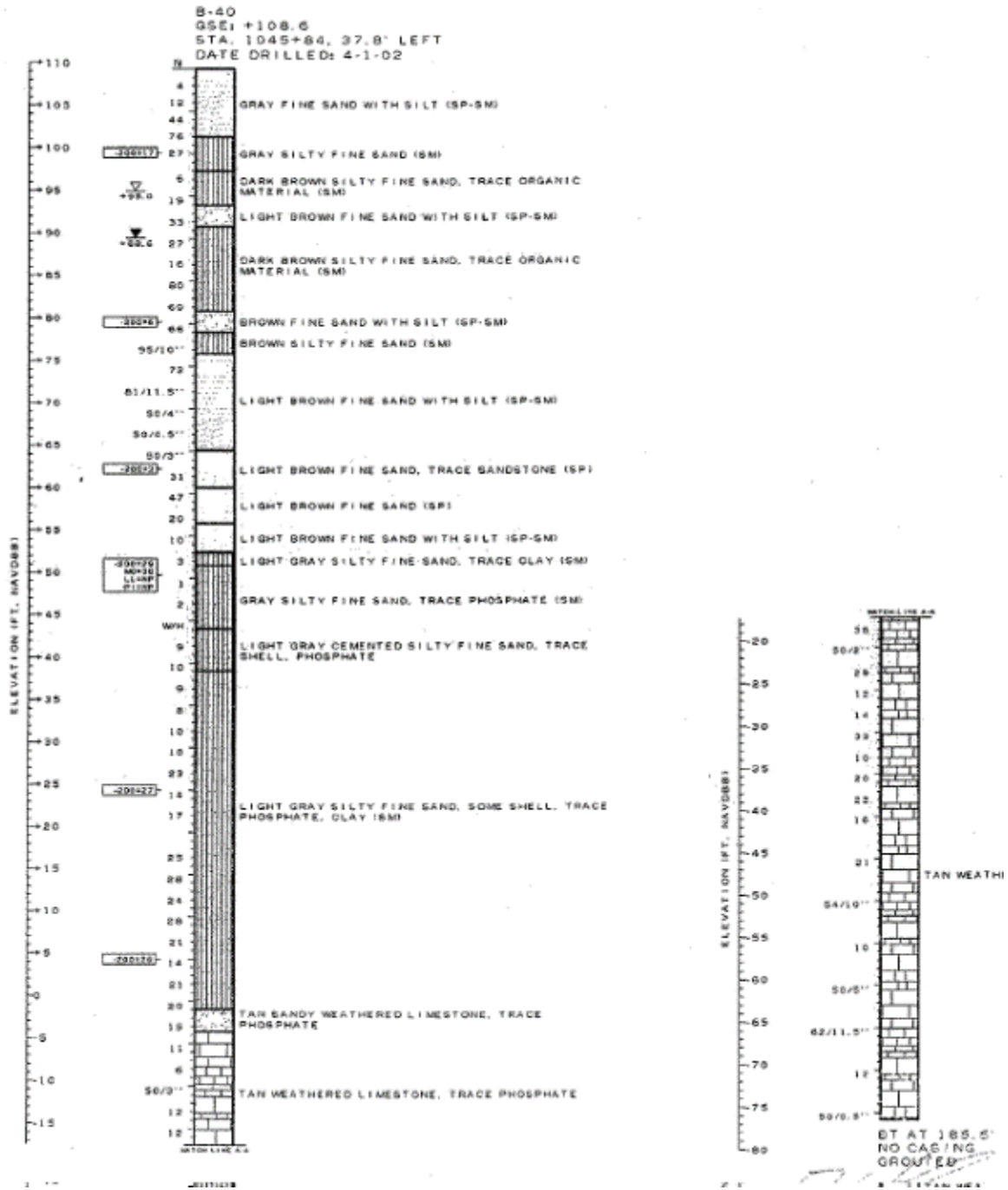
#### B.3.4.1. I-4 / US-192 Interchange

##### B.3.4.1.1. SPT B-27 (Ramp BD EB1P3)

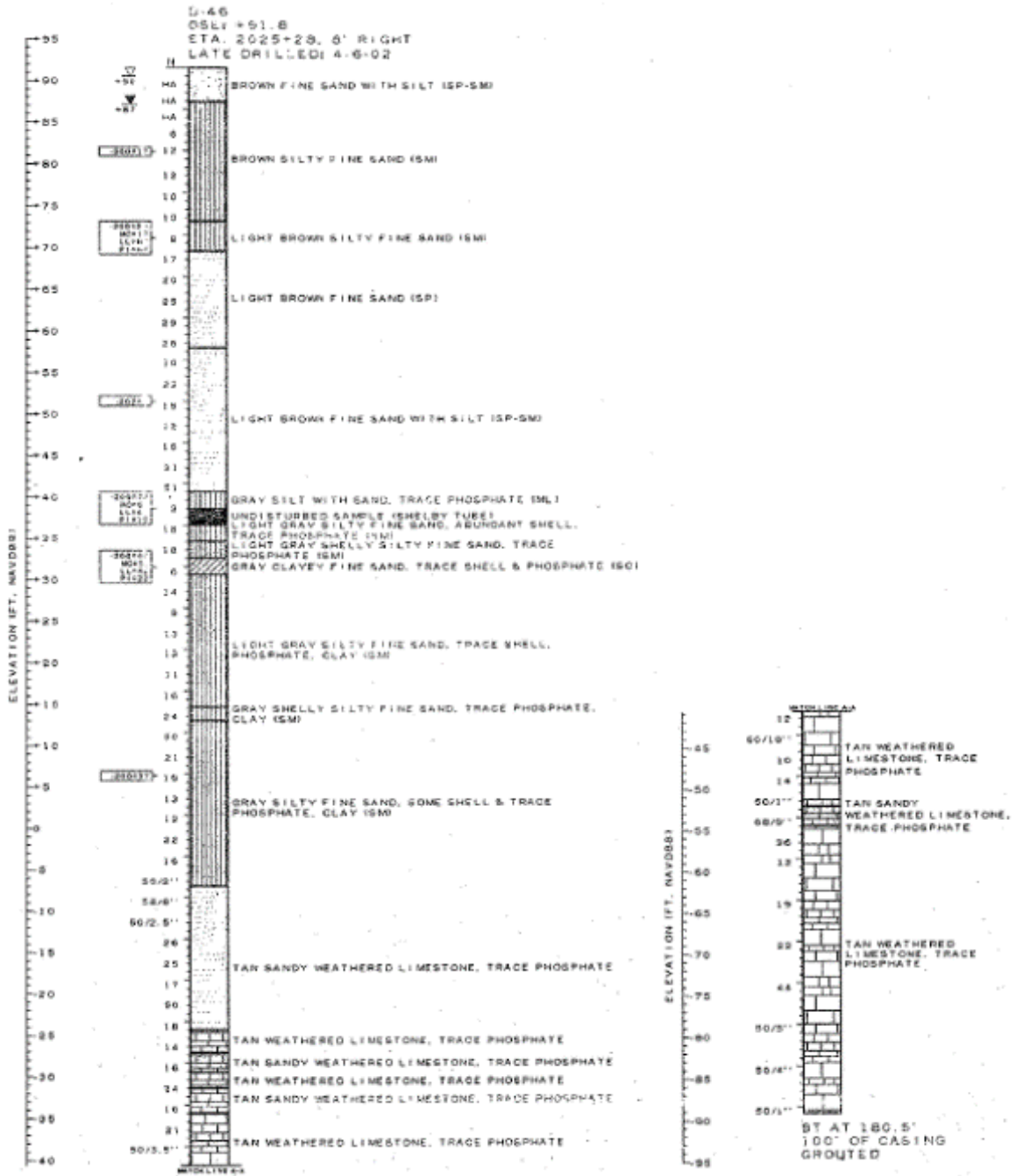




B.3.4.1.3. C.4.1.3. SPT B-41 (Ramp CA P8P4)

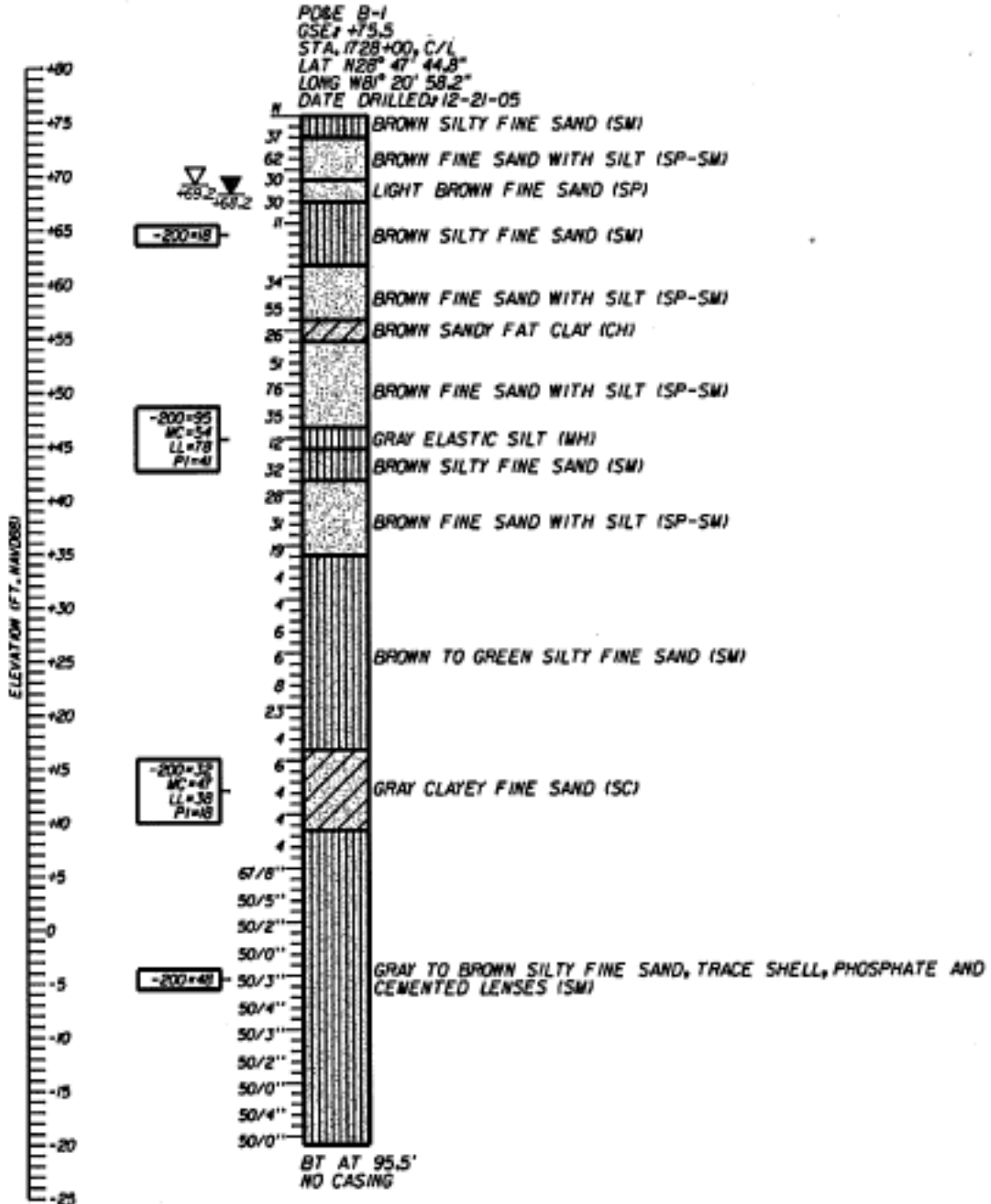


B.3.4.1.4. C.4.1.4 SPT B-46 (Ramp D2 P2P8)



B.3.4.2. C.4.2. SR-417 and International Parkway

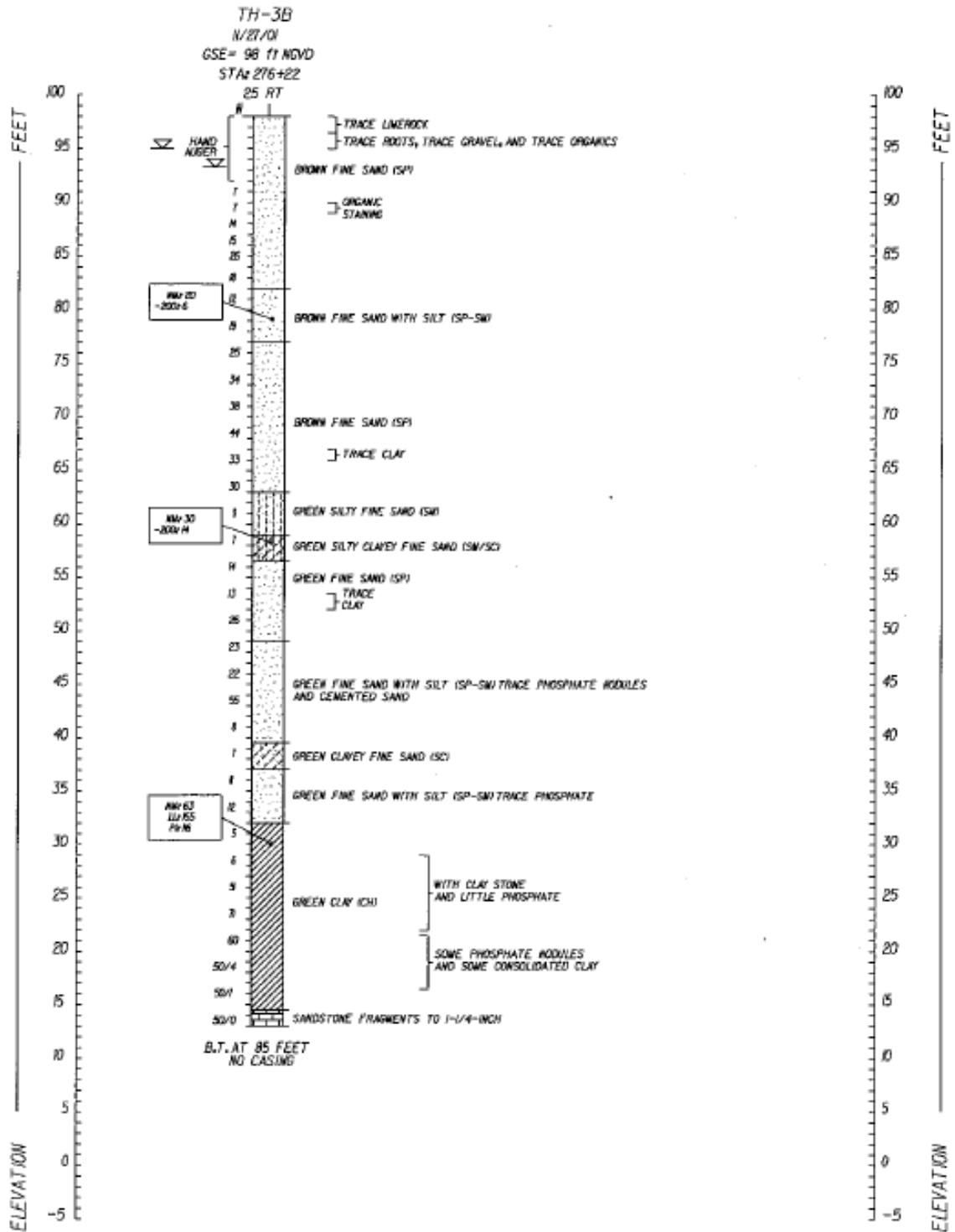
B.3.4.2.1. C.4.2.1 SPT B-1 (EB1P14)





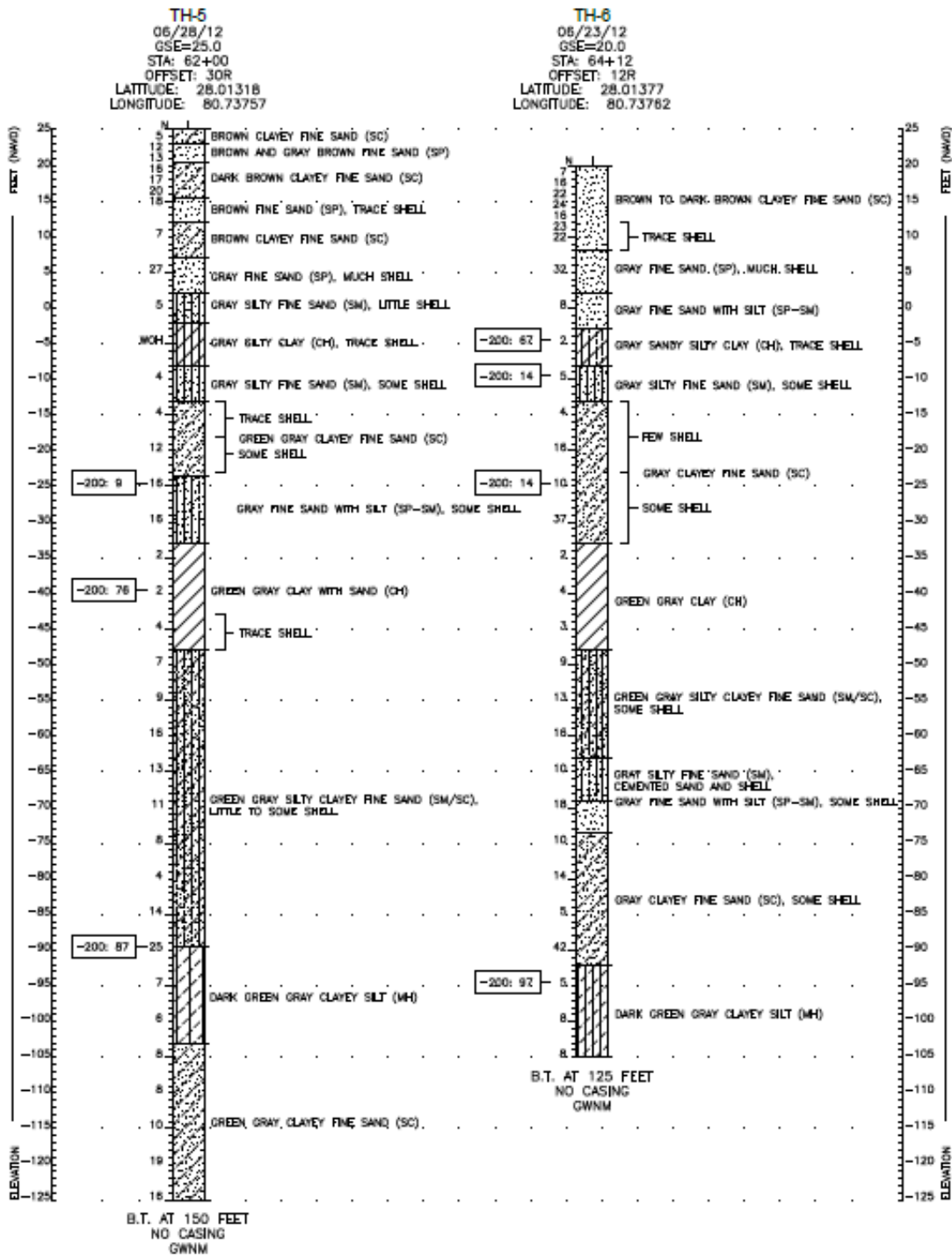


B.3.4.3.2. C.4.3.2. SPT TH-3B (P3P10, EB)

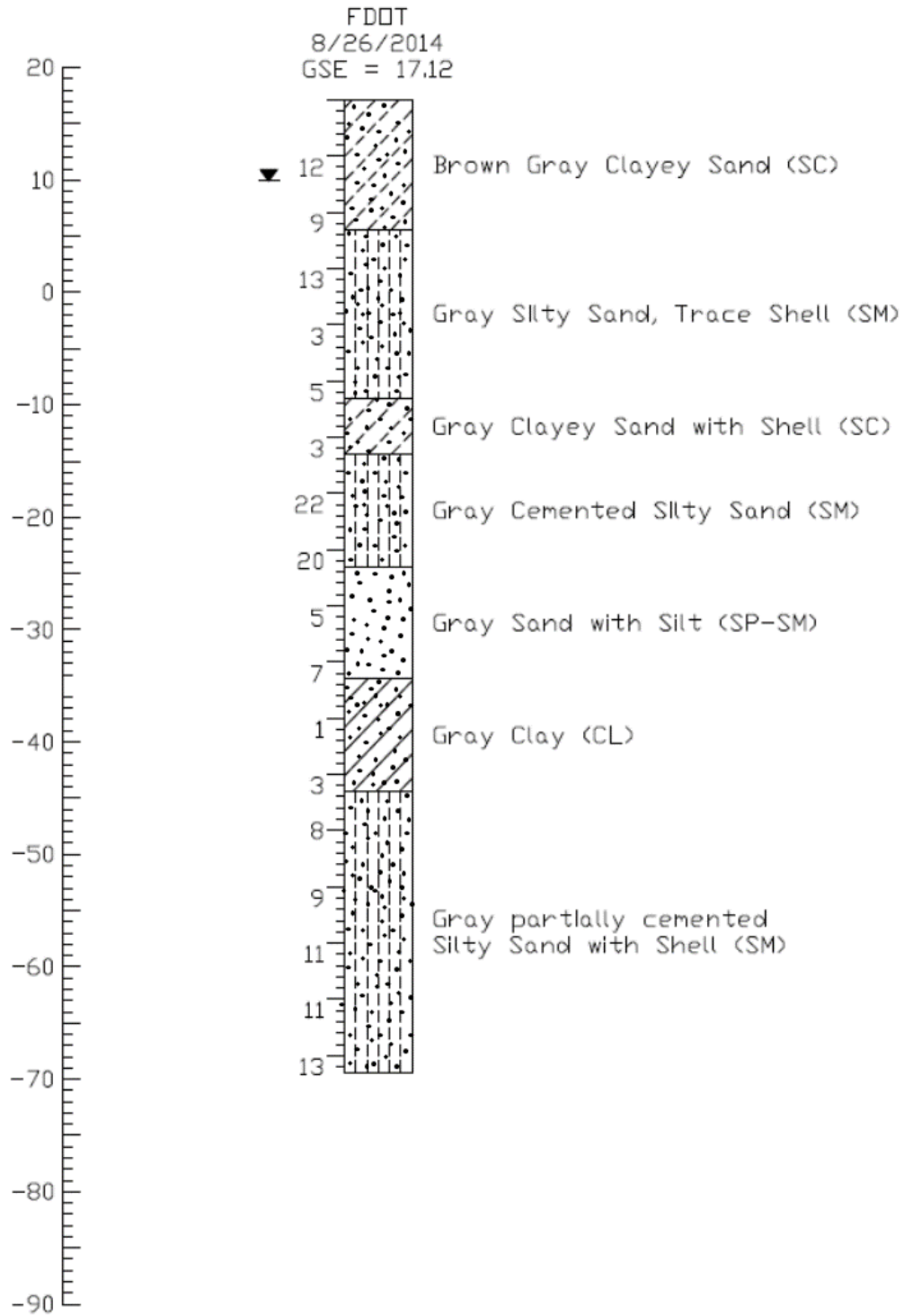


### B.3.4.4. C.4.4. Heritage Parkway

#### B.3.4.4.1. C.4.4.1 SPT TH-5 (EB1P1) & SPT TH-6 (EB5P1)

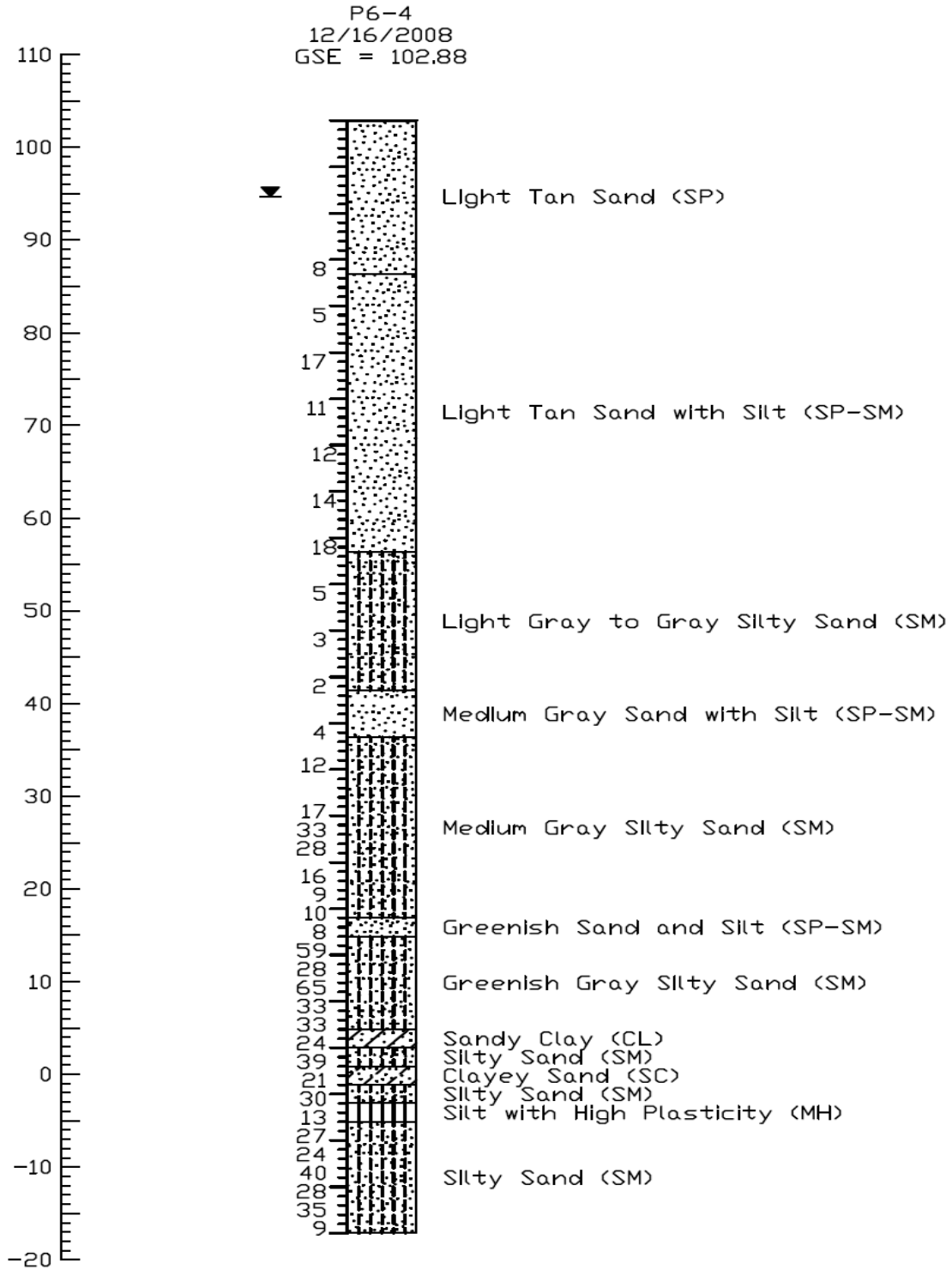


**B.3.4.4.2. C.4.4.2. SPT FDOT Heritage (P3P1)**



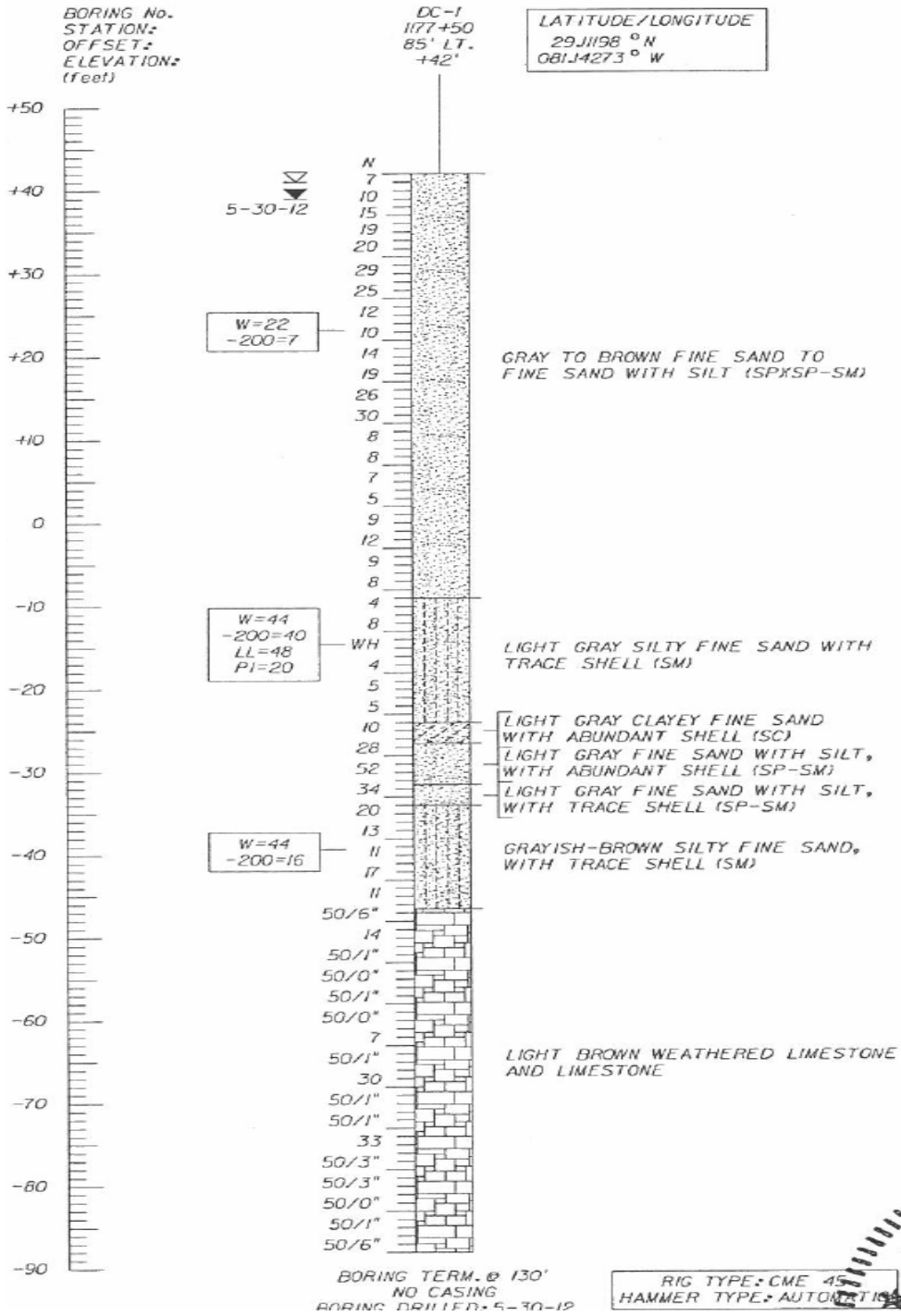
**B.3.4.5. C.4.5. Anderson Street Overpass**

**B.3.4.5.1. C.4.5.1. SPT P6-4 (P6P5, P6P6)**



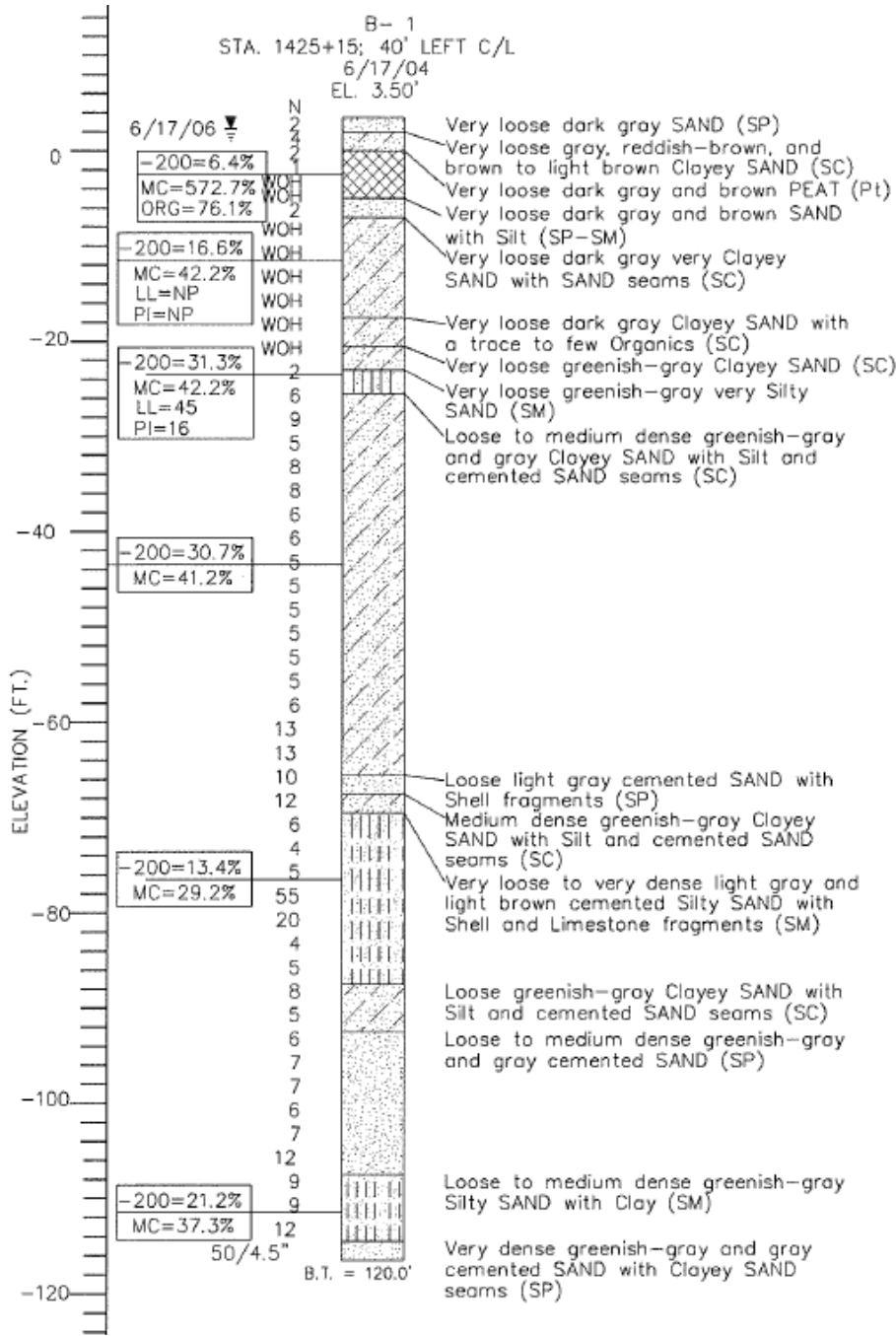
**B.3.4.6. C.4.6. I-4 Widening Daytona**

**B.3.4.6.1. C.4.6.1. SPT DC-1 (EB 3-1, P5)**

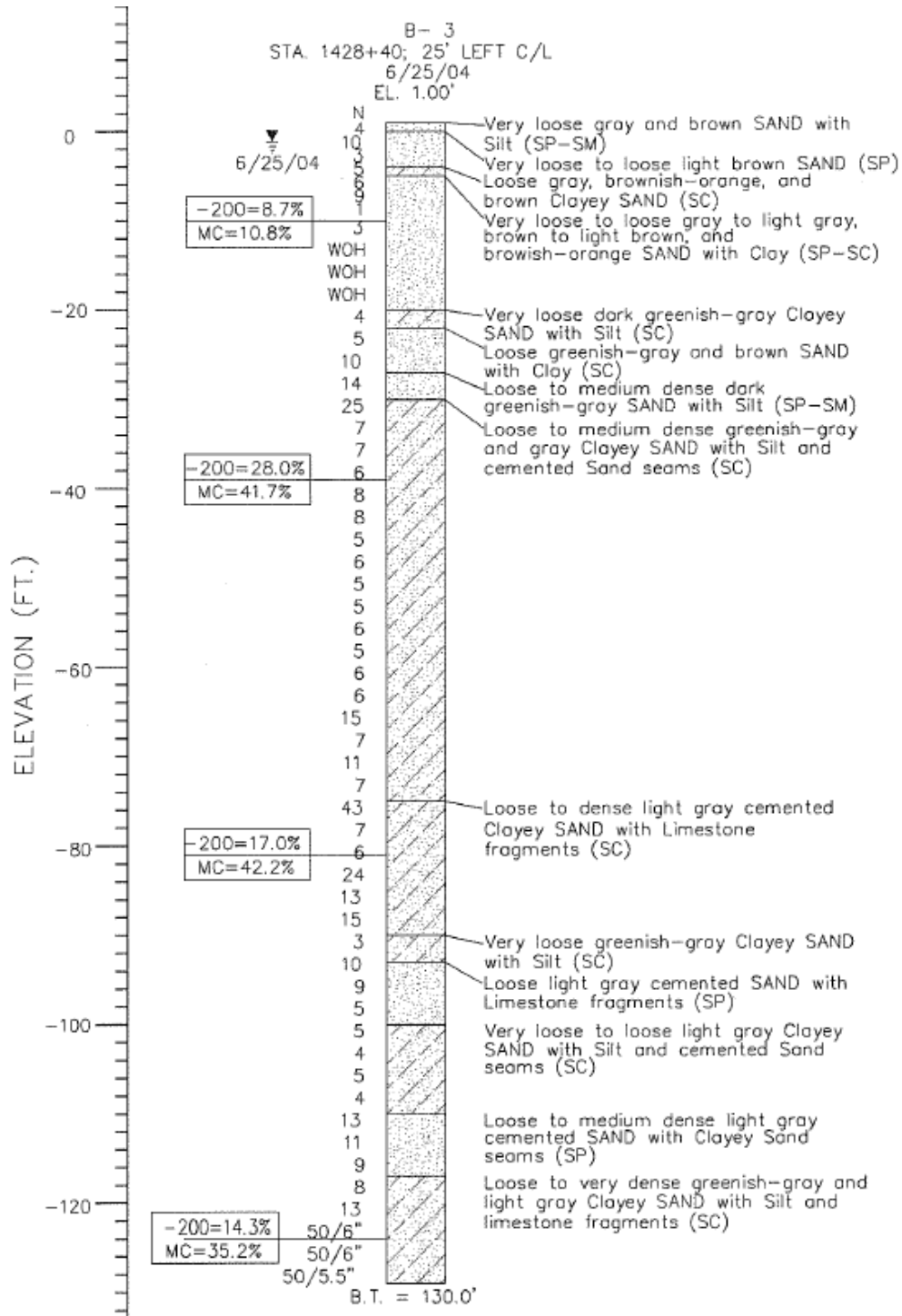


### B.3.4.7. C.4.7. SR-83 over Ramsey Branch

#### B.3.4.7.1. C.4.7.1. SPT B-1 (EB1P1)

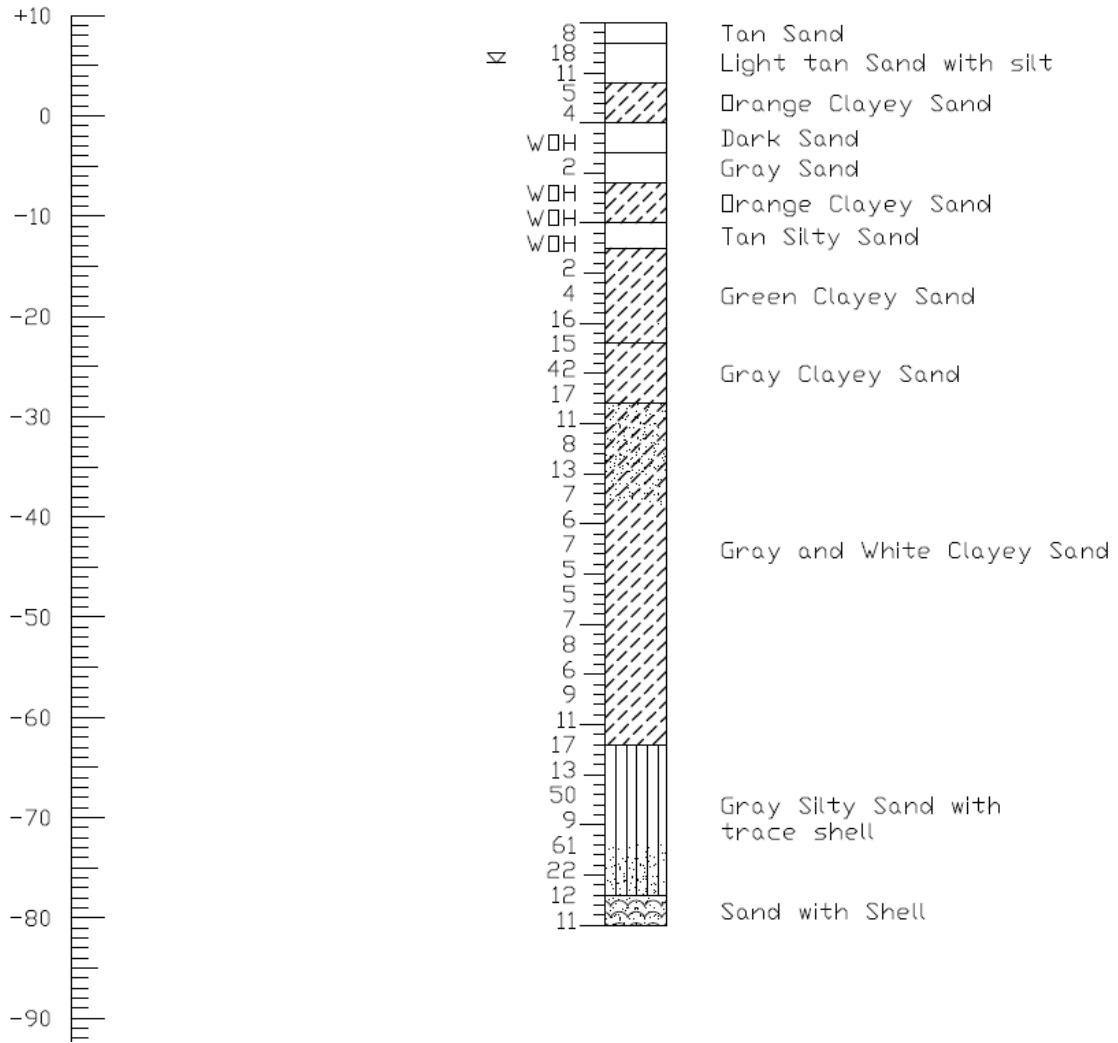


**B.3.4.7.2. C.4.7.2. SPT B-3 (P4P5)**



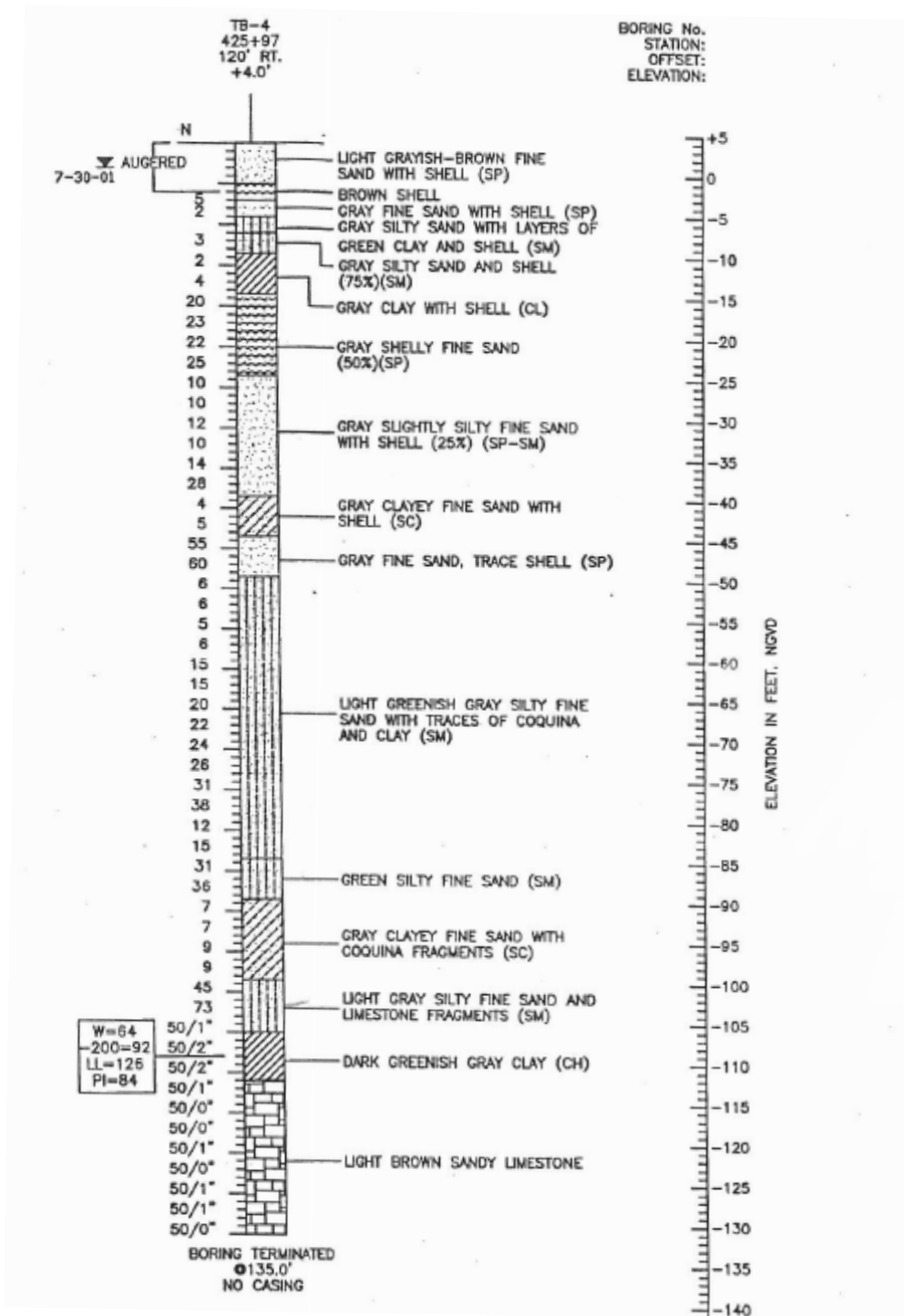
**B.3.4.7.3. C.4.7.3. SPT FDOT Ramsey (EB5P2)**

Ramsey Branch SPT  
 Sta approx 1248+60, 25' East of CL  
 Elevation: +9.3'  
 Water Table: +5.3'

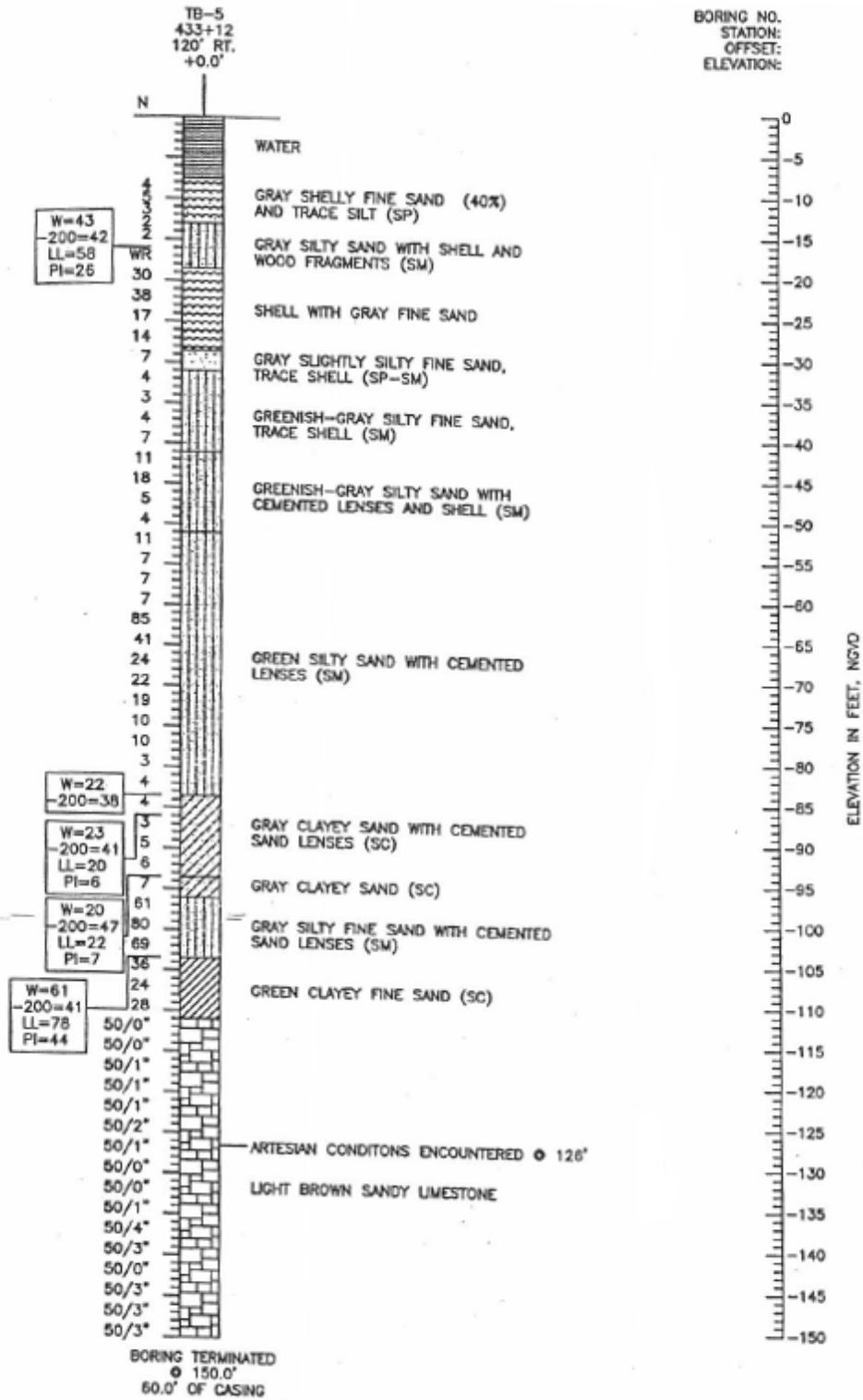


B.3.4.8. C.4.8. SR-528 over Indian River

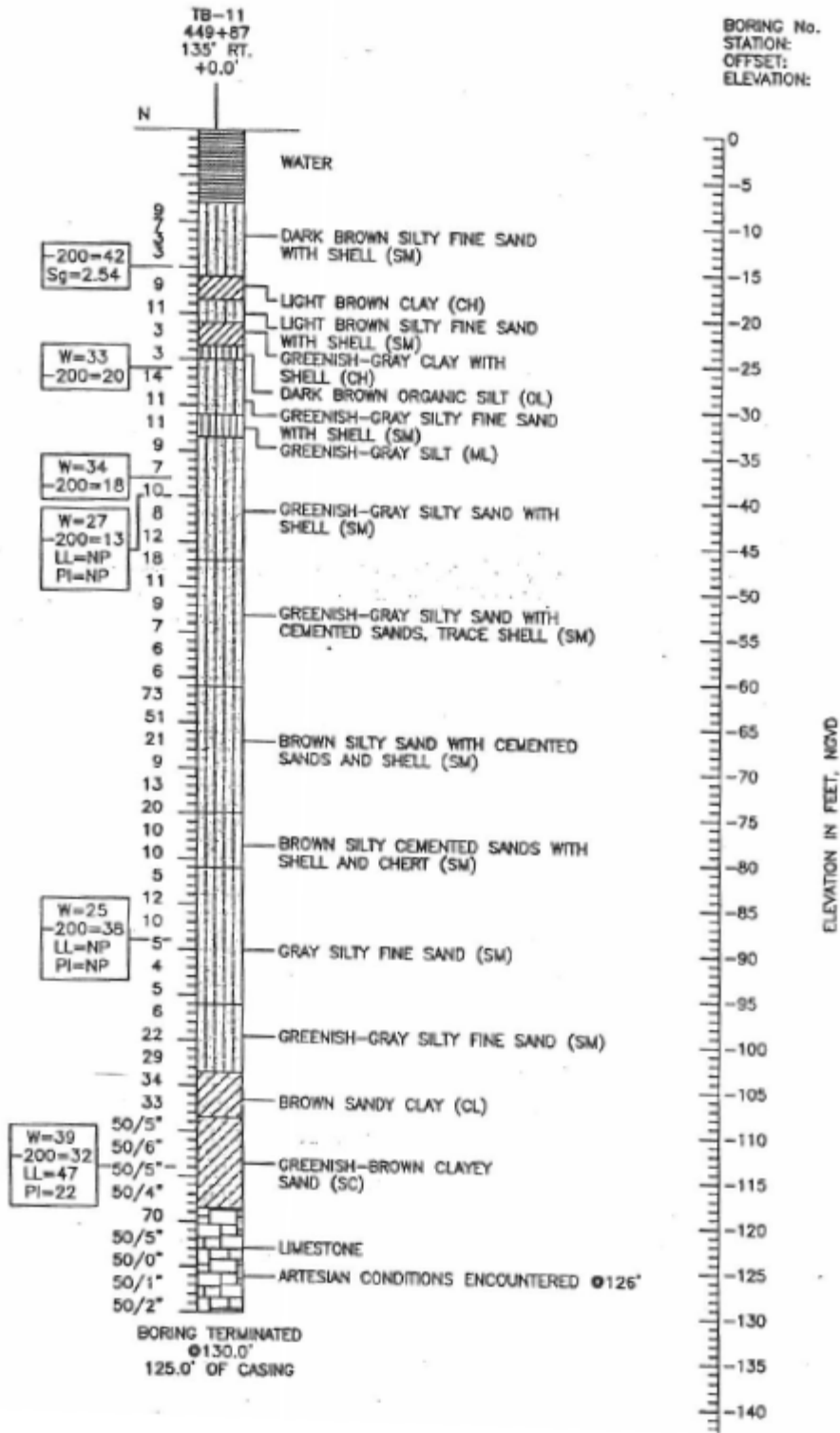
B.3.4.8.1. C.4.8.1. SPT TB-4 (P4P7)



B.3.4.8.2. C.4.8.2. SPT TB-5 (P9P3)

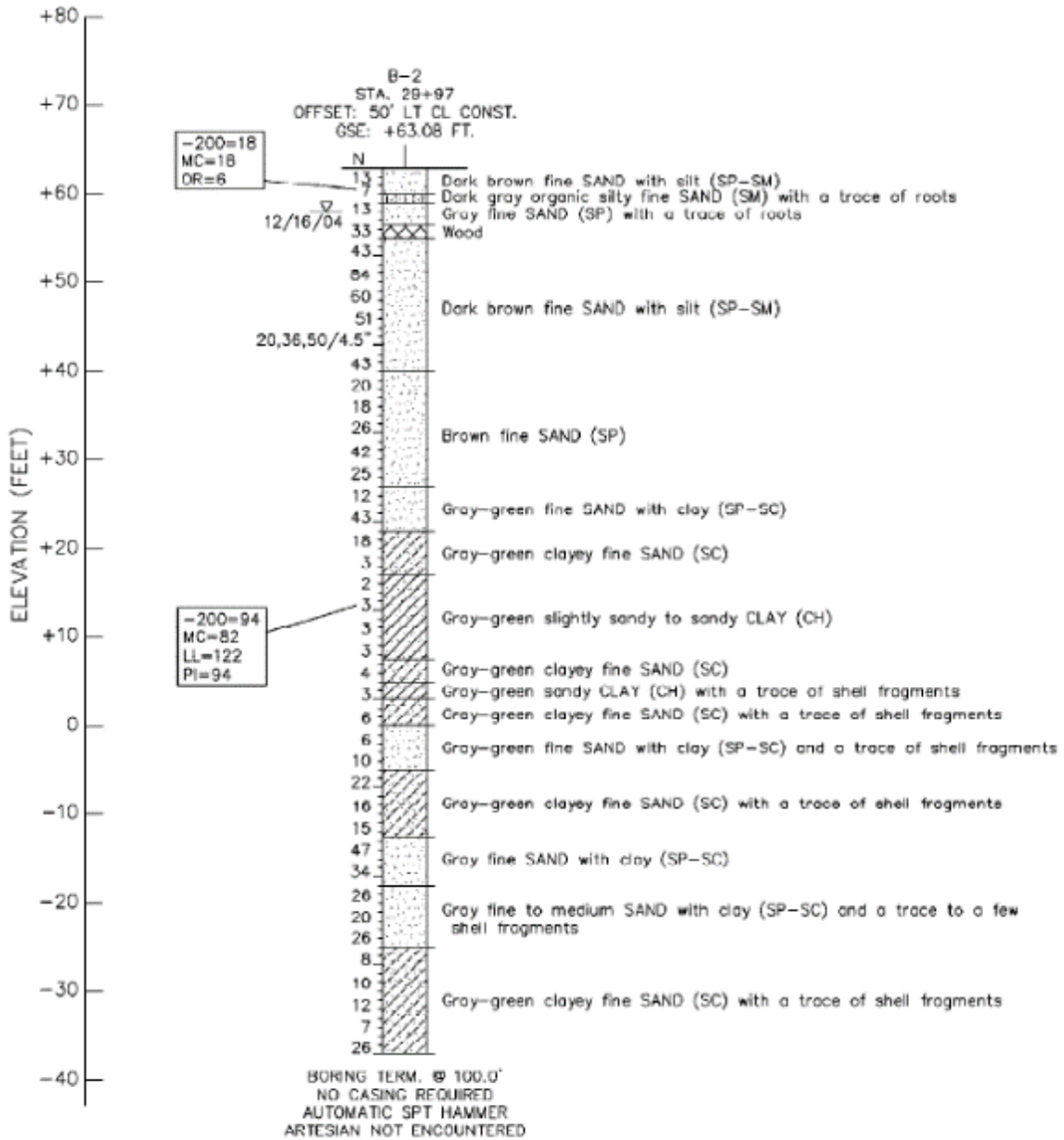


B.3.4.8.3. C.4.8.3. SPT TB-11 (P20P6)



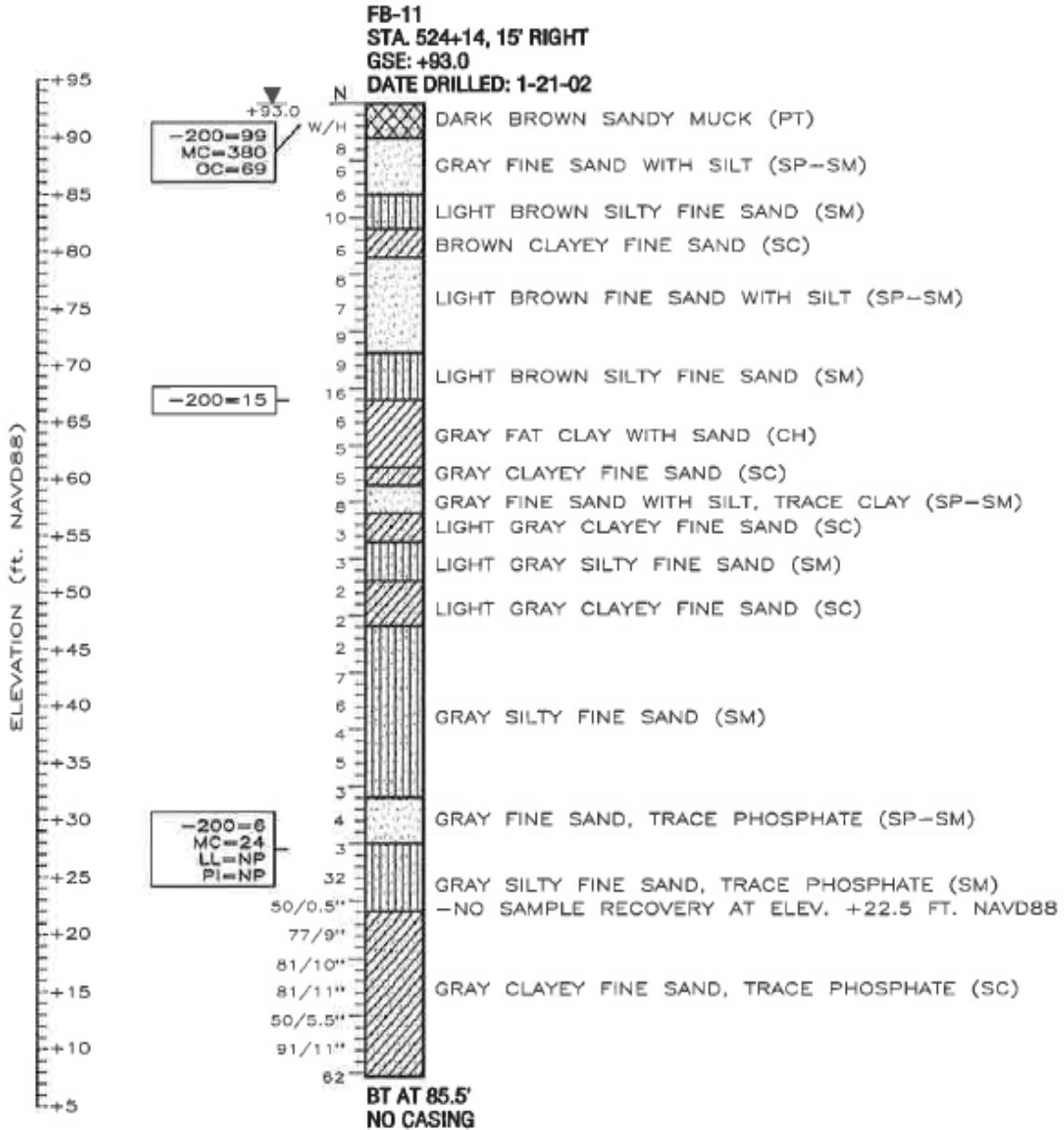
### B.3.4.9. C.4.9. I-10 and Chaff33 Road Overpass

#### B.3.4.9.1. C.4.9.1. SPT B-2 (P2P9)

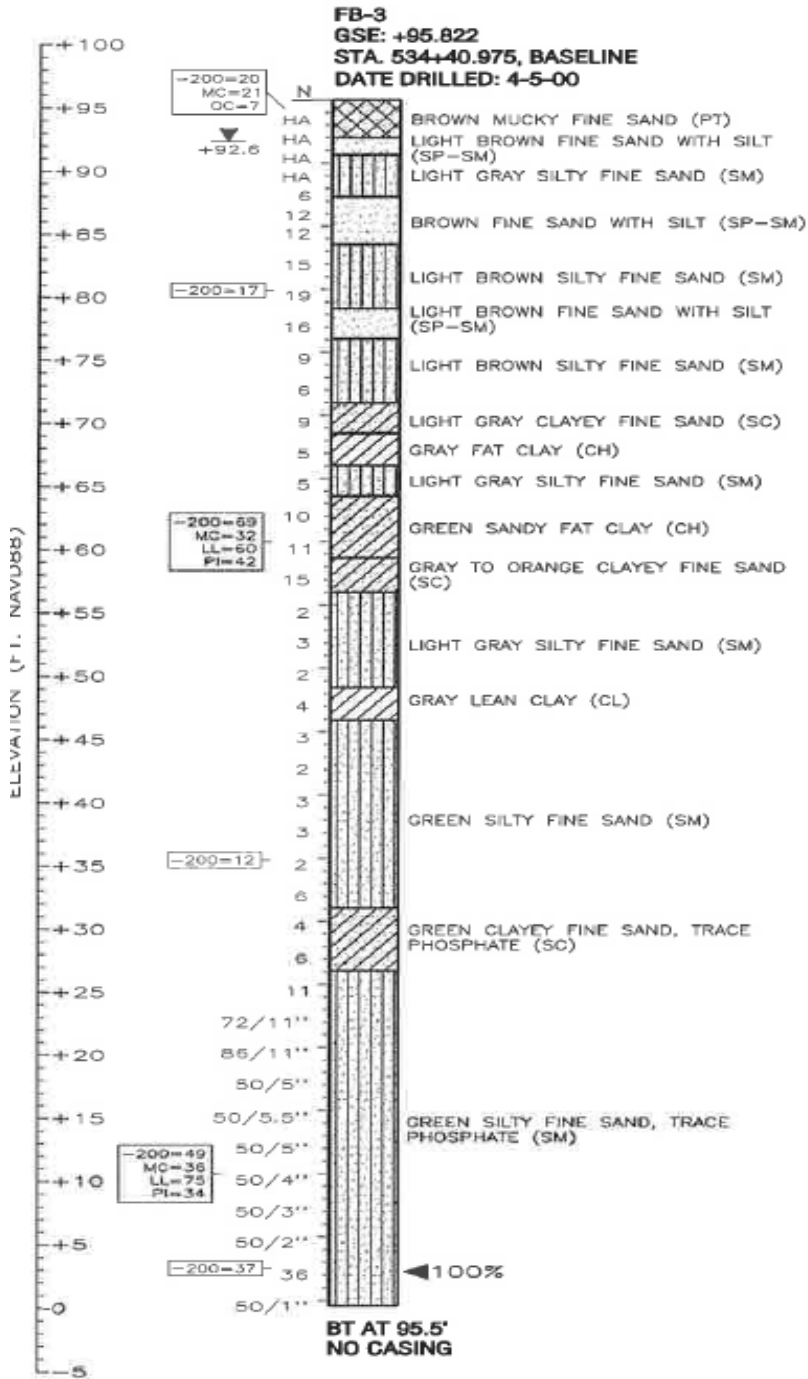


**B.3.4.10. C.4.10. I-4 and John Young Parkway**

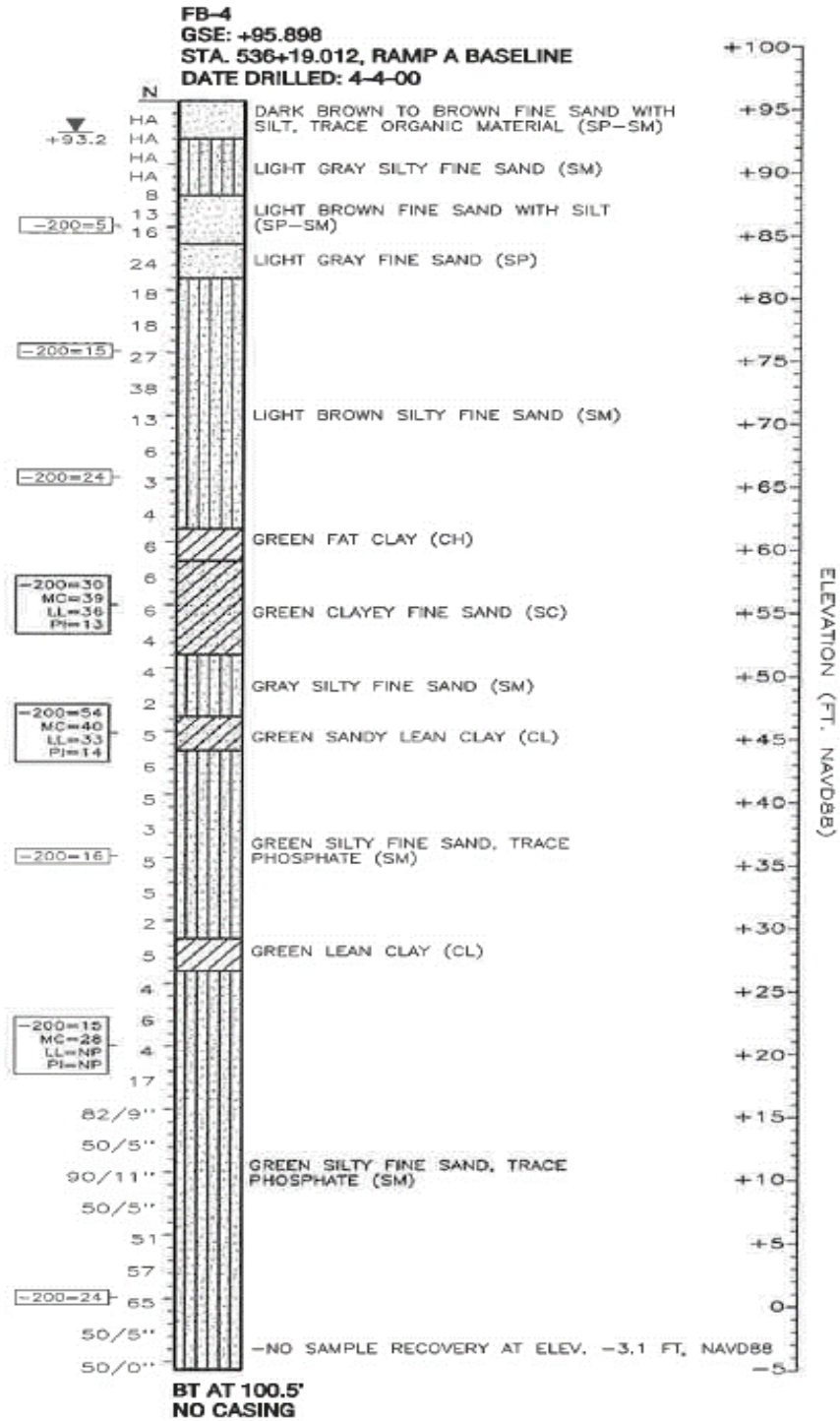
**B.3.4.10.1. C.4.10.1. SPT FB-11 (Ramp A P2P1)**



B.3.4.10.2. C.4.10.2. SPT FB-3 (Ramp A P9P12)

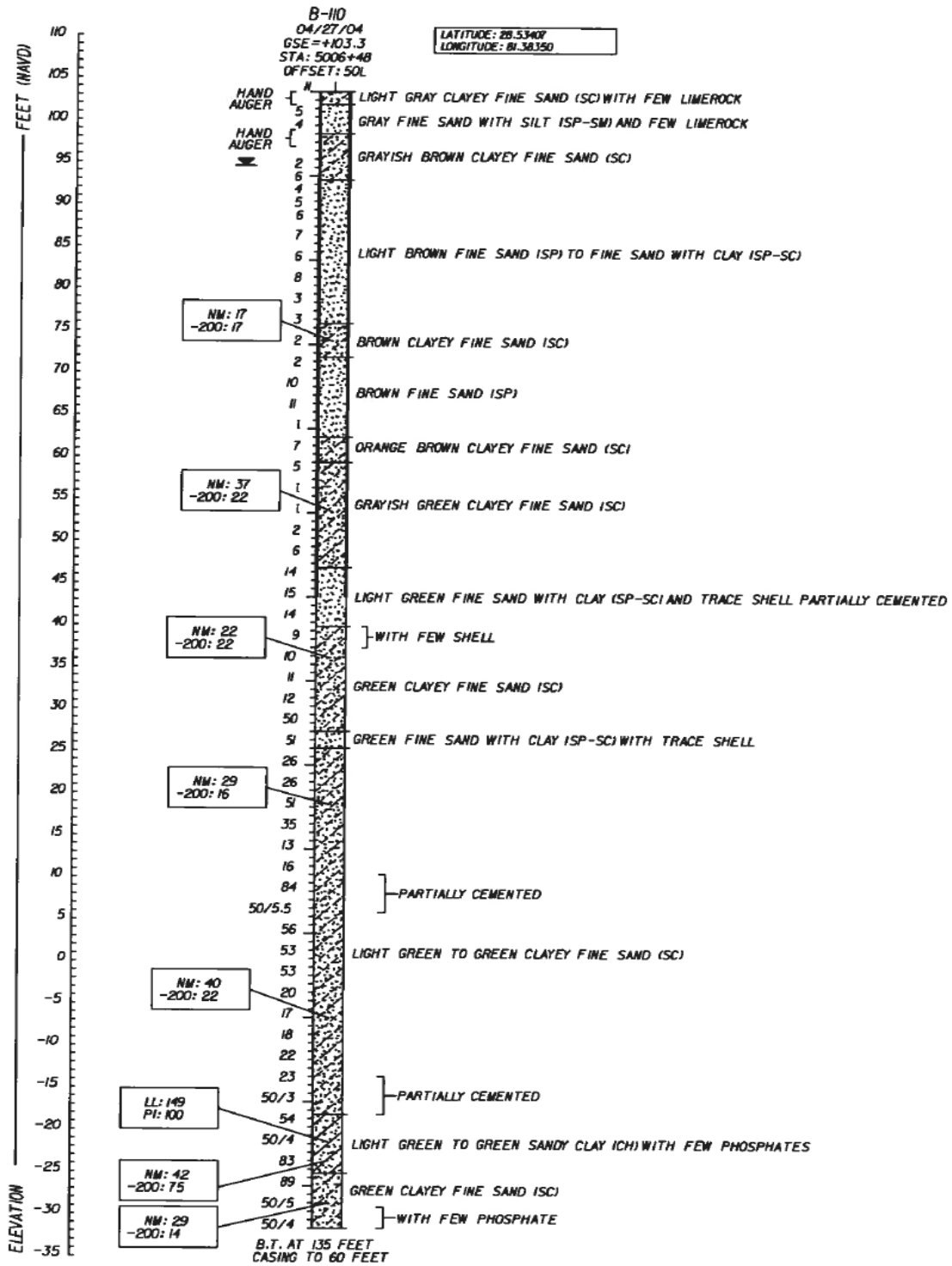


B.3.4.10.3. C.4.10.3. SPT FB-4 (Ramp A P10P14)



B.3.4.11. C.4.11. I-4 and SR-408 Intersection

B.3.4.11.1. C.4.11.1. SPT B-110 (Ramp B5 P2P5)



# B.4. Test Pile Driving Logs

## B.4.1. I-4 / US-192 Interchange

### B.4.1.1. Test Pile EB1P3 (Ramp BD)

May 27 2005 8:59AM

H. W. Lochner

407-396-0055

p. 2

#### PILE DRIVING INFORMATION

TEST Pile

STATE PROJECT NO. 242531-1-52-01 DATE 5-26-05 STATION NO. B62+28.5  
 PILE SIZE 24" LENGTH 162' BENT/PIER NO. 1 PILE NO. 3  
 HAMMER TYPE ICE 120S RATED ENERGY 120K OPERATING RATE VARIOUS  
 TEMPLATE ELEV 94.77 MIN TIP ELEV 455.58 PILE CUTOFF ELEV 116.96  
 DRIVING CRITERIA P.D.A.

PILE CUSHION THICKNESS AND MATERIAL 9" PLYWOOD  
 HAMMER CUSHION THICKNESS AND MATERIAL 5" NYLON 2 1/2" (2 1/2" ALUM.)  
 WEATHER PLY CLOUD TEMP 85° START TIME 2:58 STOP TIME 7:14

#### PILE DATA

PAY ITEM NO. 455-143-5 WORK ORDER NO. \_\_\_\_\_  
 MANUFACTURED BY SCP B.M. ELEV. \_\_\_\_\_ GROUND ROD READ. \_\_\_\_\_  
 DATE CAST 1-29-05-RTT ROD READ. \_\_\_\_\_ PILE HEAD ROD READ \_\_\_\_\_  
2-7-05-X42 MANUFACTURER'S PILE NO. X40 H.I. \_\_\_\_\_ PILE HEAD ELEV. 167.77  
 PILE HEAD CHAMFER PLAN PILE TIP ELEV. -1.23  
 PILE TIP CHAMFER \_\_\_\_\_ GROUND ELEV. 55.0  
 PILE DRIVING INSPECTOR MEL PICQUET

SPICE EACH	CUTOFF TYPE CODE	POINT PROTECTOR	PREFORMED HOLE	PDA	PILE REDRIVE	ISOLATED DRIVING	EXTRACTION	30X SPICE	PILE TYPE CODE	BATTER	TOTAL PILE		PENETRATION	BUILD UP	
											FURNISHED	DRIVEN		AUTHORIZED	ACTUAL
X	X	X	X	X	X	X	X	X	X	XXX.XXX	XXX.XXX	XXX.XXX	XXX.XXX	XXX.XXX	XXX.XXX
											169.000	118.130	56.230		

NOTES: CONTR choice to furnish 169' TOTAL in lieu of 162' Authorized

Length - PLAN SH E-7 X40=80' X27=89'

① START DRIVE 2:58 ② adjust STROKE + ③ adjust STROKE - ④ stop change Pile

Cushion - RE Hook PDA Wires 2:29-3:50 Restrict ⑤ 1/2" rebound - 1" ⑥ STOP 4:16

Now Pile Cushion Move template out of way ⑦ Restrict 4:50 ⑧ stop side plates up splices 6:44 Restart Drive

⑨ stop 7:14 Good Pile Met Bearing

SIGNATURE OF INSPECTOR: Mel Picquet

Bridge # 190194

PILE DRIVING LOG

TEST PILE EB-1 (3) Pile

Depth	Blows	Stroke/Pressure	Note No.	Depth	Blows	Stroke/Pressure	Note No.	Depth	Blows	Stroke/Pressure	Note No.	Depth	Blows	Stroke/Pressure	Note No.
1				34	52	7.0	(2)	67	48	6.9	(5)	100			
2				35	44	7.4		68	59	6.6		101			
3				36	41	7.2		69	87	6.5		102			
4				37	41	7.0		70	73	6.6		103			
5				38	34	6.9		71	79	6.8		104			
6				39	31	6.8		72	142	6.6		105			
7				40	36	6.8		73 <sup>37</sup>	178	8.3	(7)	106			
8				41	27	6.7		74	109	6.8	(5)	107			
9				42	24	6.7		75	127	6.9		108			
10				43	24	6.7		76	103	7.7		109			
11				44	25	6.7		77	79	7.8		110			
12				45	29	6.8		78	70	7.8		111			
13				46	29	6.8		79	241	6.5	(8)	112			
14				47	27	6.8		80	255	6.7	(10)	113			
15				48	23	6.8		81	76	8.6		114			
16				49	32	6.8		82	65	8.4		115			
17				50	38	6.9		83	51	8.5		116			
18				51	38	7.1		84	51	8.3		117			
19				52	41	7.1		85	49	8.2		118			
20				53	37	7.2		86	46	8.3		119			
21				54	40	7.2	(3)	87	47	8.3		120			
22				55	37	7.2		88	45	8.3		121			
23				56	38	7.1		89	47	8.3		122			
24				57	42	6.9		90	44	8.3		123			
25				58	39	6.8		91	43	8.3		124			
26	2		(1)	59	40	6.8		92	47	8.3		125			
27	12	7.5		60	35	6.9		93	60	8.4		126			
28	20	7.0		61	38	6.9	(4)	94	130	8.2		127			
29	32	6.9		62	38	7.6		95	103	8.0		128			
30	40	7.1		63	38	7.3		96	124	8.0	(9)	129			
31	51	7.0		64	36	7.4	(5)	97				130			
32	55	7.0		65	38	7.5		98				131			
	49	7.0		66	34	7.2		99				132			

B.4.1.2. D.1.2. Test Pile P7P10 (Ramp CA)

PILE DRIVING INFORMATION

TEST PILE

FIN PROJ. ID # 242531-1-52-01 DATE 9-14-05 STATION NO. 1046+19  
 PILE SIZE 24" LENGTH 116' BENT/PIER NO. 7 PILE NO. 10  
 HAMMER TYPE JCF-120F RATED ENERGY 120,000 OPERATING RATE VARIES  
 TEMPLATE ELEV 94.56 MAIN TIP ELEV 455-6.8 PILE CUTOFF ELEV 77.00  
 DRIVING CRITERIA \_\_\_\_\_

PILE CUSHION THICKNESS AND MATERIAL 9' plywood  
 HAMMER CUSHION THICKNESS AND MATERIAL 5" compressed ceramic fiber / Adv  
 WEATHER clear TEMP 87° START TIME 9:26AM STOP TIME \_\_\_\_\_

PILE DATA

PAY ITEM NO. 455-143-5 WORK ORDER NO. \_\_\_\_\_  
 MANUFACTURED BY S.C.P B.M. ELEV 92.12 GROUND ROD READ \_\_\_\_\_  
 DATE CAST \_\_\_\_\_ ROD READ +10.26 PILE HEAD ROD READ \_\_\_\_\_  
 MANUFACTURER'S PILE NO. X- H.I. 101.18 PILE HEAD ELEV. \_\_\_\_\_  
 PILE HEAD CHAMFER PLAN PILE TIP ELEV. \_\_\_\_\_  
 PILE TIP CHAMFER \_\_\_\_\_ GROUND ELEV. \_\_\_\_\_  
 PILE DRIVING INSPECTOR GLEN TRUESDALE

SPACE EACH	CUTOFF TYPE CODE	PREFORMED HOLE	PCA	PILE REMOVE	ISOLATED DRIVING	EXTRACTOR	PILE TYPE CODE	BATTER	TOTAL PILE		PENETRATION	BUILD UP	
									FURNISHED	DRIVEN		AUTHORIZED	ACTUAL
	1	1	1				1		116.600				

NOTES: PRE FORMED HOLE +55.0 (1) STARTER DRIVING AT 9:26AM  
(2) STOPPED DRIVING 9:57AM, TO CHANGE PILE CUSHION. STARTER RUNNING WITH  
980 TONS BLANK. (3) CONTINUED DRIVING AT 10:58AM (WITH A.C.A.)  
(4) STOPPED DRIVING AT 11:35AM, CHANGE PILE CUSHION. (5) CONTINUED DRIVING  
AT 11:03PM (6) STOPPED DRIVING AT 11:28PM, CHANGE PILE CUSHION.  
(7) CONTINUED DRIVING AT 2:15PM. (8) STOPPED DRIVING AT 2:25PM CHANGE PILE CUSHION  
(9) CONTINUED DRIVING AT 2:53PM. (10) CONTINUED DRIVING AT 3:24PM  
 SIGNATURE OF INSPECTOR: Glen Truesdale  
(11) STOPPED AT 3:20PM, TO MAKE SNOT MARKS. (12) EMPLOYER DRIVING AT 3:37PM  
AT THE 101.003 MARK. TO 1ST. SNOT COIT 26 BLOWS WITH A 9.2 STAKE.  
 NOTE: MANTY BIRLOTT, WITH G.R.L. CALL PILE GOOD.

PILE TEST PILE

77.0 NT 66

### PILE DRIVING LOG

Depth	Blows	Penetration	Notes												
				4	55	8.6		7	48	7.6		100	80	7.3	ⓐ
				5	42	8.6		8	48	7.7		100	80	7.3	ⓐ
				6	42	8.5		9	51	7.9		8	126	8.1	ⓐ
				7	39	8.4		70	42	7.6		3			ⓐ
				8	37	8.2		1	49	7.8		4			
				9	36	7.6		2	51	7.0		5			
				40	42	7.5		3	58	6.8	1/4"	6			
				1	36	7.2		4	49	7.1	1/4"	7			
				2	37	7.0		75	72	6.9	1/4"	8			
				3	35	7.0		6	82	6.8	1/4"	9			
10				4	41	6.7		7	102	6.7	1/2"	110			
				5	54	6.2		8	126	6.3	1/2"	1			
				6	54	6.4		9	136	7.3	1/4"	2			
				7	49	6.7		80	143	7.3	1/4"	3			
15				8	51	6.4		1	111	8.0	1/4"	4			
	26	8.0	ⓐ	9	50	6.6		2	154	7.3	1/2"	5			
	48	7.9		50	50	6.7		3	121	7.7	1/2"	116			
	63	8.0		1	55	6.5		4	120	7.6	3/4"				
	67	8.4		2	60	6.1		85	250	6.6	1/2"				ⓐ - Stanton Driving
20	87	7.7		3	50	6.8		6	109	7.7	ⓐ				9:26 AM on 7-11-07
	56	8.4		4	52	6.8		7	110	7.5	1/4"				ⓐ - Stopped AT 7:52 PM
	92	8.7		5	40	7.4		8	85	7.8	1/4"				Ta. Bays for 1.000
	91	9.4		6	43	7.6		9	69	7.9	1/4"				Stanton Driving
	80	9.1		7	41	7.6		90	60	7.9	1/4"				only 988 blows
25	89	9.2		8	41	7.0		1	58	7.8	1/4"				ⓐ - continuation driving
	56	9.2		9	50	6.6		2	75	7.0	1/4"				AT 10:58 AM with
	64	9.1		60	59	6.7	ⓐ	3	73	7.0	1/4"				G.A.L. P.O.R.
	61	9.8		1	64	7.0	ⓐ	4	72	7.0	1/4"				ⓐ - Stopped Driving
	61	8.8	ⓐ	2	59	6.5		95	74	6.9					AT 11:27 AM, alloy
30	113	7.9	ⓐ	3	63	6.3		6	88	7.0					pile driving
	1	77	8.2	4	46	7.0		7	88	7.0					ⓐ - continuation driving
	2	75	8.3	5	60	6.8		8	89	7.2					AT 11:03 PM
	3	67	8.4	6	46	7.2		9	78	7.2	ⓐ				ⓐ - Stanton Driving

ⓐ - continuation driving AT 2:16 PM  
 ⓐ - stopped AT 2:25 PM, alloy condition

(7' 1.19 PM) 1:28 PM alloy pile 1.25

B.4.1.3. D.1.3. Test Pile P8P4 (Ramp CA)

**PILE DRIVING INFORMATION**

FIN PROJ. ID# 242531-1.52-01 DATE 8/19/1 STATION NO. 1048+00  
 PILE SIZE 24" LENGTH 96' BENT/PIER NO. 8 PILE NO. 4  
 HAMMER TYPE ICE-1205 RATED ENERGY 120,000 OPERATING RATE VARIABLES  
 TEMPLATE ELEV. 88.11 MAIN TIP ELEV 4551.5.8 PILE CUTOFF ELEV 82.00  
 DRIVING CRITERIA 100 Blows P/FT 2 FT 8' STAKE  
 PILE CUSHION THICKNESS AND MATERIAL 9" ply wood  
 HAMMER CUSHION THICKNESS AND MATERIAL 5" COMPRESSED CERAMIC FIBER / ALUM.  
 WEATHER P/Cloudy TEMP 96 START TIME 1:45 STOP TIME 6:05 PM

**PILE DATA**

PAY ITEM NO. 455-24.5 WORK ORDER NO. \_\_\_\_\_  
 MANUFACTURED BY S.C.P B.M. ELEV \_\_\_\_\_ GROUND ROD READ \_\_\_\_\_  
 DATE CAST \_\_\_\_\_ ROD READ \_\_\_\_\_ PILE HEAD ROD READ \_\_\_\_\_  
 MANUFACTURER'S PILE NO. X H.I. \_\_\_\_\_ PILE HEAD ELEV. 91.11  
 PILE HEAD CHAMFER 3 planes PILE TIP ELEV. -4.89  
 PILE TIP CHAMFER \_\_\_\_\_ GROUND ELEV. 90.84  
 PILE DRIVING INSPECTOR M.A. SHALLOTT: HADDAY

SPICE EACH	CUTOFF TYPE CODE	PREFORMED HOLE	PDA	PILE REDRIVE	ISOLATED DRIVING	EXTRACTION	PILE TYPE CODE	BATTER	TOTAL PILE		PENETRATION	BUILD UP	
									FURNISHED	DRIVEN		AUTHORIZED	ACTUAL
	1	1	1						96	86.89	59.89		

NOTES: PREFORMED HOLE + 55  
 (1) START AT 1:45 PM (2) STOP AT 1:40 PLACED PDA GAUGES  
 (3) START AT 2:22 PM (4) STOP CHANGE CUSHION AT 2:59 PM  
 (5) START AT 3:42 PM (6) START REBOUNDS AT 64' MARK ON PILE  
 (7) STOP CHANGE CUSHION AT 4:07 PM (8) START AT 4:22 PM  
 (9) STOP CHANGE CUSHION AT 5:08 (10) START AT 5:37 PM (11) STOP  
 REBOUNDS AT 82' (12) STOP AT 5:30 MOVED PDA GAUGE (13) START AT 5:56 PM  
 SIGNATURE OF INSPECTOR: STOP AT 6:08 GOOD PILE M.A. SHALLOTT: HADDAY

### PILE DRIVING LOG

Depth	Time	Pressure	Temp	Depth	Time	Pressure	Temp	Depth	Time	Pressure	Temp	Notes
1				24	40	7.0		67	89	6.8	3/4	
				25	35	7.1		68	104	7.3		
				26	32	7.0		69	95	7.5		
				27	31	6.9		70	89	8.1		
5				38	31	7.0		71	102	8.1		
				39	29	7.0		72	132	7.3		
				40	32	7.1		73	164	6.5	(7)	
				41	30	7.1		74	135	7.5	(8)	
				42	34	7.1		75	175	7.4		
10				43	30	7.1		76	135	8.0		
11				44	33	7.1		77	85	8.5		
12				45	35	7.1		78	74	8.3		
13	↓			46	36	7.1		79	115	7.9		
14	9	6.5	(1)	47	39	7.2		80	203	6.8	(9)	
15	12	6.7		48	40	7.2		81	78	8.0	(10)	
16	11	6.7		49	38	7.3		82	75	8.0	(11)	
17	15	6.8		50	42	7.3		83	79	8.1		
18	18	6.9	(2)	51	36	7.2		84	79	8.2		
19	17	6.4	(3)	52	37	7.3		85	67	8.7		
20	23	6.7		53	34	7.4		86	52	8.8		
21	24	6.3		54	36	7.3		87	49	8.9		
22	28	6.9		55	40	7.3		88	59	8.8		
23	31	7.0		56	36	7.4		89	62	8.6		
24	32	7.1		57	38	7.0		90	88	8.6	(12)	
25	40	7.1		58	37	7.4		91	88	8.3	(13)	
26	40	7.1		59	39	7.1		92	102	8.3		
27	48	7.0		60	33	7.3	(4)	93	114	8.2	(14)	
28	50	7.2		61	51	7.1	(5)	94				
29	47	7.2		62	49	6.2		95				
30	50	7.1		63	46	7.2		96				
31	44	7.3		64	51	7.0	(6)					
32	44	7.1		65	57	6.9	↓					
33	44	6.8		66	47	6.9	↓					

**B.4.1.4. D.1.4. Test Pile P2P8 (Ramp D2)**

**PILE DRIVING INFORMATION**

STATE PROJECT NO. 242531-1-52-01 DATE 6/6/05 STATION NO. 2024+61.8  
 PILE SIZE 24" LENGTH 100 ~~EDM~~ / PIER NO. 2 PILE NO. 8  
 HAMMER TYPE ICE 120S RATED ENERGY 120 K OPERATING RATE VARIABLES  
 TEMPLATE ELEV 93.83 MIN TIP ELEV. 455.58 PILE CUTOFF ELEV 87.0  
 DRIVING CRITERIA \_\_\_\_\_

PILE CUSHION THICKNESS AND MATERIAL 9" PLYWOOD  
 HAMMER CUSHION THICKNESS AND MATERIAL 5" NYLON  
 WEATHER CLOUDY TEMP 78° START TIME 7:58 STOP TIME 8:10 PM 6/10:55 AM

**PILE DATA**  
 PAY ITEM NO. 455-34-5 WORK ORDER NO. \_\_\_\_\_  
 MANUFACTURED BY \_\_\_\_\_ B.M. ELEV 90.3 GROUND ROD READ. 419  
 DATE CAST 3/26/05 ROD READ. 5.68 PILE HEAD ROD READ \_\_\_\_\_  
 MANUFACTURER'S PILE NO. X70 H.I. 95.99 PILE HEAD ELEV. \_\_\_\_\_  
 PILE HEAD CHAMFER PLAN PILE TIP ELEV. \_\_\_\_\_  
 PILE TIP CHAMFER \_\_\_\_\_ GROUND ELEV. 91.8  
 PILE DRIVING INSPECTOR \_\_\_\_\_

SPICE EACH	CUTOFF TYPE CODE	POINT PROTECTOR	PREFORMED HOLE	POA	PILE REDRIVE	ISOLATED DRIVING	EXTRACTION	30% SPLICE	PILE TYPE CODE	BATTER	TOTAL PILE		PENETRATION	BUILD UP	
											FURNISHED	DRIVEN		AUTHORIZED	ACTUAL
X	X	X	X	X	X	X	X	X	X	XXX.XXX	XXX.XXX	XXX.XXX	XXX.XXX	XXX.XXX	XXX.XXX

NOTES: PREDRILL TO ELEV +45  
① START AT 7:58 PM ② STOP AT 8:10 PM ③ START DRIVING WITH PDA AT 10:55 AM 6/7/05 ④ STOP AT 11:18 CHACK PDA GAUGE ⑤ START AT 11:24 AM ⑥ STOP AT 11:27 AM CHACK PDA GAUGE ⑦ START AT 11:36 AM ⑧ STOP CHANGE CUSHION ⑨ START AT 12:20 PM ⑩ STOP AT 12:48 PM  
NO BEARING WILL BACK TO PILE: AFTER DRIVING REST OF THE PILE.  
 SIGNATURE OF INSPECTOR: Redrive 112 79 blows / 3/4 inch

PILE DRIVING LOG

Depth	Blows	Stroke/Pressure	Note No.	Depth	Blows	Stroke/Pressure	Note No.	Depth	Blows	Stroke/Pressure	Note No.	Depth	Blows	Stroke/Pressure	Note No.
1				34				67	31	7.7		100			
				35				68	25	7.8					
				36	18	6.6	①	69	27	7.8					
				37	23	6.7		70	25	7.7					
5				38	23	6.7		71	27	7.6					
				39	22	6.7		72	29	7.5					
				40	28	6.6		73	40	7.1	④				
				41	27	6.6		74	35	7.6	⑤				
				42	23	6.6		75	38	7.5	⑥				
10				43	25	6.6		76	41	7.7	⑦				
				44	30	6.6		77	63	7.1					
				45	29	6.6		78	79	7.2					
				46	31	6.7		79	71	7.3					
				47	33	6.7		80	77	7.1					
15				48	34	6.7		81	90	7.3					
				49	40	6.8		82	108	7.2					
				50	42	6.8	②	83	145	7.1	81				
				51	49	6.6	③	84	90	7.2	8				
				52	42	7.2		85	155	6.8					
20				53	38	7.2		86	145	7.1					
				54	42	7.1		87	127	7.4					
				55	41	7.2		88	83	7.4					
				56	41	7.4		89	79	7.5					
				57	43	7.5		90	101	7.4					
25				58	50	7.7		91	79	7.4					
				59	45	7.6		92	86	7.4					
				60	44	7.6		93	71	7.5					
				61	42	7.5		94	68	7.5	10				
				62	41	7.6		95	194	7.5	11				
30				63	36	7.6		96							
				64	36	7.7		97							
				65	36	7.7		98							
33				66	32	7.7		99							

## **B.4.2. SR-417 and International Parkway**

### **B.4.2.1. Test Pile EB1P14**

No Log

From PDA File:

Reference Elevation = +81.03 feet

Estimated from SPT B-1:

GSE = 72.30 feet

### **B.4.2.2. Test Pile EB2P5**

No Log

From PDA File:

Reference Elevation = +77.45 feet

Estimated form SPT B-2:

GSE = 72.30 feet

### B.4.3. SR-50 and SR-436

#### B.4.3.1. Test Pile EB4P10

### PILE DRIVING INFORMATION

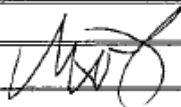
FIN PROJ. ID # 239203-2-52-01 DATE 7/25/08 STATION NO. 277+63.38  
 PILE SIZE 24x24 LENGTH 120 LF BENT PIER NO. 4EB PILE NO. 10  
 HAMMER TYPE AFE D62-22 RATED ENERGY 154,482 ft<sup>2</sup>/lb OPERATING RATE Variable  
 TEMPLATE ELEV 101.605 MAIN TIP ELEV +20 PILE CUTOFF ELEV 112.412  
 DRIVING CRITERIA PDA  
 PILE CUSHION THICKNESS AND MATERIAL 1 1/2" Plywood  
 HAMMER CUSHION THICKNESS AND MATERIAL 2" Con Best, 1 1/2" Aluminum  
 WEATHER Partly Cloudy TEMP 92°F START TIME 9:12A STOP TIME 9:37A

#### PILE DATA

PAY ITEM NO. 455-143-5 WORK ORDER NO. \_\_\_\_\_  
 MANUFACTURED BY S.C.P. B.M. ELEV 99.415 GROUND ROD READ 4.47  
 DATE CAST 11/8/07 ROD READ 3.85 PILE HEAD ROD READ 36.84 (taped, inverted read)  
 MANUFACTURER'S PILE NO. T-4 H.I. 103.265 PILE HEAD ELEV. 140.105  
 PILE HEAD CHAMFER 3" PILE TIP ELEV. +20.105  
 PILE TIP CHAMFER 3" GROUND ELEV. 98.795  
 PILE DRIVING INSPECTOR MARK FABISEK

SPICE EACH	CUTOFF TYPE CODE	PREFORMED HOLE	PDA	PILE REDRIVE	ISOLATED DRIVING	EXTRACTION	PILE TYPE CODE	BATTER	TOTAL PILE		PENETRATION	BUILD UP	
									FURNISHED	DRIVEN		AUTHORIZED	ACTUAL
0	1	1	1	0	0		1	-	120 LF	92.307	78.69	-	-

NOTES: ① 7/24/08: 7:54A - Begin auger pre-forming ~~at~~ 8:14am end pre-forming @ 21.33.795. ② Place pile in preformed hole 8:51am. ③ 7/25/08, 9:07A - 9:12A Begin driving pile ④ Stop driving 9:37A, Practical Refusal: 20+ Blows per inch.

SIGNATURE OF INSPECTOR: 

End Bent 4 East  
Pile 10

### PILE DRIVING LOG

9:07  
9:37 am

Depth	Blows	Stroke Pressure	Note No.	Depth	Blows	Stroke Pressure	Note No.	Depth	Blows	Stroke Pressure	Note No.	Depth	Blows	Stroke Pressure	Note No.
			①	58	25	5.44		91							
				59	23	5.91		92							
27			②	60	23	5.89		93							
28				61	21	5.80		94							
29	3	6.02	③	62	19	5.61		95							
30	3	6.66		63	22	5.69		96							
31	3	6.66		64	24	5.78		97							
32	5	5.68		65	25	6.01		98							
33	5	6.11		66	26	5.95		99							
34	14	4.35		67	26	5.81	↓ FS	100							
35	9	4.36		68	40	5.34		101							
36	10	4.42		69	43	5.72	↑	102							
37	10	4.62		70	40	6.04		103							
38	8	4.44		71	39	6.08		104							
39	8	4.40		72	35	6.19		105							
40	6	5.50		73	31	6.04		106							
41	9	4.44		74	28	5.83		107							
42	6	5.32		75	34	6.32		108							
43	13	4.28		76	41	6.39		109							
44	14	4.44		77	44	6.58		110							
45	11	5.20		78	34	6.55		111							
46	14	4.96		79	31	6.59	↓	112							
47	16	5.02		80	36	6.59		113							
48	15	5.01		81	57	6.56		114							
49	16	5.18		82	148 @ 6.02		↑ ⊕	115							
50	17	5.23		83			Practically refusal								
51	14	5.31		84											
52	16	5.27		85											
53	16	5.37		86											
54	18	5.11		87											
55	21	5.02		88											
56	19	5.10		89											
57	22	5.17		90											

↑ FS: Fuel Settings



Pier 3 East Banna  
Pile 10

### PILE DRIVING LOG

0 10:32  
10:36 10:37 11:04 11:19 11:21/4m

Depth	Blows	Stroke Pressure	Note No.	Depth	Blows	Stroke Pressure	Note No.	Depth	Blows	Stroke Pressure	Note No.	Depth	Blows	Stroke Pressure	Note No.
			①	58	23	5.97		91							
				59	23	6.18		92							
27				60	25	6.23		93							
28				61	32	6.16		94							
29				62	37	6.20		95							
30				63	32	6.48		96							
31				64	30	6.62		97							
32				65	32	6.59		98							
33	5	5.19	②	66	35	6.65		99							
34	6	5.26		67	45	6.79		100							
35	6	5.21		68	50	6.89									
36	5	4.13		69	50	7.02	↑ FS								
37	4	4.67		70	43	7.36	↑								
38	7	4.72		71	39	7.26									
39	5	4.48		72	28	7.10									
40	5	4.51		73	26	7.15									
41	4	4.43		74	31	7.32									
42	4	4.00		75	36	7.46									
43	5	4.48	③	76	42	7.61	→ min 1.5								
44	3	4.73		77	41	7.59									
45	6	4.86		78	39	7.61									
46	10	4.92		79	31	7.08									
47	12	5.71		80	35	6.84	↓								
48	15	5.02		81	60	7.10									
49	14	5.07		82	116	7.62	④	Practical Refusal Set Check		208 blows					
50	15	5.22		83				15 min 63 Blows @		5.28 strike					
51	14	5.41		84						81.6" total					
52	14	5.09		85											
53	13	5.37		86											
54	15	5.37		87											
55	22	5.40		88											
56	22	5.57		89											
57	26	5.72		90											

↑↓: Fuel Setting

# B.4.4. Heritage Parkway

## B.4.4.1. Test Pile EB1P1

Page No. 1 113-12-60-6322A 700-010-00  
Construction  
11/11

### PILE DRIVING INFORMATION

Structure Number: BOC-1

FIN PROJ. ID # 4283461-58-01 01-0-2012/BLM DATE 12/17/12 STATION NO. 62+05.85

PILE SIZE 18.0x18.0 ACTUAL/AUTH LENGTH 121.0 ft BENT/PIER NO. EB 1 PILE NO. 1

HAMMER TYPE APE 36-32 RATED ENERGY 83,875 ft lb OPERATING RATE 37-52 BPM

REF. ELEV SN 07041 (D19) +33.12 ft MIN. TIP ELEV -50.00 ft PILE CUTOFF ELEV +28.7 ft

DRIVING CRITERIA Test Pile - PDA by GRL (John Antarana) and Mahamud

PILE CUSHION THICKNESS AND MATERIAL 12 inches plywood

HAMMER CUSHION THICKNESS AND MATERIAL 2 inches nylon

WEATHER Pt cl TEMP 78°F START TIME 11:50 am STOP TIME 1:39 pm

### PILE DATA

PAY ITEM NO. \_\_\_\_\_ WORK ORDER NO. \_\_\_\_\_

MANUFACTURED BY Dura Stress T.B.M./B.M. ELEV +27.77 ft GROUND ROD READ \_\_\_\_\_

DATE CAST 11-14-12 ROD READ \_\_\_\_\_ PILE HEAD ROD READ \_\_\_\_\_

MANUFACTURER'S PILE NO. K7-5 H.I. \_\_\_\_\_ PILE HEAD ELEV. +30.87 ft

PILE HEAD CHAMFER 3.0 inches PILE TIP ELEV. +28.7 ft

PILE TIP CHAMFER 3.0 inches GROUND ELEV. +22.0 ft

QUALIFIED INSPECTOR'S NAME: James Dunaway TIN #: D 500-445-48

SPICE / EACH	PERFORMED HOLE	DYNAMIC LOAD TEST	PAY SET CHECK	NO PAY SET CHECK	REDRIVE	EXTRACTION	DRIVING OF SPICE	PILE TYPE CODE	BATTER	PILE LENGTH		EXTENSION / BUILD UP		
										ORIGINAL FURNISHED	TOTAL LENGTH WITH EXTENSION	PENETRATION BELOW GROUND	AUTHORIZED	ACTUAL
0	0	0	0	0	0	0	0	1	0	121.000	—	112.13 ft 41.88 ft	0	0

NOTES: 12/17/12 Predrilled 23 ft with 24 inch auger. 1) Pile set at 26.0 ft at ref,  
hammer cushion OK, New pile cushion, No hammer cut, Ref. = 33.12 ft, Start @ 11:50 am fs #1  
 2) Stop at 11:58 am to place PDA sensors, start @ 12:26 pm  
 3) Stop at 12:24 pm to change fs to #1, start @ 12:35 pm  
 4) Stop at 12:52 to remove partial template and for set checks. See next page

For Trainee experience evidence only:  
 Name of CTQP Trainee being supervised by the Qualified Inspector: \_\_\_\_\_  
 CTQP Trainee  
 I certify the Pile Driving Record accuracy and that the named above Trainee has observed the full pile installation:  
James Dunaway  
 Qualified Inspector (Signature)

### PILE DRIVING LOG

Structure No. <u>B0C-1</u>	Bent/Pier No. <u>EB1</u>	Pile No. <u>1</u>
----------------------------	--------------------------	-------------------

Depth	Blows	Stroke/ Pressure	Note No.	Depth	Blows	Stroke/ Pressure	Note No.	Depth	Blows	Stroke/ Pressure	Note No.	Depth	Blows	Stroke/ Pressure	Note No.
12	17	12		33	15	5.3		66	11	7.2		99	18	6.1	
1				34	7	4.9		67	9	7.2		100	22	6.3	
2				35				68	9	7.2		101	36	6.5	
3				36				69	9	6.9	#2	102	36	6.4	
4				37	↓			70	8	6.9		103	30	6.4	
5				38	1			71	10	6.5	#1, #3	104	25	6.4	
6				39	↓			72	13	5.5		105	24	6.4	
7				40	1			73	13	5.6		106	26	6.4	
8				41	↓			74	12	5.7		107	25	6.5	
9				42	2			75	12	5.7		108	26	6.5	
10				43	2			76	13	5.6		109	24	6.6	
11				44	2			77	13	5.7		110	26	6.6	
12				45	1			78	12	5.7		111	29	6.6	
13				46	1			79	12	5.6		112	32	6.7	
14				47	↓			80	13	5.6		113	36	6.8	#2
15				48	1			81	13	5.7		114	32	6.7	#2
16				49	3			82	14	5.7		115	36	6.8	
17				50	5	4.7		83	13	5.7		116	51	6.7	
18				51	5	4.4		84	12	5.7		117	42	6.6	
19				52	5	4.4		85	14	5.7		118	39	6.6	
20				53	6	4.6		86	13	5.8		119	36	6.6	
21				54	7	4.5		87	14	5.7		120	35	6.5	
22				55	12	5.3		88	14	5.7		121	36	6.6	
23				56	25	5.6		89	16	5.8		122	50	6.7	
24				57	26	5.7		90	23	6.1	#2	123	60	6.7	
25				58	19	6.0	#2	91	20	6.8	#2	124 <del>1000</del> F.O.D. 5:15 pm			
26	↓		6	59	31	6.1	#3	92	19	6.9		Set check			
27	17	5.9	#90	60	39	6.9	#3	93	19	7.0	#1	Top = +31.12 ft elev			
28	29	7.1		61	35	7.5		94	26	6.3		Tip = -89.88 ft elev.			
29	27	6.6		62	32	7.5		95	24	6.2		500 ± kips			
30	37	5.8		63	34	7.7		96	20	6.0		Set check 6			
31	37	5.6		64	31	7.9	#4	97	19	5.9		Top = +30.87 ft elev			
32	22	5.6		65	19	7.5		98	18	6.0		Tip = -90.13 ft elev.			

CO 20.0 ft

B.4.4.2. D.4.2. Test Pile B3P1

Page No. 1

113-12-60-6322A

700-010-60  
Construction  
11/11

**PILE DRIVING INFORMATION**

Structure Number: B0C-1

FIN PROJ. ID # 4283467-58-01 DATE 12-20-12 STATION NO. 63+25.85

PILE SIZE 18x18 ACTUAL/AUTH LENGTH 121.0 ft BENT/PIER NO. IB-3 PILE NO. 1

HAMMER TYPE APE 36-32 RATED ENERGY 83,875 ft.lbs. OPERATING RATE 37-52 BPM

REF. ELEV +21.75 ft MIN. TIP ELEV -50.0 ft PILE CUTOFF ELEV +28.1 ft

DRIVING CRITERIA Test Pile - PDA by GRL (Ryan Gissal)

PILE CUSHION THICKNESS AND MATERIAL 12 inches plywood

HAMMER CUSHION THICKNESS AND MATERIAL 2 inches nylon

WEATHER Pt Cl TEMP 81°F START TIME 2:01 pm STOP TIME 5:19 pm

**PILE DATA**

PAY ITEM NO. \_\_\_\_\_ WORK ORDER NO. \_\_\_\_\_

MANUFACTURED BY Dura Stress T.B.M./B.M. ELEV +24.77 ft GROUND ROD READ \_\_\_\_\_

DATE CAST 11/14/12 ROD READ \_\_\_\_\_ PILE HEAD ROD READ \_\_\_\_\_

MANUFACTURER'S PILE NO. KT-1 H.I. \_\_\_\_\_ PILE HEAD ELEV. +29.50 ft

PILE HEAD CHAMFER 30 inches PILE TIP ELEV. -91.50 ft

PILE TIP CHAMFER 3.0 inches GROUND ELEV. +9.0 Existing Plan = +7.0 ft ±

QUALIFIED INSPECTOR'S NAME: James Dunaway TIN #: D500 445 48

SPICE / EACH	PERFORMED HOLE	DYNAMIC LOAD TEST	PAY SET CHECK	NO PAY SET CHECK	REDRIVE	EXTRACTION	DRIVING OF SPLICE	PILE TYPE CODE	BATTER	PILE LENGTH		PENETRATION BELOW GROUND	EXTENSION / BUILD UP	
										ORIGINAL FURNISHED	TOTAL LENGTH WITH EXTENSION		AUTHORIZED	ACTUAL
0	1	0	0	0	0	0	0	1	0	121.000	—	84.0 ft	0	0

NOTES: 12/20/12 Predrilled 23 ft with 24 inch auger. 1) Pile set at 21.75 ft at ref. New pile cushion No hammer wt, Ref. = 21.75 ft, Start at 2:01 pm @ fs #1  
 2) Stop @ 60 blows until here @ 2:07 pm  
 3) Stop at 2:42 pm Set check: Start @ 1", 6 @ 2.1 2", 8 @ 7.1 3", 8 @ 6.9, 600 hits, stop 3:15  
 4) Stop at 3:26 pm for set check old pile cushion = 7.0 inches

For Trainee experience evidence only:  
Name of CTQP Trainee being supervised by the Qualified Inspector: \_\_\_\_\_

CTQP Trainee

I certify the Pile Driving Record accuracy and that the named above Trainee has observed the full pile installation:

James Dunaway  
Qualified Inspector (Signature)

### PILE DRIVING LOG

Structure No. <u>BOC-1</u>	Bent/Pier No. <u>IB-3</u>	Pile No. <u>1</u>
----------------------------	---------------------------	-------------------

Depth	Blows	Stroke/ Pressure	Note No.	Depth	Blows	Stroke/ Pressure	Note No.	Depth	Blows	Stroke/ Pressure	Note No.	Depth	Blows	Stroke/ Pressure	Note No.
12	20	12		33	2			66	12	5.8		99	31	6.7	
1				34				67	9	5.9		100	35	6.8	
2				35	↓			68	13	5.8		101	36	6.8	
3				36	2			69	13	5.8		102	40	6.8	
4				37	2			70	14	5.9		103	36	6.9	
5				38	3	4.3		71	14	5.9		104	79	6.8	settle
6				39	6	5.6		72	28	5.9		105	63	6.6	
7				40	6	5.6		73	15	6.1		106	48	6.8	
8				41	7	5.5		74	15	6.1		107	46	6.7	
9				42	15	5.4	2								
10				43	31	5.5		75	9	6.1		108	43	6.7	
11				44	31	5.5		76	14	6.0		109	44	6.9	
12				45	34	5.5		77	15	6.0		110	53	6.9	
13				46	34	5.8		78	19	6.2		111	66	7.0	
14				47	53	5.8		79	22	6.3		112	51	6.8	
15				48	58	7.3	fs#2	80	24	6.3		113	36	6.7	4
16				49	48	6.9		81	23	6.3		113.35	set checked	5	3126
17				50	50	6.9		82	27	6.5			FOD		5118
18				51	51	7.1		83	31	6.5			Top 729.50	ft elev	
19				52	53	7.1		84	32	6.3			Tip 720	ft elev	
20				53	29	6.9		85	24	6.4			-91.50	ft elev	
21				54	17	6.7		86	22	6.2					
22				55	13	6.6	fs#1	87	19	6.3					
23				56	12	6.6		88	27	6.6					
24				57	13	6.5		89	36	7.0					
25				58	14	6.5		90	43	6.6					
26				59	13	6.8		91	43	6.1					
27				60	16	6.6		92	33	6.2					
28				61	17	6.1		93	33	6.1					
29				62	17	6.0		94	30	6.2					
30				63	18	6.0		95	30	6.3					
31	1			64	17	5.7		96	26	6.6					
32				65	15	5.8		97	29	6.6					
								98	29	6.7					

B.4.4.3. D.4.3. Test Pile EB5P1

Page No. 1

Palm Bay Parkway  
113-12-60-6322A

700-010-80  
Construction  
11/11

**PILE DRIVING INFORMATION**

Structure Number: BOC-1

FIN PROJ. ID # 428346-1-58-01 DATE 12/20/12 STATION NO. 64+45.85  
 PILE SIZE 18"x18" ACTUAL/AUTH LENGTH 121.0 ft BENT/PIER NO. EB-5 PILE NO. 1  
 HAMMER TYPE APF 36-32 RATED ENERGY 83,875 ft lbs OPERATING RATE 37-52 BPM  
 REF. ELEV +22.46 ft MIN. TIP ELEV -50.0 ft PILE CUTOFF ELEV 28.7 ft  
 DRIVING CRITERIA Test Pile - PDA by GRL (Ryan Gissal)

PILE CUSHION THICKNESS AND MATERIAL 12 inches plywood  
 HAMMER CUSHION THICKNESS AND MATERIAL 2 inches nylon  
 WEATHER PTCI TEMP 79°F START TIME 4:15 pm STOP TIME 5:30 pm

**PILE DATA**

PAY ITEM NO. \_\_\_\_\_ WORK ORDER NO. \_\_\_\_\_  
 MANUFACTURED BY Dura Stress T.B.M./B.M. ELEV +24.77 ft GROUND ROD READ \_\_\_\_\_  
 DATE CAST 11/14/12 ROD READ \_\_\_\_\_ PILE HEAD ROD READ \_\_\_\_\_  
 MANUFACTURER'S PILE NO. KT-4 H.I. \_\_\_\_\_ PILE HEAD ELEV. +39.61 ft  
 PILE HEAD CHAMFER 3.0 inches PILE TIP ELEV. -81.39 ft  
 PILE TIP CHAMFER 3.0 inches GROUND ELEV. +20.8 ft existing, Plan = +22.0 ft ±  
 QUALIFIED INSPECTOR'S NAME: James Dunaway TIN # D500 445 48

SPICE / EACH	PERFORMED HOLE	DYNAMIC LOAD TEST	PAY SET CHECK	NO PAY SET CHECK	REDRIVE	EXTRACTION	DRIVING OF SPLICE	PILE TYPE CODE	BATTER	PILE LENGTH		PENETRATION BELOW GROUND	EXTENSION / BUILD UP	
										ORIGINAL FURNISHED	TOTAL LENGTH WITH EXTENSION		AUTHORIZED	ACTUAL
0	0	0	0	0	0	0	0	1	0	121.000	-	102.19 ft	0	0

NOTES: 12/20/12, Predrilled 23 ft with 24 inch auger. 1) Pile set at 1933 ft at ref. +22.46 ft  
New pile cushion, No hammer wt, Start at 4:15 pm fs #1  
2) Stop 90 blows until 4:22 pm  
3) Stop at 4:58 pm Set check used cushion, after IB-3, Start at 5:29  
1" = 9 blows 7.0 2" = 9 blows 6.0 3" = 11 blows 6.9  
Stop at 5:30 pm, Old cushion = 7.25 inches. Top = +39.61 ft elev. Tip = -81.39 ft elev

For Trainee experience evidence only:  
 Name of CTQP Trainee being supervised by the Qualified Inspector: \_\_\_\_\_  
 CTQP Trainee

I certify the Pile Driving Record accuracy and that the named above Trainee has observed the full pile installation:  
James Dunaway  
 Qualified Inspector (Signature)

42834671-58-01 /  
103-12-60-6322A  
**PILE DRIVING LOG**

Structure No. <u>B06-1</u>	Bent/Pier No. <u>EB-5</u>	Pile No. <u>1</u>
----------------------------	---------------------------	-------------------

Depth	Blows	Stroke/ Pressure	Note No.												
12	20		12	33	3			66	15	5.5		99	31	6.7	
1				34	2			67	14	5.6		100	33	6.9	
2				35	4			68	14	5.6		101	37	6.9	
3				36	3			69	15	5.6		102	40	7.0	
4				37	↓			70	15	5.7		103	40	6.9	
5				38	1			71	17	5.8		103.5	18	5.8	4:58
6				39	2			72	18	5.8		104			700 blows
7				40	3	3.4		73	16	5.7		106		Top = 107.61 ft ele	
8				41	2			74	19	5.8		107		Tip = 81.39 ft ele	
9				42	5	5.8		75	20	5.9		108			
10				43	9	4.8		76	20	5.9		109			
11				44	15	5.5		77	19	5.9		110			
12				45	35	5.6	2 #2	78	21	5.9		111			
13				46	34	5.7		79	26	6.0		112			
14				47	31	5.7		80	30	6.2		113			
15				48	40	6.0		81	28	6.1		114			
16				49	53	5.8		82	29	6.2		114			
17				50	56	5.9		83	32	6.2					
18				51	61	5.9		84	34	6.3					
19				52	68	6.0		85	32	6.6					
20	8	4.9	1) 103	53	70	6.0		86	31	6.3					
21	8	5.6		54	48	5.9		87	26	6.5					
22	5	4.2		55	24	5.6		88	25	6.2					
23	3			56	17	5.5		89	30	6.5					
24	2			57	15	5.4		90	43	6.6					
25	↓			58	14	5.5		91	48	6.7					
26	↓			59	14	5.5		92	42	6.7					
27	1			60	13	5.8		93	36	6.6					
28	1			61	13	5.6		94	34	6.5					
29	1			62	13	5.6		95	34	6.6					
30	↓			63	12	5.6		96	34	6.6					
31	5			64	13	5.5		97	32	6.8					
32	4			65	15	5.5		98	32	6.7					

1.46  
5'

# B.4.5. Anderson Street Overpass

## B.4.5.1. Test Pile P6P5

### Anderson St. PILE DRIVING INFORMATIC

FIN PROJ. ID # 242484-2-52-01 DATE 10-27-06 STATION NO. 4613+22.27  
 PILE SIZE 24 in<sup>2</sup> LENGTH 124' BENT/PIER NO. 6 PILE NO. 5  
 HAMMER TYPE Dainag 062 RATED ENERGY 90,500 ft<sup>2</sup>/lb OPERATING RATE Variable  
 TEMPLATE ELEV 105.58 MAIN TIP ELEV 455.58 PILE CUTOFF ELEV 96.0  
 DRIVING CRITERIA P.D.A. - TEST PILE  
 PILE CUSHION THICKNESS AND MATERIAL 12" plywood - 16" plywood  
 HAMMER CUSHION THICKNESS AND MATERIAL 1" Miscarta, 1/2" Alum, 1/2" Alum  
 WEATHER Cloudy TEMP 88 START TIME 3:08 STOP TIME 3:30

PILE DATA  
 PAY ITEM NO. 465-143-5 WORK ORDER NO. N/A  
 MANUFACTURED BY Southern Conc. Products B.M. ELEV 105.08 GROUND ROD READ +3.00  
 DATE CAST 6-9-06 ROD READ +2.50 PILE HEAD ROD READ \_\_\_\_\_  
 MANUFACTURER'S PILE NO. CAI-10 H.I. 107.58 PILE HEAD ELEV. \_\_\_\_\_  
 PILE HEAD CHAMFER 3" PILE TIP ELEV. \_\_\_\_\_  
 PILE TIP CHAMFER 3" GROUND ELEV. 104.58  
 PILE DRIVING INSPECTOR Arnold Lord

SPICE No EACH	CUTOFF TYPE CODE	PREFORMED HOLE	P.O.A.	PILE REDRIVE	ISOLATED DRIVING	EXTRACTION	PILE TYPE CODE	BATTER	TOTAL PILE		PENETRATION	BUILD UP	
									FURNISHED	DRIVEN		AUTHORIZED	ACTUAL
1	0	0	1	0	0	0	0	0	124			0	0

- NOTES: ① Piled First 0-10 in pre-drill hole ② start @ 11:40  
 ③ Stopped @ 12:00 PM To add 62' splice. ④ start @ 2:40 PM  
 ⑤ Stopped @ 2:55 PM To Align the pile head and checking the splice.  
 ⑥ start @ 3:08 PM ⑦ Stopped @ 3:30 PM  
 ⑧ 10-30-06 set Check Start @ 8:40 AM  
 ⑨ 10-30-06 set Check Stopped @ 8:45 AM  
 ⑩ 10-30-06 start Driving @ 8:50 AM. ⑪ To stop stop @ 9:55 AM  
 SIGNATURE OF INSPECTOR: Arnold Lord **SCANNED**  
 ⑪ 10-30-06 stop Driving @ 9:55 AM  
 ⑫ 10-30-06 New 16" plywood pile cushion start @ 9:50 AM  
 ⑬ 10-30-06 stop @ 10:00 AM

HNTB  
 Doc#:

Anderson St.  
 Pier # 6  
 Pile # 5

### PILE DRIVING LOG

Depth	Blows	Stroke/Pressure	Note No.	Depth	Blows	Stroke/Pressure	Note No.	Depth	Blows	Stroke/Pressure	Note No.	Depth	Blows	Stroke/Pressure	Note No.
			①	40	20	6.14		73	11	6.78		100-1"	120	6.35	③
				41	17	6.13		74	11	6.74		103	m/3/4"	rebound	
			in predrill Hole	42	16	6.01		75	12	6.81		104	= 100-1"		
10				43	17	5.92		76	13	6.84		105			
11	5	5.62	②	44	14	5.86		77	14	6.85		106			
12	10	5.30		45	10	5.79	③	78	16	6.80		107			
13	15	5.29		46	11	5.59	④	79	14	6.81		108			
14	21	5.60		47	13	5.56		80	12	6.83		109			
15	23	5.79		48	13	5.47		81	14	6.85		110			
16	23	5.79		49	16	5.38		82	13	6.76					
17	22	5.75		50	16	6.27		83	13	6.73					
18	23	5.76		51	10	6.46		84	14	6.78					
19	23	5.72		52	8	6.43		85	12	6.68					
20	23	5.80		53	8	6.35		86	11	6.72					
21	26	5.77		54	8	6.50		87	12	6.55					
22	26	5.81		55	9	6.58		88	13	6.70					
23	27	5.87		56	8	6.49		89	15	6.85					
24	27	5.88		57	8	6.59		90	36	7.11					
25	26	6.04		58	10	6.52		91	52	7.01	1/4" rebound				
26	26	6.13		59	10	6.51		92	47	6.97	1/4" rebound				
27	27	6.10		60	10	6.51		93	45	6.91	1/2" rebound				
28	27	6.06		61	9	5.58	⑤	94	53	6.99	1/2" rebound				
29	27	6.01		62	12	6.62	⑥	95	111	6.75	1/2" rebound				
30	25	5.98		63	9	6.70		96	140	6.97	1/2" rebound				
31	24	6.01		64	13	6.69	96 1/2"	97	254	6.97	1" rebound	⑦			
32	23	6.06		65	10	6.69		98	10-30-06	Set Check					
33	22	6.06		66	11	6.66		99	Depth Blows	St. Note					
34	19	6.11		67	11	6.58		100	97-2'	13	7.81	⑧	⑨		
35	19	6.08		68	10	6.75		101	= 97'	17"					
36	20	6.10		69	10	6.78		102	156	6.48	⑩	⑪	1/2" rebound		
37	20	6.03		70	12	6.65		103	98	0'					
38	19	5.93		71	11	6.83		104	109	140	7.18	⑫	1/2" rebound		
39	20	6.10		72	10	6.83		105	106	200	7.27		3/4" rebound		

B.4.5.2. D.5.2. Test Pile P6P6

Anderson St. **PILE DRIVING INFORMATION**

FIN PROJ. ID # 242484-2-52-01 DATE 11-7-06 STATION NO. 4013+22.00  
 PILE SIZE 24 in LENGTH 110 BENT/PIER NO. 6 PILE NO. 6  
 HAMMER TYPE Delmag D62 RATED ENERGY 90,500 ft/lb OPERATING RATE Variable  
 TEMPLATE ELEV 107.08 MAIN TIP ELEV 455-5.8 PILE CUTOFF ELEV 96.0  
 DRIVING CRITERIA SEE ATTACHMENT Pg 166 - Instrumented Piling

---

PILE CUSHION THICKNESS AND MATERIAL 12" Plywood cap  
 HAMMER CUSHION THICKNESS AND MATERIAL 1/2" Alum 1" Microbars 1/2 Alum 1" comb  
 WEATHER Cloudy TEMP 85° START TIME 11-7-06 8:30 AM STOP TIME 4:10 pm  
11-8-06 7:50 AM 8:05 pm

PILE DATA  
 PAY ITEM NO. 455-34-5 WORK ORDER NO. N/A  
 MANUFACTURED BY Standard Concrete Products B.M. ELEV 105.025 GROUND ROD READ 5.00  
 DATE CAST 10-19-06 ROD READ 2.205 PILE HEAD ROD READ \_\_\_\_\_  
 MANUFACTURER'S PILE NO. CA1-74 H.I. 107.88 PILE HEAD ELEV. \_\_\_\_\_  
 PILE HEAD CHAMFER 3" PILE TIP ELEV. \_\_\_\_\_  
 PILE TIP CHAMFER 3" GROUND ELEV. 102.88

PILE DRIVING INSPECTOR Arnold Lord

SPRINKLE EACH	CUTOFF TYPE CODE	PREFORMED HOLE	PDA	PILE REDRIVE	ISOLATED DRIVING	EXTRACTION	PILE TYPE CODE	BATTER	TOTAL PILE		PENETRATION	BUILD UP	
									FURNISHED	DRIVEN		AUTHORIZED	ACTUAL
0	0	0	1	0	0	0	2	0	110			0	0

NOTES: Instrumented Piling  
 ① Placed First 0-19 in pre-drill hole.  
 ② Start @ 8:30 AM ③ Stopped @ 8:37 AM To Hook up the gauges.  
 ④ Start @ 9:10 AM ⑤ Stopped @ 9:35 AM To Remove Template  
 ⑥ Start @ 2:00 PM ⑦ Stopped @ 2:35 To change Pile Cushion  
 ⑧ Start @ 2:55 PM ⑨ Stopped @ 3:30 PM Ran out of fuel  
 ⑩ Start @ 4:00 PM ⑪ Stopped @ 4:10 PM.  
SET Check 11-8-06 ⑫ Start @ 8:50 AM ⑬ Stopped @ 8:55 AM  
 SIGNATURE OF INSPECTOR: Arnold Lord  
Set Check 11-8-06 ⑭ Start @ 8:05 AM ⑮ Stopped @ 8:05 AM

Anderson St.  
 Pier # 6 North Footing  
 Pile # 6

### PILE DRIVING LOG

Depth	Blows	Stroke/ Pressure	Note No.	Depth	Blows	Stroke/ Pressure	Note No.	Depth	Blows	Stroke/ Pressure	Note No.	Depth	Blows	Stroke/ Pressure	Note No.
0	Placed		①	49	10	5.61		82	27	6.22		Set Check			
	in prod. 11			50	5	6.79		83	27	6.26		11-8-06			
	↓ Hole			51	6	7.96		84	26	6.26		1" 10	6.90		
19				52	7	5.38		85	28	6.24		1" 10	6.68		
20	7	6.21	② FS #1	53	7	5.40		86	28	6.28					
21	7	5.65		54	6	6.52		87	29	6.18					
22	9	5.53		55	8	5.46		88	27	6.39					
23	7	5.59		56	9	5.48		89	26	6.30					
24	11	5.55		57	9	5.43		90	30	6.39					
25	11	5.64		58	9	5.45		91	32	6.45					
26	12	5.69		59	8	5.42		92	51	6.67	FS				
27	16	5.75		60	8	5.39		93	45	7.47	FS				
28	16	5.83		61	8	5.43		94	37	7.33					
29	16	5.85		62	8	5.45		95	21	7.26					
30	16	5.81	③	63	8	5.46		95.4	29	6.95					
31	16	5.82	④	64	9	5.44		96	95	7.00	FS#2				
32	18	5.82		65	9	5.54		97	98	7.74	FS#3				
33	17	5.84		66	9	5.63		98	85	8.19	FS#4				
34	17	5.83		67	10	5.58		99	85	8.03					
35	15	5.83		68	11	5.66		100	103	7.97					
36	16	5.83		69	11	5.74		101	110	7.96	FS#5				
37	15	5.85		70	11	5.78		102	109	7.98	FS#6				
38	16	5.85		71	13	5.69		103	123	7.88	FS#7				
39	17	6.78		72	16	5.64		103-10	243	7.06	FS#8				
40	18	5.84		73	14	5.83		104	13	7.39	FS#9				
41	16	5.87		74	14	5.80		105	141	7.22	FS#10				
42	18	5.83		75	12	5.92		106	365	7.01	FS#11				
43	20	5.88		76	17	6.04		107	157	7.90	FS#12				
44	20	5.96		77	21	6.11		108	105	8.33	FS#13				
45	18	5.92		78	24	6.14		109	8166	6.94	FS#14				
46	15	5.77		79	25	6.15		110	33	6.38	FS#15				
47	15	5.69		80	24	6.46		111	256	6.41	FS#16				
48	9	6.57		81	25	6.28									

# B.4.6. I-4 Widening Daytona

## B.4.6.1. Test Pile EB3-1, P5

Page No. 1/2

700-010-60  
Construction  
11/11

### PILE DRIVING INFORMATION

Structure Number: 790207 I-4 over Deer Crossing

FIN PROJ. ID # 408464-1-52-1 DATE 9-24-13 STATION NO. 1178+00  
 PILE SIZE 24" SQ ACTUAL/AUTH LENGTH 115' BENT/PIER NO. EB3-1 PILE NO. 5  
 HAMMER TYPE APE D-46-42 ~~SP-111#200605391~~ RATED ENERGY 114,109 FT/LBS OPERATING RATE VARIES  
 REF. ELEV +52.18 MIN. TIP ELEV -3 PILE CUTOFF ELEV +51.6  
 DRIVING CRITERIA TEST PILE

PILE CUSHION THICKNESS AND MATERIAL \_\_\_\_\_  
 HAMMER CUSHION THICKNESS AND MATERIAL 3 1/2" MICARTA 2X 1" ALUM 3 X 1/2"  
 WEATHER Cloudy TEMP 70° START TIME 9:43am STOP TIME 11:45am

#### PILE DATA

PAY ITEM NO. N/A WORK ORDER NO. N/A  
 MANUFACTURED BY DURASTRESS T.B.M./B.M. ELEV N/A GROUND ROD READ N/A  
 DATE CAST \_\_\_\_\_ ROD READ N/A PILE HEAD ROD READ N/A  
 MANUFACTURER'S PILE NO. H-18 H.I. N/A PILE HEAD ELEV. 65.18'  
 PILE HEAD CHAMFER 3/4" X 3" PILE TIP ELEV. -49.82'  
 PILE TIP CHAMFER 3/4" X 3" GROUND ELEV. +46.18'  
 QUALIFIED INSPECTOR'S NAME: Michael Harrington TIN # 465255860

SPICE / LEACH	PERFORMED HOLE	DYNAMIC LOAD TEST	PAY SET CHECK	NO PAY SET CHECK	REDRIVE	EXTRACTION	DRIVING OF SPLICE	PILE TYPE CODE	BATTER	PILE LENGTH		PENETRATION BELOW GROUND	EXTENSION / BUILD UP	
										ORIGINAL FURNISHED	TOTAL LENGTH WITH EXTENSION		AUTHORIZED	ACTUAL
0.00		1.00	0.00	0.00	0.00	0.00	0.00	1.0	0.000	115'	115'	96'	0.000	0.000

NOTES: ① Fuel setting # 1

② Fuel setting # 2

③ Fuel setting # 3

④ Fuel setting # 4

⑤ Start Driving

⑥ Stop Driving

⑦ Stopped to hook up PDA gauges @ 9:55am - 10:20am

⑧ Stopped to change cushion

For Trainee experience evidence only:

Name of CTQP Trainee being supervised by the Qualified Inspector: \_\_\_\_\_

CTQP Trainee

I certify the Pile Driving Record accuracy and that the named above Trainee has observed the full pile installation:

Allen Hill

Qualified Inspector (Signature)

# PILE DRIVING LOG

Construct  
17

Structure No. 790207	Bent/Pier No. EB 3-1	Pile No. 5
----------------------	----------------------	------------

Depth	Blows	Stroke/Pressure	Note No.	Depth	Blows	Stroke/Pressure	Note No.	Depth	Blows	Stroke/Pressure	Note No.	Depth	Blows	Stroke/Pressure	Note No.
0-1				33-34	24	6.12	170psi	66-67	44	7.00	170psi	91-92	68	9.07	200psi
1-2				34-35	16	5.57	170psi	67-68	41	7.08	170psi	92-93	92	9.83	200psi
2-3				35-36	26	5.93	170psi	68-69	43	7.15	170psi	93-94	93	9.25	200psi
3-4				36-37	31	5.78	170psi	69-70	41	7.16	170psi				
4-5				37-38	73	5.04	170psi	70-71	36	7.11	170psi				
5-6				38-39	43	5.99	170psi	71-72	39	7.28	170psi				
6-7				39-40	54	5.96	170psi	72-73	40	7.28	170psi				
7-8				40-41	51	5.94	170psi	73-74	39	7.22	170psi				
8-9				41-42	64	5.92	170psi	74-75	40	6.74	170psi				
9-10				42-43	50	6.04	170psi	75-76	38	7.30	170psi				
10-11				43-44	51	6.80	170psi	76-77	49	7.25	170psi				
11-12				44-45	53	6.05	170psi	77-78	39	7.37	170psi				
12-13				45-46	36	6.34	170psi	78-79	60	7.44	170psi				
13-14				46-47	41	6.35	170psi	79-80	87	7.54	200psi				
14-15				47-48	43	6.20	170psi	80-81	72	8.16	200psi				
15-16				48-49	40	6.23	170psi	81-82	105	8.24	200psi				
16-17				49-50	46	6.23	170psi	82-83	92	8.47	200psi				
17-18				50-51	48	6.26	170psi	83-84	101	8.58	200psi				
18-19				51-52	47	6.34	170psi	84-85	37/85	8.27	200psi	84"			
19-20				52-53	53	6.41	170psi	85-86	84	8.21	200psi	1"	12	7.88	
20-21				53-54	51	6.44	170psi	86-87	75	8.30	200psi	2"	13	7.79	
21-22				54-55	56	6.52	170psi	87-88	61	8.26	200psi	3"	12	7.96	
22-23				55-56	45	6.94	190psi	88-89	61	8.22	200psi				
23-24				56-57	42	7.11	170psi	89-90	53	8.23	200psi				
24-25				57-58	47	7.12	170psi	90-91	50	8.27	200psi				
25-26				58-59	46	7.27	190psi	91-92	56	8.37	200psi				
26-27				59-60	43	7.28	170psi	92-93	55	8.52	200psi				
27-28				60-61	39	7.31	170psi	93-94	56	8.47	200psi				
28-29				61-62	34	7.38	170psi	94-95	53	8.53	200psi				
29-30				62-63	39	6.98	170psi	95-96	60	8.72	200psi				
30-31				63-64	42	6.77	170psi	96-97	59	8.21	200psi				
31-32				64-65	50	6.88	170psi	97-98	60	8.91	200psi				
32-33				65-66	45	7.61	170psi	98-99	52	8.94	200psi				

## **B.4.7. SR-83 over Ramsey Branch**

### **B.4.7.1. Test Pile EB1P1**

No Log

From PDA File:

Reference Elevation = +9.47 feet

Estimated from pre-construction survey:

GSE = +1.45 feet

B.4.7.2. D.7.2. Test Pile P4P5

Page No. 1

700-010-60  
 Constructor  
 6'2" 11/11"

**PILE DRIVING INFORMATION**

Structure Number: 600190

FIN PROJ. ID # 220679-1-52-01 DATE 10-7-13 STATION NO. 1427+94.80  
 PILE SIZE 24" ACTUAL/AUTH LENGTH 120 BENT/PIER NO. 4 PILE NO. 5  
 HAMMER TYPE PF 50-42 RATED ENERGY 124587 FT/LB OPERATING RATE \_\_\_\_\_  
 REF. ELEV +10.18 MIN. TIP ELEV -48 PILE CUTOFF ELEV +6.6  
 DRIVING CRITERIA TEST PILE PDA Replacement Test pile

PILE CUSHION THICKNESS AND MATERIAL 15" New Plywood  
 HAMMER CUSHION THICKNESS AND MATERIAL 3 1/2" 3-1/2" Aluminum Plates, 2-1" MICARTA PLATES  
 WEATHER PARTLY Cloudy TEMP 81° START TIME 4:12 PM STOP TIME 6:50 PM  
 10-7-13 10-7-13

**PILE DATA**

PAY ITEM NO. 0455143-5 WORK ORDER NO. \_\_\_\_\_  
 MANUFACTURED BY CDS Manufacturing T.B.M./B.M. ELEV 12.173 GROUND ROD READ 15.97  
 DATE CAST 10-3-13 ROD READ 3.78 PILE HEAD ROD READ 4.12  
 MANUFACTURER'S PILE NO. 45331 TP6 H.I. 15.97 PILE HEAD ELEV. +11.85  
 PILE HEAD CHAMFER 3" x 3/4" PILE TIP ELEV. -108.15  
 PILE TIP CHAMFER 3" x 3/4" GROUND ELEV. 0.0  
 QUALIFIED INSPECTOR'S NAME: Spence Moldovan TIN #: M43149758

SPICE / EACH	PERFORMED HOLE	DYNAMIC LOAD TEST	PAY SET CHECK	NO PAY SET CHECK	REDRIVE	EXTRACTION	DRIVING OF SPICE	PILE TYPE CODE	BATTER	PILE LENGTH		PENETRATION BELOW GROUND	EXTENSION / BUILD UP	
										ORIGINAL FURNISHED	TOTAL LENGTH WITH EXTENSION		AUTHORIZED	ACTUAL
0	52	0	0	2	0	0	0	1	0	120		108.15	0	0

NOTES: (A) Contractor Elected to predrill pilot hole on 10-4-13 starting at 9:20 AM ground elevation 0.4 ending at elevation -52 at 10:40 AM Contractor elected to ream and remove sediment from 12:20 PM to 12:40 PM Contractor reamed pilot hole & removed sediment from elevation -43 to -52 (B) Contractor received and unloaded pile from 10:00 AM to 10:30 AM 10-7-13. Note Pile is only 4 days old

For Trainee experience evidence only:

Name of CTQP Trainee being supervised by the Qualified Inspector: \_\_\_\_\_

CTQP Trainee

I certify the Pile Driving Record accuracy and that the named above Trainee has observed the full pile installation:

\_\_\_\_\_  
 Qualified Inspector (Signature)

### PILE DRIVING LOG

700-  
Construcción  
11/1

Structure No. <u>600190</u>	Bent/Pier No. <u>4</u>	Pile No. <u>5</u>
-----------------------------	------------------------	-------------------

Depth	Blows	Stroke/ Pressure	Note No.												
1		WOP		34	8	6.55	(3)	67	131	6.68	(9)	100	36	6.68	
2				35	13	6.36		68	110	6.88		101	40	6.68	
3				36	14	5.80		69	163	6.13	(10/11)	102	38	6.69	
4				37	16	5.58		70	106	5.96	(12)	103	40	6.75	
5				38	18	5.84		71	173	6.50	(13)	104	42	6.76	
6				39	20	5.49		72	183	6.67		105	40	7.03	
7				40	9	5.49		73	94	6.94	(14)(15)	106	37	7.09	
8				41	4	5.49		74	38	7.44	(16)	107	38	7.04	
9				42	4	5.19		75	33	7.23		108	44	7.00	
10				43	4	5.65		76	39	7.05	(17)	109	44	7.03	
11				44	8	5.71		77	41	7.07		110	44	7.24	
12				45	6	5.63		78	35	6.82		111	45	7.30	
13				46	6	5.67		79	38	6.79	(18)	112	41	7.19	
14				47	7	5.66		80	40	6.89		113	41	7.36	
15				48	10	5.62		81	41	6.94		114	40	7.27	
16				49	17	5.59		82	39	7.08		115	39	7.39	(20)
17				50	14	5.78		83	44	7.35		116	85	7.57	(21)
18				51	14	5.78	(4)	84	48	7.44		117	69	7.55	
19				52	8	6.82	(5)	85	59	7.61		118	70	7.46	(23)
20				53	8	5.78		86	71	7.66					
21				54	7	5.30		87	84	7.62					
22				55	7	6.80		88	77	7.71					
23				56	7	5.64		89	61	7.60					
24				57	8	5.66		90	52	7.54				First Set check	
25				58	11	5.72		91	46	7.55		1"	9	8.78	(21)
26				59	13	5.89		92	40	7.67		1/2"	4	8.78	
27				60	13	5.88	(6)	93	35	7.67				Second Set check	
28				61	27	6.31	(7)	94	32	7.67					
29				(62)	19	6.41		95	34	6.92	(19)	1"	4	8.09	(24)
30				63	37	6.26		96	31	6.80		2"	4	8.09	
31		WOP		64	41	6.06	(8)	97	39	6.70		1/2	2	8.09	
32		↓	(1)	65	104	5.95		98	39	6.68					
33		W.O.H	(2)	66	196	5.76		99	42	6.70					

Foot  
min  
115

At F mark 54 appeared pile shifted to the north east by approx 2" N.E.

<p>Ⓒ OBSERVATION SAG 1/8" BETWEEN COLLIES DURING HAULING NOTE SAG APPEARED APPROX 1" TO 1/2" NO OTHER BLEMISHES OR CRACKING WAS PRESENT DURING INSPECTION</p>
<p>Ⓓ CONTRACTOR PERFORMED OVER REMAINING OF PILE HOLE FROM 12:45 PM TO 12:58 PM ELEVATION 0.4 TO -52 NO RESISTANCE AUGERED HOLE RANGES FROM 20' - 52 FOOT MARK 62 TO -28 FOOT MARK 38 AND 22" FROM ELEV -28 FOOT MARK 38 TO 0 FOOT MARK 10</p>
<p>Ⓔ SET PILE 11:15 PM TO 1:45 PM</p>
<p>Ⓘ W.O.P FOOT MARK 0 TIP ELEVATION 0.00 TO FOOT MARK 32 ELEV -22</p>
<p>Ⓚ W.O.H + DRY FIRE FOOT MARK 32 ELEV -22 TO FOOT MARK 33 -23</p>
<p>Ⓛ STARTED DRIVING FUEL SETTING 1 AT 4:12 PM</p>
<p>Ⓜ STOPPED TO MAKE CONNECTION TO PDA GAUGES 4:16 PM</p>
<p>Ⓝ RESTARTED AT 4:25 PM</p>
<p>Ⓟ STOPPED AT 4:27 PM PROBLEMS WITH PDA SHORT GAUGE CONNECTION</p>
<p>Ⓠ START BACK AT 4:39 PM</p>
<p>Ⓡ 1/2" TO 3/4" REBOUND AT FOOT MARK 64</p>
<p>Ⓢ INCREASED TO FUEL SETTING 2 FOOT MARK 67</p>
<p>Ⓣ DECREASED TO FUEL SETTING 1 FOOT MARK 69</p>
<p>NOTE OBSERVATION OF WELD BROKE ON TOP PACKET AND PILE BINDING ON BOTTOM PACKET</p>
<p>Ⓤ STOPPED AT FOOT MARK 69 AT 4:56 PM ALSO CHANGED CUSHION CHANGE THICKNESS TO 18" NEW PLYWOOD OLD CUSHION FOUND TO BE 11 1/2" THICK NOTE</p>
<p>Ⓡ STARTED BACK 5:40 PM FUEL SETTING 1 69 TO 70</p>
<p>Ⓢ FUEL SETTING 2 AT FOOT MARK 70 TO 71</p>
<p>Ⓣ FUEL SETTING 3 AT FOOT MARK 72 TO 73</p>
<p>Ⓤ STOPPED AT 5:55 PM PACKET BROKE CONTRACTOR ELECTED TO REWELD FOOT MARK 73</p>
<p>Ⓡ RESTARTED AT 6:07 PM FUEL SETTING 3</p>
<p>Ⓢ BACK DOWN TO FUEL SETTING 2 FOOT MARK 75 TO 76</p>
<p>Ⓣ FOOT MARK 79 REBOUND IS GONE</p>
<p>Ⓤ FUEL SETTING 1 FOOT MARK 85 TO 95</p>
<p>Ⓡ STOPPED AT 6:50 PM FOOT MARK 115 ELEVATION -104.82 WILL SET CHECKS TO 8-13</p>

<p>21</p>	<p>10-8-13</p>	<p>Performed Set</p>	<p>Check from</p>	<p>9:35<sup>AM</sup></p>	<p>stopped at</p>	<p>9:36<sup>AM</sup></p>	
<p>22</p>	<p>Redrive</p>	<p>9:40<sup>AM</sup></p>	<p>Foot MARK</p>	<p>115</p>	<p>FUEL</p>	<p>Setting 1</p>	
<p>23</p>	<p>Stopped redrive</p>	<p>at 9:46<sup>AM</sup></p>	<p>ENDING redrive</p>	<p>with piston</p>	<p>Set</p>	<p>CHECK IN 1 hour</p>	<p>1100 KIP Tip 107.82 Stopping At 9:50<sup>AM</sup></p>
<p>24</p>	<p>Second Set</p>	<p>Check continued</p>	<p>at 11:25<sup>AM</sup></p>	<p>ENDING at</p>	<p>11:26<sup>AM</sup></p>	<p>2 1/2"</p>	

**B.4.7.3. D.7.3. Test Pile EB5P2**

Page No. 1

700-010-60  
Construction  
11/11

**PILE DRIVING INFORMATION**

Structure Number: 600190

FIN PROJ. ID# 220679-1-52-01 DATE 10-2-13 STATION NO. 1428+57.00 52' LGE  
 PILE SIZE 24" ACTUAL/AUTH LENGTH 95 <sup>TEST PILE</sup> END BENT/PIER NO. 5 PILE NO. 2  
 HAMMER TYPE APE 50-42 RATED ENERGY 124582 FT/LB OPERATING RATE \_\_\_\_\_  
 REF. ELEV. 11.37 MIN. TIP ELEV. NA PILE CUTOFF ELEV. 6.5  
 DRIVING CRITERIA TEST PILE - PDA

PILE CUSHION THICKNESS AND MATERIAL 15" NEW Plywood  
 HAMMER CUSHION THICKNESS AND MATERIAL 3 1/2" 3-1/2" Aluminum Plate, 2-1" MICARTA Plate  
 WEATHER Sunny TEMP 80 START TIME 9:07 AM STOP TIME 1:07 PM

**PILE DATA**

PAY ITEM NO. 455-143-5 WORK ORDER NO. \_\_\_\_\_  
 MANUFACTURED BY CDS Manufacturing T.B.M./B.M. ELEV. 12.713 GROUND ROD READ 7.013  
 DATE CAST 6-11-13 ROD READ 3.5 PILE HEAD ROD READ .213  
 MANUFACTURER'S PILE NO. TP-2 H.I. 16.213 PILE HEAD ELEV. +16  
 PILE HEAD CHAMFER 3" x 3/4" PILE TIP ELEV. -79  
 PILE TIP CHAMFER 3" x 3/4" GROUND ELEV. ORIGINAL 7.4 Backfilled to +9.2  
 QUALIFIED INSPECTOR'S NAME: Spence Moldovan TIN# 1M43149758

SPUCE / EACH	PERFORMED HOLE	DYNAMIC LOAD TEST	PAY SET CHECK	NO PAY SET CHECK	REDRIVE	EXTRACTION	DRIVING OF SPLICE	PILE TYPE CODE	BATTER	PILE LENGTH		PENETRATION BELOW GROUND	EXTENSION / BUILD UP	
										ORIGINAL FURNISHED	TOTAL LENGTH WITH EXTENSION		AUTHORIZED	ACTUAL
0	52	⊕	⊕	⊕	⊕	⊕	⊕	1	⊕	95	⊕	88.2	⊕	⊕

NOTES (A) Contractor started predrilling on 9-26-13 started at elevation +9.173 4:45 PM encountered dense green clay material at elevation -17.6. Stopped Auger at 5:50 PM elevation -17.6, (B) 9-27-13 Contractor continued to predrill pilot hole at 7:00 AM elevation -17.6 continued until 8:27 AM elevation -23.63, stopped at this time, started using punch at 8:50 AM elevation -23.63 to elevation -32.00 stopping at 9:30 AM

For Trainee experience evidence only:

Name of CTQP Trainee being supervised by the Qualified Inspector: \_\_\_\_\_

CTQP Trainee

I certify the Pile Driving Record accuracy and that the named above Trainee has observed the full pile installation:

\_\_\_\_\_  
Qualified Inspector (Signature)

### PILE DRIVING LOG

Structure No. <u>600190</u>	Bent/Pier No. <u>END BENT 5</u>	Pile No. <u>2</u>
-----------------------------	---------------------------------	-------------------

Depth	Blows	Stroke/ Pressure	Note No.												
1				34				67	81	6.9		100			
2				35	7	6.24		68	76	7.02		101			
3				36	7	5.95		69	70	7.12	(6)	102			
4				37	6	5.84		70	116	6.27	(7)	103			
5				38	9	5.66		71	72	7.2	(8)	104			
6				39	4	5.83		72	52	7.5	(9)	105			
7				40	4	5.48		73	93	6.98					
8				41	5	5.48		74	141	6.66					
9				42	5	5.48		75	89	6.87					
10				43	6	5.81		76	66	6.86					
11				44	7	5.40		77	96	6.86					
12				45	7	5.35		78	61	7.01	(10)				
13				46	10	5.33		79	44	7.10					
14				47	6	6.06		80	24	7.15					
15				48	10	5.78		81	24	7.15					
16				49	11	5.54		82	29	7.10					
17				50	10	5.66		83	27	7.10	(11)				
18				51	17	5.71		84	53	6.91	(12)				
19				52	10	5.45		85	68	6.36					
20				53	10	5.75		86	55	7.21	(13)				
21				54	10	6.05		87	57	7.57					
22				55	10	5.81		88	62	7.24					
23				56	17	5.79		89	75	7.07					
24				57	12	5.93		90	70	7.32	(14)				
25				58	15	6.07	(X4)	91"	(5)	8.5	(15)				
26				59	30	5.93		92"	5	8.45					
27				60	26	5.81		93"							
28				61	46	5.80		94"							
29				62	58	5.84		95"							
30				63	108	5.80		96"							
31		WOP	(1)	64	143	5.82	(5)	97"							
32		Dry Fire WOP		65	89	6.33		98"							
33				66	82	6.69		99"							

<p>③ STARTED BACK ON 9-30-13 ASSEMBLED NEW AUGER UNIT - 7:00AM TO 5:30PM</p>
<p>④ 10-1-13 CONTRACTOR COMPLETED ASSEMBLY OF PILE AUGER FROM 7:00AM ENDING AT 2:55PM</p>
<p>RESTARTED AUGERING AT 3:55<sup>PM</sup> ELEVATION -10 OVERBURDEN TO ELEVATION -28 4:04PM ORIGINAL ELEVATION, PREDRILLED -28.00, PREDRILLED ON THIS DAY FROM -28 TO ELEVATION -45 FROM 4:04PM TO 4:25PM STOPPING ON DAY.</p>
<p>⑤ 10-2-13 CONTRACTOR REAMED SIDEWALLS AND REMOVED OVERBURDEN FROM PILOT HOLE. FROM + PLACED PILE. NO BEARING P.I.P. 40' FT + 62' FT</p>
<p>① WEIGHT OF PILE PENETRATION FROM FOOT MARK 1 ELEV 11.37 TO FOOT MARK 31 ELEVATION -19.63</p>
<p>② DRY FIRE + WEIGHT OF HAMMER FOOT MARK 31 ELEVATION -19.63 TO W.D.H 31-33 DRY FIRE 33-34</p>
<p>③ STARTED ON FUEL SETTING #1 AT 9:07AM-</p>
<p>④ REBOUND 59 FT MARK 1/2 TO 3/4"</p>
<p>⑤ FUEL SETTING 2 FOOT MARK 64</p>
<p>⑥ FUEL SETTING 1 FOOT MARK 69</p>
<p>⑦ FUEL SETTING 2 FOOT MARK 70</p>
<p>⑧ STOPPED AT 9:45AM TO CHANGE PILE CUSHION FOOT MARK 71 ELEV -59.63 EXISTING CUSHION 1 1/4" THICK</p>
<p>⑨ START BACK AT 10:12AM FUEL SETTING 2 WHEN STARTED BACK FIRST LITTLE OR NO REBOUND THEN PILE BACK UP WITH 1/2 TO 3/4" REBOUND FT MARK 72</p>
<p>⑩ FOOT MARK 78 ELEVATION 66.63 LESS THAN 1/4" REBOUND</p>
<p>⑪ STOPPED AT 10:30AM TO CUT TOP <sup>PARTIAL</sup> COMPLETE FOR HAMMER TO PASS THROUGH FOOT MARK 83 ELEVATION -71.63</p>
<p>⑫ START BACK AT 11:15PM USING FUEL SETTING 1</p>
<p>⑬ FUEL SETTING 2 FOOT MARK 85</p>
<p>⑭ STOPPED AT 11:27<sup>PM</sup> WITH WILL PERFORMED SET CHECK TO ONE HOUR</p>
<p>⑮ SET CHECK STARTS 1:02PM → 10 BLOW TO 2" AT 8.5 STROKES ENDING AT 1:07PM MEETING OR EXCEEDING PROJECT CRITERIA</p>

REF = 11.37

BOTTOM OF P.I.P. NOTE -45 FT MARK 56.37

## **B.4.8. SR-528 over Indian River**

### **B.4.8.1. Test Pile P4P7**

No Log

From PDA File:

Reference Elevation = +11.48 feet

Estimated from pre-construction survey:

GSE = +4.50 feet

### **B.4.8.2. Test Pile P9P3**

No Log

From PDA File:

Reference Elevation = +5.87 feet

Estimated from pre-construction survey:

GSE = -7.50 feet

### **B.4.8.3. Test Pile P20P6**

No Log

From PDA File:

Reference Elevation = +6.23 feet

Estimated from pre-construction survey:

GSE = -8.00 feet

# B.4.9. I-10 and Chaffee Road Overpass

## B.4.9.1. Test Pile P2P9

### PILE DRIVING INFORMATION

STATE PROJECT NO. 213272-4-52-01 DATE 06/15/09 STATION NO. 129+98  
 PILE SIZE 18" LENGTH 89.0' ~~PIER~~ PIER NO. 2 PILE NO. 9  
 HAMMER TYPE PILECO D36 RATED ENERGY 83,750 ft-lb OPERATING RATE 18'  
 TEMPLATE ELEV 66.05 MIN TIP ELEV -15.00 PILE CUTOFF ELEV 58.50  
 DRIVING CRITERIA TEST PILE, PDA & EDC PREFOR IN ELFT. +30'  
(33.23' deep)  
 PILE CUSHION THICKNESS AND MATERIAL 12" PLYWOOD  
 HAMMER CUSHION THICKNESS AND MATERIAL 2" MARGITA/ALUMN.  
 WEATHER CLEAR TEMP 95° START TIME 1:35pm STOP TIME 2:39pm

PILE DATA 455137-PDA  
455146-EDC  
 PAY ITEM NO. 455143-3 - TEST PILE WORK ORDER NO.  
 MANUFACTURED BY DURASTRESS B.M. ELEV 62.89 GROUND ROD READ. 5.10  
 DATE CAST 02/02/09 ROD READ 5.04 PILE HEAD ROD READ  
 MANUFACTURER'S PILE NO. AA4 H.I. 68.33 PILE HEAD ELEV.  
 PILE HEAD CHAMPHER 3/4"x3" PILE TIP ELEV. -18.20  
 PILE TIP CHAMPHER 3/4"x3" GROUND ELEV. 63.23  
 PILE DRIVING INSPECTOR CLIFFORD WHITESIDE  
 Prefor in To +30' = 33.23' deep from ground BUT PAID TO TWO PER PLANS. P11 & P6'

SPICE EACH	CUTOFF TYPE CODE	POINT PROTECTOR	PREFORMED HOLE	PDA	PILE REBIVE	ISOLATED DRIVING	EXTRACTION	30% SPICE	PILE TYPE CODE	BATTER	TOTAL PILE		PENETRATION	BUILD UP	
											FURNISHED	DRIVEN		AUTHORIZED	ACTUAL
X	X	X	X	X	X	X	X	X	X	XXX.XXX	XXX.XXX	XXX.XXX	XXX.XXX	XXX.XXX	XXX.XXX
0	1	0	1	1EA	0	0	0	0	1	000.000	059.000	076.700	081.420	000.000	000.000

NOTES: TEST PILE; PREFORMED HOLE TO +30' EL.; PDA BY CNA 9500 HWANG AND  
EDC BY MIKE WORSHAM. START DRIVE AT 1:35pm WITH SPICE & THIN 1" HEAVY 2"-3" REBARRED THROUGHT  
drive TO THE 2 1/2" MARK. STOP DRIVE AT 1:43pm AT THE 74.5 MARK. REMOVE TOP IRON PILE SOCKET. START MARK AT 1:50pm  
SWEL TAKES 2" AT THE 74.5 MARK TO THE 74.2 MARK. EQUAL TEST. STOP DRIVE AT 2:00pm TO REMOVE BOTTOM IRON PLATE & PUT A 1/2 HOUR  
SET CHECK TO 2 1/2" MARKS. 3" MARKS. START DRIVE AT 2:39pm. STOP DRIVE AT 2:50pm. PER CHANGE 500.

SIGNATURE OF INSPECTOR: Clifford Whiteside

CHAFFEE RD  
PIER 2 TEST PILE 9

PILE DRIVING LOG  
TEMPER = 66.05

Depth	Blows	Stroke Pressure	Note No.	Depth	Blows	Stroke Pressure	Note No.	Depth	Blows	Stroke Pressure	Note No.	Depth	Blows	Stroke Pressure	Note No.
				36				69	9	5.96					
				37	4	6.79	①	70	12	5.83					
				38	7	6.15		71	12	6.23					
				39	10	6.13		72	13	6.27					
				40	12	6.86		73	17	4.64					
				41	12	6.76		74	16	5.12					
				42	29	7.00		75	10	5.14	②				
				43	10	5.05		76	14	5.17	155				
				44	7	6.50		77	15	4.90					
				45	6	6.50		78	28	6.20					
				46	5	5.87		79	84	6.38	③				
				47	6	6.24		80	119	7.61	④				
				48	3	6.2		81	67	7.27	⑤				
				49	3	6.60		82	60	8.09					
				50	3			83	70	8.23					
18				51	2	7.07		84	61	8.14	⑥				
19				52	5	6.67		84'-1"	5	6.54					
20				53	3			84'-2"	4	9.64					
21				54	4	6.77		84'-3"	5	6.99	⑦				
22				55	5	6.81									
23				56	7	6.14									
24				57	7	5.98									
25				58	6	6.13									
26				59	6	6.01									
27				60	7	6.03									
28				61	9	6.04									
29				62	7	6.16									
30				63	9	5.72									
31				64	8	6.07									
32				65	9	6.14									
33				66	10	6.10									
34				67	10	5.84									
35				68	9	5.92									

**B.4.10. I-4 and John Young Parkway**

**B.4.10.1. Test Pile P2P1 (Ramp A)**

RAMP A

TP

**PILE DRIVING INFORMATION**

STATE FIN PROJ. ID 242493-1-52-01 DATE 4-27-04 STATION NO. 524+02.2  
 PILE SIZE 24" LENGTH 91 BENT/PIER NO. P2 PILE NO. 1  
 HAMMER TYPE ICE RATED ENERGY 120,000 <sup>FT LB</sup> OPERATING RATE 120,000 <sup>FT LB</sup>  
 TEMPLATE ELEV 98.192 MAIN TIP ELEV NA PILE CUTOFF ELEV 86.00  
 DRIVING CRITERIA TEST PILE

PILE CUSHION THICKNESS AND MATERIAL 5' PLASTICIZED BLUE NYLON  
 HAMMER CUSHION THICKNESS AND MATERIAL 11" PLYWOOD  
 WEATHER OVERCAST TEMP 78 START TIME 9:42 AM STOP TIME 10:06 AM

**PILE DATA**

PAY ITEM NO. 455-143-5 WORK ORDER NO. REQUIRED STRIKE AND PILE  
 MANUFACTURED BY STANDARD PILE PRODUCTS B.M. ELEV 95.382 GROUND ROD READ 5.43  
 DATE CAST 1-16-04 ROD READ 5.12 PILE HEAD ROD READ \_\_\_\_\_  
 MANUFACTURER'S PILE NO. G9 H.I. 100,502 PILE HEAD ELEV. \_\_\_\_\_  
 PILE HEAD CHAMFER 1/2" x 4" PILE TIP ELEV. \_\_\_\_\_  
 PILE TIP CHAMFER 1/2" x 8" GROUND ELEV. 95.472  
 PILE DRIVING INSPECTOR R. KOPYAN

SPICE EACH	CUTOFF TYPE CODE	POINT PROTECTOR	PERFORATED HOLE	PDA	PILE REDRIVE	ISOLATED DRIVING	EXTRACTION	30% SPICE	PILE TYPE CODE	BATTER	TOTAL PILE		PENETRATION	BUILD UP	
											FURNISHED	DRIVEN		AUTHORIZED	ACTUAL

NOTES: TEST PILE ① 4-29-04 2:24 PM S&T CHECK  
② STOP 2:26 PM

SIGNATURE OF INSPECTOR: R. Kopyan

# PILE DRIVING LOG

Depth	Blows	Stroke/Pressure	Note No.	Depth	Blows	Stroke/Pressure	Note No.	Depth	Blows	Stroke/Pressure	Note No.	Depth	Blows	Stroke/Pressure	Note No.
1	1			33	34	2	5.5	66	67	5	6.4				
1	2			34	35	3	5.6	67	68	5	6.4				
2	3			35	36	3	5.6	68	69	4	6.4				
3	4			36	37	3	5.6	69	70	6	6.3				
4	5			37	38	4	5.7	70	71	6	6.4				
5	6			38	39	4	5.7	71	72	7	6.7				
6	7			39	40	3	5.9	72	73	7	6.7				
7	8	AUGER		40	41	3	5.9	73	74	70	9.4				
8	9		41	42	3	5.9	74	75	45	9.3					
9	10		42	43	3	5.9	75	76	96	8.9					
10	11		43	44	3	5.9	76	77	106	9.0					
11	12		44	45	3	5.9	77	78	128	9.6	3/4	TO 1	REED	JUD	
12	13		45	46	3	6.0	78	79	154	10.0					
13	14		46	47	3	6.0	79	80	7	8.9	①				
14	15		47	48	4	5.8	80	81	10	10.2					
15	16		48	49	4	5.9	81	82	26	8.7	②				
16	17		49	50	3	5.7									
17	18	50	51	3	5.8	83	84								
18	19	X GRD		51	52	3	5.8	84	85						
19	20		52	53	3	5.8	85	86							
20	21	↓ TKNT NTD		53	54	3	5.8	86	87						
21	22		54	55	3	5.8	87	88							
22	23	2	5.4	55	56	4	7.0	88	89						
23	24	4	5.4	56	57	4	7.0	89	90						
24	25	3	5.4	57	58	4	6.7	90	91						
25	26	3	5.4	58	59	4	6.7	91	92						
26	27	3	5.4	59	60	4	6.5	92	93						
27	28	3	5.4	60	61	4	6.5	93	94						
28	29	3	5.5	61	62	4	6.5	94	95						
29	30	3	5.5	62	63	4	6.4	95	96						
30	31	3	5.5	63	64	4	6.4	96	97						
31	32	3	5.5	64	65	4	6.4	97	98						
32	33	3	5.5	65	66	4	6.4	98	99						

B.4.10.2. D.10.2. Test Pile P9P12 (Ramp A)

TP

PILE DRIVING INFORMATION

STATE FIN PROJ. ID 242493-1-52.01 DATE \_\_\_\_\_ STATION NO. 53447.00  
 PILE SIZE 24" LENGTH 90 BENT/PIER NO. P9 PILE NO. 12  
 HAMMER TYPE ICE RATED ENERGY 120,000 ft-lb OPERATING RATE 125,000 %  
 TEMPLATE ELEV 99.330 MAIN TIP ELEV NA PILE CUTOFF ELEV 84.500  
 DRIVING CRITERIA TEST PILE

PILE CUSHION THICKNESS AND MATERIAL 5" PLACTICIZED BLUE NYLON  
 HAMMER CUSHION THICKNESS AND MATERIAL 9/2" PLYWOOD  
 WEATHER PARTLY CLOUDY TEMP 80° START TIME 4:51 PM STOP TIME 5:06 PM

PILE DATA

PAY-ITEM NO. 455-143-5 WORK ORDER NO. REQUIRE STAMP ON PILE  
 MANUFACTURED BY STANDARD CONCRETE PRODUCTS B.M. ELEV 98.310 GROUND ROD READ 5.11  
 DATE CAST 1-22-04 ROD READ 2.970 PILE HEAD ROD READ \_\_\_\_\_  
 MANUFACTURER'S PILE NO. G12 H.I. 101.318 PILE HEAD ELEV. \_\_\_\_\_  
 PILE HEAD CHAMFER 1/2" x 4" PILE TIP ELEV. \_\_\_\_\_  
 PILE TIP CHAMFER 1/2" x 4" GROUND ELEV. 96.200  
 DRIVING INSPECTOR R. KENYON

SPICE EACH	CUTOFF TYPE CODE	POINT PROTECTOR	REINFORCED HOLE	PCA	PILE REDRIVE	ISOLATED DRIVING	EXTRACTION	3/8" SPICE	PILE TYPE CODE	BATTER	TOTAL PILE		PENETRATION	BUILD UP	
											FURNISHED	DRIVEN		AUTHORIZED	ACTUAL
0	0	0	0	1	0	0	0								

NOTES: TEST PILE ① STOP 5:06 PM REBOUND TO BE ABOUT 3/4" TO 1" WRITING FOR 1 hr SBT CHECK ② START 6:06 PM ③ STOP 6:06 PM SBT CHECK ④ 7-20-04 12:02 PM SBT CHECK ⑤ 12:03 PM STOP SBT CHECK

SIGNATURE OF INSPECTOR: R. Kenyon

W: 10433 84

### PILE DRIVING LOG

Depth	Blows	Stroke/Pressure	Note No.	Depth	Blows	Stroke/Pressure	Note No.	Depth	Blows	Stroke/Pressure	Note No.	Depth	Blows	Stroke/Pressure	Note No.
0				30	2	5.9		67	4	6.1					
1	2			31	2	5.9		68	4	6.1					
2	2			35	4	5.9		69	4	6.1					
3	4			36	4	5.9		70	4	6.1					
4	5			37	4	5.9		71	5	6.2					
5	6			38	4	5.7		72	3	6.4					
6	7			39	4	5.7		73	5	6.4					
7	8			40	3	5.7		74	5	6.4					
8	9			41	3	5.9		75	4	6.4					
9	10			42	4	5.9		76	7	6.4					
10	11			43	4	5.9		77	22	8.6					
11	12			44	5	6.1		78	57	7.9					
12	13			45	5	6.2		79	170	7.9					
13	14			46	2	6.2		80	227	8.2	①				1-hr set back
14	15			47	3	6.2		81	4	9.5	②				
15	16			48	3	6.2		82	5	9.7					
16	17			49	3	6.2		83	29	7.3	③				19-hr set back
17	18			50	3	6.4		84	9	9.4	④				
18	19			51	3	6.4		85	13	10.2					
19	20	2	6.4	52	3	6.8		86	15	10.2	⑤				
20	21	3	6.4	53	4	6.2									
21	22	3	6.4	54	3	6.2									
22	23	3	6.3	55	3	6.2									
23	24	3	6.4	56	4	6.2									
24	25	2	6.4	57	3	6.2									
25	26	2	6.3	58	3	6.2									
26	27	3	6.3	59	4	6.2									
27	28	2	6.3	60	3	6.2									
28	29	3	6.1	61	5	6.2									
29	30	2	6.1	62	4	6.1									
30	31	2	6.1	63	4	6.1									
31	32	2	5.9	64	3	6.1									
32	33	2	6.0	65	3	6.1									
				66	4	6.1									

B.4.10.3. D.10.3. Test Pile P10P14 (Ramp A)

**PILE DRIVING INFORMATION**

STATE FIN PROJ. ID 242493-1-52-01 DATE 4-16-04 STATION NO. 536719.00  
 PILE SIZE 24" LENGTH 90' BENT/PIER NO. P10 PILE NO. 14  
 HAMMER TYPE IC6 RATED ENERGY 120,000 FT LBS OPERATING RATE 78,500 F/W  
 TEMPLATE ELEV 98.910 MAIN TIP ELEV NA PILE CUTOFF ELEV 84.50  
 DRIVING CRITERIA OUT PILE

PILE CUSHION THICKNESS AND MATERIAL 5" PLASTICIZED BLUE NYLON  
 HAMMER CUSHION THICKNESS AND MATERIAL 9 1/2" PLYWOOD  
 WEATHER P. CLDY TEMP 72 START TIME 2:50 STOP TIME 5:00 PM

**PILE DATA**

PAY ITEM NO. 455-143-5 WORK ORDER NO. REQUIRE STAMP ON PILE  
 MANUFACTURED BY STANBARD CONCRETE PRODUCTS B.M. ELEV 96.590 GROUND ROD READ 6.340  
 DATE CAST 1-22-04 ROD READ 6.250 PILE HEAD ROD READ 10.810  
 MANUFACTURER'S PILE NO. G13 H.I. 102.840 PILE HEAD ELEV. 91.98  
 PILE HEAD CHAMFER 1/2" x 4" PILE TIP ELEV. 1.98  
 PILE TIP CHAMFER 1/2" x 4" GROUND ELEV. 95.860  
 PILE DRIVING INSPECTOR R. KRYM

SPICE EACH	CUTOFF TYPE CODE	POINT PROTECTOR	PERFORMED HOLE	PCA	PILE REGRIVE	ISOLATED DRIVING	EXTRACTION	SOL. SPICE	PILE TYPE CODE	BATTER	TOTAL PILE		PENETRATION	BUILD UP	
											FURNISHED	DRIVEN		AUTHORIZED	ACTUAL
0	1	0	0	1	0	0	0	0	1	000.000	90.000	91.620	91.910	000.000	0.0

EXCAVATE  
 NOTES: TEST PILE ① STOP 3:10 PM TOP OF PILE AT TEMPLATE. EXCAVATE  
 ② START 4:25 PM ③ STOP 4:40 PM EXCAVATE HOLE DEEPER. 3/4 TO 1"  
REBOUND ④ START 4:52 PM STOP 5:00 PM ⑤ 4-19-04 START 10:05  
 ⑥ STOP 10:07 PM 7-19-04. Get Check  
PILE DID NOT ACHIEVE 5' OF BEARING MATERIAL

SIGNATURE OF INSPECTOR: R. KRYM

# PILE DRIVING LOG

7.17'

Depth	Blows	Stroke Pressure	Hammer No.	Depth	Blows	Stroke Pressure	Hammer No.	Depth	Blows	Stroke Pressure	Hammer No.	Depth	Blows	Stroke Pressure	Hammer No.
1				33	24	5	6.2	44	67	4	6.3	1'	28	9.3	(6)
2				34	25	4	6.1	45	68	4	6.4	1'			
3				35	26	5	6.3	46	69	4	6.4	1'			
4				36	27	5	6.3	47	70	5	6.8	1'			
5				37	28	3	6.4	48	71	5	6.8				
6				38	29	5	6.4	49	72	5	6.8				
7				39	30	5	6.3	50	73	5	6.8				
8				40	31	5	6.4	51	74	5	6.8				
9				41	32	7	6.3	52	75	4	6.8				
10				42	33	3	6.3	53	76	4	6.8				
11				43	34	3	6.3	54	77	4	6.8				
12				44	35	3	6.3	55	78	4	6.8				
13				45	36	3	6.3	56	79	4	6.9				
14				46	37	3	6.2	57	80	5	6.9				
15				47	38	3	6.0	58	81	7	7.1				
16				48	39	5	6.1	59	82	7	7.1				
17				49	40	4	6.1	60	83	8	7.4				
18				50	41	4	6.0	61	84	11	7.7				
19				51	42	4	6.2	62	85	16	8.3				
20	5	6.8		52	43	4	6.2	63	86	32	8.8				
21	5	6.8		53	44	4	6.3	64	87	41	6.6				
22	2	6.8		54	45	3	6.4	65	88	60	8.6				
23	4	6.8		55	46	3	6.5	66	89	56	8.9				(1)
24	5	7.5		56	47	5	6.5	67	90	85	9.0				(2)
25	3	6.5		57	48	3	6.5	68	91	70	8.6				
26	4	6.4		58	49	5	6.4	69	92	80	8.8				
27	4	6.4		59	50	5	6.4	70	93	135	8.9				
28	5	6.0		60	51	3	6.4	71	94	120	7.6				
29	4	6.0		61	52	5	6.4	72	50	52	9.6				(3)
30	4	6.0		62	53	4	6.4	73	192	8.2					(4)
31	4	5.8		63	54	3	6.4	74	1	8	8.2				(5)
32	5	6.4		64	55	3	6.7	75	1	6	9.4				
33	5	6.4		65	56	3	6.6	76	1	18	7.9				

## **B.4.11. . I-4 and SR-408 Intersection**

### **B.4.11.1. Test Pile P2P5 (Ramp B5)**

No Log

From PDA File:

Reference Elevation = +9.47 ft

Estimated from pre-construction survey:

GSE = +1.45 feet

# B.5. FDOT Boring Logs and Lab Testing Data

## B.5.1. Heritage Parkway

### B.5.1.1. FDOT SPT Boring Log (8/26/2014)

STATE OF FLORIDA DEPARTMENT OF TRANSPORTATION  
FIELD BORING LOG

FORM 675-020-12  
MATERIALS  
0999

8/26/14

SHEET 1 OF 5

PROJECT NO. PALM BAY NAME BENT 3 PILE 1 COUNTY DUVAL DISTRICT \_\_\_\_\_  
 LOCATION 30' N 15' E OF P-1 TOWNSHIP \_\_\_\_\_ RANGE \_\_\_\_\_ SECTION \_\_\_\_\_  
 ROAD NUMBER \_\_\_\_\_ SURFACE ELEVATION 117.10  
 EQUIPMENT TYPE CME 75 RIG NO. \_\_\_\_\_ BORING NO. B-1  
 DATE STARTED 8-26-14 COMPLETED 8-27-14 DRILLED BY SWID, SHEPPARD, ST.  
 LOGGED BY T. BRITTON BORING TYPE: AUGER, WASHED, PERCUSSION, ROTARY, \_\_\_\_\_  
 WATER TABLE: 0 HR. \_\_\_\_\_ 24 HRS. 1, 2 HRS. \_\_\_\_\_  
 CASED, UNCASED, DRILLING MUD \_\_\_\_\_

SAMPLE CONDITIONS:  DISTURBED  GOOD  LOST  CORE SAMPLE  
 SAMPLE TYPES: A AUGER SB SPLIT BARREL S SHELBY TUBE RC ROCK CORE \_\_\_\_\_ SIZE  
 TESTS: W.C. WATER CONTENT (%) T TORVANE (TSF) V IN-SITU VANE TEST (TSF)

ELEV. (FT.)	DEPTH (FT.)	S.P.T. BLOWS	MATERIAL DESCRIPTION	SAMPLES			TESTS	REMARKS
				CON.	NO. TYPE	REC. (%)		
	5							
	6	4	BROWN & GRAY CLAYEY SAND		S-1	60		
	7							
	10							
	11	4	GRAYISH GREEN SILTY SAND		S-2	50		
	12							
	15							
	16	4	GRAY SAND WITH SHELL		S-3	60		
	17							
	18							
	19							
	20							



STATE OF FLORIDA DEPARTMENT OF TRANSPORTATION  
**FIELD BORING LOG**

FORM 675-020-12  
 MATERIALS  
 06/99

SHEET 3 OF 5

PROJECT NO. PAINTWAY NAME BENT 3 P-1 COUNTY \_\_\_\_\_ DISTRICT \_\_\_\_\_  
 LOCATION \_\_\_\_\_ TOWNSHIP \_\_\_\_\_ RANGE \_\_\_\_\_ SECTION \_\_\_\_\_  
 ROAD NUMBER \_\_\_\_\_ SURFACE ELEVATION \_\_\_\_\_  
 EQUIPMENT TYPE \_\_\_\_\_ RIG NO. \_\_\_\_\_ BORING NO. B-1  
 DATE STARTED \_\_\_\_\_ COMPLETED \_\_\_\_\_ DRILLED BY \_\_\_\_\_  
 LOGGED BY \_\_\_\_\_ BORING TYPE: AUGER, WASHED, PERCUSSION, ROTARY, \_\_\_\_\_  
 CASED, UNCASD, DRILLING MUD, \_\_\_\_\_  
 WATER TABLE: 0 HR. \_\_\_\_\_ 24 HRS. \_\_\_\_\_ HRS. \_\_\_\_\_

SAMPLE CONDITIONS:  DISTURBED  GOOD  LOST  CORE SAMPLE  
 SAMPLE TYPES: A: AUGER SB: SPLIT BARREL S: SHELBY TUBE RC: ROCK CORE \_\_\_\_\_ SIZE  
 TESTS: W.C.: WATER CONTENT (%) T: TORVANE (TSF) V: IN-SITU VANE TEST (TSF)

ELEV. (FT.)	DEPTH (FT.)	S.P.T. BLOWS	MATERIAL DESCRIPTION	SAMPLES			TESTS	REMARKS
				CON.	NO. TYPE	REC. (%)		
	40	8	GRAY SAND		5-8	50		
	41	9	ABUNDANT SHELL					
			SHELBY TUBE					SAMPLE FELL OUT
	45	1			5-9			HARD DRILLING
		4						HOLE COLLAPSED
								WASH ABUNDANT SHELL
	50	3	GRAY SAND		5-10	15%		HARD DRILLING
		4	& SHELL					
		3						
	55	WOH	GRAY CLAY		5-11	70%		
		1						
			SHELBY TUBE			60% GOOD		
	60							

STATE OF FLORIDA DEPARTMENT OF TRANSPORTATION  
**FIELD BORING LOG**

FORM 675-020-12  
 MATERIALS  
 .0699

SHEET 4 OF 5

PROJECT NO. PALM ONE NAME BENT 3 P-1 COUNTY \_\_\_\_\_ DISTRICT 2  
 LOCATION \_\_\_\_\_ TOWNSHIP \_\_\_\_\_ RANGE \_\_\_\_\_ SECTION \_\_\_\_\_  
 ROAD NUMBER \_\_\_\_\_ SURFACE ELEVATION \_\_\_\_\_  
 EQUIPMENT TYPE \_\_\_\_\_ RIG NO. \_\_\_\_\_ BORING NO. B1  
 DATE STARTED \_\_\_\_\_ COMPLETED \_\_\_\_\_ DRILLED BY \_\_\_\_\_  
 LOGGED BY \_\_\_\_\_ BORING TYPE: AUGER, WASHED, PERCUSSION, ROTARY, \_\_\_\_\_  
 CASED, UNCASD, DRILLING MUD, \_\_\_\_\_  
 WATER TABLE: 0 HR. \_\_\_\_\_ 24 HRS. \_\_\_\_\_ HRS. \_\_\_\_\_

**SAMPLE CONDITIONS:**  **SAMPLE TYPES:** A: AUGER SB: SPLIT BARREL S: SHELBY TUBE RC: ROCK CORE \_\_\_\_\_ SIZE  
**TESTS:** W.C.: WATER CONTENT (%) T: TORVANE (TSF) V: IN-SITU VANE TEST (TSF)

ELEV. (FT.)	DEPTH (FT.)	S.P.T. BLOWS	MATERIAL DESCRIPTION	SAMPLES			TESTS	REMARKS
				CON.	NO. TYPE	REC. (%)		
	60		GRAY CLAY		5-12	75%		
			SHELBY TUBE			75%		
	64		GRAY SANDY CLAY TRACE SHELL		5-13	75%		
	70		GRAY SILTY SAND WITH SHELL / SLIGHTLY COMPACTED		5-14	70%		
	75		LIGHT GRAY CEMENTED SAND & SHELL		5-15	40%		
	80							

STATE OF FLORIDA DEPARTMENT OF TRANSPORTATION  
**FIELD BORING LOG**

FLORIDA DEPARTMENT OF  
 MATERIALS  
 0859

SHEET 5 OF 5

PROJECT NO. PALM BAY NAME BENT 3 P-1 COUNTY 5 DISTRICT \_\_\_\_\_  
 LOCATION \_\_\_\_\_ TOWNSHIP \_\_\_\_\_ RANGE \_\_\_\_\_ SECTION \_\_\_\_\_  
 ROAD NUMBER \_\_\_\_\_ SURFACE ELEVATION \_\_\_\_\_  
 EQUIPMENT TYPE \_\_\_\_\_ RIG NO. \_\_\_\_\_ BORING NO. B-1  
 DATE STARTED 8-26-14 COMPLETED 8-27-14 DRILLED BY \_\_\_\_\_  
 LOGGED BY \_\_\_\_\_ BORING TYPE: AUGER, WASHED, PERCUSSION, ROTARY, \_\_\_\_\_  
 CASED, UNCASD, DRILLING MUD, \_\_\_\_\_  
 WATER TABLE: 0 HR. \_\_\_\_\_ 24 HRS. \_\_\_\_\_ HRS. \_\_\_\_\_

SAMPLE CONDITIONS:  DISTURBED  GOOD  LOST  CORE SAMPLE

SAMPLE TYPES: A: AUGER SB: SPLIT BARREL S: SHELBY TUBE RC: ROCK CORE \_\_\_\_\_ SIZE

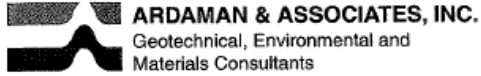
TESTS: W.C.: WATER CONTENT (%) T: TORVANE (TSF) V: IN-SITU VANE TEST (TSF)

ELEV. (FT.)	DEPTH (FT.)	S.P.T. BLOWS	MATERIAL DESCRIPTION	SAMPLES			TESTS	REMARKS
				CON.	NO. TYPE	REC. (%)		
	86	5 4 7	SAME AS S-15		S-16	70%		
	89	5 6 7	SAME AS S-14		S-17	60%		
	90		SHELBY TUBE			Ø		LOST SAMPLE
	95							Boring Term Equipment Max
	100							



# B.5.2. Anderson Overpass

## B.5.2.1. FDOT SPT Boring Log P6-4



SPT-AAI-A5-P6-4

BORING LOG				GENERAL DATA	
DEPTH FT.	BLOWS PER 6" N VALUE	SAMPLE NO.	DESCRIPTION OF MATERIAL	% RECOVERY	FILE NO. _____
5			Hand Augered		CLIENT: _____
10			Hand Augered Drilled (Washed)		SITE: _____
15	3 4 4	1	Light Tan Sand Soft Sand		HOLE NO. _____ SHEET _____ OF _____
20	2 3 2	2			LOCATION OF BORING _____
25	7 7 10	3			DATE <u>16 Dec 08</u>
30	5 6 5	4			CASING: INSIDE DIAMETER _____ IN. OUTSIDE DIAMETER _____ IN. DEPTH OF CASING _____ FT.
35					SPOON: INSIDE DIAMETER _____ IN. OUTSIDE DIAMETER _____ IN.
					HAMMER: HAMMER WEIGHT _____ LB. DROP OF HAMMER _____ IN.
					ELEVATION: GROUND SURFACE _____ FT.
					GWL: DATE 1st _____ DATE 2nd _____ ACTUAL ELEVATION _____
					DRILLING CREW: <u>Lee &amp; Lance</u>
					REMARKS: <u>Safety Hammer</u>

A0154A (12/03)



FILE NO. \_\_\_\_\_ BORING NO. \_\_\_\_\_ SHEET OF \_\_\_\_\_

DEPTH FT.	BLOWS PER 6"	N VALUE	SAMPLE NO.	DESCRIPTION OF MATERIAL	% RECOVERY	DEPTH FT.	BLOWS PER 6"	N VALUE	SAMPLE NO.	DESCRIPTION OF MATERIAL	% RECOVERY
37	12	5				75	17	13		0.5 tsf Greenish Gray Clayey Sand Med. Dense	
40	14	6		Slightly Compacted Light Tan Sand ? Trace silt.		75	33	14		1.6 tsf Very Dense Dark Greenish Gray Clayey Sand	
45	18	7		Light Gray ? Silty (fine) Sand Med Dense		80	28	15		1.3 tsf Dense & Lower MC 1.75 tsf	
50	5	8		Med. Gray - Dense Clayey 1 tsf		80	16	16		DRILLED THROUGH 1.25 tsf	
55	3	9		0.5 tsf		85	9	17		1.10 tsf	
60	2	10		0.5 tsf		85	10	18		Med. Compaction High MC 0.75 tsf No voids	
65	11	11		Greenish Gray		90	8	19		4.4 tsf	
70	13	12				90	59	20		0.5 tsf	
						90	28	21		4.5 tsf 2.5 tsf 3.75 tsf 4.8 tsf	
						95	16	22		LESS THAN 30" Blow ~ 24" REVIEW * PDA *	NL
						95	33	23		4.5 tsf 1.6 tsf 2.8 tsf 3.8 tsf 4.5	NL
						100	17	24		4.4	NL
						100	39	26		3.25 tsf 4.0 tsf 2.5 tsf 4.5 tsf	NL
						105	21	27		4.5 tsf	
							13	28			

A0154B (1/92)



ARDAMAN & ASSOCIATES, INC.  
Geotechnical, Environmental and  
Materials Consultants

STP-AAI-AS-P6-4

FILE NO. BORING NO. SHEET OF

DEPTH FT.	BLOWS PER FT.	W VALUE	SAMPLE NO.	DESCRIPTION OF MATERIAL	% RECOVERY	DEPTH FT.	BLOWS PER FT.	W VALUE	SAMPLE NO.	DESCRIPTION OF MATERIAL	% RECOVERY
108											
109	5		28								
110	9										
111	13		29								
112	16			2.0							
113	17		30								
114	13			3.5							
115	18										
116	21		31	2.0							
117	20										
118	19		40	4.5							
119	13		30	8.5							
120	29										
121	15		28	2.25							
122	17										
123	18		35	4.0							
124	17		39	4.5							
125	7		9	4.5							
126	5										
127											
128											
129											
130											
131											
132											
133											
134											
135											
136											
137											
138											
139											
140											
141											
142											
143											
144											
145											
146											
147											
148											
149											
150											

B.5.2.2. E.2.2. SPT P6-4 Lab Data

SAMPLE NUMBER	DEPTH (FT)	PERCENT MOISTURE	#10 SIEVE	#40 SIEVE	#60 SIEVE	#100 SIEVE	#200 SIEVE	clay SIEVE	SAND	SILT	CLAY	LL/PI	D10	D30	D50	D60	Cc	Cu	AASHTO CLASS	USCS CLASS
1	15.5-16.5	29.6	100	99.6	97.0	41.8	3.7	2	96	2	2	NP	0.085	0.125	0.17	0.18	1.0212	2.1176	A-3	SP
2	20.0-21.5	29.1	100	99.6	97.1	72.2	5.9	3	94	3	3	NP	0.0785	0.096	0.125	0.14	0.8386	1.7834	A-3	SP-SM
3	25.5-26.5	22.4	100	98.8	85.3	28.5	10.7	7	89	4	7	NP	0.075	0.16	0.185	0.2	1.7067	2.6667	A-2-4	SP-SM
4	30.0-31.5	25.0	100	99.8	97.5	37.0	6.2	5	94	1	5	NP	0.082	0.135	0.175	0.185	1.2014	2.2561	A-3	SP-SM
5	35.0-36.5	24.7	98	97.8	96.9	75.6	9.5	6	90	4	6	NP	0.0755	0.0925	0.12	0.1375	0.8242	1.8212	A-3	SP-SM
6	40.0-41.5	24.7	99	98.3	97.1	64.3	8.9	6	91	3	6	NP	0.076	0.098	0.133	0.15	0.8425	1.9737	A-3	SP-SM
7	45.0-46.5	23.0	100	99.3	98.3	49.9	7.5	4	92	4	4	NP	0.078	0.1125	0.158	0.175	0.9272	2.2436	A-3	SP-SM
8	50.0-51.5	50.9	100	95.2	92.3	86.7	46.0	27	54	19	27	47/18	0.039	0.057	0.08	0.095	0.8769	2.4359	A-7-6	SM
9	55.0-56.5	40.1	100	96.8	87.1	60.7	29.2	5	71	24	5	NP	0.048	0.076	0.124	0.16	0.7521	3.3333	A-2-4	SM
10	60.0-61.5	38.2	100	81.6	43.6	23.0	14.0	6	86	8	6	NP	0.056	0.18	0.125	0.32	1.808	5.7143	A-2-4	SM
11	65.0-66.5	33.4	100	95.6	76.6	24.5	9.4	3	91	6	3	NP	0.074	0.17	0.193	0.22	1.7752	2.973	A-3	SP-SM
12	68.5-70.0	33.5	100	97.2	90.7	70.0	15.1	1	85	14	1	NP	0.075	0.17	0.121	0.22	1.7515	2.9333	A-2-4	SM
13	73.5-75.0	33.3	99	94.3	78.2	26.8	17.1	5	83	12	5	NP	0.044	0.17	0.192	0.215	3.055	4.8864	A-2-4	SM
14	75.0-77.0	32.4	99	96.0	91.1	74.1	16.8	6	83	11	6	NP	0.069	0.089	0.117	0.135	0.8503	1.9565	A-2-4	SM
15	77.0-79.0	31.7	100	94.7	87.6	72.9	15.2	4	85	11	4	NP	0.07	0.092	0.118	0.135	0.6772	1.9286	A-2-4	SM
16	80.0-82.0	31.9	99	90.0	80.5	66.2	15.5	5	84	11	5	NP	0.07	0.092	0.126	0.15	0.8061	2.1429	A-2-4	SM
18	84.0-86.0	28.3	87	63.5	48.8	37.3	15.9	7	84	9	7	NP	0.0615	0.125	0.264	0.38	0.6686	6.1789	A-2-4	SM
19	86.0-88.0	29.0	85	54.2	39.4	29.8	11.3	3	89	8	3	NP	0.07	0.165	0.3667	0.57	0.6823	8.1429	A-2-4	SP-SM
20	88.0-90.0	15.7	83	69.0	51.9	33.3	25.5	3	74	23	3	NP	0.006	0.12	0.239	0.325	7.3846	54.167	A-2-4	SM
21	90.0-92.0	24.8	100	83.9	52.8	26.4	22.9	4	77	19	4	NP	0.006	0.17	0.242	0.285	16.901	47.5	A-2-4	SM
22	92.0-94.0	23.8	99	87.5	62.4	44.4	40.9	6	59	35	6	NP	0.003	0.025	0.181	0.24	0.8681	80	A-4	SM
23	94.0-96.0	30.0	99	88.3	76.8	54.3	31.3	8	69	23	8	NP	0.0028	0.065	0.138	0.18	8.3829	64.286	A-2-4	SM
24	96.0-98.0	53.2	99	92.7	87.4	69.0	32.8	20	67	13	20	NP	0.002	0.036	0.106	0.135	4.8	67.5	A-2-4	SM
25	98.0-100.0	32.8	100	93.5	87.5	74.0	50.0	18	50	32	18	44/23	0.002	0.008	0.076	0.11	0.2909	55	A-7-6	CL
26	100.0-104.0	34.4	100	91.8	79.4	48.4	26.3	17	74	9	17	NP	0.002	0.084	0.162	0.185	19.07	92.5	A-2-4	SM
27	102.0-104.0	49.9	98	95.8	93.5	77.4	42.6	25	57	18	25	67/37	0.002	0.0057	0.087	0.11	0.1477	55	A-7-6	SC
28	104.0-106.0	58.6	80.2	71.9	68.9	58.1	39.7	35	60	5	35	86/42	0.002	0.002	0.114	0.17	0.0118	85	A-3	SM
29	106.0-108.0	42.0	92.8	88.1	85.1	79.9	74.1	11	26	63	11	85/43	0.002	0.006	0.019	0.034	0.5294	17	A-7-6	MH
30	108.0-110.0	40.5	85.5	76.5	59.1	34.4	25.6	10	75	16	10	45/14	0.002	0.115	0.208	0.265	24.953	132.5	A-2-7	SM
31	110.0-112.0	44.7	94.9	83.5	67.4	41.5	27.6	13	72	14	13	51/21	0.002	0.085	0.182	0.215	16.802	107.5	A-2-7	SM
32	112.0-114.0	48.1	92.3	80.2	65.3	43.3	31.2	26	69	5	26	56/19	0.002	0.035	0.1805	0.215	2.8488	107.5	A-2-7	SM
33	114.0-116.0	27.2	67	53.0	40.8	28.3	21.0	2	79	19	2	40/13	0.0093	0.17	0.372	0.95	3.2711	102.15	A-2-7	SM
34	116.0-118.0	36.4	93	81.1	68.3	50.8	38.6	8	61	31	8	NP	0.0027	0.029	0.153	0.2	1.5574	74.074	A-4	SM
35	119.0-120.0	50.4	76	58.5	49.9	40.5	32.1	13	68	19	13	NP	0.002	0.052	0.256	0.5	2.704	250	A-2-4	SM

### B.5.3. SR-83 over Ramsey Branch

#### B.5.3.1. FDOT SPT Boring Log (6/25/2014)

STATE OF FLORIDA  
DEPARTMENT OF TRANSPORTATION  
FIELD BORING LOG

BORING NO. 7

ELEVATION \_\_\_\_\_

PAGE 1 OF 7

PROJECT NO. Ramsey Branch Bridge B.I. NO. \_\_\_\_\_ BRIDGE NO. \_\_\_\_\_  
 ROAD NO. SR 83 03, Walker Co. STATION NL \_\_\_\_\_ OFFSET \_\_\_\_\_  
 TYPE BORING  AUGER  STANDARD  OTHER \_\_\_\_\_ TOWNSHIP \_\_\_\_\_  
 EQUIPMENT TYPE CME-75 DOT NUMBER 23890 RANGE \_\_\_\_\_  
 DATE STARTED 6-25-14 DATE COMPLETE 6-25-14 SECTION \_\_\_\_\_  
 DRILLED BY Porter LOGGED BY Shiver  
 WATER TABLE 4ft 0-HOURS 3 1/2 feet 24-HOURS \_\_\_\_\_ HOURS \_\_\_\_\_

Depth M	Depth Ft	SPT Blows	Materials Description	Sample		Core Run		Sample Rec.		Sample Test		Remarks
				Number		From	To	Inches	%	Type	Type	
1		2	tan sand with some white and dark sand	1	0	1.5		100	SB			
	1	2										
	2	8										
		6	light tan sand with silts	2	2	3.5		100				
	3	8										
	4	10										
	6	light tan sand with some silt	3	4	5.5		100					
5	6											
6	3											
2	2	2	Orange Clay Sand	4	6	7.5		100				
	7	2										
	8	3										
3		1	Orange clay sand	5	8	9.5	20			Set 10 foot of casing starting mixing mud		
	9	2										
	10	1										

General Notes:  $Sf_{2.} = 2 \text{ approx. } 134B+60, 45' \text{ AT. } 9$

Sample Type:  
 A- Auger  
 SB- Split Barrel  
 ST- Shelby Tube  
 CB- Core Barrel  
 Test Type:  
 SV- Shear Vane  
 T- Torvane  
 WC- Water Content

Depth M	Depth Ft	SPT Blows	Materials Description	Sample Number	Core From	Run To	Sample Inches	Rec. X	Sample Type	Test Type	Remarks
4	11	W 0	Woh mucky sand dark color	6	11	12.5	21		SB		
	12	h									
	13	l									
5	14	l	gray sand	7	13.5	15	15				
	15	l									
	16										
6	17	W 0	Woh clay sand tan and orange color	8	16	17.5	24				
	18	h									
	19										
7	20		Woh Orange clay Sand	9	18.5	20	24				
	21										
	22										
7	23	W 0	Siltysand tan color	10	21	22.5	24				
	24	h									
	25	l									
7	23	W 0	green clay sand	11	23.5	25	24				
	24	h									
	25	l									

General Notes:

Sample Type:

- A- Auger
- SB- Split Barrel
- ST- Shelby Tube
- CB- Core Barrel

Test Type:

- SV- Shear Vane
- T- Torvane
- WC- Water Content

Depth M	Depth Ft	SPT Blows	Materials Description	Sample Number	Core From	Run To	Sample Rec. Inches	Rec. %	Sample Type	Test Type	Remarks
8	26		green clay sand	12	26	22.5	19		SB		
		1									
	27	2									
9		2	green clay sand	13	28.5	30	16				
	28	3									
	29	6									
10		10	green clay	14	31	32.5	17				
	30										
	31	3									
11		6	gray clay	15	33.0	35	24				
	32	9									
	33										
12		3	gray clay	16	36	37.5	24				
	34	28									
		14									
12			gray sandy clay	17	38.5	40	18				
	35										
	36	2									
	39	5									
	40	6									

General Notes:

Sample Type:

- A- Auger
- SB- Split Barrel
- ST- Shelby Tube
- CB- Core Barrel

Test Type:

- SV- Shear Vane
- T- Torvane
- WC- Water Content

Depth M.	Depth Ft	SPT Blows	Materials Description	Sample Number	Core From	Run To	Sample Rec. Inches	Rec. %	Sample Type	Test Type	Remarks
									SB		
	41	2	gray sandy clay	18	41	42.5	24				
		3									
	42	5									
13	43		gray sandy clay	19	43.5	45	24				
		3									
	44	5									
		8									
	45										
14	46	2	changes from gray to green color clay with trace of white mixed in	20	46	47.5	24				
		3									
	47	4									
	48		gray <sup>green</sup> clay with small trace of white	21	48.5	50	24				
		2									
15	49	3									
		3									
	50		gray sandy clay	22	51	52.5	24				
		2									
	51	3									
	52	4									
16	53		gray sandy clay	23	53.5	55	24				
		2									
	54	2									
		3									
	55										

General Notes:

Sample Type:

A- Auger  
SB- Split Barrel  
ST- Shelby Tube  
CB- Core Barrel

Test Type:

SV- Shear Vane  
T- Torvane  
WC- Water Content

Depth M	Depth Ft	SPT Blows	Materials Description	Sample Number	Core Run From	To	Sample Rec. Inches	%	Sample Type	Test Type	Remarks
17	56	2	gray sandy clay	24	56	57.5	24		SB		
		2									
	57	3									
18	58		gray sandy clay small traces of white mixed with it	25	58.5	60	24				
		2									
	59	3									
		4									
19	60		gray sandy clay	26	61	62.5	24				
		2									
	62	5									
20	63		gray sandy clay	27	62.5	65	24				
		2									
	64	2									
		4									
20	65		gray sandy clay small traces of white mixed in	28	66	67.5	24				
	66	3									
		3									
21	67	6	gray sandy clay	29	68.5	70	24				
	68	3									
	69	4									
		7									
	70										

General Notes:

Sample Type:      Test Type:  
 A- Auger            SV- Shear Vane  
 SB- Split Barrel    T- Torvane  
 ST- Shelby Tube    WC- Water Content  
 CB- Core Barrel

Depth M	Depth Ft	SPT Blows	Materials Description	Sample Number	Core From	Run To	Sample Inches	Rec. %	Sample Type	Test Type	Remarks
22	71	3	Sandy clay gray Just starting to bit dark gray hard clay	30	71	72.5	29		SB		
		7									
		72	10								
	73	7	Gray silt sand with shell	31	73.5	75	20				
		7									
	74	6									
23	75		Silt sand Shell	32	76	77.5	21				
		76									7
											7
		77									43
24	78	6	Silt sand and shell	33	78.5	80	21				
											5
		79	4								
		80									
25	81	5	a little silt sand shell	34	81	82.5	17				
											25
		82	36								
		83	37	Silt Sand shell	35	83.5	85	17			
			14								
		84	8								
		85									

General Notes:

Sample Type:

- A- Auger
- SB- Split Barrel
- ST- Shelby Tube
- CB- Core Barrel

Test Type:

- SV- Shear Vane
- T- Torvane
- WC- Water Content

Depth M	Depth Ft	SPT Blows	Materials Description	Sample Number	Core Run		Sample Rec. Inches	Sample % Type	Test Type	Remarks
					From	To				
26			Silt sand					SB		hole trying to close up a little
	86	114	Shell	36	86	87.5	17			
		6								
	87	6								
			Sand with shell							
	88			37	88.5	90	21			
27		9								
	89	5								
		6								
	90									
			End of boring - 90'							
	91									
28	92									
	93									
	94									
29	95									
	96									
	97									
	98									
30	99									
	100									

General Notes:

Sample Type:  
 A- Auger  
 SB- Split Barrel  
 ST- Shelby Tube  
 CB- Core Barrel  
 Test Type:  
 SV- Shear Vane  
 T- Torvane  
 WC- Water Content



## B.6. Additional Figures

### B.6.1. Effective Internal Angle of Friction versus Rebound

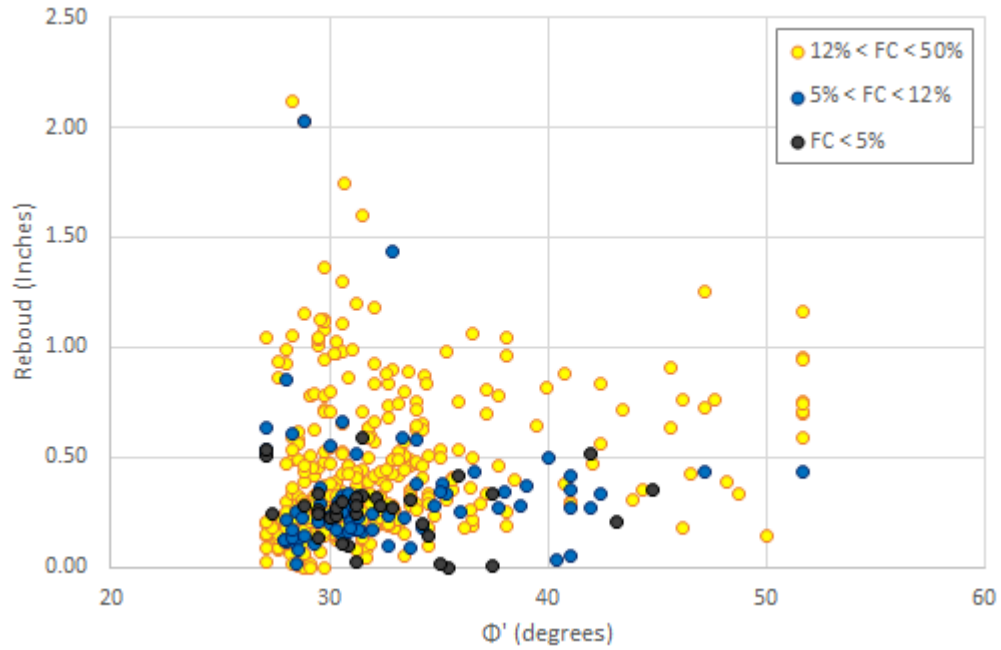


Figure F.1.  $\Phi'$  (Peck, 1974) versus rebound

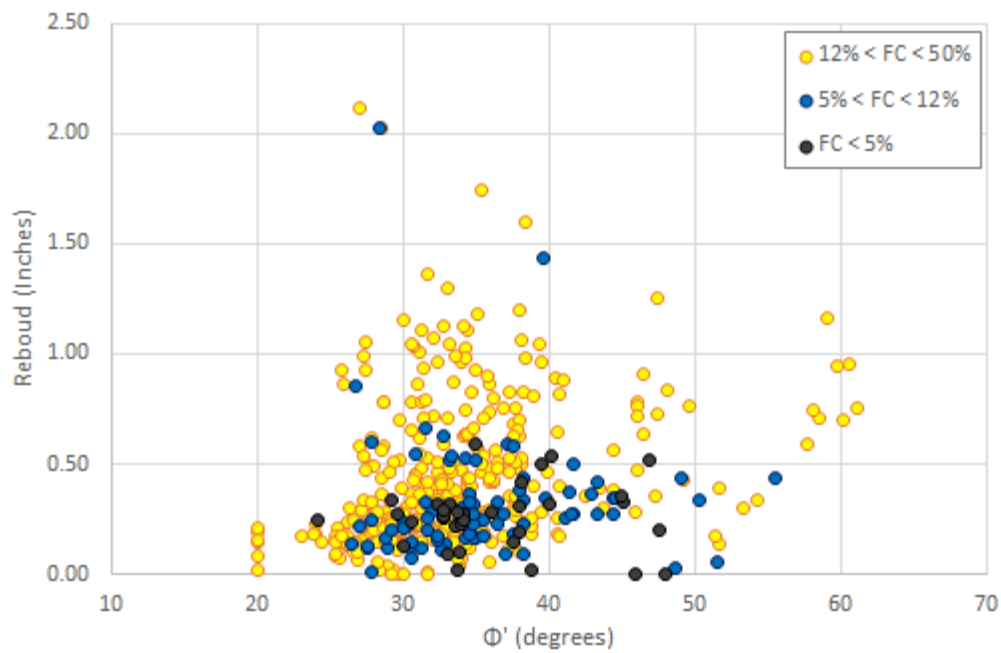


Figure F.2.  $\Phi'$  (Hatanaka and Uchida, 1996) versus rebound

### B.6.2. . Cohesion from unconfined compressive strength versus Rebound

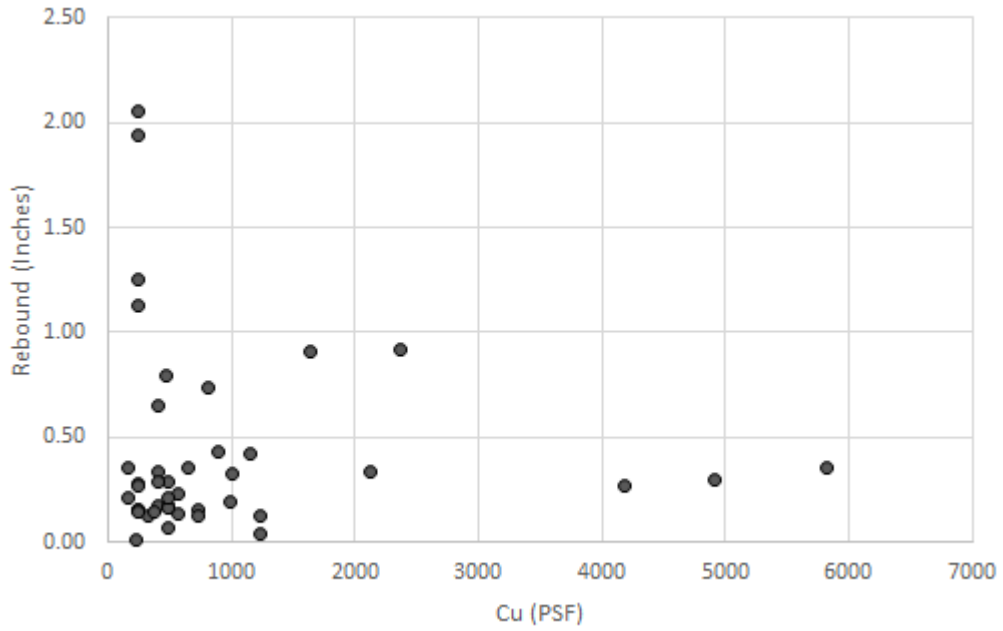


Figure F.3.  $q_u$  (Hettiarachchi and Brown, 2009) versus rebound

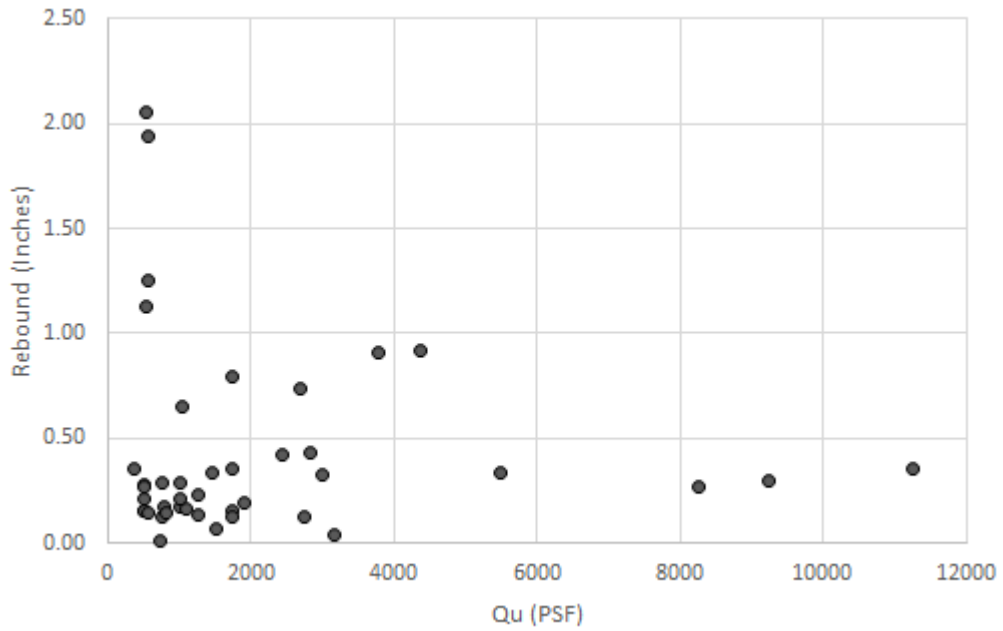


Figure F.4.  $q_u$  (CDOT, 2014) versus rebound

## **Appendix C- Results from Standard Undrained Triaxial Tests**

Table C-1- Summary of HPR Phase II Sites Tested to Obtain Thin Walled Tube Samples

Site Name and Test Pile Description		Pile Length (ft)	Pile Shape	Hammer Type	Max Rebound (in)
<b>I4/ US-192</b>	Ramp CA Pier 6 Pile 16	110	2-ft Square PCP	Single Acting Diesel ICE 120 S	0.7
	Ramp CA Pier 7	116			0.8
	Ramp CA Pier 8	96			0.96
	West Bound End Bent 1	162			0.85
	Ramp BD End Bent 1	162			1
<b>I-4 / Osceola Parkway</b>	Pier 2	100	2-ft Square PCP	Single Acting Diesel ICE 120 S	0.97
	Pier 3	100			0.7
	Pier 4	100			0.97
<b>I-10 at Chaffee Road</b>	End Bent 1	89	1.5-ft Square PCP	Single Acting Diesel Pileco D35-32	2.6
	End Bent 3	89			2.6
<b>SR-83 Over Ramsey Branch</b>	End Bent 5	95	1.5-ft Square PCP	Single Acting Diesel APE D50-42	1.4
<b>SR 417 / International Parkway</b>	End Bent 1	105	2-ft Square PCP	Single Acting APE D46-42	0.4
	End Bent 3	105			0.31
<b>Palm Bay Parkway</b>	Int. Bent 3	121	1.5-ft Square PCP	Single Acting Diesel APE D36-32	0.6
	End Bent 5	121			0.55

Note: High rebound sites or > 0.5 inches rebound are unshaded;

Nonrebound sites or < 0.25 inches rebound are shaded

## C.1. Test results – Cohesionless soils

Table C-2 Soil classification, percentage sand, silt, clay and fines by weight, and particle size distribution for cohesionless rebound and nonrebound soils for all thin walled tube sample sites.

	Depth		Elevation		GSE	Rebound	Sand	Silt	Clay	Fine	D10	D30	D60	Cu	Cc	Classification	
	ft	in	ft	in												mm	mm
Rebound > 0.5 in	75	76	14	13	89	0.74	56	36	8	44	0.004	0.049	0.118	30	5	SM	A-4
	80	81	9	8	89	0.78	74	20	6	26	0.007	0.085	0.185	28	6	SM	A-2.4
	85	87	4	2	89	0.79	88	5	7	12	0.063	0.130	0.230	4	1	SM	A-2.4
	80	82	15	13	95	0.62	66	27	7	34	0.005	0.069	0.110	24	10	SM	A-2.4
	70	72	19	17	89	0.50	56	34	9	44	0.002	0.075	0.110	61	28	SM	A-4
	70	72	20	18	90	0.88	55	37	9	45	0.003	0.051	0.093	37	11	SM	A-4
	70	72	20	18	90	0.69	72	21	8	29	0.004	0.077	0.110	31	15	SM	A-2.4
	75	77	15	13	90	0.58	72	21	7	28	0.003	0.078	0.110	34	17	SM	A-2.4
	80	82	12	10	92	0.76	68	19	13	33	0.071	0.103	0.150	2	1	SM	A-2.4
	64	66	-54	-57	9	1.12	65	20	16	36	0.019	0.130	0.150	2	1	SM	A-2.4
Rebound < 0.2 in	42	44	27	25	68.5	0.145	87	4	9	13	0.006	0.100	0.150	27	12	SM	A-2.4
	58	60	11	9	68.5	0.140	67	19	14	33	0.068	0.110	0.150	2	1	SM	A-2.4
	58	61	11	8	68.5	0.140	87	11	2	13	0.066	0.100	0.150	2	1	SM	A-2.4
	55	57	14	12	68.5	0.050	62	24	14	38	0.052	0.110	0.150	2	1	SM	A-4
	60	62	35	33	95.0	0.160	87	5	8	13	0.007	0.220	2.000	303	4	SM	A-1-b
	45	47	45	43	90.3	0.165	81	15	4	19	0.009	0.140	0.220	24	10	SM	A-2.4
	55	57	35	33	90.3	0.220	76	16	8	24	0.004	0.120	0.235	67	18	SM	A-2.4
	46	47	44	43	90.1	0.140	75	20	6	26	0.004	0.130	0.280	68	15	SM	A-2.4
	55	57	35	33	90.3	0.185	76	14	10	24	0.002	0.096	0.180	113	32	SM	A-2.4
	50	52	42	40	91.8	0.195	84	11	4	16	0.013	0.145	0.210	16	8	SM	A-2.4
Averages Rebound	75	77	7	6	82	0.74	67	24	9	33	0.011	0.070	0.130	31	12		
Averages NonRebound	52	54	30	28	82	0.15	78	14	8	22	0.014	0.117	0.365	78	12		
Averages Overall	64	66	19	17	82	0.45	73	19	8	27	0.012	0.094	0.247	54	12		

USCS=Unified Soil Classification System; AASHTO = American Association of State Highway and Transportation Officials;  $C_u = \frac{D_{60}}{D_{10}}$ ;  $C_c = \frac{D_{30}^2 - D_{10} D_{60}}{D_{10}^2}$

Table C-3 List of physical properties from triaxial test samples retrieved from cohesionless rebound and nonrebound soils for all thin walled tube sample sites.

	Depth		Elevation		GSE	Rebound	Unit Wt.	Dry Unit Wt.	Void ratio	Porosity, (n)	Degree of saturation (S)	Moisture	Permeability
	ft	ft	ft	ft									
I-4&Osceola Pier 2	75	76	14	13	89	0.74	111	89	0.94	48	73	25	3.47E-07
I-4&Osceola Pier 2	80	81	9	8	89	0.78	118	92	0.78	44	93	28	3.87E-07
I-4&Osceola Pier 2	85	87	4	2	89	0.79	121	102	0.65	39	79	19	4.98E-05
I-4&192 Pier 6 pile 4	80	82	15	13	95	0.62	110	79	1.14	53	93	39	NA
I-4&192 B4 Pier 7 Pile 10	70	72	19	17	89	0.50	106	71	1.38	58	97	49	NA
I-4&192 Pier 8 pile 4	70	72	20	18	90	0.88	107	73	1.30	57	95	46	4.98E-07
I-4&192 Ramp BD EB1 Pile 3	70	72	20	18	90	0.69	111	82	1.03	51	90	35	5.20E-07
I-4&192 Ramp BD EB1 Pile 3	75	77	15	13	90	0.58	110	76	1.24	55	98	44	2.96E-06
I-4&192 WB EB Pile 1	80	82	12	10	92	0.76	106	75	1.28	56	88	41	NA
Ramsey Branch Bridge	64	66	-54	-57	9	1.12	112	81	1.12	53	96	39	4.84E-06
I-4&417 EB1	42	44	27	25	68.5	0.145	119	98	0.71	41	83	22	NA
I-4&417 EB1	58	60	11	9	68.5	0.140	108	75	1.32	57	93	44	NA
I-4&417 EB1	58	61	11	8	68.5	0.140	120	94	0.80	45	93	27	2.7E-05
I-4&417 EB2	55	57	14	12	68.5	0.050	104	73	1.36	58	88	44	1.6E-07
I-4&192 Pier 6 Pile 4	60	62	35	33	95.0	0.160	117	89	0.96	49	93	32	NA
I-4&192 Pier 8 Pile 4	45	47	45	43	90.3	0.165	116	90	0.85	46	89	28	3.8E-05
I-4&192 Pier 8 Pile 4	55	57	35	33	90.3	0.220	119	96	0.81	45	82	24	2.3E-05
I-4&192 Ramp BD EB1 Pile 3	46	47	44	43	90.1	0.140	124	102	0.67	40	89	22	1.2E-05
I-4&192 South of Ramp BD EB3	55	57	35	33	90.3	0.185	120	96	0.79	44	85	24	NA
I-4&192 B6 WB EB1 Pile 1	50	52	42	40	91.8	0.195	118	93	0.80	44	90	27	1.4E-05
<b>Averages Rebound</b>	75	77	7	6	82	0.74	111	82	1.09	51	90	37	8.48E-06
Averages NonRebound	52	54	30	28	82	0.15	116	90	0.91	47	89	29	1.91E-05
Averages Overall	64	66	19	17	82	0.45	114	86	1.00	49	89	33	1.34E-05

Table C-4 Standard undrained triaxial tests results on cohesionless soils for all thin walled tube sample sites

	Depth		Elevation		GSE	Rebound	Confining Pressure	Max Dev. Stress	$\Delta u$ @ Max Dev. Stress	Strain @ Max Dev. Stress	Af	Et	Es	$\phi$	$\phi'$
	ft	ft	ft	ft											
Rebound > 0.5 in	75	76	14	13	89	0.74	30	29	22	15.50	0.67	45.01	22.52	19	40
	80	81	9	8	89	0.78	32	59	6	15.50	0.10	34.96	9.60	29	32
	85	87	4	2	89	0.79	34	250	-59	7.93	-0.23	175.31	43.59	52	35
	80	82	15	13	95	0.62	32	66	9	10.42	0.16	95.08	37.66	30	36
	70	72	19	17	89	0.50	30	48	96	15.12	1.96	94.08	9.33	26	34
	70	72	20	18	90	0.88	24	60	11	2.75	0.19	99.47	6.72	34	45
	70	72	20	18	90	0.69	25	53	2	15.50	0.01	128.57	7.68	31	32
	75	77	15	13	90	0.58	27	69	3	12.31	0.04	80.00	12.79	34	36
	80	82	12	10	92	0.76	27	60	12	3.92	0.20	95.65	33.98	32	42
	64	66	-54	-57	9	1.12	29	51	15	9.97	0.20	81.90	31.24	28	40
Rebound < 0.2 in	42	44	27	25	68.5	0.145	17	65	-22	6.05	-0.33	36.67	12.16	41	27
	58	60	11	9	68.5	0.140	24	27	NA	15.42	NA	125.00	45.40	23	43
	58	61	11	8	68.5	0.140	24	201	-59	15.00	-0.29	75.36	15.05	54	33
	55	57	14	12	68.5	0.050	24	54	2	14.97	0.04	113.23	31.54	32	34
	60	62	35	33	95.0	0.160	24	51	14	15.50	0.27	103.78	25.78	31	45
	45	47	45	43	90.3	0.165	18	21	9	15.45	0.45	54.51	12.93	21	33
	55	57	35	33	90.3	0.220	21	43	10	12.86	0.23	81.10	23.26	30	41
	46	47	44	43	90.1	0.140	18	59	0	15.32	-0.01	104.25	18.14	38	38
	55	57	35	33	90.3	0.185	20	61	4	8.93	0.06	11.70	11.70	37	41
	50	52	42	40	91.8	0.195	20	49	-1	15.42	-0.03	11.43	6.29	33	32
Averages Rebound	75	77	7	6	82	0.142	29	74	12	11	0.33	93	28	31	37
Averages NonRebound	52	54	30	28	82	0.154	21	63	-5	13	0.04	78	20	34	37
Averages Overall	64	66	19	17	82	0.148	25	69	4	12	0.20	86	24	33	37

Af = Skempton's pore water coefficient at failure,  $E_t$  = Tangent modulus;  $E_s$  = Secant modulus;  $\phi$  = Angle of Friction;  $\phi'$  = effective friction angle

## C.2. Tests results- Cohesive soils

Table C-5 Soil classification, percent sand, silt, clay and fines by weight, Atterberg limits and particle size distribution for rebound and nonrebound cohesive soils for thin walled tube sample sites.

	Depth		Elevation		GSE	Rebound	Sand	Silt	Clay	Fine	D10	D30	D60	Classification	
	ft	ft	ft	ft										AASHTO	USCS
Rebound > 0.5 in	50	52	13	11	63	2.04	23	28	49	77	0.007	0.007	0.007	CH	A-7-6
	54	56	9	7	63	1.34	42	21	37	58	0.080	0.080	0.080	CH	A-7-6
	52	55	11	8	63	1.40	9	30	61	91	0.002	0.002	0.002	CH	A-7-6
	60	63	3	0	63	2.15	18	29	53	82	0.004	0.004	0.004	CH	A-7-6
Rebound < 0.2 in	31	33.5	-22	-24	9	0.81	25	25	50	75	0.009	0.009	0.009	CH	A-7-6
	55	57	-29	-31	26	0.49	12	57	31	88	0.002	0.002	0.013	CH	A-7-6
	62	64	-36	-38	26.1	0.140	13	57	30	87	0.002	0.002	0.018	CL	A-7-6
	57	59	-32	-34	24.9	0.215	13	69	19	87	0.006	0.006	0.030	CL	A-7-6
Averages	50	53	-2	-5	48	1.368	21	32	47	79	0.002	0.002	0.019		
NonRebound	60	62	-34	-36	25	0.178	13	63	24	87	0.004	0.004	0.024		
Overall	53	55	-10	-13	42	1.071	19	39	41	81	0.003	0.003	0.020		

USCS=Unified Soil Classification System; AASHTO = American Association of State Highway and Transportation Officials;  $C_u = \frac{D_{60}}{D_{10}}$ ;  $C_c = \frac{D_{30}^2}{D_{60} \times D_{10}}$

Table C-6 List of physical properties of triaxial test samples retrieved from rebound and nonrebound cohesive soils for all thin walled tube sample sites.

	Depth		Elevation		GSE	Rebound	Unit Wt.	Dry Unit Wt.	Void ratio	Porosity (n)	Degree of Saturation (S)	Permeability	Moisture (%)	LL	PL	PI	Activity of a clay
	ft	ft	ft	ft													
Charlree Rd EB 3	50	52	13	11	63	2.04	97	57	1.87	65	98	NA	69	71	25	45	0.92
	54	56	9	7	63	1.34	102	74	1.20	55	81	NA	37	51	19	33	0.87
	52	55	11	8	63	1.40	92	53	2.12	68	93	1.43E-08	75	92	29	63	1.03
	60	63	3	0	63	2.15	90	48	2.50	71	96	1.01E-08	90	77	25	52	0.98
Ramsay Branch Bridge	31	33.5	-22	-24	9	0.81	109	85	1.14	53	74	7.40E-07	29	82	23	59	1.19
Palm bay Parkway IB 4 Pile 10	55	57	-29	-31	26	0.49	95	55	2.05	67	95	8.94E-08	73	53	24	30	0.96
Palm bay Parkway IB 4 Pile 10	62	64	-36	-38	26.1	0.140	104	68	1.50	60	98	1.04E-07	54	43	19	24	0.81
Palm bay Parkway EB 5 P1	57	59	-32	-34	24.9	0.215	101	67	1.55	61	90	6.28E-07	51	44	21	24	1.30
Averages Rebound	59	53	-2	-5	48	1.37	98	62	1.81	63	89	2.13E-07	62	71	24	47	1
Averages NonRebound	60	62	-34	-36	25	0.18	103	67	1.52	60	94	3.66E-07	53	44	20	24	1
Averages Overall	53	55	-10	-13	42	1.07	99	63	1.74	63	91	2.64E-07	60	64	23	41	1

LL= Liquid Limit; PL =Plastic Limit; PI= Plasticity index; Activity of a clay =  $\frac{PI}{\% \text{ Clay particles less than } 2 \mu\text{m}}$

Table C-7 Summary of standard undrained triaxial tests results for all cohesion soils retrieved from all thin walled tube sample sites

	Depth		Elevation		GSE	Rebound	Confining Pressure	Max Dev. Stress	Au @ Max Dev. Stress	Strain @ Max Dev. Stress	Af	Et	Es	$\phi$	$\phi'$
	ft	in	ft	in											
Charltee Rd EB 3	50	52	13	11	63	2.04	20	25.94	13.84	1.78	0.53	36.5	31.5	23.2	42.7
	54	56	9	7	63	1.34	22	18.26	15.26	2.56	0.83	95.8	30.8	17.1	35.1
	52	55	11	8	63	1.40	17	18.17	10.23	3.12	0.17	35.3	23.3	20.4	35.0
Charltee Rd EB 3	60	63	3	0	63	2.15	19	13.94	8.57	3.09	0.22	61.6	36.5	16.8	30.7
	31	33.5	-22	-24	9	0.81	17	55.61	7.64	4.24	0.08	89.0	2.5	38.4	48.4
Palm Bay Parkway IB 4 Pile 10	55	57	-29	-31	26	0.49	23	23.35	14.13	1.29	0.61	94.4	72.0	19.7	34.6
Palm bay Parkway IB 4 Pile 10	62	64	-36	-38	26.1	0.140	25	31.45	16.91	1.17	0.54	124.7	116.0	22.7	41.3
Palm bay Parkway EB 5 P1	57	59	-32	-34	24.9	0.215	24	29.85	16.26	1.93	0.54	113.4	77.6	22.5	41.2
Averages Rebound	50	53	-2	-5	48	1.368	20	25.88	11.61	2.68	0.41	69	33	23	38
Averages NonRebound	60	62	-34	-36	25	0.178	25	30.65	16.59	1.55	0.54	119	97	23	41
Averages Overall	53	55	-10	-13	42	1.071	21	27.07	12.86	2.40	0.44	81	49	23	39

$A_f$  = Skempton's pore water coefficient at failure,  $E_t$  = tangent modulus;  $E_s$  = secant modulus;  $\phi$  = friction angle;  $\phi'$  = effective friction angle

## **Appendix D- Results from Cyclic Triaxial Tests**

# D.1. Tests results - Cohesionless soils

Table D-1 Soil classification, percent, sand, silt, clay and fine by weight, and particle size distribution for all rebound and nonrebound cohesionless soils.

	Depth		Elevation		GSE	Rebound	Sand	Silt	Clay	Fine	D10	D30	D60	Cu	Cc	Classification	
	ft	ft	ft	ft												AASHTO	USCS
Rebound > 0.5 in	75	76	14	13	89	0.74	36	54	10	64	0.002	0.03	0.07	38.2	9.9	ML	A-4
	80	81	9	8	89	0.78	65	23	12	35	0.001	0.06	0.11	83.0	26.0	SP-SM	A-2-4
	85	87	4	2	89	0.79	71	18	12	30	0.001	0.08	0.14	115.2	32.9	SP-SM	A-2-4
	80	82	15	13	95	0.62	69	24	7	31	0.004	0.07	0.11	31.4	14.2	SM	A-2-4
	65	66	25	24	90	0.67	73	23	4	27	0.008	0.08	0.11	14.1	7.7	SM	A-2-4
	70	72	20	18	90	0.88	54	38	8	46	0.002	0.04	0.09	45.8	10.2	SM	A-4
	75	77	15	13	90	0.58	70	20	10	30	0.002	0.08	0.11	57.9	26.9	SM	A-2-4
	80	82	12	10	92	0.76	76	16	8	24	0.002	0.07	0.10	103.1	31.9	SM	A-2-4
	31	34	-22	-24	9	0.81	79	10	10	21	0.002	0.11	0.19	103.1	31.9	SM	A-2-4
	42	44	27	25	69	0.15	86	3	11	14	0.002	0.10	0.15	103.1	31.9	SM	A-2-4
Rebound < 0.2 in	57	58	12	11	69	0.14	76	15	9	25	0.00	0.08	0.12	60.0	28.0	SM	A-2-4
	60	62	35	33	95	0.16	88	6	6	13	0.01	0.20	1.30	130.0	3.0	SW-SM	A-1-b
	45	47	45	43	90	0.17	87	9	4	13	0.032	0.14	0.2	6.3	3.1	SM	A-2-4
	46	47	44	43	90	0.14	55	35	11	45	0.00	0.01	0.18	105.9	0.3	SM	A-4
	55	57	35	33	90	0.19	74	16	10	26	0.00	0.09	0.18	112.5	28.1	SM	A-2-4
	50	52	42	40	92	0.20	80	12	9	21	0.00	0.12	0.21	100	32.7	SM	A-2-4
	71	73	11	10	82	1	66	25	9	34	0.002	0.069	0.115	63	21		
	52	54	31	29	83	0.158	76	16	8	24	0.009	0.100	0.307	75	14		
	62	64	20	18	83	0.474	70	21	9	30	0.006	0.083	0.201	68	18		
	Averages Rebound																
Averages NonRebound																	
Averages Overall																	

USCS=Unified Soil Classification System; AASHTO = American Association of State Highway and Transportation Officials;  $C_u = \frac{D_{60}}{D_{10}}$ ;  $C_c = \frac{D_{30}^2}{D_{60} \times D_{10}}$

Table D-2 Cyclic test results for all cohesionless soils from all thin walled tube sample sites

	Depth		Elevation		GSE	Rebound	Confining Pressure	Number of Cyclic Causing 1 % Strain	Number of Cyclic Causing 2.5 % Strain	Number of Cyclic Causing 5 % Strain	Number of Cyclic Causing 10 % Strain	Number of Cyclic Causing 15 % Strain	Number of Cyclic Causing 20 % Strain	
	ft	in	ft	in										
Rebound > 0.5 in	I-4/Osceola Pier 2 Pile 8	75	76	14	13	89	0.74	30	8464	◆	◆	◆	◆	
	I-4/Osceola Pier 2 Pile 8	80	81	9	8	89	0.78	32	8464	◆	◆	◆	◆	
	I-4/Osceola B1 Pier 2 Pile 8	85	87	4	2	89	0.79	34	2127	7409	◆	◆	◆	
	I-4&192 Pier 6 pile 4	80	82	15	13	95	0.62	32	3180	4660	6687	8119	◆	
	I-4&192 Pier 8 pile 4	65	66	25	24	90	0.67	24	6441	◆	◆	◆	◆	
	I-4&192 Ramp BD EB1 Pile 3	70	72	20	18	90	0.88	24	4587	7595	◆	◆	◆	
	I-4&192 WB EndBent1 Pile 3	75	77	15	13	90	0.58	27	5234	3444	4233	5389	6452	7110
	I-4/192 WB EndBent1 Pile 1	80	82	12	10	92	0.76	27	5339	6762	8235	◆	◆	
	Ramsey Branch Bridge	31	34	##	-24	9	0.81	17	6	3334	5929	7545	8420	◆
	I-4&417 pile 14	42	44	27	25	69	0.15	17	1061	1082	1147	1440	2021	2174
Rebound < 0.2 in	I-4&417 pile 14	57	58	12	11	69	0.14	24	3179	3582	4383	5493	6393	7182
	I-4&417 EB1 pile 14	58	61	11	8	69	0.14	24	2130	2181	2345	3163	3596	4201
	I-4&192 Pier 6 pile 4	60	62	35	33	95	0.16	24	2179	2696	3361	4263	4845	◆
	I-4&192 Pier 8 pile 4	45	47	45	43	90	0.17	18	5394	6016	6629	7985	◆	
	I-4&192 Ramp BD EB1 Pile 3	46	47	44	43	90	0.14	18	2186	3237	4235	4881	5415	5660
	I-4&192 South of Ramp BD EB3 Pile 1	55	57	35	33	90	0.19	22	2122	2182	2463	3533	4348	4785
	I-4/192 WB EB1 Pile 1	50	52	42	40	92	0.20	20	2143	2290	3193	3351	3588	3876
	Averages Rebound	71	73	41	39	82	0.228	27	4893	5534	6271	7018	7436	7110
	Averages NonRebound	52	54	31	29	83	0.158	21	2549	2908	3469	4263	4646	4998
	Averages Overall	62	64	20	18	83	0.474	24	3629	4034	4403	5015	5009	4998

Table D-3: Cyclic test results for cohesionless soils from thin walled tube sample sites (cont.)

	Depth		Elevation	GSE	Rebound	PWP @ 1% Strain	PWP @ 2.5% Strain	PWP @ 5% Strain	PWP @ 10% Strain	PWP @ 15% Strain	PWP @ 20% Strain	PWP Ratio @ 1% Strain	PWP Ratio @ 2.5% Strain	PWP Ratio @ 5% Strain	PWP Ratio @ 10% Strain	PWP Ratio @ 15% Strain	PWP Ratio @ 20% Strain		
	ft	in																	
Rebound > 0.5 in	I-4/Osceola Pier 2 Pile 8	75	76	14	13	89	0.74	16	16	16	16	0.53	0.53	0.53	0.53	0.53	0.53		
	I-4/Osceola Pier 2 Pile 8	80	81	9	8	89	0.78	11	11	11	11	0.34	0.34	0.34	0.34	0.34	0.34		
	I-4/Osceola B1 Pier 2 Pile 8	85	87	4	2	89	0.79	1.6	24.4	24.4	24.4	0.05	0.05	0.05	0.05	0.05	0.05		
	I-4&192 Pier 6 pile 4	80	82	15	13	95	0.62	26.2	29.2	28.4	28.4	0.82	0.91	0.92	0.89	0.89	0.89		
	I-4&192 Pier 8 pile 4	65	66	25	24	90	0.67	12.3	12.3	12.3	12.3	0.51	0.51	0.51	0.51	0.51	0.51		
	I-4&192 Pier 8 pile 4	70	72	20	18	90	0.88	15.9	20.7	20.7	20.7	0.66	0.86	0.86	0.86	0.86	0.86		
	I-4&192 Ramp BD EB1 Pile 3	70	72	20	18	90	0.69	0.9	16.5	19.1	19.2	0.03	0.66	0.76	0.79	0.77	0.75		
	I-4&192 Ramp BD EB1 Pile 3	75	77	15	13	90	0.58	16.0	16.0	16.0	16.0	0.59	0.59	0.59	0.59	0.59	0.59		
	I-4/192 WB EndBent1 Pile 1	80	82	12	10	92	0.76	11.4	16.3	16.9	16.9	0.42	0.60	0.63	0.63	0.63	0.63		
	Ramsay Branch Bridge	31	34	##	-24	9	0.81	0.1	10.0	8.7	6.0	6.0	0.01	0.59	0.62	0.51	0.35	0.35	
Rebound < 0.2 in	I-4&417 pile 14	42	44	27	25	69	0.15	9.6	9.7	13.4	14.3	0.56	0.57	0.79	0.83	0.84	0.84		
	I-4&417 pile 14	57	58	12	11	69	0.14	11.8	20.7	22.4	22.9	0.49	0.86	0.93	0.97	0.95	0.92		
	I-4&417 EB1 pile 14	58	61	11	8	69	0.14	17.1	19.6	21.3	21.2	0.71	0.82	0.89	0.90	0.88	0.89		
	I-4&192 Pier 6 pile 4	60	62	35	33	95	0.16	18.6	21.1	22.1	22.4	0.78	0.88	0.90	0.92	0.93	0.93		
	I-4&192 Pier 8 pile 4	45	47	45	43	90	0.17	12.0	14.8	15.4	15.4	0.67	0.82	0.85	0.85	0.85	0.85		
	I-4&192 Ramp BD EB1 Pile 3	46	47	44	43	90	0.14	11.8	14.4	14.0	13.3	0.66	0.80	0.82	0.78	0.74	0.65		
	I-4&192 South of Ramp BD EB3 Pile 1	55	57	35	33	90	0.19	11.6	11.1	20.8	20.7	0.53	0.50	0.94	0.95	0.94	0.94		
	I-4/192 WB EB1 Pile 1	50	52	42	40	92	0.20	9.8	15.9	16.8	16.4	0.49	0.80	0.83	0.84	0.82	0.82		
	Averages Rebound	71	73	11	10	82	0.78	11	19	19	13	19	0.40	0.72	0.73	0.73	0.73	0.56	0.75
	Averages NonRebound	52	54	31	29	83	0.158	13	16	19	19	18	0.61	0.76	0.87	0.88	0.87	0.85	
Averages Overall	62	64	20	18	83	0.474	12	17	18	17	18	0.49	0.74	0.82	0.84	0.80	0.83		

$PWP Ratio = \Delta u / \sigma'_v$ ; PWP = Pore Water Pressure

## D.2. Tests results- Cohesive soils

Table D-4 : Soil classification, percent sand, silt, clay and fines by weight, Atterberg limits and particle size distribution for all rebound and nonrebound cohesive soils for thin walled tube sample sites.

	Depth		Elevation		GSE	Rebound	Sand	Silt	Clay	Fine	D10	D30	D60	LL	PL	PI	Activity of a clay	Classification	
	ft	ft	ft	ft	ft	in	%	%	%	%	mm	mm	mm				A	AASHTO	USCS
Rebound > 0.5 in	70	72	19	17	89	0.500	31	54	15	69	◆	0.009	0.057	60	27	33	2.16	CH	A-7-6
	50	52	13	11	63	2.040	23	28	49	77	◆	◆	0.007	71	25	45	0.92	CH	A-7-6
	54	56	9	7	63	1.335	42	20	37	58	◆	◆	0.080	51	19	33	0.87	CH	A-7-6
	52	55	11	8	63	1.400	5	34	61	95	◆	◆	0.002	91	30	61	1.00	CH	A-7-5
	47	49	15	13	62	0.800	43	20	37	57	◆	◆	0.085	51	16	35	0.95	CH	A-7-6
	50	52	13	11	63	2.040	23	28	49	77	◆	◆	0.007	71	25	45	0.92	CH	A-7-6
Rebound < 0.2 in	54	56	9	7	63	1.335	42	20	37	58	◆	◆	0.080	51	19	33	0.87	CH	A-7-6
	55	57	14	12	69	0.050	59	14	27	41	◆	0.004	0.104	40	19	21	0.33	SC	A-6
	65	67	-40	-42	25	0.175	32	46	22	68	◆	0.004	0.038	37	18	19	0.55	CL	A-6
	62	64	-36	-38	26	0.140	9	65	26	91	◆	0.003	0.017	44	19	25	0.53	CL	A-7-6
Averages Rebound	54	56	13	11	67	1.35	30	29	41	70	0.009	0.045	64	23	41	1			
Averages NonRebound	61	63	-21	-23	40	0.12	33	42	25	67	0.003	0.053	40	19	22	0			
Averages Overall	56	58	3	1	59	0.98	31	33	36	69	0.005	0.048	57	22	35	1			

Table D-5: List of physical properties from cyclic tests retrieved from all rebound and nonrebound cohesive soils for all thin walled tube sample sites.

	Depth		Elevation		GSE	Rebound	Unit Wt.	Dry Unit Wt.	Void ratio	Porosity, (n)	Degree of Saturation (S)	Moisture	LL	PL	PI	Activity of a clay	Classification
	ft	ft	ft	ft													
Rebound > 0.5 in	70	72	19	17	89	0.50	94	60	1.78	64.08	83	55	60	27	33	2.16	AASHTO CH
	50	52	13	11	63	2.04	97	58	1.87	65.10	97	69	71	25	45	0.92	CH
	54	56	9	7	63	1.34	108	87	0.88	46.78	72	24	51	19	33	0.87	CH
	52	55	11	8	63	1.40	94	53	2.22	68.98	95	77	91	30	61	1.00	CH
	47	49	15	13	62	0.80	101	65	1.58	61.30	95	56	51	16	35	0.95	CH
	50	52	13	11	63	2.04	97	58	1.87	65.10	97	69	71	25	45	0.92	CH
	54	56	9	7	63	1.34	108	87	0.88	46.78	72	24	51	19	33	0.87	CH
Rebound < 0.2 in	55	57	14	12	69	0.05	107	74	1.33	57.01	94	45	40	19	21	0.33	SC
	65	67	-40	-42	25	0.18	111	83	1.04	51.06	88	34	37	18	19	0.55	CL
Averages Rebound	54	56	13	11	67	1.35	100	67	1.58	60	87	53	64	23	41	1.10	
	61	63	-21	-23	40	0.12	107	76	1.25	55	92	43	40	19	22	0.47	
Averages NonRebound	56	58	3	1	59	0.98	102	69	1.48	58	89	50	57	22	35	0.91	

LL= Liquid Limit; PL = Plastic Limit; PI= Plasticity index;

$$\text{Activity of a clay} = \frac{\% \text{ Clay particles less than } 2 \mu\text{m}}{PI}$$

Table D-6 Summary of cyclic triaxial tests results for all cohesion soils retrieved from all thin walled tube sample sites

	Depth		Elevation		GSE	Rebound	Confining Pressure	Number of Cyclic Causing % Strain	Number of Cyclic Causing 2.5 % Strain	Number of Cyclic Causing 5 % Strain	Number of Cyclic Causing 10 % Strain	Number of Cyclic Causing 15 % Strain	Number of Cyclic Causing 20 % Strain
	ft	in	ft	in									
Rebound > 0.5 in	70	72	19	17	89	0.50	30	4313	7611	8502	13164	8410	10660
	50	52	13	11	63	2.04	20	6	7333	8502	13164	8410	10660
	54	56	9	7	63	1.34	22	4665	5398	5768	13164	8410	10660
	52	55	11	8	63	1.40	17	8464	8464	8464	13164	8410	10660
	47	49	15	13	62	0.80	15	8464	8464	8464	13164	8410	10660
	50	52	13	11	63	2.04	20	6351	7559	7869	13164	8410	10660
	54	56	9	7	63	1.34	29	8464	8464	8464	13164	8410	10660
	55	57	14	12	69	0.05	24	2506	3750	4410	4780	4902	4902
	65	67	-40	-42	25	0.18	27	11738	12758	12994	13164	13437	13437
	62	64	-36	-38	26	0.14	25	8437	9625	9863	10290	10613	10660
Averages Rebound	54	56	13	11	67	1.35	22	5818	7026	7380	8131	8410	10660
Averages NonRebound	61	63	-21	-23	40	0.12	25	7560	8711	9089	9411	9651	10660
Averages Overall	56	58	3	1	59	0.98	23	6341	7748	8234	9091	9341	10660

Table D-7 Summary of cyclic triaxial tests results for all cohesion soils retrieved from all thin walled tube sample sites (cont.)

	Depth		Elevation		GSE	Rebound	Confining Pressure	PWP @ 1% Strain	PWP @ 2.5% Strain	PWP @ 5% Strain	PWP @ 10% Strain	PWP @ 15% Strain	PWP @ 20% Strain	PWP Ratio @ 1% Strain	PWP Ratio @ 2.5% Strain	PWP Ratio @ 5% Strain	PWP Ratio @ 10% Strain	PWP Ratio @ 15% Strain	PWP Ratio @ 20% Strain
	ft	in	ft	in															
I-48192 Pier 7	70	72	19	17	89	0.50	30	8	18	18	18	18	18	0.26	0.61	0.61	0.61	0.61	0.61
	50	52	13	11	63	2.04	20	0.03	10	13	13	13	13	0.002	0.48	0.64	0.64	0.64	0.64
Chaifree Rd EB3	54	56	9	7	63	1.34	22	16	18	19	19	19	19	0.73	0.80	0.86	0.86	0.86	0.86
	52	55	11	8	63	1.40	17	3	17	17	17	17	17	0.18	0.18	0.18	0.18	0.18	0.18
Chaifree Rd EB1	47	49	15	13	62	0.80	15	5	15	15	15	15	15	0.33	0.33	0.33	0.33	0.33	0.33
	50	52	13	11	63	2.04	20	6	8	8	9	9	9	0.32	0.41	0.42	0.44	0.46	0.46
Chaifree Rd EB3 Renom	54	56	9	7	63	1.34	29	9	19	19	19	19	19	0.31	0.31	0.31	0.31	0.31	0.31
	55	57	14	12	69	0.05	24	14	19	21	20	16	16	0.59	0.81	0.85	0.84	0.68	0.68
I-48417 EB2 Pile 5	65	67	-40	-42	25	0.18	27	21	24	24	24	23	23	0.23	0.23	0.23	0.23	0.23	0.23
	62	64	-36	-38	26	0.14	25	16	20	21	22	22	22	0.22	0.22	0.22	0.22	0.22	0.22
Average Rebound	54	56	13	11	67	1.55	22	6.74	13.47	13.37	6.80	5.21	#DIV/0!	0.30	0.58	0.64	0.44	0.46	0.46
	61	63	-21	-23	40	0.12	25	17.15	21.14	21.87	21.98	20.57	21.52	0.59	0.81	0.85	0.84	0.68	0.68
Average NonRebound	56	58	3	1	59	0.98	23	9.86	16.76	17.62	18.68	17.73	21.52	0.34	0.62	0.69	0.64	0.64	0.57
Average Overall																			

$$PWP = \text{Pore Water Pressure; } PWP \text{ Ratio} = \Delta u / \sigma'_v$$

## **Appendix E- Additional Correlations from Shelby Tube Testing**

## E.1. Physical Properties Analysis: Fine content

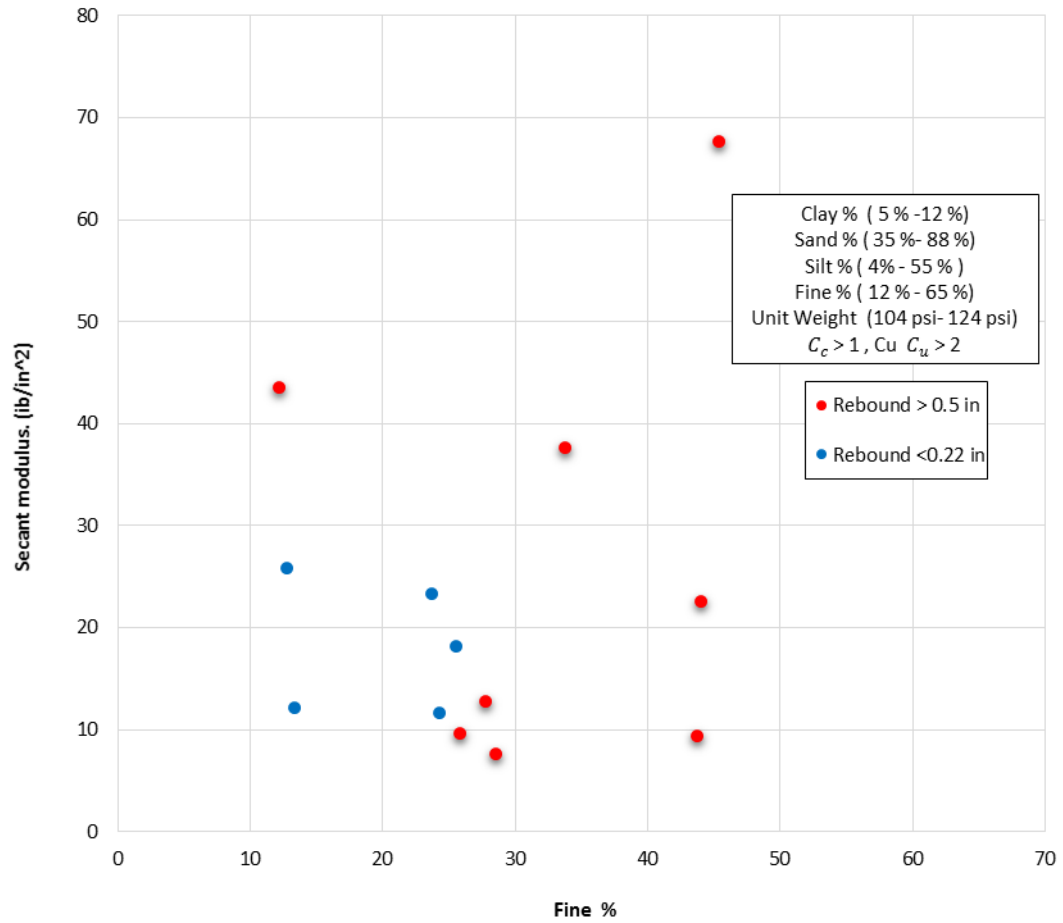


Figure F-1: Fine Content (%) Vs. Secant Modulus (psi)- Cohesionless soils (SM)

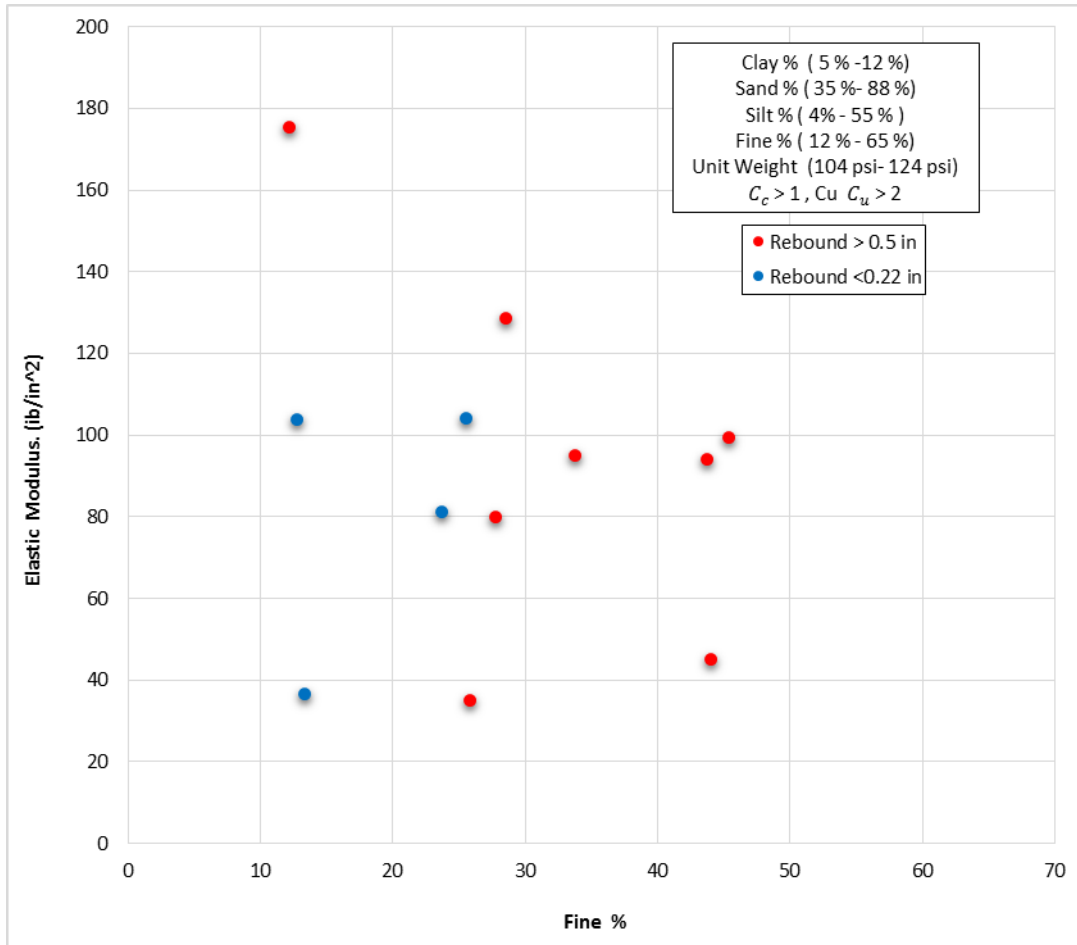


Figure F-2: Fine Content (%) Vs. Elastic Modulus (psi)- Cohesionless soils (SM)

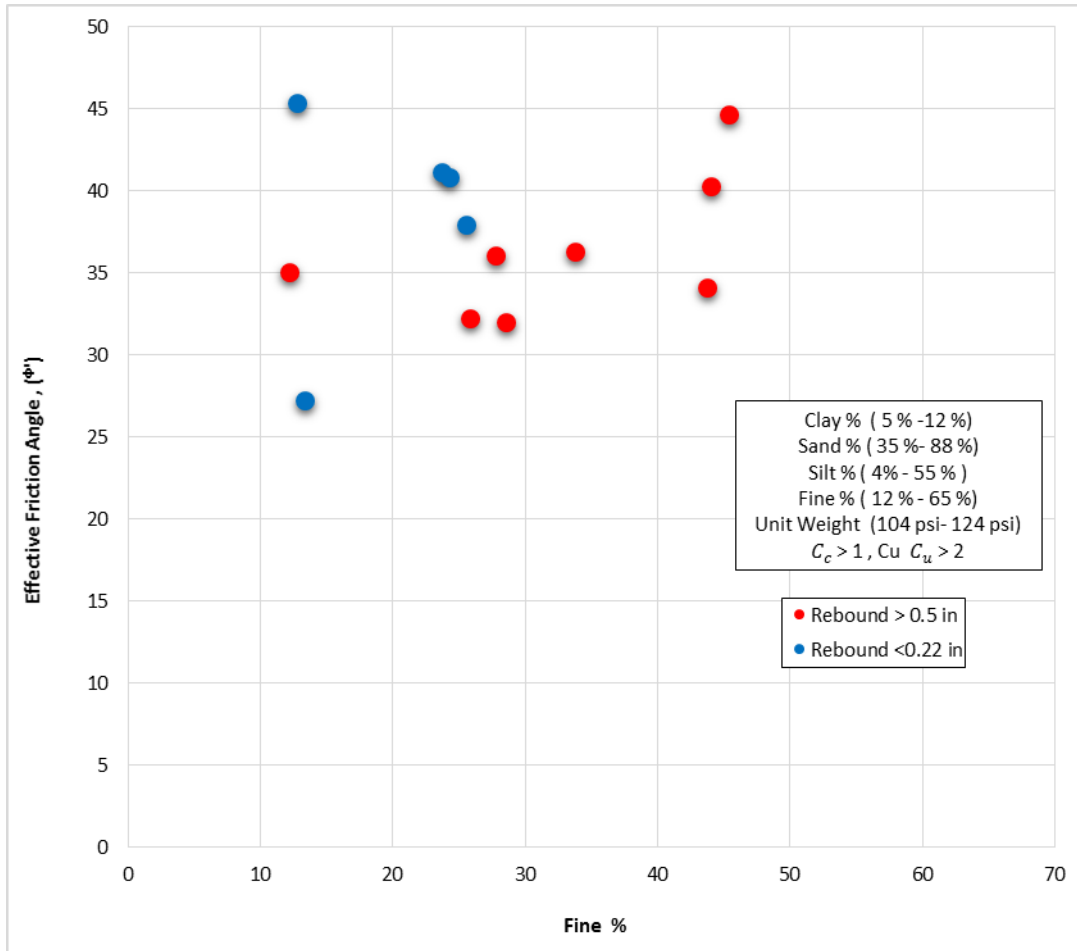


Figure F-3: Fine Content (%) Vs. Effective Friction Angle- Cohesionless soils (SM)